SYSTEMS APPLICATIONS, INC.
PREPARED FOR BUREAU
OF LAND MANAGEMENT

FEBRUARY 1983

BLM LIBRARY
88045472

FINAL AIR QUALITY TECHNICAL REPORT

UINTAH BASIN SYNFUELS DEVELOPMENT

BLM LIBRARY
RS 150A BLDG. 50
DENVER FEDERAL CENTER
P.O. BOX 25047
DENVER, CO 80225

ID 88045472

17342697

UINT
~~#3~~
SUP

TD
195
.S95
U35
1983
Suppl.

FINAL
AIR QUALITY
TECHNICAL REPORT

for the

UINTAH BASIN SYNFUELS DEVELOPMENT

ENVIRONMENTAL IMPACT STATEMENT

BLM LIBRARY
RS 150A BLDG. 50
DENVER FEDERAL CENTER
P.O. BOX 25047
DENVER, CO 80225

February 1983

Prepared by Systems Applications, Incorporated for
U.S. Department of the Interior, Bureau of Land Management

Bureau of Land Management
Library
Bldg. 50, Denver Federal Center
Denver, CO 80225

This study report was prepared by the following technical personnel at Systems Applications, Inc.:

Principal Investigators

Douglas A. Latimer
William R. Oliver
Mark A. Yocke

Contributing Technical Staff

Jody Ames
Don H. Hern
Henry Hogo
Clark D. Johnson
John E. Langstaff
Ralph E. Morris
Thomas C. Myers
Pradeep Saxena
David R. Souten

ACKNOWLEDGMENTS

We express our gratitude to Bill Wagner of the Bureau of Land Management, whose guidance, encouragement, and helpful comments were of great benefit to us and our work.

Helpful comments on the draft report were received from several people on the governmental technical review committee and from the public --far too many to thank individually.

DISCLAIMER

The conclusions regarding air quality impacts presented in this report are based on state-of-the-art regional and near-source air quality simulation models. However, these models are not approved by the U.S. Environmental Protection Agency or the states of Utah and Colorado for the purposes of regulatory permitting activities. The statements in this report regarding the applicability, conservatism, and uncertainty of models are based solely on the scientific and professional judgments of the authors. The analyses presented in this report are for information and planning purposes only. People concerned with satisfying regulatory requirements for Prevention of Significant Deterioration (PSD) permits should consult the responsible state or federal agency. Air quality impacts of the sources to be located in Utah would be evaluated separately by the State of Utah Department of Health, Division of Environment, Bureau of Air Quality, which has delegated PSD authority from EPA.

EXECUTIVE SUMMARY

This report documents an analysis of air quality impacts that was performed by Systems Applications, Inc. for the Bureau of Land Management (BLM) of synthetic fuel developments in the Uinta Basin of Utah. This analysis is to support the Environmental Impact Statement (EIS) that BLM is preparing for each of five specific synthetic fuel developments and cumulative regional impacts.

The primary objective of the study was to evaluate the air quality impacts of five synthetic fuel (oil shale and tar sands) facilities proposed to be developed in the Uinta Basin: Enercor-Mono Power (Rainbow site), Magic Circle, Paraho, Syntana-Utah, and Tosco. Three additional facilities that are at a conceptual design phase--Enercor-Mono Power (PR Springs site), Geokinetics, and Sohio--were also studied in regional scenarios. The impacts associated with two levels of oil production in the Uinta Basin of 121,400 and 320,500 barrels per day were studied.

Since cumulative regional impacts were considered to be important in this study, impacts of other industrial facilities were also examined. In the Uinta Basin these included the Moon Lake power plant (units 1 and 2), White River oil shale project (100,000 barrel per day capacity), Plateau refinery, and five other small projects. In the Piceance Basin in Colorado the air quality impacts of oil shale facilities having capacities totaling 271,000 and 639,000 barrels per day were included in regional assessments. The total synthetic fuel production capacity in the Uinta and Piceance basins studied in the low- and high-oil-production scenarios was 492,000 and 1,059,500 barrels per day, respectively.

Air quality impacts in the region were previously studied by both Systems Applications and Los Alamos Scientific Laboratory. The current study provides a more detailed analysis than did the previous policy and screening analyses. The current report is based on detailed emission inventories developed by synthetic fuel developers, Systems Applications, and PEDCo Environmental; measured meteorological conditions in the region; and additional regional data such as ambient air quality, topography, and visibility.

ANALYSIS METHODOLOGY

The methodology used in this study consisted of the following major tasks:

> Collection of Data. Emission data for the Uinta Basin synfuel facilities were collected from the developers. Information concerning Colorado point and area source emissions and Utah population projections were obtained from a study performed for the National Park Service by PEDCo. Meteorological and topographical data were collected for the region.

> Emission Inventory Development. Emission data were reviewed, checked, revised, and converted to input files for air quality modeling. Utah population data and projections were used to generate secondary area source emission files for the portion of Utah in the study region for the year 1980 baseline and for future low- and high-oil-production scenarios.

> Air Quality Modeling. With the emissions, meteorological, and topographical data as input, several air quality simulation models were applied to address specific concerns. The most extensive modeling was performed by means of the Gaussian Puff Model (GPM), which was applied to 110-km x 110-km and 180-km x 268-km, regions encompassing the Uinta Basin and the combined Uinta and Piceance basins, respectively. Impacts were computed for every 3-hour period in a year to determine maximum 3-hour, 24-hour, and annual averages for every receptor in these regions. This model, which is believed to be conservative as applied in this study, was used to identify high (conservative) estimates of worst-case impacts. Additional calculations using the Regional Transport Model (RTM) were made for four worst-case regional transport episodes identified by GPM. The EPA Gaussian, sector-average COMPLEX I Model was applied to evaluate the impact of multiple point ground-level TSP emissions within a given facility on near-source (< 5 km downwind) TSP concentrations for which the GPM calculations are inappropriate. Worst-case photochemical smog and visibility impairment scenarios were evaluated by means of EKMA and PLUVUE, respectively. Acid deposition was evaluated from GPM results.

ANALYSIS RESULTS

Although there is uncertainty in the regional modeling results of this study, this uncertainty was explicitly identified by providing high and low estimates of ground-level concentrations. Even with this uncertainty,[*] the following major conclusions were made on the basis of this study:

- Uinta Basin Site-Specifics. The air quality impacts resulting from direct emissions from the five proposed site-specific facilities in the Uinta Basin--Enercor-Mono Power, Magic Circle, Paraho, Syntana-Utah, and Tosco--when evaluated separately or together with other planned projects in the Uinta Basin, will be less than all applicable air quality standards and PSD increments. Near-source, maximum 24-hour average TSP concentrations are close to the Class II PSD increment, however.

- Uinta Basin Conceptuals. The air quality impacts resulting from direct emissions from the proposed projects in the Uinta Basin that are at a conceptual design stage--Enercor-Mono Power, Geokinetics, and the Sohio tar sands facility--will be within all applicable air quality standards and PSD increments (when emissions are treated separately or together with the site-specifics and other interrelated projects in the Uinta Basin). One exception to this general statement is the possibility that near the Sohio facility the PSD Class II increment for the maximum 24-hour average TSP concentration may be exceeded. This potential violation could be mitigated provided that better TSP emission controls can be implemented in the detailed design phase of this project.

- Piceance Basin Oil Shale Facilities. All of the proposed oil shale facilities in Colorado can be sited without exceedance of applicable air quality standards and PSD increments, except the Cathedral Bluffs facility which could violate the 24-hour average SO_2 PSD Class II increment and possibly the Class I increment in the Flat Tops Wilderness Area (see additional discussion of Flat Tops impacts below). These violations could be avoided if, as recently announced, the Cathedral Bluffs facility is not built or if better emission control technology than that assumed in this analysis could be employed. Maximum 24-hour average TSP concentrations at the site boundaries of a number of these Piceance Basin oil shale facilities will approach the Class II increment.

---

[*] Cases in which the use of a high estimate would result in a conclusion different from that of a low estimate are identified. Most of the conclusions in this summary are unequivocal even within the estimated range of uncertainty.

> Secondary Emissions. The impacts of associated regional population growth and residential and commercial development (so-called secondary impacts) will be within all applicable standards, except that total suspended particulate (TSP) concentrations, which are currently in excess of standards in some parts of the region, will be exacerbated. Most of this impact is due to windblown dust and dust raised from unpaved and gravel roads. These large particles are not respirable and do not affect regional visibility. In addition, if this fugitive dust from secondary sources is included in the consumption of the PSD increments for TSP, and mitigation measures, such as paving roadways, are not employed, it is quite likely that PSD Class II increments for TSP will be exceeded in much of the region and that PSD Class I increments for TSP in Flat Tops and Mt. Zirkel will be exceeded.*

> Flat Tops Wilderness. The existing mandatory Class I area with maximum impacts from the proposed synfuel industry in the Uinta and Piceance basins is the Flat Tops Wilderness. If secondary TSP emissions in the Piceance Basin are not mitigated and are counted in the Class I increment consumption, there most likely will be a violation of the Class I TSP increment. If not, then the Class I SO_2 increment could be constraining if all the Uinta and Piceance sources are considered conservative, high estimates of maximum 3- and 24-hour average SO_2 concentrations in Flat Tops are utilized. However, even if high estimates are used and secondary TSP emissions are included in the increment, the Uinta Basin synfuel

---

* The EPA fugitive dust policy allows the discounting of the TSP impacts that can be shown to be caused by wind-blown dust. This policy could be extended to localized dust plumes from unpaved roads as well as wind blown dust.

facilities (both the site-specific and conceptual proposals) could be operated without violations of Class I increments in Flat Tops if some of the Piceance Basin sources are not built. Indeed, the substantial emissions from the proposed Cathedral Bluffs facility dominate impacts in Flat Tops. If this project is shelved indefinitely, as recently announced, the Class I increment is not likely to be consumed in Flat Tops.

> Dinosaur and Colorado National Monuments. The Dinosaur and Colorado national monuments are currently Federal Class II areas that are under consideration for redesignation to Class I. These areas are also Colorado Category I for SO_2. It is possible, depending on what set of Uinta and Piceance basin emission sources are considered and on whether conservatively high estimates of impacts are utilized, that PSD Class I and Colorado Category I increments would be exceeded in these two areas.

> Visibility Impairment. Even for the maximum synthetic fuel development scenario studied, regional visual range (visibility) will largely be unaffected by the industrial, commercial, and residential developments. Significant, local reductions in visual range could be observed in stagnant haze layers principally in the winter. These hazes would be caused by TSP emissions from industrial facilities, windblown dust, dust from roadways, and smoke from residential wood stoves and fireplaces. These hazes would be infrequent and localized and would not affect regional visibility and views in wilderness areas. Worst-case reductions in regional visual range are anticipated to occur in the summer when sulfate formation rates are highest. Worst visual range reduction is projected to be less than 10 percent and would be principally due to sulfate aerosol formed in the atmosphere from regional SO_2 emissions from synthetic fuel facilities and power plants. The predicted high TSP concentrations from secondary emissions are not expected to greatly reduce regional visibility. They would only cause local dust clouds. Yellow-brown atmospheric plume discoloration may be visible on fewer than 50 days, primarily on mornings with clear, light-wind, stable conditions in the vicinity of synthetic fuel facilities, on the Uintah/Ouray Indian Reservation, and at Dinosaur National Monument.

> Acid Deposition. Wet and dry acid deposition in the middle of the developed areas in the Uinta and Piceance basins and in the Grand Junction area is expected to be at rates as great as those experienced currently in large areas of the eastern United States and in Europe. However, at distances beyond about 50 km from development areas, in wilderness areas, and throughout most of the region, deposition rates are expected to be typical of worldwide background conditions.

> Perspective on Air Quality Impacts. The regional air quality impacts of the proposed synthetic fuel industry can be put in perspective by comparing projected emissions to the atmosphere with other emission sources with which we have more experience. For example, the largest of the synfuel facilities in the Uinta Basin have SO_2 and NO_x emissions rates equivalent to a very well-controlled, 300-Mwe coal-fired power plant. All the projected regional emissions of SO_2 from all sources in both the Uinta and Piceance basins for the high-oil-production scenario, which are spread throughout a 15,000 square kilometer region, are the equivalent of the well-controlled emissions from 5600 Mwe of low-sulfur-coal-fired power plant capacity. Regional NO_x emissions are the equivalent of 8000 Mwe of capacity.

CONTENTS

ACKNOWLEDGMENTS.. iv

DISCLAIMER... v

EXECUTIVE SUMMARY.. vii

LIST OF ILLUSTRATIONS.. xvii

LIST OF TABLES... xxiii

1 INTRODUCTION... 1-1

1.1 SCOPE OF THE STUDY... 1-2

1.2 REPORT CONTENTS.. 1-2

2 THE AFFECTED ENVIRONMENT....................................... 2-1

2.1 TOPOGRAPHY... 2-1

2.2 METEOROLOGY AND CLIMATOLOGY.................................. 2-1

2.2.1 Wind Direction... 2-7
2.2.2 Wind Speeds.. 2-10
2.2.3 Stability.. 2-10
2.2.4 Effect of Terrain on Wind Fields........................... 2-15

2.3 EXISTING AIR QUALITY... 2-15

3 AIR QUALITY IMPACT SIGNIFICANCE CRITERIA........................ 3-1

3.1 AMBIENT AIR QUALITY STANDARDS................................ 3-1

3.2 PREVENTION OF SIGNIFICANT DETERIORATION...................... 3-3

3.3 DETERMINATION OF SIGNIFICANT VISIBILITY IMPAIRMENT........... 3-5

3.4 PROTECTION OF AIR-QUALITY-RELATED VALUES..................... 3-6

4 ANALYSIS METHODOLOGY... 4-1

4.1 DEVELOPMENT OF EMISSION INVENTORIES.......................... 4-3

4.1.1 Utah Synfuel Projects...................................... 4-7
4.1.2 Other Planned Projects (Utah).............................. 4-11
4.1.3 Utah Baseline Point Sources................................ 4-11

4.1.4 Colorado Oil Shale, Point, and Area Sources.... 4-13
4.1.5 Utah Baseline Area Sources.... 4-15
4.1.6 Utah Area Sources: Regional High-Oil-Production Scenario.... 4-31
4.1.7 Utah Area Sources: Regional Low-Oil-Production Scenario.... 4-44
4.1.8 Utah Area Source Summary.... 4-47
4.1.9 Socioeconomic Data Comparison for Utah.... 4-47
4.1.10 Concluding Remarks Pertaining to Inventory Activities.... 4-53

4.2 DESCRIPTION OF MODELING APPROACHES.... 4-54

4.2.1 Modeling Methodology.... 4-54

5 REGIONAL AIR QUALITY IMPACTS.... 5-1

5.1 CONCENTRATION ESTIMATION APPROACH.... 5-2

5.1.1 Conservatism of the Gaussian Puff Model.... 5-4
5.1.2 Comparing GPM and RTM Calculations.... 5-6
5.1.3 Qualitative Estimates of Uncertainty in Model Calculations.... 5-17

5.2 IMPACTS OF INDUSTRIAL GROWTH.... 5-19

5.2.1 Low-Oil-Production Scenario.... 5-31
5.2.2 High-Oil-Production Scenario.... 5-47

5.3 IMPACTS OF POPULATION AND ASSOCIATED GROWTH.... 5-88

5.3.1 Low-Production Scenario.... 5-88
5.3.2 High-Production Scenario.... 5-100

5.4 CUMULATIVE AIR QUALITY IMPACTS OF ALL REGIONAL EMISSIONS.... 5-100

5.4.1 SO_2 Impacts.... 5-100
5.4.2 TSP Impacts.... 5-118

5.5 PHOTOCHEMICAL SMOG.... 5-126

5.6 VISIBILITY IMPAIRMENT.... 5-135

5.6.1 Plume Discoloration.... 5-136
5.6.2 Regional Haze.... 5-144

5.7 ACID DEPOSITION.... 5-147

5.8 AIR QUALITY IMPACTS ASSOCIATED WITH CONSTRUCTION ACTIVITIES.... 5-153

6 AIR QUALITY IMPACTS OF SPECIFIC PROPOSED ACTIONS.... 6-1

6.1 ENERCOR-MONO POWER.... 6-2

6.2 MAGIC CIRCLE.. 6-2
6.3 PARAHO 6-22
6.4 SYNTANA-UTAH.. 6-22
6.5 TOSCO.. 6-22
6.6 SUMMARY AND COMPARISON WITH OTHER ANALYSES............ 6-44

APPENDIX A UPPER-LEVEL WIND ROSE STRATIFIED BY SEASON AND TIME OF DAY FOR STUDY REGION IN 1978............. A-1

APPENDIX B SURFACE (10 m) WIND ROSE STRATIFIED BY SEASON AND TIME OF DAY AT U-A, U-B SITE IN 1978............. B-1

APPENDIX C TECHNICAL DISCUSSION OF MODELS USED IN STUDY......... C-1

APPENDIX D LEVEL-1 VISIBILITY SCREENING RESULTS FOR EMISSIONS FROM ALL SYNTHETIC FUEL FACILITIES IN THE REGION AT THE HIGH OIL PRODUCTION RATES........ D-1

APPENDIX E MITIGATION MEASURES FOR SYNFUEL INDUSTRY RELATED EMISSIONS.............................. E-1

REFERENCES.. R-1

LIST OF ILLUSTRATIONS

1-1 Locations of Sources, Towns, Counties, and Mandatory and Potential Class I Areas in Study Region................. 1-5

2-1 Terrain Elevation Contours (ft MSL) in Study Region......... 2-2

2-2 Perspective of Terrain in Study Region...................... 2-3

2-3 Average Upper Air Wind Rose for Study Region................ 2-5

2-4 Wind Direction Frequency Distributions for All Morning Soundings... 2-8

2-5 Vertical Wind Direction Distribution Profiles for All Afternoon Soundings.................................. 2-9

2-6 Wind Speed Frequency Distributions for All Morning Soundings... 2-11

2-7 Wind Speed Frequency Distributions for All Afternoon Soundings... 2-12

2-8 Computed Wind Fields for Eight Synoptic Wind Directions for the Study Region (Lowest Modeled Layer from 4300 ft MSL or Terrain Elevation, to 6800 ft MSL)........... 2-17

2-9 Computed Wind Fields for Down-Slope and Up-Slope Flow Conditions and Zero Upper-Air Winds (Lowest Modeled Layer from 4300 ft MSL or Terrain Elevation, to 6800 ft MSL)... 2-25

2-10 Existing Annual Average SO_2 Concentrations ($\mu g/m^3$).......... 2-29

2-11 Correlations between TSP Emissions and Ambient Concentrations... 2-31

2-12 Model Estimates of Existing Total Suspended Particulate (TSP) Concentrations in Study Region........................ 2-32

2-13 Frequency Distribution of Visual Range at Dinosaur National Monument in Summer 1979 2-35

4-1 Overall Flow Diagram of Analysis Methodology 4-2

4-2 Schematic Diagram of Activities for the Emission Inventory Development Process 4-4

4-3 Area Emission Source Inventory for the Study Region in the Baseline Year 1980 (tons/yr/100 km^2) 4-34

4-4 Total Cumulative Population in the Uinta Basin with High-Level Synfuel Development 4-52

4-5 Schematic Diagram of Modeling Methodology 4-56

4-6 3-D Perspective of Terrain in Regional Modeling Area 4-63

4-7 Temporal Variation of First Grid Layer Depth 4-68

4-8 Schematic Diagram of Methodology for Applying the Complex-Terrain Wind Model (CTWM) in the "Composite" Mode 4-74

4-9 Spatial Distribution of Land Use Categories 4-79

5-1 24-Hour SO_2 Concentration Estimates for 27 July 1978 from Direct Source SO_2 Emissions and for the High Oil Production Scenario 5-8

5-2 Schematic Representation of Estimated Ranges in the Regional Air Quality Impacts Assessment 5-20

5-3 Impact of Direct Source Emissions from Moon Lake Unit 2 on Ground-Level SO_2 Concentrations ($\mu g/m^3$) 5-21

5-4 Impact of Direct Source Emissions from Moon Lake Unit 2 on Ground-Level TSP Concentrations ($\mu g/m^3$) 5-24

5-5 Impact of Direct Source Emissions from White River Shale Project on Ground-Level SO_2 Concentrations ($\mu g/m^3$) 5-26

5-6 Impact of Direct Source Emissions from White River Shale Project on Ground-Level TSP Concentrations ($\mu g/m^3$) 5-29

5-7 Impact of Direct Source Emissions from Uinta Basin Site-Specifics on Ground-Level SO_2 Concentrations ($\mu g/m^3$) for Low Oil Production Scenario........ 5-32

5-8 Impact of Direct Source Emissions from Uinta Basin Site-Specifics on Ground-Level TSP Concentrations ($\mu g/m^3$) for Low Oil Production Scenario........ 5-35

5-9 Impact of Direct Source Emissions from Uinta Basin Site-Specifics and Conceptuals on Ground-Level SO_2 Concentrations ($\mu g/m^3$) for Low Oil Production Scenario........ 5-37

5-10 Impact of Direct Source Emissions from Uinta Basin Site-Specifics on Ground-Level TSP Concentrations ($\mu g/m^3$) for Low Oil Production Scenario........ 5-40

5-11 Impact of Direct Source Emissions from Colorado Emission Sources on Ground-Level SO_2 Concentrations ($\mu g/m^3$) for the Low Oil Production Scenario........ 5-42

5-12 Impact of Direct Source Emissions from Colorado Point Sources on Ground-Level TSP Concentrations ($\mu g/m^3$) for Low Oil Production Scenario........ 5-45

5-13 Impact of Direct Source Emissions on Ground-Level SO_2 Concentrations ($\mu g/m^3$) for the Low Oil Production Scenario........ 5-48

5-14 Impact of Direct Source Emissions on Ground-Level TSP Concentrations ($\mu g/m^3$) for the Low Oil Production Scenario........ 5-51

5-15 Impact of Direct Source Emissions from Uinta Basin Site-Specifics on Ground-Level SO_2 Concentrations ($\mu g/m^3$) for the High Oil Production Scenario........ 5-53

5-16 Impact of Direct Source Emissions from Uinta Basin Site-Specifics on Ground-Level TSP Concentrations ($\mu g/m^3$) for the High Oil Production Scenario........ 5-56

5-17 Impact of Direct Source Emissions from Uinta Basin Site-Specifics and Conceptuals on Ground-Level SO_2 Concentrations ($\mu g/m^3$) for the High Oil Production Scenario.......... 5-58

5-18 Impact of Direct Source Emissions from Uinta Basin Site-Specifics and Conceptuals on Ground-Level TSP Concentrations ($\mu g/m^3$) for the High Oil Production Scenario.......... 5-61

5-19 Maximum 24-Hour Average, Near-Source TSP Concentrations ($\mu g/m^3$) Resulting from Direct Source Emissions from the Sohio Conceptual Tar Sands Facility on the Basis of COMPLEX-I Calculations.......... 5-64

5-20 Impact of Direct Source Emissions from Colorado Point Sources on Ground-Level SO_2 Concentrations ($\mu g/m^3$) for the High Oil Production Scenario.......... 5-65

5-21 Impact of Direct Source Emissions from Colorado Point Sources on Ground-Level TSP Concentrations ($\mu g/m^3$) for the High Oil Production Scenario.......... 5-68

5-22 Maximum 24-Hour Average Near Source TSP Concentrations Resulting from Direct Source Emissions from Oil Shale Facilities in the Piceance Basin of Colorado Based on COMPLEX-I.......... 5-70

5-23 Maximum Near-Source SO_2 Concentrations Resulting from Direct Source Emissions from Cathedral Bluffs on the Basis of COMPLEX-I Calculations.......... 5-81

5-24 Impact of Direct Source Emissions on Ground-Level SO_2 Concentrations ($\mu g/m^3$) for the High Oil Production Scenario.......... 5-83

5-25 Impact of Direct Source Emissions on Ground-Level TSP Concentrations ($\mu g/m^3$) for the High Oil Production Scenario.......... 5-86

5-26 Impact of Area Source Emissions on Ground-Level SO_2 Concentrations ($\mu g/m^3$) for the Low Oil Production Scenario.......... 5-89

5-27 Impact of Area Source Emissions on Ground-Level TSP Concentrations ($\mu g/m^3$) for the Low Oil Production Scenario 5-92

5-28 Area Source Emission Densities for Low Oil Production Scenario (tons/yr/100 km^2) 5-94

5-29 Impact of Area Source Emissions on Ground-Level SO_2 Concentrations ($\mu g/m^3$) for the High Oil Production Scenario 5-101

5-30 Impact of Area Source Emissions on Ground-Level TSP Concentrations ($\mu g/m^3$) for the High Oil Production Scenario 5-104

5-31 Area Source Emission Densities for High Oil Production Scenario (tons/yr/100 km^2) 5-106

5-32 Summary of SO_2 Concentration Estimates for Various Averaging Times Compared to Air Quality Standards and PSD Increments 5-119

5-33 Summary of TSP Concentration Estimates for Various Averaging Times Compared to Ambient Air Quality Standards and PSD Increments for Both the Low and High Oil Production Scenarios 5-125

5-34 Two Trajectories Modeled for Worst-Case Photochemical Oxidant (Ozone) Impact 5-131

5-35 Cumulative Frequency of Perceptible Plume Discoloration Resulting from Emissions from Various Uinta Basin Sources at Dinosaur National Monument 5-140

5-36 Cumulative Frequency of Perceptible Plume Discoloration Resulting from Emissions from Various Uinta Basin Sources at Uintah and Ouray Indian Reservation 5-142

5-37 Annual Sulfur Anion Dry Deposition ($G/M^2/yr$) for the High Oil Production Scenario 5-149

5-38 Annual Nitrogen Anion Dry Deposition ($G/M^2/yr$) for the High Oil Production Scenario 5-150

6-1 Ground-Level SO_2 Concentrations (μ/m^3) due to Enercor-Mono Power Emissions.................................. 6-5

6-2 Ground-Level TSP Concentrations ($\mu g/m^3$) due to Enercor-Mono Power Emissions.................................. 6-8

6-3 Ground-Level SO_2 Concentrations ($\mu g/m^3$) due to Magic Circle Emissions.. 6-14

6-4 Ground-Level TSP Concentrations ($\mu g/m^3$) due to Magic Circle Emissions.. 6-17

6-5 Ground-Level SO_2 Concentrations ($\mu g/m^3$) due to Paraho Emissions.. 6-26

6-6 Ground-Level TSP Concentrations ($\mu g/m^3$) due to Paraho Emissions.. 6-29

6-7 Ground-Level SO_2 Concentrations ($\mu g/m^3$) due to Syntana-Utah Emissions.. 6-37

6-8 Ground-Level TSP Concentrations ($\mu g/m^3$) due to Syntana-Utah Emissions.. 6-40

6-9 Ground-Level SO_2 Concentrations ($\mu g/m^3$) due to Tosco Emissions... 6-48

6-10 Ground-Level TSP Concentrations ($\mu g/m^3$) due to Tosco Emissions... 6-51

LIST OF TABLES

1-1 Uinta Basin Synthetic Fuel Facilities........................ 1-3

1-2 Piceance Basin Oil Shale Facilities........................... 1-4

1-3 Industrial Facilities in Study Region......................... 1-6

2-1 Frequency of Occurrence of Atmospheric Stability at the 500-m Level (AGL)...................................... 2-13

2-2 Seasonal and Annual-Average Morning and Afternoon Mixed-Layer Heights and Wind Speeds for Grand Junction, Colorado.. 2-16

2-3 Measured Ambient Concentrations of Total Suspended Particulates (TSP) in Study Region........................... 2-27

3-1 Applicable State and Federal Ambient Air Quality Standards... 3-2

3-2 Prevention of Significant Deterioration Increments.......... 3-3

3-3 EPA Significant (de minimis) Emission Rates.................. 3-4

3-4 Categories of Potential Air Quality Impacts on Air-Quality-Related Values of Class I Areas.................. 3-7

4-1 Production and Emission Rates for Utah Synfuel Projects--High-Oil-Production Scenario.............................. 4-9

4-2 Production and Emission Rates for Utah Synfuel Projects--Low-Oil-Production Scenario............................... 4-10

4-3 Emission Totals for Other Planned Projects in Utah.......... 4-12

4-4 Emission Totals for Baseline Point Sources in Utah.......... 4-14

4-5 Emission Totals for Colorado Oil Shale Projects............. 4-16

4-6 Emission Totals for Non-Oil Shale Sources in Colorado....... 4-18

4-7 Area Source Categorization Scheme........................... 4-19

4-8 Emission Factors for 1980 Baseline......................... 4-21

4-9 Area Source Spatial Allocation Parameters.................. 4-30

4-10 1980 Baseline Area Source Emission Inventory for Uintah County... 4-32

4-11 1980 Baseline Area Source Emission Inventory for Grand County.. 4-33

4-12 Emission Factors for On-Road Motor Vehicles (Exhaust) for 1990.. 4-40

4-13 Area Source Projection Parameters.......................... 4-41

4-14 Regional High Oil Production Scenario Area Source Emission Inventory for Uintah County........................ 4-45

4-15 Regional High Oil Production Scenario Area Source Emission Inventory for Grand County......................... 4-46

4-16 Regional Low Oil Production Scenario Area Source Emission Inventory for Uintah County........................ 4-48

4-17 Regional Low Oil Production Scenario Area Source Emission Inventory for Grand County......................... 4-49

4-18 Emission Totals for Area Sources in Utah................... 4-50

4-19 Total Population for 1990 Regional Scenarios (NPS).......... 4-51

4-20 Summary of the Relative Capabilities of the Models Used in This Study.. 4-60

4-21 Morning Stable Layer Depths from the Four Upper-Air Stations, and the Average Used by RTM....................... 4-67

4-22 USGS Land Use Categories................................... 4-77

4-23 Land Use Categories, Surface Roughness Lengths, and Deposition Velocities for the Study Area.................. 4-80

5-1 Summary of Ambient Air Quality Impacts Associated with the Low Oil Production Scenario.......................... 5-112

5-2 Summary of Ambient Air Quality Impacts Associated with the High Oil Production Scenario......................... 5-115

5-3 Summary of Ambient Air Quality Impacts Associated with the Low Oil Production Scenario.......................... 5-121

5-4 Summary of Ambient Air Quality Impacts Associated with the High Oil Production Scenario......................... 5-123

5-5 Summary of EKMA Results for Trajectory 1.................... 5-127

5-6 Summary of EKMA Results for Trajectory 2.................... 5-128

5-7 Magnitude [Δ(L*a*b*)] of Plume Discoloration................ 5-129

5-8 Particle Size Distributions and Deposition Velocities Assumed in Visibility Model Simulations....................... 5-133

5-9 Worst-Case Reduction of Visual Range for a View from Flat Tops Wilderness Area Looking Toward the Northwest... 5-134

5-10 Summary of World-Wide Wet and Dry, Sulfuric and Nitric Acid Deposition Measurements......................... 5-138

6-1 Summary of PSD Increment Consumption by Enercor-Mono Power.. 6-3

6-2 Summary of Maximum Ambient Air Quality Impacts of Enercor-Mono Power Compared with Applicable Standards.............. 6-4

6-3 Level-1 Screening Analysis Results for Visibility Impacts of Enercor-Mono Power................................ 6-10

6-4 Summary of PSD Increment Consumption by Magic Circle........ 6-11

6-5 Summary of Maximum Ambient Air Quality Impacts of Magic Circle Compared with Applicable Standards............. 6-13

6-6 Level-1 Screening Analysis Results for Visibility Impacts of Magic Circle.. 6-21

6-7 Summary of PSD Increment Consumption by Paraho.............. 6-23

6-8 Summary of Maximum Ambient Air Quality Impacts of Paraho Compared with Applicable Standards.................. 6-25

6-9 Level-1 Screening Analysis Results for Visibility Impacts of Paraho.. 6-33

6-10 Summary of PSD Increment Consumption by Syntana............. 6-34

6-11 Summary of Maximum Ambient Air Quality Impacts of Syntana Compared with Applicable Standards................. 6-36

6-12 Level-1 Screening Analysis Results for Visibility Impacts of Syntana....................................... 6-43

6-13 Summary of PSD Increment Consumption by Tosco............... 6-45

6-14 Summary of Maximum Ambient Air Quality Impacts of Tosco Compared with Applicable Standards................... 6-47

6-15 Level-1 Screening Analysis Results for Visibility Impacts of Tosco... 6-55

6-16 Summary of Model Approaches Used by Applicants.............. 6-56

6-17 Comparison of Worst-Case Calculations of 24-Hour Concentrations near Specific Proposed Synthetic Fuel Facilities.. 6-57

1 INTRODUCTION

Plans are being made to produce synthetic fuels from oil shale and tar sand deposits in the Piceance Basin of Colorado and the Uinta Basin of Utah. The air quality impact of this development is an important environmental concern to government, industry, and many citizens. This concern arises because of the substantial industrial development and population growth that is projected in a region that currently has nearly pristine air quality, surrounded by several national parks, national monuments, and wilderness areas. Concerns related to air quality impacts range from such regulatory issues as consumption of Prevention of Significant Deterioration (PSD) increments and ground-level concentrations compared with federal and state ambient air quality standards to air quality impacts that are not regulated by specific numerical limits, such as visibility impairment and acid deposition. Air quality impacts of individual industrial facilities, cumulative regional industrial development (primarily energy-related) and cumulative regional development associated with population growth are concerns that were analyzed in this study.

This report documents an analysis of air quality impacts that was performed by Systems Applications, Inc. for the Bureau of Land Management (BLM) of synthetic fuel development in the Uinta Basin of Utah. This analysis is to support the Environmental Impact Statement (EIS) that BLM is preparing for each of five specific synthetic fuel developments and cumulative regional impacts. The cumulative impacts of regional emissions to the atmosphere from these five projects, from other planned energy developments in the Uinta and Piceance basins, and from additional development and activities associated with regional population growth were studied.

The current study is more detailed than the previous policy and screening analyses of air quality impacts in the region performed by both Systems Applications (Anderson et al., 1980 and 1981; Latimer and Doyle, 1981) and Los Alamos Scientific Laboratory (Williams et al., 1981). The current report is based on (1) detailed emission inventories developed by synthetic fuel developers, Systems Applications, and PEDCo Environmental, Inc. (1981); (2) measured meteorological conditions in the region; and (3) additional regional data such as ambient air quality, topography, and visibility.

1.1 SCOPE OF THE STUDY

The primary objective of the study was to evaluate the air quality impacts of five synthetic fuel facilities proposed to be developed in the Uinta Basin: Enercor-Mono Power (Rainbow site), Magic Circle, Paraho, Syntana-Utah, and Tosco. Three additional facilities that are in a conceptual-design phase--Enercor-Mono Power (PR Springs site), Geokinetics, and Sohio--were also studied in regional scenarios. The impacts associated with two levels of production from each of these facilities was studied. Table 1-1 summarizes the production levels.

Since cumulative regional impacts were considered to be important in this study, other industrial facilities were also examined. In the Uinta Basin these included the Moon Lake power plant (units 1 and 2), White River oil shale project (100,000 barrel per day capacity), Plateau refinery, and five other small projects. In the Piceance Basin in Colorado, the air quality impacts of the oil shale facilities listed in table 1-2 were included in regional assessments. The total synthetic fuel production in the Uinta and Piceance basins studied in the high- and low-oil-production scenarios was 1,059,500 and 492,000 barrels per day, respectively.

Figure 1-1 shows the 180 x 268-km region studied in this analysis and the locations of the major industrial facilities, towns, and state and county boundaries. Also shown are Flat Tops Wilderness Area, the only federal PSD Class I area in the study region, and Dinosaur and Colorado national monuments, which are currently federal Class II and Colorado category I areas but may potentially be redesignated federal Class I. Outside, but adjacent to the study region, are the Mt. Zirkel and Maroon Bells/Snowmass wilderness areas, which are currently Federal Class I areas, and the Uinta Primitive Area, which may be redesignated Class I. Table 1-3 provides a legend for the industrial facilities (shown in figure 1-1) that were studied in the regional air quality analysis.

1.2 REPORT CONTENTS

This report is divided into six sections. Section 2 discusses the topography, climatology, meteorology, and existing air quality of the study region shown in figure 1-1. The criteria for judging the significance of air quality impacts, such as federal and state ambient air quality standards and Prevention of Significant Deterioration (PSD)

TABLE 1-1. UINTA BASIN SYNTHETIC FUEL FACILITIES

Project	Oil-Production Capacity (bpd) Low Production	High Production
Enercor-Mono Power		
Rainbow[a] (tar sand)	5,000	5,000
P.R. Springs[b] (tar sand)	15,000	50,000
Magic Circle[a] (oil shale)	16,400	31,500
Paraho[a] (oil shale)	10,500	42,000
Syntana-Utah[a] (oil shale)	16,500	57,000
Tosco[a] (oil shale)	22,000	45,000
Geokinetics (oil shale)		
Lofreco (in-situ)[b]	20,000	50,000
Agency Draw[b]	11,000	20,000
Sohio Shale Oil[b] (tar sand)	5,000	20,000
Total	121,400	320,500

Note: bpd = barrels per calendar day.

[a] Site-specific project.

[b] Conceptual project.

TABLE 1-2. PICEANCE BASIN OIL SHALE FACILITIES*

Project	Oil-Production Capacity (bpd)	
	Low Production	High Production
Cathedral Bluffs	94,000	94,000
Chevron	15,000	100,000
Colony	47,000	47,000
Exxon	0	47,000
Getty	0	15,000
Mobil	0	50,000
Multimineral	0	50,000
Naval Oil Shale Reserve	0	50,000
Rio Blanco	50,000	86,000
Superior	15,000	15,000
Union	50,000	50,000
Total	271,000	639,000

---

* Development plans in Colorado are uncertain as suggested by several recent project modifications, delays, and cancellations. Therefore, the low- and high-production scenarios assumed for Colorado are quite speculative and indicative of general development plans at the time this study was started.

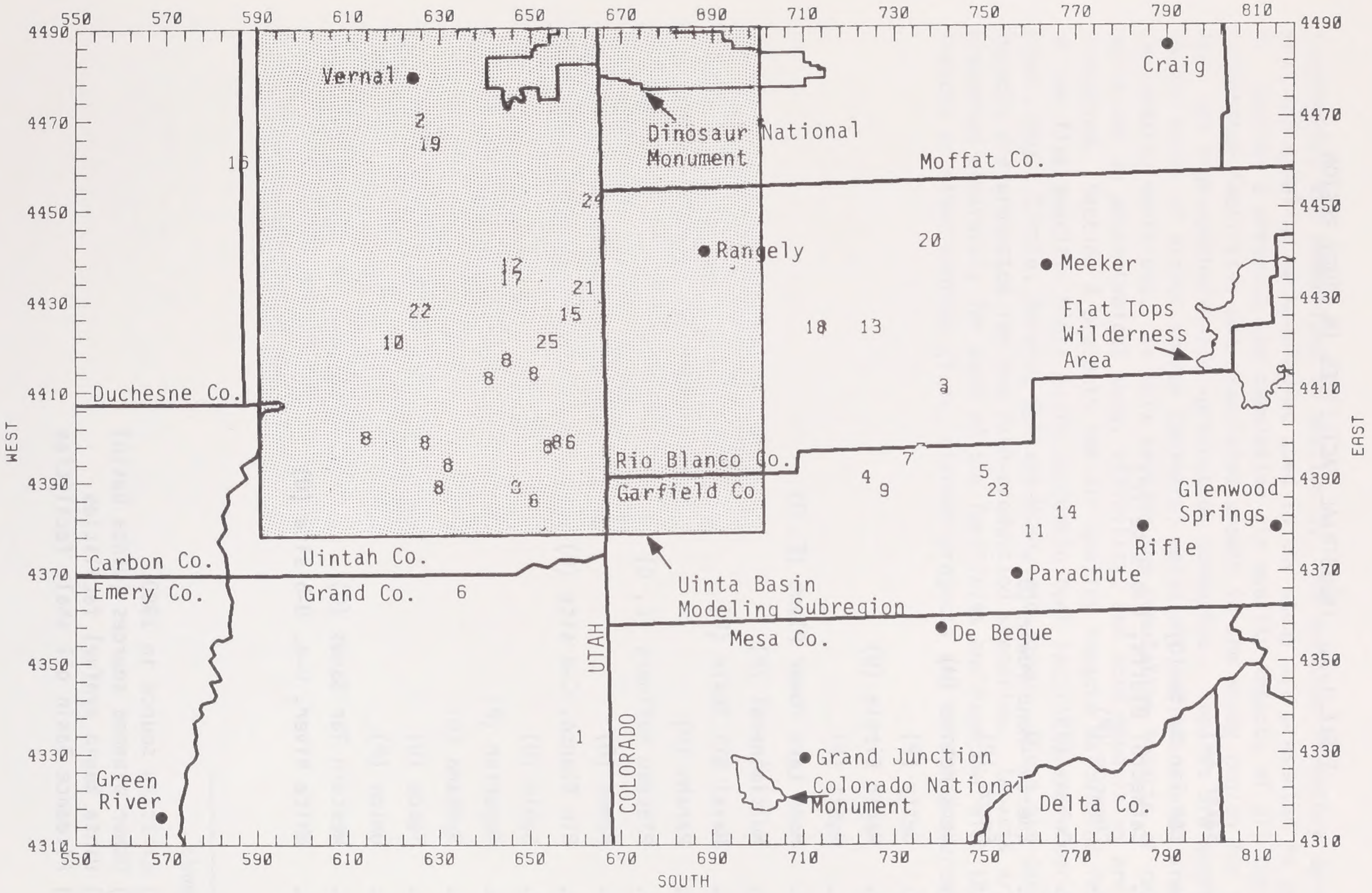

FIGURE 1-1. LOCATIONS OF SOURCES, TOWNS, COUNTIES, AND MANDATORY AND POTENTIAL CLASS I AREAS IN STUDY REGION

TABLE 1-3. INDUSTRIAL FACILITIES IN STUDY REGION

1. Baker (O)
2. C&A Tar Sands (O)
3. Cathedral Bluffs, C-b site (P)
4. Chevron (P)
5. Colony (P)
6. Enercor-Mono Power (U)
7. Exxon (P)
8. Geokinetics (U)
9. Getty (P)
10. Magic Circle (U)
11. Mobil (P)
12. Moon Lake Power Plant (E, O)
13. Multimineral (P)
14. Naval Oil Shale (P)
15. Paraho (U)
16. Plateau Refinery (E, O)
17. Ramex (O)
18. Rio Blanco, C-a site (P)
19. Sohio (U)
20. Superior (P)
21. Syntana (U)
22. Tosco (U)
23. Union (P)
24. Western Tar Sands (O)
25. White River, U-a, U-b site (O)

Legend:

(E) Existing source in 1980
(O) Other planned sources (Uinta Basin)
(U) Uinta Basin synfuel facilities
(P) Piceance Basin oil shale facilities

increments, are summarized in section 3. The emission inventory development and modeling methodologies used in the study are presented in section 4. Section 5 presents the cumulative air quality impacts of all the industrial facilities and associated growth in the study region for the low- and high-synthetic-fuel-production scenarios. Impacts are segregated on the basis of direct source (primary) emissions and associated area (secondary) emissions. In this section the cumulative impacts of regional emissions on photochemical smog, visibility, and acid deposition are also presented. Section 6 presents the air quality impacts calculated for each of the five specific Uinta Basin synthetic fuel facilities--Enercor-Mono Power, Magic Circle, Paraho, Syntana-Utah, and Tosco. These air quality impacts are projected for the high-production scenarios. Impacts are presented separately for each of the facilities and together with the impacts of other sources (i.e., planned projects and existing sources).

2 THE AFFECTED ENVIRONMENT[*]

In this section we discuss the topography, climatology (including wind direction, wind speed, and atmospheric stability), and existing air quality of the study region.

2.1 TOPOGRAPHY

The 180 x 268-km study region (see figure 1-1) in which oil shale and tar sands development is planned is on the western slope of the Rockies in eastern Utah and northwestern Colorado. It is characterized by complex terrain (i.e., mountains and valleys), but large portions of the region are relatively flat plateaus. Figures 2-1 and 2-2 show terrain elevation contours and a perspective plot of the study region. Note the Colorado River cutting through the southern portion of the region near Grand Junction. The Uinta Basin is in relatively flat, high plateau country in the northwestern portion of the study region. The region becomes progressively more elevated, rugged, and mountainous to the east, where parts of the Flat Tops Wilderness Area lie above 10,000 ft MSL.

2.2 METEOROLOGY AND CLIMATOLOGY

The climate of the region is arid. Because of the typically dry atmosphere, there is a high frequency of occurrence of bright, sunny days and clear nights. The clear atmosphere, in turn, allows rapid heating of the ground surface during daylight hours and rapid cooling in the dark. Since heated air rises and cooled air falls, winds tend to blow up-slope during daytime and down-slope at night.

The up- and down-slope cycle occurs at all geographic scales; that is, the tendency can be noted on canyon walls, river courses, mountains, and mountain range slopes. The larger the horizontal scale of the geographic feature, the greater is the volume of air that moves, and the

---

[*] Portions of this section were excerpted from appendix H, entitled "Meteorological Characterization," by Anderson et al. (1981).

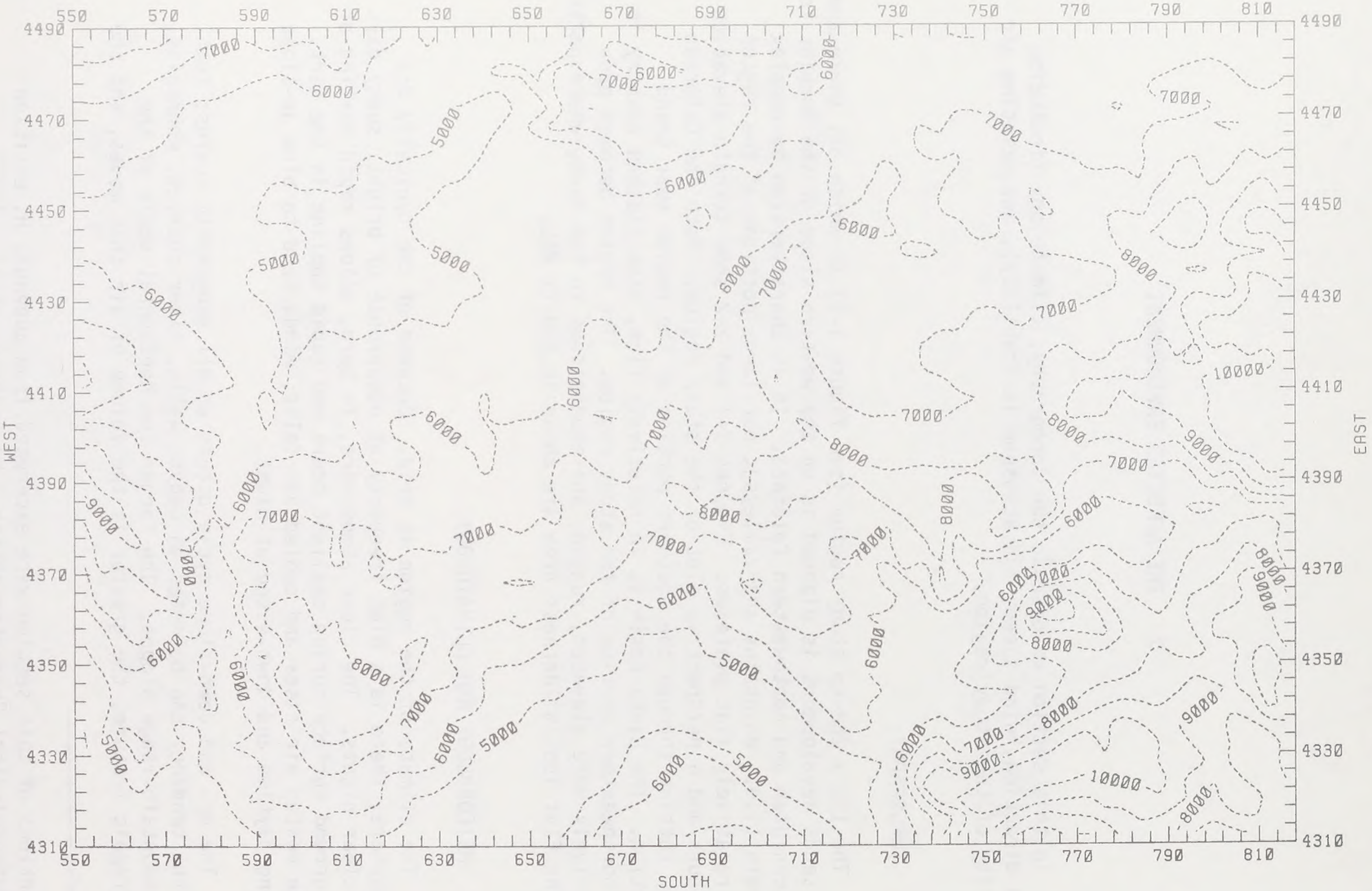

FIGURE 2-1. TERRAIN ELEVATION CONTOURS (FT MSL) IN STUDY REGION

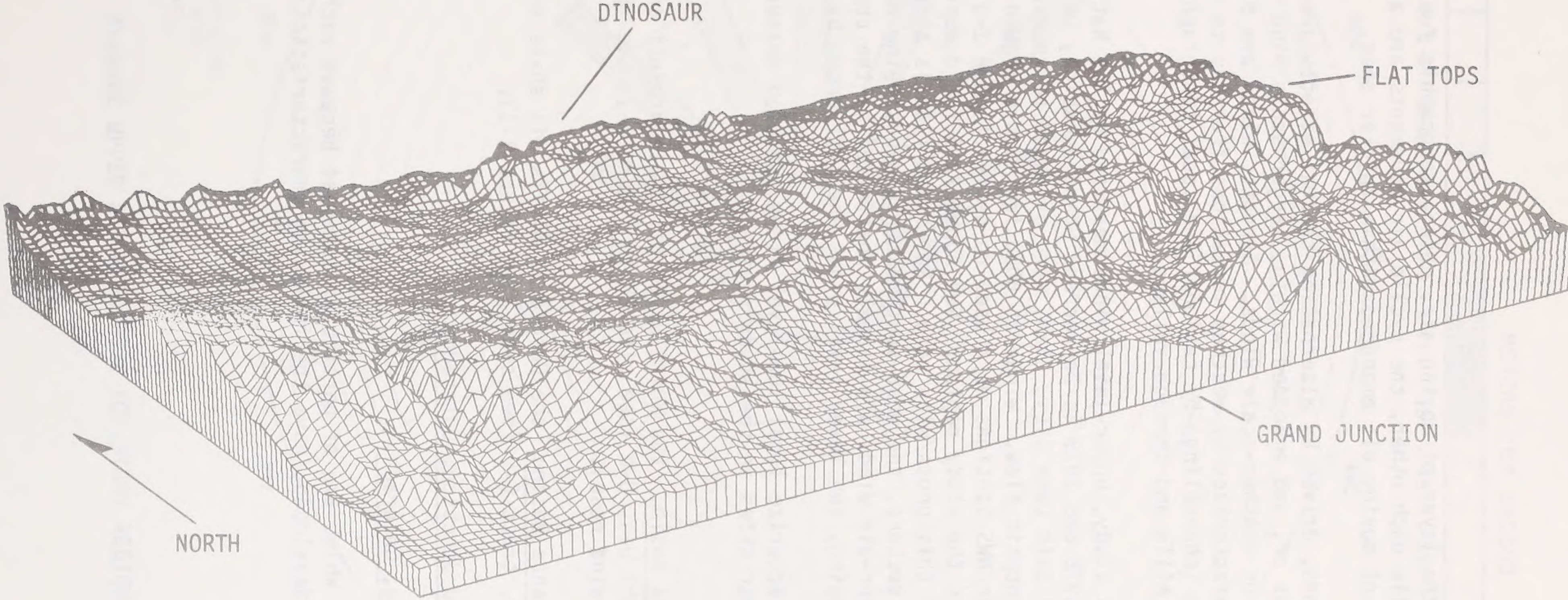

FIGURE 2-2. PERSPECTIVE OF TERRAIN IN STUDY REGION

Note: Dark internal boundaries delineate the Uinta Basin subregion.

thicker is the layer of moving air. Since geographic features of many scales overlie each other, the cyclic air movements are also complex, with thin layers of moving air embedded within thicker ones.

The winds, driven by alternating thermal effects are, in turn, perturbations of, and embedded within, larger-scale wind systems called "synoptic," or weather-scale winds. Synoptic winds are predominantly west to east, characterized by weather variations from day to day and significant guiding (channeling) by regional and local topography; that is, winds blow around hills and through valleys.

In this study, upper-level winds measured by the National Weather Service in 1978 and 1979 in Denver and Grand Junction, Colorado; Lander, Wyoming; and Salt Lake City, Utah, were averaged to characterize the upper-air synoptic flow. Winds at 6000 feet above ground level from each of these four NWS stations were used to derive figure 2-3, which shows a wind rose for the study region. See Appendix A for a more detailed breakdown of this gross wind rose. Note that flow is almost always from the western sectors, the west-southwesterly winds being most frequent. Although upper-air winds are largely unaffected by the complex terrain in the study region, the lower-level winds are influenced by such terrain.

To characterize local low-level flows, we used measurements at the following four sites in the study region:

> Uinta Basin: the White River oil shale project site, tracts U-a, U-b (see site 25 in figure 1-1; see Appendix B for wind rose).

> Piceance Basin: the Cathedral Bluffs oil shale project site, tract C-b (see site 3 in figure 1-1).

> Grand Junction, Colorado.

> Craig, Colorado.

These areas, which are of particular interest because each will be intensively developed, have the following characteristics:

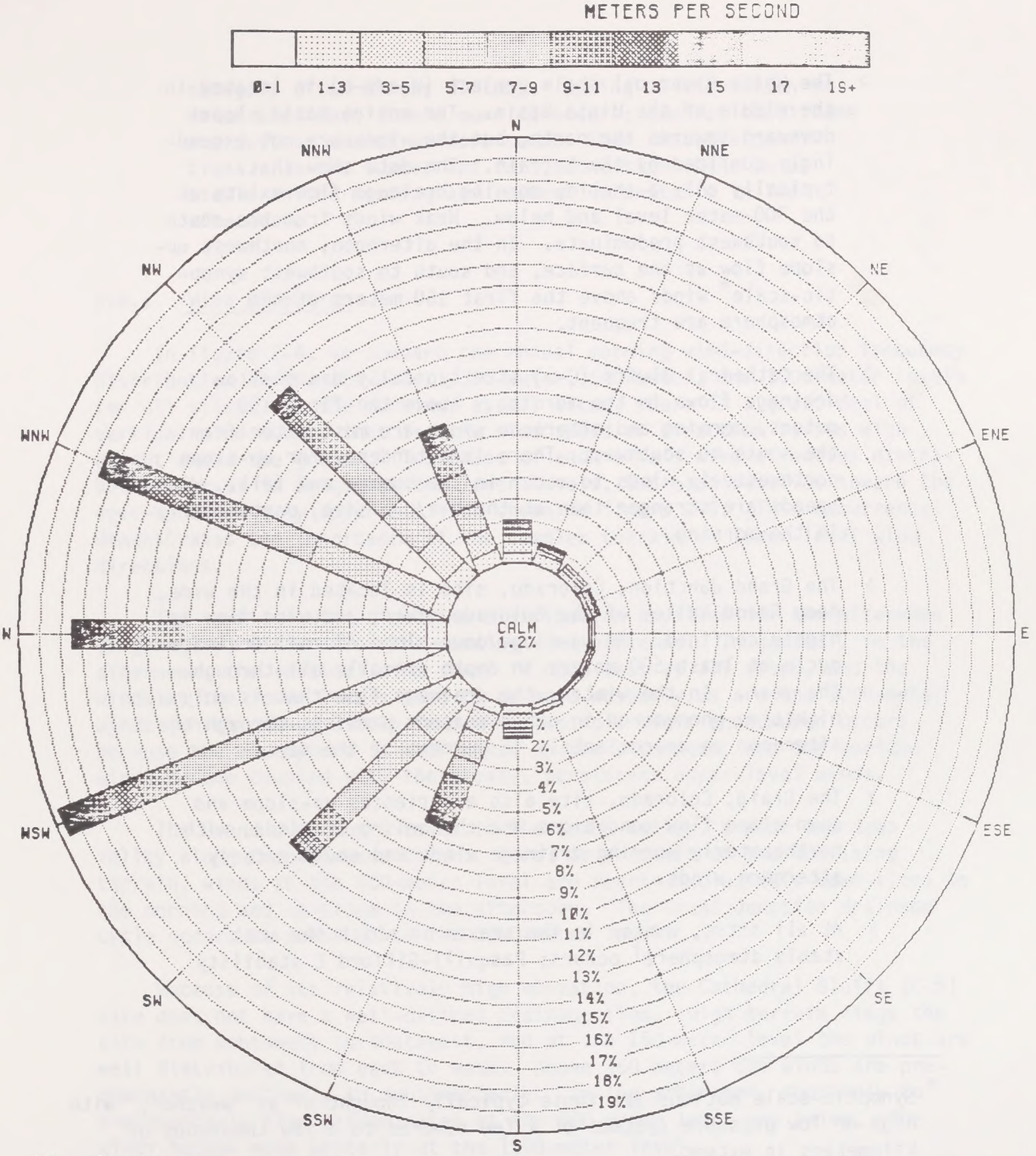

Note: Based on the average of winds measured at NWS sites 6000 feet above ground level.

FIGURE 2-3. AVERAGE UPPER AIR WIND ROSE FOR STUDY REGION

- The White River oil shale project (U-a/U-b) is located in the middle of the Uinta Basin. The entire basin slopes downward towards the north, but the winds are not exceedingly confined by the terrain. The data show that typically only a shallow morning drainage flow exists at the 300-meter level and below. Weak winds from the south to southwest predominate. In the afternoon, northwest up-slope flow at the surface, and south to southwest synoptic-scale[*] winds above the first 150 meters of the atmosphere are frequent.

- The Cathedral Bluffs (C-b) site typically has shallow drainage flows in the morning. Above the first 150 meters, morning and afternoon winds are most often from the south to southwest. There is a tendency for up-slope northwesterly winds to occur in the summer and fall. Wind speeds are stronger than at the U-a/U-b site, particularly in the morning.

- The Grand Junction, Colorado, site is located in the wide, deep Grand Valley of the Colorado river, and wind flow is highly confined. An up-slope/down-slope diurnal drainage cycle at least 500 meters in depth prevails all through the year. In the winter, the drainage flow that is only a nighttime phenomenon in other seasons persists through the afternoon on approximately 15 percent of the days.

- The Craig, Colorado, site also experiences up-slope and down-slope flow conditions and channeling of winds, with northeasterly morning drainage winds and southwesterly afternoon winds.

- At all sites, winter is the season in which the most stable atmosphere[†] occurs; Pasquill-Gifford E stability category often exists all day. Spring is the season in which the least stable morning occurs; neutral conditions are just as common or more common than unstable conditions. In the summer and fall, conditions tend to be stable in the morning and neutral or unstable in the afternoon.

---

[*] Synoptic-scale motions are those typically thought of as "weather," with high or low pressure systems of a few hundred to a few thousands of kilometers in extent.

[†] A stable atmosphere is one in which turbulent air motions tend to die out. In the Pasquill-Gifford classification system, the most unstable, turbulent air is classed "A," the most stable, smooth air "G". D represents a neutrally stable condition.

2.2.1 Wind Direction

In figure 2-4, we compare the annual morning wind-direction frequency distribution at the 150-meter, 300-meter, 500-meter, and 1000-meter levels for all sites. In the morning, at all sites, there is a great deal of vertical wind shear, that is, the wind speed or direction varies with height above the ground. The shape of each site's wind-direction distribution curves is unique at the lower levels, but each resolves toward the west-southwesterly upper-air flow shown in figure 2-5. This occurrence demonstrates the importance of the complex terrain on lower-level wind directions.

The vertical wind-direction distribution profiles for the afternoon (figure 2-5) differ from the morning wind patterns. In general, in the afternoon, the vertical wind shear is much less at all sites, and the winds at the lower levels tend to be more westerly as are the 1000-meter winds (which change little from the morning). This phenomenon occurs because the atmosphere is well mixed in the afternoon, and the surface winds become coupled with the steady, persistent upper-level winds.

The Grand Junction site is in the Grand Valley, a wide and deep valley along the Colorado River. Here, as a result of the confining terrain, winds at the 500-meter level are nearly exclusively down-slope in the morning and up-slope in the afternoon. The Grand Junction drainage cycle occurs at least up to the 1000-meter level.

Because of its relatively high elevation, the Cathedral Bluffs (C-b) site does not have a well-defined drainage flow. High terrain rings the site from southwest to southeast, and at the 150-meter level the winds are well distributed from east to west. Above 150 meters the winds are predominantly southerly to southwesterly. In the afternoon, southerly to southwesterly flow predominates at the 500-meter level and below. The winds become more westerly at the 1000-meter level.

A diurnal wind cycle is evident at Craig and at the White River project (U-a/U-b) as well. At Craig, a morning east-drainage wind dominates up to the the 300-meter level. In the afternoon, the up-slope

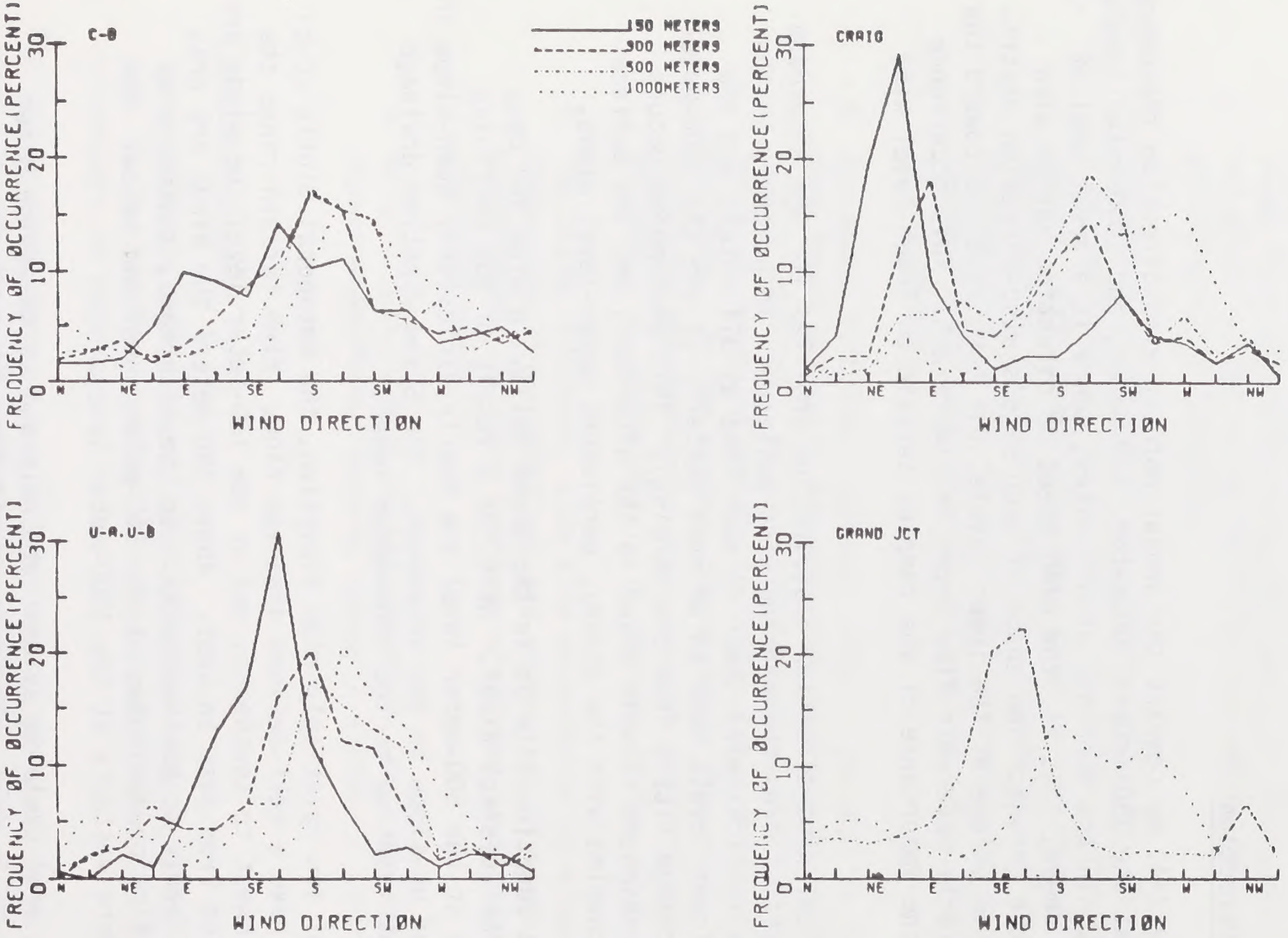

FIGURE 2-4. WIND DIRECTION FREQUENCY DISTRIBUTIONS FOR ALL MORNING SOUNDINGS

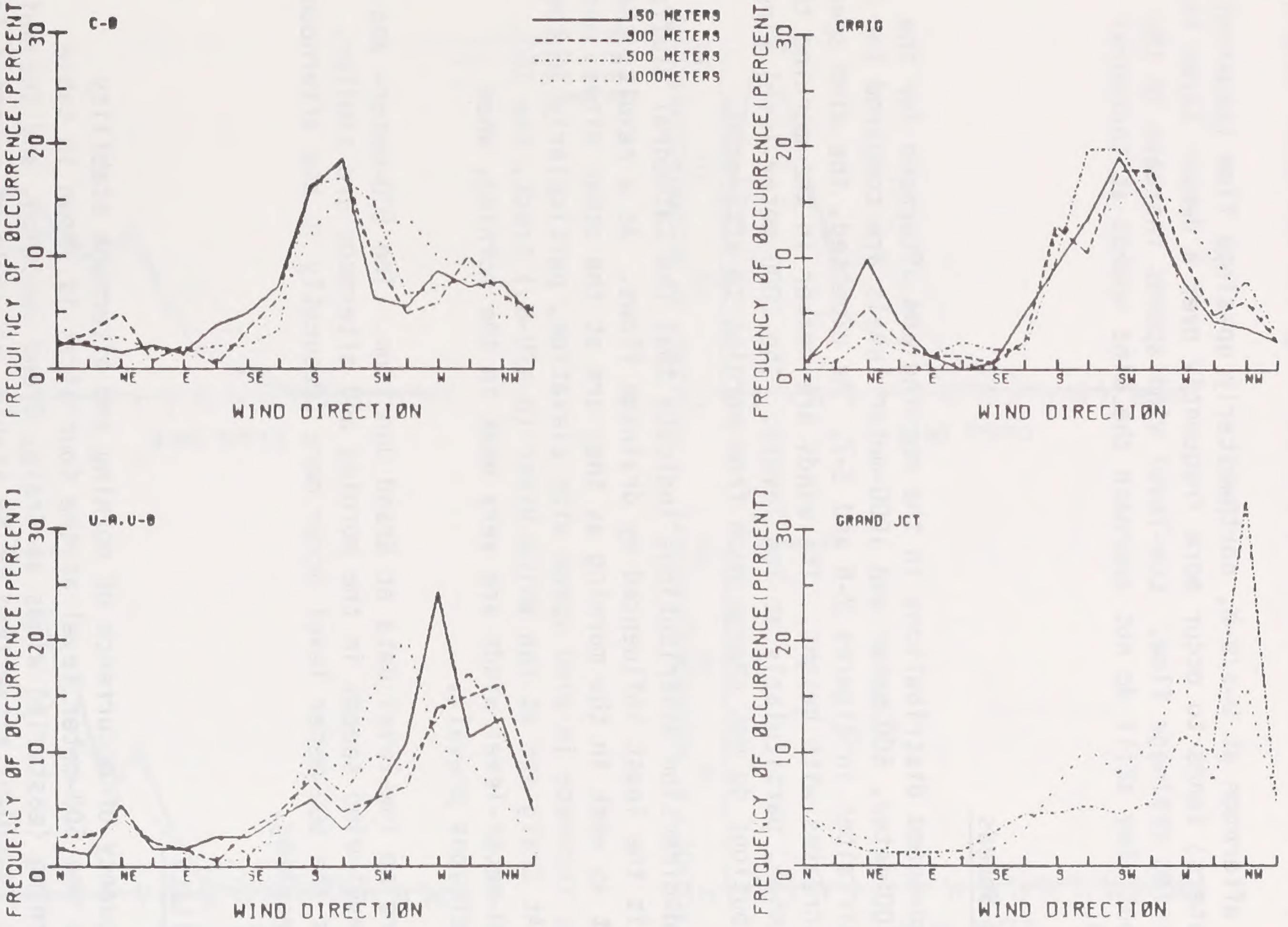

FIGURE 2-5. VERTICAL WIND DIRECTION DISTRIBUTION PROFILES FOR ALL AFTERNOON SOUNDINGS

and synoptic-scale winds reinforce each other, and the winds are predominantly westerly. The morning drainage flow on the U-a/U-b tract is shallower than that at Craig. At U-a/U-b, the drainage flow is from the southeast, and is evident at the 150-meter level. However, the wind direction distribution shifts towards the south by the 300-meter level.

In the afternoon at U-a/U-b, northwesterly up-slope flow (penetrating up to 500 meters) tends to occur more frequently over a deeper layer than does the morning drainage flow. Low-level wind speeds increase in the afternoon, but they still do not approach the wind speeds at Cathedral Bluffs (C-b).

2.2.2 Wind Speeds

The wind-speed distributions in the morning and afternoon for the 150-meter, 300-meter, 500-meter and 1000-meter levels are compared for the four upper-air sites in figures 2-6 and 2-7. As expected, the wind speed typically increases with height. The winds are weaker in the morning than in the afternoon, particularly at low levels. The 1000-meter-level wind-speed distributions do not change much from morning to afternoon.

The wind-direction distributions indicate that the Cathedral Bluffs (C-b) tract is the least influenced by drainage flows. As a result, the winds are not as weak in the morning as they are at the other sites, and there is less increase in wind speed with elevation, particularly in the afternoon. At Craig and at the White River (U-a/U-b,) tract, the 150-meter and 300-meter-level winds are very weak in the morning, when drainage conditions prevail.

There are no low-level data at Grand Junction. The 500-meter- and 1000-meter-level wind speeds in the morning and afternoon are similar. Weak winds at the 500-meter level occur more frequently in the afternoon than in the morning.

2.2.3 Stability

The frequency of occurrence of morning and afternoon stability categories at the 500-meter level at the four sites is shown in table 2-1. The morning (easterly) winds at Craig, Grand Junction, and the White River project (U-a/U-b) sites tend to be stable, as would be expected for these drainage flows. At the C-b site, where drainage flows are not as organized, neutral conditions predominate in the morning. The atmosphere is neutral most of the time at the 500-meter level in the afternoon at all sites.

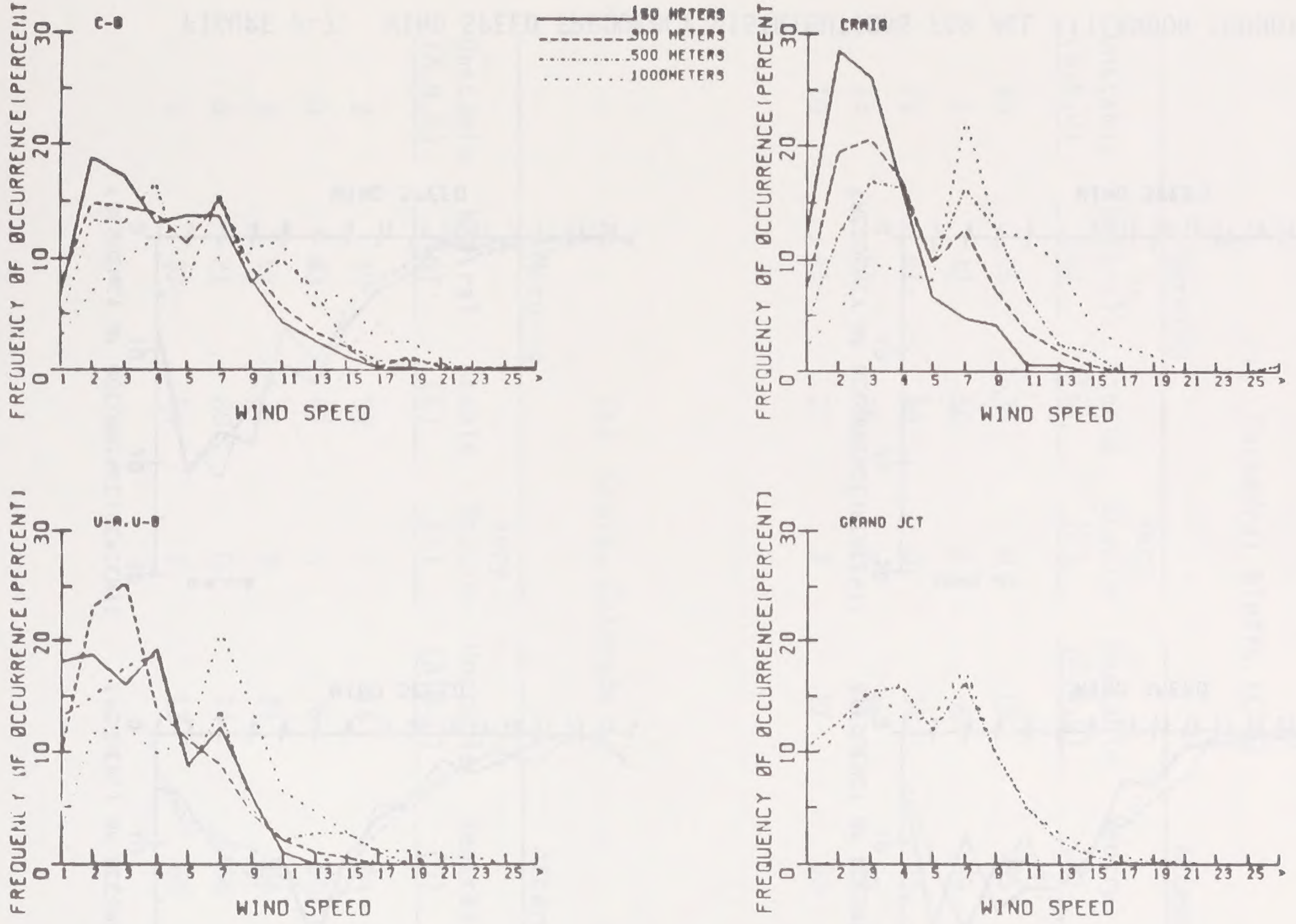

FIGURE 2-6. WIND SPEED FREQUENCY DISTRIBUTIONS FOR ALL MORNING SOUNDINGS

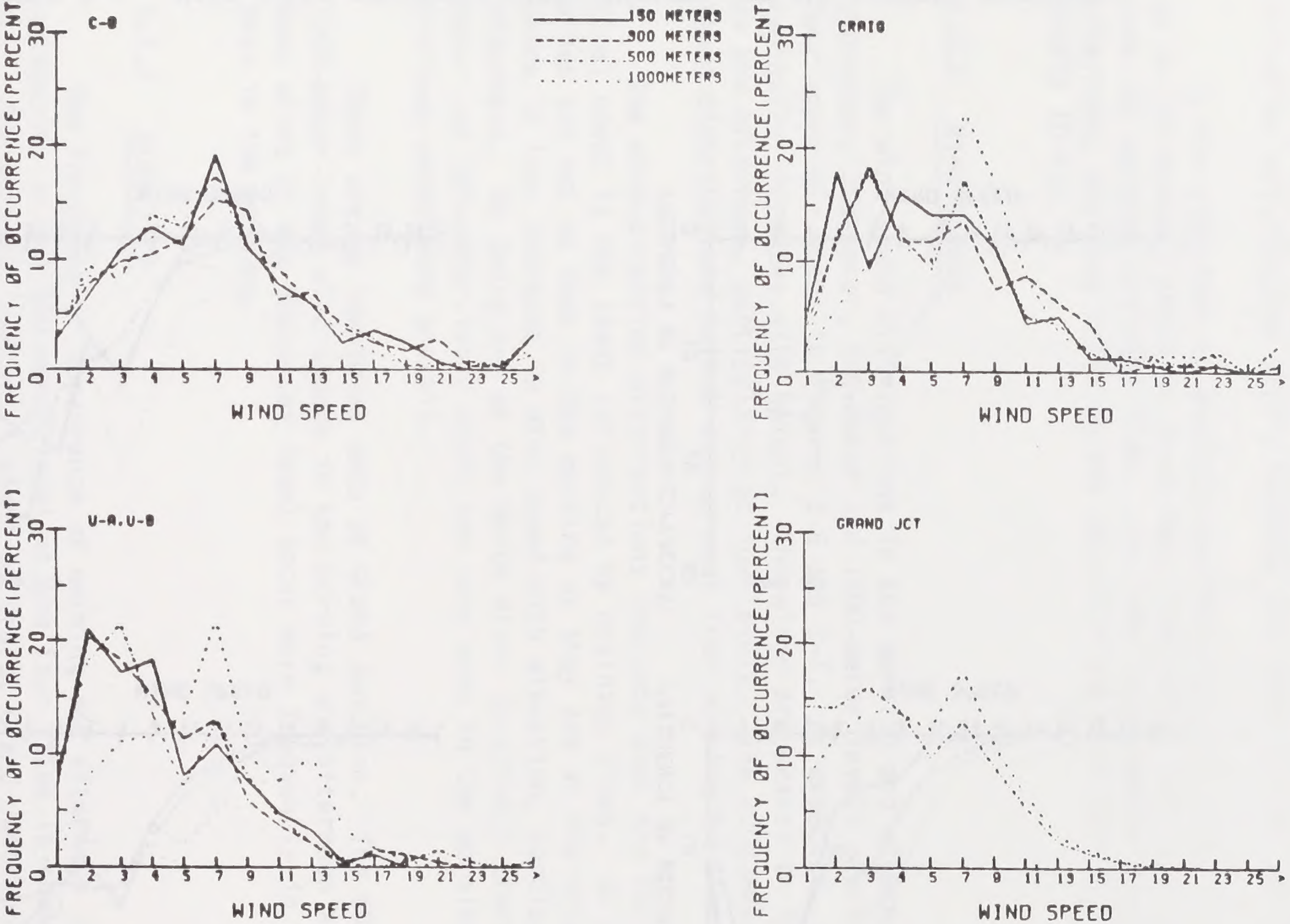

FIGURE 2-7. WIND SPEED FREQUENCY DISTRIBUTIONS FOR ALL AFTERNOON SOUNDINGS

TABLE 2-1. FREQUENCY OF OCCURRENCE OF ATMOSPHERIC STABILITY AT THE 500-m LEVEL (AGL)

(percent)

(a) Cathedral Bluffs (C-b)

	Morning				Afternoon			
	Unstable (A,B,C)	Neutral (D)	Stable (E)	Very Stable (F)	Unstable (A,B,C)	Neutral (D)	Stable (E)	Very Stable (F)
Annual	10	55	34	0	19	55	27	0
Winter	2	48	50	0	6	69	25	0
Spring	11	61	28	0	34	54	12	0
Summer	13	51	36	0	45	32	23	0
Fall	10	61	27	2	17	63	21	0

(b) Craig, Colorado

	Morning				Afternoon			
	Unstable (A,B,C)	Neutral (D)	Stable (E)	Very Stable (F)	Unstable (A,B,C)	Neutral (D)	Stable (E)	Very Stable (F)
Annual	2	39	59	1	16	64	20	0
Winter	0	43	57	0	6	65	29	0
Spring	5	56	39	0	31	54	14	0
Summer	0	21	80	0	14	66	20	0
Fall	2	37	59	2	13	69	18	0

TABLE 2-1 (Concluded)

(c) White River (U-a, U-b)

	Morning				Afternoon			
	Unstable (A,B,C)	Neutral (D)	Stable (E)	Very Stable (F)	Unstable (A,B,C)	Neutral (D)	Stable (E)	Very Stable (F)
Annual	1	25	74	0	16	52	31	2
Winter	0	33	65	2	6	40	50	4
Spring	0	29	71	0	26	64	10	0
Summer	0	14	87	0	29	54	17	0
Fall	2	24	74	0	10	53	36	2

(d) Grand Junction, Colorado

	Morning				Afternoon			
	Unstable (A,B,C)	Neutral (D)	Stable (E)	Very Stable (F)	Unstable (A,B,C)	Neutral (D)	Stable (E)	Very Stable (F)
Annual	2	52	44	2	1	84	13	2
Winter	6	33	56	6	3	51	40	7
Spring	1	68	31	0	0	96	3	0
Summer	0	57	43	0	0	98	2	0
Fall	1	49	49	1	0	91	9	90

The morning and afternoon mixing depths for Grand Junction have been determined by Holzworth and are listed in table 2-2. Because of increased surface heating, the summer afternoon mixing depths are more than three times the average winter value.

2.2.4 Effect of Terrain on Wind Fields

The descriptions in this section of the effect of the complex terrain (hills, mountains, and valleys) in the study region are substantiated by the wind field modeling work performed as part of this analysis (see section 4). Figure 2-8 displays the computed wind fields for the lowest of the three atmospheric layers modeled, which is about 2500 feet (780 meters) thick and extends from the terrain or 4300 feet above mean sea level (MSL), whichever is highest, to 6800 feet MSL. Note in the figures that winds are channeled through valleys (the White, Green, and Colorado river basins), and winds are both accelerated and decelerated by the effects of complex terrain. Nominal synoptic winds of 10 m/s from indicated directions were assumed for these model calculations. (Clear plastic overlays showing various geographical features and terrain elevations are provided inside the back cover of this report.) The reader is encouraged to use these over the figures throughout this report so that the locations of important geographical features and sources can be identified.

Figure 2-9 shows similar plots for a zero upper air (synoptic) wind and two conditions of strong down- and up-slope flow induced by nocturnal terrain cooling and daytime heating, respectively. The nominal wind speed of 10 m/s was chosen for illustration purposes only; actual down- and up-slope flows would generally be expected to have much lower speeds. See Section 4.2 for discussion of techniques by which these nominal wind fields were scaled on the basis of measured winds.

2.3 EXISTING AIR QUALITY

The existing air quality of the study region is typical of a largely undeveloped region in the western United States. The measured long-term average concentrations of the criteria pollutants in the Uinta Basin are well within ambient air quality standards except in populated areas where particulate emissions from various man-made sources, windblown dust, and emissions from dirt and general roads may cause exceedances of standards. A summary of baseline air quality in the Uinta nd Piceance Basins is provided in Table 2-3.

TABLE 2-2. SEASONAL AND ANNUAL-AVERAGE MORNING AND AFTERNOON MIXED-LAYER HEIGHTS AND WIND SPEEDS FOR GRAND JUNCTION, COLORADO

	Morning		Afternoon	
Season	Height (m)	Wind Speed (m/s)	Height (m)	Wind Speed (m/s)
Winter	329	3.4	1160	3.4
Spring	628	5.4	3166	6.6
Summer	307	4.7	3940	6.1
Autumn	273	3.9	2133	4.6
Annual	384	4.3	2600	5.2

Source: Holzworth (1972)

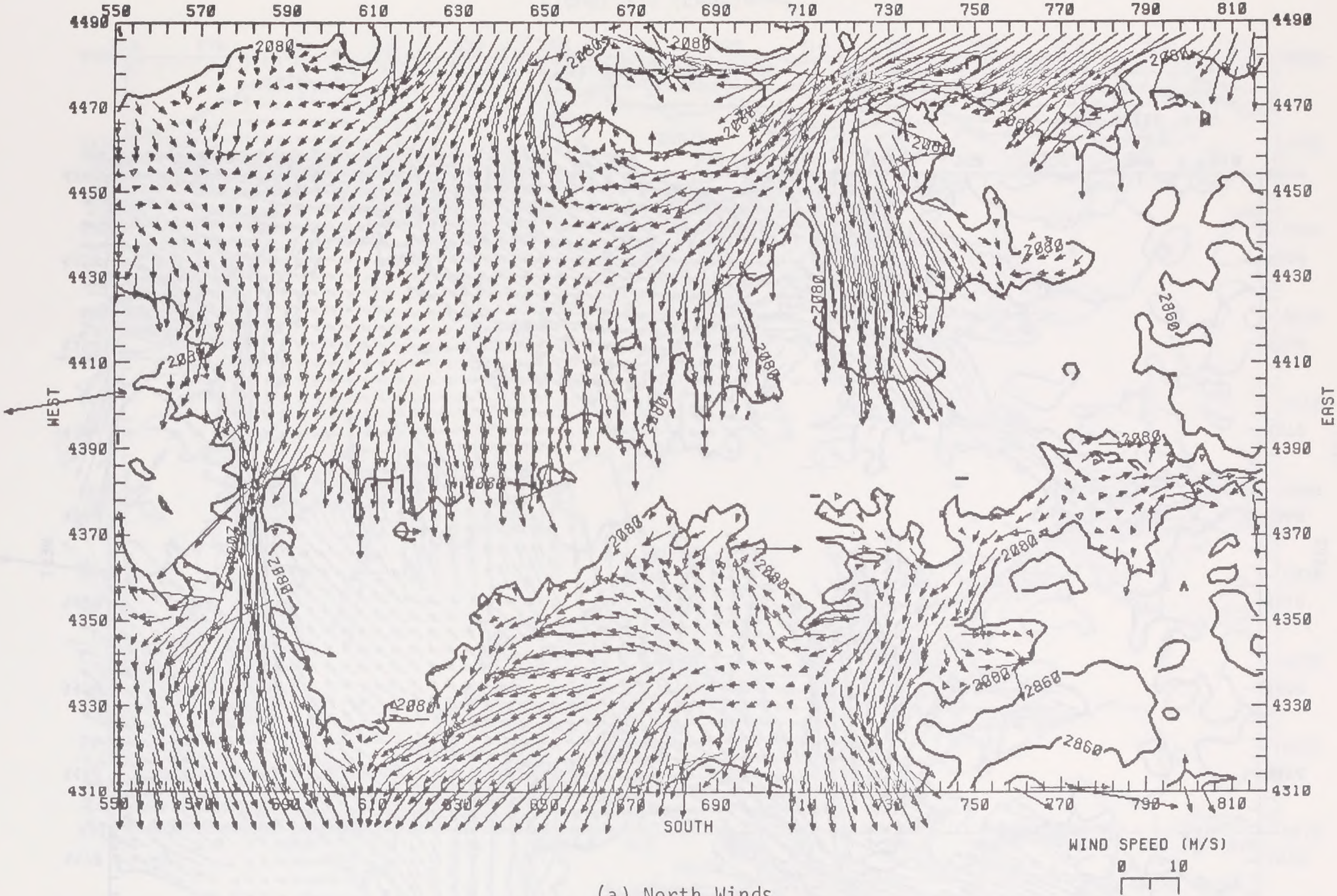

(a) North Winds

FIGURE 2-8. COMPUTED WIND FIELDS FOR EIGHT SYNOPTIC WIND DIRECTIONS FOR THE STUDY REGION (LOWEST MODELED LAYER FROM 4300 FT MSL OR TERRAIN ELEVATION, TO 6800 FT MSL)

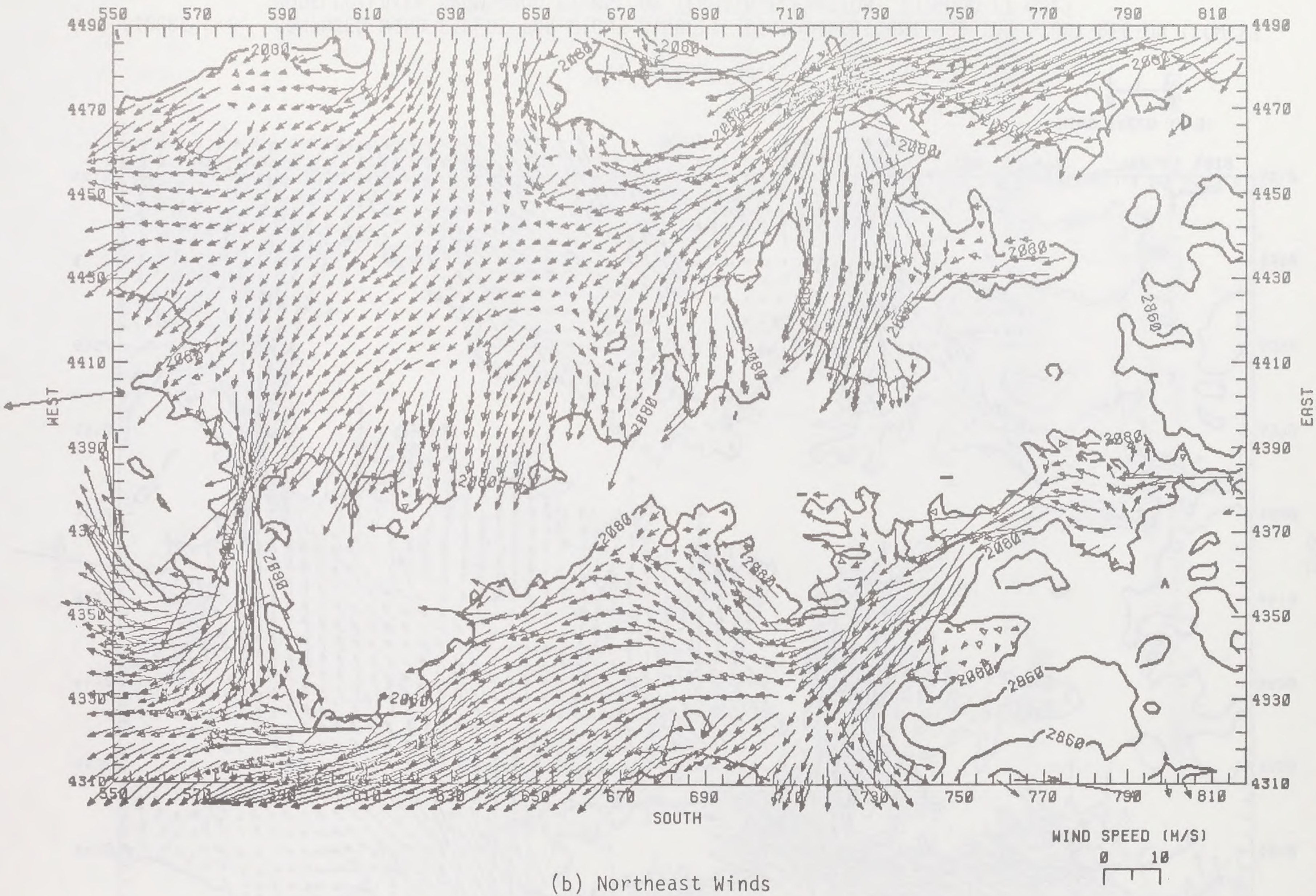

(b) Northeast Winds

FIGURE 2-8 (Continued)

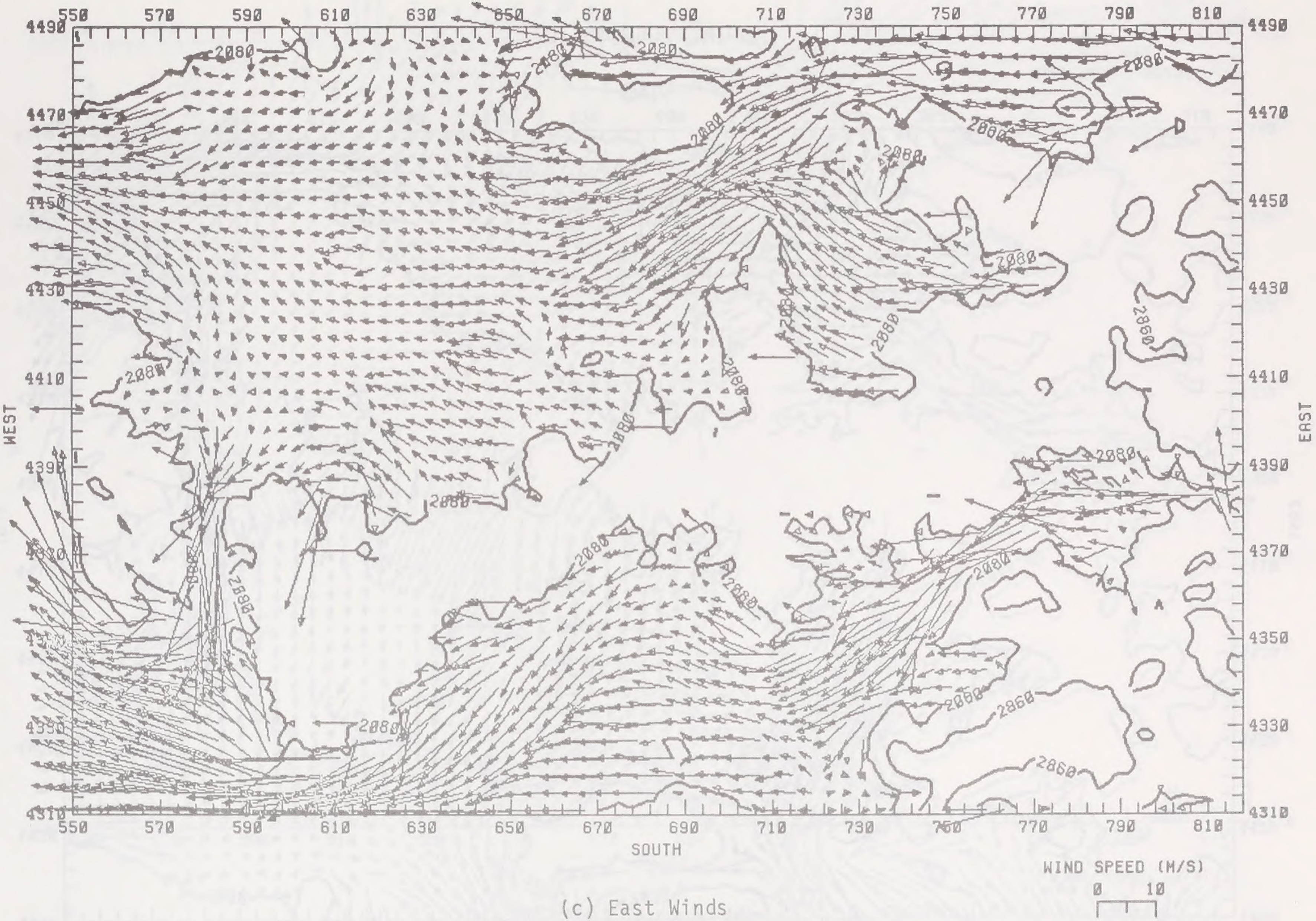

(c) East Winds

FIGURE 2-8 (Continued)

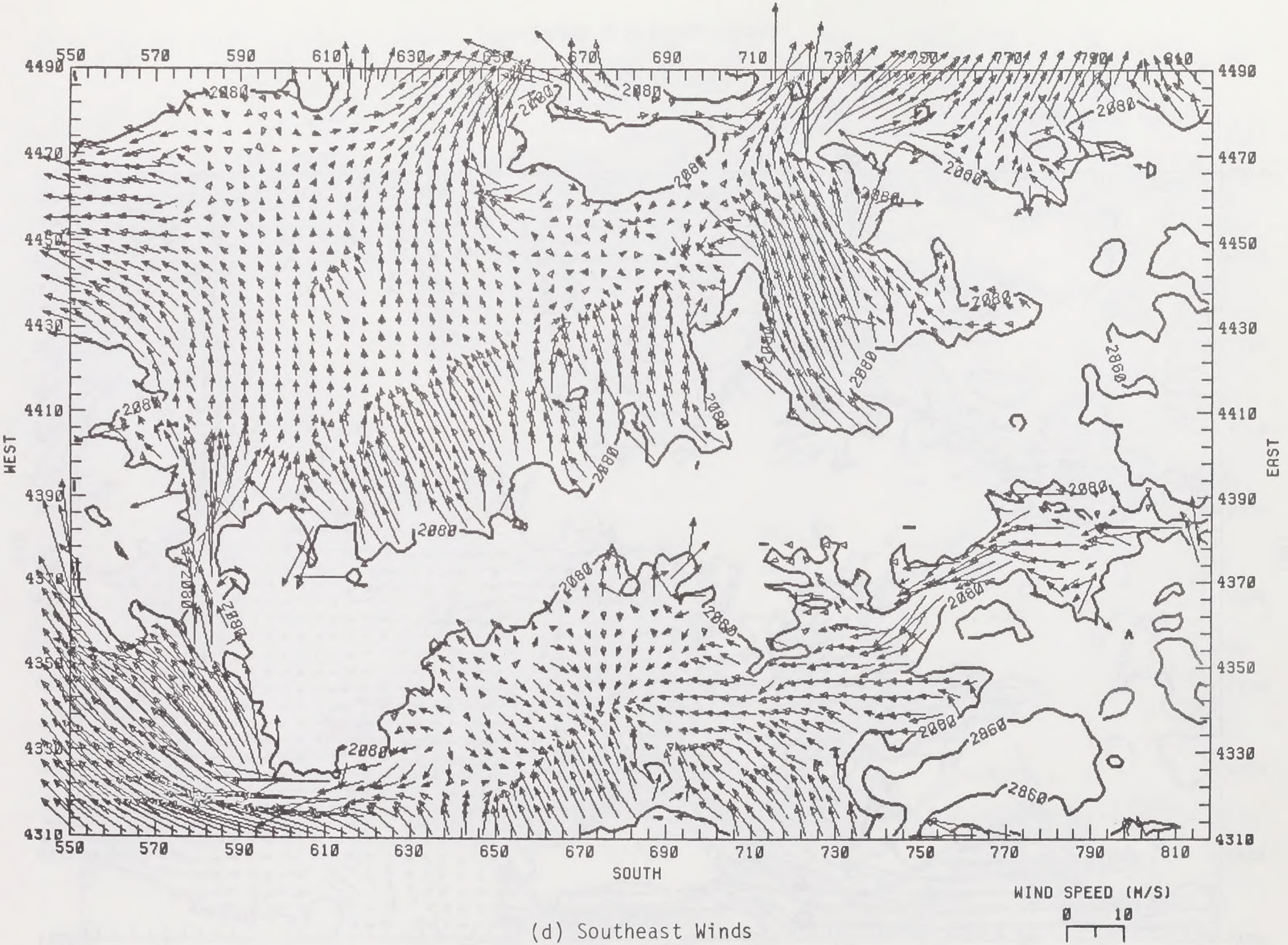

(d) Southeast Winds

FIGURE 2-8 (Continued)

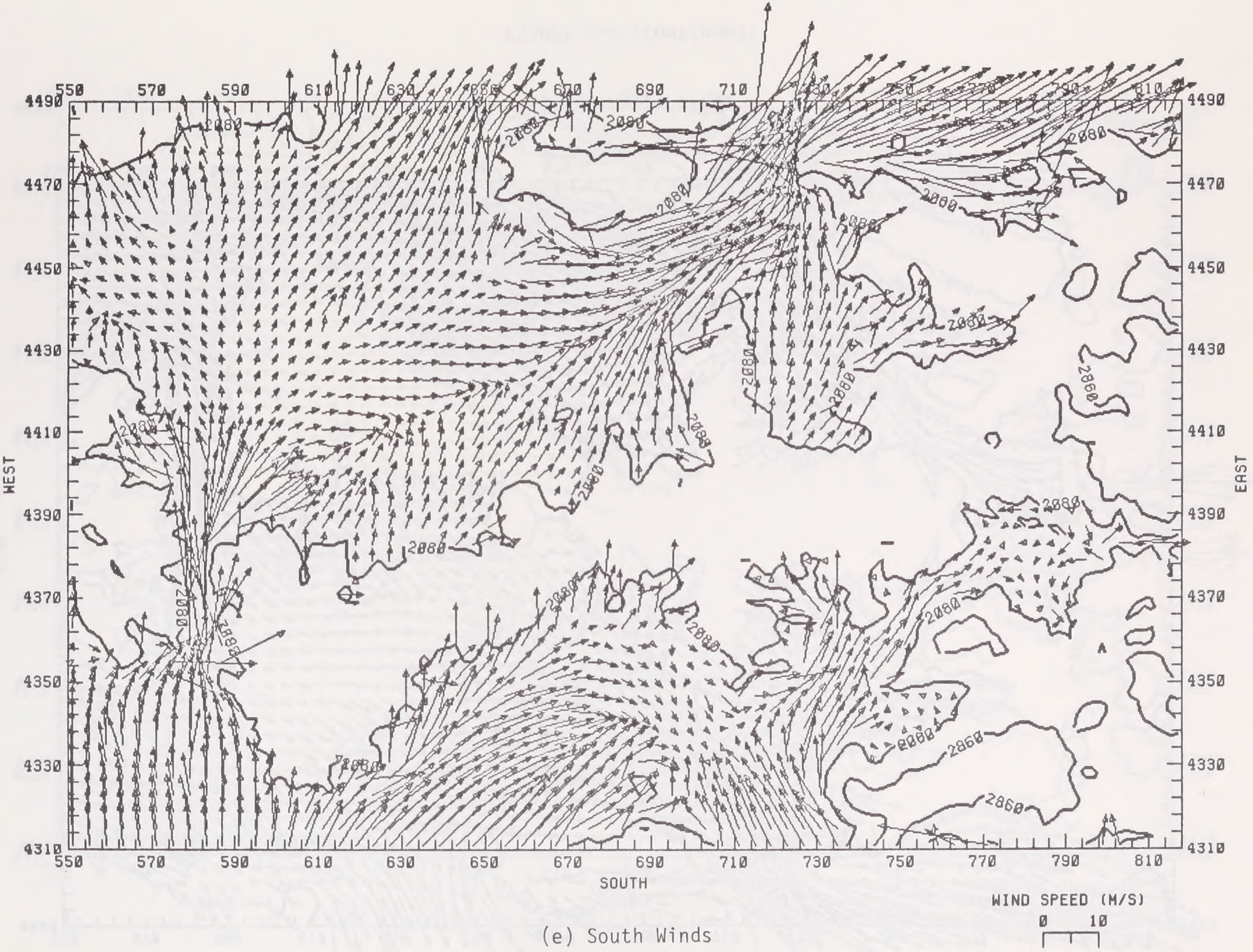

(e) South Winds

FIGURE 2-8 (Continued)

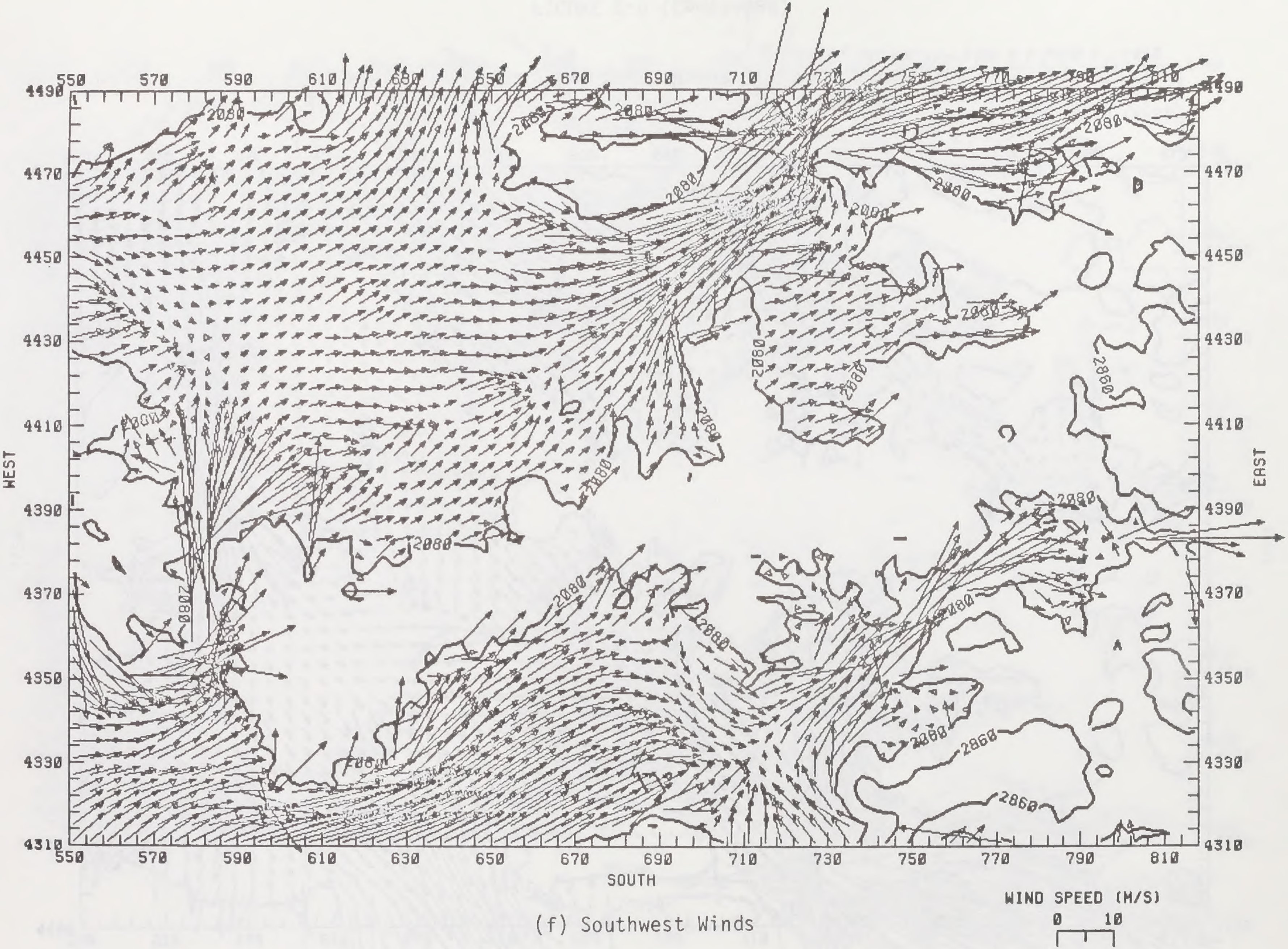

(f) Southwest Winds

FIGURE 2-8 (Continued)

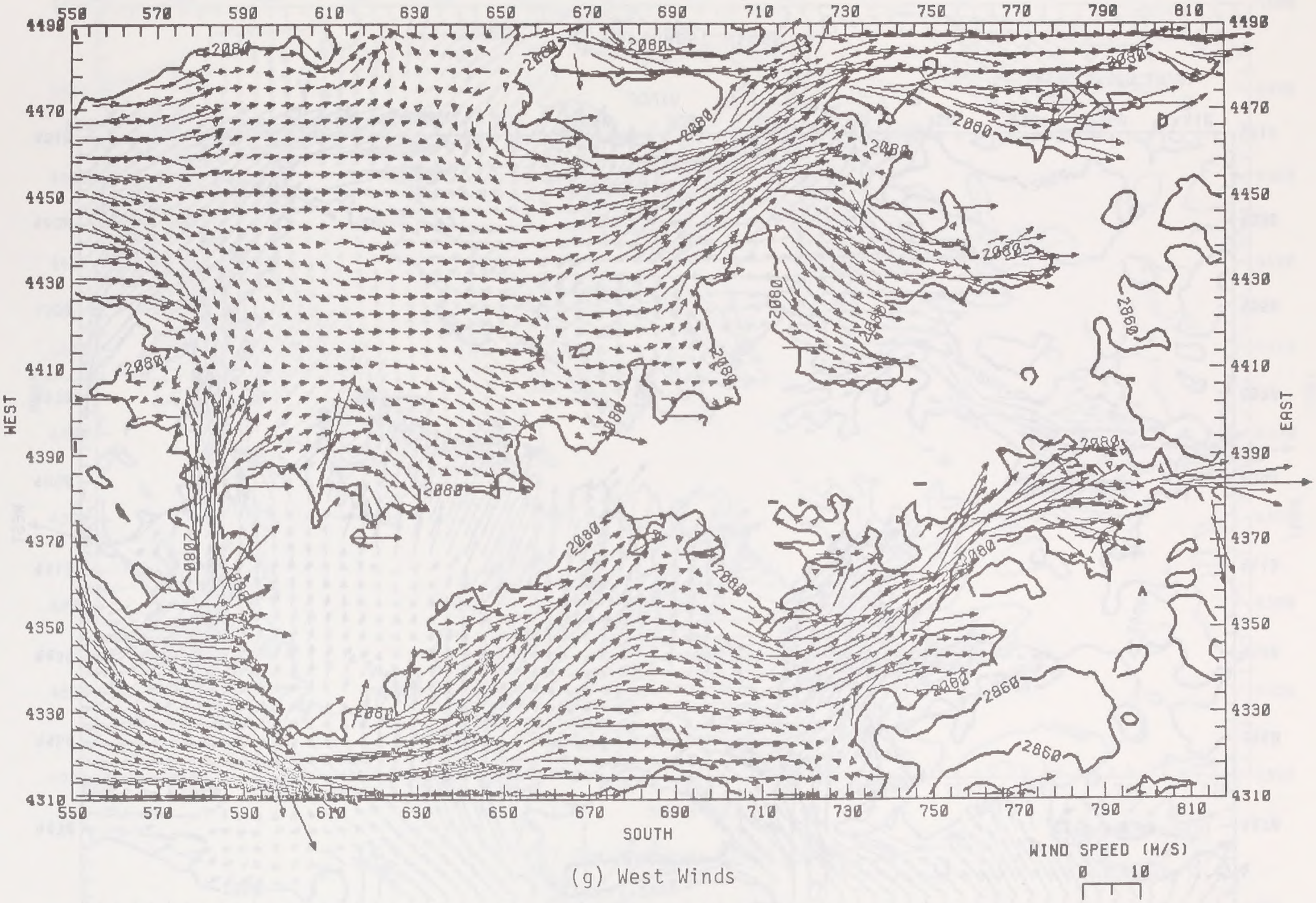

(g) West Winds

FIGURE 2-8 (Continued)

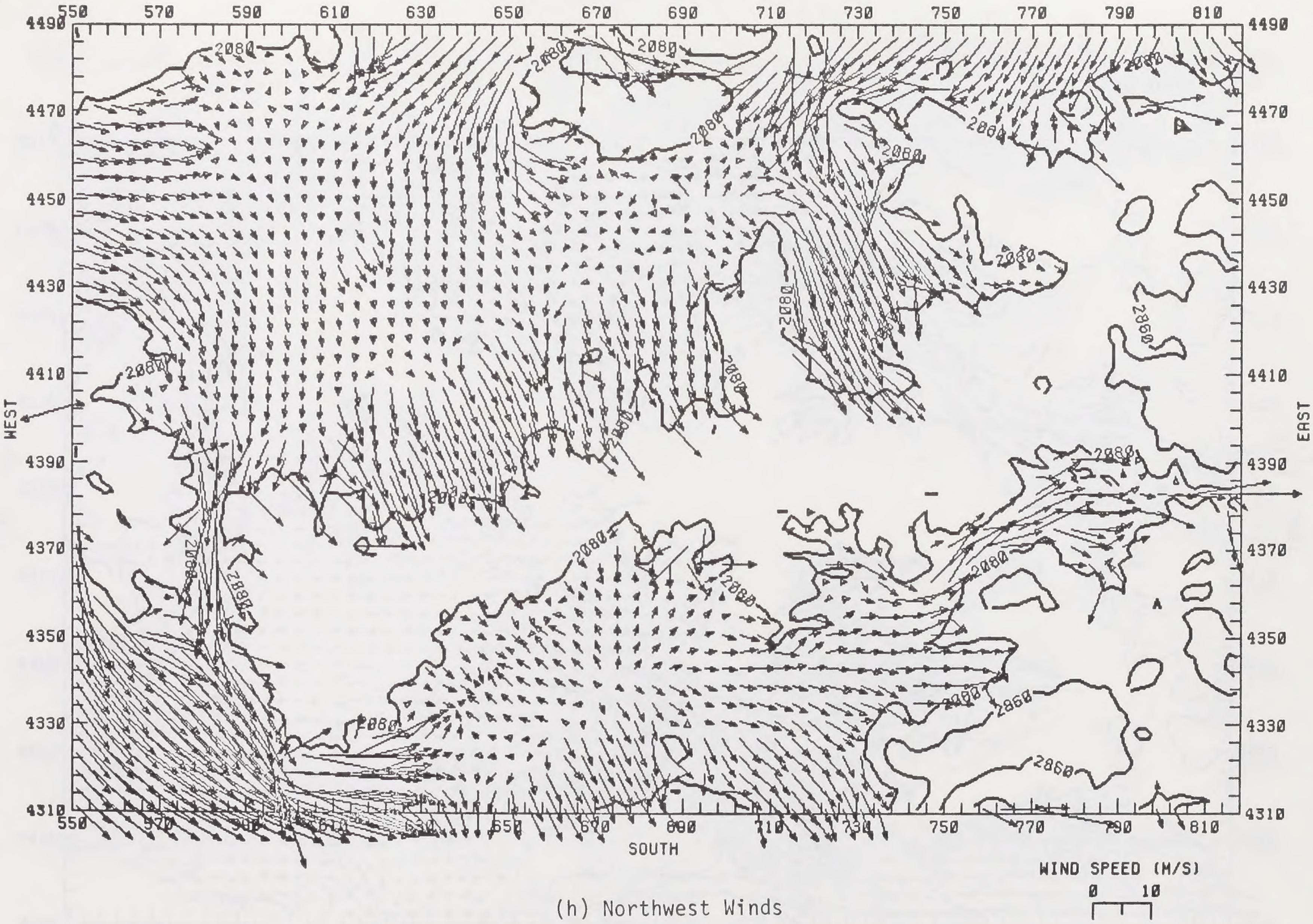

(h) Northwest Winds

FIGURE 2-8 (Concluded)

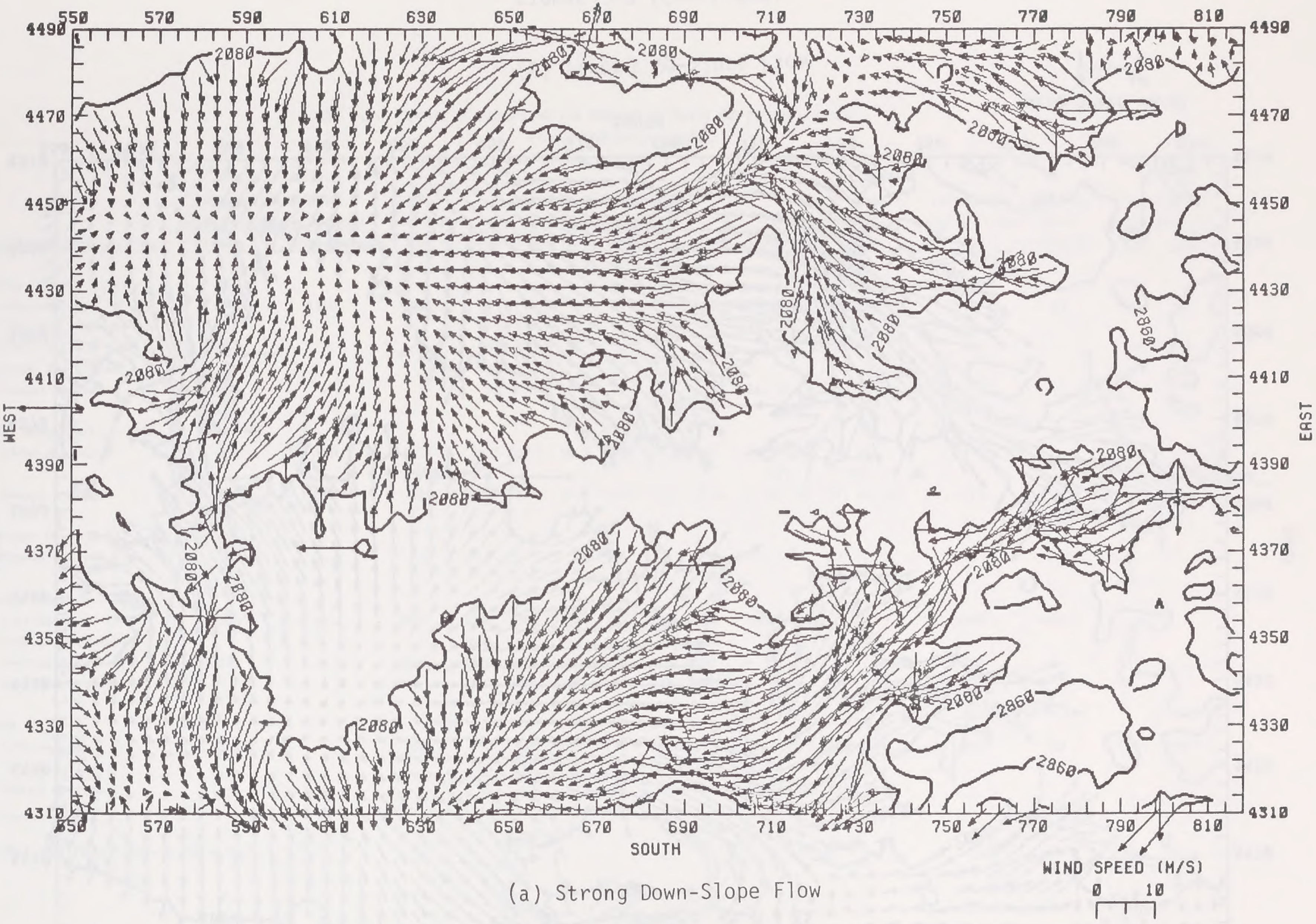

(a) Strong Down-Slope Flow

FIGURE 2-9. COMPUTED WIND FIELDS FOR DOWN-SLOPE AND UP-SLOPE FLOW CONDITIONS AND ZERO UPPER-AIR WINDS (LOWEST MODELED LAYER FROM 4300 FT MSL OR TERRAIN ELEVATION, TO 6800 FT MSL)

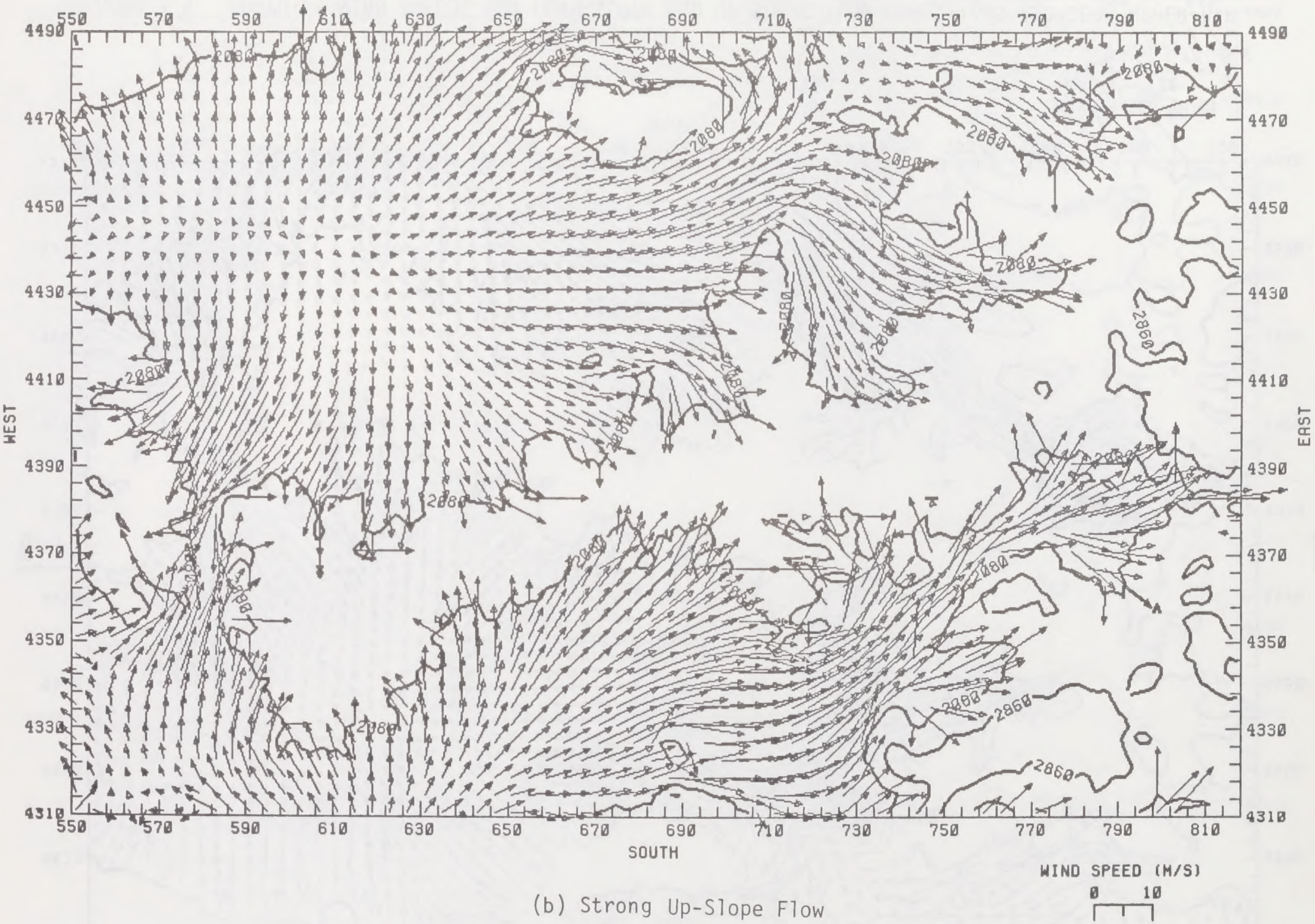

(b) Strong Up-Slope Flow

FIGURE 2-9 (Concluded)

TABLE 2-3. SUMMARY OF BACKGROUND AIR QUALITY IN UINTA AND PICEANCE BASINS
(Concentrations in $\mu g/m^3$)

	National Ambient Air Quality Standards (NAAQS)		Tosco-Sand Wash	White River Shale Project (U-a, U-b, A6)						Rio Blanco (C-a)		Cathedral Bluffs (C-b)	Chevron Site	Naval Oil Shale Reserve	
Pollutant/Averaging Time	Primary	Secondary	1980	1975	1976	1977	1978	1979	1980	1975-1976	1978	1978	1980-81	1980	1981
Sulfur Dioxide (SO_2)															
3-hr maximum	--	1300	4.5	15	5	15	27	113	16	234, 130	78, 286	88	21	44	118
3-hr 2nd highest				15	5	10	25	47	16						
24-hr maximum	365	--	2	10	0	10	14	14	9			43		13	69
24-hr 2nd highest				10	0	5	13	6	8						
Annual average	80	--	1	3	0	1	3	0	1	26, 26	26, 26	1	3		
Total Susp. Partic. (TSP)															
24-hr maximum	260	150	83.5	74.7	101.2	58.3	62.7	52.9	127	211, 102, 281	59, 60, 160	178		30	37
Annual average	75	60	19	24.5	23.5	22.2	15.0	12.5	19.6	9, 9, 15	14, 13, 26	11			
Nitrogen Dioxide NO_2															
Annual average	100	--	5.5	5	5	0	1	1	2	17, 11*	11*	10*	4		
Carbon Monoxide (CO)															
1-hr maximum	40,000	--	7400	3000	3000	1000	700	1800	2500	4800, 6900	--	2800	5400		
1-hr 2nd highest				2000	2700	900	600	900	1900						
8-hr maximum	10,000	--	4500	1300	1800	600	400	500	1500			1700			
8-hr 2nd highest				700	1700	600	400	500	1400						
Ozone (O_3)															
1-hr maximum	240	--	160	150	140	160	137	151	143	136, 178	176, 144	160	148	206	265
1-hr 2nd highest				150	140	160	135	149	143						
Annual average	--	--		70	63	61	72	73	68	68,62	114, 76				

---

* Total NO_x concentrations ($NO + NO_2$).

Ambient measurements of SO_2 and NO_2 were also made by the state of Utah in Green River and Vernal, Utah, during the years 1977 to 1980. SO_2 concentrations were essentially zero, and the NO_2 annual concentrations ranged from zero to 20 $\mu g/m^3$.

On the basis of an emission inventory developed for the region for the 1980 baseline year, as discussed in Section 4.1, the annual-average SO_2 concentration was modeled using the Gaussian puff model described in Section 4.2. The results are shown in figure 2-10. Note that concentrations are essentially zero except in the Grand Junction, Colorado, area, where SO_2 concentrations are higher than 6 $\mu g/m^3$.

More ambient data were available for TSP than for other criteria pollutants for the study region. Table 2-4 summarizes measurements made by the states of Utah and Colorado in the study region. For most of the sites in the study area, TSP ambient air quality standards are exceeded. The primary cause of these exceedances is most likely windblown dust and dust from unpaved and gravel roads.

Utilizing the TSP emission inventory developed for the study region, we looked specifically at the emissions in locations for which we had TSP ambient data. We found a high correlation between local TSP emissions and ambient concentrations, as shown in figure 2-11. On the basis of these correlations, we developed the following empirical models:

$$\chi = 55 + 0.267\ d \quad \text{for maximum 24-hour average}$$
$$\chi = 17 + 0.061\ d \quad \text{for geometric mean}$$

where χ is the ambient maximum 24-hour average or annual geometric mean TSP concentration in $\mu g/m^3$ and d is the particle emission density in tons per year per 100 km^2.

These models were used to calculate impacts of secondary TSP emissions for the low and high oil production scenarios (see Section 5). The existing baseline ambient TSP concentrations for the study region are displayed in figure 2-12. Ambient annual-average TSP concentrations in excess of the air quality standards are predicted to exist in the Colorado River basin (near Grand Junction and Rifle) in the southeastern portion of the study region, and near Craig, Colorado, and Vernal, Utah. We estimate that annual-average TSP concentrations in most other sites in the study area are currently in the range of 20 to 40 $\mu g/m^3$.

Visual-range (visibility) measurements were made by the National Park Service during the period 1978 to 1979 at Dinosaur National Monument at the northern edge of the study region. Visibility in the region is usually quite good--the mean visual range is 178 to 192 km in the summer,

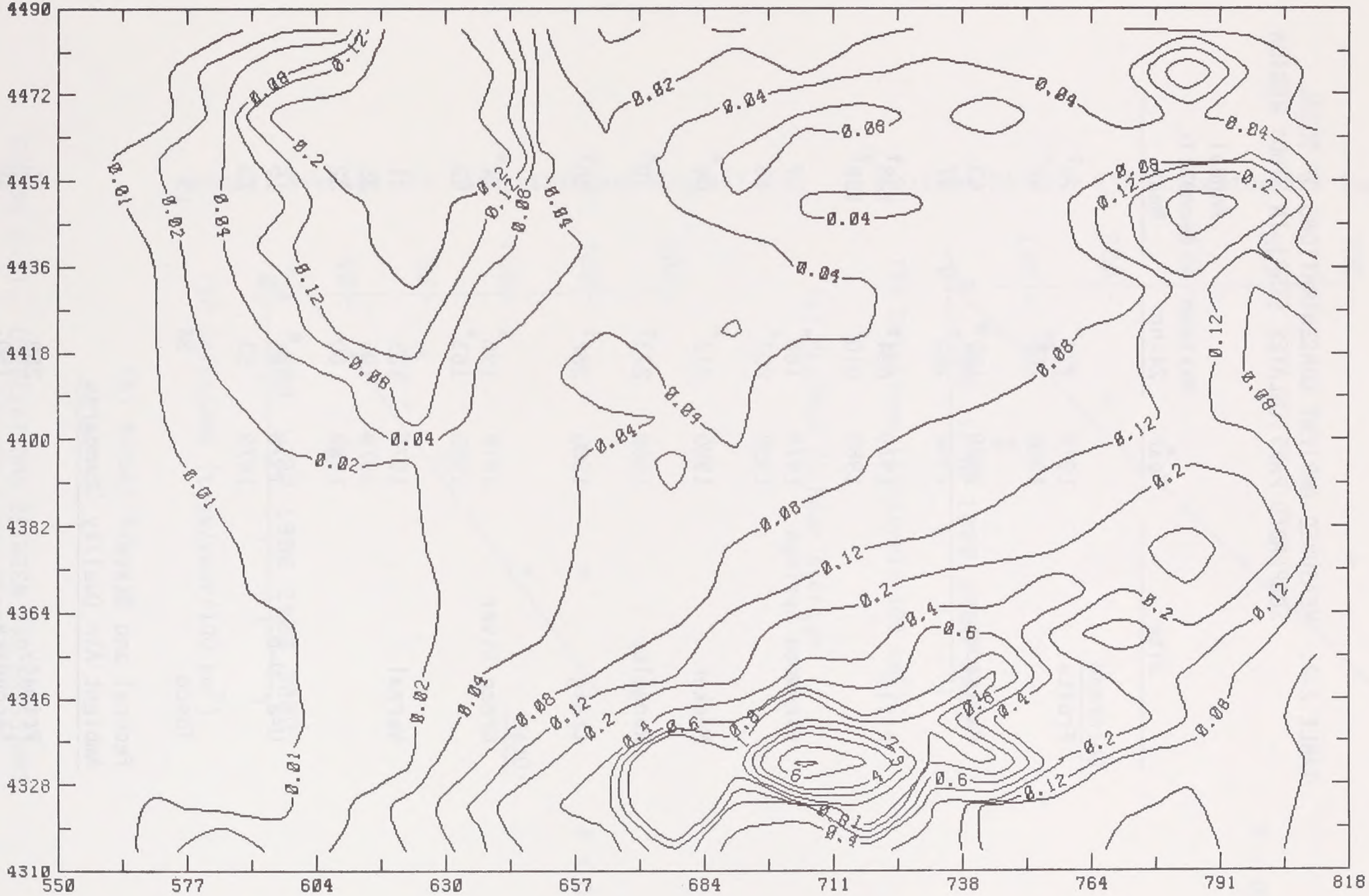

FIGURE 2-10. EXISTING ANNUAL AVERAGE SO_2 CONCENTRATIONS (µg/m^3)

TABLE 2-4. MEASURED AMBIENT CONCENTRATIONS OF TOTAL SUSPENDED PARTICULATES (TSP) IN STUDY REGION

Site	Year	Maximum 24-hr	Annual Geometric Mean
Colorado			
Fruita	1979	173[*]	76[†]
	1980	166[*]	69[*]
Palisade	1979	130	43
	1980	163[*]	47
Rifle	1979	694[†]	128[†]
	1980	510[†]	156[†]
Glenwood Springs	1979	188[*]	57
	1980	203[*]	68[*]
Meeker	1980	212[*]	66[*]
Rangeley	1980	273[†]	70[*]
Craig	1980	382[†]	86[†]
Utah			
Green River	1979	196[*]	64[*]
	1980	163[*]	53
Vernal	1978	105	31
	1979	106	35
	1980	80	32
U-a, U-b	1978	63	15
	1979	53	13
Tosco		84	19
Federal and State Ambient Air Quality Standards			
Primary		260	75
Secondary		150	60

---

[*] Exceedance of secondary standard.

[†] Exceedance of primary and secondary standards.

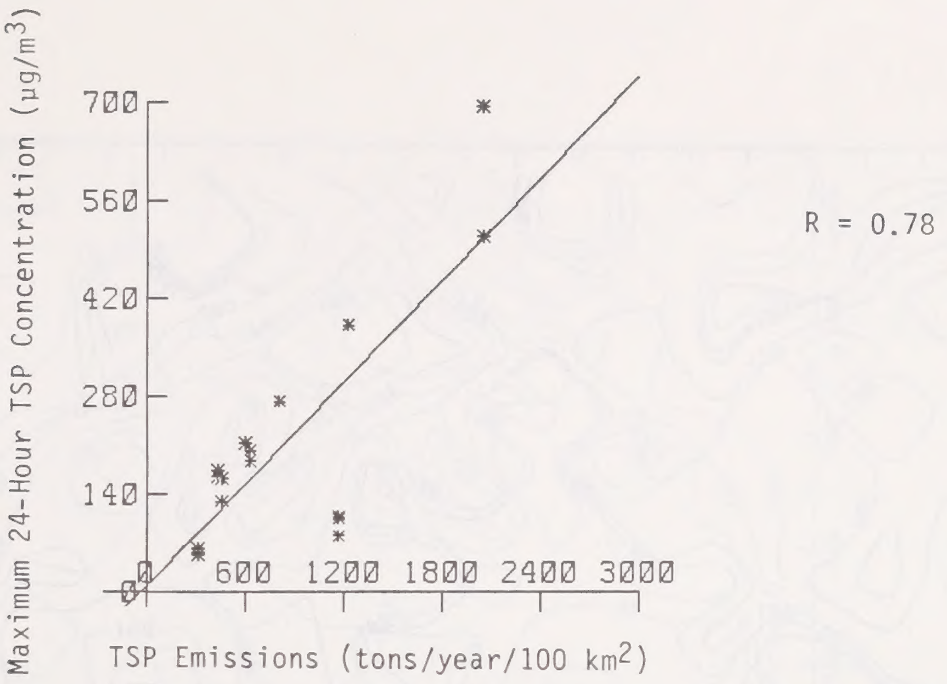

(a) Maximum 24-Hour Average

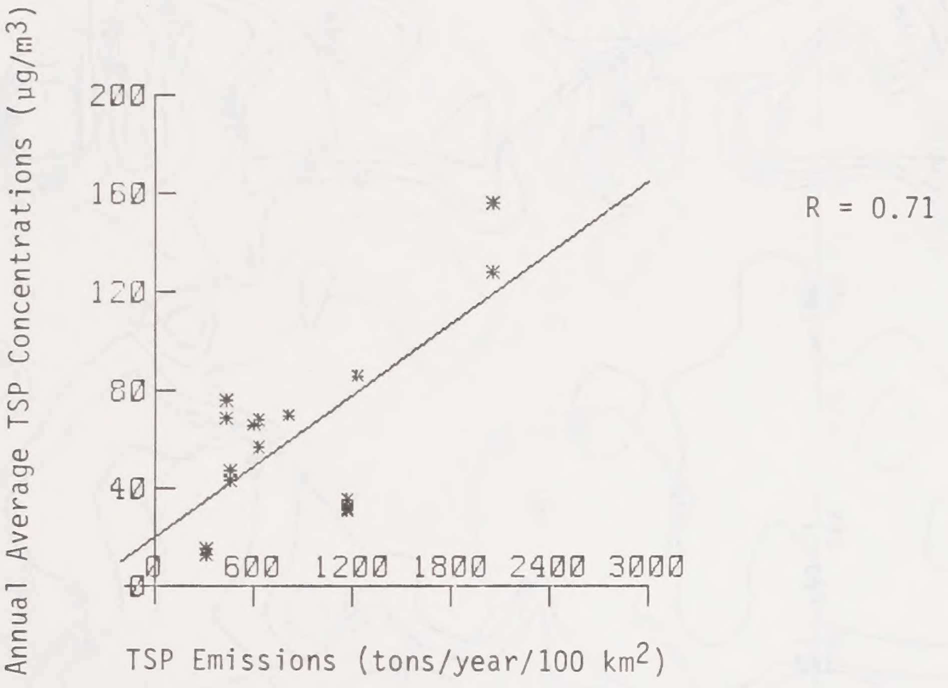

(b) Annual Average

FIGURE 2-11. CORRELATIONS BETWEEN TSP EMISSIONS AND AMBIENT CONCENTRATIONS

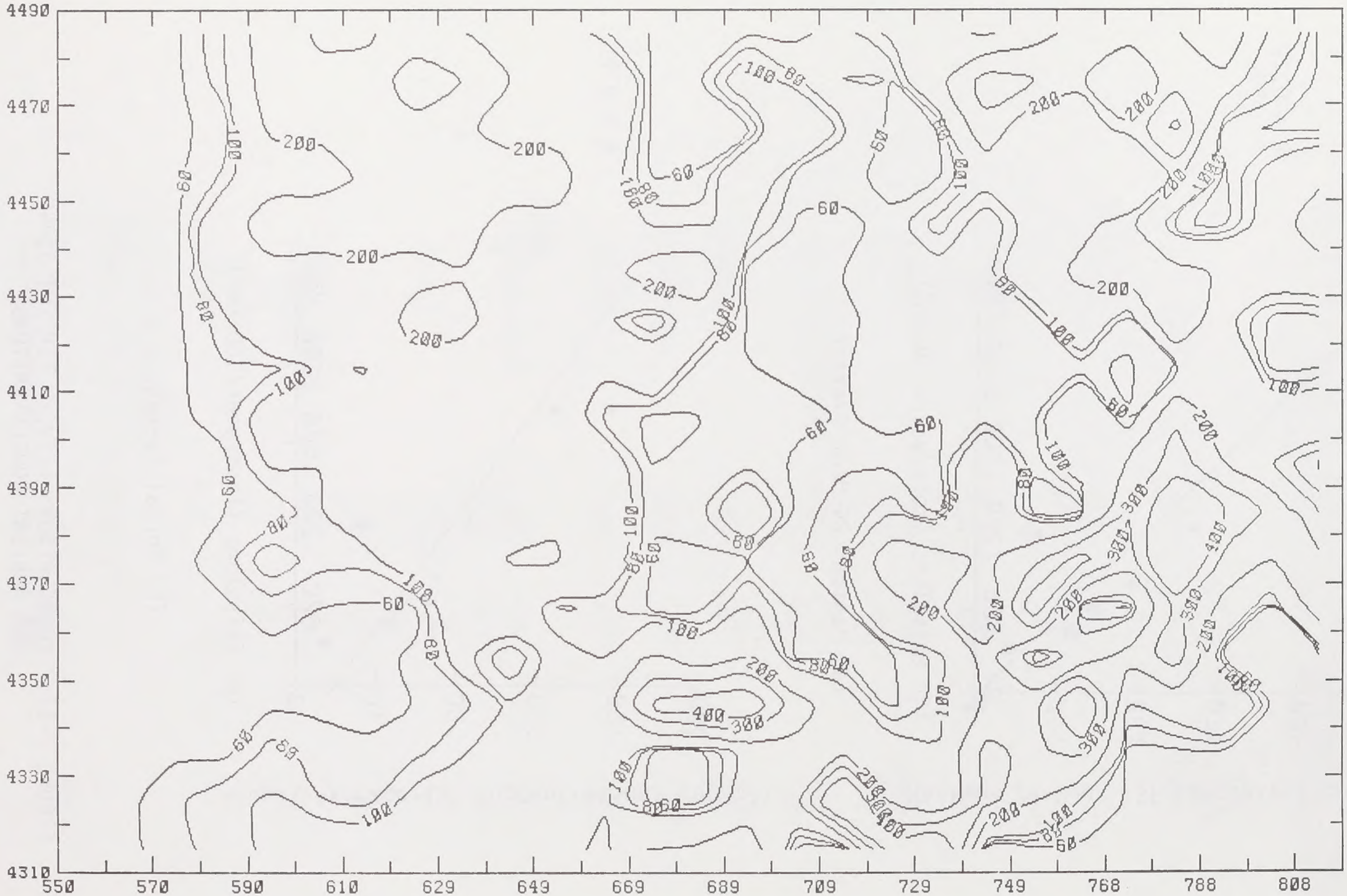

(a) Maximum 24-Hour Average

FIGURE 2-12. MODEL ESTIMATES OF EXISTING TOTAL SUSPENDED PARTICULATE (TSP) CONCENTRATIONS IN STUDY REGION

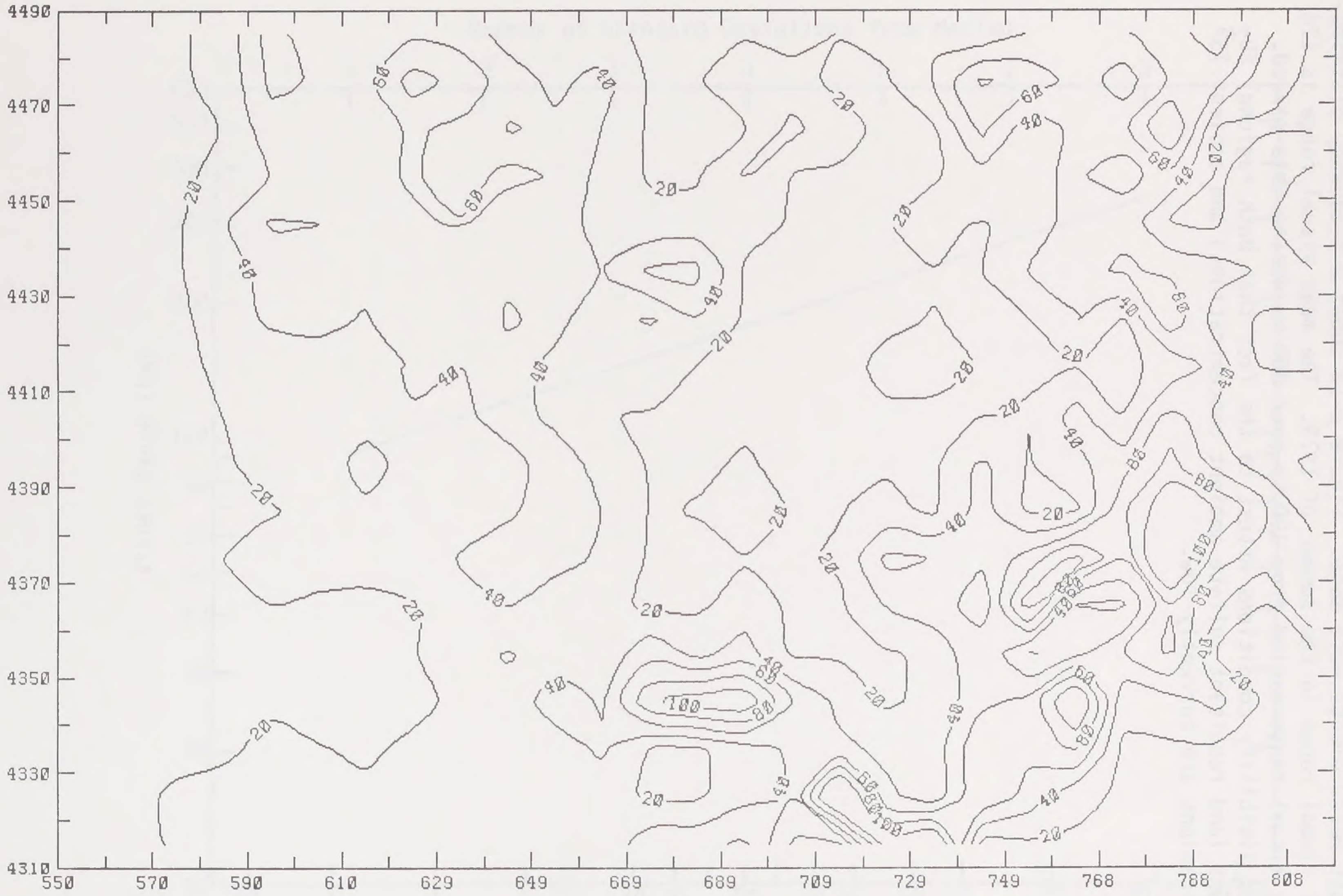

(b) Annual Average

FIGURE 2-12 (Concluded)

when most measurements were made. Figure 2-13 shows a frequency distribution of visual range in the summer of 1979. The mean visual range is 178 km, but visual range varied from 100 to over 300 km during this period. The good visibility conditions attest to the fact that both regional SO_2 emissions (and resultant sulfate ambient concentrations) and ambient TSP concentrations are currently low.

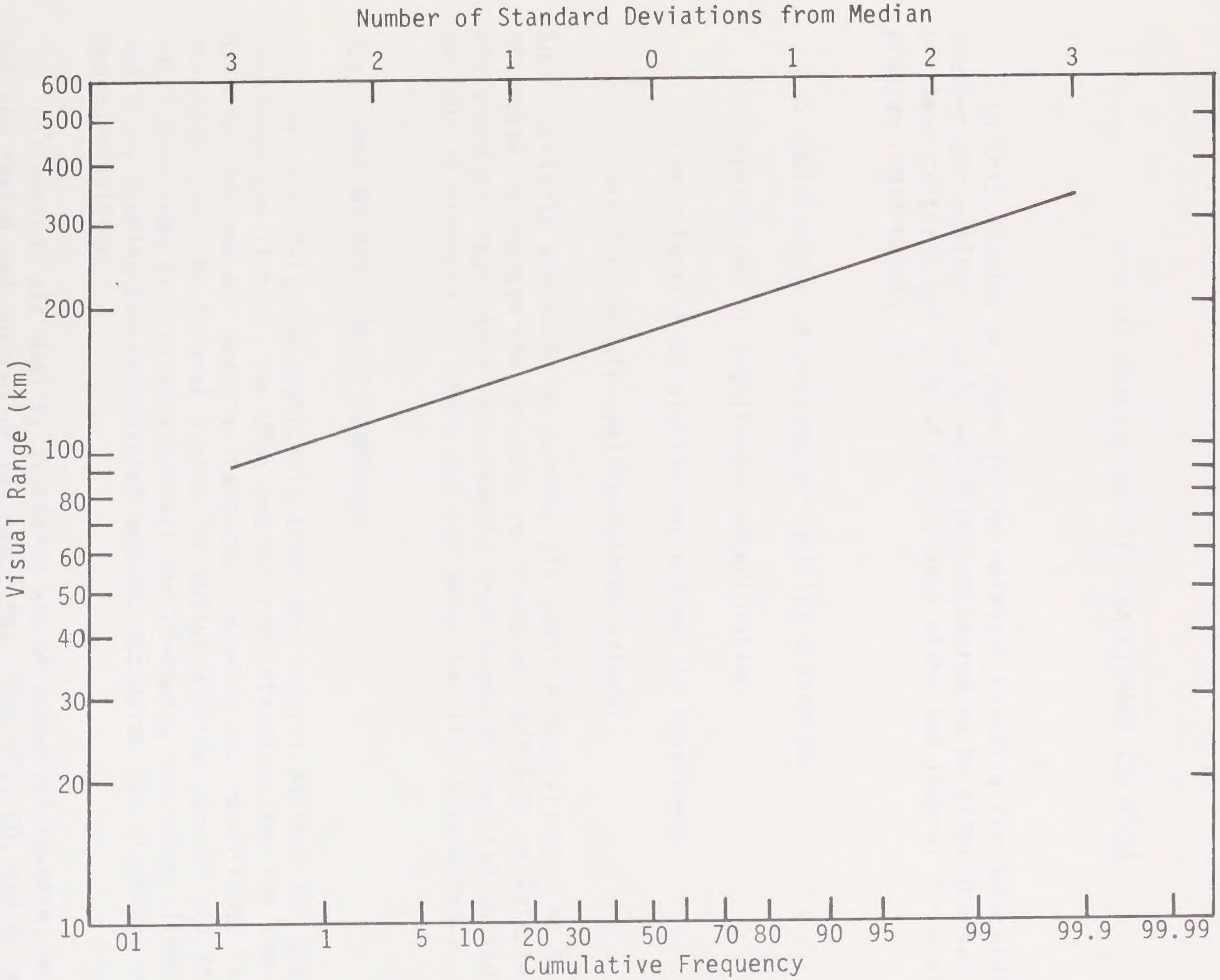

Source: Walther and Newburn (1980)

FIGURE 2-13. FREQUENCY DISTRIBUTION OF VISUAL RANGE AT DINOSAUR NATIONAL MONUMENT IN SUMMER 1979

3 AIR QUALITY IMPACT SIGNIFICANCE CRITERIA

In this section we identify the relevant criteria for determining whether air quality impacts would be considered to be significant. Most of these criteria are part of established state and federal air quality program requirements for

- Maintenance of ambient air quality standards
- Prevention of significant deterioration
- Determination of significant visibility impairment
- Protection of air-quality-related values.

These criteria are based on current air quality regulations. We have not attempted to address the possible revisions or additions to existing statutory and regulatory requirements that might be expected during the periods of proposed oil shale and tar sands facility development.

3.1 AMBIENT AIR QUALITY STANDARDS

In table 3-1, the applicable state and federal ambient air quality standards are listed. The Utah and Colorado standards are the same as the National Ambient Air Quality Standards. Wyoming has established tighter standards than the federal limits for sulfur dioxide (annual and 24-hour), total suspended particulates (annual and 24-hour), and ozone (1-hour). In addition, Wyoming has established ambient standards for fluorides and hydrogen sulfide.

All ambient air quality standards are of potential concern; however, for the region and sources of interest, SO_2, TSP, NO_2, CO, and O_3 are the pollutants of principal concern.

TABLE 3-1. APPLICABLE STATE AND FEDERAL AMBIENT AIR QUALITY STANDARDS ($\mu g/m^3$)

Pollutant	Federal	Utah	Colorado	Wyoming
SO_2				
(annual)	80	80	80	60
(24-hour)	365	365	365	260
(3-hour secondary)	1300	1300	1300	1300
TSP				
Primary				
(annual)	75	75	75	60
(24-hour)	260	260	260	150
Secondary				
(annual)	60	60	60	
(24-hour)	150	150	150	
CO				
(8-hour)	10,000	10,000	10,000	10,000
(1-hour)	40,000	40,000	40,000	40,000
O_3				
(1-hour)	240	240	240	160
NO_2				
(annual)	100	100	100	100
Flourides as HF				
(24-hour)				0.8
Lead				
(1/4 year)	1.5			
H_2S				
(30-minute average)				70

3.2 PREVENTION OF SIGNIFICANT DETERIORATION

The U.S. EPA and state (Utah and Wyoming) prevention of significant deterioration requirements allow only a limited increase in the second-highest short-term TSP and SO_2 concentrations and annual-average TSP and SO_2 concentrations associated with emissions from a new source. These SO_2 and TSP increments are listed in table 3-2 for each area classification (I, II, and III).

TABLE 3-2. PREVENTION OF SIGNIFICANT DETERIORATION INCREMENTS

		Maximum Allowable Concentrations ($\mu g/m^3$)		
Pollutant	Averaging Time	Class I	Class II	Class III
SO_2	Annual	2	20	40
	24-hr	5	91	182
	3-hr	25	512	700
TSP	Annual	5	19	37
	24-hr	10	37	75

Currently, no areas within Utah, Colorado, or Wyoming are designated Class III. Existing Class I areas that are likely to be most affected by development (see Latimer and Doyle, 1981) in the study area include

> Flat Tops Wilderness

> Mt. Zirkel Wilderness

> Maroon Bells/Snowmass Wilderness.

These wilderness areas are all at distances of 50 km or more from the oil shale and tar sands development regions. Since all other areas within the study area are designated Class II, near-source impacts are evaluated against the PSD Class II increments.

Several requirements of PSD review apply only to pollutants emitted in significant amounts; these significant, or de minimis, levels are presented in table 3-3. These values provide criteria for determining whether specific pollutant emissions for a source are significant, thus requiring ambient air quality modeling.

TABLE 3-3. EPA SIGNIFICANT (DE MINIMIS) EMISSION RATES

Pollutant	Emission Rate (tons/year)
Carbon monoxide	100
Nitrogen oxides	40
Sulfur dioxide	40
Total suspended particulates	25
Ozone (volatile organic compounds)	40
Lead	0.6
Asbestos	0.007
Beryllium	0.0004
Mercury	0.1
Vinyl chloride	1.0
Fluorides	3
Sulfuric acid mist	7
Total reduced sulfur (including H_2S)	10
Reduced sulfur (including H_2S)	10
Hydrogen sulfide	10

In addition to the federal PSD requirements, the state of Colorado has adopted standards for sulfur dioxide (SO_2) expressed as allowable amounts of increase in ambient concentrations over an established baseline. Like PSD, these standards have been adopted for three categories (I, II, and III) of land areas or regions. The increment limits for these state categories are the same as the PSD Class I, II, and III increments for SO_2. Colorado has included national monuments in category I, and two national monuments, Colorado and Dinosaur, are located within the study area. These two national monuments may also be redesignated federal Class I PSD areas. Also, to the northwest of the study region is the Uinta Primitive Area, an area of special concern that may also at some future date be redesignated Class I.

3.3 DETERMINATION OF SIGNIFICANT VISIBILITY IMPAIRMENT

Currently there are no clear objective criteria for judging adverse visibility impairment in Class I areas. However, the EPA visibility regulations, promulgated on 2 December 1980 (Federal Register, pp. 80084-80095) state that adverse visibility impairment will be determined on a ". . . case-by-case basis taking into account the geographic extent, intensity, duration, frequency and time of visibility impairments, and how these factors correlate with (1) times of visitor use of the federal class I area and (2) the frequency and timing of natural conditions."

More objective criteria for determining adverse visibility impairment are outlined in the EPA document entitled "Workbook for Estimating Visibility Impairment" (Latimer and Ireson, 1980). That document suggests the following criteria: if a plume contrast or sky/terrain contrast change greater than ± 0.10, or a plume discoloration corresponding to a ΔE (*L*a*b) of 4, or a blue-red ratio of 0.9 is predicted to occur on the worst day, the probability of adverse visibility impairment cannot be ruled out.

The existing mandatory Class I areas in the study area that are currently afforded visibility protection are administered by the U.S. Forest Service (USFS). The USFS has not yet established specific criteria for judging the significance of visibility impairment, except to state that visibility effects, such as changes in contrast, coloration, and visual range, should be considered. The USFS has not identified any "integral vistas," which are views from within a Class I area of landscape features located outside an area, that are afforded visibility protection.

3.4 PROTECTION OF AIR-QUALITY-RELATED VALUES

The U.S. Forest Service has started to address the air-quality-related values of its Class I areas and has identified categories of effects that air quality impacts could have on air-quality-related values. These effects are listed in table 3-4.

The National Park Service (NPS) administers both the Dinosaur and Colorado national monuments, which are protected under the 1916 Organic Act. Although these areas are not Class I, their air-quality-related values are a major concern to the NPS.

TABLE 3-4. CATEGORIES OF POTENTIAL AIR QUALITY IMPACTS ON AIR-QUALITY-RELATED VALUES OF CLASS I AREAS

Flora and fauna effects
    Growth
    Mortality
    Reproduction
    Diversity
    Visible injury
    Succession
    Productivity

Soil effects
    Cation exchange capacity
    Base saturation
    pH
    Structure
    Metals concentration

Water effects
    pH
    Metals concentration
    Total alkalinity

Visibility effects
    Contrast
    Coloration
    Visual range

Odor effects

Cultural, archaeological, and geological effects
    Deposition
    Decomposition

4 ANALYSIS METHODOLOGY

The methodology used in this study is indicated schematically in figure 4-1 and consisted of the following major tasks:

> Collection of Data. Emission data for the Uinta Basin synfuel facilities were collected from the developers. Information concerning Colorado point and area source emissions and Utah population projections were obtained from a study performed for the National Park Service by PEDCo. Meteorological and topographical data were collected from the National Weather Service, various oil-shale tracts (U-a, U-b, C-a, C-b), and the U.S. Geological Survey.

> Emission Inventory Development. Emission data were reviewed, developed, checked, and converted to input files for air quality modeling. Utah population projections were used to generate secondary growth area source emission files for the portion of Utah in the study region.

> Air Quality Modeling. With the emissions, meteorological, and topographical data as input, several air quality simulation models were applied to address specific concerns. The most extensive modeling was performed by means of the Gaussian Puff Model (GPM), which was applied to both the 110-km x 110-km and 180-km x 268-km regions shown in figure 1-1 for every 3-hour period in a year to compute maximum 3-hour, 24-hour, and annual averages for every receptor in these regions. This conservative model was used to identify periods of worst-case impacts that were modeled with the more realistic finite-difference grid model--Regional Transport Model (RTM), which, because of its cost to run, was applied to only one worst-case regional transport day. For near-source (< 5 km downwind) TSP impacts the EPA Gaussian, sector-average COMPLEX I model was applied to take into account multiple TSP emission points within a given facility (GPM was not used

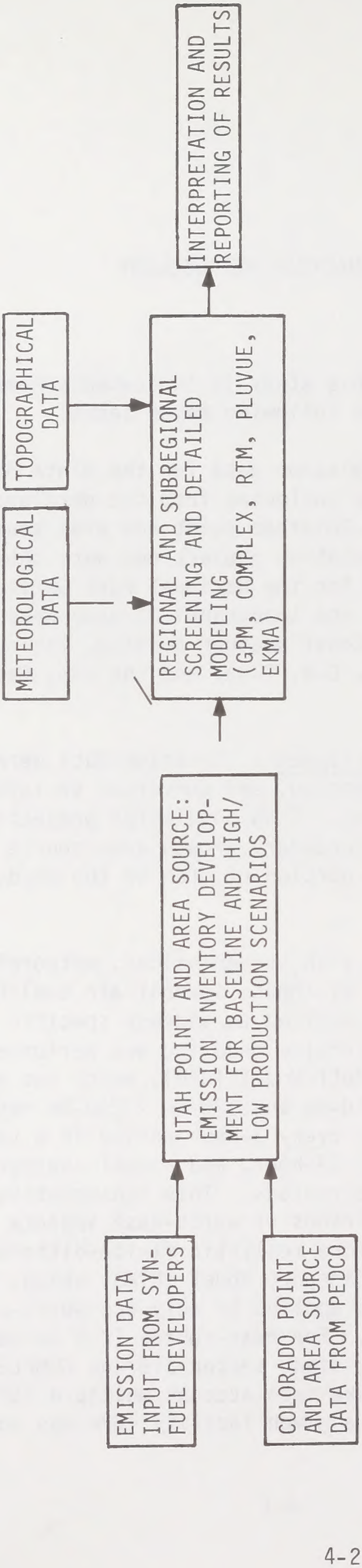
EMISSION DATA INPUT FROM SYN-FUEL DEVELOPERS
COLORADO POINT AND AREA SOURCE DATA FROM PEDCO
UTAH POINT AND AREA SOURCE: EMISSION INVENTORY DEVELOPMENT FOR BASELINE AND HIGH/LOW PRODUCTION SCENARIOS
METEOROLOGICAL DATA
TOPOGRAPHICAL DATA
REGIONAL AND SUBREGIONAL SCREENING AND DETAILED MODELING (GPM, COMPLEX, RTM, PLUVUE, EKMA)
INTERPRETATION AND REPORTING OF RESULTS

FIGURE 4-1. OVERALL FLOW DIAGRAM OF ANALYSIS METHODOLOGY

because of its cost). Worst-case photochemical smog and visibility impairment scenarios were evaluated by means of EKMA and PLUVUE, respectively. Acid deposition was evaluated from GPM results.

This chapter is divided into two major sections. Section 4.1 discusses the development of emission inventories and section 4.2 discusses the modeling methodology.

4.1 DEVELOPMENT OF EMISSION INVENTORIES

This section discusses the array of procedures used by Systems Applications to develop detailed emission inventories for the broad area encompassing the study region. Several of the characteristics of this study contributed to the large effort that was needed to complete the inventories. Principal among these was the large number of different groups of source types including proposed synfuel projects, existing point sources, other sources planned for future operation, and secondary growth sources, for which emission inventories had to be developed.

This work has resulted in the first comprehensive set of inventories for this region of the country. Figure 4-2 depicts the flow of activities for the inventory development process.

We began the inventory process by assigning the existing and proposed emission sources to specific groupings having common characteristics. Considerations of geographic location, general source type, and operational parameters were used to identify specific groups of source categories for baseline conditions and alternative scenarios of future operating conditions. Emission estimates were developed for the following source categories:

> Point sources

  - Proposed Utah oil shale and tar sands projects

  - Other planned projects in Utah

  - 1980 baseline (existing) point sources in Utah

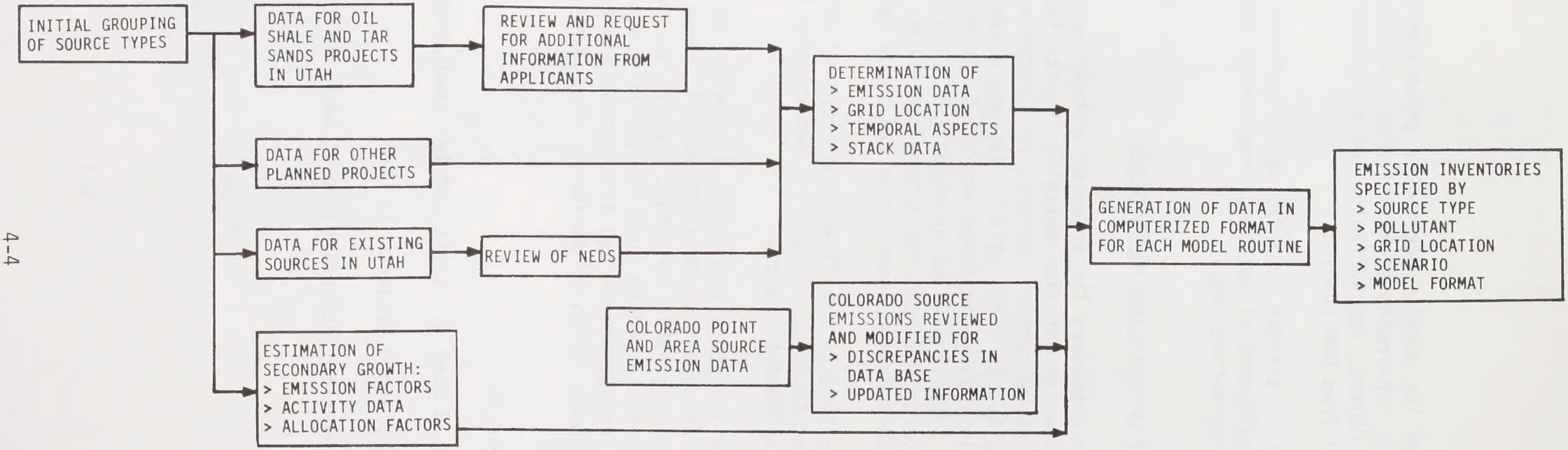
INITIAL GROUPING OF SOURCE TYPES
DATA FOR OIL SHALE AND TAR SANDS PROJECTS IN UTAH
REVIEW AND REQUEST FOR ADDITIONAL INFORMATION FROM APPLICANTS
DATA FOR OTHER PLANNED PROJECTS
DATA FOR EXISTING SOURCES IN UTAH
REVIEW OF NEDS
ESTIMATION OF SECONDARY GROWTH:
> EMISSION FACTORS
> ACTIVITY DATA
> ALLOCATION FACTORS
DETERMINATION OF
> EMISSION DATA
> GRID LOCATION
> TEMPORAL ASPECTS
> STACK DATA
COLORADO POINT AND AREA SOURCE EMISSION DATA
COLORADO SOURCE EMISSIONS REVIEWED AND MODIFIED FOR
> DISCREPANCIES IN DATA BASE
> UPDATED INFORMATION
GENERATION OF DATA IN COMPUTERIZED FORMAT FOR EACH MODEL ROUTINE
EMISSION INVENTORIES SPECIFIED BY
> SOURCE TYPE
> POLLUTANT
> GRID LOCATION
> SCENARIO
> MODEL FORMAT

FIGURE 4-2. SCHEMATIC DIAGRAM OF ACTIVITIES FOR THE EMISSION INVENTORY DEVELOPMENT PROCESS

    - Proposed Colorado oil shale facilities*
    - 1980 baseline point sources in Colorado
    - Future Colorado point sources for the low- and high-oil production scenarios, respectively.
- Area sources
    - 1980 baseline area sources in Utah
    - Future (including secondary growth) Utah area sources for the low- and high-oil-production scenarios.
    - 1980 baseline area sources in Colorado
    - Future Colorado area sources for the low- and high-oil-production scenarios, respectively.

Emission estimates in each case were derived for the five criteria pollutants:

- Sulfur dioxide
- Particulate matter
- Nitrogen oxides
- Hydrocarbons
- Carbon monoxide.

Some speciation of these pollutants into sulfate, nitrogen dioxide, and reactive hydrocarbon categories was also performed. Insufficient data are available to evaluate the emissions and resultant air quality impacts of other species of potential concern such as trace metals and organic materials. Also, the potential long-term climatic effects of carbon dioxide emissions to the atmosphere were not evaluated.

As previously shown in figure 1-1, the study region consisted primarily of six counties in two states.

---

* Plans for developing oil shale resources in Colorado are currently in a state of uncertainty. This study was based on assumptions concerning these development plans.

> Utah (eastern)

- Uintah
- Grand

> Colorado (western)

- Moffat
- Rio Blanco
- Garfield
- Mesa.

Another effort conducted by PEDCo Environmental, Inc. and coordinated by the National Park Service and the Bureau of Land Management had resulted in estimates of emissions for sources located in the Colorado portion of the study region. Due to project scheduling constraints, Systems Applications developed inventories for sources located in Utah only and employed the PEDCo inventories for Colorado sources in the study region. During the course of the study, additional data were received from the State of Utah. These data were compared with the PEDCo data and found to be in reasonably close agreement. Because the derivation of the PEDCo estimates has been reported elsewhere (PEDCo, 1981), the majority of section 4.1 focuses on the development of the Utah point and area source inventories.

All emission data were developed on a gridded basis. Stack data were also derived for modeling the plume rise of individual emission points at each point source.

Baseline emission data were initially derived for all existing point and area sources in operation in 1980. Future emissions representative of various years were then estimated for the individual synfuel projects in Utah at peak operation and for the other planned projects in Utah. In a similar manner, area source emissions were projected to future years that corresponded to the specification of particular scenarios. All emission data were developed on an average basis of operating conditions without regard to considerations such as seasonal characteristics or differences in weekday/weekend operation.

The remainder of section 4.1 discusses the methods used to develop each of the point and area source emission files identified above.

4.1.1 Utah Synfuel Projects

Seven synthetic fuel (oil shale and tar sands) projects proposed for the Uinta Basin represented the principal focus for our study.

> Enercor-Mono Power (tar sands)

> Geokinetics (oil shale)

> Magic Circle (oil shale)

> Paraho (oil shale)

> Sohio (tar sands)

> Syntana-Utah (oil shale)

> Tosco (oil shale).

Distinguishing features among these projects, in addition to their operating processes, are their site locations and project plans. Each of these projects, except Enercor-Mono Power and Geokinetics, would be a single facility developed at one site. Enercor-Mono Power plans to operate facilities at two sites (Rainbow and PR Springs), and Geokinetics intends to develop facilities at 11 locations (Agency Draw and ten other sites identified as LOFRECO). Furthermore, the plans for each proposed project are currently considered to be either "conceptual" in nature or more defined and certain ("site-specific"). The site-specific projects are the Rainbow site for Enercor-Mono Power, Magic Circle, Paraho, Syntana-Utah, and Tosco. The conceptual projects include the PR Springs site for Enercor-Mono Power, Geokinetics (all sites), and Sohio.

Information was submitted by all seven project applicants for use in estimating the direct emissions* from each facility. We reviewed the materials submitted by the applicants to ensure that the estimates were reasonable, thorough, and accurate; in some cases, we requested additional information. Our review focused primarily on the following emission-related areas:

---

* All "secondary growth" emissions are considered to be area sources and are discussed later.

> Process description

> Emission factors

> Activity data

> Anticipated control technology

> Stack parameters.

The data from each applicant formed the initial basis of each project's emission estimates. Inventories for each project were constructed for both high and low levels of production. In certain instances, engineering judgment was used to complete the inventories for the synfuel projects. In addition, because of the large number of emission points at some projects, we consolidated the smaller emission rates into fewer emission points for the regional modeling cases in which this activity was technically justified; this effort reduced the complexity and cost of the regional modeling activities. In the case of near-source modeling, each emission point at a project was located by means of UTM coordinates, and stack data were developed for each point. The reader is referred to the project descriptions and numerous supporting documentation for further elaboration on the derivation of the basic emission estimates.

Tables 4-1 and 4-2 provide the production rates and direct emission totals for each of the Utah synfuel projects at the high and low levels of oil shale and tar sands production. As shown in these two tables, emission rates vary considerably from one project to another. This variation is due to several aspects of the proposed projects including process design, production rate, and emission control technology design. For example, Geokinetics proposes to employ an in-situ oil shale extraction process, unlike the other Utah projects which are above ground processes. Furthermore, Geokinetics is in an early stage of design; future designs may alter emission rates considerably from those presented in the tables. Similarly, emission levels for Sohio are quite different between the high and low oil production scenarios. This variation results from different assumed fuels and levels of control for steam generation at the Sohio tar sands facility.

Furthermore, the concept of "normalizing" emission estimates for the same pollutant to an equivalent barrel per day production rate is an overly simplistic approach to assessing source emissions and controls. For example, even for a process type which is well known and well documented, uncontrolled emission factors for fluid catalytic cracking units (from the EPA report known as AP-42) vary substantially for NO_x (37 to 145), SO_2 (100 to 525), and particulate (93 to 340) in units of pounds

TABLE 4-1. PRODUCTION AND EMISSION RATES FOR UTAH SYNFUEL PROJECTS--HIGH-OIL-PRODUCTION SCENARIO

		Emissions (kilograms per hour)*				
Project	Oil Production (barrels/day)	Sulfur Dioxide	Particulate Matter	Nitrogen Oxides†	Total Hydrocarbon	Carbon Monoxide
Enercor-Mono Power	55,000	111	233	123	38	33
Geokinetics	70,000	1799	159	744	40	22
Magic Circle	31,500	147	107	823	4	53
Paraho	42,000	182	97	482	14	72
Sohio	20,000	373	644	327	88	29
Syntana-Utah	57,000	128	129	746	81	64
Tosco	45,000	94	127	786	183	9
Total	320,500	2834	1496	4031	448	282

---

* 1 kg/hr = 9.66 tons/year.

† NO_x emissions expressed as NO_2.

TABLE 4-2. PRODUCTION AND EMISSION RATES FOR UTAH SYNFUEL PROJECTS--LOW-OIL-PRODUCTION SCENARIO

		Emissions (kilograms per hour)[*]				
Project	Oil Production (barrels/day)	Sulfur Dioxide	Particulate Matter	Nitrogen Oxides[†]	Total Hydrocarbon	Carbon Monoxide
Enercor-Mono Power	20,000	40	79	45	13	12
Geokinetics	31,000	764	71	331	18	12
Magic Circle	16,400	73	51	420	2	33
Paraho	10,500	45	54	105	3	21
Sohio	5,000	1	136	25	22	16
Syntana-Utah	16,500	40	38	230	18	19
Tosco	22,000	46	62	385	90	4
Total	121,400	1009	491	1541	166	117

---

[*] 1 kg/hr = 9.66 tons/year.

[†] NO_x emissions expressed as NO_2.

of pollutant per thousand barrels. Moreover, the range in emission factors becomes even greater when different types of catalytic crackers are considered (such as fluid vs. moving-bed).

In addition, emission controls introduce a multiplicative effect on the range in emission factors. Each project applicant proposes different types of control with varying levels of reduction. Such differences often result from the fact that some controls are not applicable to certain processes. These varying control levels are acceptable to regulatory agencies as best available control technology (BACT) because the definition of BACT inherently permits a tailoring of control technology (and the conversion efficiencies resulting from such equipment) to an individual source. Fuel sulfur and nitrogen levels also vary in the fuel burned in heaters and boilers, which affects emissions on a per unit of production basis. Thus, because processes and controls are unique, emission rates will differ for sources employing alternative equipment.

4.1.2 Other Planned Projects (Utah)

Future point sources other than the seven Utah synfuel facilities were included in the emission estimates for Uintah and Grand counties in Utah. Eight other planned projects had significant emission rates; of these, three were estimated to account for the majority of total emissions from other planned projects in Utah:

> Moon Lake power plant unit 2

> Plateau refinery expansion

> White River oil shale project.

Emissions and stack parameters for the eight other planned projects were developed from information regarding each facility's source type, operating process, activity data, and proposed controls. In some cases, the conceptual nature of a particular project required considerable judgment to estimate the emission rates. Emission totals for the larger facilities and for the other planned projects are listed in table 4-3.

4.1.3 Utah Baseline Point Sources

Emissions for existing point sources with significant emission rates were developed from available data. We first reviewed the state of Utah emission files for Utah counties within the grid region (primarily Uintah and Grand counties). Although several sources were identified by the

TABLE 4-3. EMISSION TOTALS FOR OTHER PLANNED PROJECTS IN UTAH

(kilograms per hour)

Project	Sulfur Dioxide	Particulate Matter	Nitrogen Oxides*	Total Hydrocarbon	Carbon Monoxide
Moon Lake unit 2	95	55	1012	0	0
Plateau expansion	29	44	58	245	67
White River	136	197	827	165	381
5 additional projects	195	80	99	93	6
Total	455	376	1996	503	454

---

* NO_x emissions expressed as NO_2.

state, only one was considered to be significant for this study; the others were assumed to be covered adequately by the procedures used to derive the area source files.* In addition, we reviewed the National Emission Data System files, which listed only one or two point sources in the two primary Utah counties.

As a result of these reviews, two point sources were identified for the Utah baseline point source file:

> Moon Lake power plant unit 1

> Plateau refinery.

The first power plant unit for the Moon Lake facility was placed in the existing point source file because construction of this facility has begun. The existing Plateau refinery located in Duchesne County was also included because of its relatively significant emissions. Emission and stack data for the Moon Lake power plant were taken from the EPA Prevention of Significant Deterioration permit, whereas comparable data for the existing Plateau facility were derived from the 1980 state of Utah data.

Table 4-4 lists the emission data for these two facilities. Note that total future emission rates for each of these sources can be estimated by summing the emission rates provided in tables 4-3 and 4-4 for the Moon Lake and Plateau facilities.

4.1.4 Colorado Oil Shale, Point, and Area Sources

In another effort conducted by PEDCo Environmental, Inc. for the National Park Service (PEDCo, 1981), emission estimates were developed for existing and future point and area sources located in northwestern Colorado. The region included the Colorado counties of Moffat, Rio Blanco, Garfield, and Mesa. These Colorado emission estimates were used in the modeling portion of this Systems Applications study.

Colorado oil shale project emissions were developed by PEDCo for specific production rates in 1990 and 2000. These production rates correspond to the low- and high-oil-production regional scenarios developed for this study. This approach resulted in the estimation of emissions, including secondary growth, for five scenarios:

---

[*] Also, computerized versions of Utah point source emissions were not readily available.

TABLE 4-4. EMISSION TOTALS FOR BASELINE POINT SOURCES IN UTAH

(kilograms per hour)

Source	Sulfur Dioxide	Particulate Matter	Nitrogen Oxides*	Total Hydrocarbon	Carbon Monoxide
Moon Lake unit 1	95	55	1012	0	0
Plateau refinery	4	6	432	291	62
Total	99	61	1444	291	62

---

* NO_x emissions expressed as NO_2.

> 1980 baseline

> 1990 without oil shale

> 1990 with oil shale

> 2000 without oil shale

> 2000 with oil shale.

Tables 4-5 and 4-6 provide the emission totals estimated by PEDCo for point and area sources in the four Colorado counties in the study region.

4.1.5 Utah Baseline Area Sources

Available emission inventory data for existing area sources in eastern Utah were very limited. Consequently, it was necessary to develop this information from the available data concerning area source activities. The inventory was first divided into 47 area source categories shown in table 4-7. Appropriate activity data such as fuel use and traffic counts were then obtained from several information sources. These data were combined with most of the same emission factors used by PEDCo for Colorado area sources. Allocation factors were finally used to assign emissions from each category to specific 10-km x 10-km (100 km^2) grid cells. The result was a set of emission inventories by source category for each of the two primary Utah counties in the study region--Uintah and Grand. The inventories are generally representative of baseline conditions for the year 1980.

4.1.5.1 Emission Factors

In order to make the Utah area source emission inventory consistent with the Colorado inventory, it was decided to use the majority of emission factors that PEDCo (1981) used to derive the 1980 baseline inventory for four Colorado counties. Our review of these emission factors led us to conclude that they were generally in agreement with those reported in the most recent revisions of the "AP-42" data base (EPA, 1981). In some cases these factors were derived from standard methods prescribed by the EPA (1980). Table 4-8 presents the emission factors used to develop the Utah area source inventories for the following primary pollutants:

TABLE 4-5. EMISSION TOTALS FOR COLORADO OIL SHALE PROJECTS*

(a) Low-Oil-Production Scenario

Project	Oil Production (barrels/day)	Emissions (kilograms per hour)				
		Sulfur Dioxide	Particulate Matter	Nitrogen Oxides	Total Hydrocarbon	Carbon Monoxide
Colony	47,000	128	239	878	158	28
Union	50,000	336	235	885	360	370
Cathedral Bluffs	94,000	851	363	3482	45	1214
Chevron	15,000	101	70	265	108	111
Rio Blanco	50,000	51	141	420	20	190
Superior	15,000	157	36	78	32	17
Total	271,000	1624	1084	6008	723	1930

TABLE 4-5 (Concluded)

(b) High-Oil-Production Scenario

Project	Oil Production (barrels/day)	Emissions (kilograms per hour) Sulfur Dioxide	Particulate Matter	Nitrogen Oxides	Total Hydrocarbon	Carbon Monoxide
Colony	47,000	128	239	878	158	28
Union	50,000	336	235	885	360	370
Cathedral Bluffs	94,000	851	363	3482	45	1214
Chevron	100,000	672	469	1770	719	740
Rio Blanco	86,000	88	243	723	34	296
Mobil	50,000	336	235	885	360	370
Exxon	47,000	128	239	878	158	28
Superior	15,000	157	36	78	32	17
Getty	50,000	336	235	885	360	370
Multimineral	50,000	336	235	885	360	370
Naval Oil Shale	50,000	50	208	511	10	56
Total	639,000	3418	2737	11,860	2596	3859

---

* Direct project emissions only. These values differ from those in the draft report as a result of revised numbers in the Pedco report.

TABLE 4-6. EMISSION TOTALS FOR NON-OIL SHALE SOURCES IN COLORADO[*]

(kilograms per hour)

Scenario	Sulfur Dioxide	Particulate Matter	Nitrogen Oxides	Total Hydrocarbon	Carbon Monoxide
1--1980 baseline	947	14,130	2328	1194	9354
2--1990 without oil shale	1987	16,267	4441	936	5678
3--1990 with oil shale[†]	2036	20,843	4851	1225	7915
4--2000 without oil shale	2002	17,118	4404	922	5174
5--2000 with oil shale[†]	2065	23,356	4831	1242	7252

---

[*] These values differ from those in the draft report as a result of revised numbers in the Pedco report.

[†] These emission totals exclude direct oil shale project emissions (table 4-5), but include secondary growth associated with oil shale development.

TABLE 4-7. AREA SOURCE CATEGORIZATION SCHEME

- Petroleum marketing and transport
  - Truck unloading
  - Underground storage
  - Auto tank filling

- Organic solvent usage
  - Surface coating
  - Petroleum drycleaning
  - Perchloroethylene drycleaning
  - Degreasing
    - 1,1,1-trichloroethane
    - Trichloroethane
  - Graphic arts
  - Miscellaneous solvent usage

- Pesticide usage

- Fuel combustion
  - Industrial
    - Distillate oil
    - Residual oil
    - LPG
    - Natural gas

  - Commercial and institutional
    - Coal
    - Distillate oil
    - Residual oil
    - LPG
    - Natural gas

  - Residential
    - Coal
    - Distillate oil
    - LPG
    - Wood
    - Natural gas

TABLE 4-7 (Concluded)

Agricultural waste burning

Wildfires

- Construction
  - Residential
  - Commercial
  - Public and institutional
  - Roads

Agricultural wind erosion

Tilling

- Off-road mobile sources
  - Gasoline farm tractors
  - Diesel farm tractors
  - Construction equipment (diesel)
  - Other gasoline usage
  - Other diesel usage
  - Piston aircraft
  - Jet aircraft
  - Railroads

- On-road motor vehicles (exhaust)
  - State highways
  - County roads
  - Class "D" roads

- On-road motor vehicles (fugitive dust)
  - State highways (paved)
  - County roads (paved)
  - Class "D" roads (unpaved)

TABLE 4-8. EMISSION FACTORS FOR 1980 BASELINE

Source Category	Hydrocarbons		NO$_x$	SO$_2$	Particulate Matter	CO	Unit
	Reactive	Nonreactive					
Petroleum marketing and transport							
Truck unloading	7.3						lb/10^3 gal
Underground storage	1.0						lb/10^3 gal
Auto tank filling	9.7						lb/10^3 gal
Organic solvent usage							
Surface coating	6.5						lb/capita
Petroleum drycleaning	0.36						lb/capita
Perchloroethylene drycleaning	1.14						lb/capita
Degreasing							
1,1,1-trichloroethane		1.0					lb/capita
Trichloroethane	3.0						lb/capita
Graphic arts	0.8						lb/capita
Miscellaneous solvent usage	6.3						lb/capita
Pesticide usage	2.0						lb/acre
Fuel combustion							
Industrial							
Distillate oil		1.0	22.0	36.0	2.0	5.0	lb/10^3 gal
Residual oil		1.0	60.0	143.1	11.6	5.0	lb/10^3 gal
LPG		0.3	11.2	0.014	1.7	1.5	lb/10^3 gal
Natural gas		3.0	175.0	0.6	10.0	17.0	lb/10^6 ft^3
Commercial and institutional							
Coal	0.005	3.0	6.0	22.8	16.0	10.0	lb/ton
Distillate oil		1.0	22.0	36.0	2.0	5.0	lb/10^3 gal
Residual oil		1.0	60.0	143.1	11.6	5.0	lb/10^3 gal
LPG		0.7	11.0	0.014	1.8	1.9	lb/10^3 gal
Natural gas		8.0	120.0	0.6	10.0	20.0	lb/10^6 ft^3

TABLE 4-8 (Continued)

Source Category	Hydrocarbons Reactive	Hydrocarbons Nonreactive	NO_x	SO_2	Particulate Matter	CO	Unit
Residential							
Coal	0.005	20.0	3.0	22.8	20.0	90.0	lb/ton
Distillate oil		1.0	18.0	36.0	2.5	5.0	lb/10^3 gal
LPG		0.7	7.0	0.014	1.8	1.9	lb/10^3 gal
Wood	5.0		1.0		20.0	120.0	lb/ton
Natural gas		8.0	80.0	0.6	10.0	20.0	lb/10^6 ft^3
Agricultural waste burning	10.52				9.1	53.82	10^{-4} tons/(acre-year
Wildfires		11.90	1.98		8.43	69.44	Tons/(acre-year)
Construction							
Residential					1.2		Tons/(acre-month)
Commercial					1.2		Tons/(acre-month)
Public and institutional					1.2		Tons/(acre-month)
Roads					1.2		Tons/(acre-month)
Agricultural wind erosion					0.12		Tons/(acre-year)
Tilling (Grand/Uintah)					0.28/0.21		Tons/(acre-year)
Off-road mobile sources							
Gasoline farm tractors	6.84	184.5	151.0	5.31	8.0	32.60	lb/10^3 gal
Diesel farm tractors	12.1	60.7	335.0	31.2	45.7	119.0	lb/10^3 gal
Construction equipment (diesel)	6.77	29.08	407.1	31.15	26.14	95.24	lb/10^3 gal
Other gasoline usage	6.5	210.5	68.8	5.4	6.11	34.63	lb/10^3 gal
Other diesel usage	7.04	37.5	469.0	31.2	33.5	102.0	lb/10^3 gal
Piston aircraft	0.85		0.05			38.01	lb/LTO
Jet aircraft	7.38		11.99	1.36	6.20	37.08	lb/LTO
Railroads	12.5	94.0	370.0	57.0	25.0	130.0	lb/10^3 gal

TABLE 4-8 (Concluded)

Source Category	Hydrocarbons Reactive	Hydrocarbons Nonreactive	NO_x	SO_2	Particulate Matter	CO	Unit
On-road motor vehicles (exhaust)							
State highways	3.18		3.73	0.23	0.44	37.22	gm/km
County roads	4.07		2.85	0.21	0.43	49.47	gm/km
Class "D" roads	5.73		1.29	0.11	0.34	64.82	gm/km
On-road motor vehicles (fugitive dust)							
State highways (paved)					3.2		gm/km
County roads (paved)					3.2		gm/km
Class "D" roads (unpaved)					453.6		gm/km

- Reactive hydrocabons (RHC)
- Unreactive hydrocarbons (URHC)
- Oxides of nitrogen (NO_x)
- Sulfur dioxide (SO_2)
- Particulate matter (TSP)
- Carbon monoxide (CO).

Major differences from the PEDCo emission factors include the following:

- The approach prescribed in AP-42 was used to compute the emission factors for wildfires. These factors were different from those for Colorado due to different field loading factors, that is, tons of combustible material per unit land.

- An emission factor of 1.20 tons per acre per month was used for TSP from construction activity.

- The wind erosion emissions are crop-specific. The emission factor for corn, as given in AP-42, was used because for eastern Utah, corn is the major crop for which there are wind erosion emissions.

- For tilling operations, the emission factors were calculated by using appropriate soil silt content values in AP-42. These factors were different for Uintah and Grand counties.

- For some source categories [notably agricultural waste burning, on-road motor vehicles (exhaust), and aircraft], the activity data available to us were not finely divided into subcategories; therefore, some aggregation of emission factors was warranted to make them compatible with the activity data.

- The hydrocarbon emissions from on-road motor vehicles were further delineated into reactive and unreactive classes by assuming that the former constituted 90 percent of the total hydrocarbons, and the latter, the remaining 10 percent.

The fugitive dust emission factors for state highways and county roads were directly derived from AP-42 emission factors. Note that these factors do not include any tire wear, which has already been accounted for in the exhaust emission factors. The fugitive dust emission factors for class "D" roads were not directly available, however. Because of the condition of these unpaved roads, identified as class "D" by the state of Utah, their average vehicle speed is low. These roads are unimproved and are often simply tracks with sagebrush covering the middle of the path. They are best described as "primitive or less" (UDOT, 1982). For these reasons, after consulting with the Utah Department of Transportation, we assumed that the average travel speed on these roads ranges between 15 to 25 miles per hour. It was not possible to use the approach recommended in supplement 8 of AP-42 because its application is restricted to speeds above 30 miles per hour. Likewise, the county-specific emission factors provided in PEDCo (1981) for three types of unpaved roads could not be used because the speeds associated with these road types were outside the range appropriate for class "D" roads. Large variabilities in the Colorado emission factors ruled out a simple averaging process. In the absence of any better information, we assumed a particulate matter emission factor of 1 lb/km. This factor is slightly higher than that for gravel urban roads and significantly lower than that for gravel rural roads as provided in PEDCo (1981). The average speed that we have assumed for class "D" roads is in general agreement with the assumed fugitive dust emission factor.

4.1.5.2 Activity Data

For the purpose of this discussion, area sources are divided into the following classes:

> Stationary sources

> Off-road mobile sources

> On-road motor vehicles.

4.1.5.2.1 Stationary sources

Gasoline consumption figures for the base year were available in thousands of gallons for Uintah and Grand counties (NPS, 1982). These were employed to estimate the emissions from petroleum marketing and transport-related categories.

Emissions due to organic solvent usage were derived from the total population of each county. The population data were available from the NPS (1982).

The number of acres that underwent pesticide applications was available from the Census of Agriculture (DOC, 1981). These acres were exposed to pesticide applications of sprays, dusts, granules, and fumigants. Hydrocarbon emissions are primarily due to the application of liquid pesticides, but no information was available to identify the acres that experienced the application of liquid pesticides only; thus, our emission estimates may be somewhat conservative.

The state totals of fuel oil, liquid petroleum gas (LPG), and natural gas consumed by industrial sources were available from the Energy Data Reports (DOE, 1981). Use of these fuels was apportioned to each county on the basis of the population of employees involved in manufacturing. Similar fuel consumption figures were available for coal, fuel oil, and natural gas for commercial and residential sources. The population and the number of dwelling units were used to apportion the state totals to each county for commercial and institutional, and residential sources, respectively. The total gallons of LPG consumed by residential and commercial sources were not further disaggregated into each category in the Energy Data Reports. Thus, we assumed that the ratio of LPG consumed by residential sources to LPG consumed by commercial sources was equal to the similar ratio for distillate fuel oil for each county. On the basis of the PEDCo report, residential wood consumption was estimated by assuming that 48 percent of the dwelling units had fireplaces, each burning 2.8 tons of wood every year.

The agricultural waste burning emissions were based on total cropland acres available from ORNL (1982).

The ratios of the area of forested land burned in wildfires nationwide to the total forested area were averaged over five years (1975-1979). This average was then multiplied by the total forested area to obtain the area of wildfires for each county. The total forested areas were estimated from Geological Survey topographic maps.

The construction-related TSP emissions were estimated by assuming that

> Each residential construction project disturbed 0.20 acres of land for 3 months.

> Each commercial, public, and institutional project disturbed the land for six months.

> The average road width was 20 feet and the construction duration was eight months.

The NPS (1982) provided us with the number of housing units constructed, acres of commercial construction, acres of public and institutional construction, and miles of new roads constructed for each county.

The total number of agricultural acres (DOC, 1981) was employed to estimate the emissions caused by wind erosion and tilling. This included agricultural land used for the production of corn, sorghum, hay, wheat, oats, barley, and seed crops.

4.1.5.2.2 Off-road mobile sources

The sources included in this category are

> Gasoline and diesel farm tractors

> Construction equipment (diesel)

> Other gasoline and diesel usage

> Aircraft

> Railroads.

The total number of wheel tractors and self-propelled grain and bean combines was obtained from published data on agricultural activity in the state of Utah (DOC, 1981). It was assumed that 60 percent of this equipment was gasoline-powered and 35 percent was diesel-powered and that each tractor consumed 1000 gallons of fuel every year. Emissions were scaled up to account for the remaining 5 percent of the population.

The employment figures for non-building construction employees (DOC, 1980) were used as an index of diesel construction equipment activity. It was assumed that 5000 gallons of diesel were consumed per employee per year.

Other gasoline and diesel usage was based on the assumption that 13 gallons of gasoline and 7.4 gallons of diesel were consumed annually per person. County population counts were available for this purpose from the NPS (1982).

Our review showed that there are only two airports of significance in eastern Utah. Both of these airports, Vernal and Roosevelt, are relatively small. We were unable to obtain any landing and takeoff figures from airport authorities and airlines operating at the Vernal airport. However, these estimates were available in a Uinta Basin transportation study performed for the Utah Department of Transportation (VanWagoner, 1980). All local flights were assumed to be general aviation and were attributed to piston engine planes. Similarly, all itinerant flights were assumed to be commercial and were ascribed to jet planes.

No information was available to compute the emissions due to railroad operations in Grand County (no major railroads exist in Uintah County). Emission rates for Grand County were obtained by scaling railroad emission estimates for the adjoining Mesa County using the ratio of the approximate lengths of rail in each of these counties.

4.1.5.2.3 On-road motor vehicles

Link-specific annual-average daily traffic (AADT) volumes were available from the Utah Department of Transportation (UDOT, 1979) for state highways. With the help of road and topographic maps, these data were used to generate total vehicle kilometers travelled (VKMT). However, no specific traffic counts were available for county roads or class "D" roads. At the recommendation of the Utah Department of Transportation (UDOT, 1982), we used an AADT of 150 for county roads and 50 for class "D" roads. Road lengths were then estimated from general highway maps with the class "D" road system. Total VKMT were computed from these AADT volumes and road length data. Urban VKMT totals, exclusive of state highways, county roads, and class "D" roads, were also available for the cities of Vernal and Moab. These were added to VKMT for county roads.

4.1.5.3 Spatial Allocation Parameters

The emission totals by source category were spatially distributed to obtain gridded area source inventories for each county. This was accomplished by assigning an allocation parameter to each source category. Sufficient information was available to distribute these parameters over 10 x 10-km grid cells. Thus, the emission rate from a particular source category in a particular cell was obtained from

$$e = \frac{Ep}{P} ,$$

where e is the emission rate for a grid cell, E is the emission rate for the entire county, p is the value of the allocation parameter in that grid cell, and P, its value over the entire county. Table 4-9 presents the source category to allocation parameter relationships.

Population distributions were derived from the 1980 census data provided to us by the state of Utah. The population totals were allocated into appropriate grid cells by using the U.S. Bureau of Census population mappings that identify detailed population locations derived from the 1980 census.

The spatial distribution of land receiving pesticide applications was assumed to be the same as the distribution of cropland and pastures. For Uintah County, available land cover and land use maps were utilized to estimate the distribution of cropland and pastures. No such maps were available for Grand County; however, it was therefore assumed that the land not managed by any of the following agencies was potential farmland:

> Bureau of Land Management

> National Park Service

> U.S. Forest Service

> Fish and Wildlife Service.

Wilderness status maps from the state of Utah were used to determine the spatial distribution of potential farm land in Grand County. This distribution, in turn, was assumed to be an acceptable representation of the distribution of land that experienced pesticide applications. Also, this methodology was employed to spatially distribute tilled acres.

Ashley National Forest in Uintah County and Manti La Sal National Forest in Grand County were identified as the major U.S. Forest Service-administered forested areas. The Geological Survey topographic maps were used to allocate the Forest Service-administered areas, as well as other forested areas, to appropriate grid cells.

The exact locations of airports were used to grid aircraft emissions. Railroad emissions were gridded by the approximate railroad length in each grid cell.

Because gridded motor vehicle emissions were unavailable, a major effort in this study was the determination of spatially resolved exhaust and fugitive dust emissions from on-road motor vehicles. U.S. Geological Survey topographic maps and the Utah Department of Transportation general highway maps were employed to measure the road lengths in each grid cell. Such measurements were made for all three types of roads. For the

TABLE 4-9. AREA SOURCE SPATIAL ALLOCATION PARAMETERS

Source Category	Allocation Parameter
Petroleum marketing and transport	Population
Organic solvent usage	Population
Pesticide usage	Acres with pesticide application
Fuel combustion	
Industrial	Population
Commercial and institutional	Population
Residential	Population
Agricultural waste burning	Tilled acres
Wildfires	Forested acres
Construction	Population
Agricultural wind erosion	Tilled acres
Tilling	Tilled acres
Off-road mobile sources	
Gasoline farm tractors	Tilled acres
Diesel farm tractors	Tilled acres
Construction equipment (diesel)	Population
Other gasoline usage	Population
Other diesel usage	Population
Piston aircraft	Airport locations
Jet aircraft	Airport locations
Railroads	Rail locations
On-road motor vehicles (exhaust)	Vehicle kilometers travelled (by road type)
On-road motor vehicles (fugitive dust)	Vehicle kilometers travelled (by road type)

major highways, these road lengths were multiplied by the appropriate link-specific AADT (UDOT, 1979) to obtain the total VKMT in each grid cell. The AADT estimates discussed in section 4.1.5.2.3 were used for county and class "D" roads. Thus, the spatial allocation of emissions from on-road motor vehicles was an integral part of the determination of total motor vehicle emissions.

4.1.5.4 Results

Tables 4-10 and 4-11 show emissions by source category for Uintah and Grand counties for all six pollutants. These inventories are generally representative of 1980 conditions. Gridded emission totals for the entire study region are presented in figure 4-3 for grid cells with significant emission rates. Clear plastic overlays showing geographical features are provided inside the cover of this report so that the reader can find the locations of area source emissions.

4.1.6 Utah Area Sources: Regional High-Oil-Production Scenario

Gridded emission inventories were prepared for the year 1990 assuming a high level of oil production in the Uinta Basin. These emission rates were obtained by projecting 1980 baseline emissions for all 47 area source categories. Emission factors were reviewed and revised where necessary. As described below, growth factors were derived from projected socioeconomic data for the future scenario. Pollutants were then spatially distributed on the basis of future-year socioeconomic data.

4.1.6.1 Emission Factors

Emission factors given in Table 4-8 were used for all source categories except on-road motor vehicles (exhaust). The emission factors for these categories were available for 1990 from PEDCo (1981) and are given in table 4-12. As in the baseline case, 90 percent of the total hydrocarbons were assumed to be reactive.

4.1.6.2 Activity Projections

Each emission source category was related to an activity parameter based on socioeconomic information (illustrated in table 4-13) . Such socioeconomic data were available from the NPS (1982) for the high-oil-production scenario as well as for the 1980 baseline. Some of the source categories for which information was sparse are discussed below.

TABLE 4-10. 1980 BASELINE AREA SOURCE EMISSION INVENTORY FOR UINTAH COUNTY

				(tons per year)			
SOURCE	CATEGORY	RHC	URHC	NOX	SO2	TSP	CO
10	Petroleum - Truck unloading	21.66	0.00	0.00	0.00	0.00	0.00
20	Petroleum - Underground storage	17.77	0.00	0.00	0.00	0.00	0.00
30	Petroleum - Auto tank filling	28.75	0.00	0.00	0.00	0.00	0.00
40	Surface coating	66.57	0.00	0.00	0.00	0.00	0.00
50	Petroleum drycleaning	3.70	0.00	0.00	0.00	0.00	0.00
60	Perchloroethylene drycleaning	11.67	0.00	0.00	0.00	0.00	0.00
70	1,1,1-trichloroethane degreasing	0.00	10.22	0.00	0.00	0.00	0.00
80	Trichloroethane degreasing	30.74	0.00	0.00	0.00	0.00	0.00
90	Graphic arts	8.20	0.00	0.00	0.00	0.00	0.00
100	Miscellaneous solvent usage	64.65	0.00	0.00	0.00	0.00	0.00
110	Pesticide usage	22.33	0.00	0.00	0.00	0.00	0.00
120	Ind. distillate oil combustion	0.00	0.07	1.96	3.18	0.12	0.40
130	Ind. residual oil combustion	0.00	0.07	6.90	16.43	1.32	0.56
140	Ind. LPG combustion	0.00	0.00	0.09	0.00	0.00	0.00
150	Ind. natural gas combustion	0.00	0.20	15.18	0.02	0.85	1.48
160	Comm. & Inst. coal combustion	0.02	17.73	35.51	134.89	94.60	59.15
170	Comm. & Inst. distillate oil combustion	0.00	0.20	5.43	8.87	0.46	1.20
180	Comm. & Inst. residual oil combustion	0.00	0.12	11.37	27.08	2.17	0.94
190	Comm. & Inst. LPG combustion	0.00	0.02	0.67	0.00	0.07	0.07
200	Comm. & Inst. natural gas combustion	0.00	1.10	16.34	0.06	1.30	2.74
210	Res. coal combustion	0.00	19.57	2.92	22.32	19.57	88.08
220	Res. distillate oil combustion	0.00	0.03	1.17	2.35	0.11	0.30
230	Res. LPG combustion	0.00	0.02	0.31	0.00	0.07	0.07
240	Res. wood combustion	18.76	0.00	3.72	0.00	74.91	449.93
250	Res. natural gas combustion	0.00	3.27	32.63	0.19	4.08	8.18
260	Agricultural waste burning	27.80	0.00	0.00	0.00	24.00	142.30
270	Wildfires	0.00	91.14	13.95	0.00	63.86	530.10
280	Res. construction	0.00	0.00	0.00	0.00	483.11	0.00
290	Comm. construction	0.00	0.00	0.00	0.00	57.54	0.00
300	Public & Inst. construction	0.00	0.00	0.00	0.00	107.98	0.00
310	Road construction	0.00	0.00	0.00	0.00	139.56	0.00
320	Agricultural wind erosion	0.00	0.00	0.00	0.00	488.00	0.00
330	Tilling	0.00	0.00	0.00	0.00	566.40	0.00
340	Gasoline farm tractors	1.90	51.05	41.80	1.45	2.20	9.00
350	Diesel farm tractors	1.95	9.80	54.15	5.05	7.40	19.25
360	Construction equipment (diesel)	3.29	14.31	200.55	15.31	12.87	46.93
370	Other gasoline usage	0.85	28.05	9.15	0.70	0.82	4.63
380	Other diesel usage	0.54	2.88	35.58	2.36	2.52	7.78
390	Piston aircraft	3.25	0.00	0.19	0.00	0.00	145.39
400	Jet aircraft	26.57	0.00	43.16	4.90	22.32	133.49
410	Railroads	0.00	0.00	0.00	0.00	0.00	0.00
420	Motor vehicle - State highways	840.34	93.37	1095.20	67.54	129.19	10928.43
430	Motor vehicle - County roads	450.16	50.02	350.21	25.84	52.83	6078.77
440	Motor vehicle - Class "D" roads	540.74	60.08	135.29	11.51	35.60	6796.36
450	Motor vehicle - State highways (fug. dust)	0.00	0.00	0.00	0.00	939.57	0.00
460	Motor vehicle - County roads (fug. dust)	0.00	0.00	0.00	0.00	393.12	0.00
470	Motor vehicle - Class "D" roads (fug. dust)	0.00	0.00	0.00	0.00	47549.62	0.00
---	TOTAL	2192.18	453.31	2113.40	350.04	51277.16	25455.34

TABLE 4-11. 1980 BASELINE AREA SOURCE EMISSION INVENTORY FOR GRAND COUNTY

(tons per year)

SOURCE	CATEGORY	RHC	URHC	NOX	SO2	TSP	CO
10	Petroleum - Truck unloading	43.97	0.00	0.00	0.00	0.00	0.00
20	Petroleum - Underground storage	6.01	0.00	0.00	0.00	0.00	0.00
30	Petroleum - Auto tank filling	58.66	0.00	0.00	0.00	0.00	0.00
40	Surface coating	26.77	0.00	0.00	0.00	0.00	0.00
50	Petroleum drycleaning	1.47	0.00	0.00	0.00	0.00	0.00
60	Perchloroethylene drycleaning	4.71	0.00	0.00	0.00	0.00	0.00
70	1,1,1-trichloroethane degreasing	0.00	4.09	0.00	0.00	0.00	0.00
80	Trichloroethane degreasing	12.32	0.00	0.00	0.00	0.00	0.00
90	Graphic arts	3.28	0.00	0.00	0.00	0.00	0.00
100	Miscellaneous solvent usage	25.96	0.00	0.00	0.00	0.00	0.00
110	Pesticide usage	0.84	0.00	0.00	0.00	0.00	0.00
120	Ind. distillate oil combustion	0.00	0.02	0.44	0.73	0.03	0.09
130	Ind. residual oil combustion	0.00	0.02	1.54	3.70	0.30	0.13
140	Ind. LPG combustion	0.00	0.00	0.02	0.00	0.00	0.00
150	Ind. natural gas combustion	0.00	0.05	3.42	0.00	0.18	0.32
160	Comm. & Inst. coal combustion	0.01	7.10	14.22	53.93	37.86	23.16
170	Comm. & Inst. distillate oil combustion	0.00	0.09	2.14	3.52	0.18	0.49
180	Comm. & Inst. residual oil combustion	0.00	0.08	4.56	10.83	0.86	0.38
190	Comm. & Inst. LPG combustion	0.00	0.01	0.20	0.00	0.03	0.03
200	Comm. & Inst. natural gas combustion	0.00	0.43	6.52	0.02	0.51	0.98
210	Res. coal combustion	0.00	8.98	1.24	10.24	8.99	40.45
220	Res. distillate oil combustion	0.00	0.02	0.52	1.06	0.07	0.14
230	Res. LPG combustion	0.00	0.01	0.13	0.00	0.02	0.02
240	Res. wood combustion	7.53	0.00	1.48	0.00	30.82	180.70
250	Res. natural gas combustion	0.00	1.48	14.98	0.10	1.85	3.70
260	Agricultural waste burning	17.43	0.00	0.00	0.00	14.98	89.11
270	Wildfires	0.00	109.82	17.86	0.00	77.90	650.18
280	Res. construction	0.00	0.00	0.00	0.00	193.71	0.00
290	Comm. construction	0.00	0.00	0.00	0.00	21.62	0.00
300	Public & Inst. construction	0.00	0.00	0.00	0.00	43.18	0.00
310	Road construction	0.00	0.00	0.00	0.00	43.18	0.00
320	Agricultural wind erosion	0.00	0.00	0.00	0.00	69.78	0.00
330	Tilling	0.00	0.00	0.00	0.00	748.93	0.00
340	Gasoline farm tractors	0.21	5.53	4.55	0.14	0.21	0.98
350	Diesel farm tractors	0.21	1.05	6.02	0.56	0.84	2.10
360	Construction equipment (diesel)	0.67	2.87	40.70	3.11	2.59	9.53
370	Other gasoline usage	0.34	11.26	3.66	0.29	0.32	1.84
380	Other diesel usage	0.20	1.14	14.33	0.94	1.00	3.10
390	Piston aircraft	0.00	0.00	0.00	0.00	0.00	0.00
400	Jet aircraft	0.00	0.00	0.00	0.00	0.00	0.00
410	Railroads	38.96	290.72	1144.86	175.83	76.92	401.61
420	Motor vehicle - State highways	575.67	63.96	750.29	46.25	88.51	7486.57
430	Motor vehicle - County roads	313.61	34.85	244.05	17.96	36.80	4235.21
440	Motor vehicle - Class "D" roads	136.64	15.18	34.22	2.96	9.04	1717.37
450	Motor vehicle - State highways (fug. dust)	0.00	0.00	0.00	0.00	643.65	0.00
460	Motor vehicle - County roads (fug. dust)	0.00	0.00	0.00	0.00	273.89	0.00
470	Motor vehicle - Class "D" roads (fug. dust)	0.00	0.00	0.00	0.00	12015.13	0.00
---	TOTAL	1275.45	558.75	2311.92	332.16	14435.99	14848.08

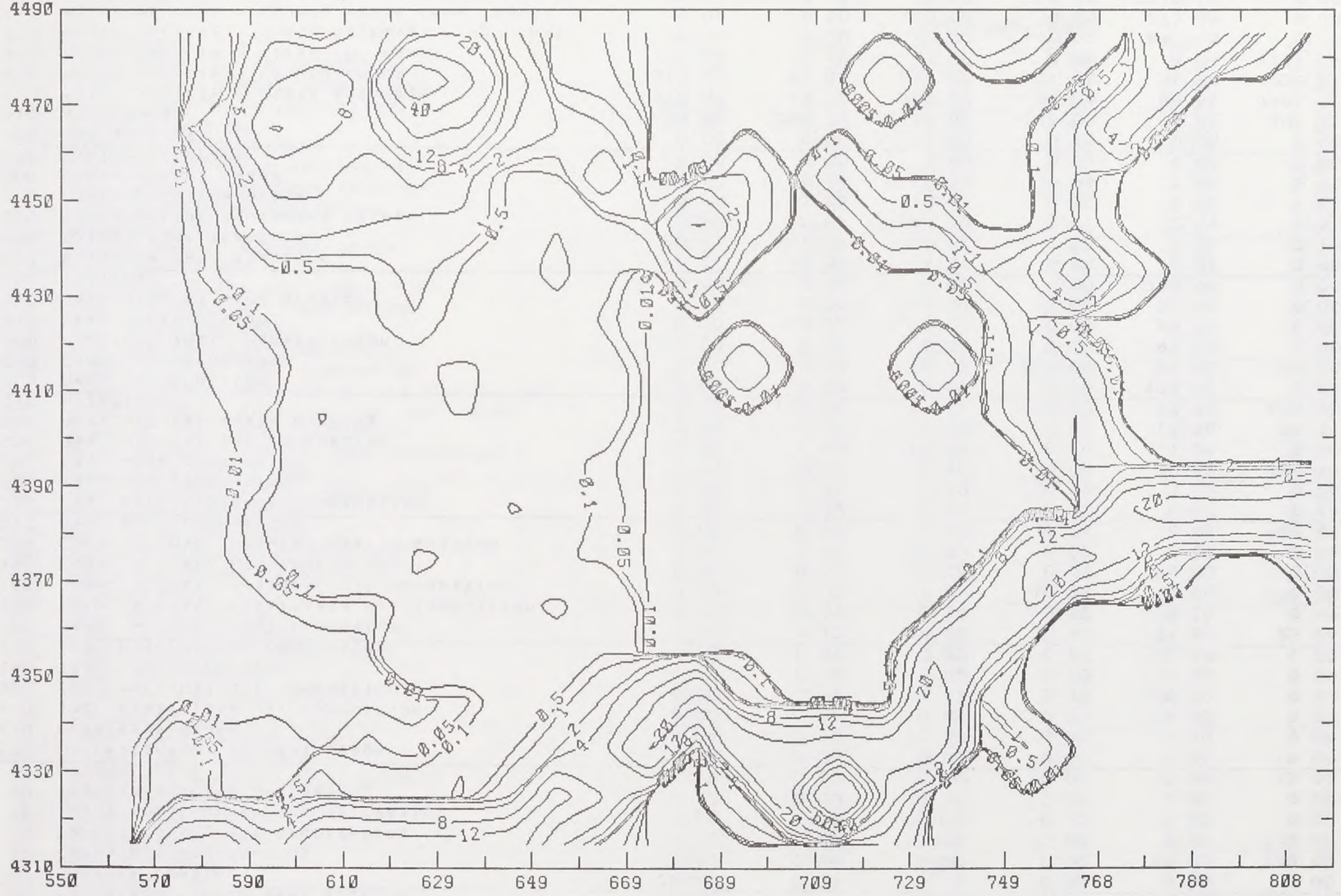

(a) SO_2

FIGURE 4-3. AREA EMISSION SOURCE INVENTORY FOR THE STUDY REGION IN THE BASELINE YEAR 1980 (tons/yr/100 km^2)

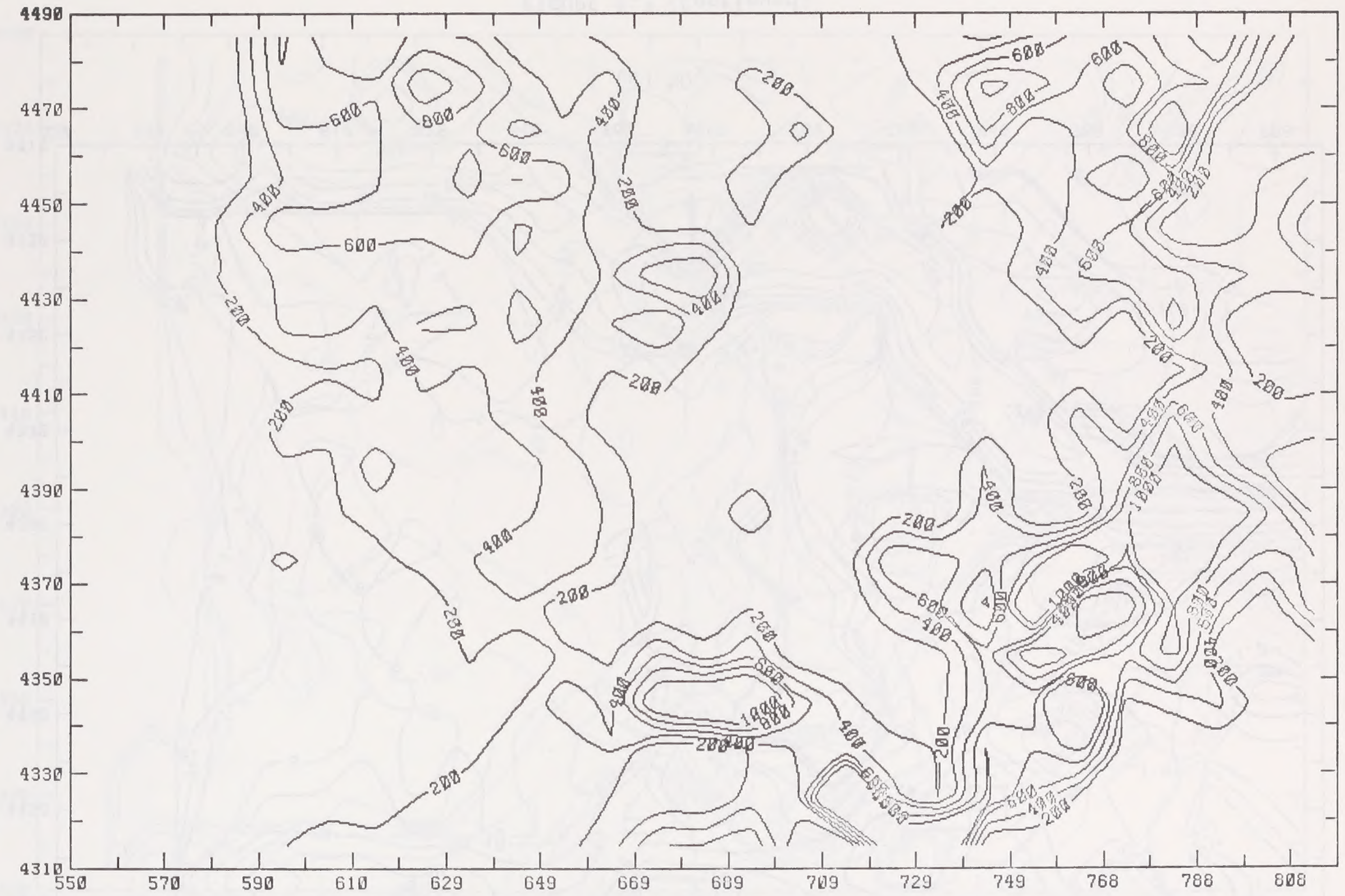

(b) TSP

FIGURE 4-3 (Continued)

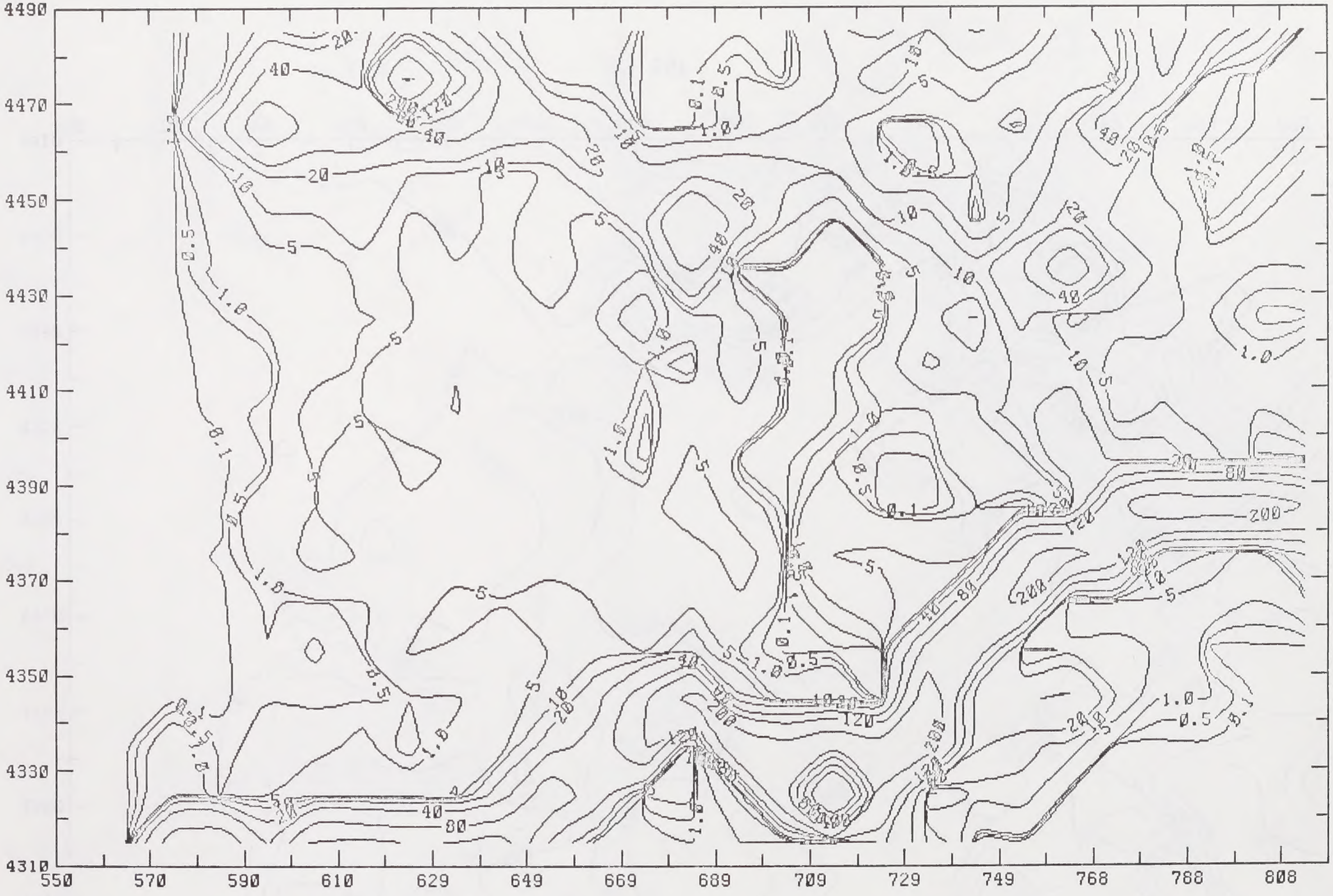

(c) NO_x

FIGURE 4-3 (Continued)

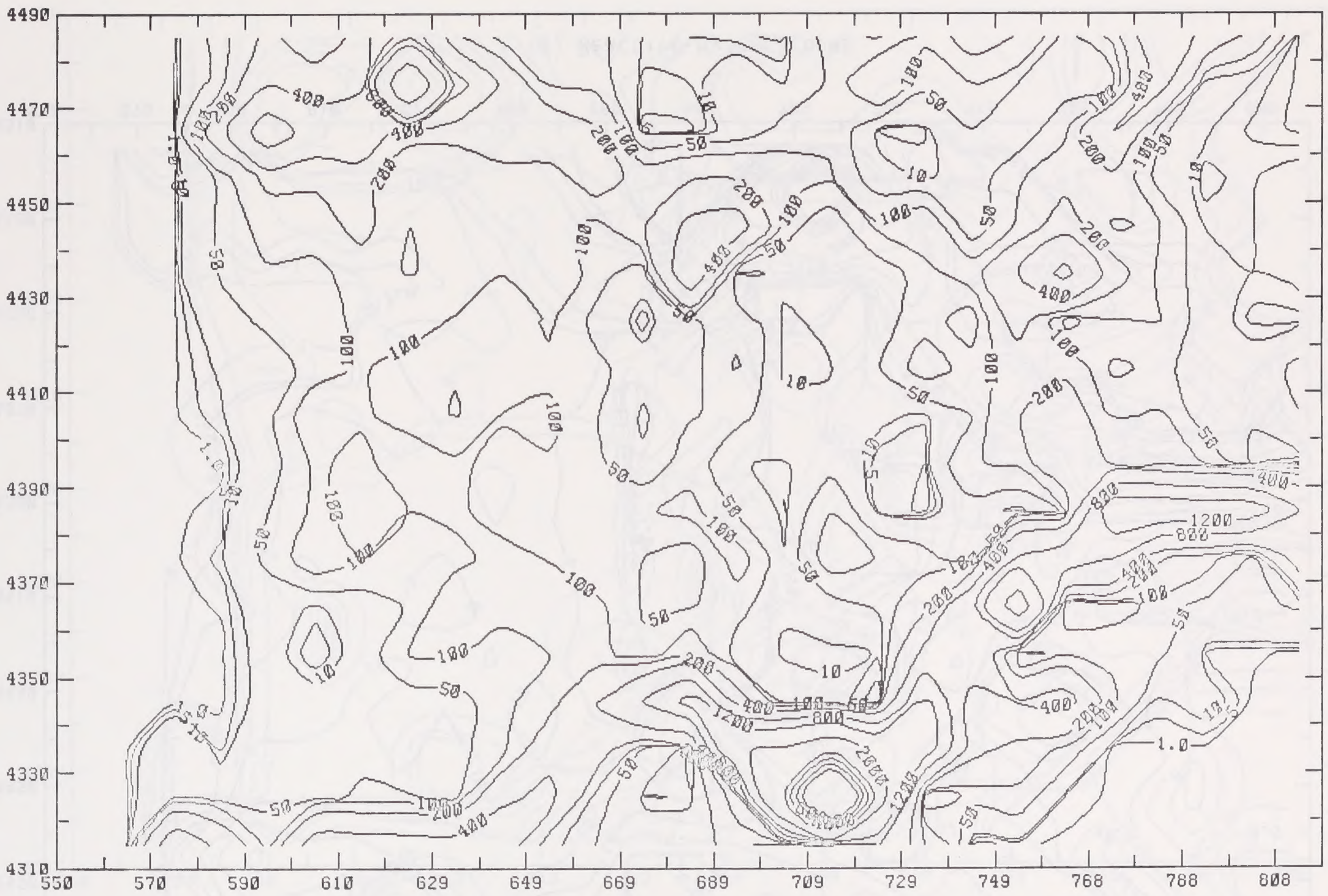

(d) CO

FIGURE 4-3 (Continued)

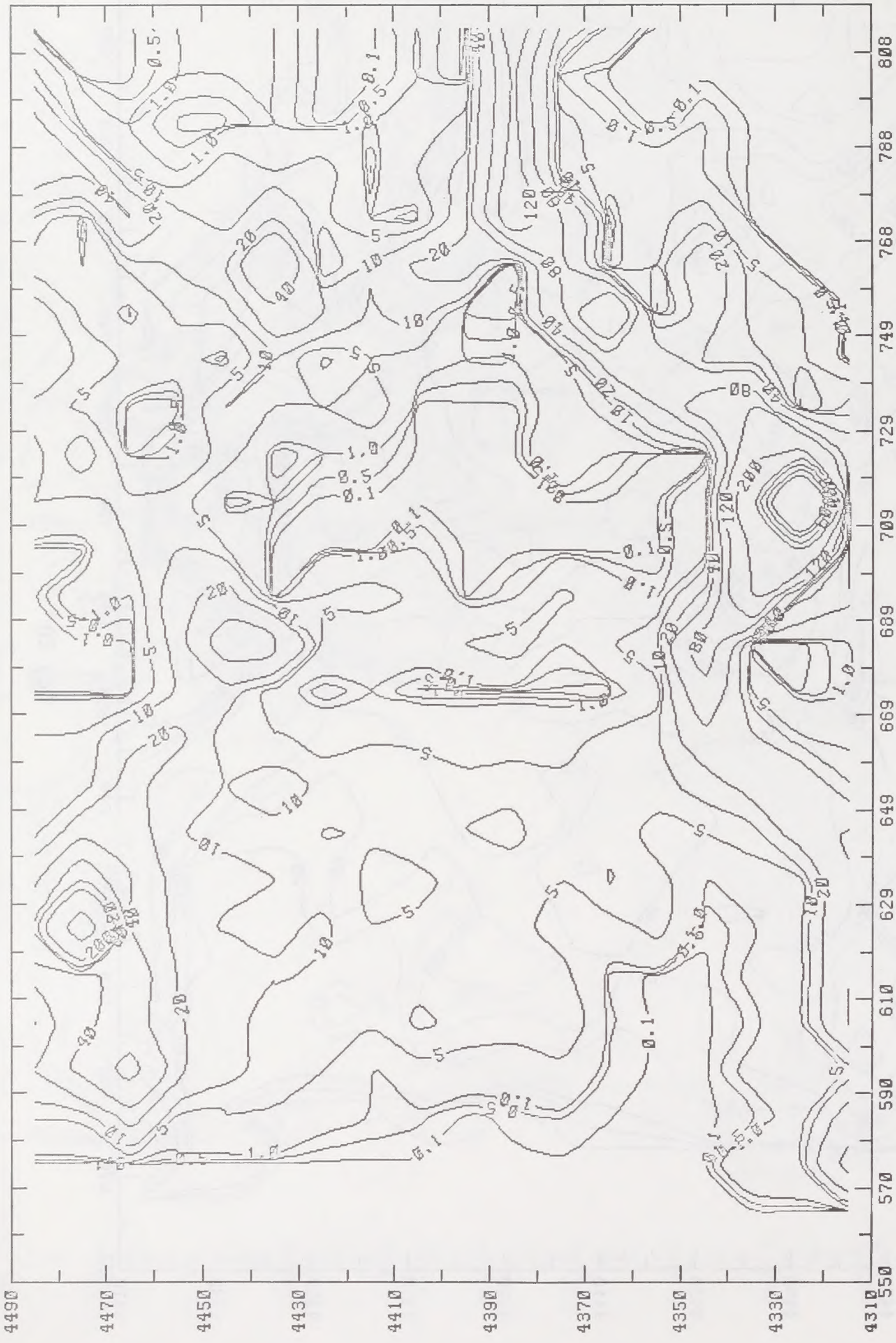

(e) Reactive Hydrocarbons

FIGURE 4-3 (Continued)

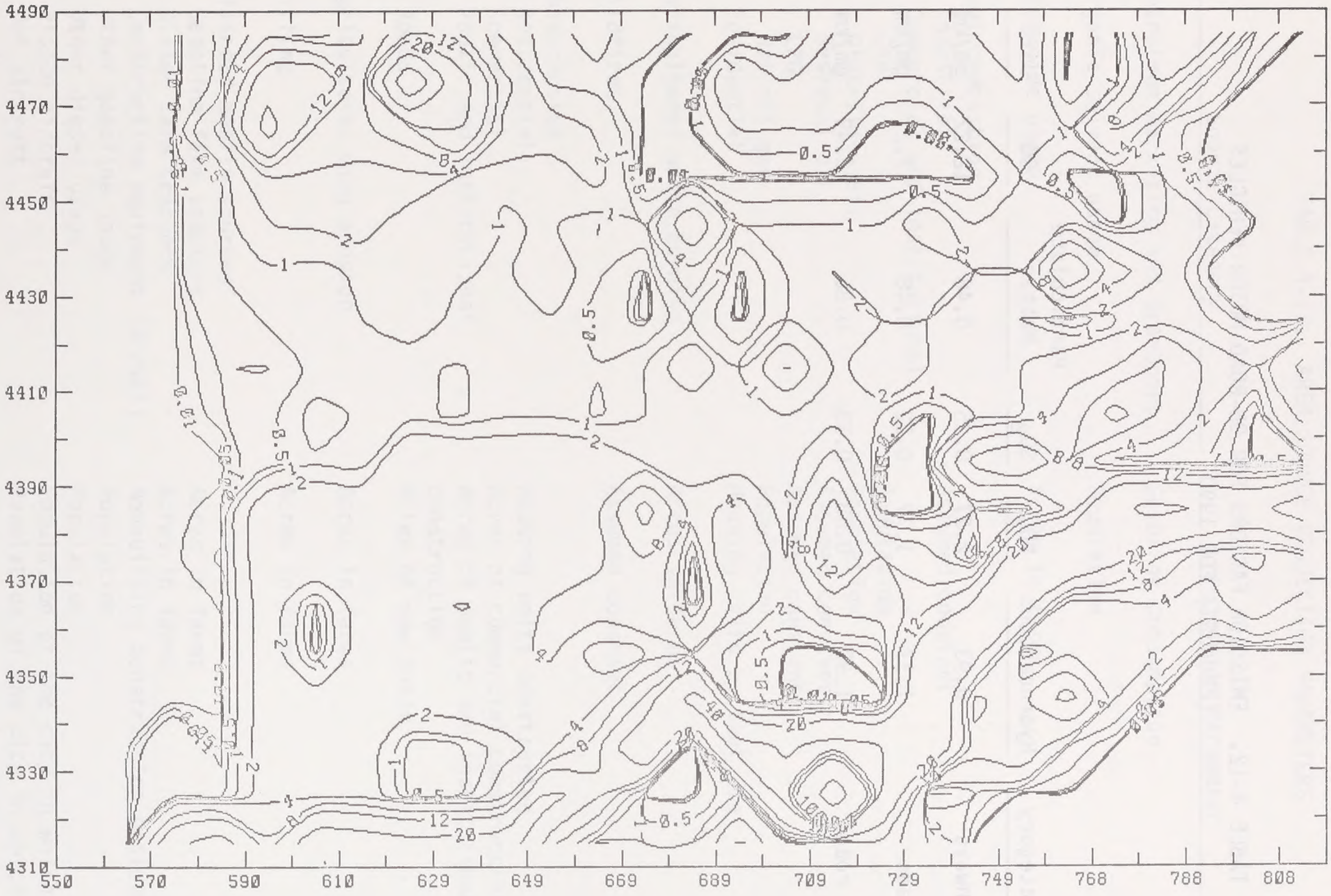

(f) Unreactive Hydrocarbons

FIGURE 4-3 (Concluded)

TABLE 4-12. EMISSION FACTORS FOR ON-ROAD MOTOR VEHICLES (EXHAUST) FOR 1990

Source Category	Hydrocarbons	NO_x	SO_2	Particulate Matter	CO	Unit
State highways	0.93	2.27	0.25	0.48	12.22	gm/km
County roads	1.37	1.77	0.22	0.48	17.21	gm/km
Class "D" roads	1.90	0.83	0.13	0.36	22.49	gm/km

TABLE 4-13. AREA SOURCE PROJECTION PARAMETERS

Source Category	Projection Parameter
Petroleum marketing and transport	Gasoline consumption
Organic solvent usage	Population
Pesticide usage	Acres in farms
Fuel combustion	
Industrial	Assumed constant
Commercial and institutional	
Coal	Population
Distillate oil	Population
Residual oil	Assumed constant
LPG	Assumed constant
Natural gas	Population
Residential	Housing units by fuel use
Agricultural waste burning	Acres in farms
Wildfires	Assumed constant
Construction	
Residential	Housing units constructed
Commercial	Acres of commercial construction
Public and institutional	Acres of public and institutional construction
Roads	Miles of new roads
Agricultural wind erosion	Acres in farms
Tilling	Acres in farms
Off-road mobile sources	
Gasoline farm tractors	Acres in farms
Diesel farm tractors	Acres in farms
Construction equipment (diesel)	Nonbuilding construction employment
Other gasoline usage	Population
Other diesel usage	Population
Piston aircraft	Population of the city in which located
Jet aircraft	Population of the city in which located
Railroads	Mining employment (excluding synfuel)

TABLE 4-13 (Concluded)

Source Category	Projection Parameter
On-road motor vehicles (exhaust)	
State highways	Population
County roads	Population
Class "D" roads	A parameter based on population (refer to text)
On-road motor vehicles (fugitive dust)	
State highways (paved)	Population
County roads (paved)	Population
Class "D" roads (unpaved)	A parameter based on population (refer to text)

No future projections of air traffic volume were available. We used the population of the city of Vernal as an index of commercial and general aviation growth in Uintah County. Both the airports included in the baseline inventory, Vernal and Roosevelt, are in the vicinity of Vernal.

It was assumed that railroads are employed mainly to haul mineral products, and thus mining employment was used as the activity parameter to project railroad emissions. There is no indication that the synfuel industry will utilize railroads significantly, and thus the mining employment related to the synfuel industry was not included.

The unavailability of pertinent data to project the emissions from class "D" roads posed a difficult situation. For the 1980 baseline, this category constitutes over 90 percent of total particulate emissions for Uintah County and over 80 percent for Grand County. Moreover, the baseline AADT estimate of 50 is an approximation, and we were cautioned (UDOT, 1982) about projecting this number. We estimate that there will be an increase in the class "D" road activity (vehicle kilometers travelled) and that this increase might range between 25 percent and 100 percent of the population increase. We would not expect an increase in VKMT for class "D" roads equivalent to the projected population growth because of the magnitude of this population increase. For example, many roads currently unimproved may be paved in the future, reflecting their increased use. This would significantly reduce particulate matter emissions from roadway travel. Furthermore, the rural nature of Uintah and Grand counties, which is directly related to class "D" road activity, will be altered dramatically by the projected population growth in the region. Fewer opportunities will be available for activities related to present class "D" road use as the area becomes more urbanized. In light of these considerations, we assumed the future VKMT increase to be 50 percent of the total county population increase; e.g., if the population doubled, then the class "D" road activity would increase by a factor of 1.5 [(2 - 1) 0.5 + 1]. It should be emphasized that a large degree of uncertainty is inherent in this estimate. The lack of relevant projections prevented a more accurate treatment.

4.1.6.3 Spatial Allocation

The source category/allocation parameter relationship presented in table 4-9 was used for the future scenarios; the revised gridded information accounted for changes in the spatial distribution of emissions with respect to the 1980 baseline. Careful examination of projected population data shows that within each county, certain areas will experience larger growth than others. In general, it was found that the urban areas were projected to undergo relatively larger population increases (NPS, 1982).

This uneven growth in population was accounted for during the preparation of the gridded population files for the future-year scenario. Furthermore, a new town in Grand County and a construction camp in Uintah County were explicitly included by allocating population to the appropriate grid cells.

Although total emissions associated with agricultural activities were reduced from the 1980 baseline because of increased population, we assumed a uniform reduction in these emissions for the appropriate grid cells in each county. For the other allocation parameters, no information was available to redistribute the emissions with respect to the 1980 baseline inventory.

4.1.6.4 Results

Emission totals for Uintah and Grand counties are presented in tables 4-14 and 4-15, respectively. Emission density maps for this high-oil-production scenario are presented in section 5.

4.1.7 Utah Area Sources: Regional Low-Oil-Production Scenario

Area source emission inventories were prepared for Uintah and Grand counties for 1990 with the assumption of a low level of oil production on a regional scale. Procedures used to develop this inventory are similar to those for the estimation of the high-oil-shale scenario.

4.1.7.1 Emission Factors

For all emission source categories, except on-road motor vehicles (exhaust), the emission factors given in table 4-8 were employed. Emission factors given in table 4-12 were used for on-road motor vehicles (exhaust).

4.1.7.2 Activity Projections

The activity parameters were derived from socioeconomic data pertaining to the low-oil-shale-development scenario for 1990 (NPS, 1982). Source category-projection parameter relationships shown in table 4-13 were used.

TABLE 4-14. REGIONAL HIGH OIL PRODUCTION SCENARIO AREA SOURCE EMISSION INVENTORY FOR UINTAH COUNTY

(tons per year)

	SOURCE CATEGORY	RHC	URHC	NOX	SO2	TSP	CO
10	Petroleum - Truck unloading	68.10	0.00	0.00	0.00	0.00	0.00
20	Petroleum - Underground storage	55.91	0.00	0.00	0.00	0.00	0.00
30	Petroleum - Auto tank filling	90.69	0.00	0.00	0.00	0.00	0.00
40	Surface coating	209.79	0.00	0.00	0.00	0.00	0.00
50	Petroleum drycleaning	11.53	0.00	0.00	0.00	0.00	0.00
60	Perchloroethylene drycleaning	36.79	0.00	0.00	0.00	0.00	0.00
70	1,1,1-trichloroethane degreasing	0.00	32.35	0.00	0.00	0.00	0.00
80	Trichloroethane degreasing	96.86	0.00	0.00	0.00	0.00	0.00
90	Graphic arts	25.74	0.00	0.00	0.00	0.00	0.00
100	Miscellaneous solvent usage	203.43	0.00	0.00	0.00	0.00	0.00
110	Pesticide usage	20.34	0.00	0.00	0.00	0.00	0.00
120	Ind. distillate oil combustion	0.00	0.07	1.96	3.17	0.12	0.43
130	Ind. residual oil combustion	0.00	0.09	6.87	16.48	1.32	0.56
140	Ind. LPG combustion	0.00	0.00	0.09	0.00	0.00	0.00
150	Ind. natural gas combustion	0.00	0.22	15.14	0.03	0.88	1.45
160	Comm. & Inst. coal combustion	0.06	55.82	111.76	424.71	298.08	186.32
170	Comm. & Inst. distillate oil combustion	0.00	0.69	17.01	27.81	1.45	3.91
180	Comm. & Inst. residual oil combustion	0.00	0.13	11.38	27.10	2.18	0.93
190	Comm. & Inst. LPG combustion	0.00	0.02	0.55	0.00	0.07	0.07
200	Comm. & Inst. natural gas combustion	0.00	3.37	51.34	0.22	4.03	8.54
210	Res. coal combustion	0.00	61.74	9.21	70.36	61.74	277.96
220	Res. distillate oil combustion	0.00	0.09	3.31	6.56	0.31	0.83
230	Res. LPG combustion	0.00	0.06	0.79	0.00	0.22	0.22
240	Res. wood combustion	63.88	0.00	12.72	0.00	255.23	1533.64
250	Res. natural gas combustion	0.00	10.22	102.92	0.69	12.97	25.74
260	Agricultural waste burning	25.33	0.00	0.00	0.00	21.86	129.64
270	Wildfires	0.00	91.14	13.95	0.00	63.86	530.10
280	Res. construction	0.00	0.00	0.00	0.00	1520.02	0.00
290	Comm. construction	0.00	0.00	0.00	0.00	179.94	0.00
300	Public & Inst. construction	0.00	0.00	0.00	0.00	338.30	0.00
310	Road construction	0.00	0.00	0.00	0.00	442.18	0.00
320	Agricultural wind erosion	0.00	0.00	0.00	0.00	444.57	0.00
330	Tilling	0.00	0.00	0.00	0.00	515.99	0.00
340	Gasoline farm tractors	1.73	46.51	38.08	1.32	2.00	8.20
350	Diesel farm tractors	1.78	8.93	49.33	4.60	6.74	17.54
360	Construction equipment (diesel)	8.22	35.47	497.62	38.07	31.92	116.48
370	Other gasoline usage	2.77	88.39	28.95	2.27	2.55	14.46
380	Other diesel usage	1.57	8.88	111.98	7.50	8.00	24.29
390	Piston aircraft	11.03	0.00	0.64	0.00	0.00	493.45
400	**Jet aircraft**	90.18	0.00	146.48	16.63	75.75	453.06
410	**Railroads**	0.00	0.00	0.00	0.00	0.00	0.00
420	**Motor vehicle - State highways**	773.95	85.99	2099.50	231.26	443.90	11299.99
430	**Motor vehicle - County roads**	477.17	53.02	685.01	85.27	185.75	6662.33
440	**Motor vehicle - Class "D" roads**	370.41	41.16	179.66	28.19	78.32	4934.16
450	**Motor vehicle - State highways (fug. dust)**	0.00	0.00	0.00	0.00	2959.64	0.00
460	**Motor vehicle - County roads (fug. dust)**	0.00	0.00	0.00	0.00	1238.32	0.00
470	**Motor vehicle - Class "D" roads (fug. dust)**	0.00	0.00	0.00	0.00	98665.48*	0.00
---	TOTAL	2647.21	624.34	4196.19	992.22	107861.84	26724.00

---

*See section 4.1.6.2 for an explanation of the uncertainty in this estimate.

TABLE 4-15. REGIONAL HIGH OIL PRODUCTION SCENARIO AREA SOURCE EMISSION INVENTORY FOR GRAND COUNTY

(tons per year)

SOURCE	CATEGORY	RHC	URHC	NOX	SO2	TSP	CO
10	Petroleum - Truck unloading	64.63	0.00	0.00	0.00	0.00	0.00
20	Petroleum - Underground storage	11.46	0.00	0.00	0.00	0.00	0.00
30	Petroleum - Auto tank filling	112.80	0.00	0.00	0.00	0.00	0.00
40	Surface coating	51.43	0.00	0.00	0.00	0.00	0.00
50	Petroleum drycleaning	2.81	0.00	0.00	0.00	0.00	0.00
60	Perchloroethylene drycleaning	8.98	0.00	0.00	0.00	0.00	0.00
70	1,1,1-trichloroethane degreasing	0.00	7.84	0.00	0.00	0.00	0.00
80	Trichloroethane degreasing	23.76	0.00	0.00	0.00	0.00	0.00
90	Graphic arts	6.30	0.00	0.00	0.00	0.00	0.00
100	Miscellaneous solvent usage	49.88	0.00	0.00	0.00	0.00	0.00
110	Pesticide usage	0.82	0.00	0.00	0.00	0.00	0.00
120	Ind. distillate oil combustion	0.00	0.02	0.44	0.71	0.03	0.10
130	Ind. residual oil combustion	0.00	0.03	1.55	3.72	0.28	0.12
140	Ind. LPG combustion	0.00	0.00	0.02	0.00	0.00	0.00
150	Ind. natural gas combustion	0.00	0.05	3.41	0.00	0.19	0.32
160	Comm. & Inst. coal combustion	0.02	13.70	27.29	103.56	72.75	44.49
170	Comm. & Inst. distillate oil combustion	0.00	0.19	4.13	6.73	0.37	0.92
180	Comm. & Inst. residual oil combustion	0.00	0.09	4.54	10.77	0.85	0.38
190	Comm. & Inst. LPG combustion	0.00	0.01	0.21	0.00	0.03	0.03
200	Comm. & Inst. natural gas combustion	0.00	0.83	12.44	0.06	0.98	1.90
210	Res. coal combustion	0.00	17.29	2.37	19.73	17.31	77.75
220	Res. distillate oil combustion	0.00	0.06	1.01	2.06	0.14	0.29
230	Res. LPG combustion	0.00	0.02	0.23	0.00	0.05	0.06
240	Res. wood combustion	14.50	0.00	2.85	0.00	59.29	347.51
250	Res. natural gas combustion	0.00	2.84	28.71	0.19	3.57	7.15
260	Agricultural waste burning	17.10	0.00	0.00	0.00	14.70	87.42
270	Wildfires	0.00	109.82	17.86	0.00	77.90	650.18
280	Res. construction	0.00	0.00	0.00	0.00	373.05	0.00
290	Comm. construction	0.00	0.00	0.00	0.00	43.22	0.00
300	Public & Inst. construction	0.00	0.00	0.00	0.00	100.79	0.00
310	Road construction	0.00	0.00	0.00	0.00	116.42	0.00
320	Agricultural wind erosion	0.00	0.00	0.00	0.00	34.82	0.00
330	Tilling	0.00	0.00	0.00	0.00	734.70	0.00
340	Gasoline farm tractors	0.21	5.42	4.46	0.14	0.21	0.96
350	Diesel farm tractors	0.21	1.03	5.91	0.55	0.82	2.06
360	Construction equipment (diesel)	1.58	6.70	94.60	7.18	6.02	22.13
370	Other gasoline usage	0.67	21.55	7.05	0.52	0.62	3.56
380	Other diesel usage	0.40	2.17	27.45	1.81	1.94	5.94
390	Piston aircraft	0.00	0.00	0.00	0.00	0.00	0.00
400	Jet aircraft	0.00	0.00	0.00	0.00	0.00	0.00
410	Railroads	100.48	749.77	2952.59	453.47	198.38	1035.75
420	Motor vehicle - State highways	323.52	35.95	877.84	96.62	185.61	4724.03
430	Motor vehicle - County roads	202.91	22.55	291.39	36.17	78.97	2833.35
440	Motor vehicle - Class "D" roads	65.86	7.32	32.00	5.10	14.00	877.58
450	Motor vehicle - State highways (fug. dust)	0.00	0.00	0.00	0.00	1237.09	0.00
460	Motor vehicle - County roads (fug. dust)	0.00	0.00	0.00	0.00	526.41	0.00
470	Motor vehicle - Class "D" roads (fug. dust)	0.00	0.00	0.00	0.00	17554.10*	0.00
----	TOTAL	1080.30	1005.23	4400.28	749.06	21455.28	10723.86

---

*See section 4.1.6.2 for an explanation of the uncertainty in this estimate.

4.1.7.3 Allocation Parameters

The procedures described for the development of the regional high scenario were used. Spatially nonuniform growth of population and a decline of agricultural activities were treated appropriately.

4.1.7.4 Results

Tables 4-16 and 4-17 show the emission totals for Uintah and Grand counties, respectively, for area sources. Spatial distributions of area source emissions are discussed in section 5.

4.1.8 Utah Area Source Summary

Table 4-18 summarizes the area source emission totals in kilograms per hour for each county and scenario. Note that approximately 80 to 90 percent of total particulate emissions from area sources are emitted as fugitive dust from unpaved roads.

4.1.9 Socioeconomic Data Comparison for Utah

The socioeconomic data used to project the Utah area source emissions to future years were developed by the NPS (1982). Because of the required schedule for completing the inventories, socioeconomic data developed by the Utah State Planning Coordinator's Office (1982) could not be employed for the air quality analysis, even though these data were used in other portions of the Uinta Basin Synfuels EIS. We have compared the Utah data to the information we used to develop the future area source inventories and conclude that although there are differences, the magnitude of the difference is within the uncertainty of the projected values. For example, the Utah 1990 baseline population data are 8.4 percent greater and 2.6 percent less than the NPS data for Uintah and Grand counties, respectively. In the case of the regional high scenario for 1990, the Utah population data are 0.9 and 8.5 percent less than the comparable total population data we used for Uintah and Grand counties (see table 4-19 and figure 4-4). For the regional low scenario in 1990, however, the projections differ because of changes in assumed locations of new population. For this scenario, the Utah population data are 26.8 percent greater for Uintah County and 17.3 percent less for Grand County when compared to the NPS data we employed. Overall for both counties combined, the Utah population data are 16.4 percent greater for the regional low scenario. One of the primary differences between the two sets of projections is that the data we used included the new town of Westwater in Grand County whereas the state of Utah data for the low scenario did not.

TABLE 4-16. REGIONAL LOW OIL PRODUCTION SCENARIO AREA SOURCE EMISSION INVENTORY FOR UINTAH COUNTY

(tons per year)

SOURCE	CATEGORY	RHC	URHC	NOX	SO2	TSP	CO
10	Petroleum - Truck unloading	44.88	0.00	0.00	0.00	0.00	0.00
20	Petroleum - Underground storage	36.97	0.00	0.00	0.00	0.00	0.00
30	Petroleum - Auto tank filling	59.64	0.00	0.00	0.00	0.00	0.00
40	Surface coating	138.24	0.00	0.00	0.00	0.00	0.00
50	Petroleum drycleaning	7.58	0.00	0.00	0.00	0.00	0.00
60	Perchloroethylene drycleaning	24.25	0.00	0.00	0.00	0.00	0.00
70	1,1,1-trichloroethane degreasing	0.00	21.30	0.00	0.00	0.00	0.00
80	Trichloroethane degreasing	63.82	0.00	0.00	0.00	0.00	0.00
90	Graphic arts	17.00	0.00	0.00	0.00	0.00	0.00
100	Miscellaneous solvent usage	134.01	0.00	0.00	0.00	0.00	0.00
110	Pesticide usage	21.33	0.00	0.00	0.00	0.00	0.00
120	Ind. distillate oil combustion	0.00	0.07	1.96	3.14	0.12	0.41
130	Ind. residual oil combustion	0.00	0.07	6.88	16.45	1.28	0.54
140	Ind. LPG combustion	0.00	0.00	0.06	0.00	0.00	0.00
150	Ind. natural gas combustion	0.00	0.22	15.13	0.03	0.86	1.49
160	Comm. & Inst. coal combustion	0.04	36.79	73.66	279.91	196.35	122.82
170	Comm. & Inst. distillate oil combustion	0.00	0.46	11.25	18.39	0.98	2.47
180	Comm. & Inst. residual oil combustion	0.00	0.13	11.36	27.08	2.18	0.93
190	Comm. & Inst. LPG combustion	0.00	0.02	0.58	0.00	0.07	0.07
200	Comm. & Inst. natural gas combustion	0.00	2.24	33.82	0.12	2.62	5.67
210	Res. coal combustion	0.00	40.61	6.00	46.27	40.61	182.74
220	Res. distillate oil combustion	0.00	0.06	2.20	4.29	0.21	0.49
230	Res. LPG combustion	0.00	0.04	0.48	0.00	0.15	0.15
240	Res. wood combustion	41.87	0.00	8.41	0.00	167.76	1006.90
250	Res. natural gas combustion	0.00	6.74	67.56	0.37	8.47	16.97
260	Agricultural waste burning	26.55	0.00	0.00	0.00	22.92	135.90
270	Wildfires	0.00	91.14	13.95	0.00	63.86	530.10
280	Res. construction	0.00	0.00	0.00	0.00	1004.45	0.00
290	Comm. construction	0.00	0.00	0.00	0.00	115.20	0.00
300	Public & Inst. construction	0.00	0.00	0.00	0.00	230.32	0.00
310	Road construction	0.00	0.00	0.00	0.00	325.66	0.00
320	Agricultural wind erosion	0.00	0.00	0.00	0.00	466.04	0.00
330	Tilling	0.00	0.00	0.00	0.00	540.91	0.00
340	Gasoline farm tractors	1.81	48.75	39.92	1.38	2.10	8.59
350	Diesel farm tractors	1.86	9.36	51.71	4.82	7.07	18.38
360	Construction equipment (diesel)	4.81	21.07	294.09	22.52	18.92	68.83
370	Other gasoline usage	1.83	58.27	19.08	1.47	1.66	9.59
380	Other diesel usage	1.06	5.92	73.91	4.90	5.23	16.15
390	Piston aircraft	7.06	0.00	0.41	0.00	0.00	315.93
400	Jet aircraft	57.74	0.00	93.79	10.65	48.50	290.07
410	Railroads	0.00	0.00	0.00	0.00	0.00	0.00
420	Motor vehicle - State highways	510.09	56.68	1384.33	152.44	292.62	7453.19
430	Motor vehicle - County roads	314.66	34.96	451.42	56.20	122.41	4388.87
440	Motor vehicle - Class "D" roads	274.70	30.52	133.12	20.89	58.03	3656.44
450	Motor vehicle - State highways (fug. dust)	0.00	0.00	0.00	0.00	1950.55	0.00
460	Motor vehicle - County roads (fug. dust)	0.00	0.00	0.00	0.00	816.11	0.00
470	Motor vehicle - Class "D" roads (fug. dust)	0.00	0.00	0.00	0.00	73131.31*	0.00
---	TOTAL	1791.68	465.40	2795.04	671.32	79643.77	18233.45

---

* See section 4.1.6.2 for an explanation of the uncertainty in the estimate.

TABLE 4-17. REGIONAL LOW OIL PRODUCTION SCENARIO AREA SOURCE EMISSION INVENTORY FOR GRAND COUNTY

(tons per year)

SOURCE CATEGORY		RHC	URHC	NOX	SO2	TSP	CO
10	Petroleum - Truck unloading	69.97	0.00	0.00	0.00	0.00	0.00
20	Petroleum - Underground storage	9.45	0.00	0.00	0.00	0.00	0.00
30	Petroleum - Auto tank filling	93.36	0.00	0.00	0.00	0.00	0.00
40	Surface coating	42.65	0.00	0.00	0.00	0.00	0.00
50	Petroleum drycleaning	2.34	0.00	0.00	0.00	0.00	0.00
60	Perchloroethylene drycleaning	7.43	0.00	0.00	0.00	0.00	0.00
70	1,1,1-trichloroethane degreasing	0.00	6.51	0.00	0.00	0.00	0.00
80	Trichloroethane degreasing	19.63	0.00	0.00	0.00	0.00	0.00
90	Graphic arts	5.20	0.00	0.00	0.00	0.00	0.00
100	Miscellaneous solvent usage	41.35	0.00	0.00	0.00	0.00	0.00
110	Pesticide usage	0.83	0.00	0.00	0.00	0.00	0.00
120	Ind. distillate oil combustion	0.00	0.01	0.43	0.71	0.04	0.10
130	Ind. residual oil combustion	0.00	0.03	1.55	3.72	0.30	0.12
140	Ind. LPG combustion	0.00	0.00	0.02	0.00	0.00	0.00
150	Ind. natural gas combustion	0.00	0.05	3.39	0.00	0.18	0.33
160	Comm. & Inst. coal combustion	0.02	11.31	22.58	85.72	60.20	36.80
170	Comm. & Inst. distillate oil combustion	0.00	0.16	3.40	5.57	0.27	0.76
180	Comm. & Inst. residual oil combustion	0.00	0.07	4.51	10.82	0.87	0.38
190	Comm. & Inst. LPG combustion	0.00	0.01	0.20	0.00	0.04	0.04
200	Comm. & Inst. natural gas combustion	0.00	0.67	10.28	0.05	0.81	1.58
210	Res. coal combustion	0.00	14.52	2.02	16.59	14.52	65.29
220	Res. distillate oil combustion	0.00	0.05	0.83	1.68	0.11	0.24
230	Res. LPG combustion	0.00	0.02	0.19	0.00	0.05	0.05
240	Res. wood combustion	11.87	0.00	2.35	0.00	48.57	285.00
250	Res. natural gas combustion	0.00	2.37	23.74	0.18	2.95	5.94
260	Agricultural waste burning	17.22	0.00	0.00	0.00	14.80	88.04
270	Wildfires	0.00	109.82	17.86	0.00	77.90	650.18
280	Res. construction	0.00	0.00	0.00	0.00	308.89	0.00
290	Comm. construction	0.00	0.00	0.00	0.00	35.99	0.00
300	Public & Inst. construction	0.00	0.00	0.00	0.00	79.17	0.00
310	Road construction	0.00	0.00	0.00	0.00	93.07	0.00
320	Agricultural wind erosion	0.00	0.00	0.00	0.00	35.06	0.00
330	Tilling	0.00	0.00	0.00	0.00	739.94	0.00
340	Gasoline farm tractors	0.21	5.46	4.50	0.14	0.21	0.97
350	Diesel farm tractors	0.21	1.04	5.95	0.55	0.83	2.07
360	Construction equipment (diesel)	1.58	6.70	94.63	7.18	6.02	22.16
370	Other gasoline usage	0.56	17.93	5.84	0.46	0.53	2.94
380	Other diesel usage	0.32	1.78	22.69	1.50	1.61	4.92
390	Piston aircraft	0.00	0.00	0.00	0.00	0.00	0.00
400	Jet aircraft	0.00	0.00	0.00	0.00	0.00	0.00
410	Railroads	100.48	749.77	2952.59	453.47	198.38	1035.75
420	Motor vehicle - State highways	267.68	29.74	726.28	79.97	153.65	3907.99
430	Motor vehicle - County roads	168.10	18.68	241.12	29.94	65.36	2346.30
440	Motor vehicle - Class "D" roads	58.48	6.50	28.37	4.53	12.42	779.69
450	Motor vehicle - State highways (fug. dust)	0.00	0.00	0.00	0.00	1024.05	0.00
460	Motor vehicle - County roads (fug. dust)	0.00	0.00	0.00	0.00	435.76	0.00
470	Motor vehicle - Class "D" roads (fug. dust)	0.00	0.00	0.00	0.00	15571.60*	0.00
---	TOTAL	718.93	983.17	4175.25	702.74	18983.89	9237.54

---

*See section 4.1.6.2 for an explanation of the uncertainty in this estimate.

TABLE 4-18. EMISSION TOTALS FOR AREA SOURCES IN UTAH

(kilograms per hour)

(a) Baseline

County	Sulfur Dioxide	Particulate Matter	Nitrogen Oxides	Total Hydrocarbon	Carbon Monoxide
Uintah	36	5310	219	274	2636
Grand	34	1495	239	190	1538

(b) Regional High Scenario

County	Sulfur Dioxide	Particulate Matter	Nitrogen Oxides	Total Hydrocarbon	Carbon Monoxide
Uintah	103	11,170	435	339	2768
Grand	78	2,222	456	216	1111

(c) Regional Low Scenario

County	Sulfur Dioxide	Particulate Matter	Nitrogen Oxides	Total Hydrocarbon	Carbon Monoxide
Uintah	70	8248	289	234	1888
Grand	73	1966	432	197	957

TABLE 4-19. TOTAL POPULATION FOR 1990 REGIONAL SCENARIOS (NPS)

Location	Scenario Low	 High
Uintah County		
Vernal	35,128	54,881
Bonanza construction camp	880	1,104
Rural area	6,556	8,606
County total	42,564	64,591
Grand County		
New town: Westwater	2,260	4,988
Moab	10,506	10,506
Rural area	347	347
County total	13,113	15,841

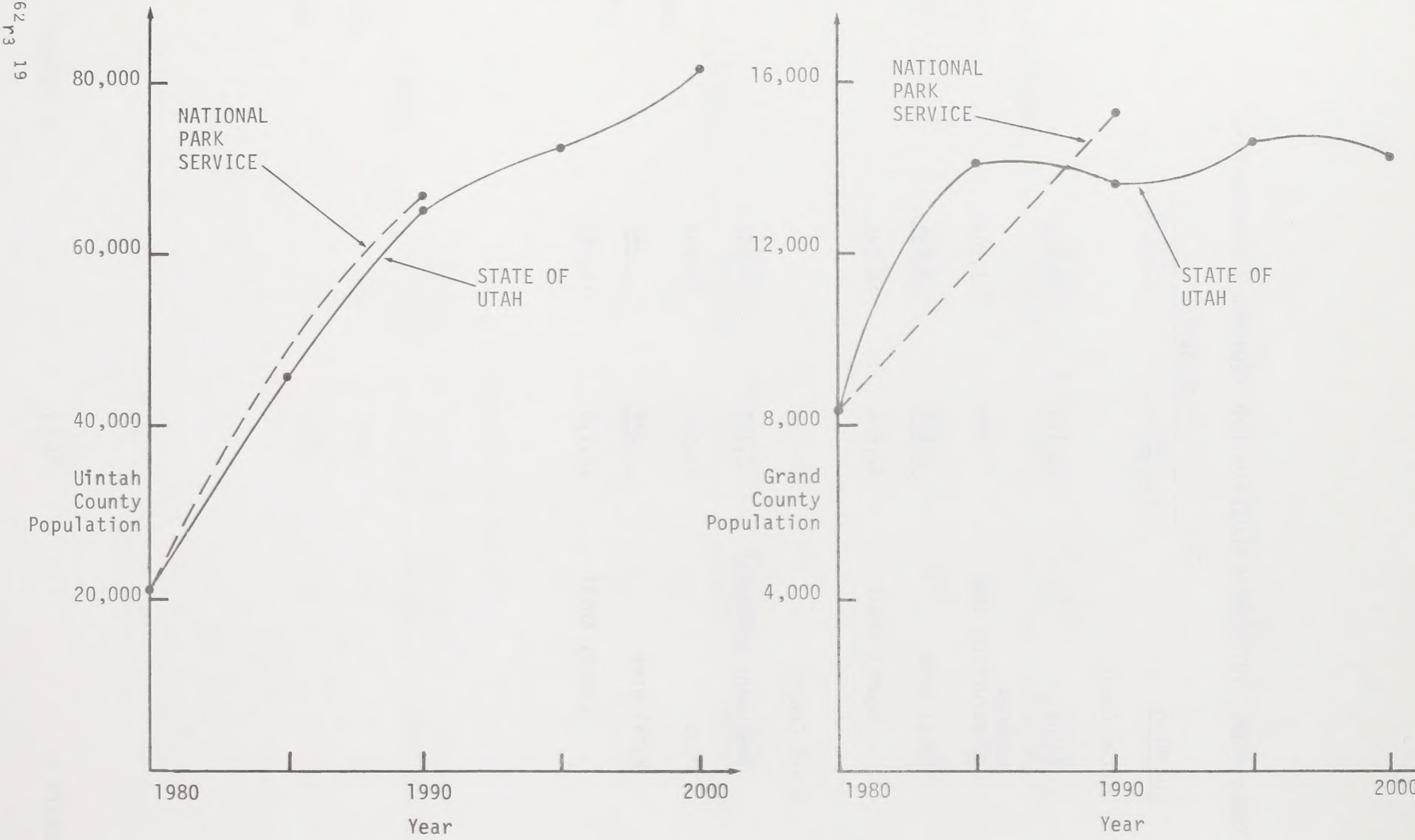

FIGURE 4-4. TOTAL CUMULATIVE POPULATION IN THE UINTA BASIN WITH HIGH-LEVEL SYNFUEL DEVELOPMENT

4.1.10 Concluding Remarks Pertaining to Inventory Activities

Previous emission inventory work, particularly in the Utah portion of the study region, has been limited primarily because of the low level of activities in this sparsely populated area. Much of our inventory development process has resulted in the first comprehensive set of emission estimates for this part of the country. Elements of the inventory process that contribute to the unique and embryonic nature of this work include the following:

> Synfuel projects. Oil shale and tar sands facilities are generally in the pilot plant stage at present. Emission factors for the several processes being proposed are uncertain, and the effectiveness of specific control technologies throughout portions of the processes remains unproven.

> Other planned projects in Utah. Little information was available relative to facility size, process description, and proposed controls for most of these future point sources.

> Area source activities and emission factors. Because of the sparse population in the region, area source activity data (e.g., commercial natural gas use, aircraft operations, and petroleum marketing) were limited in scope. Often, activity data were not available even on a countywide basis. Furthermore, emission factors have never been adapted to conditions in eastern Utah.

> Area source gridding. This study represents the first set of gridded emission inventories for eastern Utah. Information that we normally use to grid area sources was either sparse or unavailable.

> Projection techniques. Projecting emissions is always uncertain; when combined with the indeterminate and fluid nature of future energy development proposals for this region, emission projections should only be used with an understanding of their limitations.

Taking into consideration the aforementioned points as well as the large size of the study region, the cautious reviewer will understand that a large degree of uncertainty prevails in each of the inventories.

4.2 DESCRIPTION OF MODELING APPROACHES

In this section we describe the approach adopted for the analysis of regional-scale air quality and visibility impacts resulting from oil shale development in the Uinta Basin and in Colorado, and from other existing and anticipated emission sources.

4.2.1 Modeling Methodology

In this effort our aim was to apply the most sophisticated and realistic modeling methodology currently available. The complex dispersion processes that occur in the rugged terrain of the study region, the large size of the modeling region, and diverse temporal scales (3 hour, 24 hour, and annual averages) strain the capabilities of almost all routinely applied air quality models. The simple models (e.g., VALLEY, CRSTER, and COMPLEX), which have been previously applied to some of the proposed facilities studied here, are recognized as having serious shortcomings on a regional scale in this setting; among the most serious are

> Inability to treat spatially and temporally varying wind fields.

> Inability to treat spatially and temporally varying dispersion rates.

> Inability to properly treat the effects of topography, slope winds and other physical processes in complex terrain (assuming instantaneous and straight-line plume transport).

> Limited ability to treat chemical transformations and removal mechanisms.

Furthermore, the model applications carried out thus far have not been extensive (i.e., allowing the assessment of cumulative impacts from all proposed developments) or consistent enough to contribute to a comprehensive impact assessment.

To achieve the study objectives, we selected a modeling methodology to assess cumulative impacts of future oil shale and other associated and nonassociated development on a regional scale, resolved to averaging periods of 3 hours, 24 hours, and 1 year, within the states of Colorado and Utah. The methodology selected is based on the utilization of several sophisticated component models: the Systems Applications Complex-Terrain Wind Model, the Systems Applications Gaussian Puff Model, the Systems Applications Regional Transport Model, the EKMA Model, and the Systems Applications/EPA PLUVUE Model. In addition, we applied EPA's COMPLEX-I Model for calculation of concentrations very near emission sources. Even though these models have previously been used, the demanding spatial and temporal scales involved in their application required an innovative and unique approach to configuring and coupling of models so that their inputs and outputs would be complementary and meet the objectives of this study.

Figure 4-5 presents a schematic diagram of the modeling methodology used in this study showing how the various model components were coupled. Each model component was intended to serve a purpose that is specific to the strengths of its particular formulation and that complements the strengths of the other components. A summary of the strengths and weaknesses of each model as applied in this study is given in Table 4-20. Descriptions of the rationale behind the use of each model and the way each is used are given below. All models were applied in a systematic fashion allowing the impacts of individual facilities or any combination of facilities to be determined with a minimum of model runs by combining the output from separate runs.

4.2.1.1 The Use of COMPLEX-I

The first part of our approach involves the application of COMPLEX-I, which was developed by the EPA specifically for complex terrain situations (COMPLEX-I is not currently an EPA-approved model). COMPLEX-I is applied to the calculation of both SO_2 and TSP and provides impact calculations for one year with 1 hour, 3 hour, 24 hour, and annual averaging periods. COMPLEX-I is used in this study to provide near-source (within 5 to 10 km of the emissions facility) impact estimates. It was selected for the purpose because

- It is a model developed by the EPA, and it is currently being evaluated by the EPA.
- It is relatively inexpensive and simple to apply.
- A meteorological data base was available for its application.
- Near the source, its formulation is nearly equivalent to those of more sophisticated and expensive models.

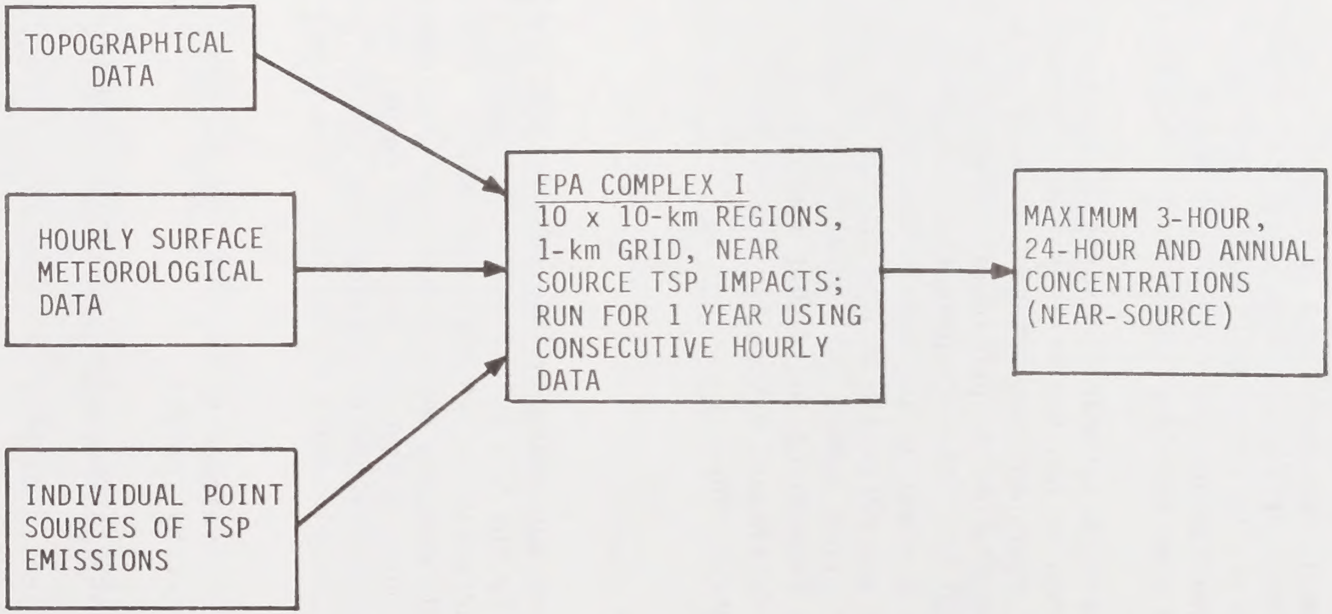
TOPOGRAPHICAL DATA
HOURLY SURFACE METEOROLOGICAL DATA
INDIVIDUAL POINT SOURCES OF TSP EMISSIONS
EPA COMPLEX I
10 x 10-km REGIONS, 1-km GRID, NEAR SOURCE TSP IMPACTS; RUN FOR 1 YEAR USING CONSECUTIVE HOURLY DATA
MAXIMUM 3-HOUR, 24-HOUR AND ANNUAL CONCENTRATIONS (NEAR-SOURCE)

(a) Detailed, Near-Source Modeling Using EPA's COMPLEX I Model

FIGURE 4-5. SCHEMATIC DIAGRAM OF MODELING METHODOLOGY

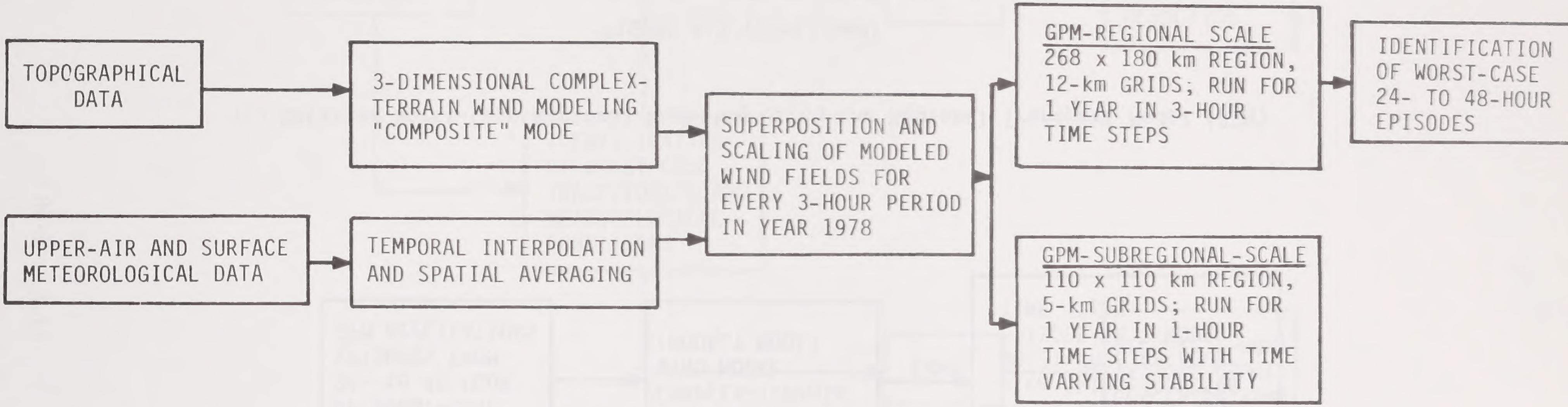
TOPOGRAPHICAL DATA
3-DIMENSIONAL COMPLEX-TERRAIN WIND MODELING "COMPOSITE" MODE
UPPER-AIR AND SURFACE METEOROLOGICAL DATA
TEMPORAL INTERPOLATION AND SPATIAL AVERAGING
SUPERPOSITION AND SCALING OF MODELED WIND FIELDS FOR EVERY 3-HOUR PERIOD IN YEAR 1978
GPM-REGIONAL SCALE
268 x 180 km REGION, 12-km GRIDS; RUN FOR 1 YEAR IN 3-HOUR TIME STEPS
GPM-SUBREGIONAL-SCALE
110 x 110 km REGION, 5-km GRIDS; RUN FOR 1 YEAR IN 1-HOUR TIME STEPS WITH TIME VARYING STABILITY
IDENTIFICATION OF WORST-CASE 24- TO 48-HOUR EPISODES

(b) Regional Impact Screening Using Gaussian Puff Model (GPM)

FIGURE 4-5 (Continued)

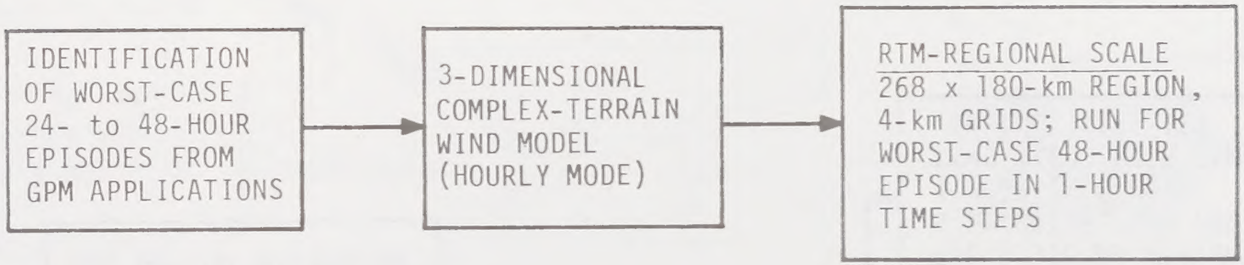
IDENTIFICATION OF WORST-CASE 24- to 48-HOUR EPISODES FROM GPM APPLICATIONS
3-DIMENSIONAL COMPLEX-TERRAIN WIND MODEL (HOURLY MODE)
RTM-REGIONAL SCALE
268 x 180-km REGION, 4-km GRIDS; RUN FOR WORST-CASE 48-HOUR EPISODE IN 1-HOUR TIME STEPS

(c) Detailed Worst-Case Regional Modeling Using the Regional Transport Model (RTM)

FIGURE 4-5 (Continued)

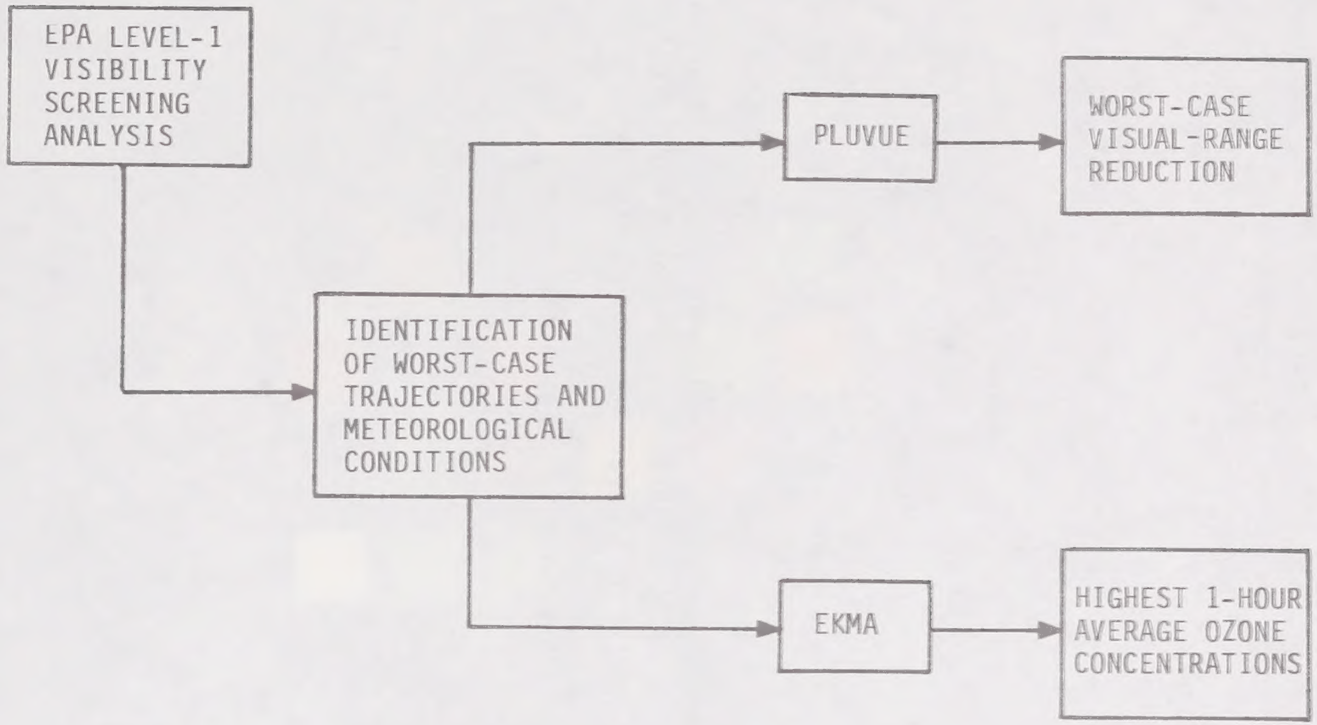
EPA LEVEL-1 VISIBILITY SCREENING ANALYSIS
IDENTIFICATION OF WORST-CASE TRAJECTORIES AND METEOROLOGICAL CONDITIONS
PLUVUE
WORST-CASE VISUAL-RANGE REDUCTION
EKMA
HIGHEST 1-HOUR AVERAGE OZONE CONCENTRATIONS

(d) Visibility and Photochemical Oxidant Modeling

FIGURE 4-5 (Concluded)

TABLE 4-20. SUMMARY OF THE RELATIVE CAPABILITIES OF THE MODELS USED IN THIS STUDY[†]

	Capabilities							
			Short Range			Medium and Long Range		
Model	Photochemistry	Visibility	3 hr	24 hr	Annual	3 hr	24 hr	Annual
GPM[*]	X	X	-	-	-	-	-	-
RTM	X	X	-	-	X	+	+	X
COMPLEX-I	X	X	+	+	+	-	-	-
PLUVUE	X	+	+	+	X	+	+	X
EKMA	+	X	+	+	X	+	+	X

[†] Capabilities of a given model in a given category that are weaker than another model in the same category are indicated by -. The model with the strongest capabilities in a category is indicated by +. Lack of capability in a category is indicated by X.

[*] As configured and applied in this study to 8760 consecutive hours (1 year).

Further, from the source (beyond 5 to 10 km), some well-known deficiencies of COMPLEX-I and other Gaussian plume models become limiting, especially in rugged terrain such as the terrain in our study area. Among the more serious of these deficiencies are

> Assumption of spatially invariant winds and dispersion

> Assumption of instantaneous transport.

More sophisticated models are required to overcome those deficiences at moderate to long transport distances. Typically, COMPLEX-I has been used for point sources only. We have modified the code to treat area sources as well by increasing the initial dimension of the plume from an area source to those of the area source itself. A technical description of COMPLEX-I can be found in Appendix C.

For Utah sources, COMPLEX-I was applied using 1978 Ua, Ub 10-meter tower wind and ΔT data. The seasonal and diurnal variations in mixing depths suggested by Holzworth (1972) were used to construct an hourly mixing depth input for both Utah and Colorado sources. For Colorado sources, either the 1975 C-a or 1975 C-b 10 meter tower data (wind and ΔT) were used, depending on the location of each emitting facility in relation to the measurement sites. For both Colorado and Utah facilities, the data collected at the site closest to the facility were used. However, if the closest monitoring site was in a significantly different terrain setting, the sites whose terrain settings were most representative of that of the facilities were used.

4.2.1.2 Use of the Gaussian Puff Model

The Systems Applications Gaussian Puff Model (GPM) was used in conjunction with the Systems Applications Complex Terrain Wind Model (CTWM) to overcome some of the major shortcomings of the COMPLEX-I model for medium- to long-range transport distances. This strategy capitalizes on the capability of GPM to accommodate spatially and temorally varying wind fields and dispersion rates and CTWM's capability to provide realistic winds in complex terrain. Detailed discussion of the technical aspects of GPM and CTWM formulations can be found in Appendix C.

GPM was adapted to provide estimates of 3-hour, 24-hour, and annual average SO_2 and TSP concentration averages within the large study region. This adaptation was accomplished by running GPM for 8760 consecutive hours (one year). During this study the GPM code was extensively "streamlined" to permit its application to an entire year without incurring exorbitant computation costs. Complex-terrain wind fields for the puff model were provided by the CTWM following a "composite" approach developed in this study (described in section 4.2.1.4), which greatly reduces the cost of preparing 8760 hourly wind fields. GPM was applied to two grids contained in the Uinta Basin--the regional-scale grid (268 km by 180 km) for the regional impacts discussed in section 5 and a sub-regional scale grid (110 km by 110 km) for the site-specific impacts discussed in section 6. Both grid regions are shown in Figure 4-6.

A regional modeling domain was used that extended far beyond the Uinta Basin where the sources being evaluated would be located. The study region was made sufficiently large to include the Flat Tops Wilderness Area, the mandatory Class I area identified in previous studies as receiving maximum air quality impacts from oil shale development. Latimer and Doyle (1981) showed that other Class I areas in Utah and Colorado would not be impacted by synthetic fuel development to the degree that Flat Tops would.

Two grid regions were employed largely because of cost. To cover the entire region of interest with sufficient receptor density would be prohibitively expensive. However, a loose receptor mesh is likely to miss the peaks in the concentration distributions, especially close to the emissions source where steep concentration gradients are more likely. The regional-scale grid is therefore intended mainly to provide concentration predictions at the larger downwind distances (e.g., greater than about 60 km downwind), whereas the subregional grid focuses on the shorter distances. Both grid region applications employ the CTWM in the "composite" mode to supply gridded hourly wind fields, and both utilize an aggregation of emissions sources (to reduce computational costs). The aggregation of emission sources probably results in GPM's overestimation of results very near the sources on either grid because an aggregated source plume is much more compact and concentrated than the composite of many individual plumes from a facility. However, in our application of the COMPLEX-I we do not aggregate sources; the results of COMPLEX-I thus do not suffer this shortcoming and are more appropriate for near-source impacts resulting from multiple point source releases.

In addition to the differences in the grid region sizes and receptor spacing between the regional and subregional applications, there are other differences between the two applications. One-hour time steps are used in the subregional applications, whereas three-hour time steps are used in the regional application. Furthermore, in the regional application, puffs are diffused assuming a Pasquill D stability class, whereas the stability class varies hourly between A and F stability in the subregional application. The assumption of D stability is made to improve computational efficiency in the regional GPM application, and is probably conservative because long-range impacts are more likely to be associated with neutral

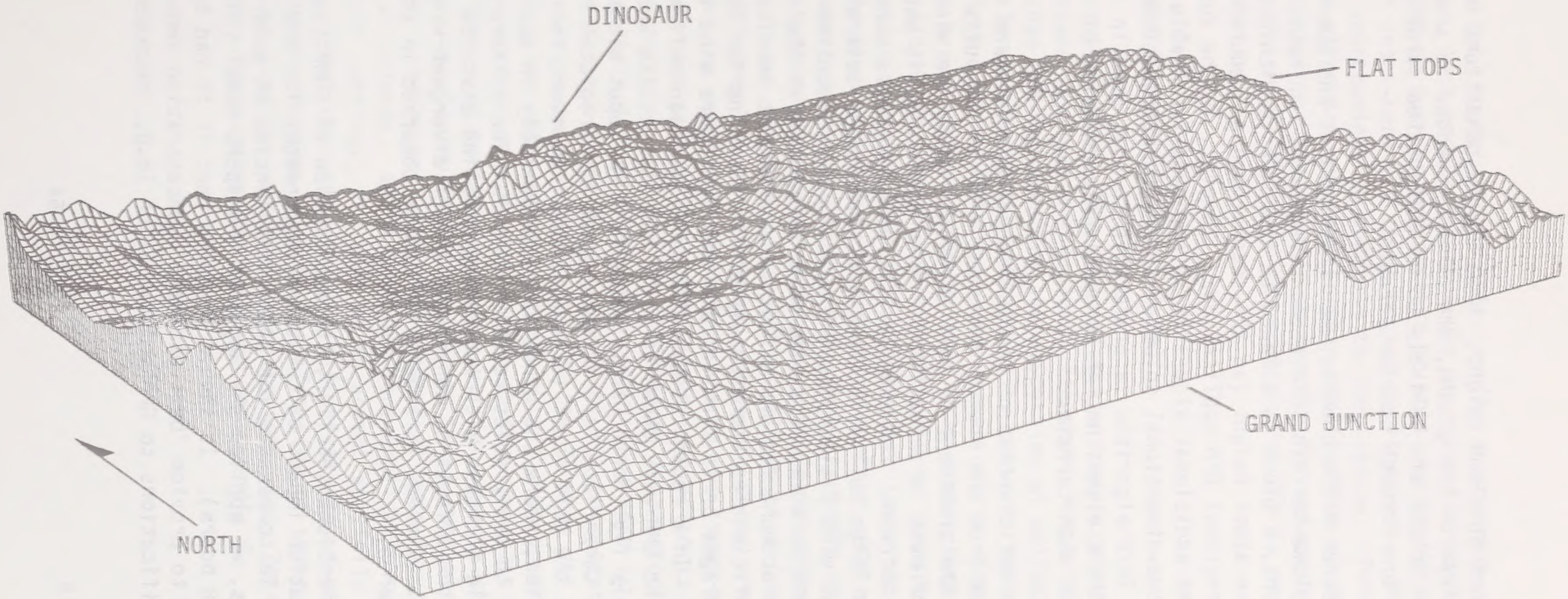

FIGURE 4-6. 3-D PERSPECTIVE OF TERRAIN IN REGIONAL MODELING AREA
(Viewed from the southwest)

Note: Dark internal boundaries delineate the sub-regional grid region.

conditions at plume height. When stable conditions occur, they usually occur close to the ground, and plumes embedded in stable flow situations near the ground are unlikely to be transported large distances in concentrated form through complex terrain.

Another difference between the regional and subregional applications is the plume-terrain interaction treatment. In neutral or unstable conditions, a plume is allowed to approach to within one-half of its effective stack height (an EPA-recommended procedure) for both regional and subregional GPM applications. However, in the subregional applications, an additional algorithm is employed for stable conditions based upon a two-dimensional solution to the equations of motion (Queney, 1947). This algorithm is preferable to that used in EPA models because, unlike EPA's algorithm, it is applicable downwind of a plume's first encounter with terrain.

The deficiencies of the puff model approach are most severe at distances from the source where the size of the puffs becomes large enough so that the treatment of puff advection using the winds at the puff's center of mass is unrealistic. This deficiency is especially important in complex terrain. For example, the pollutant mass conceptually contained within a large puff will likely be advected in several directions by a divergent wind field; yet, GPM's formulation requires that puffs remain intact and be advected by the wind velocities at their centroids, and it does not account for the effective enhancement in dispersion. However, these deficiencies are probably not as limiting for long-term concentration averages or in flat terrain settings where wind fields are fairly uniform. In a recent study, RTM and a Gaussian puff model (MESOPUFF) similar to GPM were shown to yield similar results when applied to the relatively flat North Dakota terrain. The input winds were homogeneous for that comparison, and in some cases RTM predicted higher concentrations than did the puff model (Schock, 1981). However, in this complex terrain application, where the winds vary considerably in space, GPM can be expected to overpredict relative to RTM. The differences between GPM and RTM should increase with increasing downwind distance in complex terrain because the effects of convergent and/or divergent winds accumulate with distance. Indeed, this behavior can be observed in the results presented in Chapter 5.

As mentioned earlier, the application of COMPLEX-I for near-source concentration impact calculations compensates for GPM's deficiences near source. To compensate for GPM's deficiencies at moderate to large distances, we applied the Regional Transport Model (RTM) for short periods (24 to 48 hours). It should be noted that if it had been our plan to use only GPM to provide "best estimate" concentration impacts, we would have made modifications to GPM's formulation (e.g., decomposition of puffs into subpuffs when required) to remedy the deficiencies at moderate to large distances. However, such modifications would increase the computation time required by GPM to such an extent that it would be prohibitively expensive even for short-term (24 to 28 hours) applications. RTM does not share GPM's major shortcomings at moderate to long ranges. Furthermore, RTM is a more cost-effective alternative than modification of GPM because it is currently operational and cheaper to execute for selected episodes than an enhanced version of GPM would be. The use of RTM is described in the following subsection.

4.2.1.3 Use of the Regional Transport Model

For calculations of short-term regional-scale concentration averages, we applied the Systems Applications Regional Transport Model (RTM), which is better suited than GPM for treating the dispersion of pollutants from many sources over large transport times and distances. As mentioned earlier, this is true because RTM allows for variations in wind and diffusivity across a puff whereas GPM cannot. This distinction between the model's capabilities is most pronounced after large transport times. Also, this distinction suggests that RTM will predict lower short-term peak concentrations than does GPM. As discussed earlier, GPM will tend to overpredict peak short-term concentrations because its puffs will remain compact even with nonhomogeneous and divergent wind fields present in complex terrain. Indeed, comparison of GPM and RTM results (see Chapter 5) confirms that RTM predictions are lower. However, there are other differences between the models' formulations and in the input data supplied to the two models (greater accuracy and resolution is provided in RTM's input data) that also account for differences in predictions. RTM is too costly to execute for an entire year, so its purpose is only to provide estimates of short-term (3-hour and 24-hour) concentration averages for the worst-case episode identified by GPM when run for an entire year. RTM is run with complex-terrain wind fields generated by the wind model, run in an hourly mode rather than in the composite mode (as was done for the GPM runs) to improve accuracy. For impacts closer to the source, the regional-scale application of RTM is not acceptable because of its coarse receptor spacing and lack of treatment of some important micrometeorological effects. While most previous applications of RTM have been in flat terrain settings, its ability to accept spatially and temporally varying wind, mixing depth, and diffusivity input permit its application to complex terrain. Proper specification of these inputs is the key to RTM's application in complex-terrain settings. Detailed discussions of RTM's formulation can be found in Appendix C.

4.2.1.3.1 Preparation of mixing layer depths for RTM

Mixing layer depths used with the RTM were calculated from four National Weather Service upper-air stations that lie in and around the area of study. These stations are Grand Junction, Colorado, which lies in the southern part of the study region, Denver, Colorado, which is approximately 200 km east of the region, Salt Lake City, Utah, which is approximately 100 km west of the region, and Lander, Wyoming, which is just north of the region.

The mixing layer depths were calculated for the worst-case modeling scenarios identified by the Gaussian Puff Model for the year 1978. The four upper-air stations provided temperature profiles at 5:00 a.m. and 5:00 p.m. MST. The morning temperature profiles almost always revealed a surface-based inversion. The stable mixing layer depths estimated from the morning soundings were averaged to obtain a uniform depth over the entire study area for the nighttime stable periods. Table 4-21 lists the stable layer depths at the four stations and the average values used for the modeling scenarios.

The afternoon temperature profiles on these days from the four upper-air stations revealed that no temperature inversions were present within 20,000 feet of the surface. Thus, the maximum afternoon mixing height was conservatively assumed to be about 3425 meters above sea level. Therefore, daytime mixing height grow to this maximum height above sea level. The depth of the lowest grid layer is the difference between this time varying height and local terrain height. Since RTM is a terrain-following model, the influence of the terrain is then incorporated not only through the wind provided by the Complex-Terrain Wind Model, but also through the mixing layer (the lowest grid layer) depths that vary with terrain. It is assumed that the stable layer depth is constant from 10:00 p.m. MST until two hours after sunrise, or until 8:00 a.m. MST. Then the mixing depth is allowed to rise linearly, starting at the stable layer depth, until it reaches the maximum afternoon mixing depth at 5:00 p.m. MST. The mixing height is then held constant at this height until two hours after sunset (10:00 p.m. MST), when the first layer heights drop to the morning stable layer height. Figure 4-7 illustrates the temporal variations in mixing layer depth.

The current version of the Systems Applications Regional Transport Model contains a second layer that interacts with the mixing (bottom) layer of the model whenever spatial or temporal variations occur at the mixing height field. The top of this second layer is constant over the modeling region. The region top value used in this study is 2300 meters AGL, which minimizes the dilution caused by too deep a second layer, yet retains a second-layer thickness of at least 100 meters over the entire region.

TABLE 4-21. MORNING STABLE LAYER DEPTHS FROM THE FOUR UPPER-AIR STATIONS, AND THE AVERAGE USED BY RTM (in meters)

Day	Time	Grand Junction	Denver	Salt Lake City	Lander, Wyoming	Average
207	0500	260	134	244	229	217
208	0500	143	123	478	339	271
195	0500	540	520	--	400	487
196	0500	260	800	410	503	658
292	0500	330	480	400	400	403
293	0500	415	295	95	310	279
349	0500	--	190	820	600	537
350	0500	--	210	--	--	210

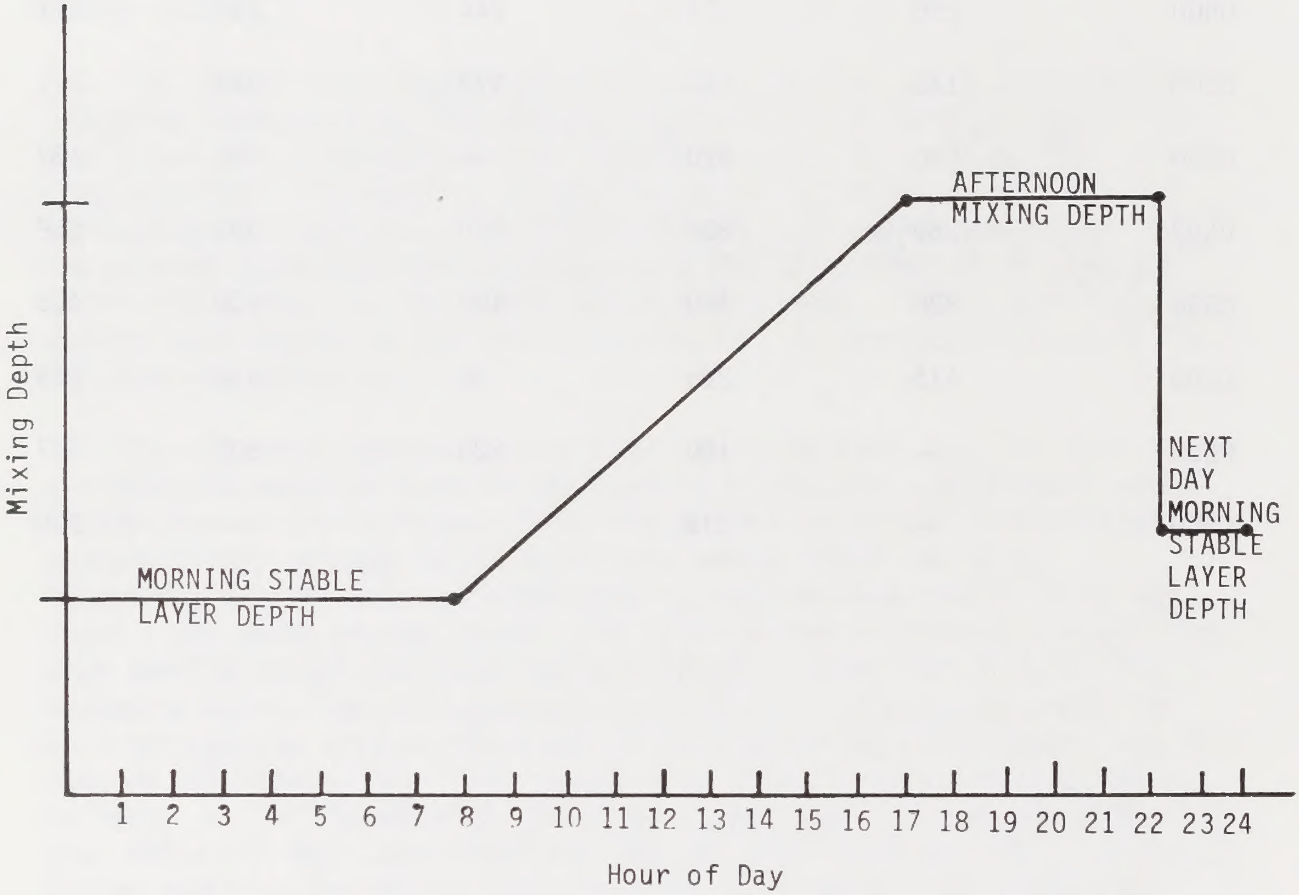

FIGURE 4-7. TEMPORAL VARIATION OF FIRST GRID LAYER DEPTH

The wind fields used by the Regional Transport Model were supplied hourly by the Complex-Terrain Wind Model (CTWM). Since RTM is a terrain-following model and CTWM is a sea-level-based model in which the terrain features are contained within the computational grid, an average of the wind fields at different vertical levels from the CTWM is used as input to RTM. For the lower RTM layer, an average of the CTWM vertical levels of wind fields contained within the RTM layer is used. Thus, when there is a low mixing layer depth, the wind field is represented mostly by the lowest CTWM layer that best represents the drainage flow associated with stable nighttime conditions. In the afternoon, a more geostrophic-like wind field develops because it has a much larger wind component from the second and sometimes the third layer of the CTWM. The upper RTM layer uses wind from the third layer of CTWM exclusively.

The surface wind speeds are needed for the surface layer of RTM. The surface wind speeds are taken from the lowest CTWM layer except when the terrain blocks this layer, in which case the second layer of the CTWM wind field is used.

4.2.1.3.2 Preparation of exposure class input to RTM

Exposure class, which is a measure of near ground-level atmospheric stability due to surface heating or cooling, is required RTM input data. For the morning hours from 0000 to 0800 and evening hours 2200 and 2300, an exposure class value of -2 is used, which corresponds to a stable Pasquill-Gifford classification. For the hours from 0900 to 2100, an exposure class value of 0 is used, which corresponds to a neutral Pasquill-Gifford classification.

4.2.1.3.3 Preparation of diffusivity input to RTM

On the regional scale, pollutant dispersal is strongly dependent on a length-scale characteristic of the effective turbulent eddies. Pertinent field observations indicate that the regional-scale horizontal diffusivity ranges in value from 10^3 to 10^5 m^2/s (Baur, 1973). In a study of the numerical simulation of the atmospheric circulation, Smagorinsky (1963) showed that nonlinear lateral diffusion can be formulated on the basis of similarity theory for turbulence in the equilibrium range (Heissenberg, 1948). Thus, the horizontal diffusivity coefficient can be derived as

$$K_H = 5/4\ (\alpha\Delta)\ |Def| ,$$

where Δ is the grid spacing, ∝ ≈ 0.28, and |Def| is the magnitude of the velocity deformation

$$|\mathrm{Def}| = \left[\left(\frac{\partial v}{\partial x} + \frac{\partial u}{\partial y}\right)^2 + \left(\frac{\partial u}{\partial x} - \frac{\partial v}{\partial y}\right)^2\right]^{1/2} .$$

The temporally and spatially varying fields of horizontal diffusivities used by RTM were calculated from the wind fields using the expressions above. The calculated values ranged from a minimum of 10^3 m^2/s to a maximum of 10^5 m^2/s.

4.2.1.3.4 Preparation of chemical reaction rate input to RTM

The homogeneous oxidation of SO_2 to $SO_4^=$ is a function of the intensity of solar radiation. The Regional Transport Model allows this oxidation to vary spatially and temporally over the modeling region. The model treats the oxidation rate as a function of the solar zenith angle, or the solar intensity in the absence of cloud cover. RTM calculates the oxidation rate for each grid cell and time on the basis of user-prescribed maximum noontime oxidation rate at the southernmost latitude, and the minimum nighttime oxidation rate for the region. The maximum oxidation rate used for this application is 1.32 percent per hour reported by Altshuller (1979). Less is known about the minimum nighttime oxidation rate of SO_2, but the minimum nighttime oxidation rate used here is 0.01 percent per hour.

4.2.1.4 Use of the Complex-Terrain Wind Model

The Systems Applications Complex-Terrain Wind Model (CTWM) is a three-dimensional diagnostic model that solves the equation of mass continuity including parameterizations of the physical processes occurring in complex terrain. The model assumes steady-state conditions, and given boundary conditions and information about the stability, terrain, surface roughness, and temperature distributions within the modeling region, the model calculates a three-dimensional gridded wind field. A complete description of the formulation of CTWM can be found in Appendix C.

In the past, CTWM has been applied to many different complex terrain settings, and has usually been applied for one-hour periods. To model a 24-hour episode, for example, 24 one-hour runs would be made. This same method of CTWM application was used to generate wind fields for the RTM simulations of 24- to 48-hour episodes.

The upper-air wind data from each of the four National Weather Service monitoring sites at Salt Lake City, Utah; Lander, Colorado; Grand Junction, Colorado; and Denver, Colorado, provided wind information along the edges of the region at 12-hour intervals. The flow vectors for the intervening hours were obtained by means of linear interpolation. An examination of these data and the surface wind measurements collected at four U-a and U-b sites allowed the determination of wind model boundary conditions for the modeling region for each hour of each day modeled. The wind model was exercised on a 67 x 45 grid of 4-km cells. The origin was at 550. E, 4310. N, UTM zone 12. The grid extended 268 km to the east and 180 km to the north. The bottom of the modeling region was chosen to be 4260 feet above MSL, and the top, 11,940 feet above MSL. The region was divided into three layers of equal thickness, approximately 3280 feet each. Up-slope and down-slope flow parameters were determined as described in Appendix C.

However, for the GPM simulation of an entire year, the hourly mode of CTWM application would be too costly. Instead, a novel method of application was devised for this study, which is considerably less costly than the hourly approach. The new method is called the "composite" mode and involves the following steps:

(1) Temporally interpolate between 0000Z and 1200Z upper-level soundings of wind at Salt Lake, Lander, Grand Junction, and Denver to yield hourly values at each site for the entire year.

(2) Vector average the hourly upper level winds measured at the four sites and interpolated in step 1.

(3) Determine the characteristics of up- and down-slope flow regimes. This is accomplished by comparing the surface-level wind direction at the U-a, U-b site in the Uinta Basin with the average upper-level wind directions from step (2) at the same hour and with the terrain slope at each surface monitoring station. Generalize several slope wind regimes.

(4) Apply a methodology for automatic (by computer) identification of 8760 hourly wind regimes (for an entire year) and creation of an hourly data input file to be used later. Regimes are identified using average upper-level flow direction and speed in the region and the intensity of up-slope and down-slope winds. The methodology includes the following elements for each hour of the year:

- Check several stations for measured surface wind direction to the slope wind input parameter.

- Check average upper-level wind speed and direction from step (2).

- Determine what component of average upper-level flow is aiding or retarding slope flow. Then determine the prevailing slope flow regime using the measured slope winds (minus the component of the upper-level flow).

(5) Run wind model for 16 cardinal upper-level wind directions and an arbitrary wind speed of 10 m/sec and store the resulting wind field output files.

(6) Run wind model for six slope wind regimes with zero upper-level wind velocity and store the resulting wind field output files. The six slope regimes are identified in step (3).

(7) Calculate composite wind field for each hour of the year (8760 hours/year). The steps for calculating a composite wind field for each hour are

- Scale the wind field output file (i.e., multiplication of all wind speeds by a scaler) whose assumed upper-level wind direction is closest to the mean upper-level flow direction occurring during the hour. The scaling factor is computed by dividing the mean upper-level wind velocity for the hour by the arbitrary velocity assumed in the wind model runs. Scaling of wind fields is allowable because the CTWM is based upon the solution of an eliptical partial differential equation. Hence, the result of multiplying a predicted wind field by a factor is identical to the wind field predicted by the model after multiplying the driving wind (boundary condition) input by the same factor. The former, however, is considerably less costly.

- Superimpose (vector addition) the wind field output file for the slope wind category appropriate for the hour upon the wind field file scaled by upper-level wind conditions for the hour. Superpositioning of model output is also a mathematically valid operation given the form of the model equations.

An illustration of the methodology applied to a hypothetical situation is provided in Figure 4-8. The main disadvantage of the "composite" mode of application is the requirement that the upper-level flow (boundary condition) be represented by an average wind speed and direction. The hourly mode allows both horizontal and vertical variations of this boundary condition and hence is capable of more realistic results. However, the "composite" mode was tested by comparison of surface winds measured at several sites in the modeling region during 25 randomly selected hours during 1978 with the corresponding winds predicted by the model. The comparison showed that the predicted surface wind directions were within 45° of the measured wind directions on all but two occasions. Predicted wind speeds were within 30 percent of the measured wind speeds in all but four instances where they were within 60 percent of the measured speeds.

4.2.1.5 Use of EKMA and PLUVUE

A two-dimensional photochemical model has been proposed to address the possible impacts of photochemical pollutant (O_3 or oxidant) due to secondary development associated with the proposed facilities. The two-dimensional photochemical model (OZIPM or Level II-EKMA) is that used in the development of ozone isopleths for control strategy purposes (Whitten and Hogo, 1978). Although the OZIPM was developed to facilitate the Empirical Kinetics Modeling Approach (EKMA), it can be used to perform single trajectory (or two-dimensional) calculation for ozone prediction. The "trajectory" mode of the OZIPM (or EKMA) model has been used in several studies for comparison purposes with more sophisticated three-dimensional grid models (Whitten, Hogo, and Johnson, 1981; Whitten and Hogo, 1981; Hogo, Whitten, and Reynolds, 1982). Although the OZIPM (and the EKMA procedure) is traditionally known as an urban photochemical box model, it can also be used in rural areas.

The OZIPM is a Lagrangian model that follows a parcel of air assumed to vary through space and time on the basis of some assumption of wind speed and wind direction. The parcel of air contains initial concentrations of hydrocarbon and NO_x that react according to a chemical mechanism. During the course of the transport of the puff along the trajectory, fresh emissions are introduced and the parcel is allowed to diffuse within a layer aloft. Pollutant concentrations are assumed to be spatially constant; therefore, there is no horizontal exchange of reactant concentrations.

The "trajectory" mode of the OZIPM computer code is used to consider impacts due to specific sources in rural areas if the horizontal area (or size) of the parcel is small in relation to the size of the source. In this situation the horizontal exchange of reactants is not important.

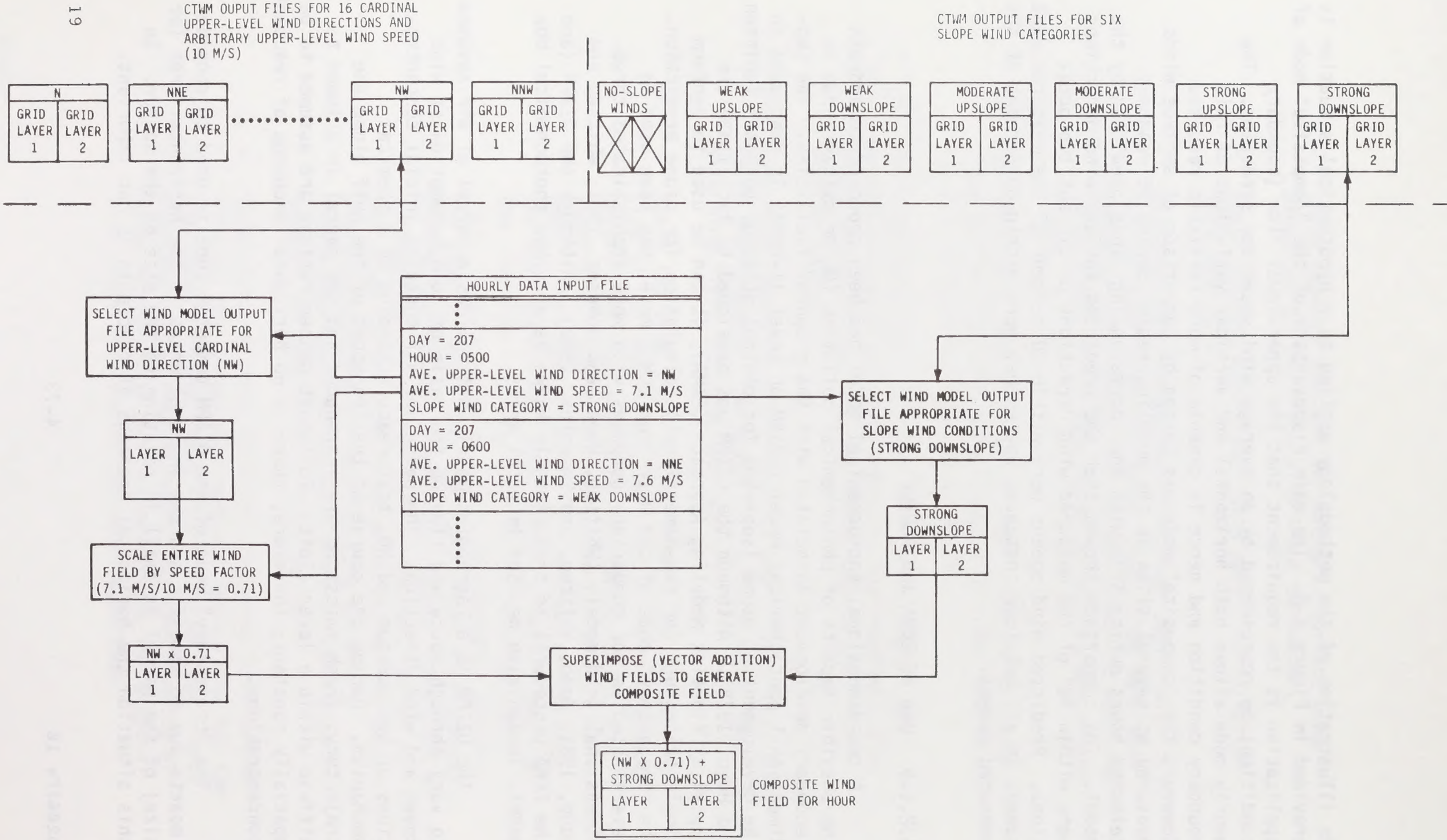
CTWM OUPUT FILES FOR 16 CARDINAL UPPER-LEVEL WIND DIRECTIONS AND ARBITRARY UPPER-LEVEL WIND SPEED (10 M/S)
CTWM OUTPUT FILES FOR SIX SLOPE WIND CATEGORIES
N
NNE
NW
NNW
GRID LAYER 1
GRID LAYER 2
NO-SLOPE WINDS
WEAK UPSLOPE
WEAK DOWNSLOPE
MODERATE UPSLOPE
MODERATE DOWNSLOPE
STRONG UPSLOPE
STRONG DOWNSLOPE
HOURLY DATA INPUT FILE
DAY = 207
HOUR = 0500
AVE. UPPER-LEVEL WIND DIRECTION = NW
AVE. UPPER-LEVEL WIND SPEED = 7.1 M/S
SLOPE WIND CATEGORY = STRONG DOWNSLOPE
DAY = 207
HOUR = 0600
AVE. UPPER-LEVEL WIND DIRECTION = NNE
AVE. UPPER-LEVEL WIND SPEED = 7.6 M/S
SLOPE WIND CATEGORY = WEAK DOWNSLOPE
SELECT WIND MODEL OUTPUT FILE APPROPRIATE FOR UPPER-LEVEL CARDINAL WIND DIRECTION (NW)
NW
LAYER 1
LAYER 2
SCALE ENTIRE WIND FIELD BY SPEED FACTOR (7.1 M/S/10 M/S = 0.71)
NW x 0.71
SELECT WIND MODEL OUTPUT FILE APPROPRIATE FOR SLOPE WIND CONDITIONS (STRONG DOWNSLOPE)
STRONG DOWNSLOPE
SUPERIMPOSE (VECTOR ADDITION) WIND FIELDS TO GENERATE COMPOSITE FIELD
(NW X 0.71) + STRONG DOWNSLOPE
COMPOSITE WIND FIELD FOR HOUR

FIGURE 4-8. SCHEMATIC DIAGRAM OF METHODOLOGY FOR APPLYING THE COMPLEX-TERRAIN WIND MODEL (CTWM) IN THE "COMPOSITE" MODE (HYPOTHETICAL HOURLY INPUT DATA ARE USED IN THIS EXAMPLE)

For this study, a slightly modified version of the OZIPM computer code was used (Hogo and Whitten, 1982). The Carbon-Bond Mechanism (CBM), which is a photochemical kinetics mechanism developed for urban air quality models (Killus and Whitten, 1981), was used for the present study. Although the CBM is primarily used for urban air quality studies, all reactions that are important in rural areas (such as those involving terpenes) are also found in the CBM. The only reaction not included in the CBM and which may be of concern is that involving methane. The reactivity of methane is small enough that exclusion of methane chemistry has virtually no impact on ozone predictions. A technical discussion of the formulation of OZIPM (and EKMA) is provided in Appendix C.

The potential for visibility impacts due to primary particulate emission and secondary particulate formation was addressed using PLUVUE. PLUVUE has most often been used to address the visibility impacts of isolated, elevated point sources. However, the model is capable of treating multiple ground-level sources, including both point and area sources. A discussion of PLUVUE's formulation can be found in Appendix C.

4.2.1.6 Preparation of Time-Invariant Terrain and Surface Cover Model Input Data for RTM, GPM, CTWM, and COMPLEX-I

The Regional Transport Model, the Gaussian Puff Model, and the Complex-Terrain Wind Model require some spatially varying, time-invariant input data. These data include average terrain heights (required by COMPLEX-I, RTM, CTWM, and GPM), roughness lengths as a function of location (required by CTWM and RTM), and deposition velocity as a function of location (required by RTM).

The Gaussian Puff Model and Complex-Terrain Wind Model require gridded values of average terrain heights. These gridded values were extracted from a tape acquired from the National Geophysical and Solar-Terrestrial Data Center. The tape provides gridded terrain heights on a 30-second grid for the entire United States. The data are also used to prepare receptor height information for COMPLEX-I.

RTM, GPM, and CTWM also require aerodynamic roughness characteristics of the underlying terrain. The interaction of the atmospheric boundary layer with the underlying surface will modify the wind in lower-level flows. Indirectly, through the modification of wind profiles and turbulent diffusivities, the terrain surface can affect the ultimate concentration distribution at the ground. Surface roughness, then, is a key parameter of these wind and air quality models.

In general, the surface roughness length, z_0, for a given surface cover may vary as a function of wind speed, wind direction, and season. In extensive studies of z_0 performed in the Sacramento, California (Myrup and Morgan, 1972) and Philadelphia, Pennsylvania (Slade, 1968) areas, it was found that the surface roughness length z_0 varied greatly as a function of season and wind direction. The variation of z_0 as a function of wind speed is especially important over water (Garratt, 1977) or tall deformable plants (Geiger, 1971). However, as a first approximation an average roughness length for a given surface type can be assigned.

The determination of roughness lengths for this study area is made from United States Geological Survey maps. Land-use categories defined by the USGS maps are given in table 4-22. The study area was divided into 2-km grids, and each grid cell was assigned a USGS land-use category (see figure 4-9). These land-use categories define the most prominent vegetation type for this area from which the average surface roughness length can be estimated. The deposition velocities for SO_2, SO_4, and TSP are also functions of vegetation type. Table 4-23 contains the USGS land-use categories used in this study and the roughness lengths and deposition velocities defined for each category. The deposition velocities used in this study were reported by McMahon and Denison (1978) in their survey of empirical atmospheric deposition parameters. It should be noted that the particulate deposition velocity is sometimes intended to represent both the deposition of fine particulates and the settling of larger particulates. The values used here are more representative of deposition velocities than of settling velocities because settling of larger particulates usually occurs close to the source, whereas deposition processes are more important on the regional scale. The Gaussian Puff Model uses spatially constant deposition velocities of 1 and 0.5 centimeter per second for SO_2 and TSP, respectively.

TABLE 4-22. USGS LAND USE CATEGORIES

Category No.	Description
	Urban
11	Residential
12	Commercial and services
13	Industrial
14	Transportation, communications, utilities
15	Industrial and commercial complexes
16	Mixed urban or built-up land
17	Other urban or built-up land
	Agricultural
21	Cropland and pasture
22	Orchards, groves, vineyards, nurseries, horticultural areas
23	Confined feeding operations
24	Other
	Rangeland
31	Herbaceous
32	Shrub and brush
33	Mixed
	Forest land
41	Deciduous
42	Evergreen
43	Mixed
	Water
51	Streams and canals
52	Lakes
53	Reservoirs
54	Bays and estuaries
	Wetland
61	Forested
62	Nonforested

TABLE 4-22 (Concluded)

Category No.	Description
	Barren land
71	Dry salt flats
72	Beaches
73	Sandy areas other than beaches
74	Base-exposed rock
75	Strip mines, quarries, gravel pits
76	Transitional areas
77	Mixed
	Tundra
81	Shrub and brush
82	Herbaceous
83	Bare ground
84	Wet
85	Mixed
	Perennial snow or ice
91	Perennial snowfields
92	Glaciers

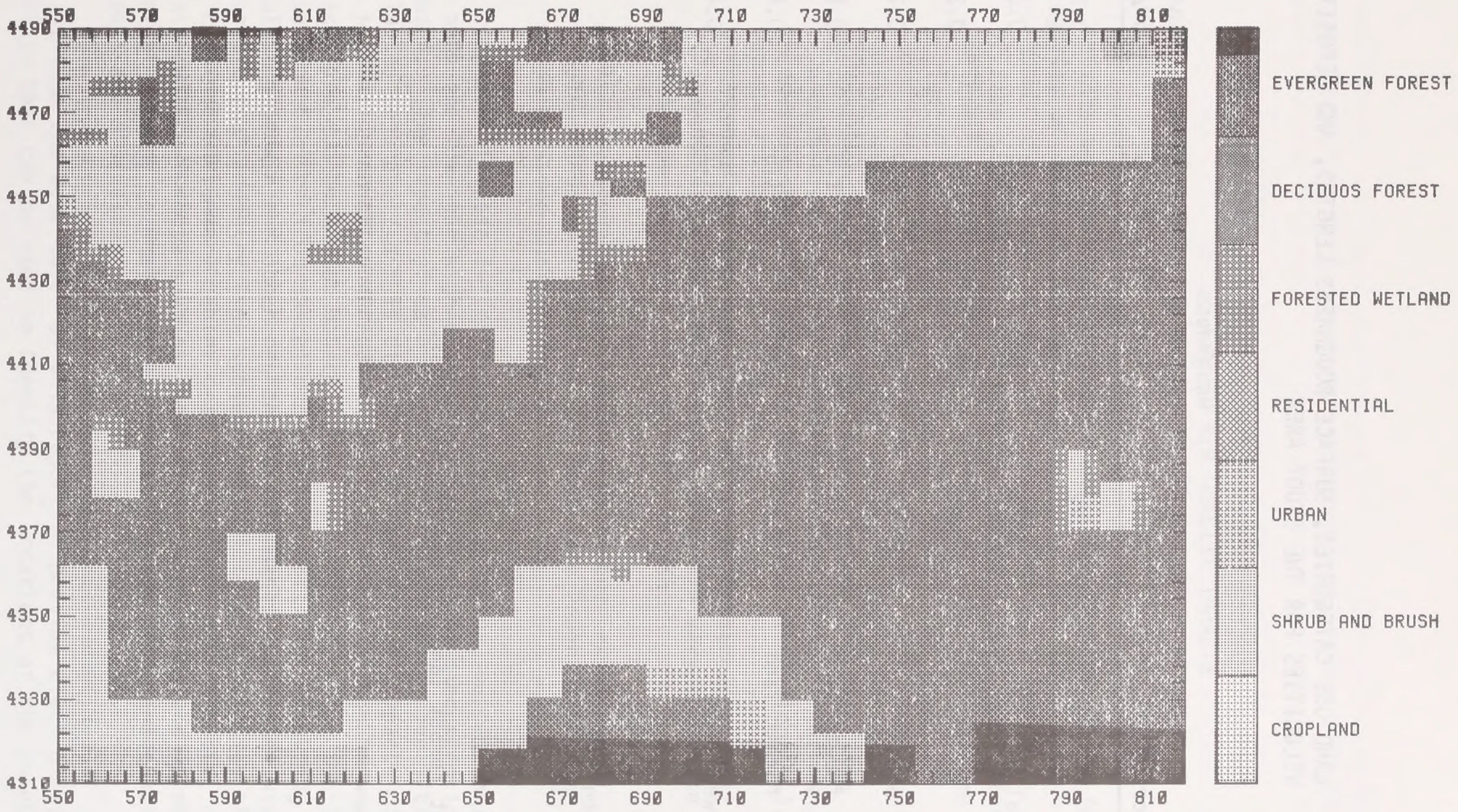

FIGURE 4-9. SPATIAL DISTRIBUTION OF LAND USE CATEGORIES

TABLE 4-23. LAND USE CATEGORIES, SURFACE ROUGHNESS LENGTHS, AND DEPOSITION VELOCITIES FOR THE STUDY AREA

Category Number	Description	Percent of Area	Roughness Length Z_0 (cm)	Deposition	Velocity	(cm/s)[*]
				SO_2	SO_4	TSP
10	Urban	1.22	40[†]	1.5	0.3	0.5
11	Residential	0.08	60[†]	1.5	0.3	0.5
21	Cropland	0.45	25[§]	1.0	0.2	0.4
32	Shrub and brush	34.03	35[§]	0.9	0.2	0.4
41	Deciduous forest land	0.12	270[**]	1.5	0.5	0.7
42	Evergreen forest land	62.60	280[††]	1.5	0.5	0.7
61	Forested wet lands	1.48	150[§§]	1.1	0.4	0.6

---

[*] McMahon and Denison (1978)
[†] Myrup and Morgan (1972)
[§] Ranzieri (1975)
[**] Szeicz (1969)
[††] Sellers (1965)
[§§] Assumed 50 percent forest land, 50 percent wet lands.

5 REGIONAL AIR QUALITY IMPACTS

In this section we examine the cumulative impacts of the following categories of emission sources:

> Five site-specific Uinta Basin synthetic fuel facilities (Enercor-Mono Power, Magic Circle, Paraho, Syntana, and Tosco).

> Five site-specific and four conceptual Uinta Basin synthetic fuel facilities (including the multiple-site Geokinetics oil shale development and the Sohio tar sands development, both at a conceptual stage of development).

> Colorado oil shale development in the Piceance Basin at several sites (all development plans are very uncertain at this time for this category of sources).

> All the above sources together plus other existing or planned projects such as the Moon Lake Power Plant and White River Shale Project.

Impacts of these different subsets of emission sources were evaluated for both the low- and high-oil-production scenarios discussed in sections 1 and 4. (The impact of each of the five site-specific facilities was evaluated separately and is discussed in section 6.) Impacts of the low- and high-oil-production scenarios were also broken out as to whether impacts are due to direct source emissions from industrial facilities (see subsection 5.2) or from so-called secondary emissions resulting from population growth and other regional developments associated with the synthetic fuel industry (see subsection 5.3). All categories of impacts are combined in summary tables (see subsection 5.4). Finally, other types of air quality impacts such as cumulative regional impacts on photochemical oxidant (ozone), visibility, acid deposition, and construction impacts are discussed.

Inside the back cover of this report we provide clear plastic overlays that can be used to identify the locations of the point sources, geographical features, and terrain elevations in the study region. The graphic scale of the plots is indicated by the UTM coordinates (in kilometers).

5.1 CONCENTRATION ESTIMATION APPROACH

As discussed in Section 4, a variety of modeling approaches were used in the analysis of regional air quality impacts; principally, the following models were used:

> Gaussian Puff Model (GPM) applied for every 3-hour period in the modeled year (1978).

> COMPLEX-I applied for every 3-hour period in the modeled year for receptors near sources for which individual emission points were aggregated in GPM calculations.

> Regional Transport Model (RTM) applied for every hour in four 48-hour episodes of interest with respect to long-range transport and regional impacts at sensitive receptors (Flat Tops Wilderness and Dinosaur National Monument).

Because each of these models has distinct strengths and limitations, as stated in Section 4, it is difficult to obtain a consistent, overall picture of potential future air quality impacts on the basis of one model. For example, we know that because of source aggregation, GPM is not well-suited to the calculation of near-source impacts, especially for sources with multiple ground-level release points. We also suspect that assumptions regarding puff diffusion used in GPM are not appropriate particularly at large distances downwind from a source. Thus, it appears appropriate to supplement the estimates of near-source and long-range ground-level air quality impacts calculated using GPM with additional estimates on the basis of COMPLEX-I and RTM calculations, respectively.

We believe that individual model results must be interpreted with considerable care. For the reasons stated in the following subsections, we believe that for some applications* GPM is conservative. To use GPM results without qualifications, in our opinion, could result in significant overestimates of both short- and long-range air quality impacts. It should be recalled that the basic intent in using GPM in the analysis was to identify by screening a year's meteorological data worst-case episodes with regard to maximum impacts at distant sensitive receptors for more detailed analysis with RTM.

Some government agencies that have reviewed the draft report of this study have commented that higher concentrations (larger air quality impacts) than those estimated here cannot be ruled out. We agree with this judgement. Since most of the sources that were modeled in this study are not currently in operation and since sufficient air quality monitoring data are not available in the region, it is not possible to rigorously evaluate the performance of GPM and other models in the region. Statements regarding the adequacy and conservatism of various models can be based solely on experience with other similar models in different settings and theoretical considerations. Therefore, model interpretation is not a rigorous, unambiguous process.

We, as authors of this report, are responsible for the model calculations and the assumptions upon which they are based. The estimated ranges of concentrations presented in this study are our best estimates of future impacts based on the data available to us at this time. However, state and federal regulatory agencies may use quite different modeling approaches and interpret model results differently in permit decisions.

5.1.1 Conservatism of the Gaussian Puff Model

The modeling plan calls for the use of GPM as a conservative screening model for identifying potential worst-case days at sensitive receptor areas and for estimating annual average concentration impacts. The plan also calls for the use of another model, RTM, to examine in greater detail the worst-case days. Clearly, assumptions made in formulating or applying a screening model affect the degree of conservatism of its concentration predictions. In line with the scope of the work, assumptions made in the applications of GPM in this study were intended to be conservative and realistic given the emphasis of the investigation on regional-scale transport to sensitive, complex terrain receptor areas.

---

* Those of principal interest to the practice of air quality management: maximum and second-highest short-term concentrations at receptors near sources and at sensitive receptors (Class I areas) far downwind.

Certainly, a simpler screening model, such as EPA's VALLEY Model, will yield higher concentrations than GPM in some locations but assumptions made in VALLEY are inappropriate or unrealistically conservative for regional-scale transport problems (Lantz, et al., 1976; Burt, 1977). Furthermore, as with any screening model, one can never be sure that the predicted worst-case day will be the true worst-case day. Assumptions made in the modeling analysis can greatly affect what day is identified. More realistic yet still conservative assumptions should more likely lead to the correct identification of worst-case days than inappropriate or less realistic, more conservative assumptions.

The Gaussian Puff Model is expected to be conservative, especially close to the emissions sources (say less than 25 km) and at large downwind distances (say 50-60 km downwind). This expectation is based on several factors.

First, the GPM model results are expected to be generally conservative for near-source impacts (< 25 km) where there are multiple, ground-level releases of emissions (e.g., TSP) at a given facility. In this analysis, because of cost considerations, multiple emissions (there are as many as 30 TSP emission sources at oil shale facilities) are treated as emissions from a single point in the center of the emission source. Furthermore, wind field definition in GPM is based upon upper-level wind characterization, which is appropriate for long-range transport. For short-range, near-source calculations, lower-level or surface winds are more appropriate, and these exhibit greater temporal variability than upper-level winds and hence would result in lower concentration averages. To more rigorously model the near-source impacts of multiple ground-level emissions, we used COMPLEX-I (see Section 6).

At all distances, including both near-source and far-source cases, the use of Pasquill-Gifford Class D stability dispersion coefficients that were derived for flat-terrain should tend toward conservative predictions in complex terrain. Many studies have shown that the dispersion potential in complex terrain is enhanced many fold, 10 to 15 times, over flat terrain dispersion rates (Howard et al., 1974; Start et al., 1974; Shearer et al., 1977; Kao and Turner, 1976; Bass et al., 1981). Even in stable flow conditions in complex terrain, Pasquill-Gifford Class D dispersion coefficients are likely to be conservative. Also, additional dilution is expected to result from daytime heating and resulting convective mixing throughout the mixed layer. These processes rapidly result in uniform vertical mixing throughout the mixed layer (the convective boundary layer), which is typically 1000 meters to over 4000 meters thick. By comparison, the vertical dispersion coefficient for Pasquill D stability at 50 km is 320 meters. Dispersion conditions during the daytime are often A, B, or C.

The treatment of plume-terrain interaction used in GPM is also expected to be conservative for regional-scale transport considerations. We assume that the plume centerline may approach elevated terrain features to within one-half of its effective plume height. The assumption is identical to the worst-case treatment used for neutral stability in EPA screening models (Irwin and Turner, 1981; Pierce and Turner, 1980). However, recent studies (Bass et al., 1981; Egan, 1975; Lavery et al., 1982) indicate that this assumption is the worst-case in neutral conditions and sometimes in stable conditions except over three-dimensional terrain features (isolated hills as opposed to long ridges); very few isolated terrain features existed within our modeling region. This behavior is not surprising when one considers that air can flow over and around isolated terrain obstacles, but is constrained to flow only over the top of two-dimensional features, in which case the mass and momentum requirements prevent large streamline compression. A more conservative treatment of plume impingement on terrain obstacles, such as the 10 m miss height used in VALLEY, are also of questionable validity after a plume's first encounter with terrain (Burt, 1977); a considerable amount of high terrain lies between the major emission sources and the most sensitive receptors in this regional-scale analysis. It is unlikely that any plumes which impinge on near-source terrain features could be transported large distances in concentrated form because of the enhanced diffusion which is generated in the proximity of the terrain.

At increasing distances from the source, a basic deficiency in the puff modeling approach becomes more limiting. At large distances the size of the puffs becomes large enough so that the treatment of puff advection using the winds at the puff's center of mass is unrealistic. This deficiency is especially important in complex terrain. For example, the pollutant mass conceptually contained within a large puff will likely be advected in several directions by a divergent wind field. Yet GPM's formulation requires that puffs remain intact and be advected by the wind velocities at their centroids, and it does not account for the effective enhancement in dispersion. However, these deficiencies are probably not as limiting for long-term concentrations, such as annual averages, because compact puffs will impact receptors less often, thereby offsetting the higher short-term impacts, or in flat terrain settings where wind fields are fairly uniform. In a recent study, RTM and a Gaussian puff model (MESOPUFF) similar to GPM were shown to yield similar results when applied to the relatively flat North Dakota terrain. The input winds were homogeneous for that comparison, and in some cases RTM predicted higher concentrations than did the puff model (Schock, 1981). However, in this complex-terrain application, where the winds vary considerably in space, GPM can be expected to overpredict relative to RTM. The differences between GPM and RTM should increase with increasing downwind distance in complex terrain because the effects of convergent and/or divergent winds accumulate with distance. Indeed this behavior can be observed in the results described in the next subsection.

Other factors which weigh in favor of conservatism in GPM are found in its treatment of deposition and transformation of pollutants. Only dry deposition is accounted for in GPM. Scavenging of pollutants by precipitation or clouds, which tends to reduce the atmospheric pollutant burden, is not accounted for. Also, only treatment of homogeneous gas-phase conversion of SO_2 to SO_4 is included in GPM. Heterogeneous conversion processes, which also reduce the atmospheric burden of SO_2 (Altshuller, 1979), are not considered.

5.1.2 Comparing GPM and RTM Calculations

Another way to evaluate the potential conservatism of GPM is to compare GPM results with those of other regional models that are expected to be more realistic, such as RTM (see Section 4.2).

Comparisons between GPM and RTM calculations of regional 24-hour average SO_2 concentrations were performed on four days of particular interest, assuming a high-oil-production scenario. These days are as follows:

> 27 July 1978, a day for which GPM calculated highest concentrations several kilometers west of Flat Tops Wilderness.

> 20 October 1978, a day for which GPM calculated highest concentrations within Flat Tops.

> 15 July 1978, a day for which GPM calculated the second highest 24-hour average concentrations in Dinosaur. (On the day with the highest concentrations modeled by GPM in Dinosaur, 1 May 1978, significant precipitation occurred, which would have scavenged SO_2 in the atmosphere.)

> 16 December 1978, a day during a high-pressure stagnation episode when surface winds were light and decoupled from rather strong upper-air winds. (GPM calculations indicated relatively low regional SO_2 concentrations on this day because GPM was driven by the strong, upper-air winds, not the light, decoupled lower-level winds.)

5.1.2.1 27 July 1978, Worst-Case Impacts

The first comparison between GPM and RTM was performed for a day (27 July 1978) in the year modeled with GPM that resulted in the highest 24-hour average SO_2 concentration in the vicinity of the Flat Tops Wilderness. This 24-hour SO_2 concentration was predicted by GPM to be 19 $\mu g/m^3$ and to occur to the west of Flat Tops. (The highest modeled 24-hour concentration within Flat Tops occurred on 20 October 1978 and was 12 $\mu g/m^3$.) The Regional Transport Model, RTM (see discussion of this model in Section 4.2, and Appendix C), was exercised for the meteorological conditions on this 27 July 1978 day. Figure 5-1(a) and (b) compare the 24-hour average SO_2 concentrations using these two models for this one day.

It should be noted that RTM was exercised and initiated with a background SO_2 concentration of 1.5 $\mu g/m^3$. Although some of this background SO_2 is transformed to sulfate and/or deposited during the RTM simulation, it is possible that up to 1.5 $\mu g/m^3$ of the RTM-calculated SO_2 concentration is the assumed background. Thus, one must be careful interpreting the RTM isopleth maps because between 0 and 1.5 $\mu g/m^3$ of the calculated SO_2 concentrations could be part of the assumed background value. Subtracting anywhere from 0 to 1.5 $\mu g/m^3$ would give an indication of the incremental inpact of sources in the region. There is uncertainty in the amount of 24-hour average background SO_2 at any receptor point in the region because it is not known how much of the 1.5 $\mu g/m^3$ is deposited or converted. Thus, RTM results are stated with a 1.5 $\mu g/m^3$ uncertainty range.

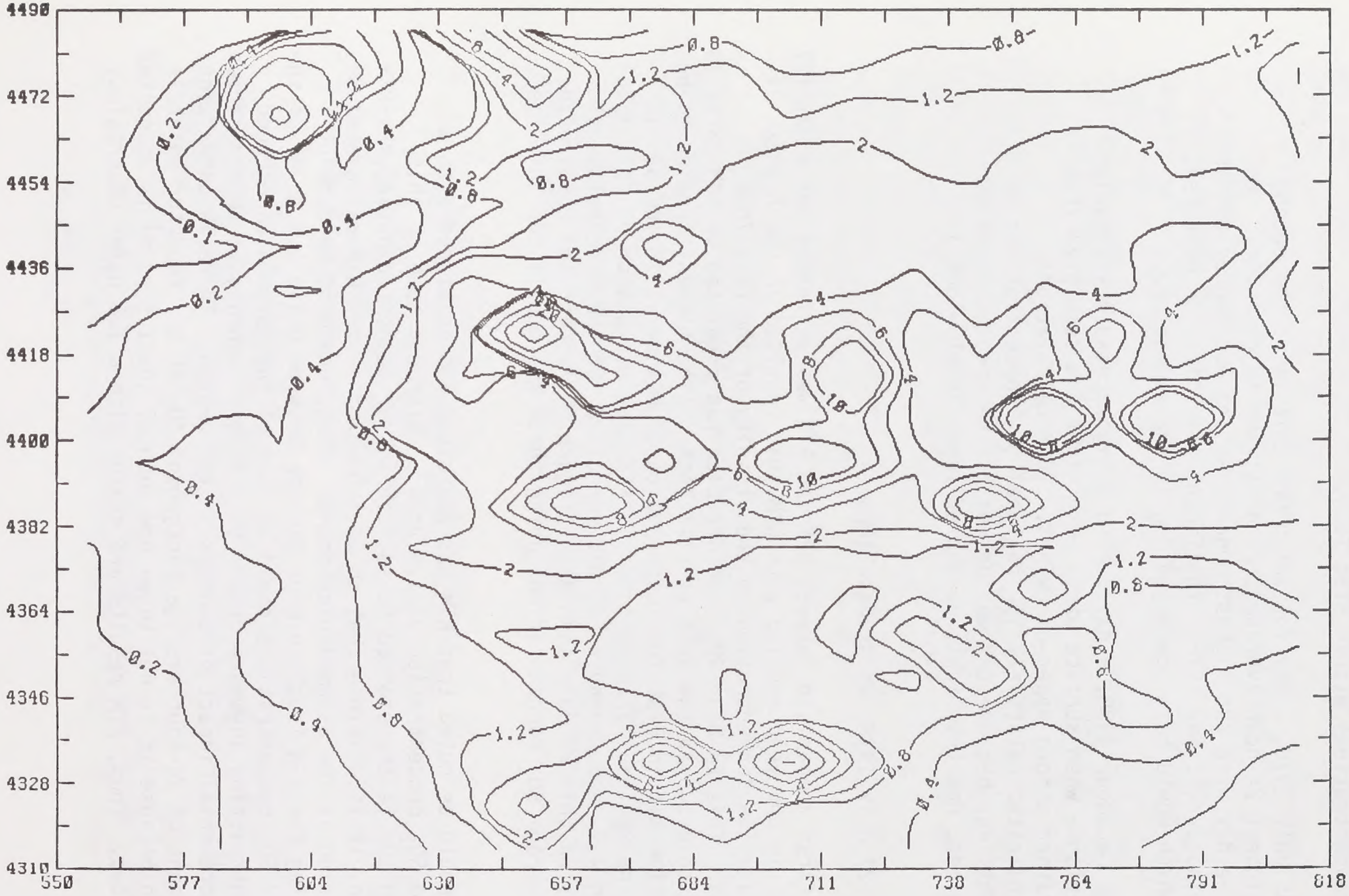

(a) 27 July 1978, on the basis of GPM calculations

FIGURE 5-1. COMPARISONS OF 24-HOUR SO_2 CONCENTRATION ESTIMATES ON FOUR WORST-CASE DAYS IN 1978 WITH IMPACTS RESULTING FROM DIRECT SOURCE SO_2 EMISSIONS DURING THE HIGH-OIL-PRODUCTION SCENARIO

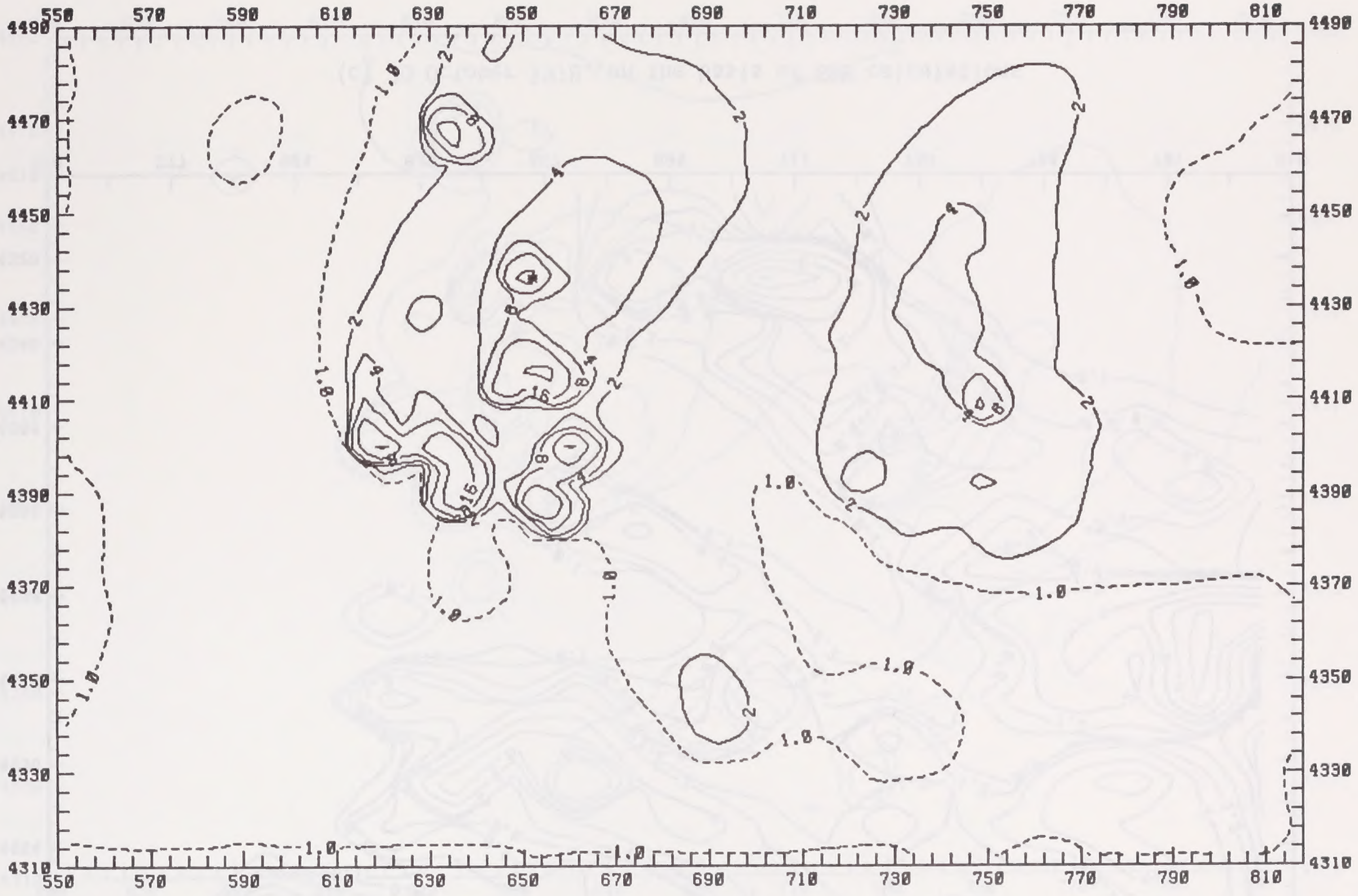

(b) 27 July 1978, on the basis of RTM calculations

FIGURE 5-1 (Continued)

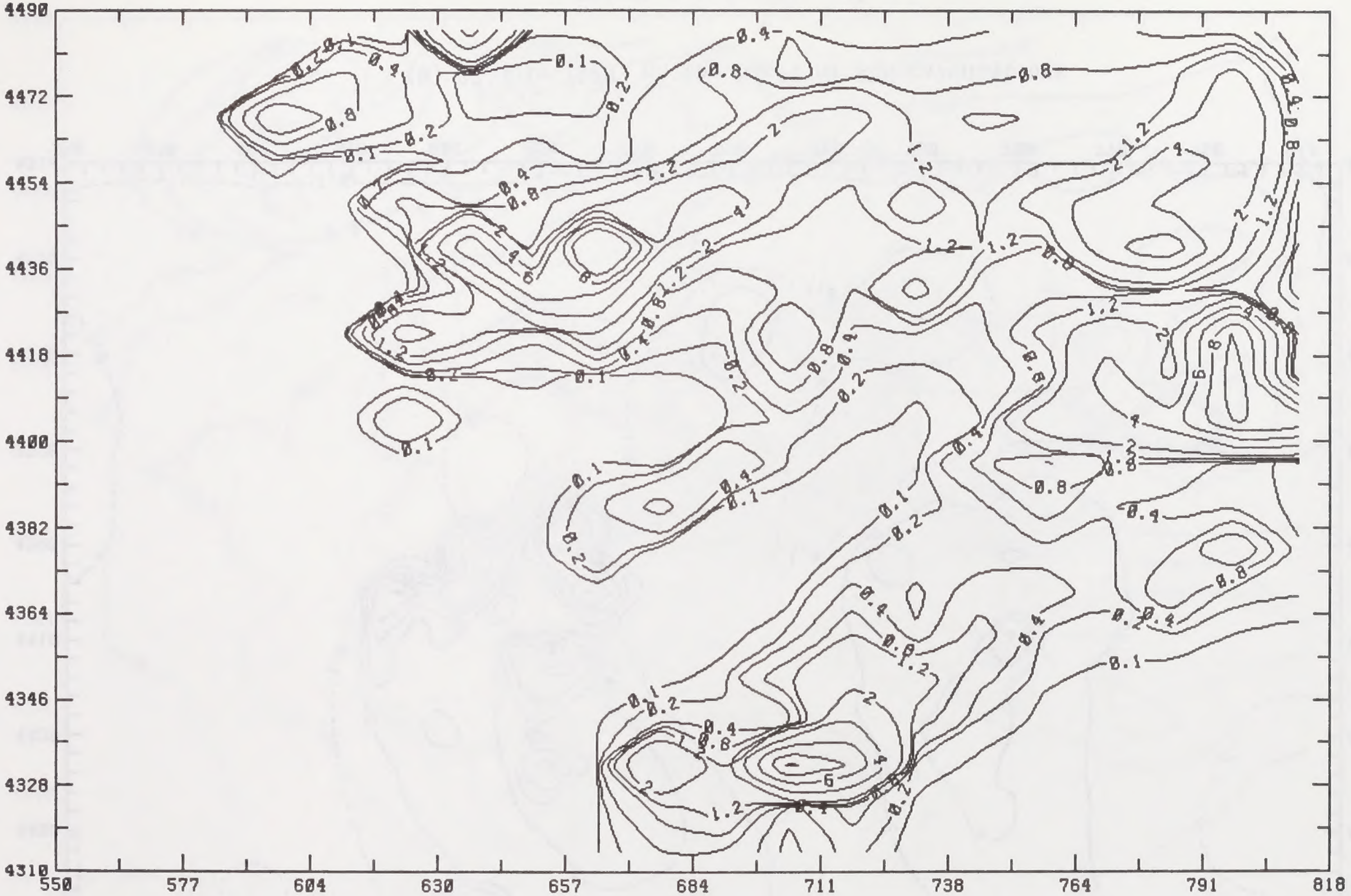

(c) 20 October 1978, on the basis of GPM calculations

FIGURE 5-1 (Continued)

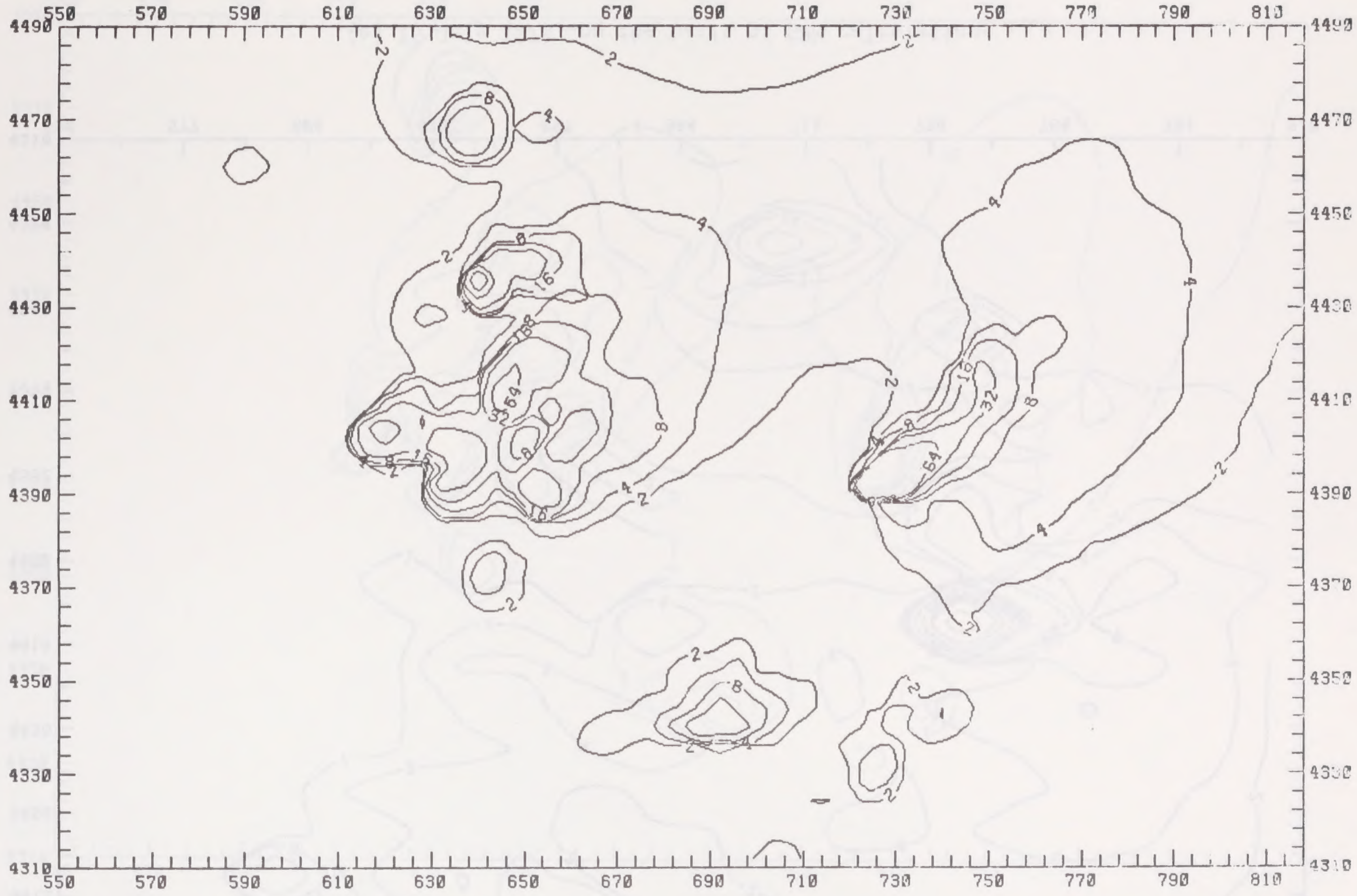

(d) 20 October 1978, on the basis of RTM calculations

Note:
Concentration isopleths greater than 64 μg/m^3 near the Chevron facility have been deleted to correct an error in emission source aggregation.

FIGURE 5-1 (Continued)

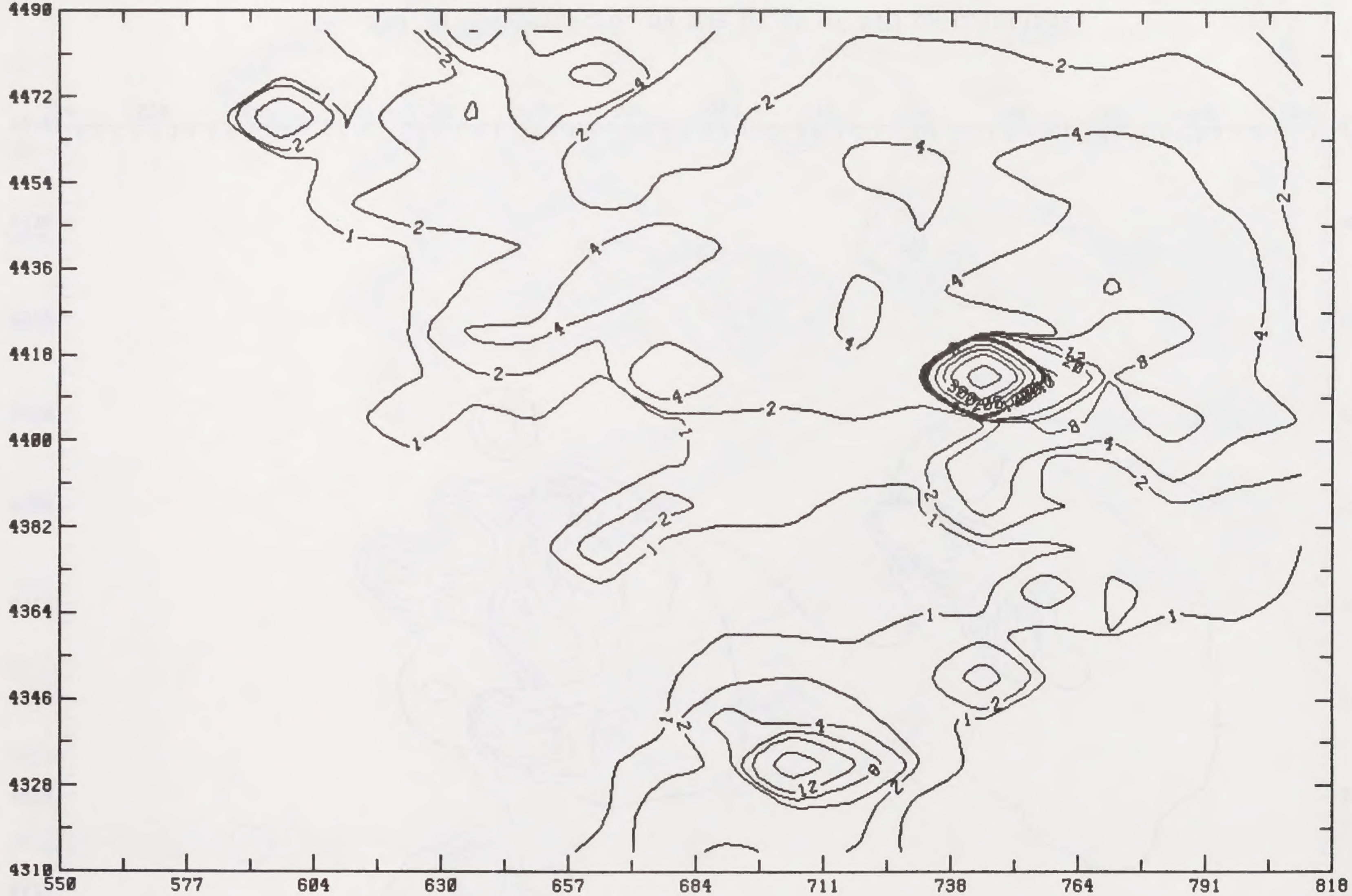

(e) 15 July 1978, on the basis of GPM calculations

FIGURE 5-1 (Continued)

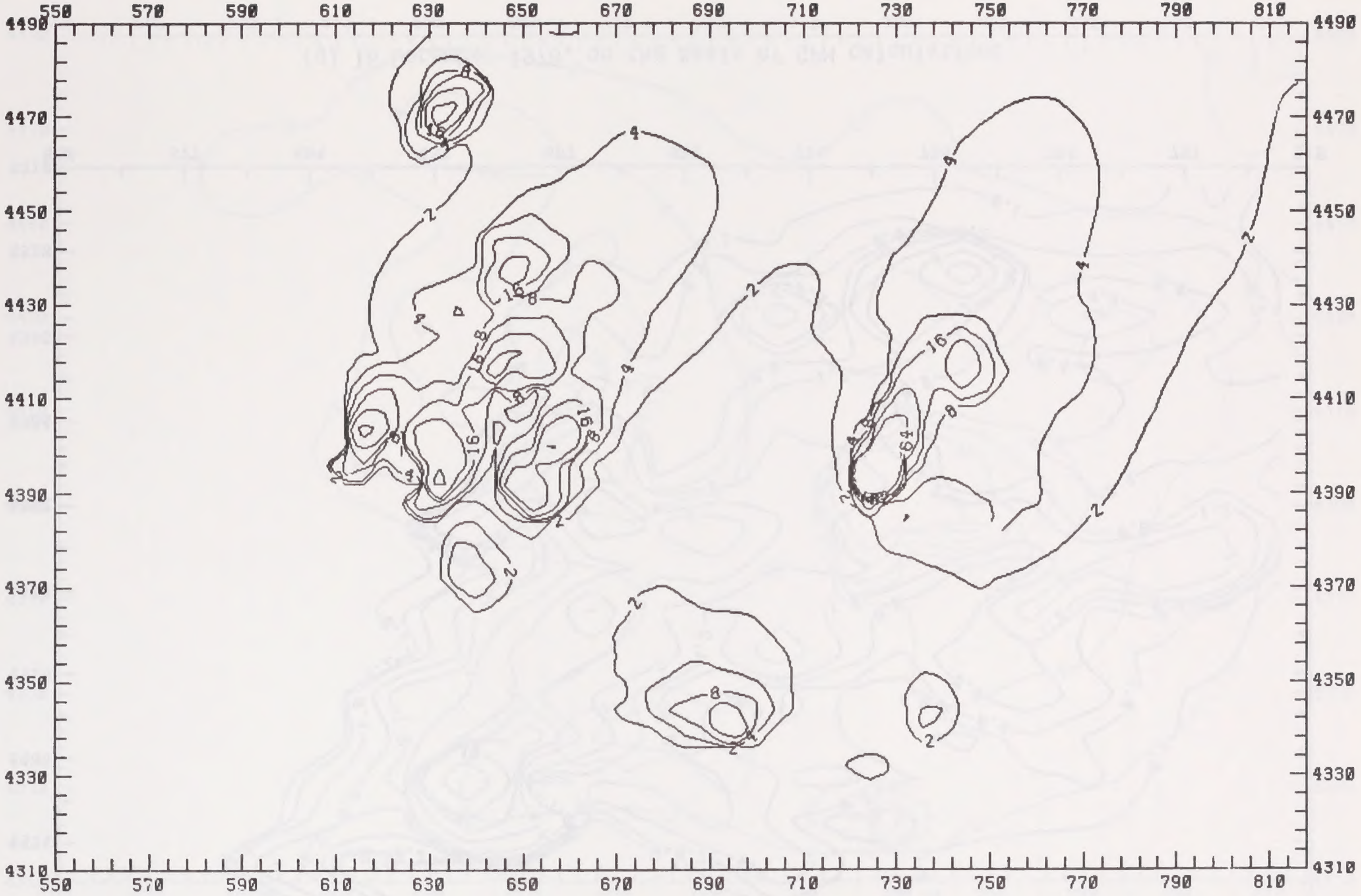

(f) 15 July 1978, on the basis of RTM calculations

Note:
Concentration isopleths greater than 64 μg/m^3 near the Chevron facility have been deleted to correct an error in emission source aggregation.

FIGURE 5-1 (Continued)

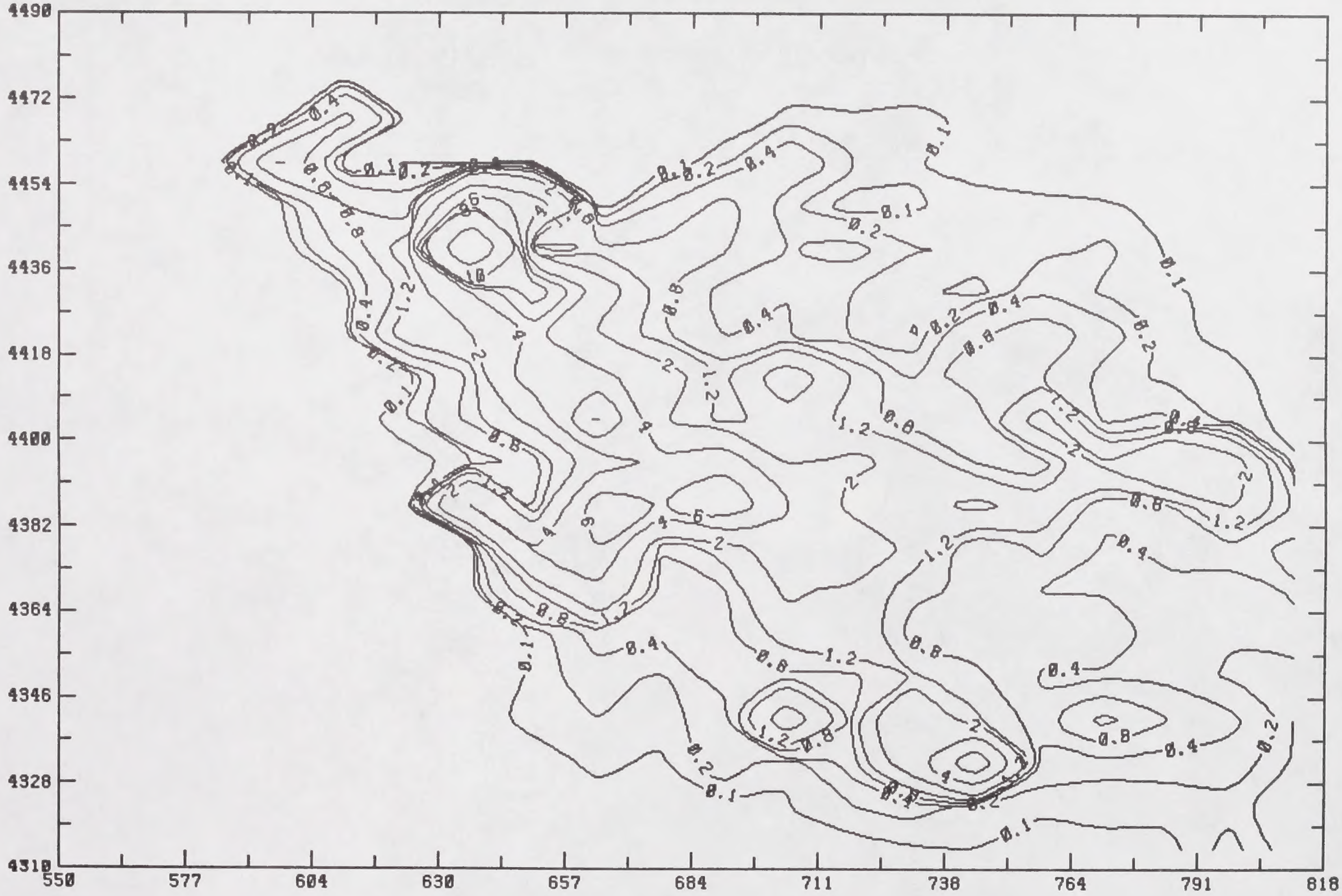

(g) 16 December 1978, on the basis of GPM calculations

FIGURE 5-1 (Continued)

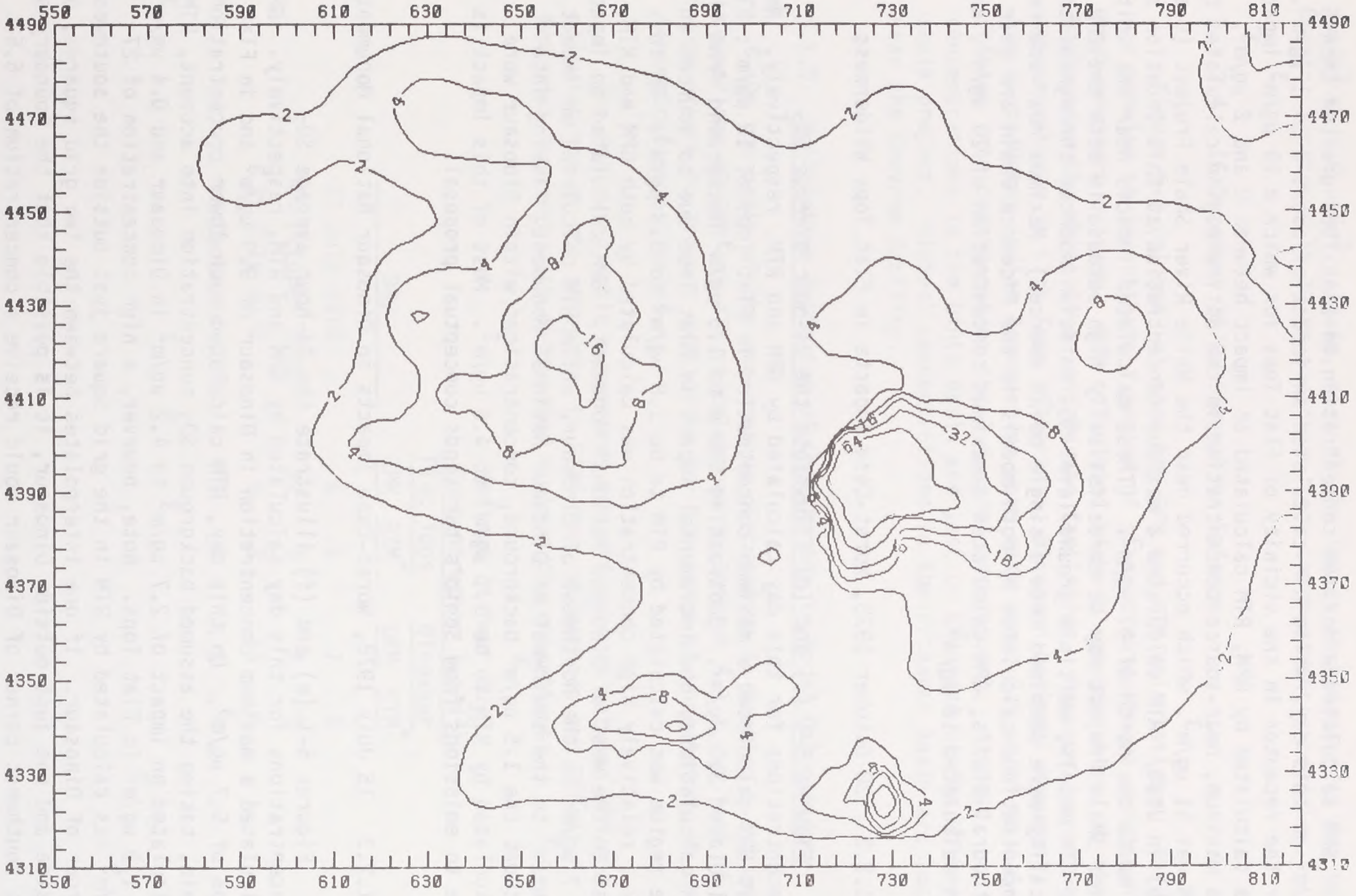

(h) 16 December 1978, on the basis of RTM calculations

Note:
Concentration isopleths greater than 64 μg/m^3 near the Chevron facility have been deleted to correct an error in emission source aggregation.

FIGURE 5-1 (Concluded)

GPM calculated a maximum concentration in Flat Tops greater than 6 $\mu g/m^3$ on this day, while RTM calculated an impact of about 0 to 1 $\mu g/m^3$. For the receptor in the vicinity of Flat Tops for which a 19 $\mu g/m^3$ impact was calculated by GPM, RTM calculated an impact between 0 and 2 $\mu g/m^3$. The maximum, near-source concentration in the entire region calculated by GPM was 51 $\mu g/m^3$, which occurred near the White River Shale Project (U-a, U-b) in Utah. RTM calculated a maximum concentration at this location and 20 km to the north of 41 $\mu g/m^3$. (These calculated impacts near the White River Shale Project may be unrealistically high because in both the GPM and RTM models, multiple ground-level SO_2 emission sources throughout the facility were combined into a single point source.) Maximum near-source concentrations calculated by both models in the Piceance Basin are near Cathedral Bluffs; GPM calculated a maximum concentration of 20 $\mu g/m^3$, and RTM calculated 16 $\mu g/m^3$.

5.1.2.2 20 October 1978, Worst-Case Impacts in Flat Tops Wilderness

Figures 5-1 (c) and (d) illustrate the 24-hour average SO_2 concentrations for this day calculated by GPM and RTM, respectively. Note that GPM calculated a maximum concentration in Flat Tops of 12 $\mu g/m^3$; RTM calculated 3.3 $\mu g/m^3$. Subtracting the 0 to 1.5 $\mu g/m^3$ background from the RTM calculations, the incremental impact in Flat Tops due to sources in the region was calculated by RTM to be 1.8 $\mu g/m^3$ to 3.3 $\mu g/m^3$. On this day a relatively high concentration was calculated by both GPM and RTM just to the west of Dinosaur National Monument. GPM calculated an impact of 7 $\mu g/m^3$ to the northwest of Dinosaur, while RTM calculated an impact of 8 $\mu g/m^3$ to the southwest of Dinosaur National Monument. Taking into account the 1.5 $\mu g/m^3$ background, concentrations within Dinosaur were calculated by RTM to be 3.1 $\mu g/m^3$ to 4.6 $\mu g/m^3$. Most of this impact is due to emissions from Sohio's tar sands conceptual proposal.

5.1.2.3 15 July 1978, Worst-Case Impacts in Dinosaur National Monument

Figures 5-1 (e) and (f) illustrate the 24-hour average SO_2 concentrations for this day calculated by GPM and RTM, respectively. GPM calculated a maximum concentration in Dinosaur of 9.8 $\mu g/m^3$ and in Flat Tops of 5.7 $\mu g/m^3$. On this day, RTM calculated much lower concentrations; again, taking the assumed background SO_2 concentration into account, RTM calculated an impact of 2.7 $\mu g/m^3$ to 4.2 $\mu g/m^3$ in Dinosaur and 0.4 $\mu g/m^3$ to 1.9 $\mu g/m^3$ in Flat Tops. Note, however, a high concentration of 27 $\mu g/m^3$ was calculated by RTM in the grid square just outside the southwest corner of Dinosaur. If one interpolates between the two grid squares, one inside and one just outside Dinosaur, it is possible that the boundary at the southwest corner of Dinosaur would receive a concentration of 6.5

$\mu g/m^3$ to 8.0 $\mu g/m^3$. Again, most of the impact in Dinosaur is due to Sohio, located only 20 km southwest from the monument's boundary.

5.1.2.4 16 December 1978, Stagnation Episode

Figure 5-1 (g) and (h) show the GPM and RTM calculations. This day was modeled to investigate a period of stagnation during a persistent, high-pressure episode. RTM calculated highest concentrations in the Uinta Basin near the White River and Paraho facilities. Maximum incremental concentrations in Flat Tops Wilderness, Dinosaur National Monument, and the Uinta/Ouray Indian Reservation were each about 2.5 $\mu g/m^3$ to 4.0 $\mu g/m^3$ (taking into consideration the 1.5 $\mu g/m^3$ background). Highest concentrations in the Uinta Basin are just to the east of the White River shale project. Highest concentrations in the Piceance Basin are located near the Chevron facility.

5.1.3 Qualitative Estimates of Uncertainty in Model Calculations

On the basis of the qualitative discussions in Section 5.1.1 and the comparison of GPM and RTM calculations in Section 5.1.2, we feel it is appropriate to account explicitly for the range of uncertainty in these concentration estimates.

The following table summarizes the differences between GPM and RTM calculations at the receptors in Flat Tops Wilderness and Dinosaur National Monument with calculated maximum concentrations:

	Maximum 24-hour SO_2 Concentration ($\mu g/m^3$)			
	Flat Tops		Dinosaur	
Day	GPM	RTM*	GPM	RTM*
27 July 1978	6	1	7	3
20 October 1978	12	3	7	5
15 July 1978	6	2	10	8
16 December 1978	< 1	4	< 1	4

	Maximum 3-hour SO_2 Concentrations ($\mu g/m^3$)			
	Flat Tops		Dinosaur	
Day	GPM	RTM*	GPM	RTM*
27 July 1978	34	3	46	8
20 October 1978	76	6	54	16
15 July 1978	10	3	30	16
16 December 1978	1	8	< 1	8

---

* These concentrations are conservatively high because they include an assumed background SO_2 concentration of between 0 and 1.5 $\mu g/m^3$.

In the sensitive receptor areas--Flat Tops and Dinosaur--RTM calculated maximum concentrations lower than GPM-calculated maxima. The most significant difference between RTM and GPM calculations occurred at Flat Tops. RTM results were similar to GPM results in Dinosaur because impacts were dominated by emissions from Sohio, only 20 km distant. Near-source impacts are modeled in a similar manner (using Gaussian puffs) in RTM and GPM, so it is not surprising that calculated maximum impacts in Dinosaur are similar, using the two models. The average ratio of GPM to RTM 24-hour average impacts in Flat Tops is 4 to 6, depending on whether or not the assumed background SO_2 concentrations is subtracted. Ratios of GPM to RTM 3-hour average impacts are even higher (greater than 10). RTM calculations of 24-hour average impacts in Flat Tops are in the range 1 $\mu g/m^3$ to 4 $\mu g/m^3$, less than the 5 $\mu g/m^3$ PSD Class I increment; GPM results are in the range 6 $\mu g/m^3$ to 12 $\mu g/m^3$, in excess of the increment. Impacts on the stagnation day (16 December) calculated by RTM were larger than those calculated by GPM because it was found that lower-level winds on this day were decoupled from upper-level winds used to drive GPM. But it should be noted that the RTM calculations on this day were not larger than the maximum concentrations calculated by GPM on other days. Even during this stagnation episode, RTM-calculated concentrations in Flat Tops and Dinosaur were a factor of 3 lower than GPM-calculated maxima.

By comparing the GPM and RTM isopleths in Figure 5-1, one can see that on these four episode days, for Class II receptors, in some cases RTM calculated higher concentrations than GPM. These differences, in general, resulted from somewhat different wind field specifications in the GPM and RTM applications. One can see that RTM calculations for all receptors on the four episode days are less than the Class II increment of 91 $\mu g/m^3$. By overlaying the maximum 24-hour SO_2 isopleths calculated using GPM (the clear plastic overlay is provided inside the back cover of the report) one can also see that RTM concentrations on the four episode days are less than maxima calculated by GPM in the entire modeled year. To provide meaningful comparisons between GPM maxima and RTM calculations for receptors other than Flat Tops and Dinosaur, different days (on which GPM calculated maximum impacts) would need to be modeled with RTM.

To account for the expected conservatism of GPM, we have projected air quality impacts by using ranges of concentrations, with the GPM predictions being at or near the high end of that range. The size of this range is estimated to be an order of magnitude (a factor of 10) for the maximum 3-hour and 24-hour concentrations. This range is based on our professional judgment as to the uncertainty of concentration estimates and our belief that GPM calculations of maximum concentrations are probably conservative (i.e., that concentration estimates predicted on the basis of GPM will be greater than actual concentrations). The GPM model is expected to be less conservative for annual averages than for short-term averages because underestimates of horizontal dispersion are cancelled out in the process of averaging concentrations over an entire year. GPM is still expected, however, to be somewhat conservative because it underestimates vertical dispersion. The empirical model used to calculate TSP concentrations from area source emission densities (described in Section 2) is expected to be unbiased since it is a least-squares fit, but it could underestimate or overestimate actual concentrations by an estimated factor of 2, or perhaps more if our estimates of fugitive dust emissions are inaccurate.

Concentration estimate ranges are thus constructed as shown schematically in Figure 5-2. Any conclusions about the magnitude and significance of air quality impact should be made recognizing that model estimates of regional impact are uncertain at this time.

5.2 IMPACTS OF INDUSTRIAL GROWTH

In this subsection the calculated impacts of various subsets of the Uinta and Piceance basin emission sources are described for both the low- and high-oil-production scenarios.

Common to these scenarios is the assumption that other (interrelated) projects in the Uinta Basin would be developed. Thus, regional impact scenarios including the impacts of these other sources. Dominating the emissions (and impacts) in this other source category are the Moon Lake Power Plant (Unit 1 is included in the 1980 baseline and Unit 2 is considered an interrelated source for the purposes of this analysis) and the White River Shale Project (WRSP). The SO_2 and TSP air quality impacts associated with direct source emissions from these facilities are displayed in Figures 5-3 through 5-6. Because of the problems associated

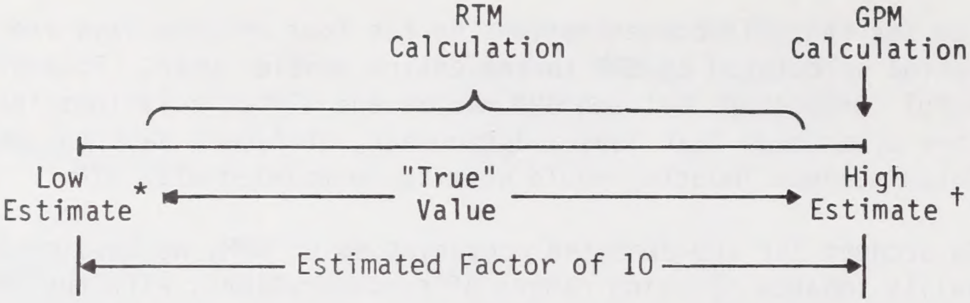

(a) Estimates for maximum 3-hour and 24-hour average concentrations.

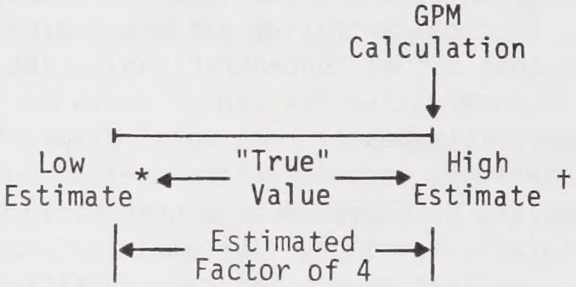

(b) Estimates for annual average concentrations.

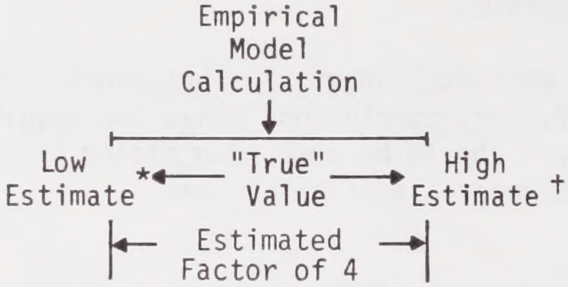

(c) Estimates for area source TSP concentrations using empirical model.

---

* The "low estimate" most likely underestimates the air quality impact.

† The "high estimate" is conservative in that it most likely overestimates the air quality impact.

FIGURE 5-2. SCHEMATIC REPRESENTATION OF ESTIMATED RANGES IN THE REGIONAL AIR QUALITY IMPACTS ASSESSMENT

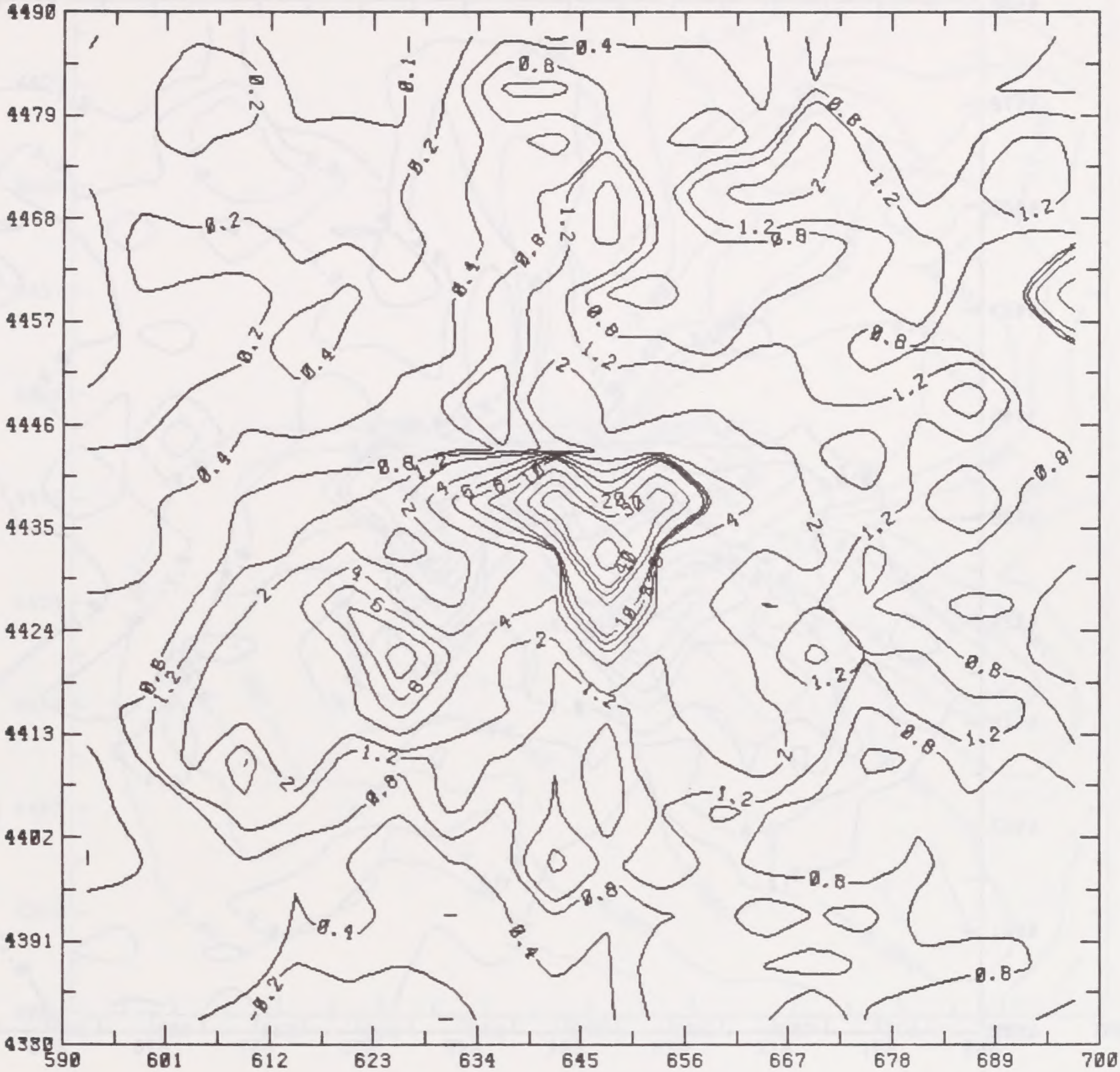

Note: These are believed to be conservatively high estimates of impacts and are non-simultaneous maxima calculated on the basis of one year's meteorological data.

(a) Maximum 3-hour average

FIGURE 5-3. IMPACT OF DIRECT SOURCE EMISSIONS FROM MOON LAKE UNIT 2 ON GROUND-LEVEL SO_2 CONCENTRATIONS ($\mu g/m^3$)

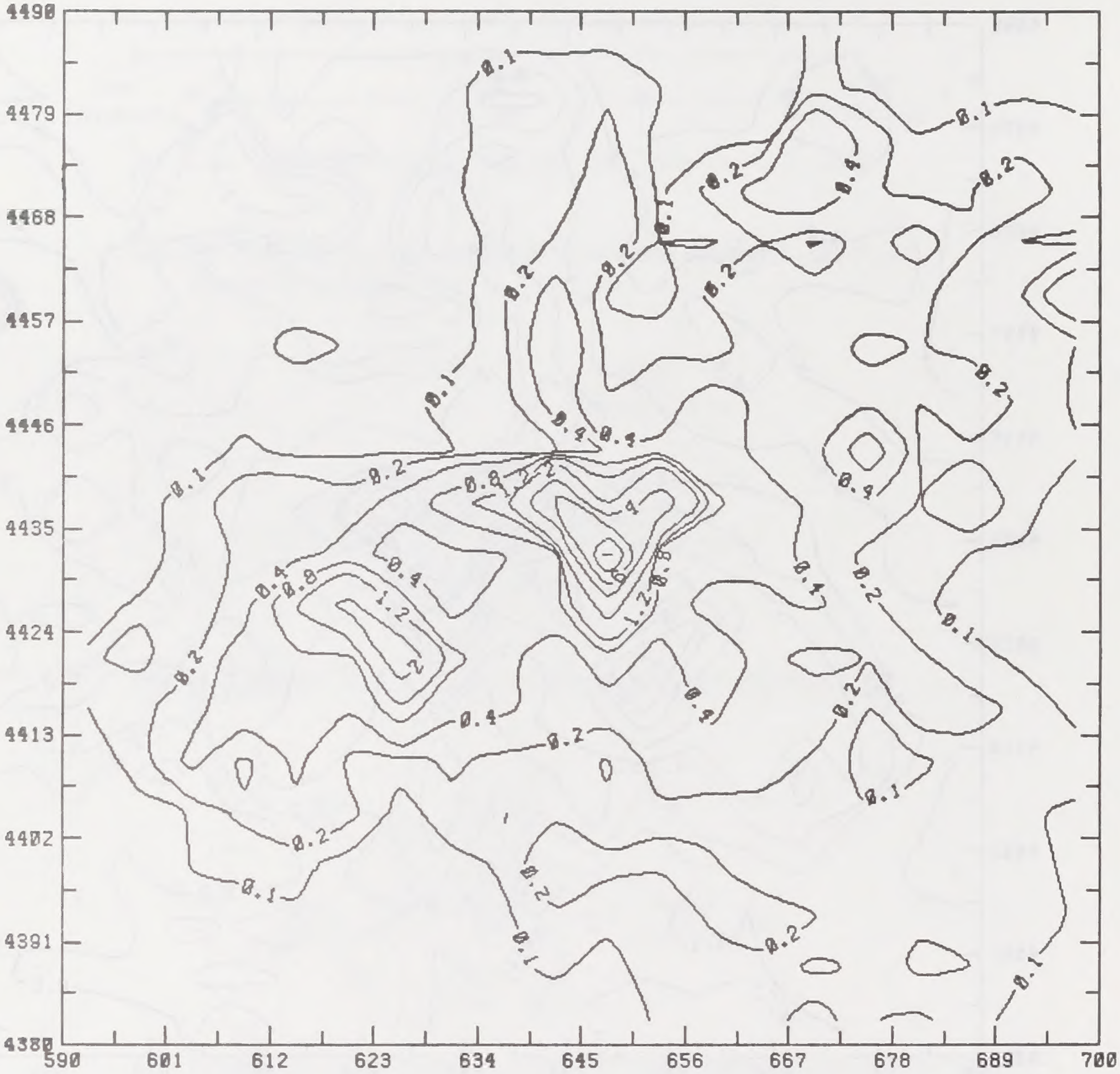

Note: These are believed to be conservatively high estimates of impacts and are non-simultaneous maxima calculated on the basis of one year's meteorological data.

(b) Maximum 24-hour average

FIGURE 5-3 (Continued)

FIGURE 5-3 (Concluded)

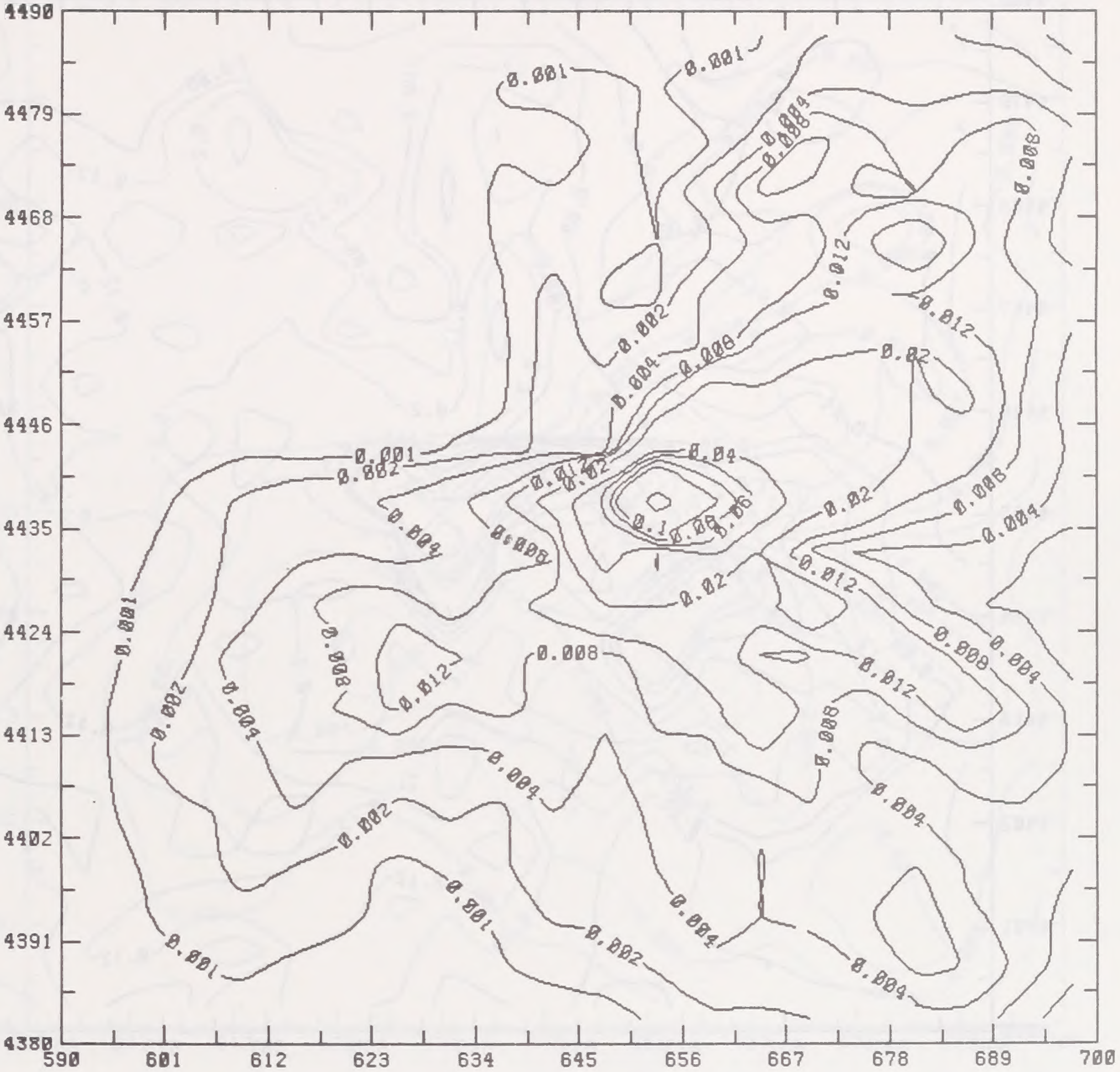

Note: These are believed to be conservatively high estimates of impacts.

(c) Annual Average

FIGURE 5-3 (Concluded)

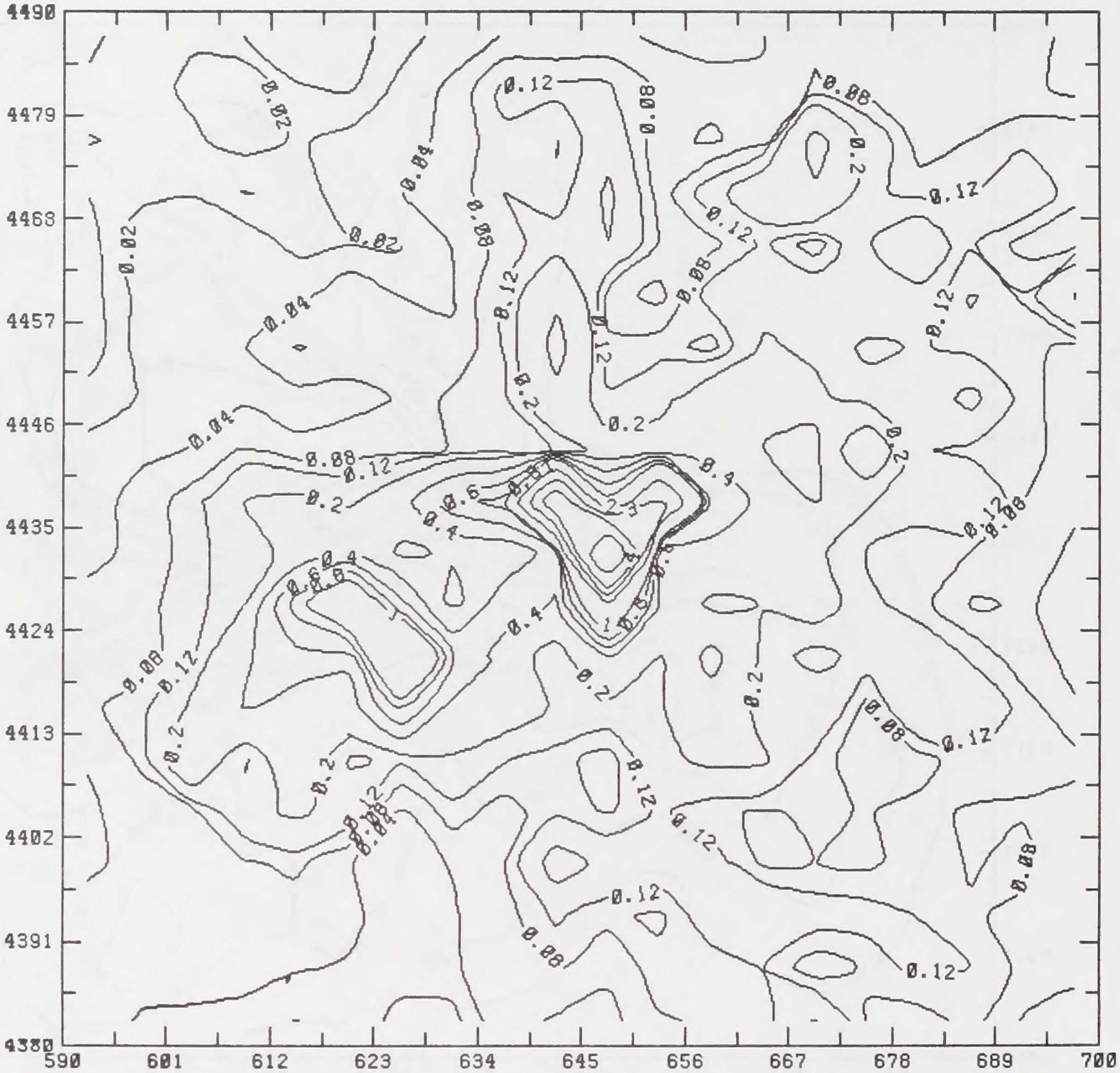

Note: These are believed to be conservatively high estimates of impacts and are non-simultaneous maxima calculated on the basis of one year's meteorological data.

(a) Maximum 24-hour average

FIGURE 5-4. IMPACT OF DIRECT SOURCE EMISSIONS FROM MOON LAKE UNIT 2 ON GROUND-LEVEL TSP CONCENTRATIONS (μg/m^3)

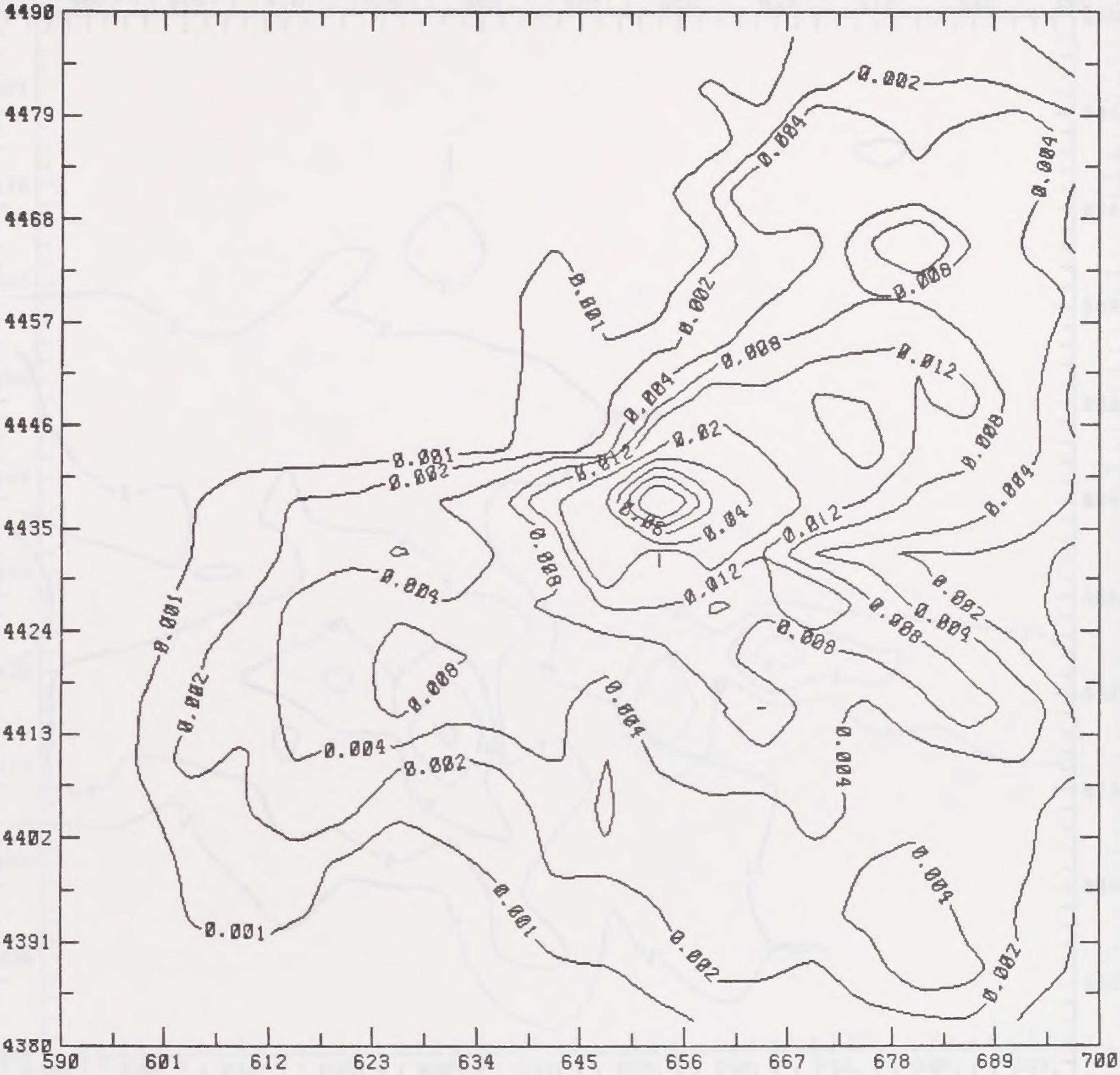

Note: These are believed to be conservatively high estimates of impacts.

(b) Annual average

FIGURE 5-4 (Concluded)

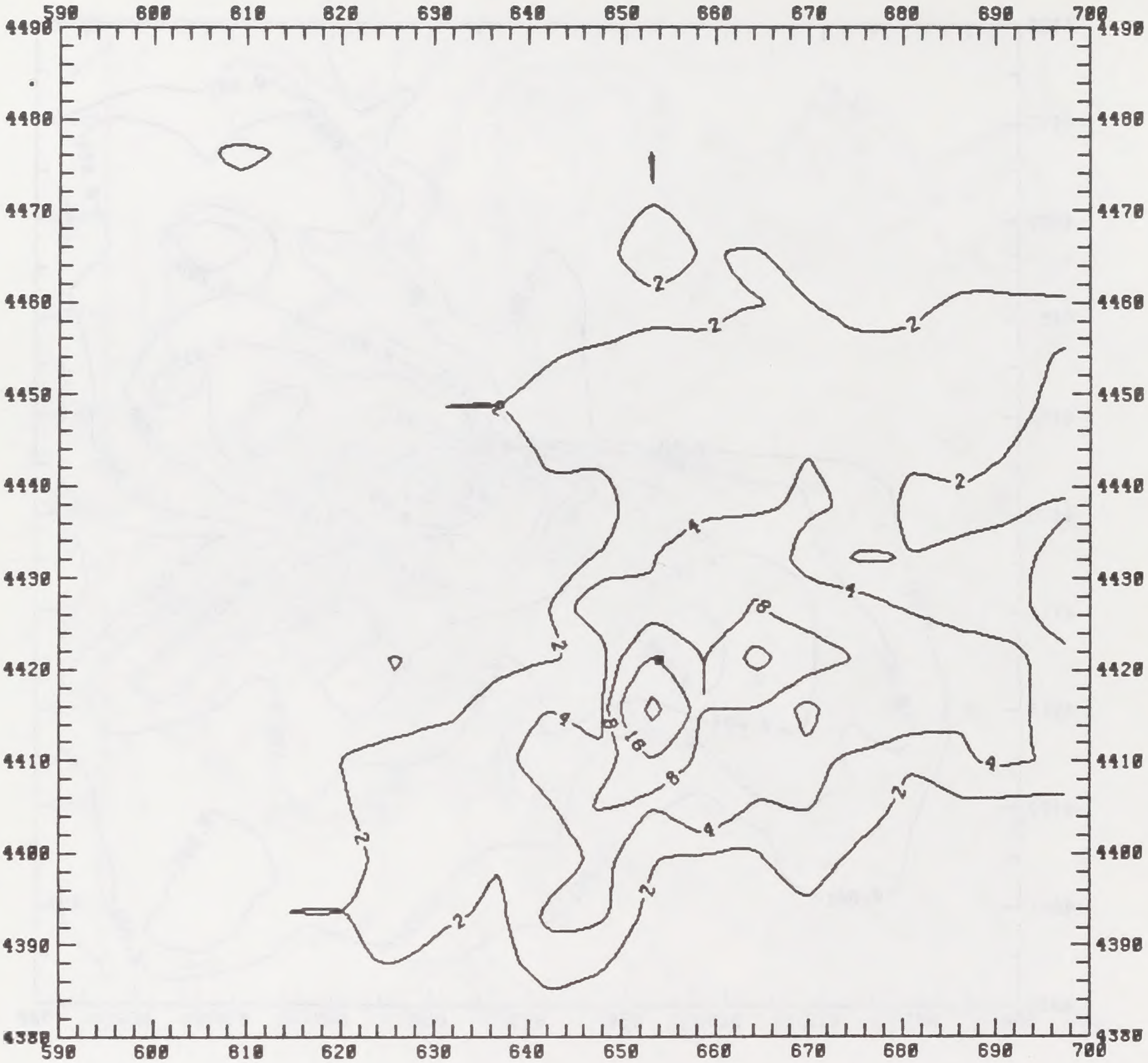

Note: These are believed to be conservatively high estimates of impacts and are non-simultaneous maxima calculated on the basis of one year's meteorological data.

(a) Maximum 3-hour average

FIGURE 5-5. IMPACT OF DIRECT SOURCE EMISSIONS FROM WHITE RIVER SHALE PROJECT ON GROUND-LEVEL SO_2 CONCENTRATIONS ($\mu g/m^3$)

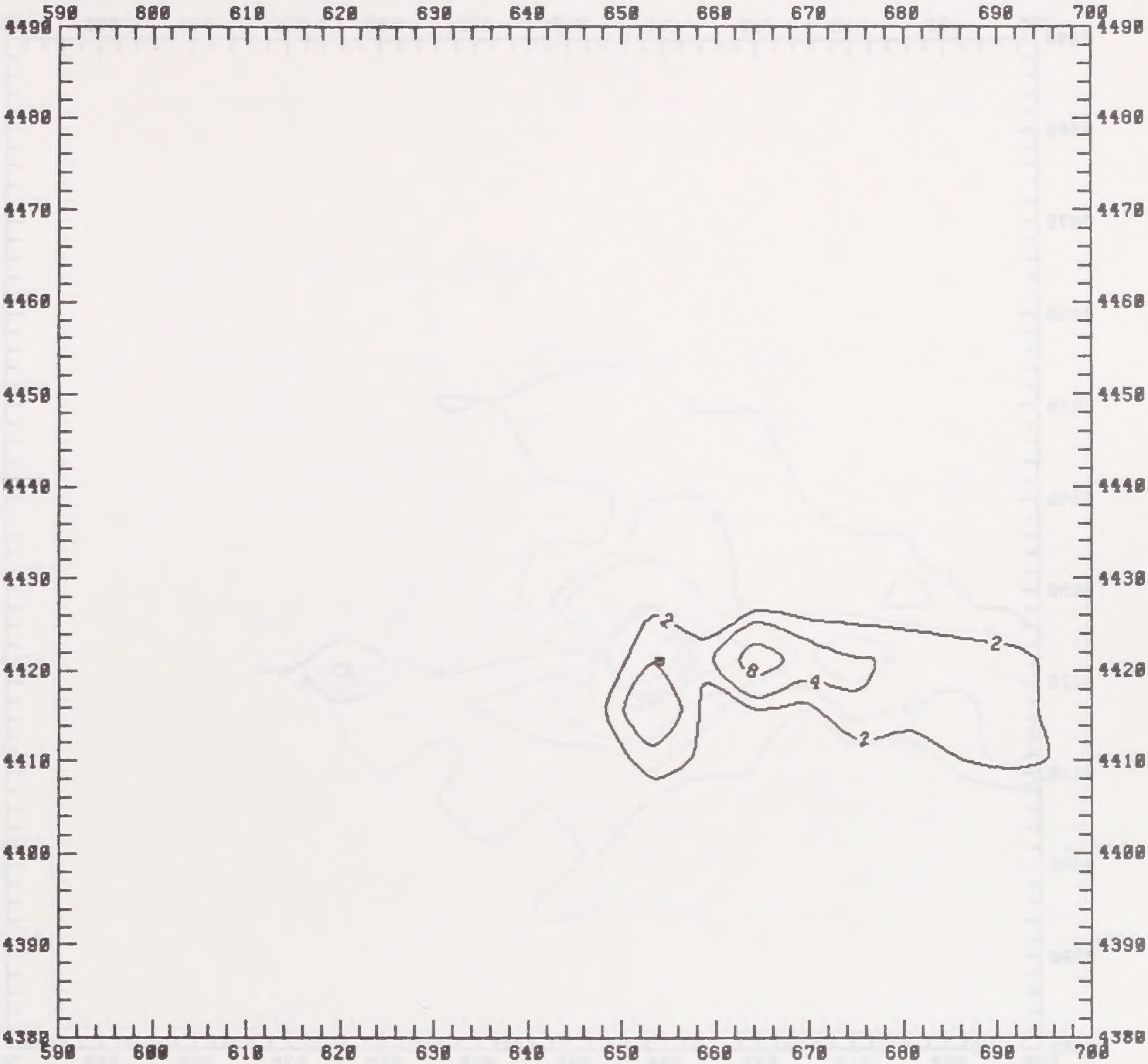

Note: These are believed to be conservatively high estimates of impacts and are non-simultaneous maxima calculated on the basis of one year's meteorological data.

(b) Maximum 24-hour average

FIGURE 5-5 (Continued)

Note: These are believed to be conservatively
high estimates of impacts.

(c) Annual average

FIGURE 5-5 (Concluded)

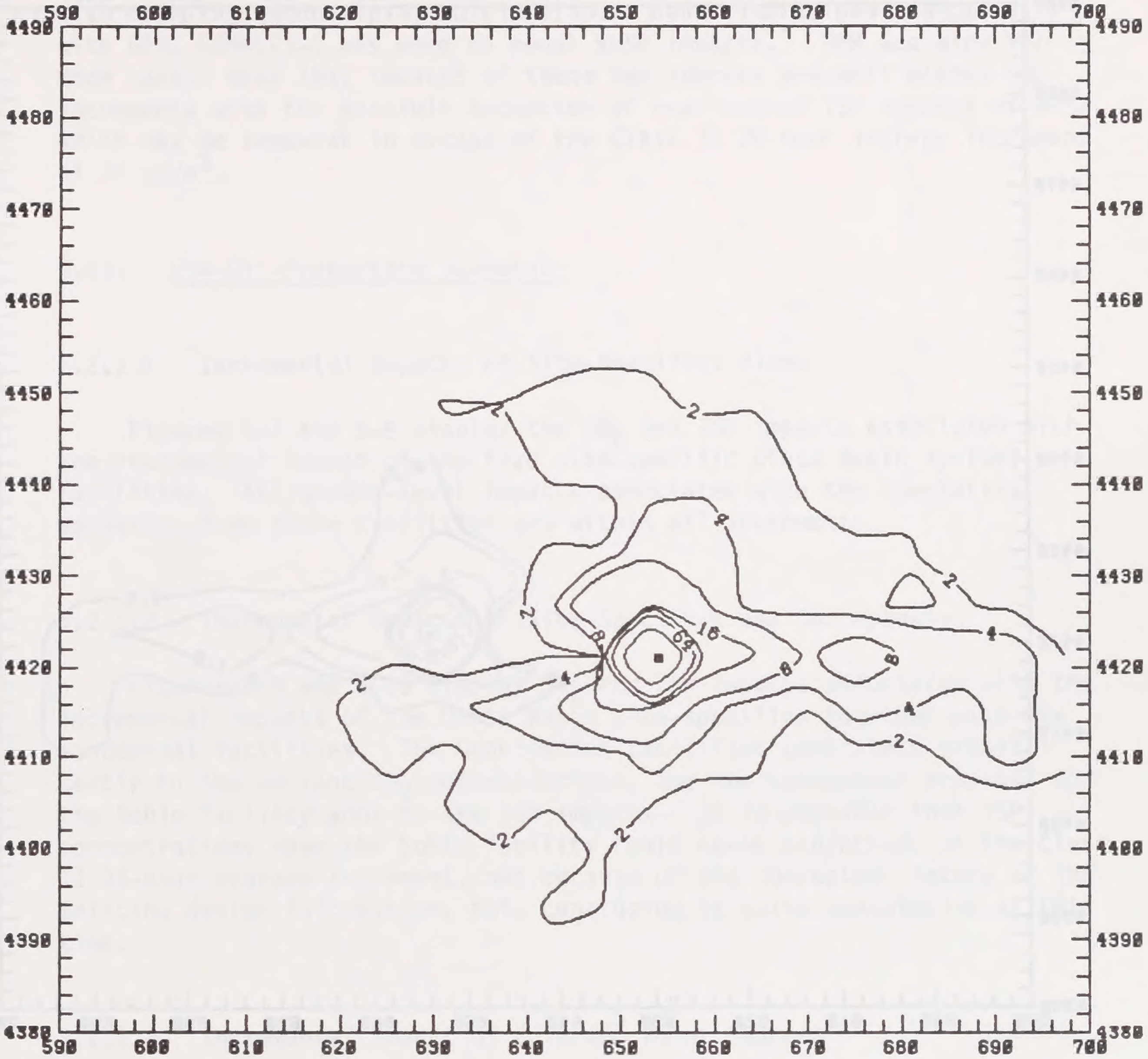

Note: These are believed to be conservatively high estimates of impacts and are non-simultaneous maxima calculated on the basis of one year's meteorological data.

(a) Maximum 24-hour average

FIGURE 5-6. IMPACT OF DIRECT SOURCE EMISSIONS FROM WHITE RIVER SHALE PROJECT ON GROUND-LEVEL TSP CONCENTRATIONS ($\mu g/m^3$)

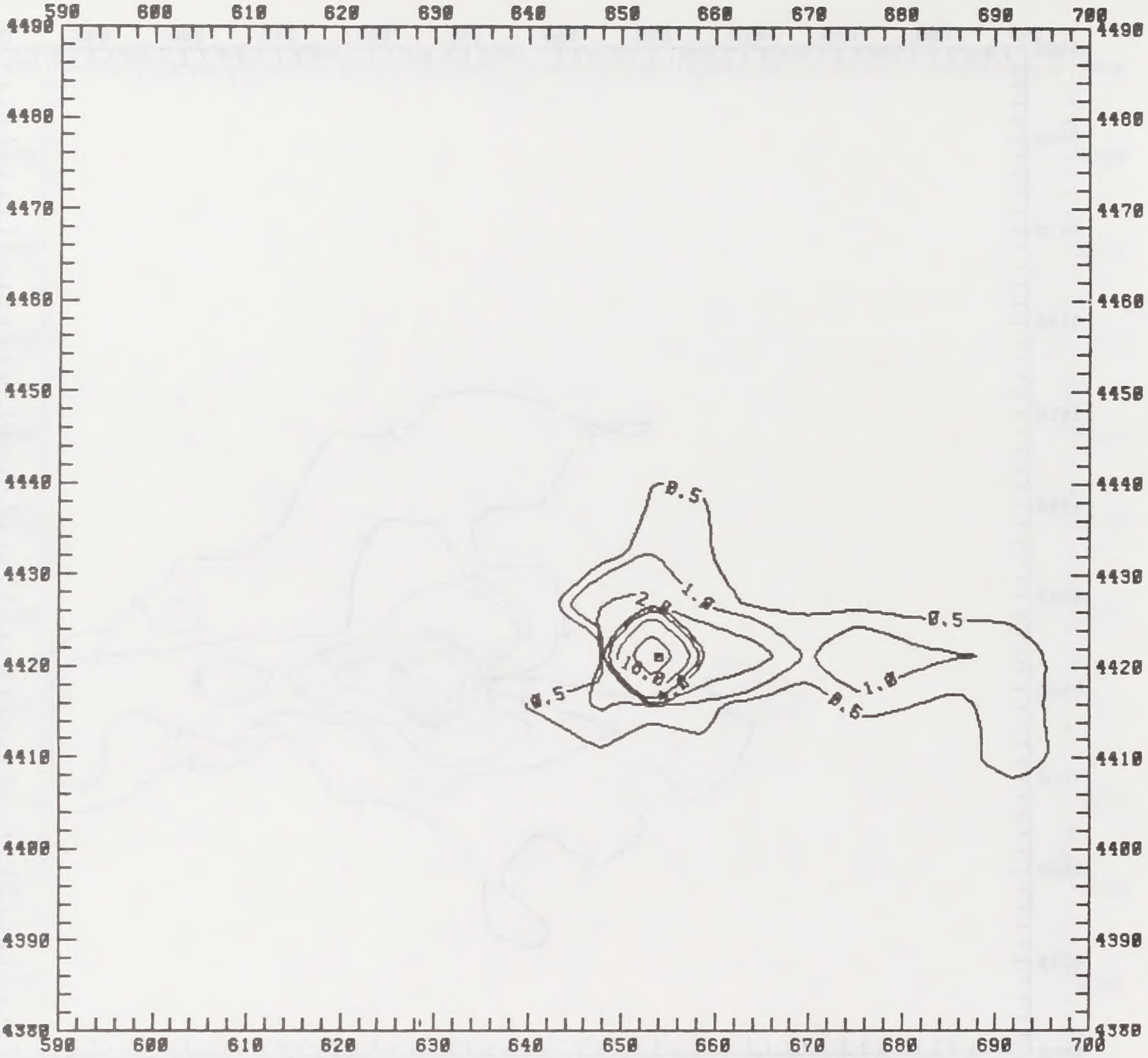

Note: These are believed to be conservatively high estimates of impacts.

(b) Annual Average

FIGURE 5-6 (Concluded)

with modeling ground-level multiple point source emissions economically with GPM, COMPLEX-I was used to model WRSP impacts.* GPM was used for Moon Lake. Note that impacts of these two sources are well within PSD increments with the possible exception of near-source TSP impacts of WRSP, which may be somewhat in excess of the Class II 24-hour average increment of 37 $\mu g/m^3$.

5.2.1 Low-Oil-Production Scenario

5.2.1.1 Incremental Impacts of Site-Specifics Alone

Figures 5-7 and 5-8 display the SO_2 and TSP impacts associated with the incremental impact of the five site-specific Uinta Basin synfuel facilities. All ground-level impacts associated with the cumulative emissions from these facilities are within all increments.

5.2.1.2 Incremental Impacts of Site-Specifics and Conceptuals

Figures 5-9 and 5-10 display SO_2 and TSP impacts associated with the incremental impacts of the Uinta Basin site-specifics together with the conceptual facilities. The Geokinetics facilities contribute significantly to the ambient SO_2 concentrations, and the conceptual proposal for the Sohio facility adds to the TSP impacts. It is possible that TSP concentrations near the Sohio facility could cause violations of the Class II 24-hour average increment, but because of the conceptual nature of the existing design information, this conclusion is quite speculative at this time.

5.2.1.3 Incremental Impact of Colorado Point Sources

Figures 5-11 and 5-12 display the incremental impacts of Piceance Basin oil shale facilities and other (existing) point sources near Grand Junction. The impacts of the Colorado sources are based on a development scenario (see section 4) that is highly speculative, especially considering project delays, cancellations, and modifications announced in recent

---

* Inappropriate isopleths in GPM regional plots near WRSP and near other facilities for TSP impacts have been replaced with corrected values based on COMPLEX-I. GPM calculations are overly conservative near sources with multiple ground-level release points because in GPM multiple emissions are treated as one (see section 4.2).

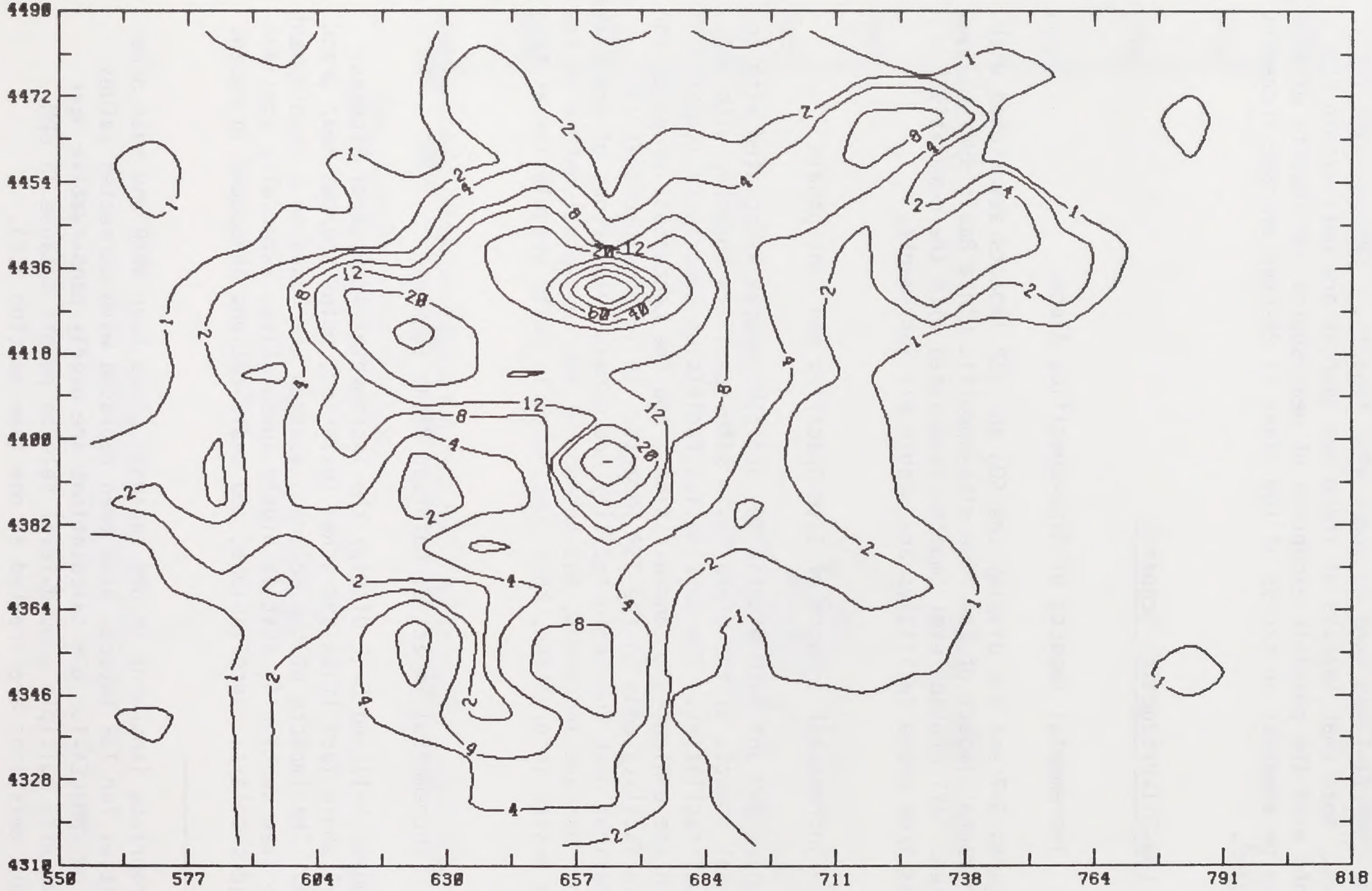

Note: These are believed to be conservatively high estimates of impacts and are non-simultaneous maxima calculated on the basis of one year's meteorological data.

(a) Maximum 3-hour average

FIGURE 5-7. IMPACT OF DIRECT SOURCE EMISSIONS FROM UINTA BASIN SITE-SPECIFICS ON GROUND-LEVEL SO_2 CONCENTRATIONS ($\mu g/m^3$) FOR LOW OIL PRODUCTION SCENARIO

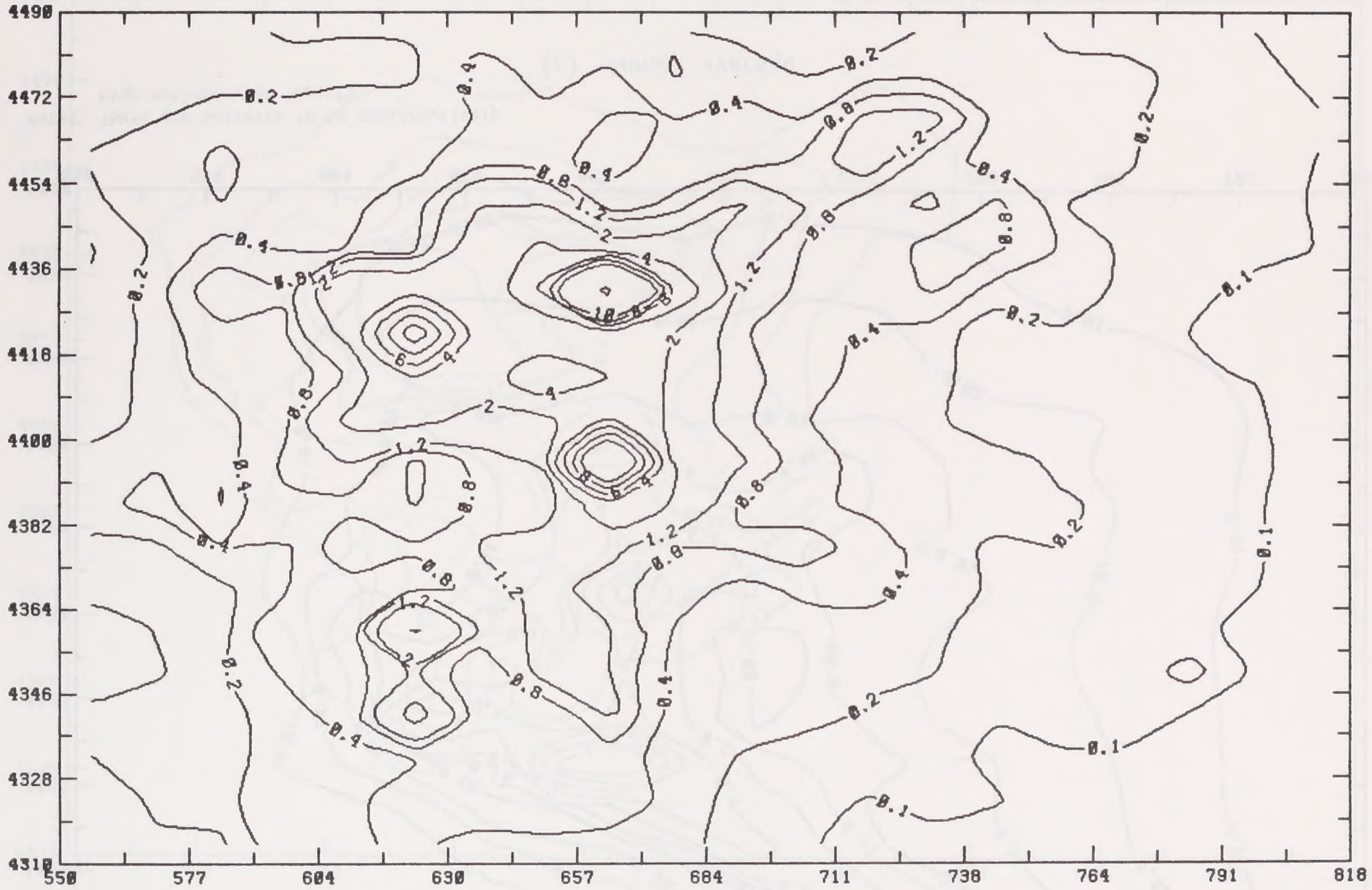

Note: These are believed to be conservatively high estimates of impacts and are non-simultaneous maxima calculated on the basis of one year's meteorological data.

(b) Maximum 24-hour average

FIGURE 5-7 (Continued)

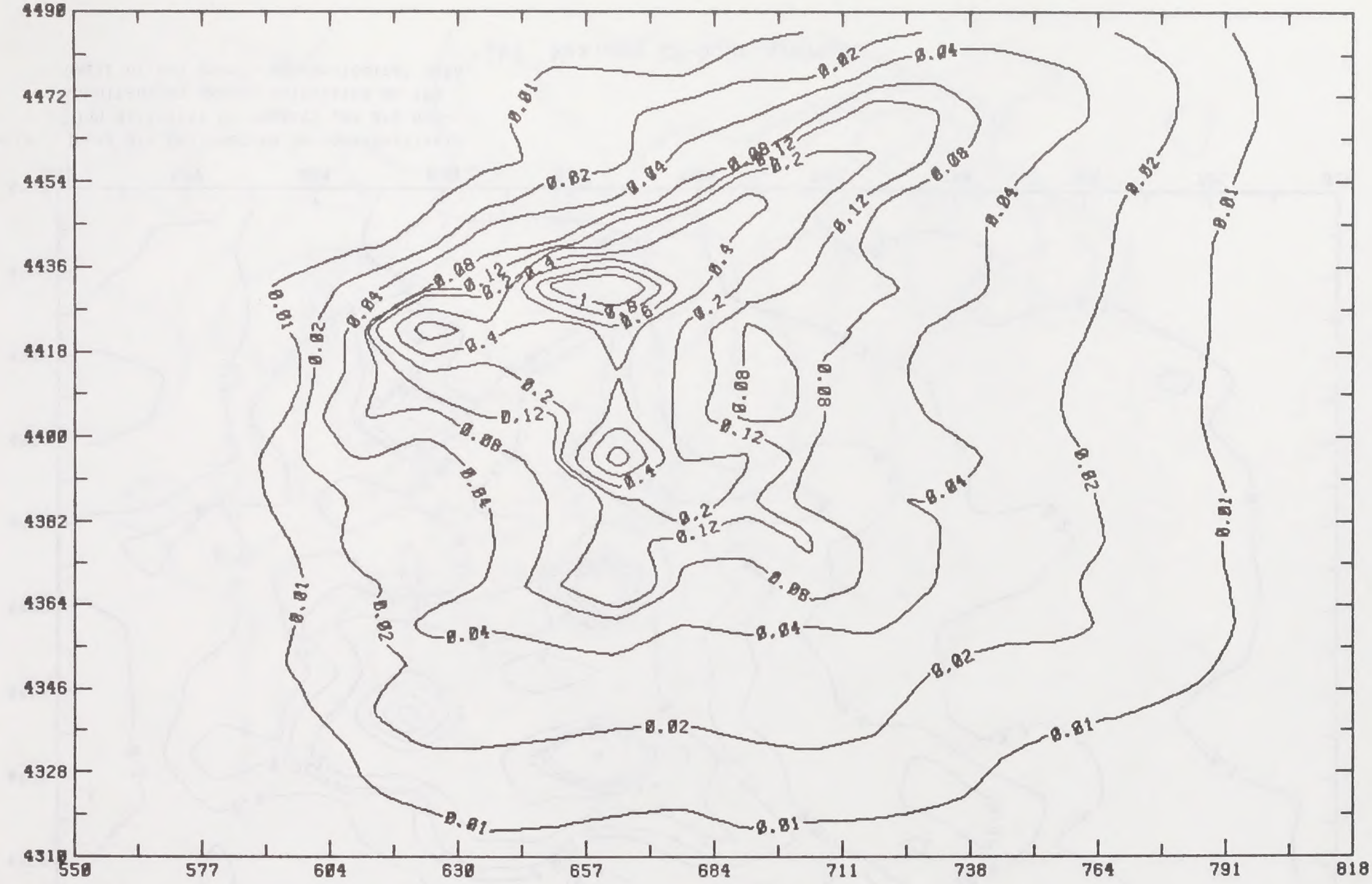

Note: These are believed to be conservatively high estimates of impacts.

(c) Annual average

FIGURE 5-7 (Concluded)

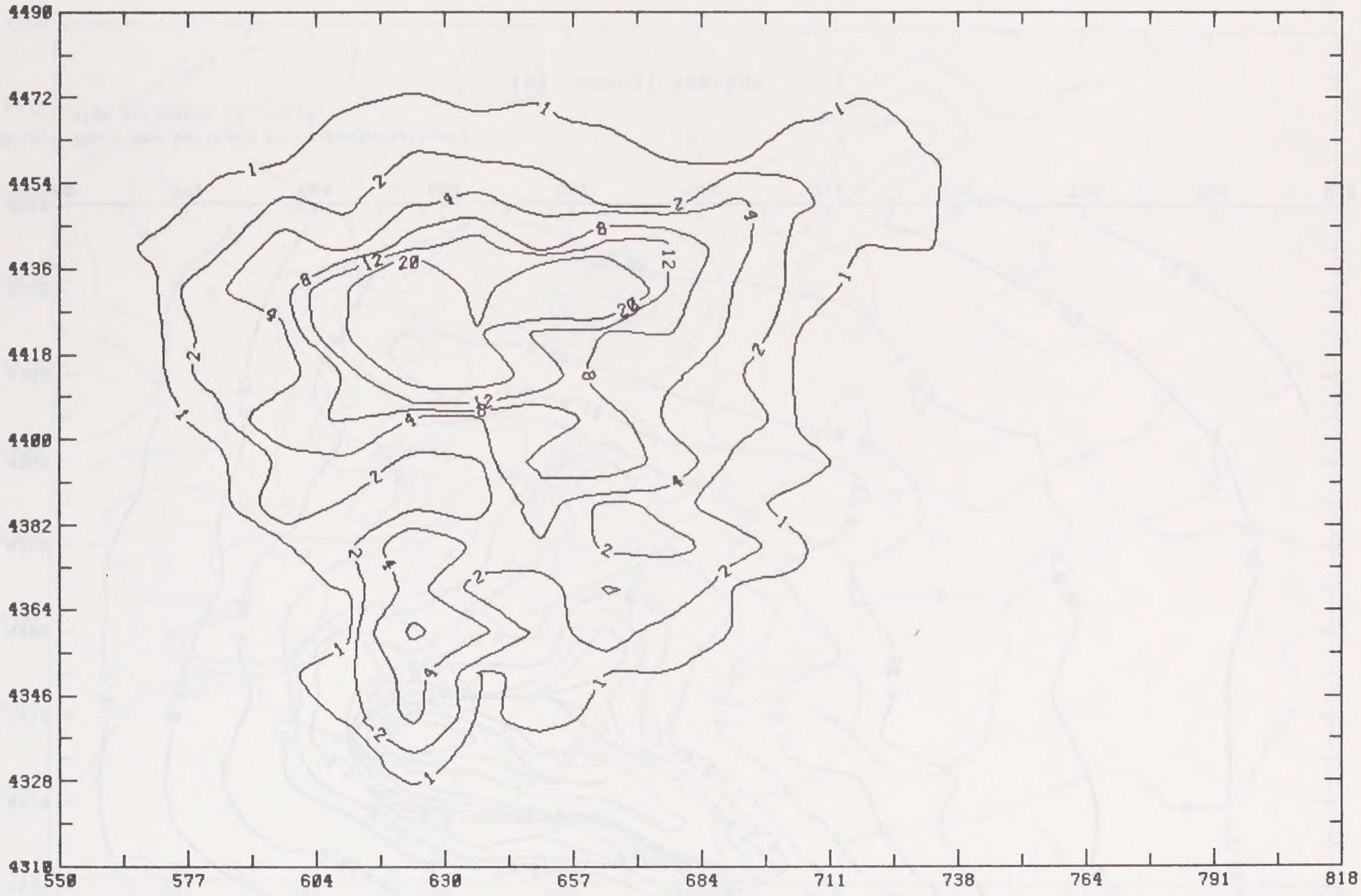

Note: These are believed to be conservatively high estimates of impacts and are non-simultaneous maxima calculated on the basis of one year's meteorological data.

(a) Maximum 24-hour average

FIGURE 5-8. IMPACT OF DIRECT SOURCE EMISSIONS FROM UINTA BASIN SITE-SPECIFICS ON GROUND-LEVEL TSP CONCENTRATIONS ($\mu g/m^3$) FOR LOW OIL PRODUCTION SCENARIO

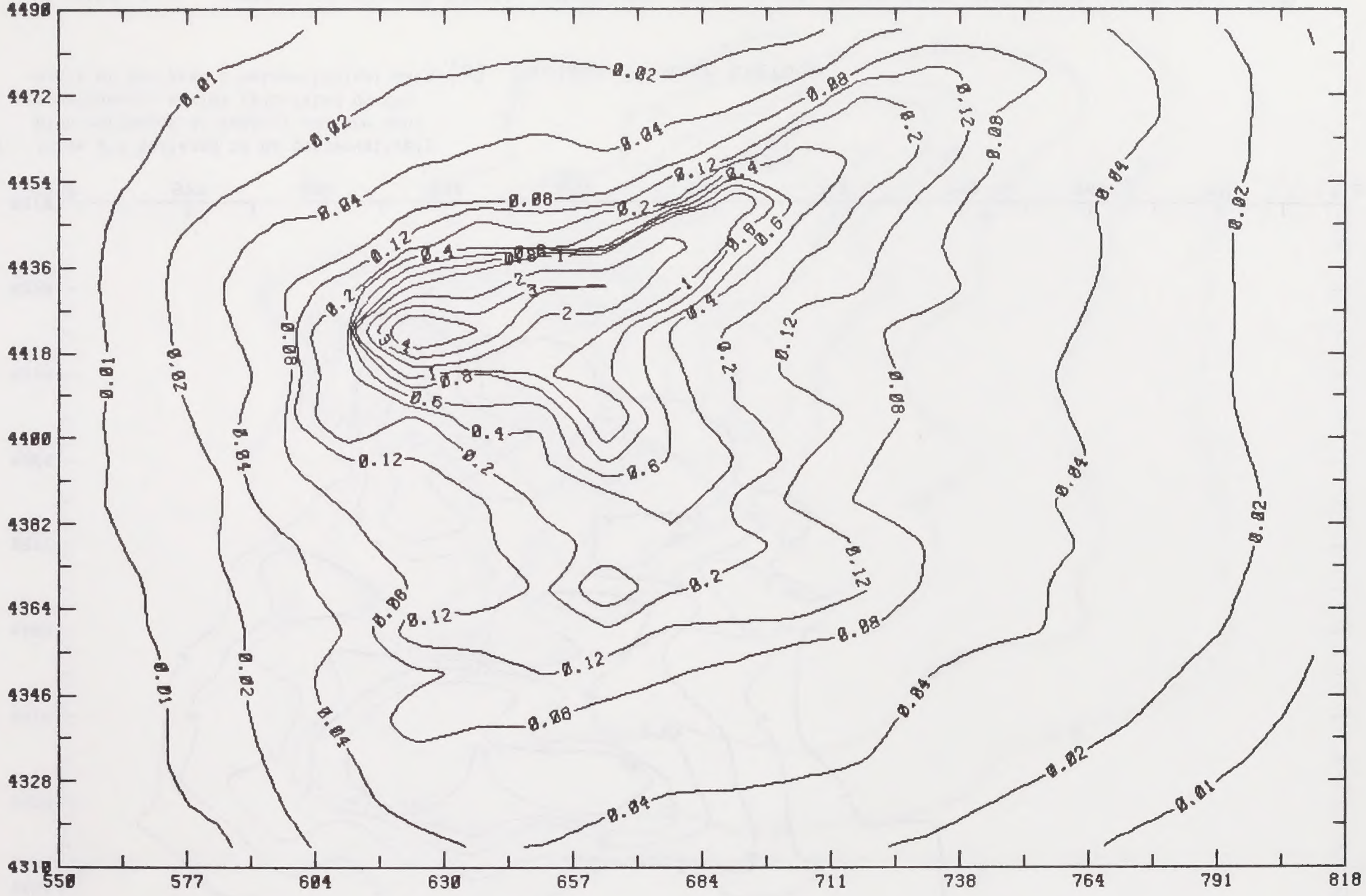

Note: These are believed to be conservatively high estimates of impacts.

(b) Annual average

FIGURE 5-8 (Concluded)

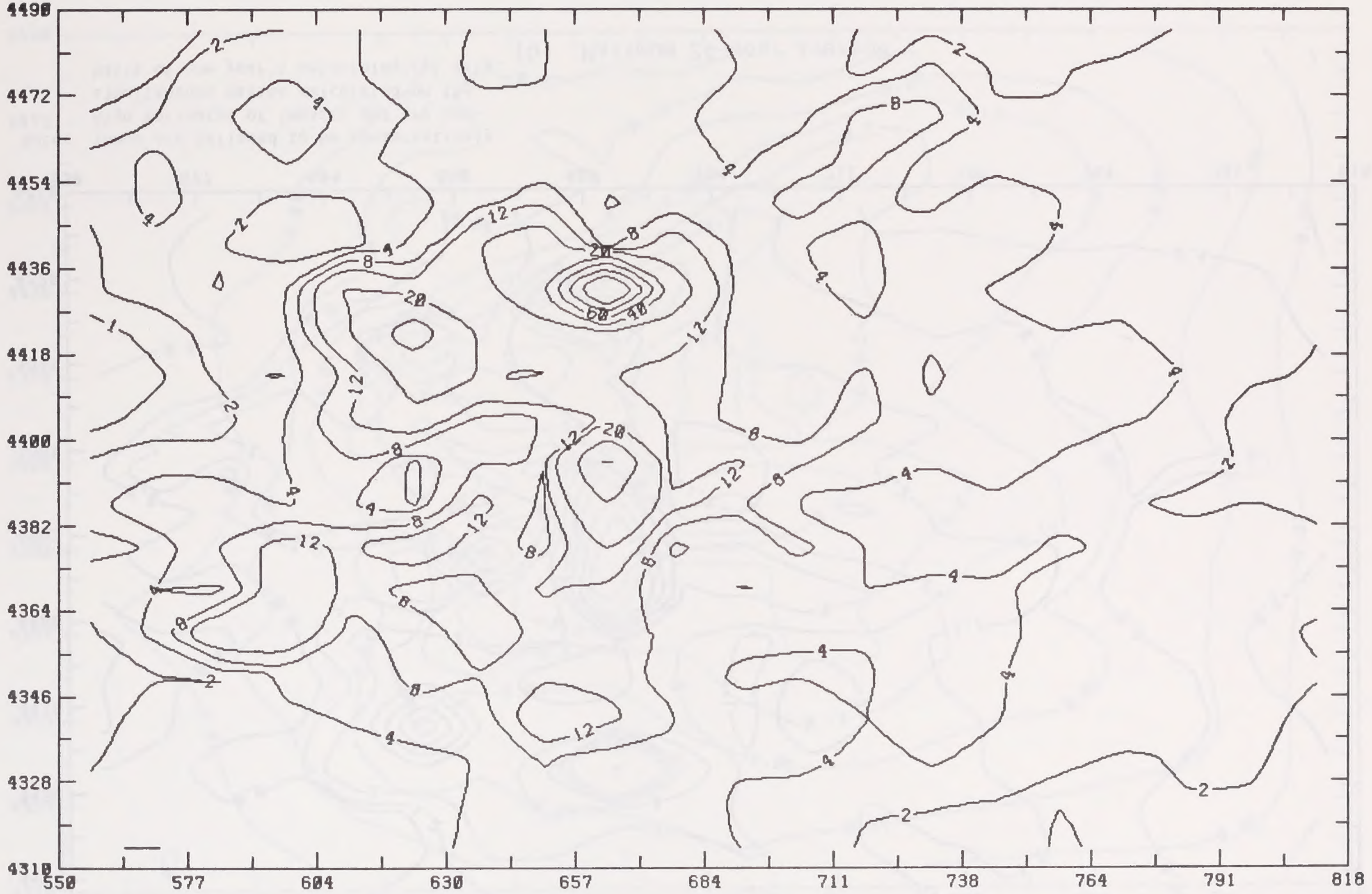

Note: These are believed to be conservatively high estimates of impacts and are non-simultaneous maxima calculated on the basis of one year's meteorological data.

(a) Maximum 3-hour average

FIGURE 5-9. IMPACT OF DIRECT SOURCE EMISSIONS FROM UINTA BASIN SITE-SPECIFICS AND CONCEPTUALS ON GROUND-LEVEL SO_2 CONCENTRATIONS (μg/m3) FOR LOW OIL PRODUCTION SCENARIO

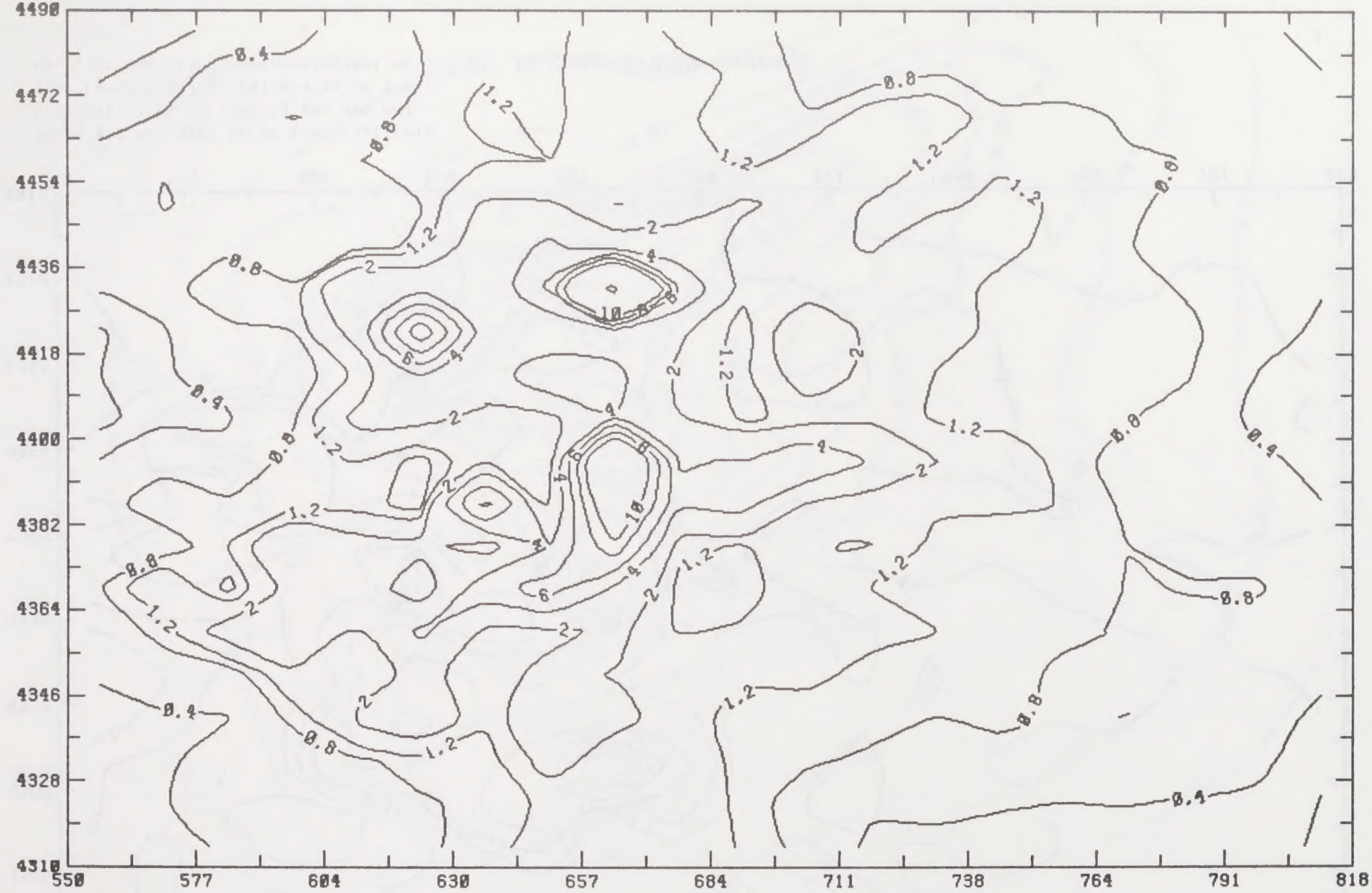

Note: These are believed to be conservatively high estimates of impacts and are non-simultaneous maxima calculated on the basis of one year's meteorological data.

(b) Maximum 24-hour average

FIGURE 5-9 (Continued)

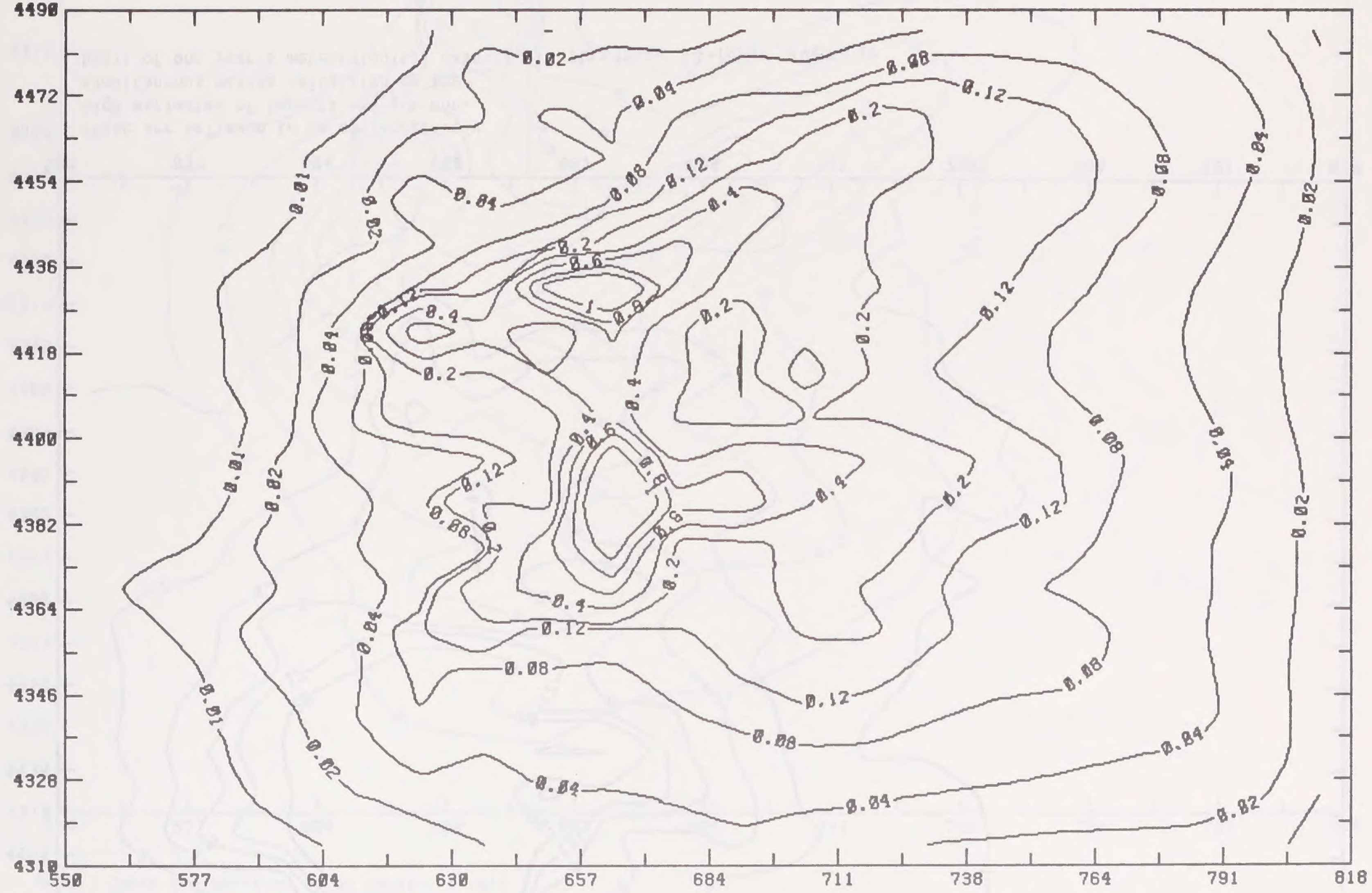

Note: These are believed to be conservatively high estimates of impacts.

(c) Annual average

FIGURE 5-9 (Concluded)

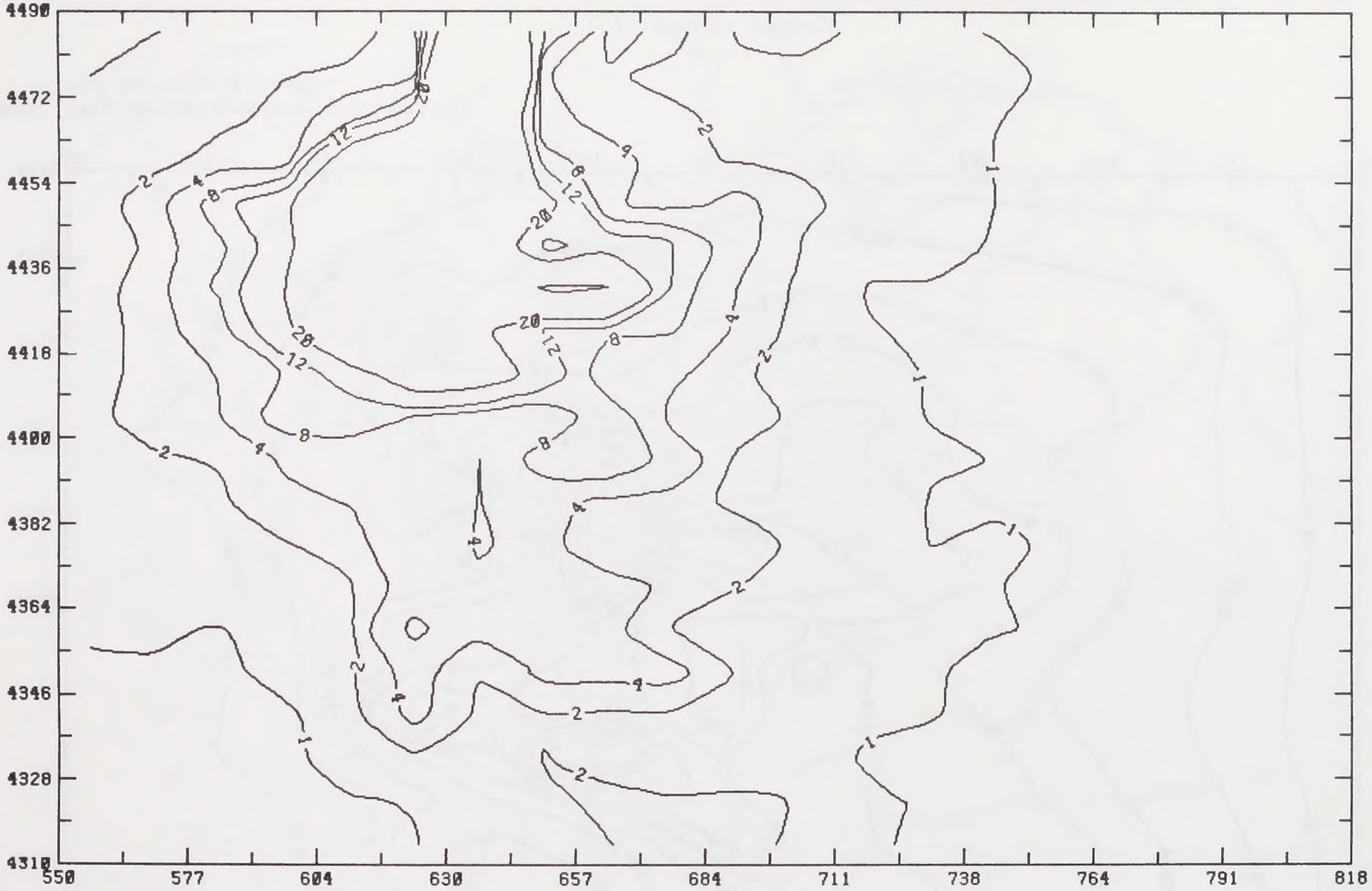

Note: These are believed to be conservatively high estimates of impacts and are non-simultaneous maxima calculated on the basis of one year's meteorological data.

(a) Maximum 24-hour average

FIGURE 5-10. IMPACT OF DIRECT SOURCE EMISSIONS FROM UINTA BASIN SITE SPECIFICS ON GROUND-LEVEL TSP CONCENTRATIONS ($\mu g/m^3$) FOR LOW OIL PRODUCTION SCENARIO

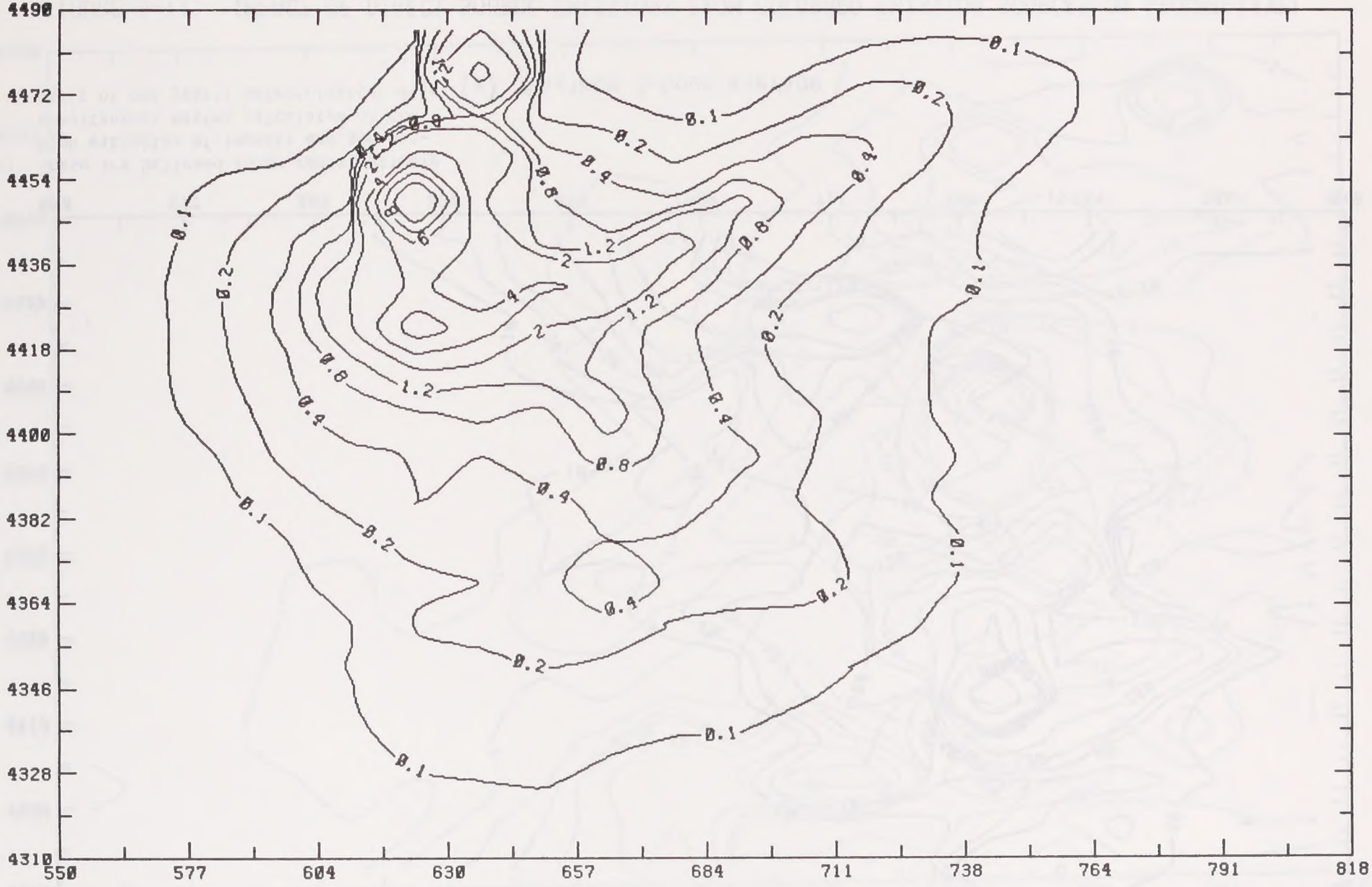

Note: These are believed to be conservatively
high estimates of impacts.

(b) Annual Average

FIGURE 5-10 (Concluded)

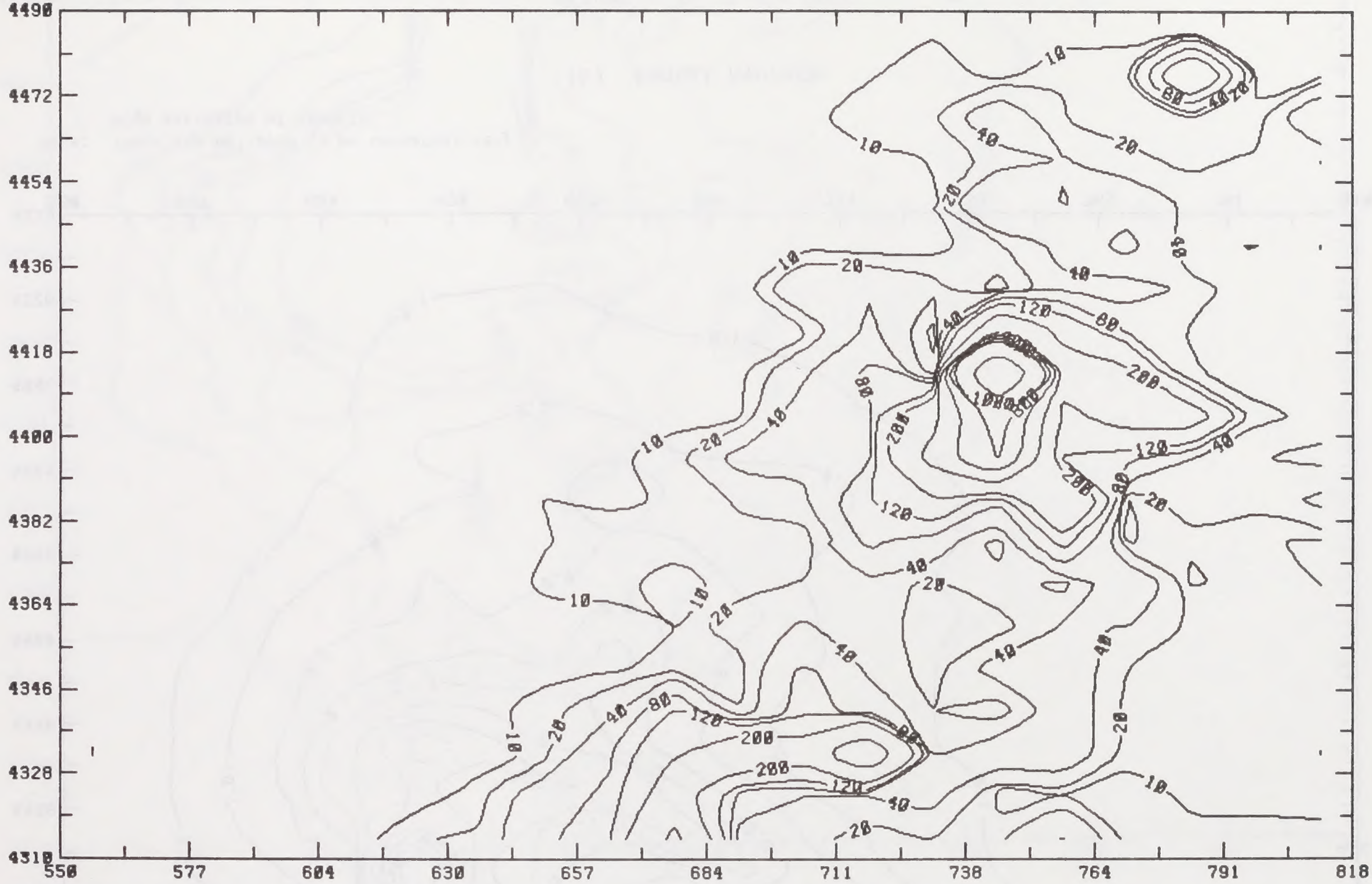

Note: These are believed to be conservatively high estimates of impacts and are non-simultaneous maxima calculated on the basis of one year's meteorological data.

(a) Maximum 3-hour average

FIGURE 5-11. IMPACT OF DIRECT SOURCE EMISSIONS FROM COLORADO EMISSION SOURCES ON GROUND-LEVEL SO_2 CONCENTRATIONS (μg/m^3) FOR THE LOW OIL PRODUCTION SCENARIO

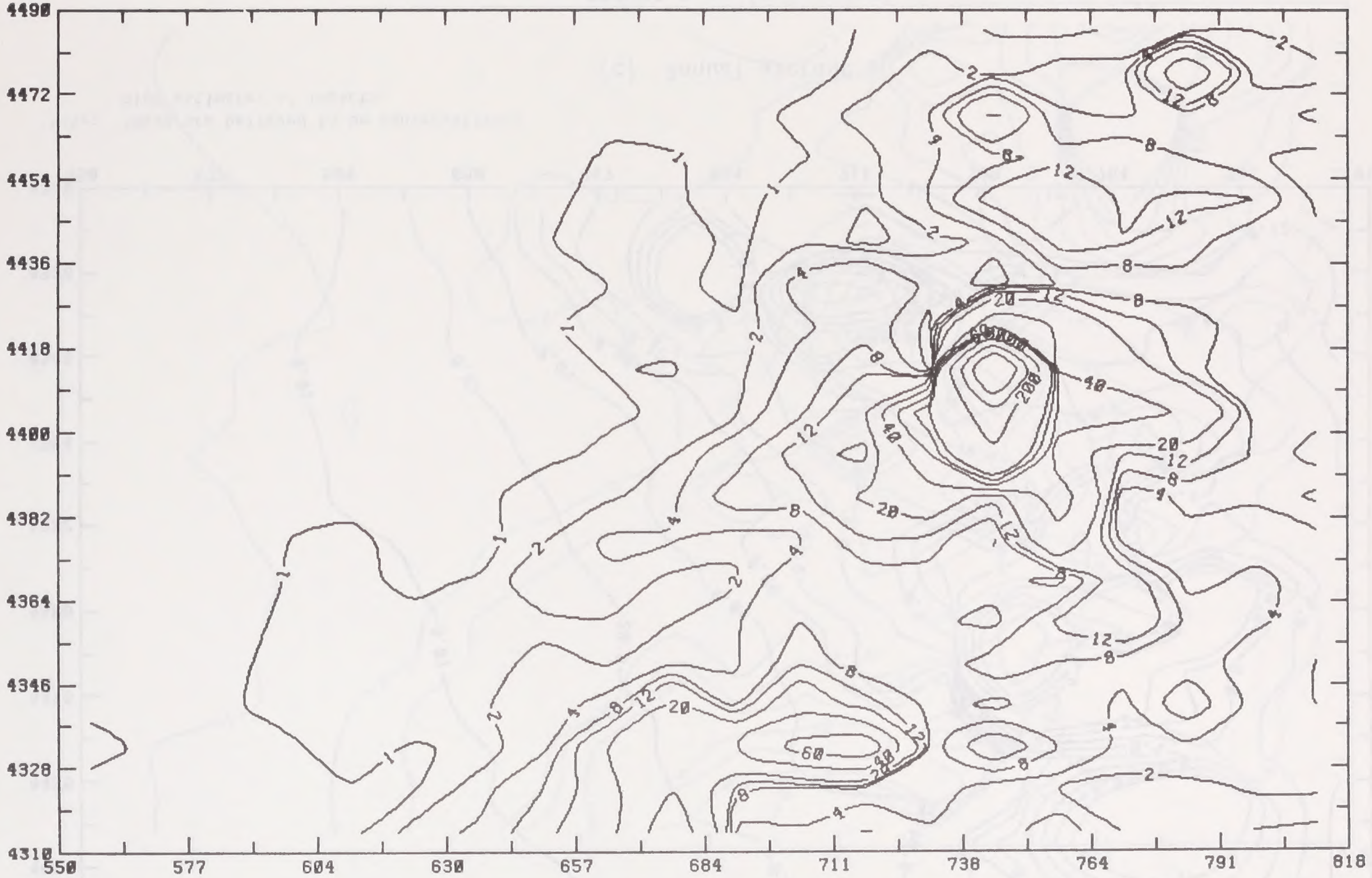

Note: These are believed to be conservatively high estimates of impacts and are non-simultaneous maxima calculated on the basis of one year's meteorological data.

(b) Maximum 24-hour average

FIGURE 5-11 (Continued)

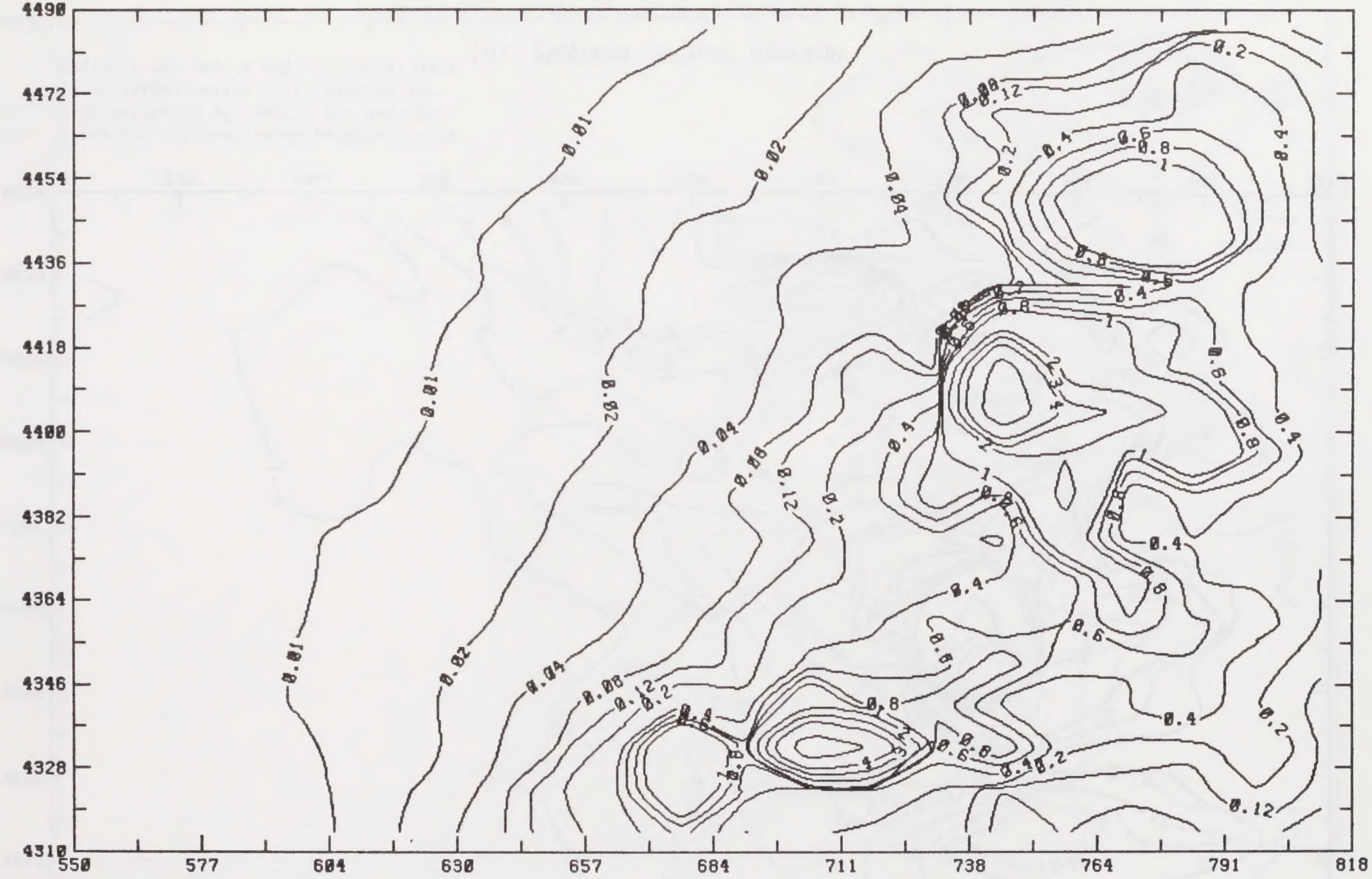

Note: These are believed to be conservatively high estimates of impacts.

(c) Annual average

FIGURE 5-11 (Concluded)

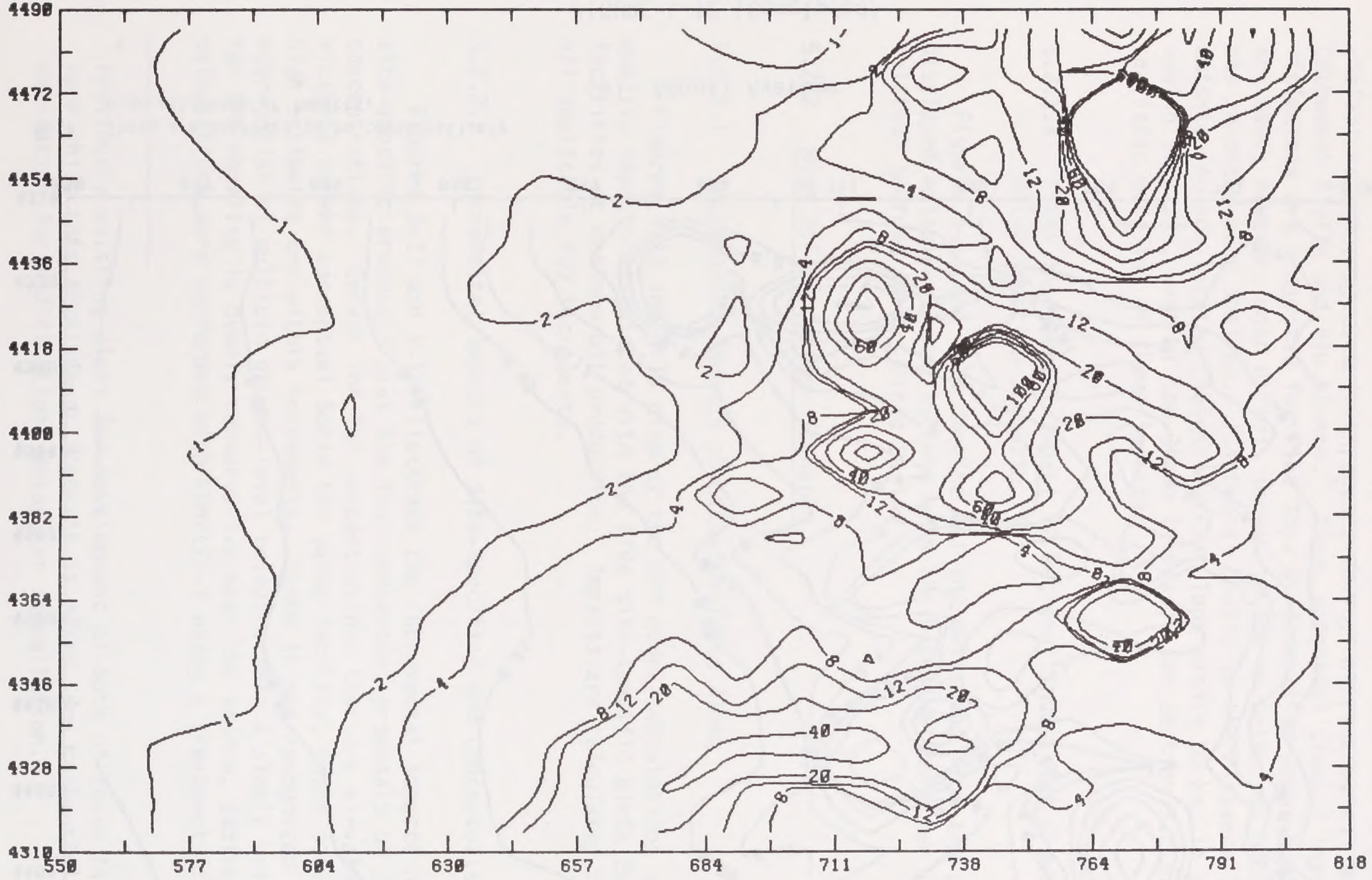

Note: These are believed to be conservatively high estimates of impacts and are non-simultaneous maxima calculated on the basis of one year's meteorological data.

(a) Maximum 24-hour average

FIGURE 5-12. IMPACT OF DIRECT SOURCE EMISSIONS FROM COLORADO POINT SOURCES ON GROUND-LEVEL TSP CONCENTRATIONS ($\mu g/m^3$) FOR LOW OIL PRODUCTION SCENARIO

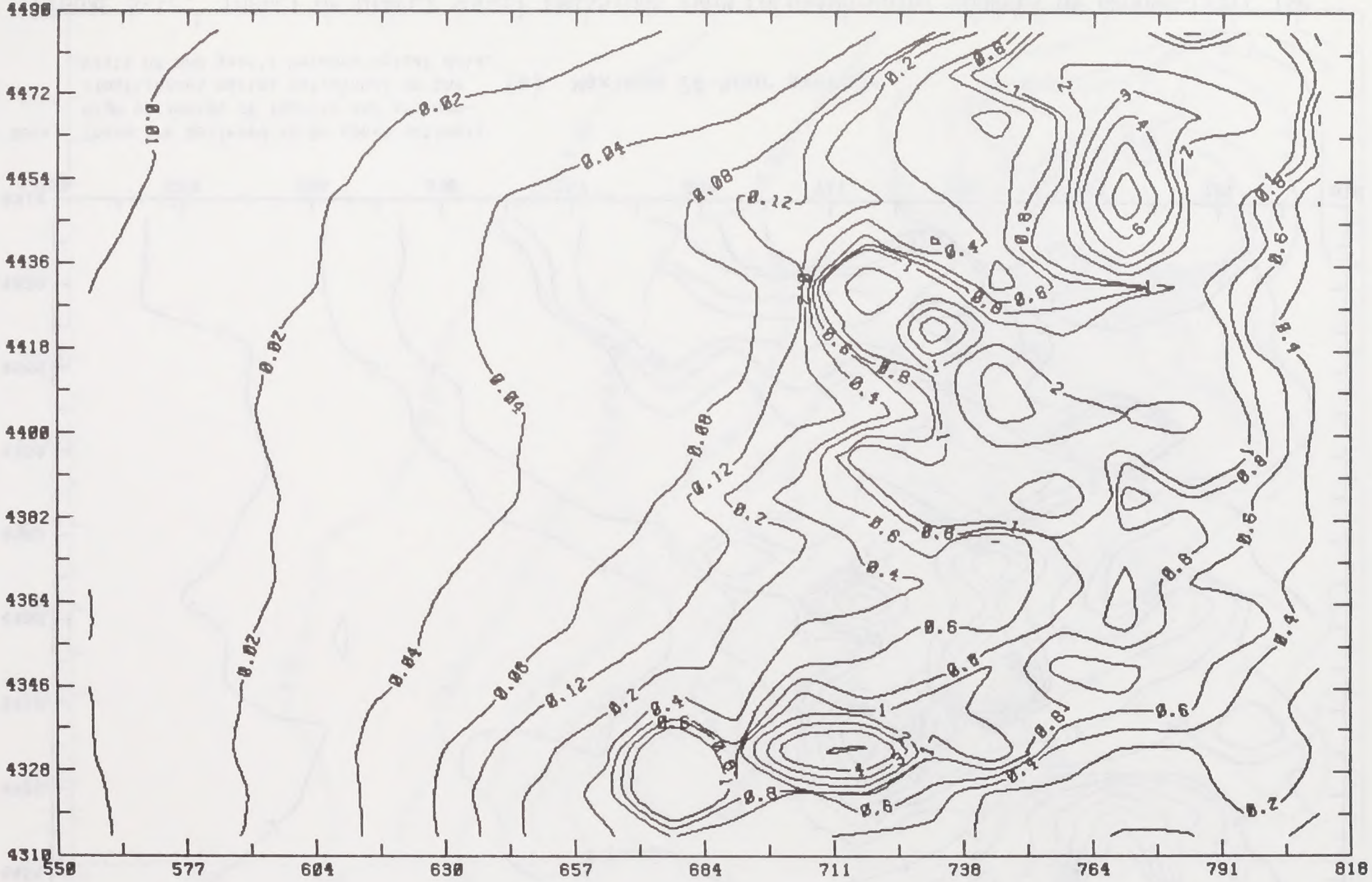

Note: These are believed to be conservatively high estimates of impacts.

(b) Annual Average

FIGURE 5-12 (Concluded)

months. With this important caveat stated, several potential problems are identified with PSD Class I and II increments. Potential Class II violations are projected (with conservative, high estimates) near Cathedral Bluffs and Rio Blanco.[*] Also, potential Class I increment violations are projected for Flat Tops Wilderness if upper-bound estimates are used; however, most of this impact is due to Cathedral Bluffs, which has recently been shelved. (Cathedral Bluffs is the Piceance Basin emission source located closest to Flat Tops within 60 km, in a generally upwind location, west of the Class I area.) See Section 5.2.2.3 for more realistic modeling of these impacts.

5.2.1.4 Total Incremental Impact of Regional Industrial Growth for Low-Oil-Production Scenario

Figures 5-13 and 5-14 combine all the emissions from the previously displayed emission source subsets with the baseline and other (inter-related) sources in the Uinta Basin.

5.2.2 High Oil Production Scenario

5.2.2.1 Incremental Impacts of Site-Specifics Alone

Figures 5-15 and 5-16 display the GPM model calculations of air quality impacts associated with the five site-specific Uinta Basin facilities at maximum oil production. Impacts are calculated to be within all applicable PSD increments.

5.2.2.2 Incremental Impacts of Site-Specifics and Conceptuals

Figures 5-17 and 5-18 illustrate the incremental impacts of the five site-specific proposals plus the four conceptual proposals on SO_2 and TSP concentrations. Except for TSP concentrations that are elevated in the vicinity of the conceptual Sohio tar sands facility, these conservative, high estimates are within increments. Since it was recognized that the aggregation of multiple ground-level releases into a single point source for GPM modeling is overly conservative near the source, additional calculations were performed with COMPLEX-I using a treatment of multiple

---

[*] Previously existing plans for development of both of these facilities, upon which this development scenario is based, are currently under evaluation for modification, delay, or cancellation.

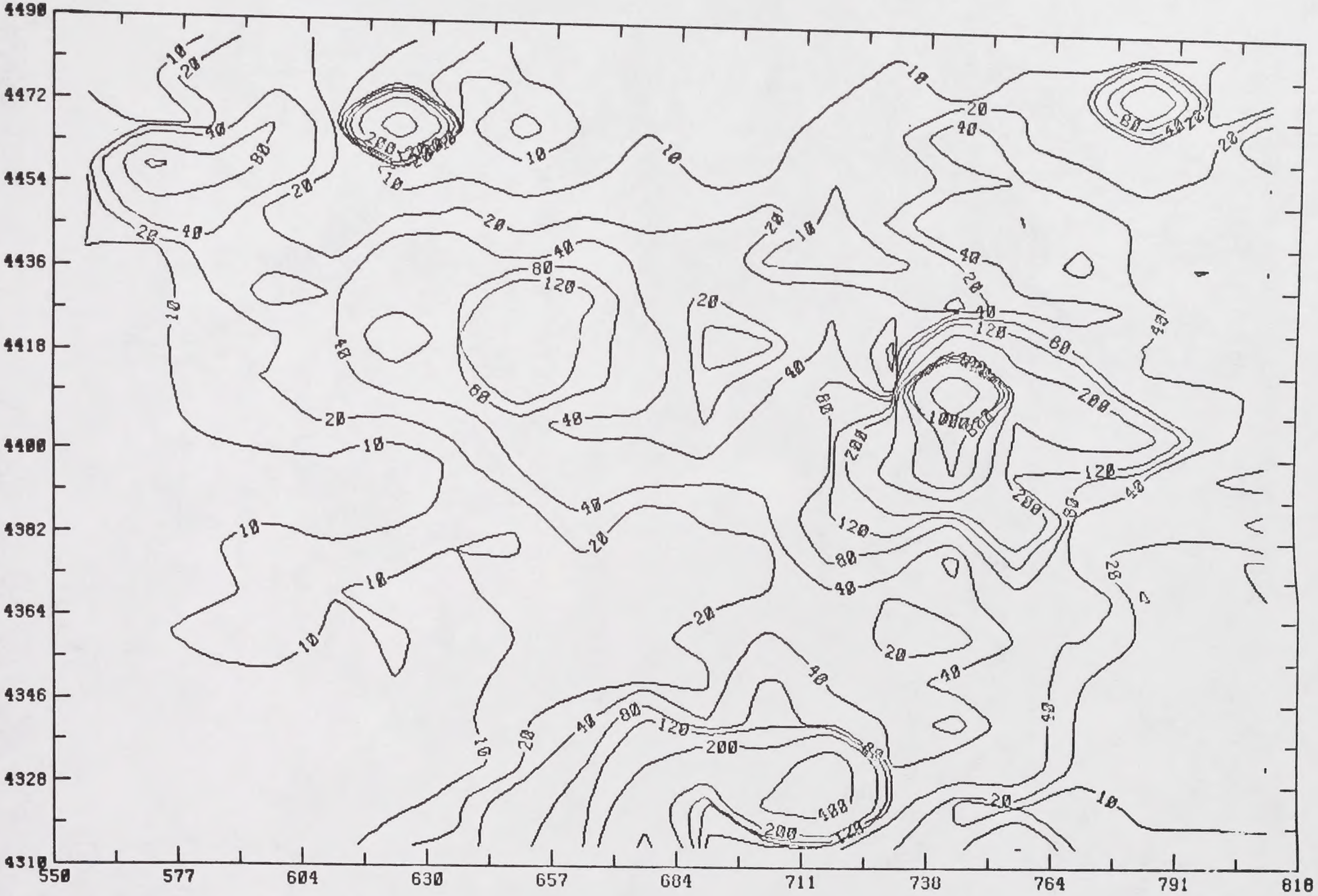

Note: These are believed to be conservatively high estimates of impacts and are non-simultaneous maxima calculated on the basis of one year's meteorological data.

(a) Maximum 3-Hour Average

FIGURE 5-13. IMPACT OF DIRECT SOURCE EMISSIONS ON GROUND-LEVEL SO_2 CONCENTRATIONS (μg/m^3) FOR THE LOW OIL PRODUCTION SCENARIO

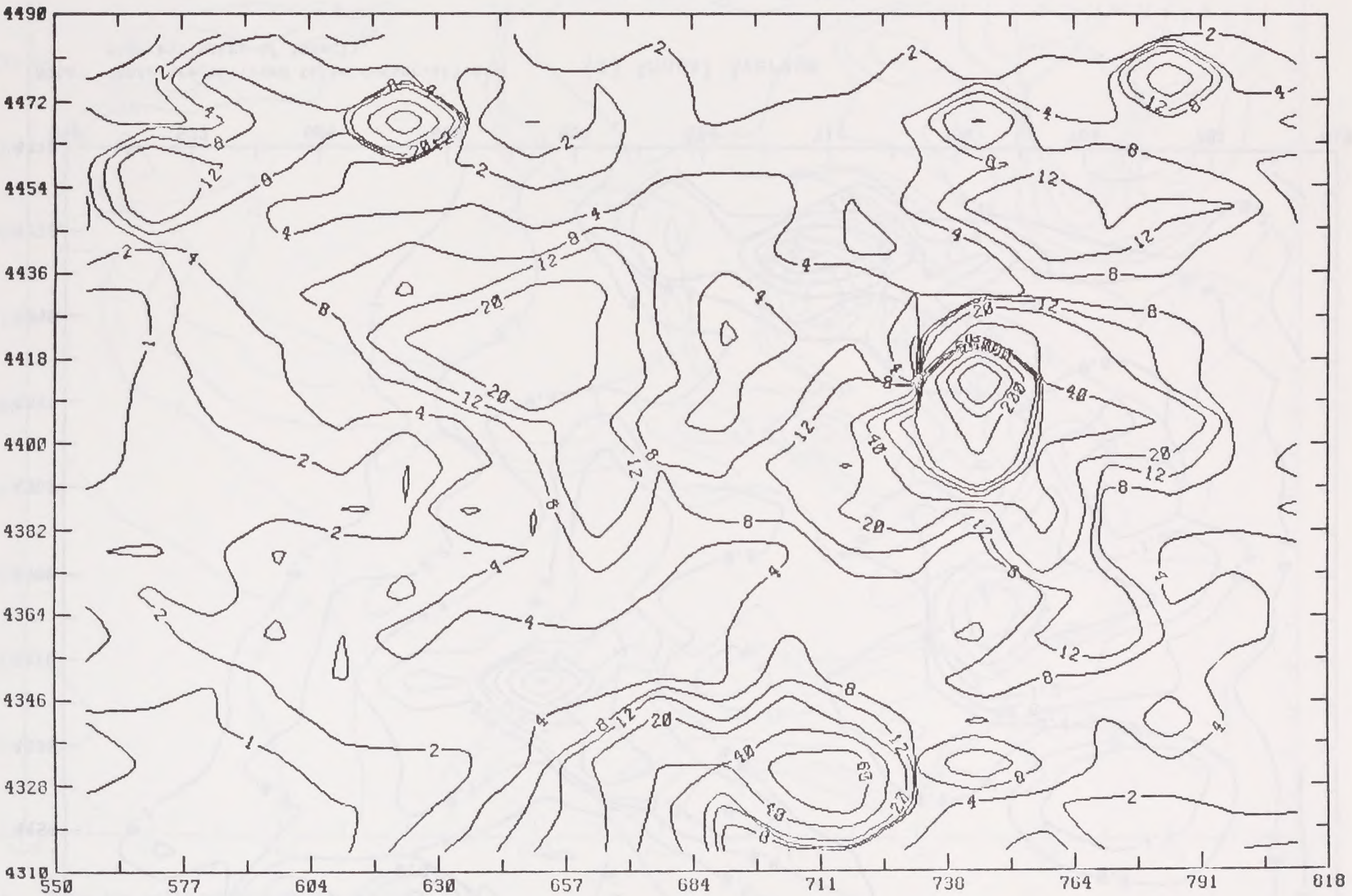

Note: These are believed to be conservatively high estimates of impacts and are non-simultaneous maxima calculated on the basis of one year's meteorological data.

(b) Maximum 24-Hour Averages

FIGURE 5-13 (Continued)

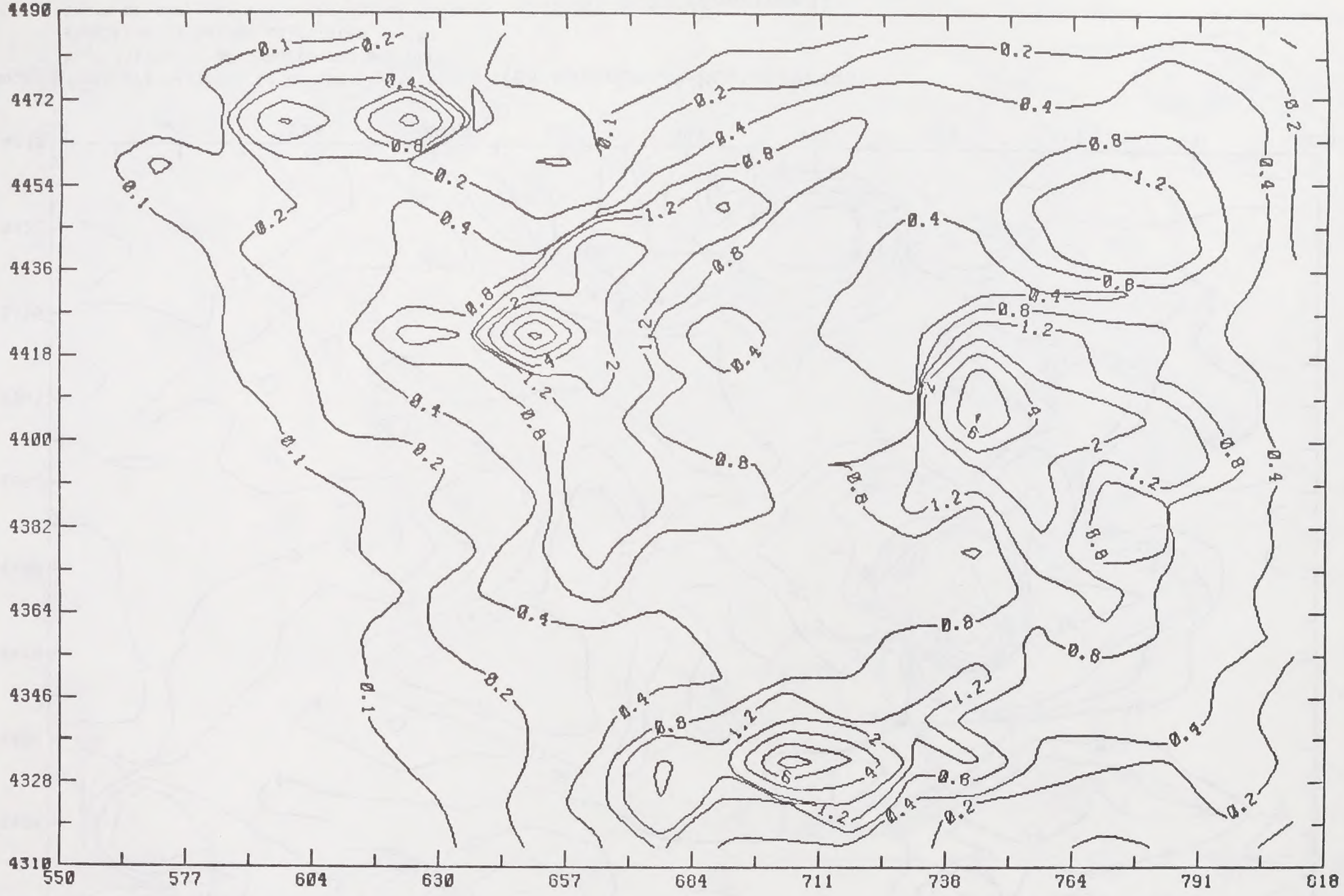

Note: These are believed to be conservatively high estimates of impacts.

(c) Annual Average

FIGURE 5-13 (Concluded)

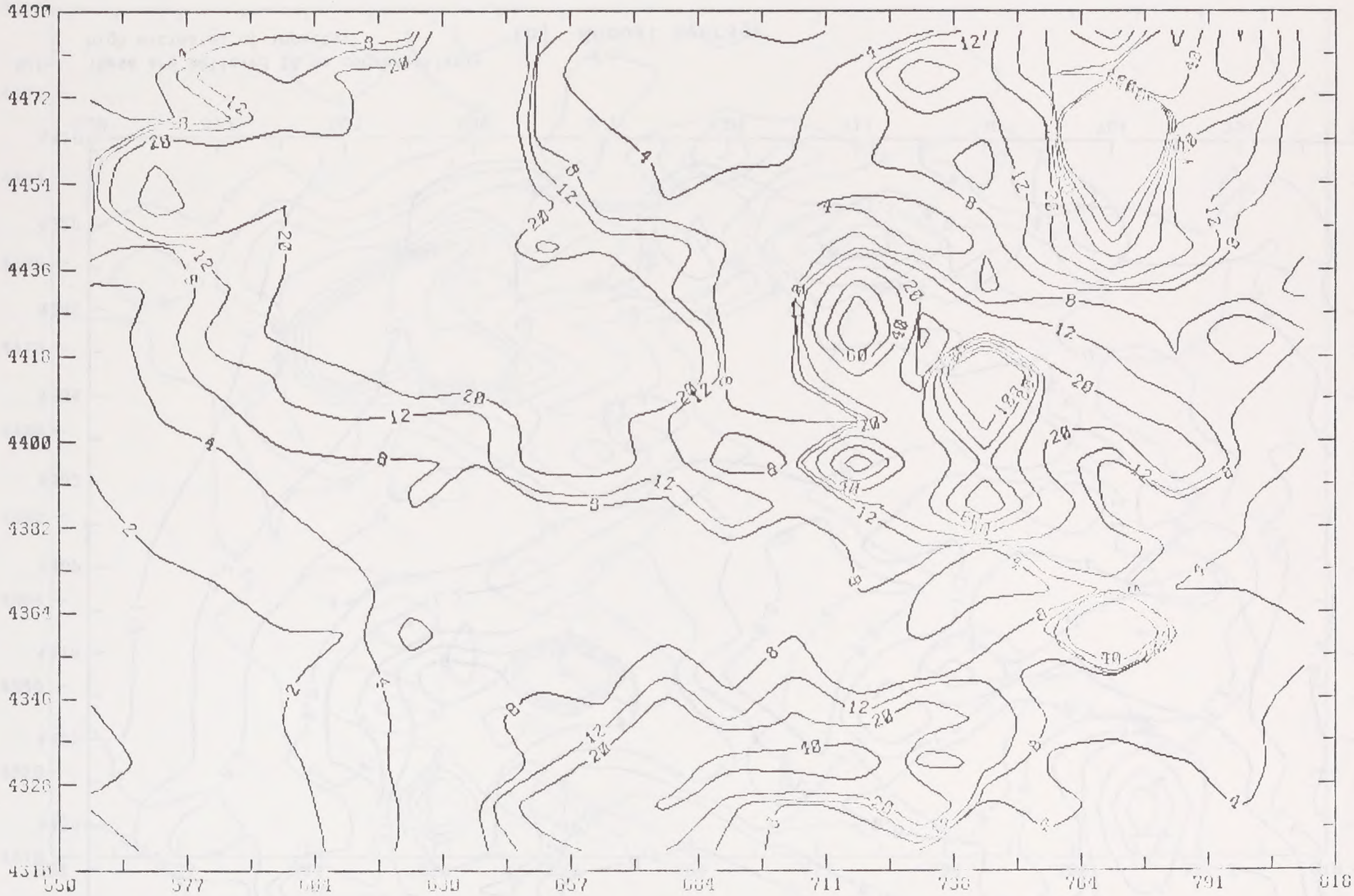

Note: These are believed to be conservatively high estimates of impacts and are non-simultaneous maxima calculated on the basis of one year's meteorological data.

(a) Maximum 24-hour average

FIGURE 5-14. IMPACT OF DIRECT SOURCE EMISSIONS ON GROUND-LEVEL TSP CONCENTRATIONS ($\mu g/m^3$) FOR THE LOW OIL PRODUCTION SCENARIO

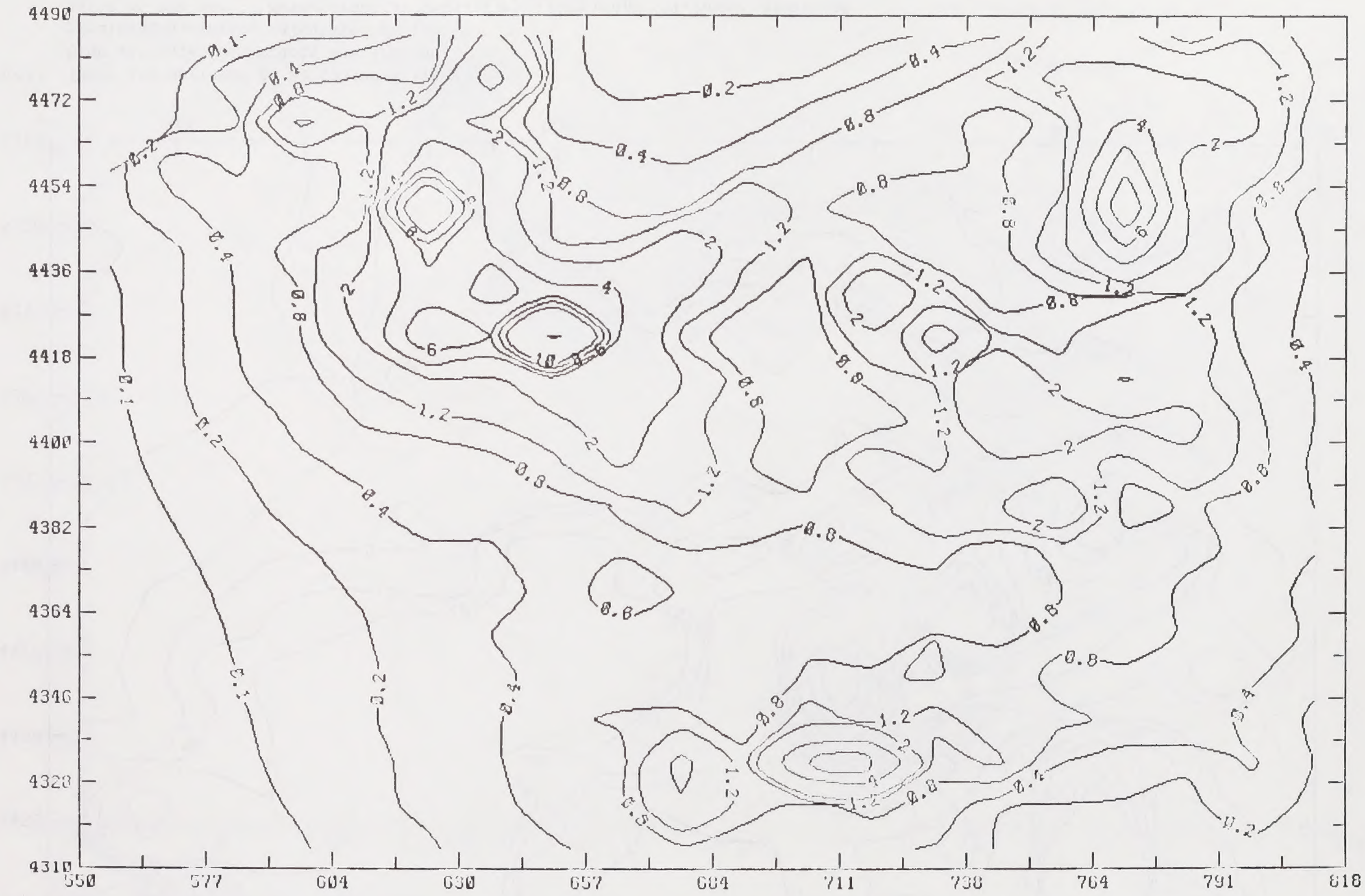

Note: These are believed to be conservatively high estimates of impacts.

(b) Annual average

FIGURE 5-14 (Concluded)

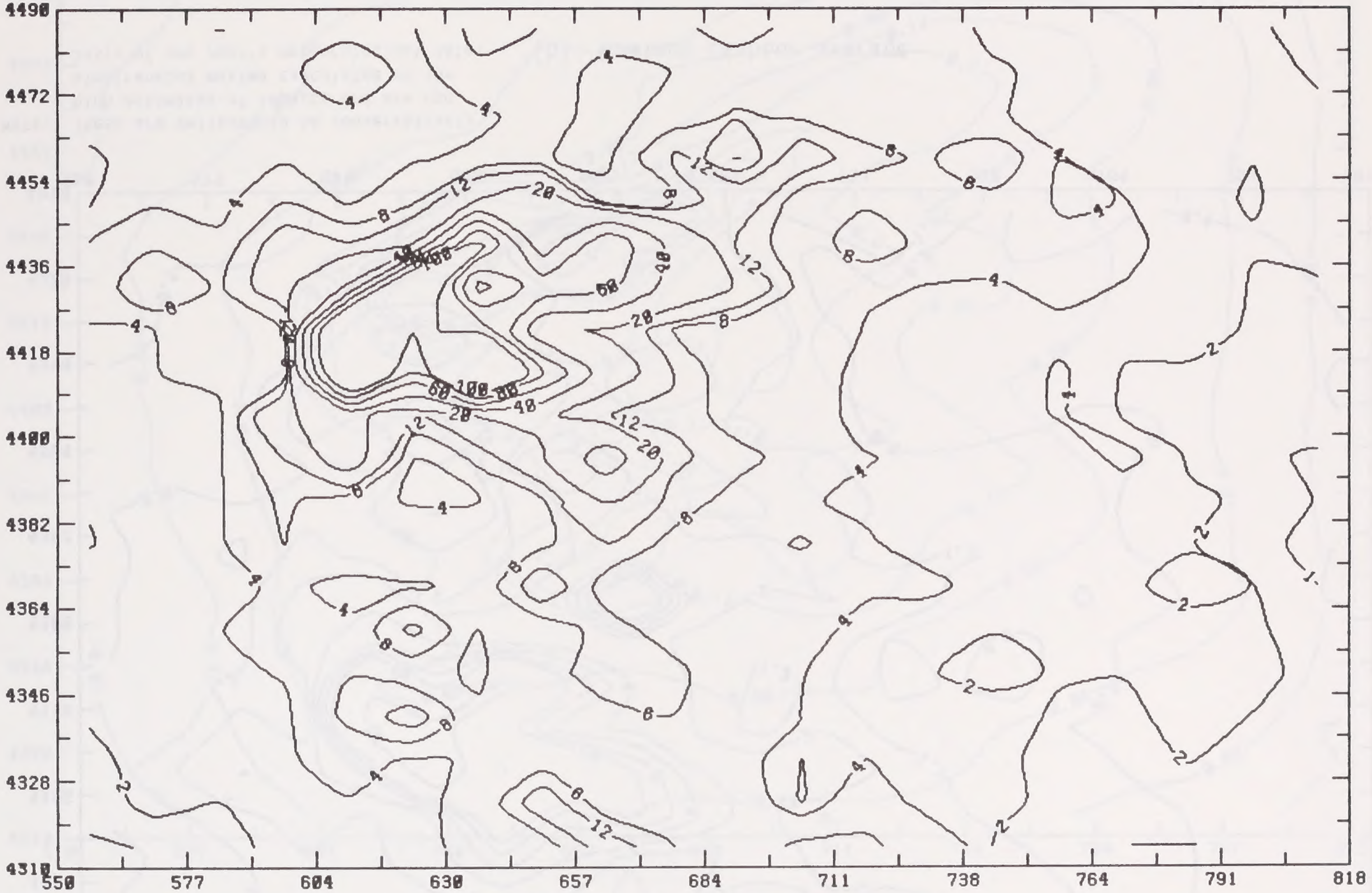

Note: These are believed to be conservatively high estimates of impacts and are non-simultaneous maxima calculated on the basis of one year's meteorological data.

(a) Maximum 3-hour average

FIGURE 5-15. IMPACT OF DIRECT SOURCE EMISSIONS FROM UINTA BASIN SITE-SPECIFICS ON GROUND-LEVEL SO_2 CONCENTRATIONS ($\mu g/m^3$) FOR THE HIGH OIL PRODUCTION SCENARIO

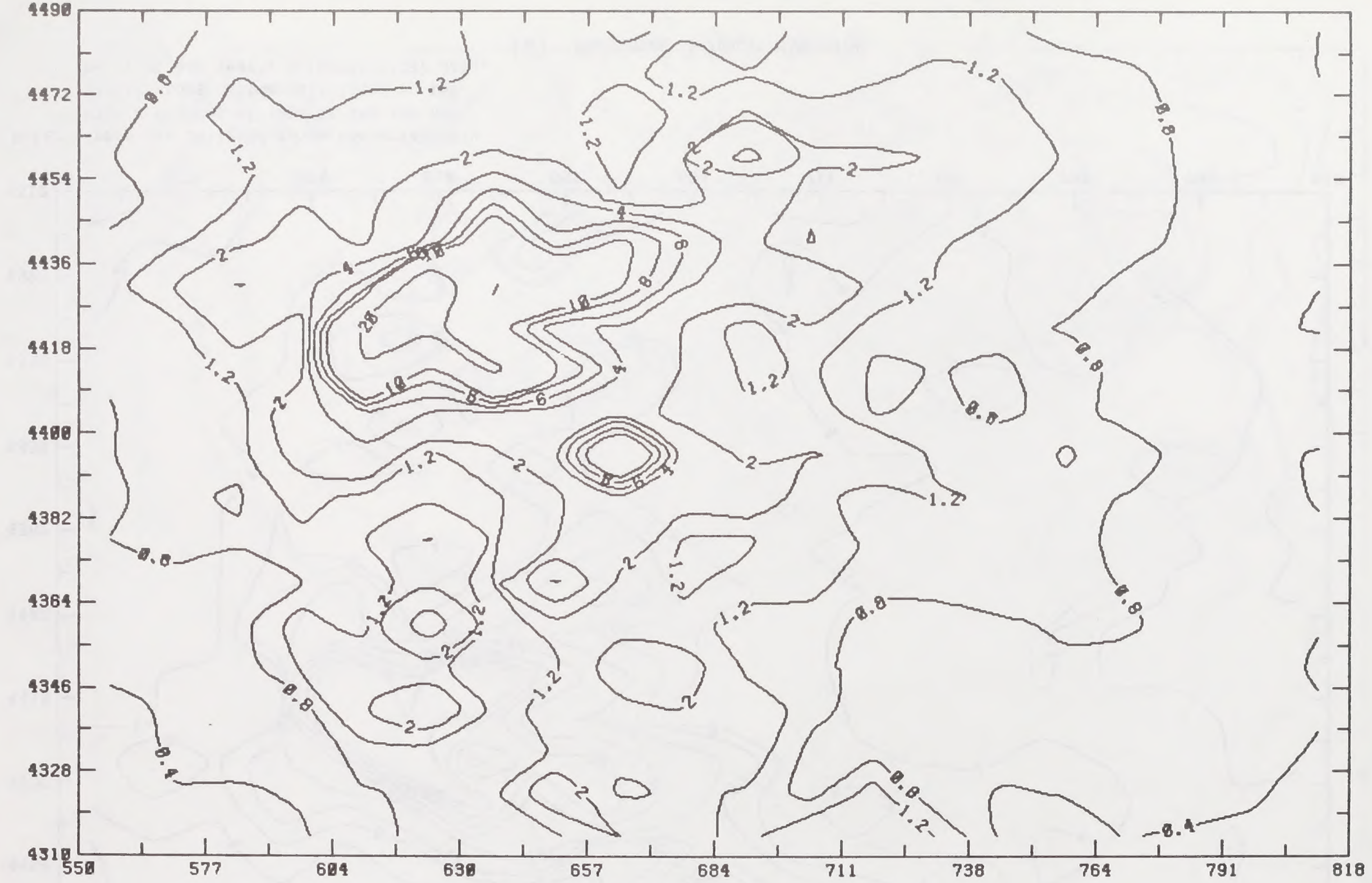

Note: These are believed to be conservatively high estimates of impacts and are non-simultaneous maxima calculated on the basis of one year's meteorological data.

(b) Maximum 24-hour average

FIGURE 5-15 (Continued)

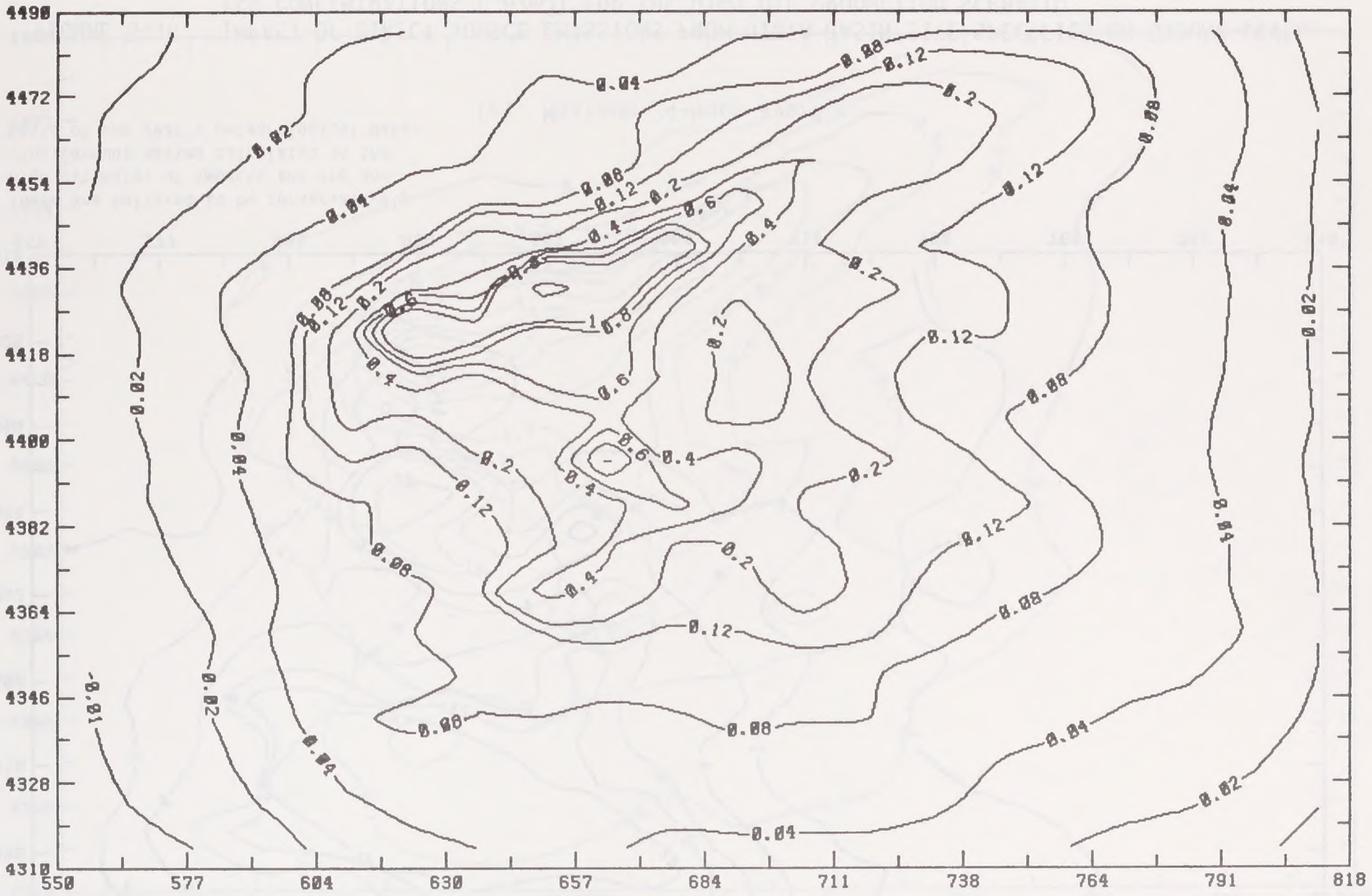

Note: These are believed to be conservatively high estimates of impacts.

(c) Annual average

FIGURE 5-15 (Concluded)

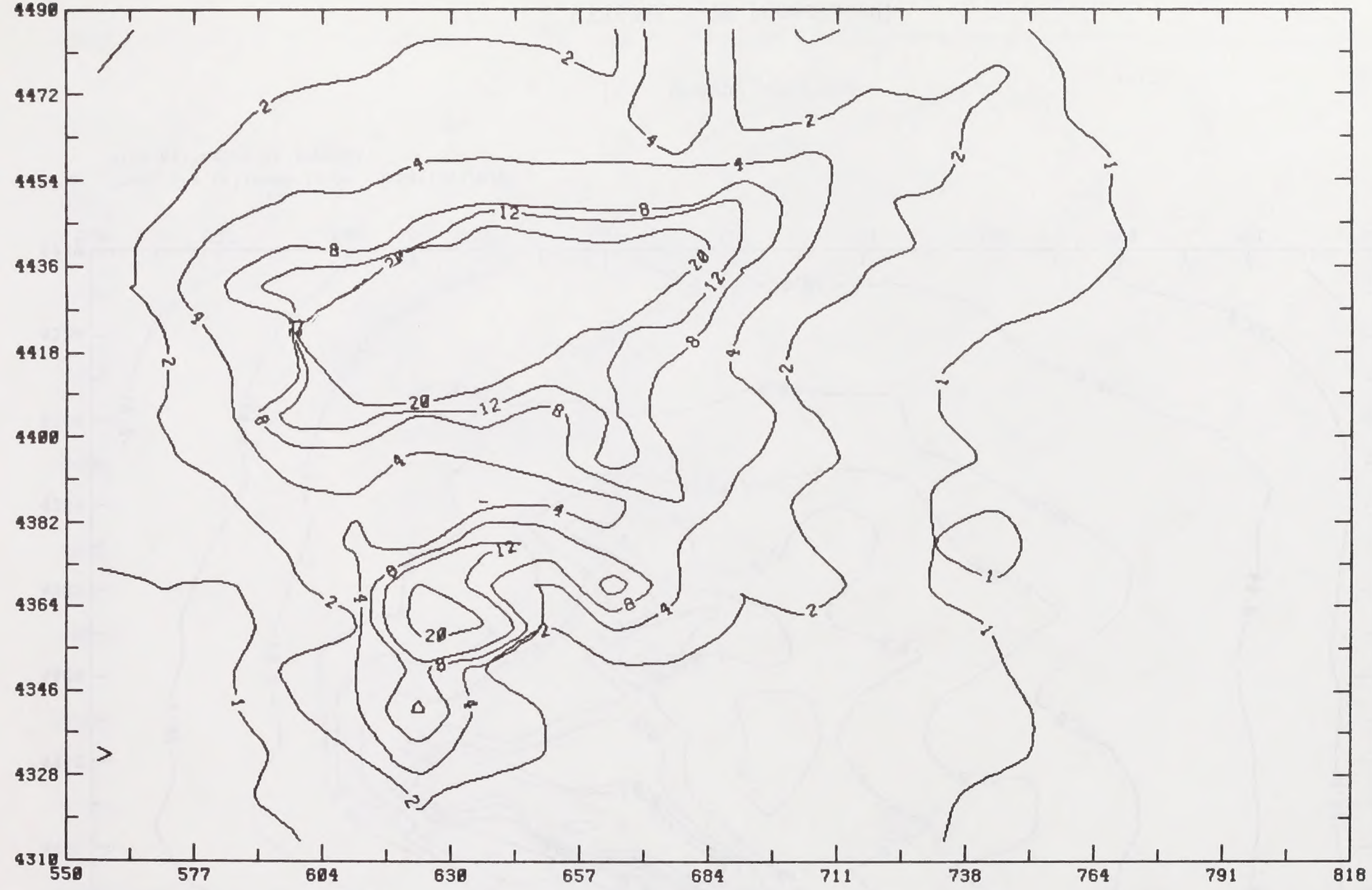

Note: These are believed to be conservatively high estimates of impacts and are non-simultaneous maxima calculated on the basis of one year's meteorological data.

(a) Maximum 24-hour average

FIGURE 5-16. IMPACT OF DIRECT SOURCE EMISSIONS FROM UINTA BASIN SITE-SPECIFICS ON GROUND-LEVEL TSP CONCENTRATIONS ($\mu g/m^3$) FOR THE HIGH OIL PRODUCTION SCENARIO

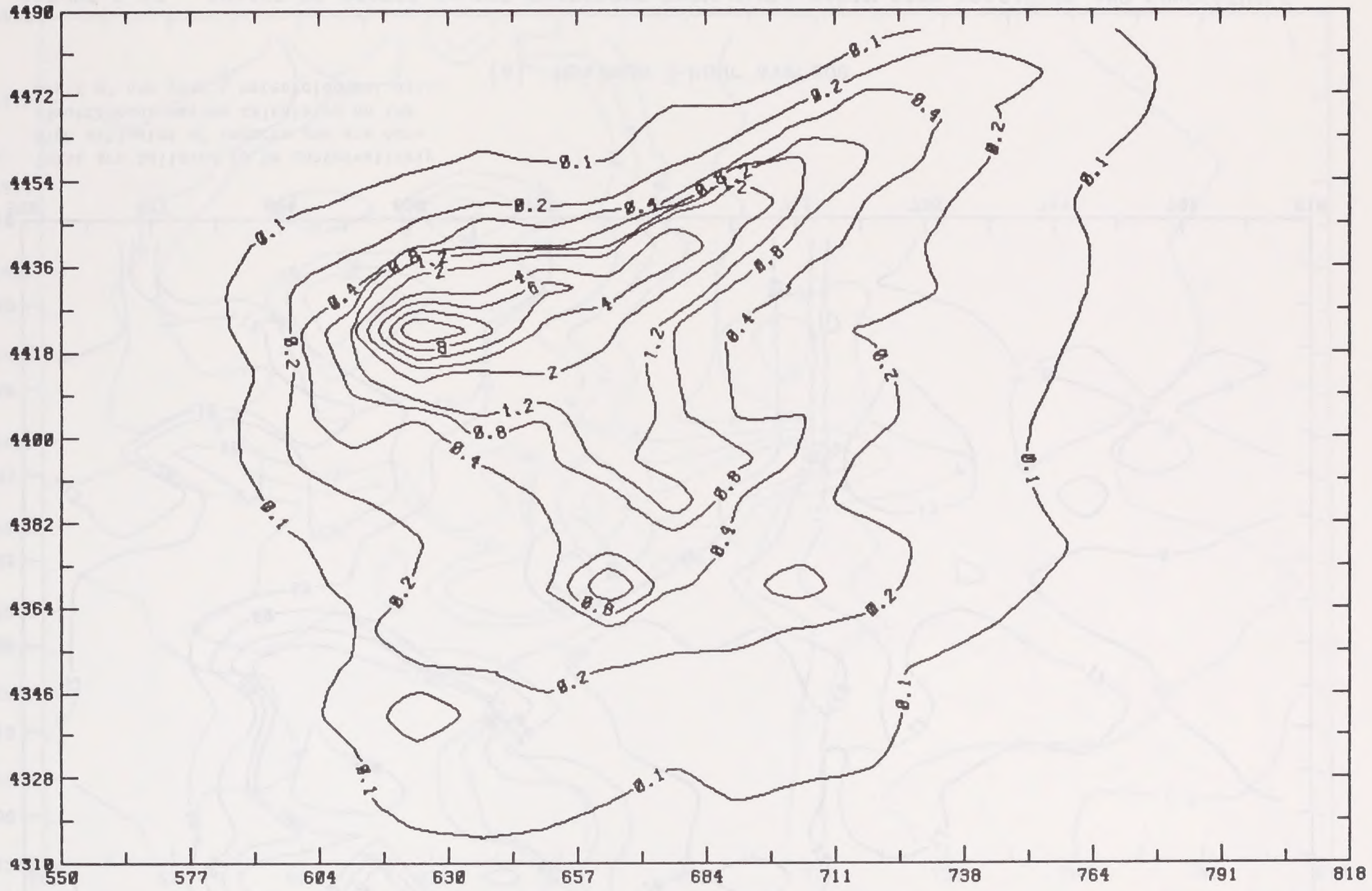

Note: These are believed to be conservatively high estimates of impacts.

(b) Annual average

FIGURE 5-16 (Concluded)

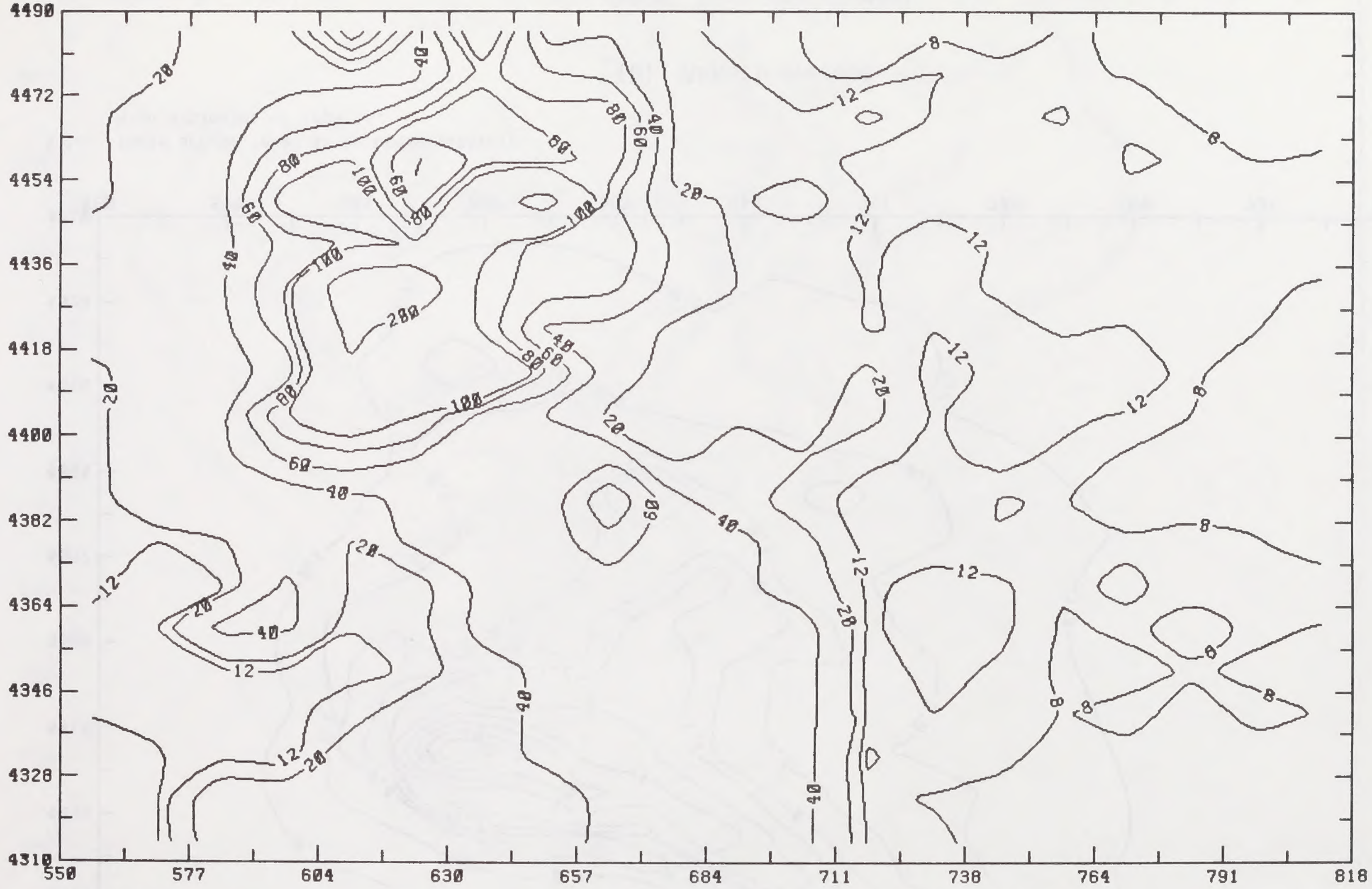

Note: These are believed to be conservatively high estimates of impacts and are non-simultaneous maxima calculated on the basis of one year's meteorological data.

(a) Maximum 3-hour average

FIGURE 5-17. IMPACT OF DIRECT SOURCE EMISSIONS FROM UINTA BASIN SITE-SPECIFICS AND CONCEPTUALS ON GROUND-LEVEL SO_2 CONCENTRATIONS ($\mu g/m^3$) FOR THE HIGH OIL PRODUCTION SCENARIO

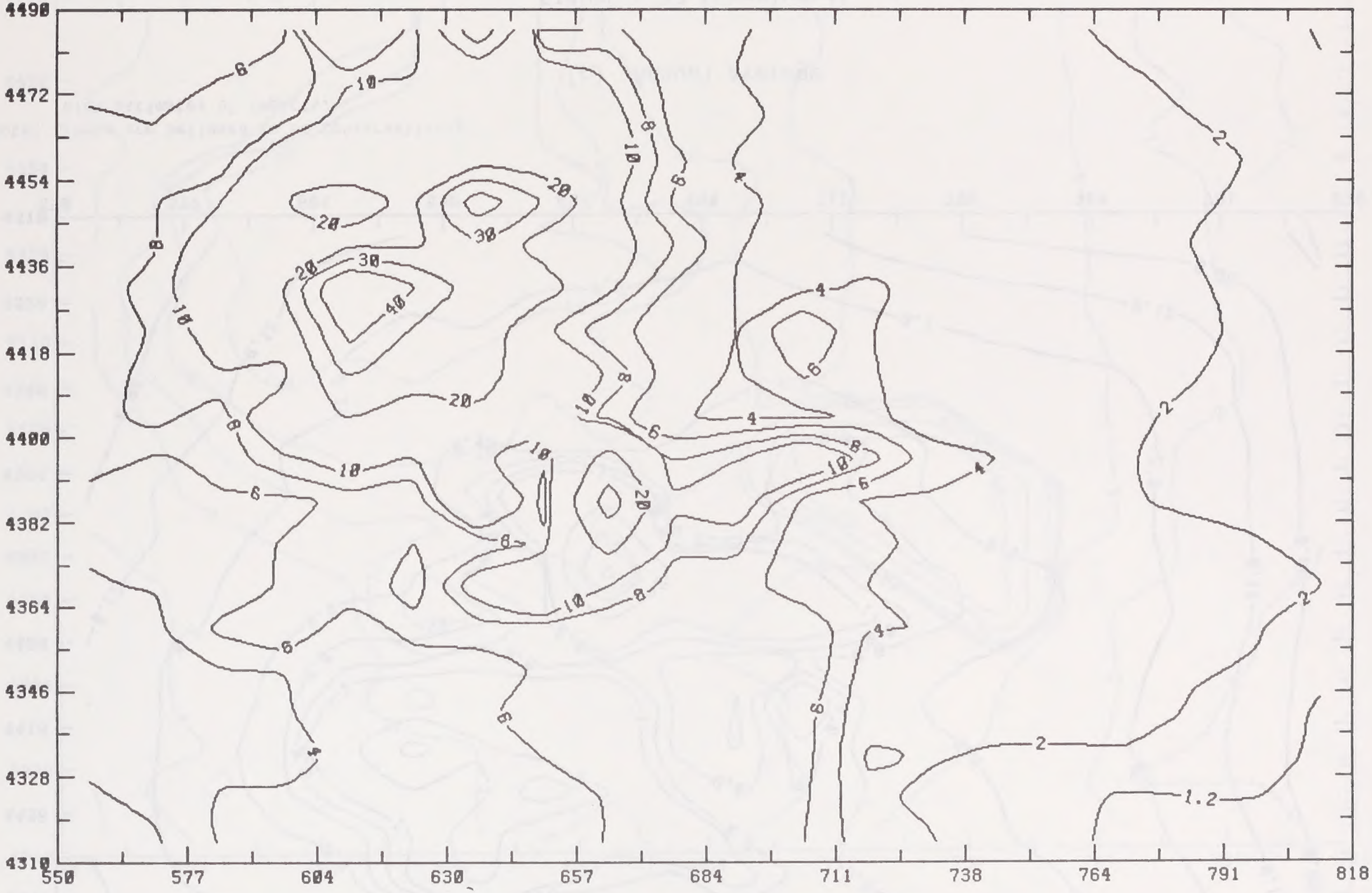

Note: These are believed to be conservatively high estimates of impacts and are non-simultaneous maxima calculated on the basis of one year's meteorological data.

(b) Maximum 24-hour average

FIGURE 5-17 (Continued)

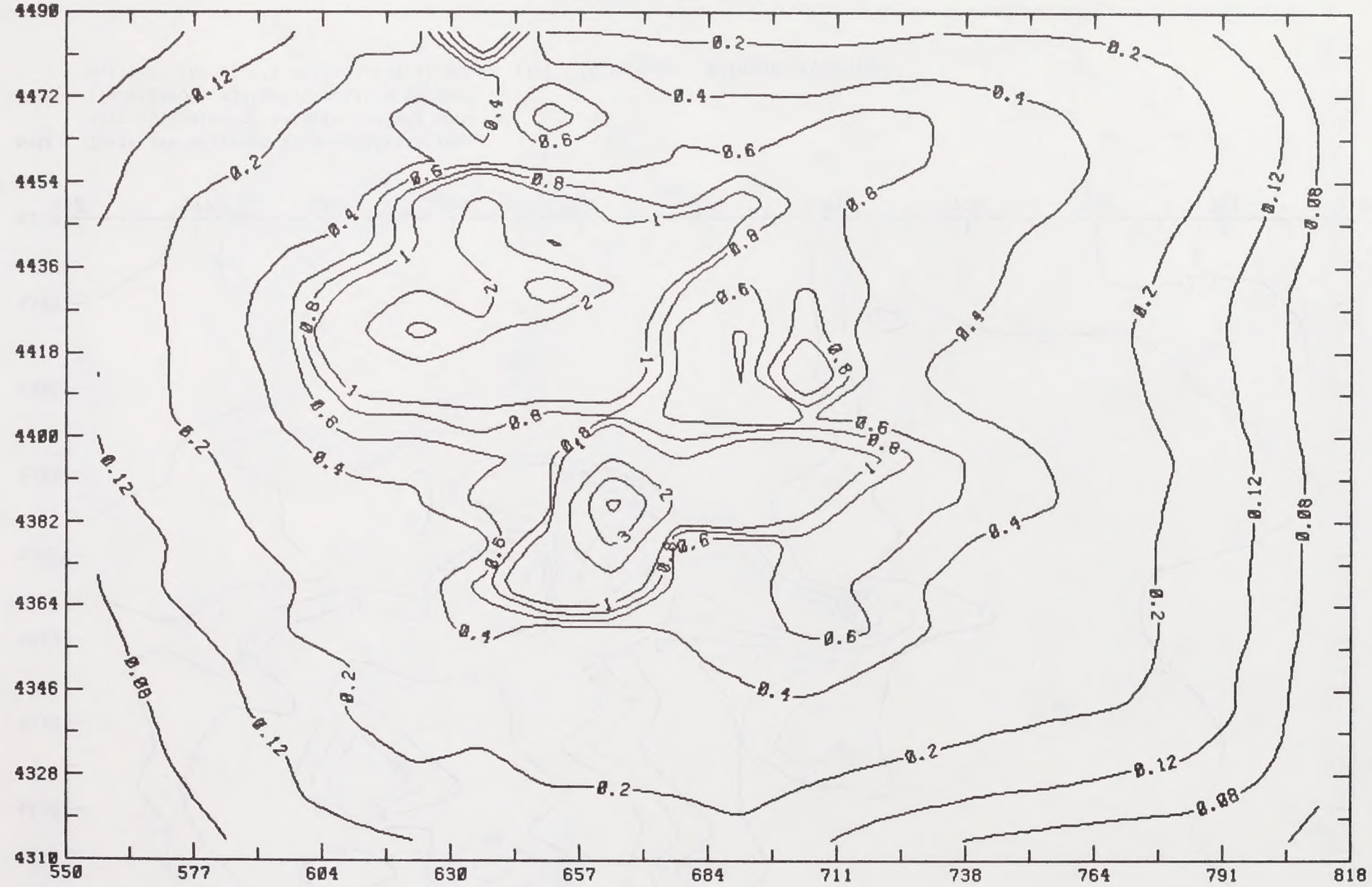

Note: These are believed to be conservatively high estimates of impacts.

(c) Annual average

FIGURE 5-17 (Concluded)

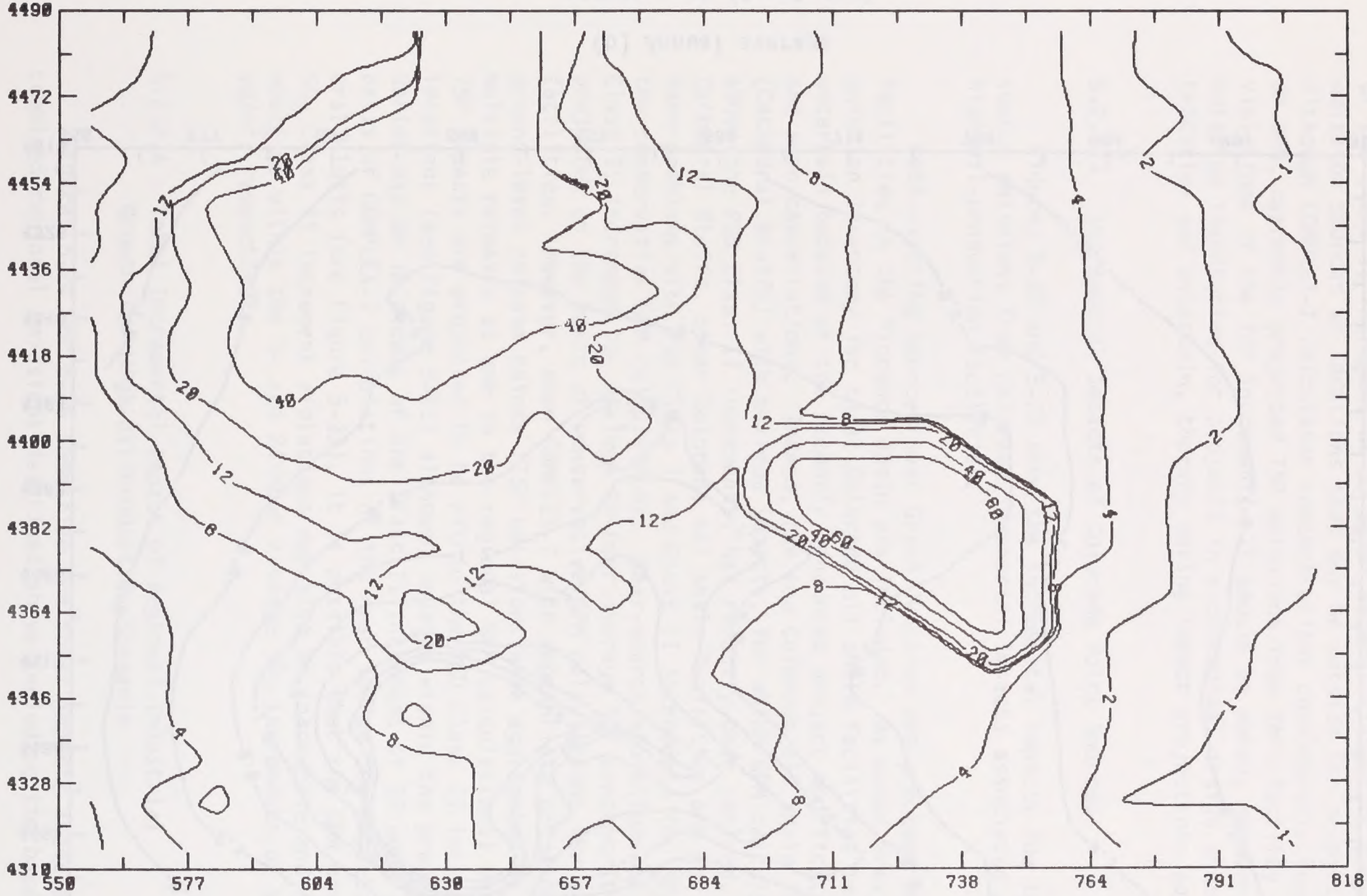

Note: These are believed to be conservatively high estimates of impacts and are non-simultaneous maxima calculated on the basis of one year's meteorological data.

(a) Maximum 24-hour average

FIGURE 5-18. IMPACT OF DIRECT SOURCE EMISSIONS FROM UINTA BASIN SITE-SPECIFICS AND CONCEPTUALS ON GROUND-LEVEL TSP CONCENTRATIONS ($\mu g/m^3$) FOR THE HIGH OIL PRODUCTION SCENARIO

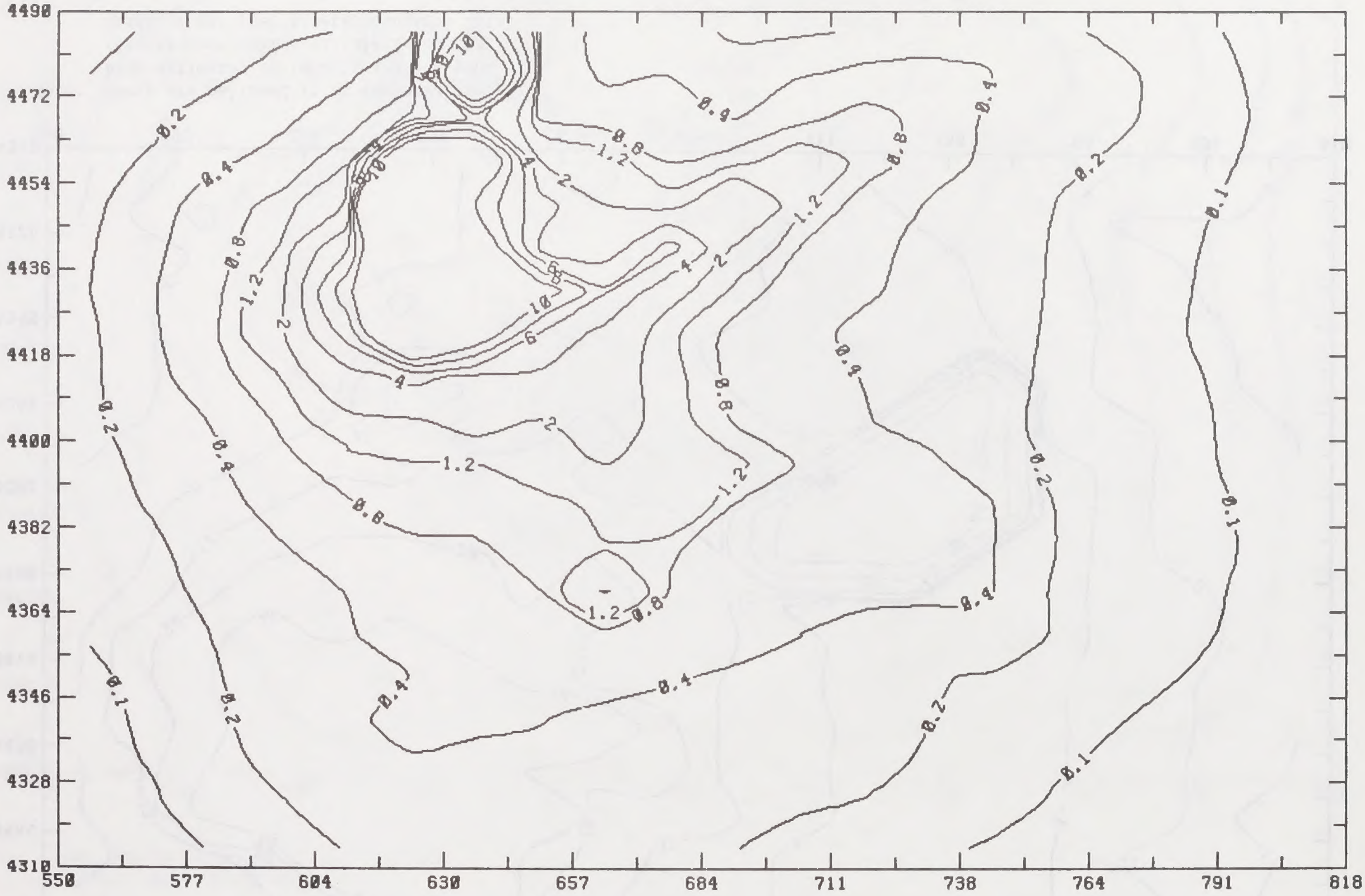

(b) Annual average

FIGURE 5-18 (Concluded)

sources (see Figure 5-19). These calculations show TSP impacts in excess of the Class II increment of 37 µg/m^3 several kilometers away from emission sources at locations that may be outside the property boundary. Although COMPLEX-I calculates concentrations considerably lower than those of GPM, currently projected TSP emissions from this facility could cause violations of the TSP increment. It should be noted, however, that emission inventories for projects in a conceptual design phase are tentative and uncertain, thereby making impact projections speculative.

5.2.2.3 Incremental Impacts of Colorado Point Sources

Figures 5-20 and 5-21 show the incremental impacts due to direct source emissions from Colorado industrial impacts associated with the high-oil-production facilities.

Both existing sources near Grand Junction and proposed oil shale facilities in the Piceance Basin are included. As noted previously, the emission inventory for these Colorado oil shale facilities is very uncertain because of the recently announced project modifications, delays, and even cancellations. Indeed, the one Colorado oil shale facility (Cathedral Bluffs) with maximum impacts, for which GPM calculates impacts above the PSD Class II increments, has recently been shelved. Except for Cathedral Bluffs, other Colorado oil shale facilities are not projected to have problems with PSD Class I and Class II increments for SO_2, based on the conservative GPM calculations. Near-source violations of the PSD Class II increment for maximum 24-hour average TSP concentrations are projected on the basis of conservative GPM calculations for several facilities. However, when COMPLEX-I with appropriate gridding of multiple ground-level release points (TSP emissions were aggregated by treating multiple releases as one in the regional GPM calculations) was applied, TSP impacts are projected to be within the PSD Class II increments at all locations (see Figure 5-22) although impacts within the property boundaries may be in excess of the Class II increment of 37 µg/m^3. On the basis of COMPLEX-I calculations of the near source SO_2 impacts of Cathedral Bluffs (see Figure 5-23), it is possible that the GPM projections of SO_2 Class II increment violations may also be inaccurate and that impacts would be within the 3- and 24-hour average SO_2 increments of 512 and 91 µg/m^3, respectively.

5.2.2.4 Total Incremental Impact of Regional Industrial Growth for High-Oil-Production Scenario

Figures 5-24 and 5-25 summarize the total impacts associated with the combined regional emissions described above including the baseline and

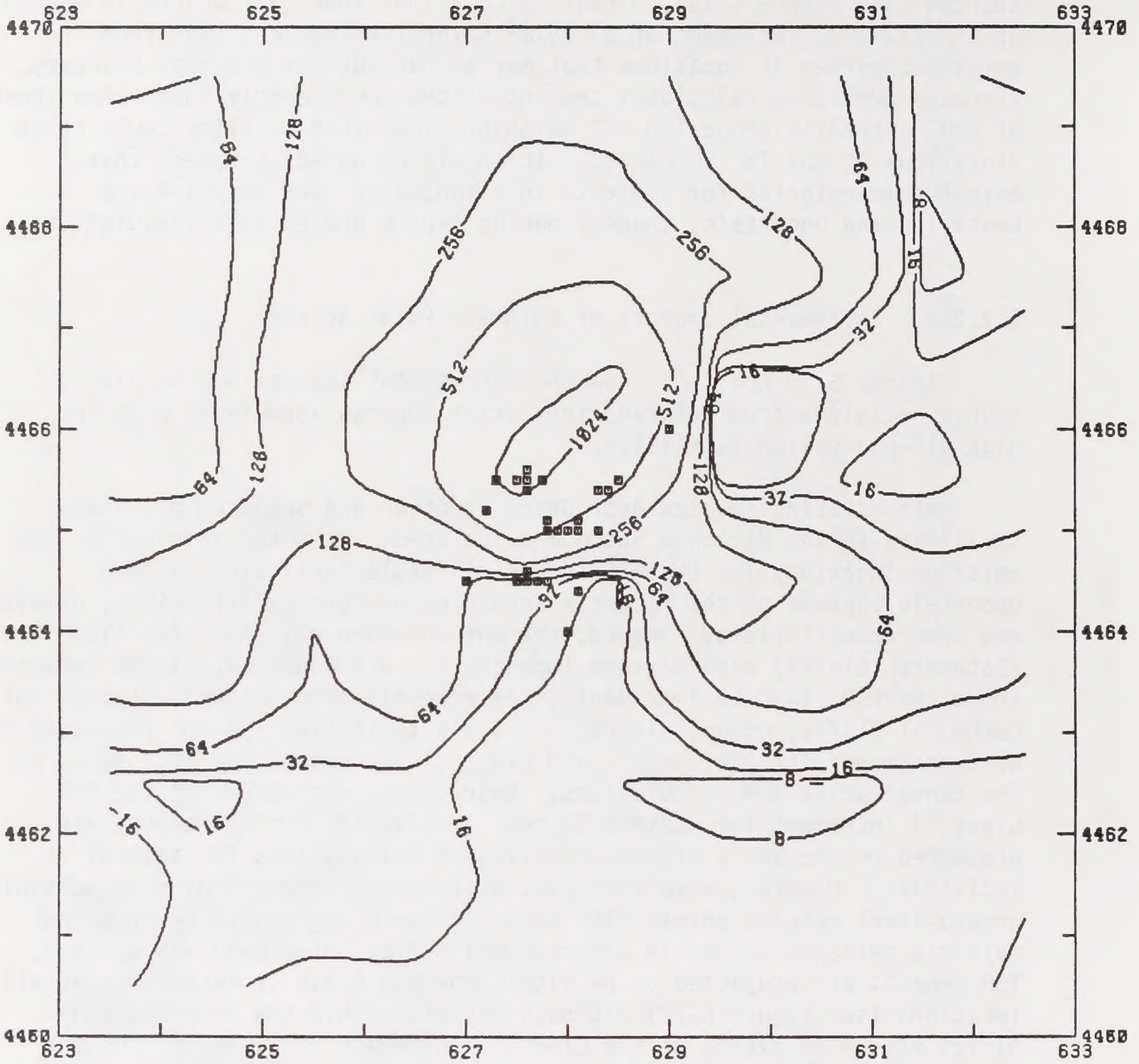

Note: These are believed to be conservatively high estimates of impacts and are non-simultaneous maxima calculated on the basis of one year's meteorological data.

▣ Point Sources

FIGURE 5-19. MAXIMUM 24-HOUR AVERAGE, NEAR-SOURCE TSP CONCENTRATIONS ($\mu g/m^3$) RESULTING FROM DIRECT SOURCE EMISSIONS FROM THE SOHIO CONCEPTUAL TAR SANDS FACILITY ON THE BASIS OF COMPLEX-I CALCULATIONS

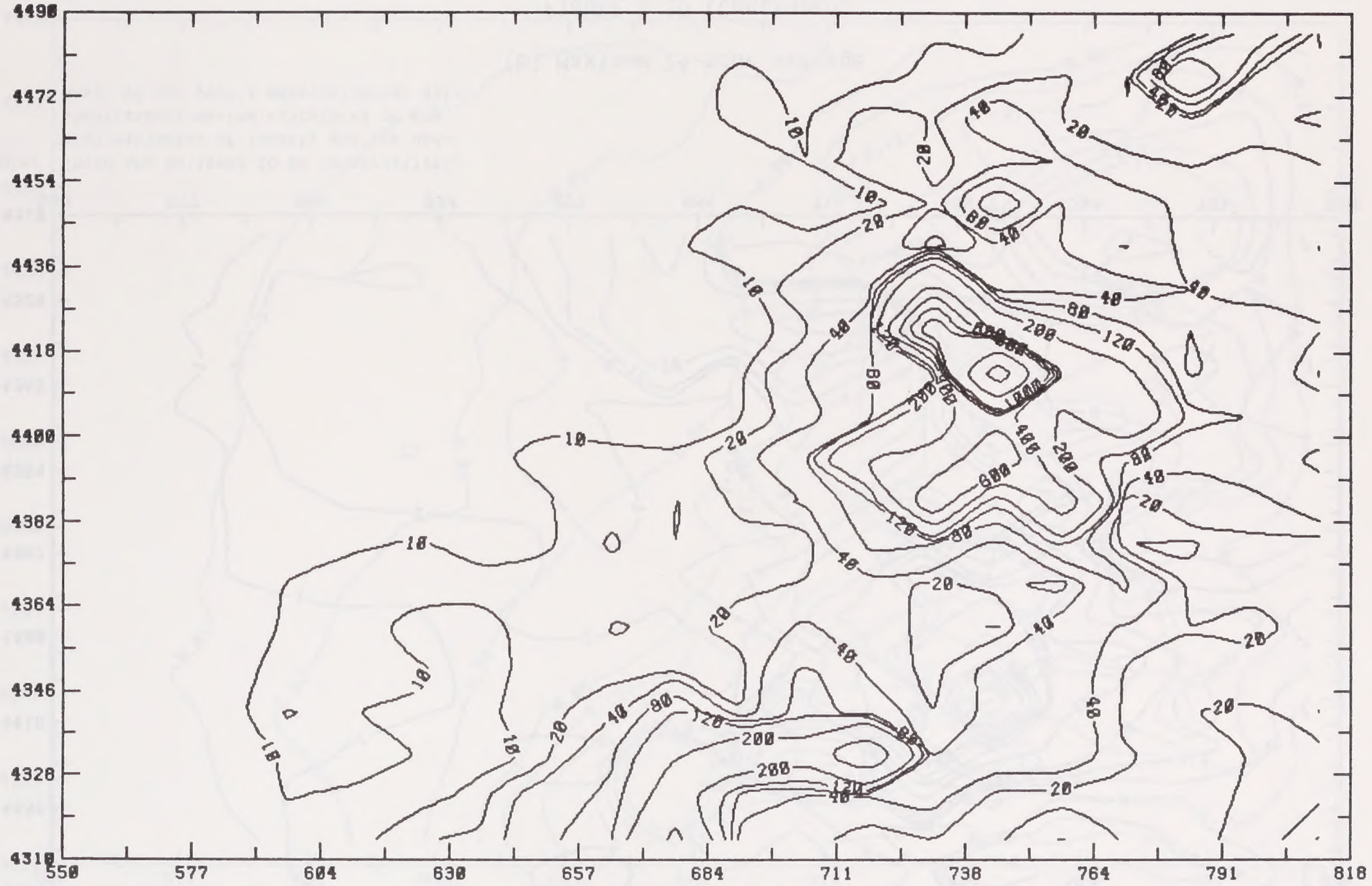

Note: These are believed to be conservatively high estimates of impacts and are non-simultaneous maxima calculated on the basis of one year's meteorological data.

(a) Maximum 3-hour average

FIGURE 5-20. IMPACT OF DIRECT SOURCE EMISSIONS FROM COLORADO POINT SOURCES ON GROUND-LEVEL SO_2 CONCENTRATIONS ($\mu g/m^3$) FOR THE HIGH OIL PRODUCTION SCENARIO

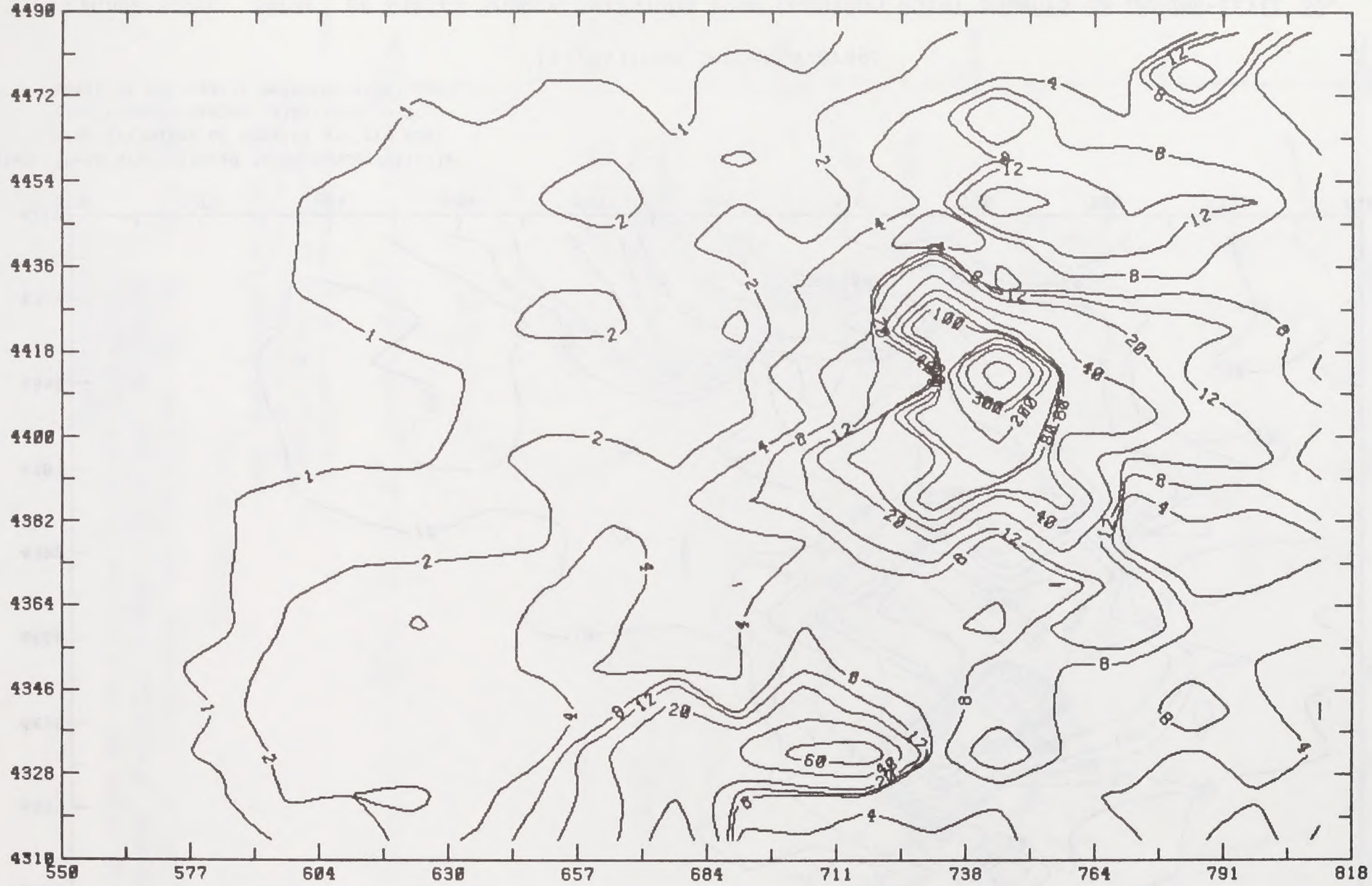

Note: These are believed to be conservatively high estimates of impacts and are non-simultaneous maxima calculated on the basis of one year's meteorological data.

(b) Maximum 24-hour average

FIGURE 5-20 (Continued)

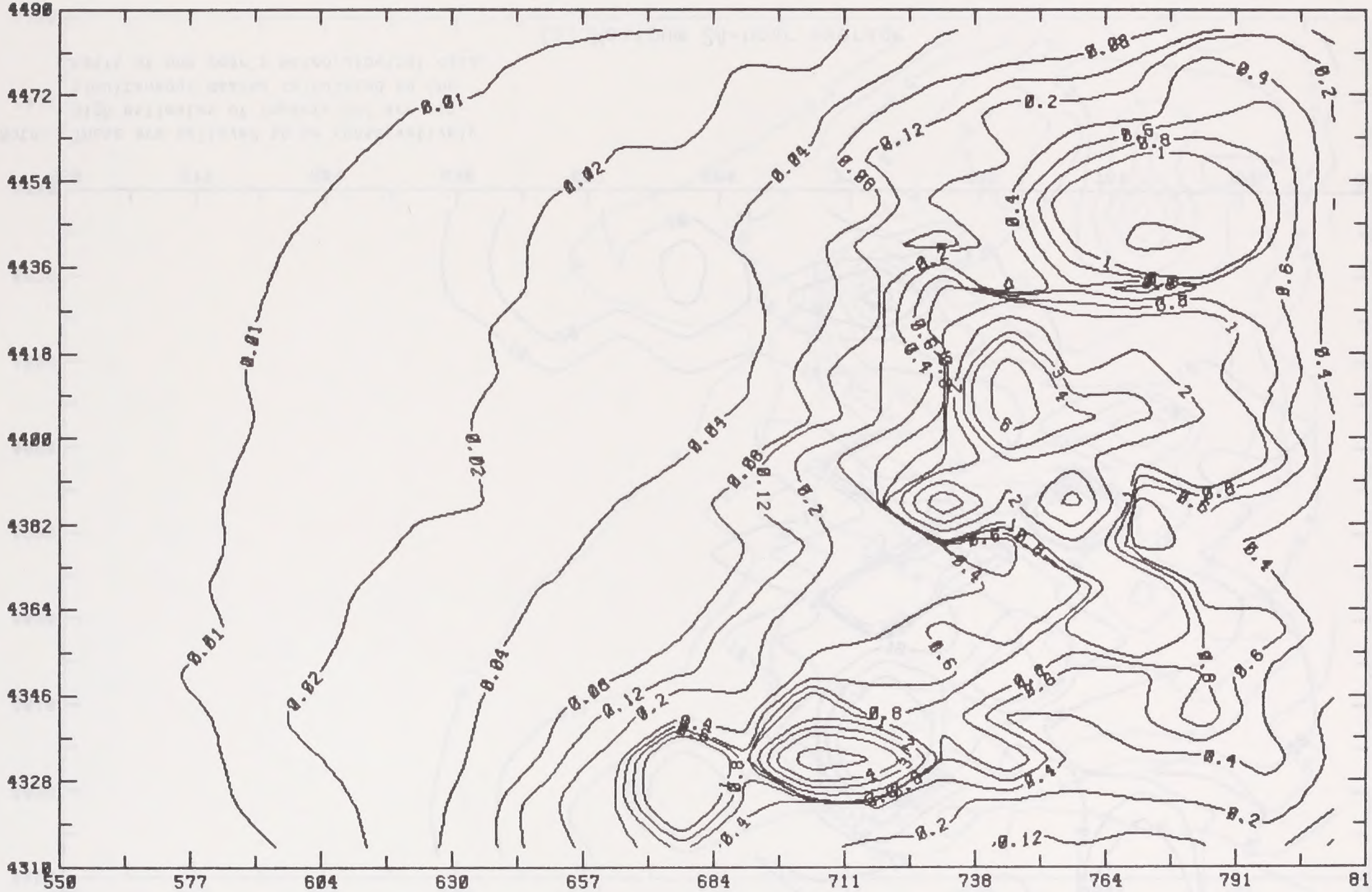

Note: These are believed to be conservatively high estimates of impacts.

(c) Annual average

FIGURE 5-20 (Concluded)

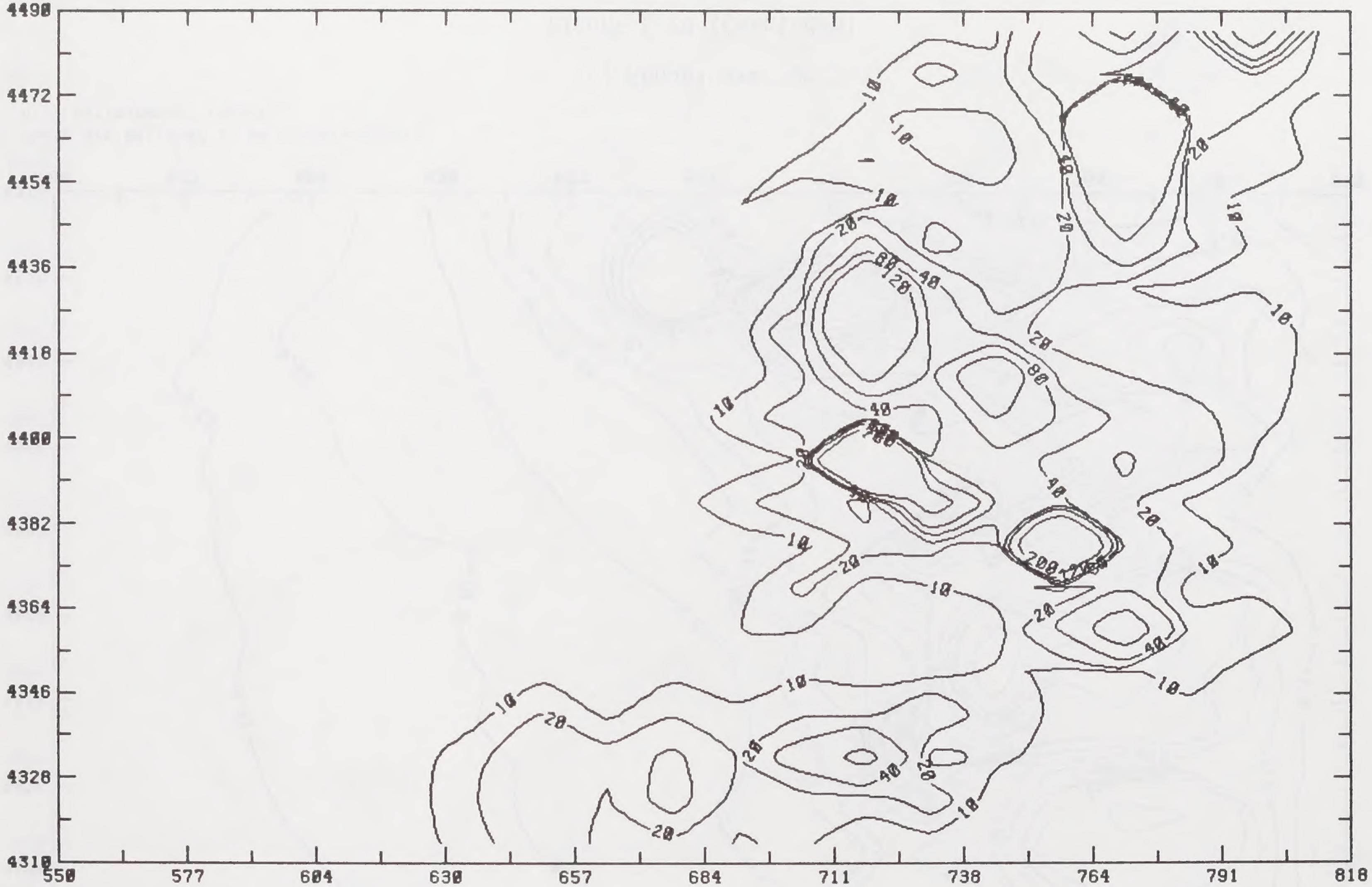

Note: These are believed to be conservatively high estimates of impacts and are non-simultaneous maxima calculated on the basis of one year's meteorological data.

(a) Maximum 24-hour average

FIGURE 5-21. IMPACT OF DIRECT SOURCE EMISSIONS FROM COLORADO POINT SOURCES ON GROUND-LEVEL TSP CONCENTRATIONS ($\mu g/m^3$) FOR THE HIGH OIL PRODUCTION SCENARIO

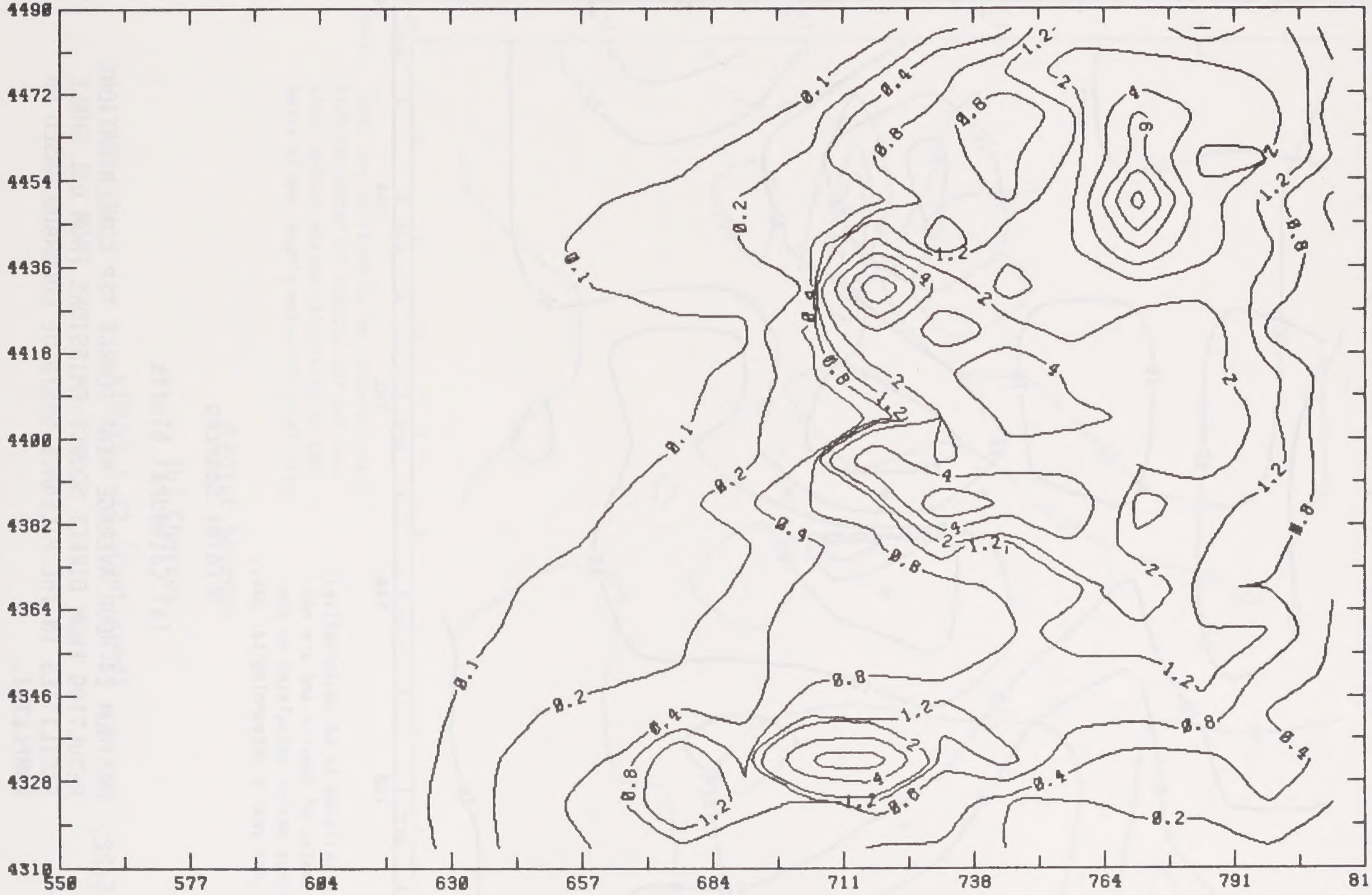

(b) Annual average

FIGURE 5-21 (Concluded)

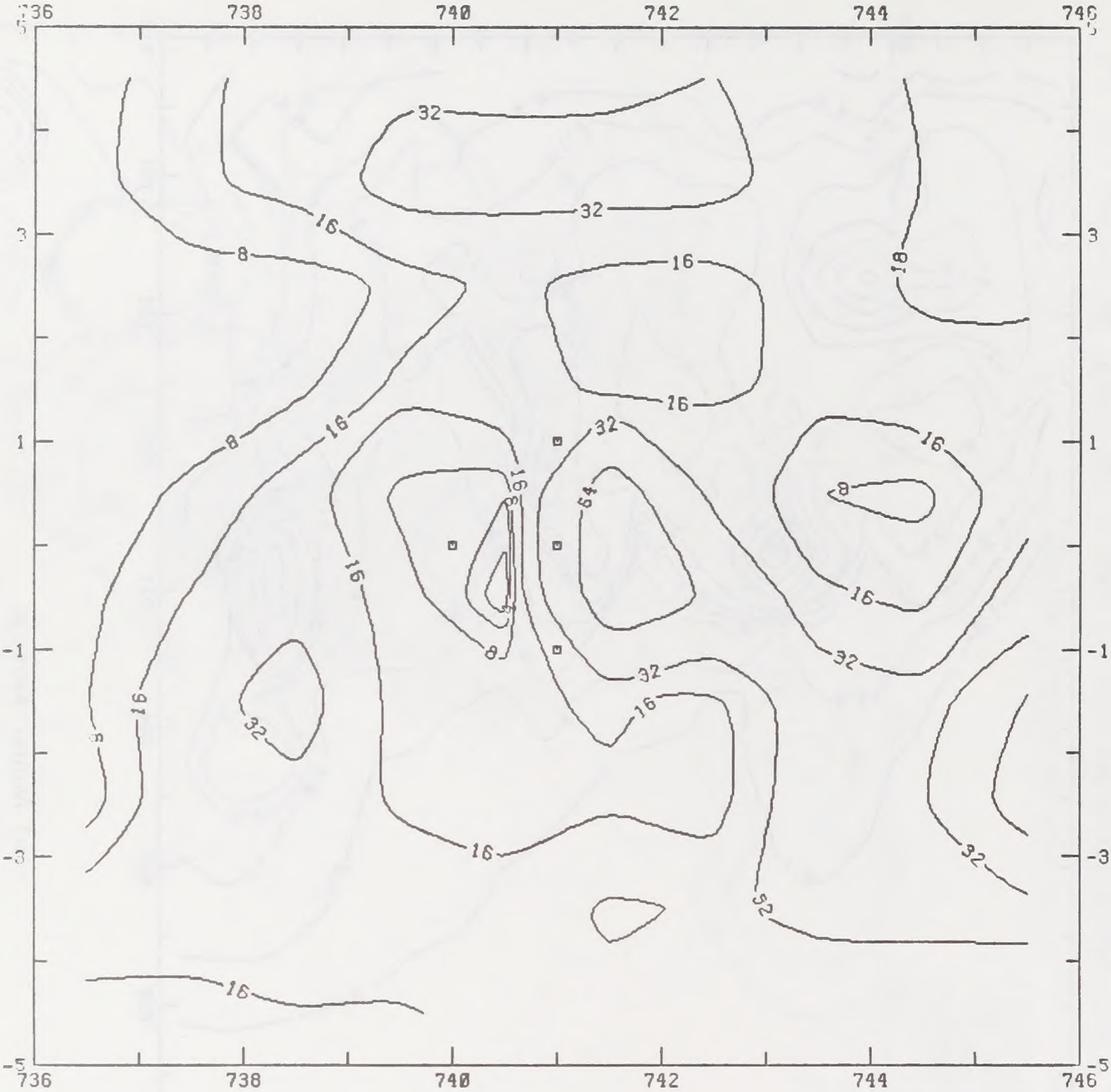

Note: These are believed to be conservatively high estimates of impacts and are non-simultaneous maxima calculated on the basis of one year's meteorological data.

▣ Point Sources

(a) Cathedral Bluffs

FIGURE 5-22. MAXIMUM 24-HOUR AVERAGE NEAR SOURCE TSP CONCENTRATIONS RESULTING FROM DIRECT SOURCE EMISSIONS FROM OIL SHALE FACILITIES IN THE PICEANCE BASIN OF COLORADO BASED ON COMPLEX-I.

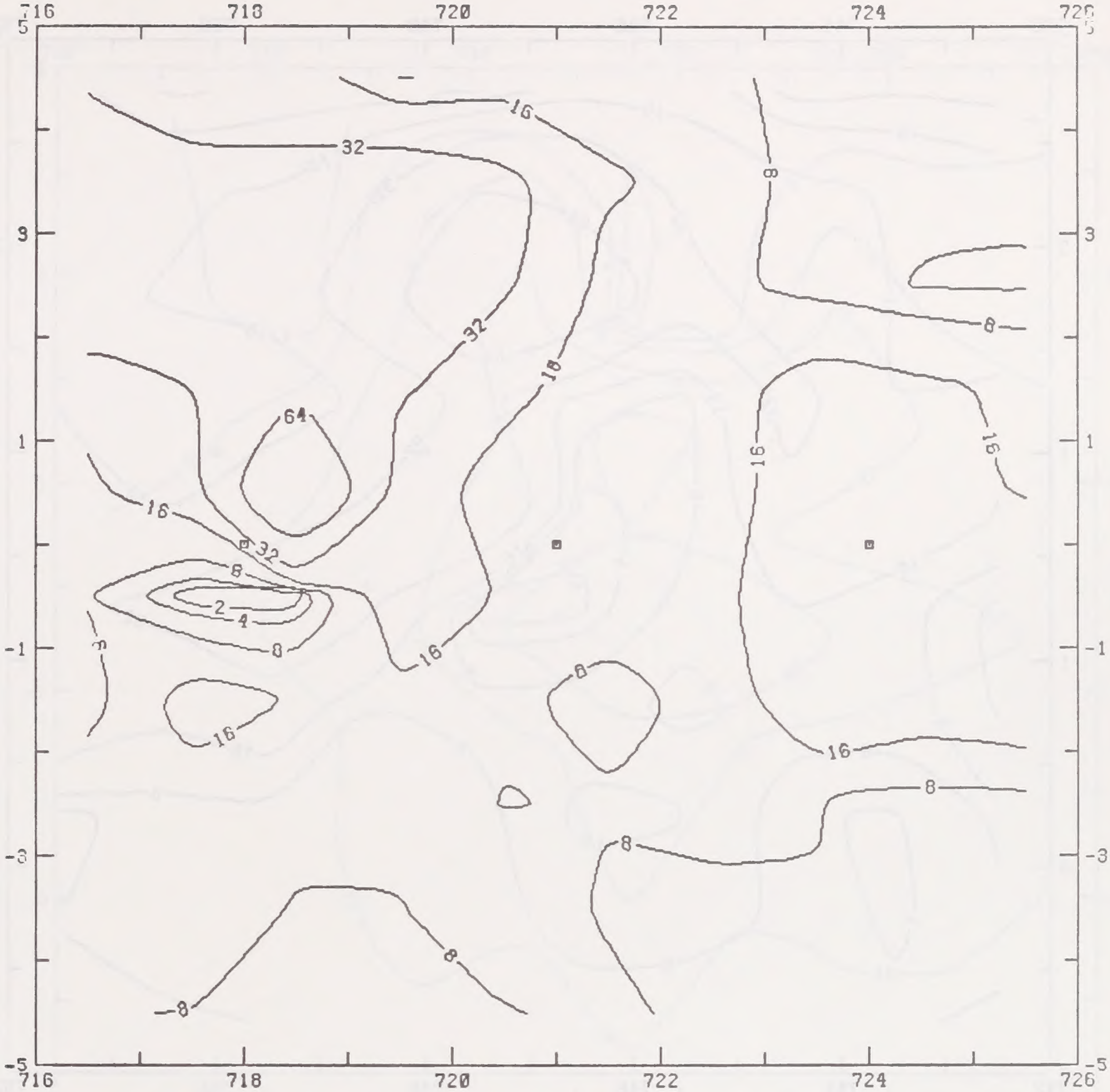

Note: These are believed to be conservatively high estimates of impacts and are non-simultaneous maxima calculated on the basis of one year's meteorological data.

□ Point Sources

(b) Chevron

FIGURE 5-22 (Continued)

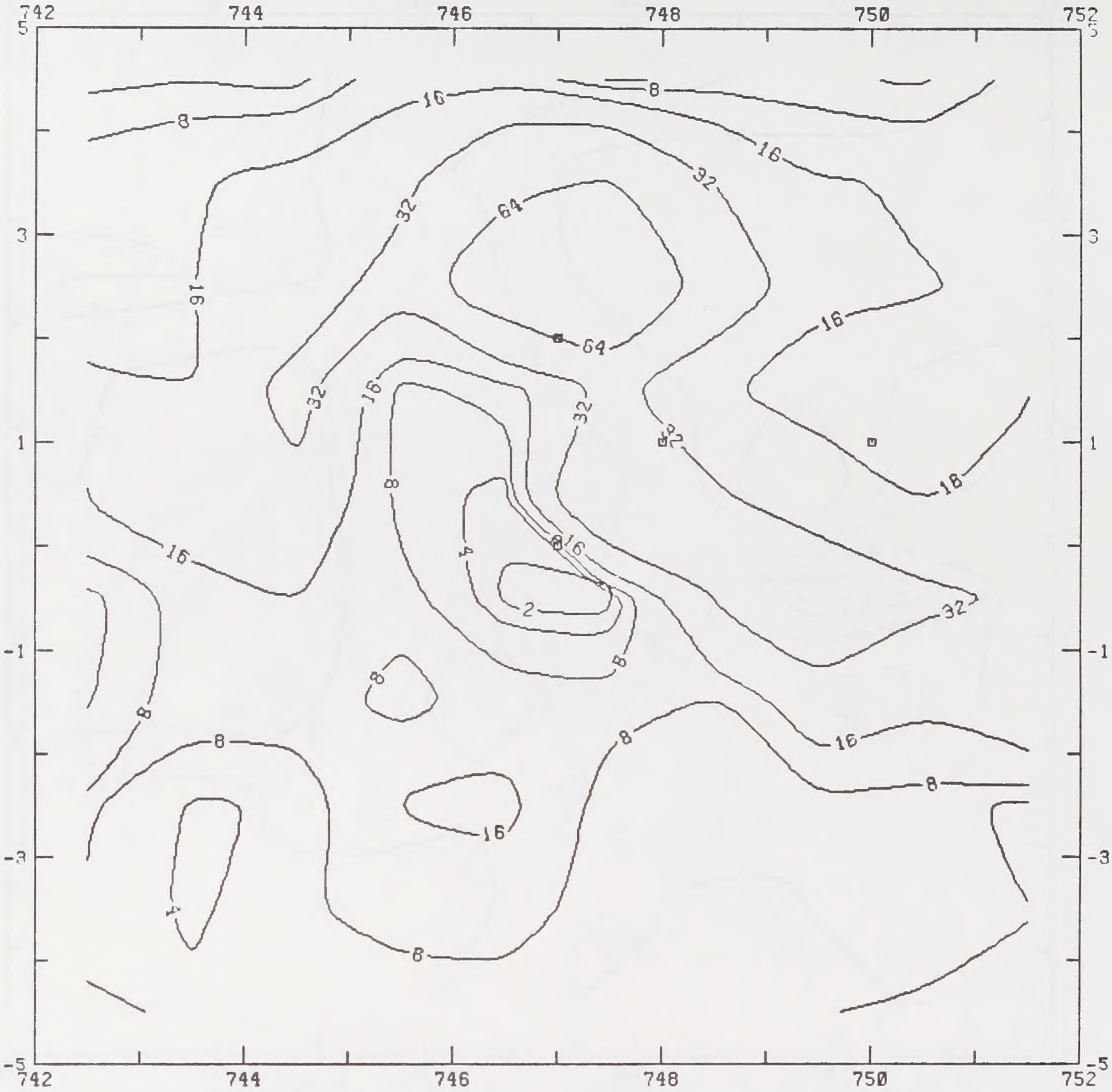

Note: These are believed to be conservatively high estimates of impacts and are non-simultaneous maxima calculated on the basis of one year's meteorological data.

◘ Point Sources

(c) Colony

FIGURE 5-22 (Continued)

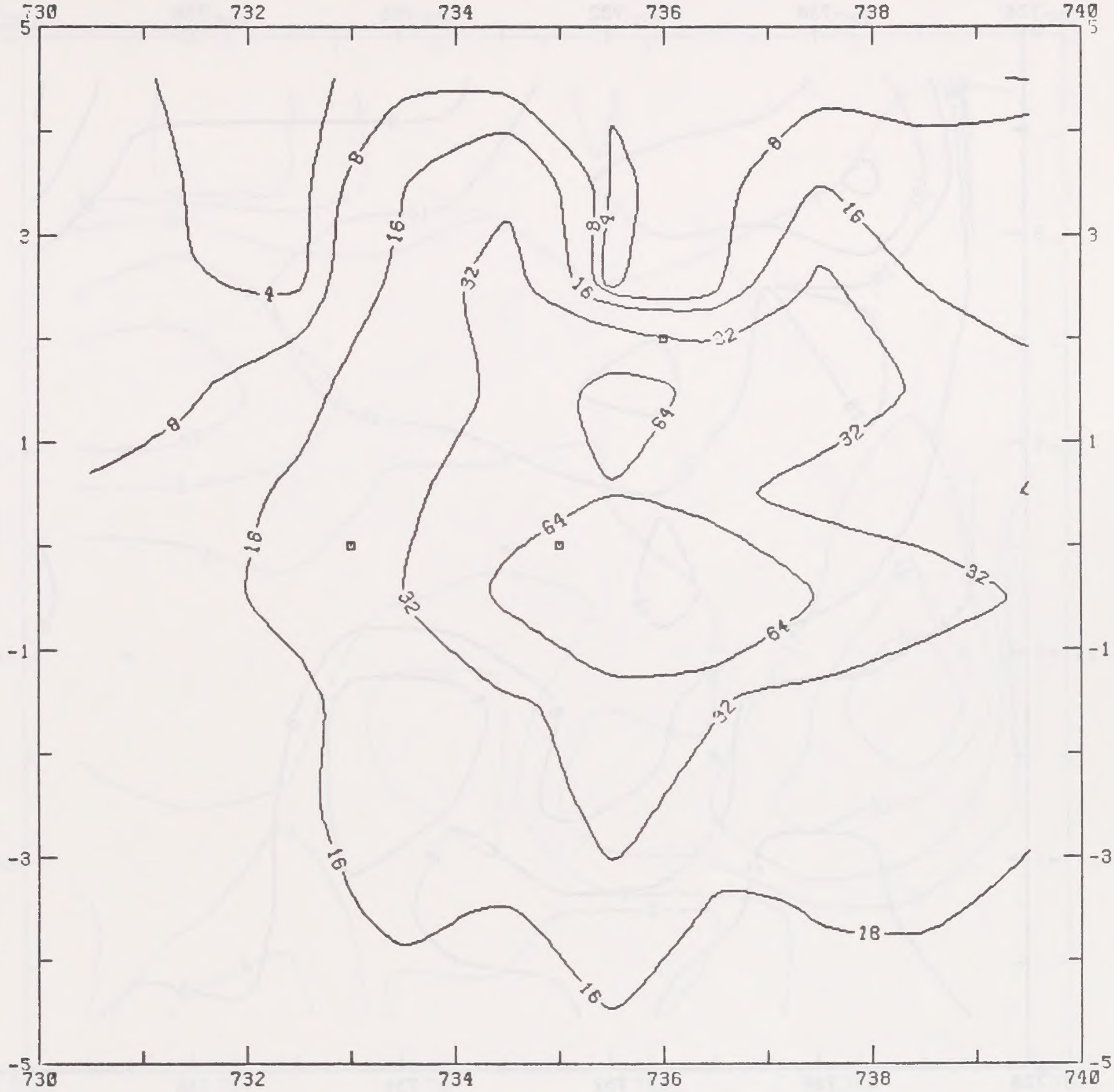

Note: These are believed to be conservatively high estimates of impacts and are non-simultaneous maxima calculated on the basis of one year's meteorological data.

▫ Point Sources

(d) Exxon

FIGURE 5-22 (Continued)

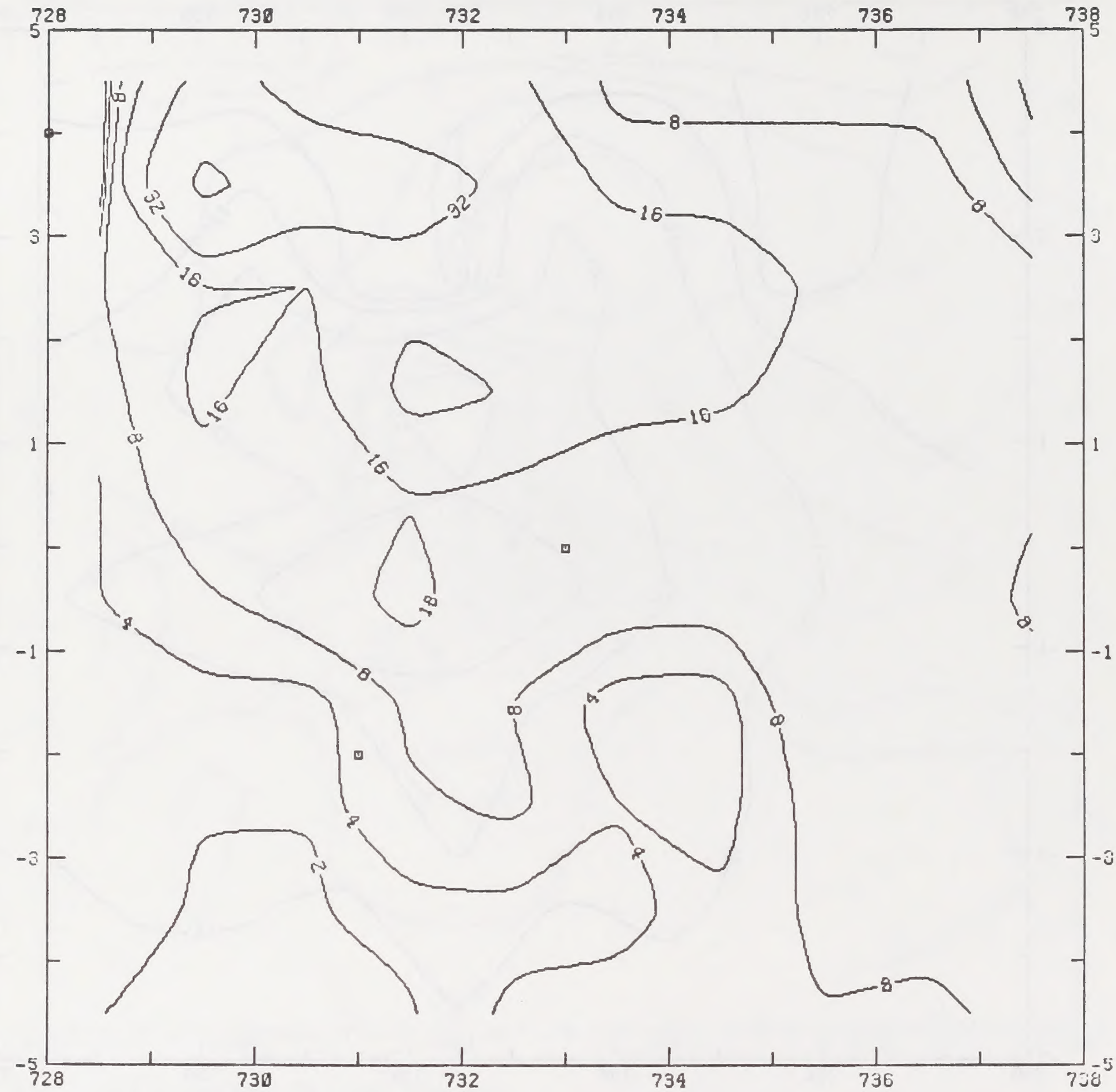

Note: These are believed to be conservatively high estimates of impacts and are non-simultaneous maxima calculated on the basis of one year's meteorological data.

⊡ Point Sources

(e) Getty

FIGURE 5-22 (Continued)

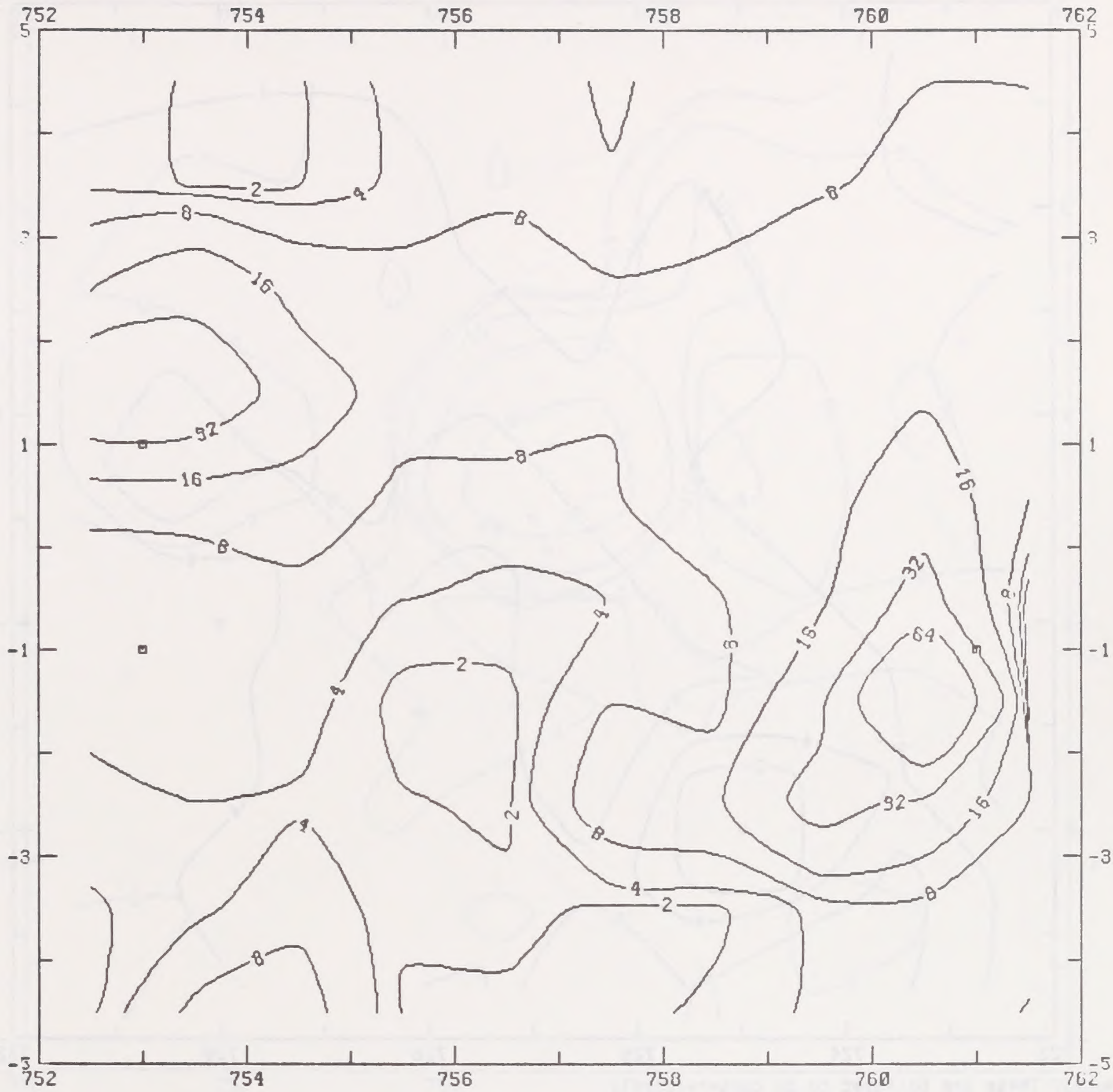

Note: These are believed to be conservatively high estimates of impacts and are non-simultaneous maxima calculated on the basis of one year's meteorological data.

◘ Point Sources

(f) Mobil

FIGURE 5-22 (Continued)

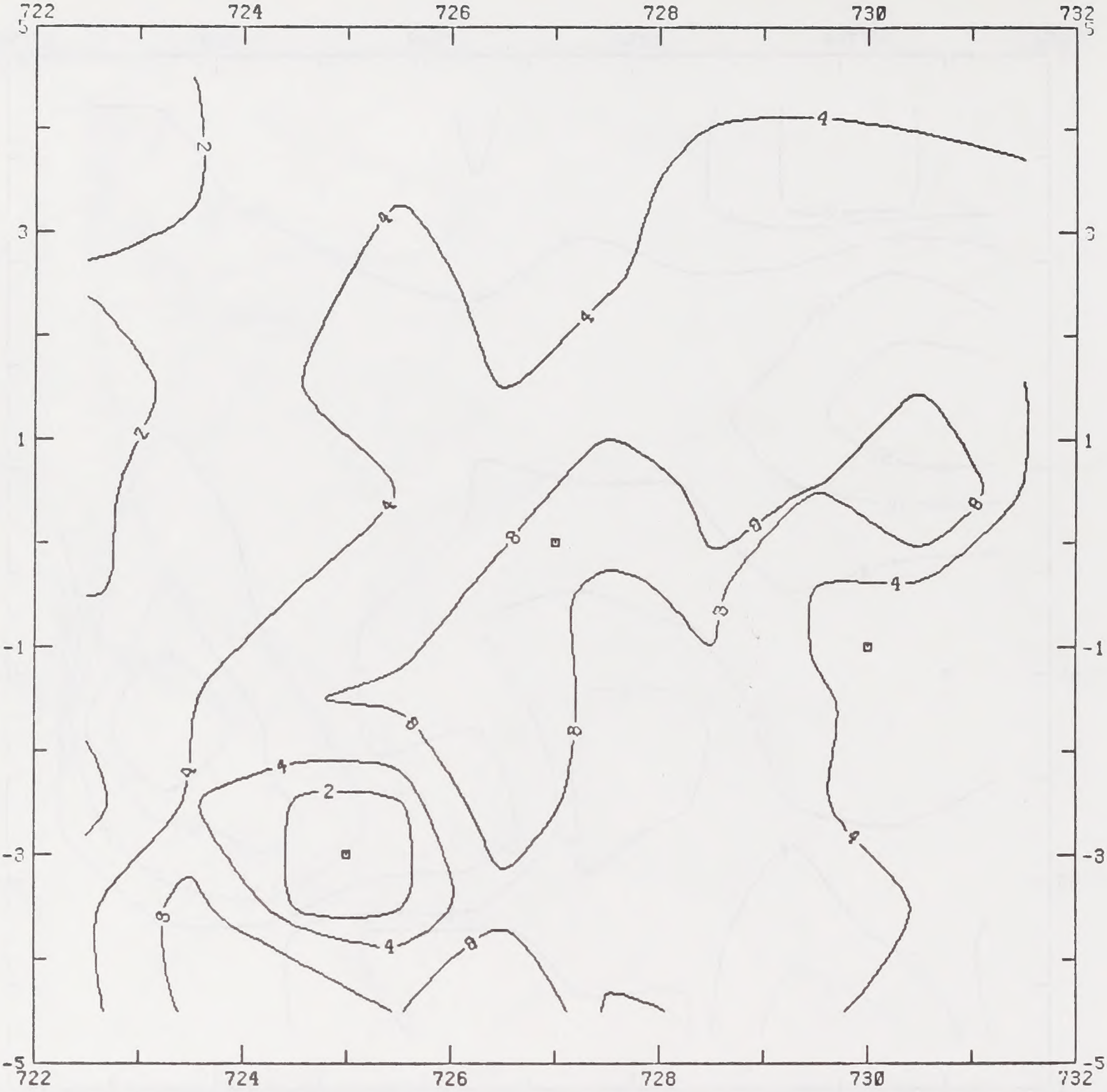

Note: These are believed to be conservatively high estimates of impacts and are non-simultaneous maxima calculated on the basis of one year's meteorological data.

▫ Point Sources

(g) Multi Mineral

FIGURE 5-22 (Continued)

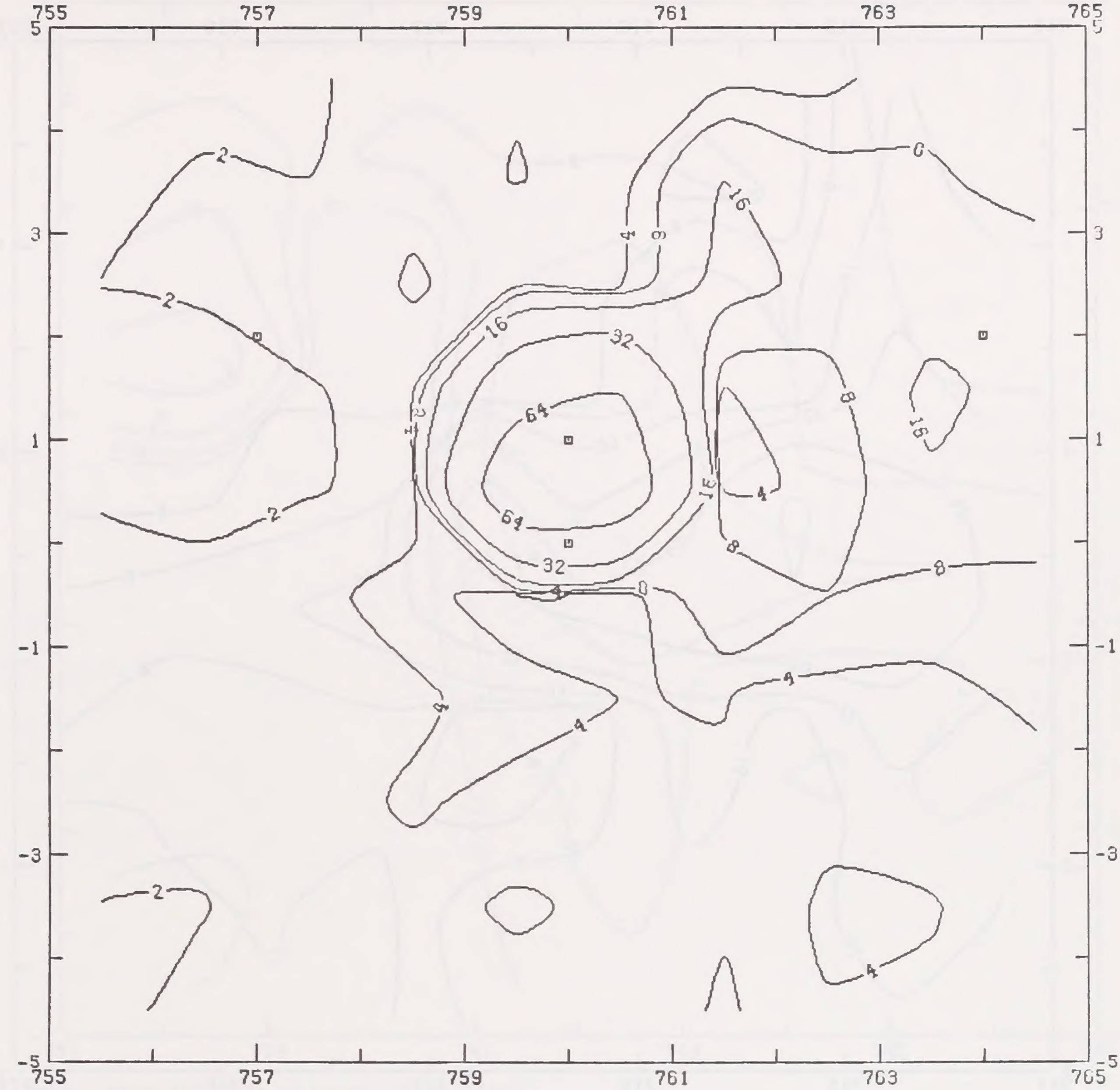

Note: These are believed to be conservatively high estimates of impacts and are non-simultaneous maxima calculated on the basis of one year's meteorological data.

□ Point Sources

(h) Naval Oil Shale Reserve

FIGURE 5-22 (Continued)

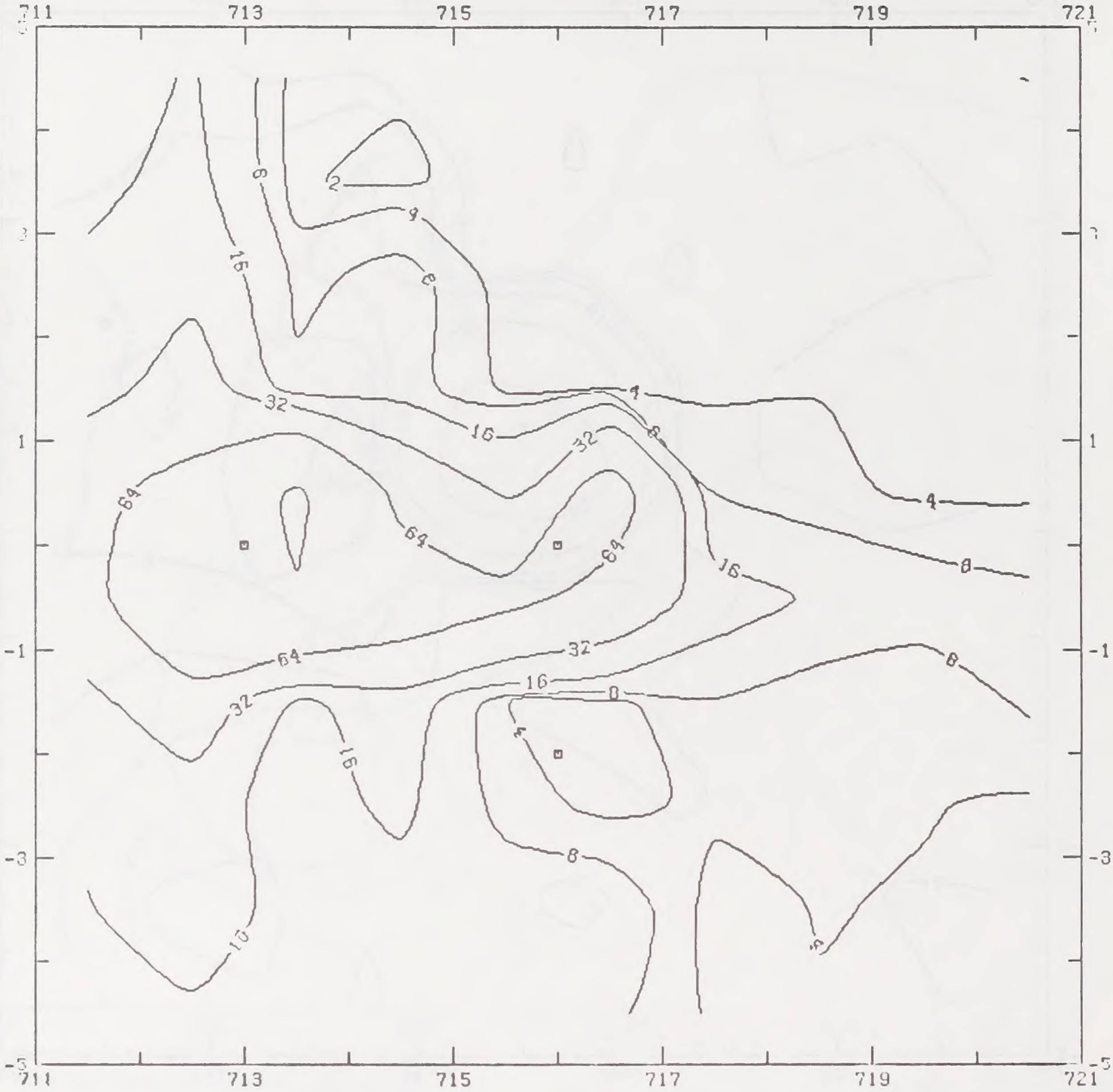

Note: These are believed to be conservatively high estimates of impacts and are non-simultaneous maxima calculated on the basis of one year's meteorological data.

□ Point Sources

(i) Rio Blanco

FIGURE 5-22 (Continued)

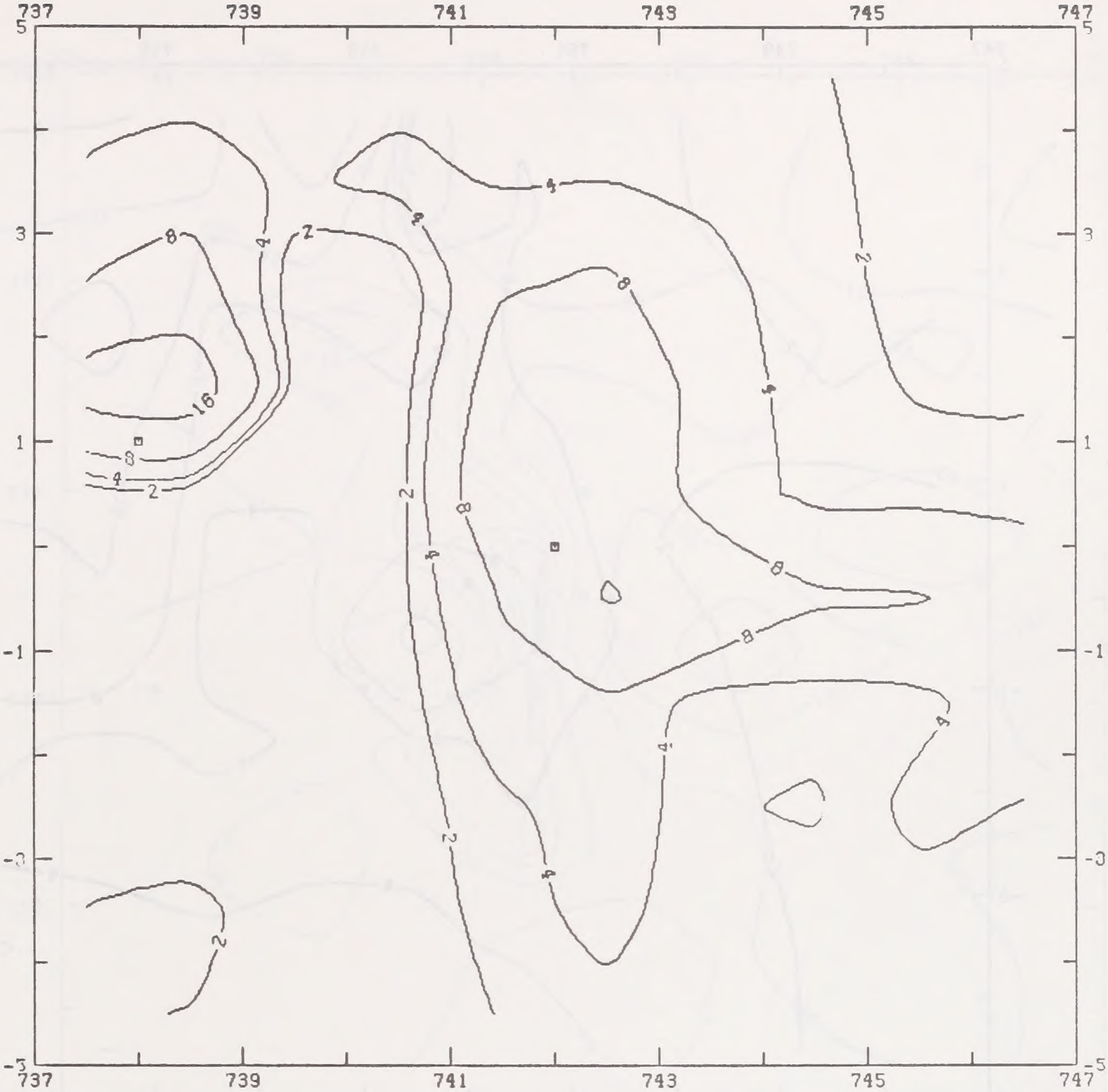

Note: These are believed to be conservatively high estimates of impacts and are non-simultaneous maxima calculated on the basis of one year's meteorological data.

▣ Point Sources

(j) Superior

FIGURE 5-22 (Continued)

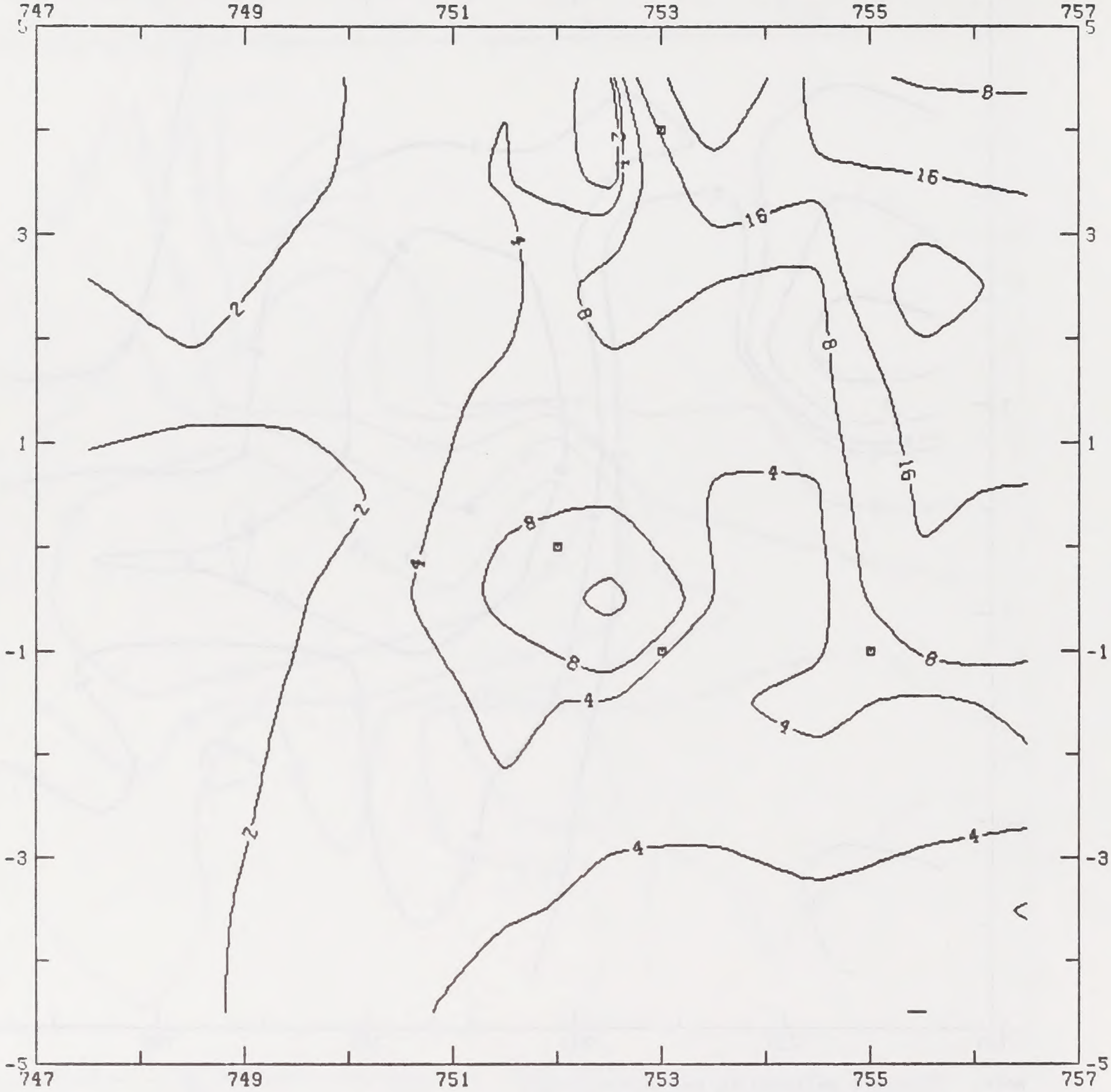

Note: These are believed to be conservatively high estimates of impacts and are non-simultaneous maxima calculated on the basis of one year's meteorological data.

◘ Point Sources

(k) Union

FIGURE 5-22 (Concluded)

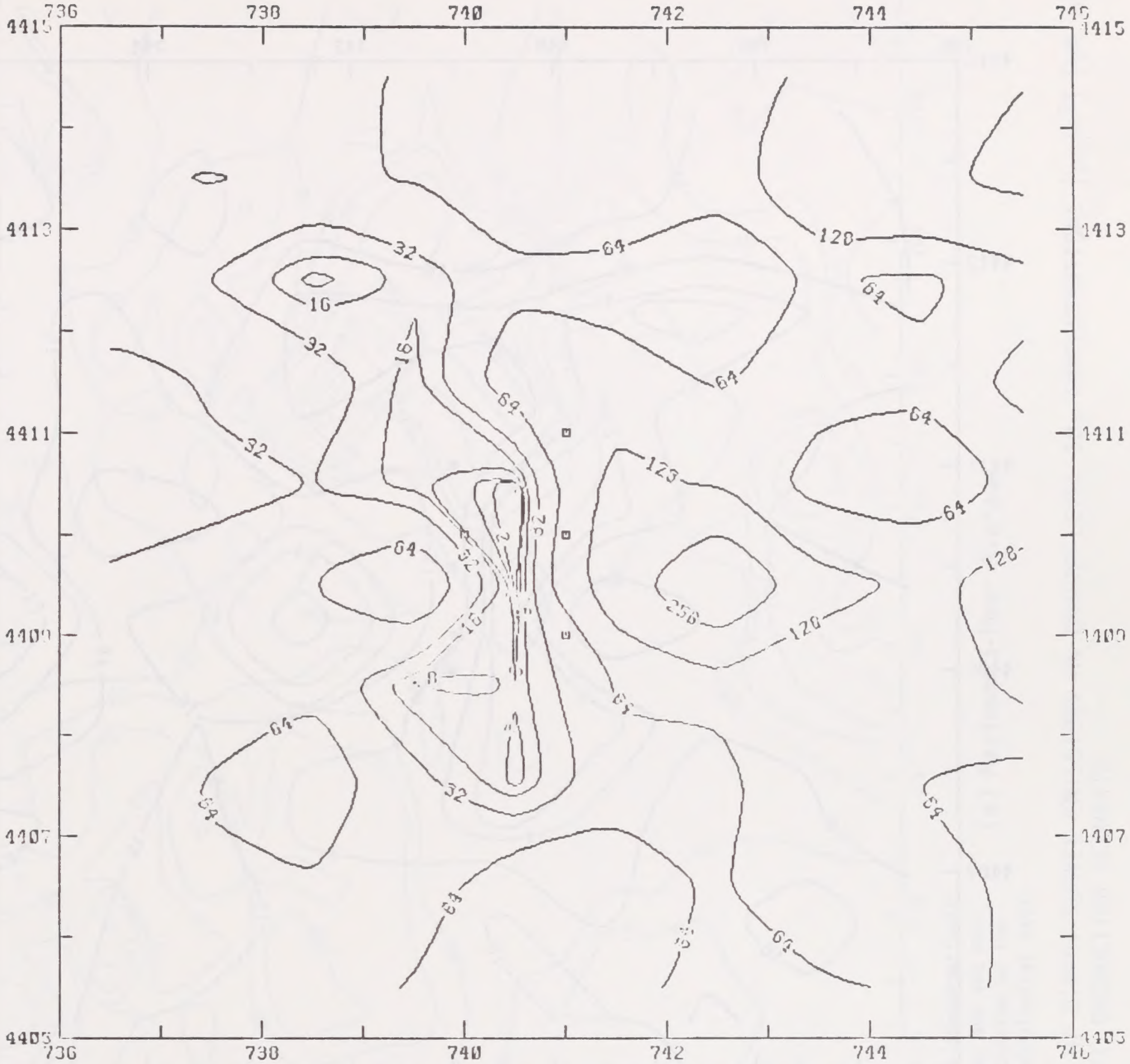

Note: These are believed to be conservatively high estimates of impacts and are non-simultaneous maxima calculated on the basis of one year's meteorological data.

▣ Point Sources

(a) Maximum 3-hour average

FIGURE 5-23. MAXIMUM NEAR-SOURCE SO_2 CONCENTRATIONS RESULTING FROM DIRECT SOURCE EMISSIONS FROM CATHEDRAL BLUFFS ON THE BASIS OF COMPLEX-I CALCULATIONS

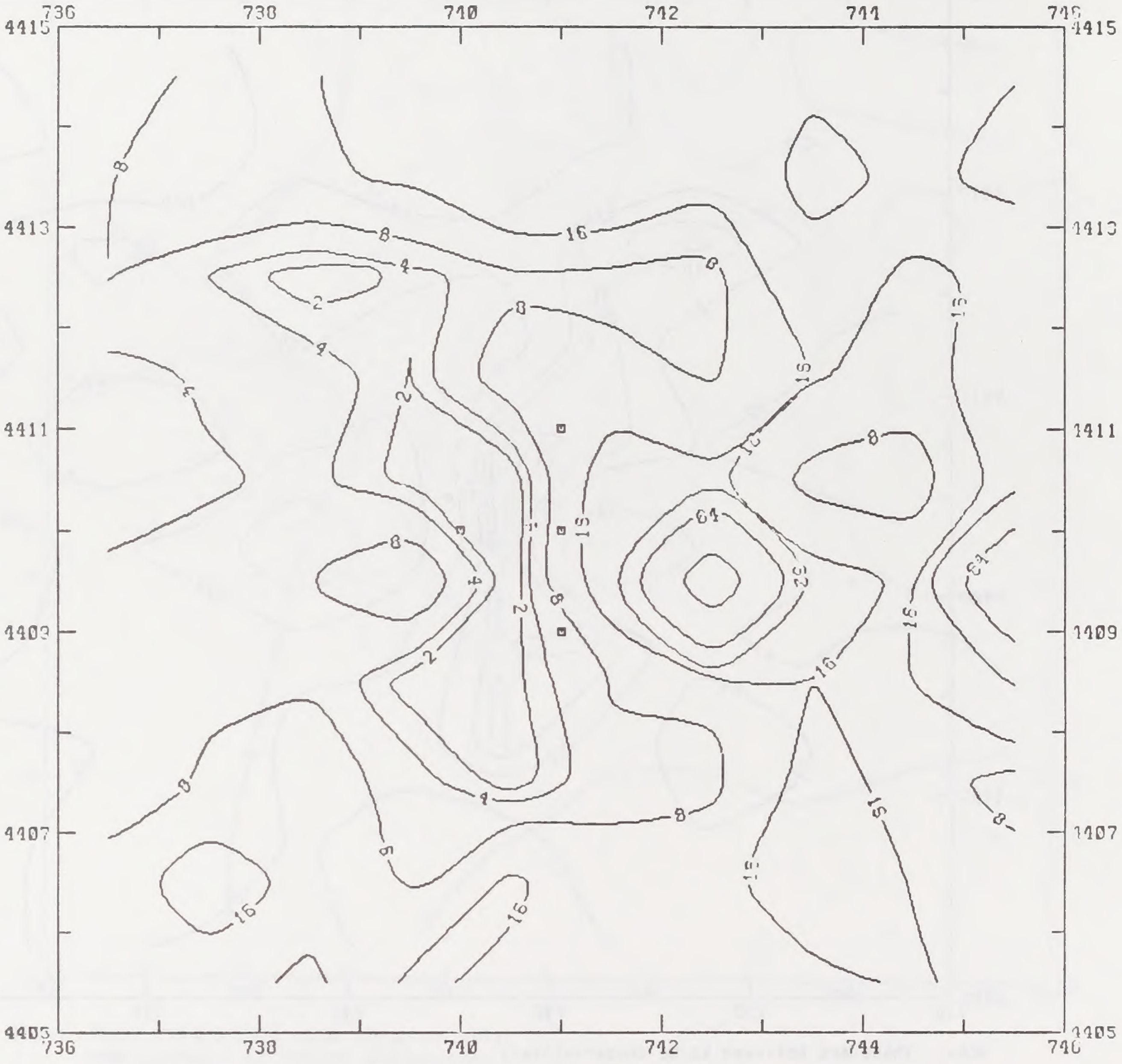

Note: These are believed to be conservatively high estimates of impacts and are non-simultaneous maxima calculated on the basis of one year's meteorological data.

◘ Point Sources

(b) Maximum 24-hour average

FIGURE 5-23 (Concluded)

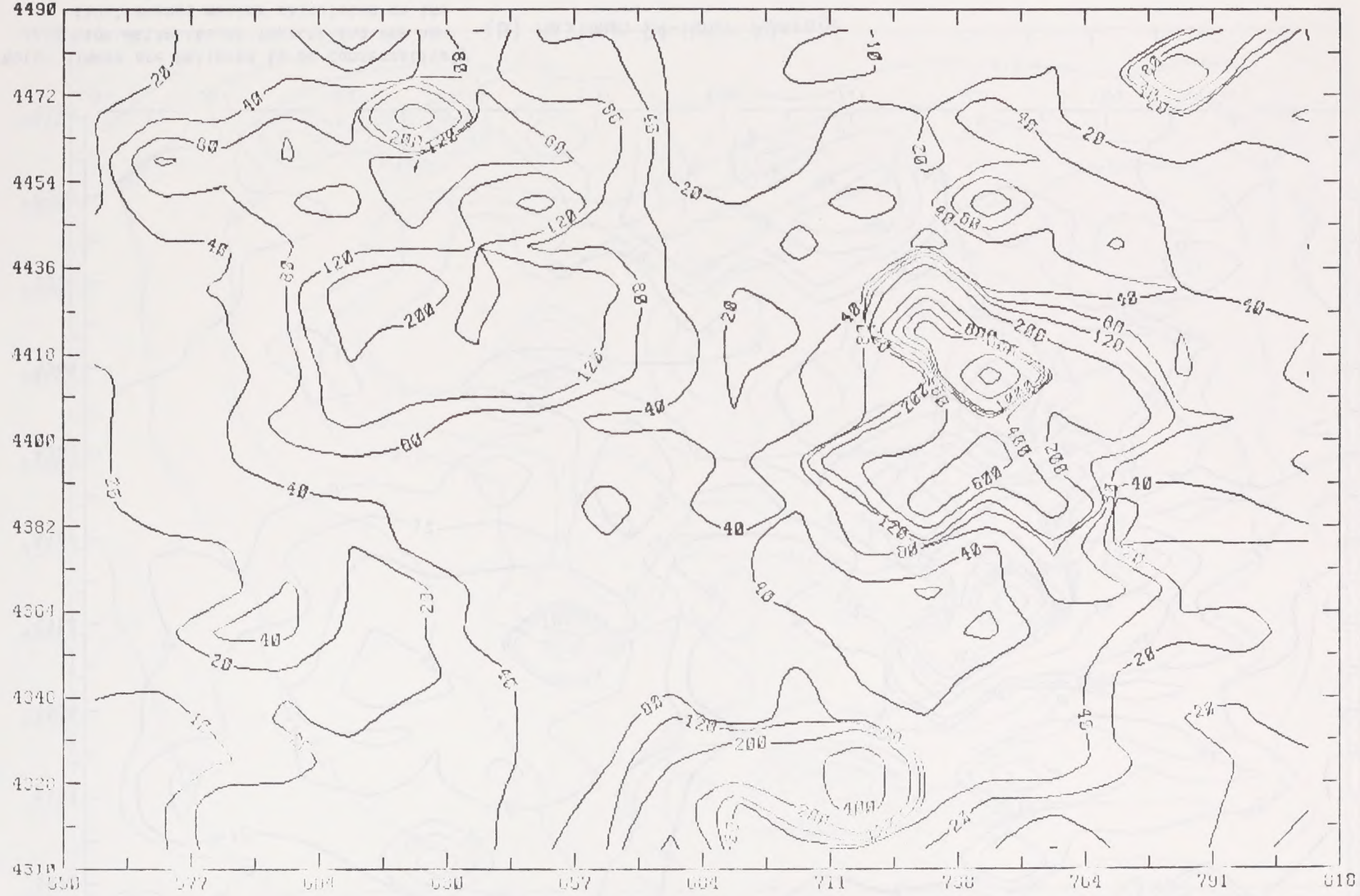

Note: These are believed to be conservatively high estimates of impacts and are non-simultaneous maxima calculated on the basis of one year's meteorological data.

(a) Maximum 3-Hour Average

FIGURE 5-24. IMPACT OF DIRECT SOURCE EMISSIONS ON GROUND-LEVEL SO_2 CONCENTRATIONS ($\mu g/m^3$) FOR THE HIGH OIL PRODUCTION SCENARIO

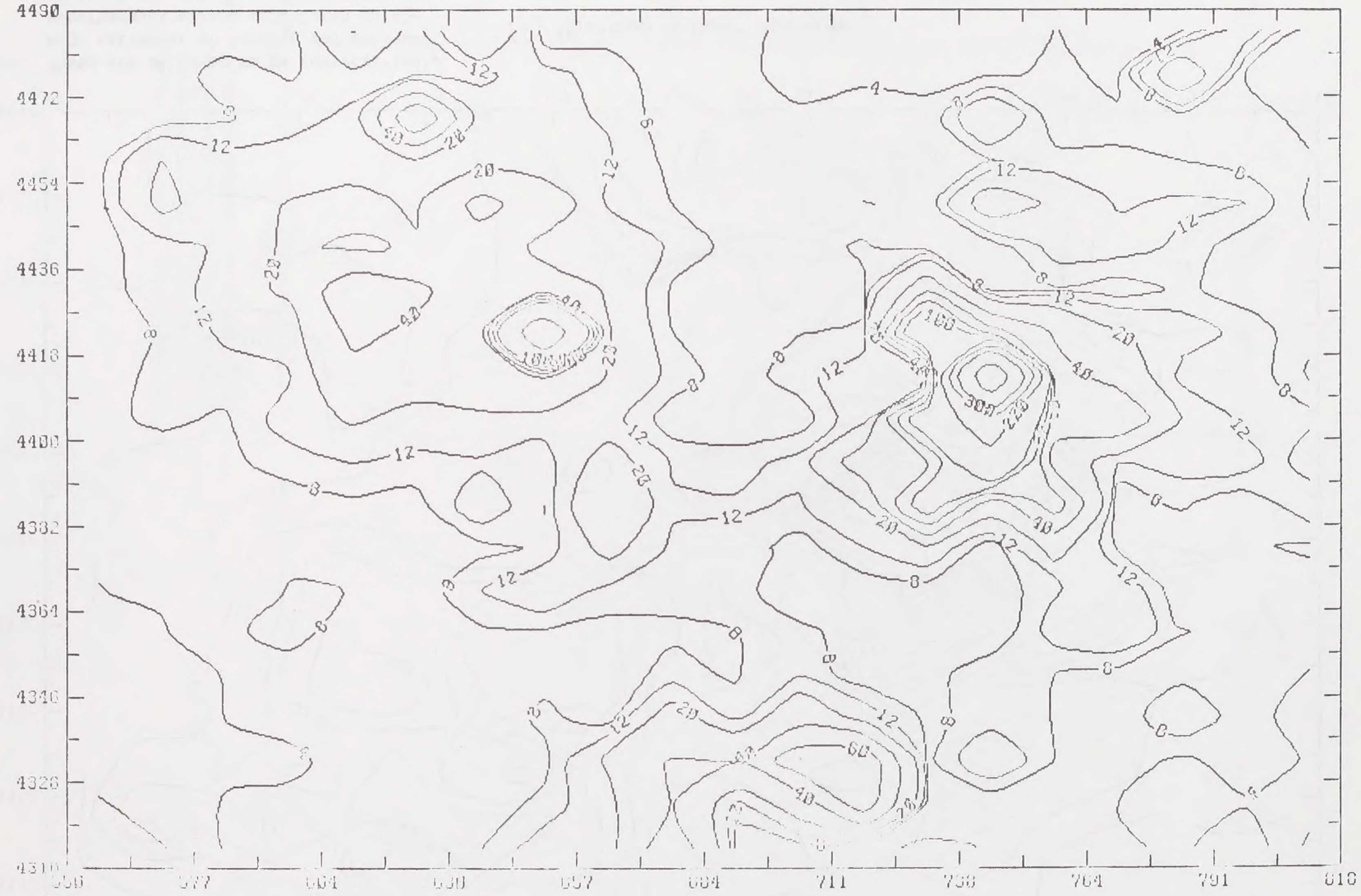

Note: These are believed to be conservatively high estimates of impacts and are non-simultaneous maxima calculated on the basis of one year's meteorological data.

(b) Maximum 24-Hour Average

FIGURE 5-24 (Continued)

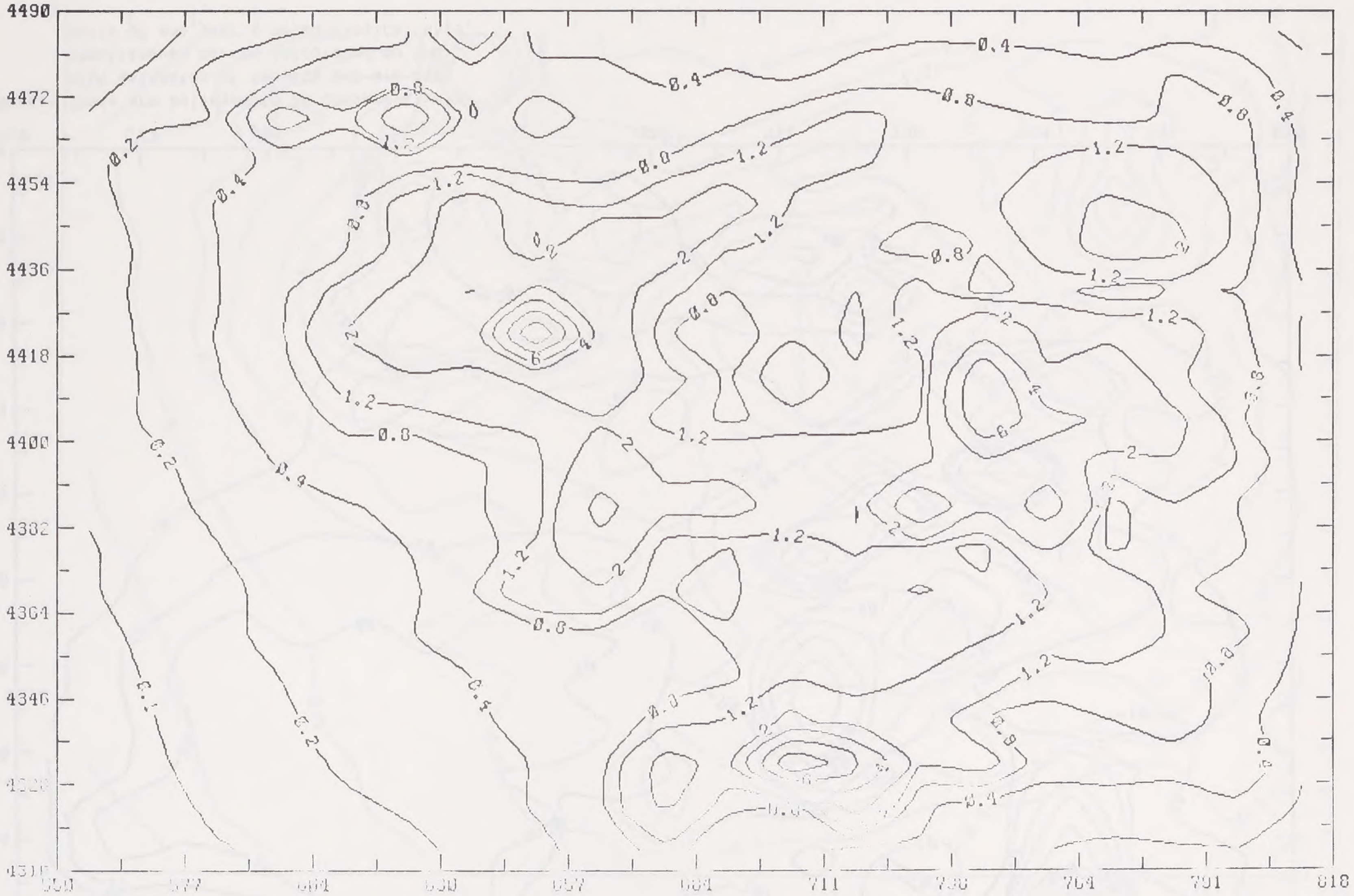

Note: These are believed to be conservatively high estimates of impacts.

(c) Annual Average

FIGURE 5-24 (Concluded)

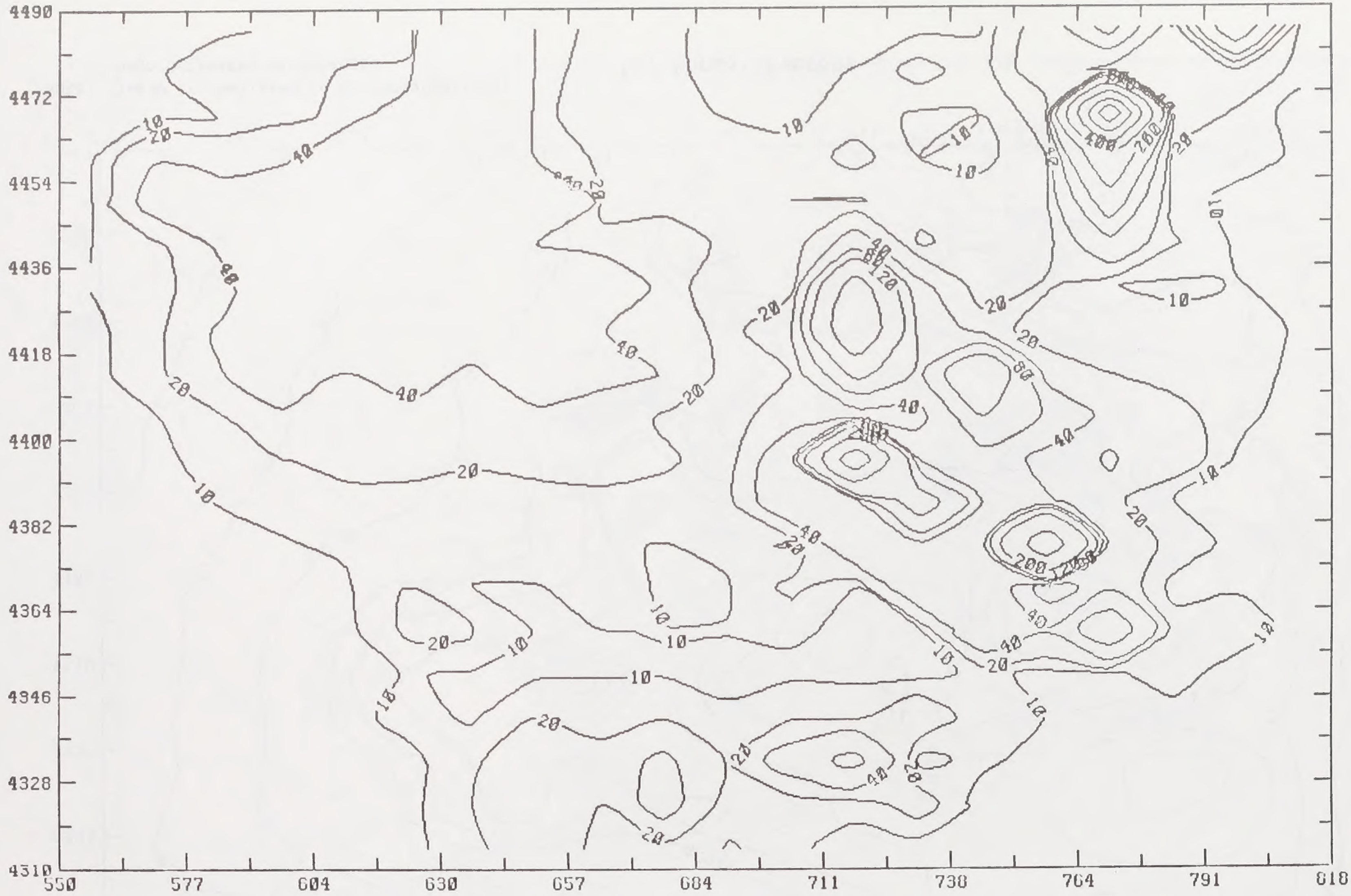

Note: These are believed to be conservatively high estimates of impacts and are non-simultaneous maxima calculated on the basis of one year's meteorological data.

(a) Maximum 24-hour average

FIGURE 5-25. IMPACT OF DIRECT SOURCE EMISSIONS ON GROUND-LEVEL TSP CONCENTRATIONS ($\mu g/m^3$) FOR THE HIGH OIL PRODUCTION SCENARIO

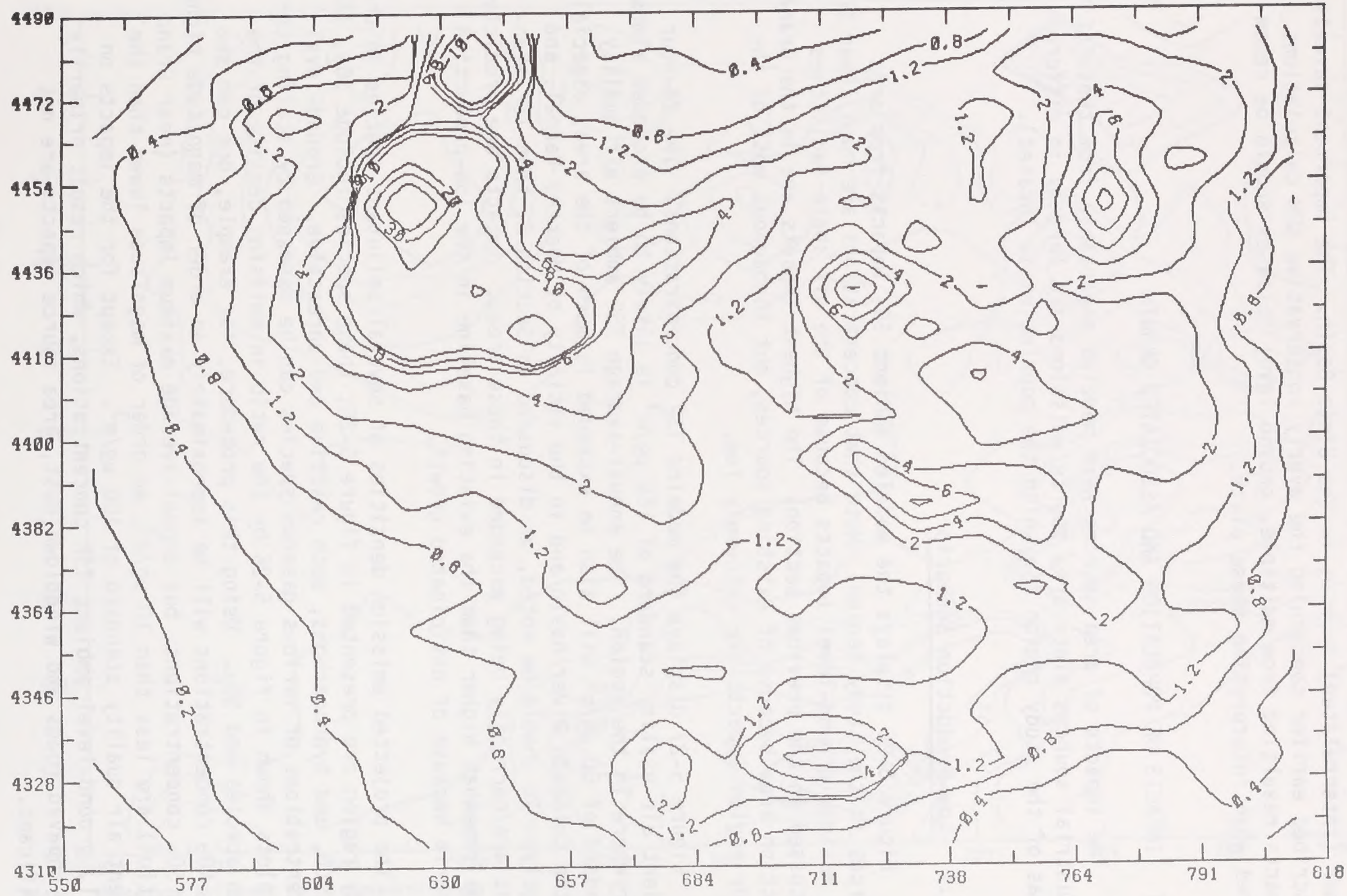

Note: These are believed to be conservatively high estimates of impacts.

(b) Annual average

FIGURE 5-25 (Concluded)

other (interrelated) sources in the Uinta Basin. The important caveats described earlier concerning the overly conservative GPM calculations of impacts resulting from multiple, ground-level releases should be remembered when interpreting these plots.

5.3 IMPACTS OF POPULATION AND ASSOCIATED GROWTH

The impacts of area sources were modeled separately from those of the industrial sources since area source emissions are largely in different areas of the study region (in which the population is located).

5.3.1 Low-Production Scenario

Figure 5-26 displays the modeled ambient SO_2 impacts from area sources in the study region. Note that concentrations are much lower than the maximum ground-level impacts because of the oil shale facilities discussed in the previous section. The highest impacts are in the Grand Junction area because of existing sources, but throughout most of the study region impacts are extremely low.

Figure 5-27 displays the modeled TSP concentrations. The 24-hour ambient air quality standard of 150 $\mu g/m^3$ is likely to be exceeded almost everywhere in the region. The annual-average TSP ambient air quality standard of 60 $\mu g/m^3$ will also be exceeded in much of the area, especially in the Colorado River basin and in the vicinity of Meeker, Vernal, and Rangely. It should be noted, as discussed in Section 2, that TSP standards are currently being exceeded in these areas. Impacts are predicted to be somewhat higher than the existing baseline in the low-production scenario because of anticipated growth.

The projected emission densities of several pollutant species in the study region are presented in figure 5-28; these species include SO_2, TSP, NO_x, CO, and hydrocarbons, both reactive and unreactive. Ground-level concentrations of various gaseous species can be assessed by scaling the SO_2 plots shown in figure 5-26 by the ratio in emission density of the given species and SO_2. Using this procedure, for example, one can see that NO_2 concentrations will be approximately an order of magnitude higher than SO_2 concentrations, but annual-average maximum impacts (near Grand Junction) are less than 10 $\mu g/m^3$, an order of magnitude lower than the ambient air quality standard of 100 $\mu g/m^3$. Except for the impacts on local, ground-level ambient TSP concentrations, which result primarily from unpaved roads and windblown dust, area source impacts are not significant.

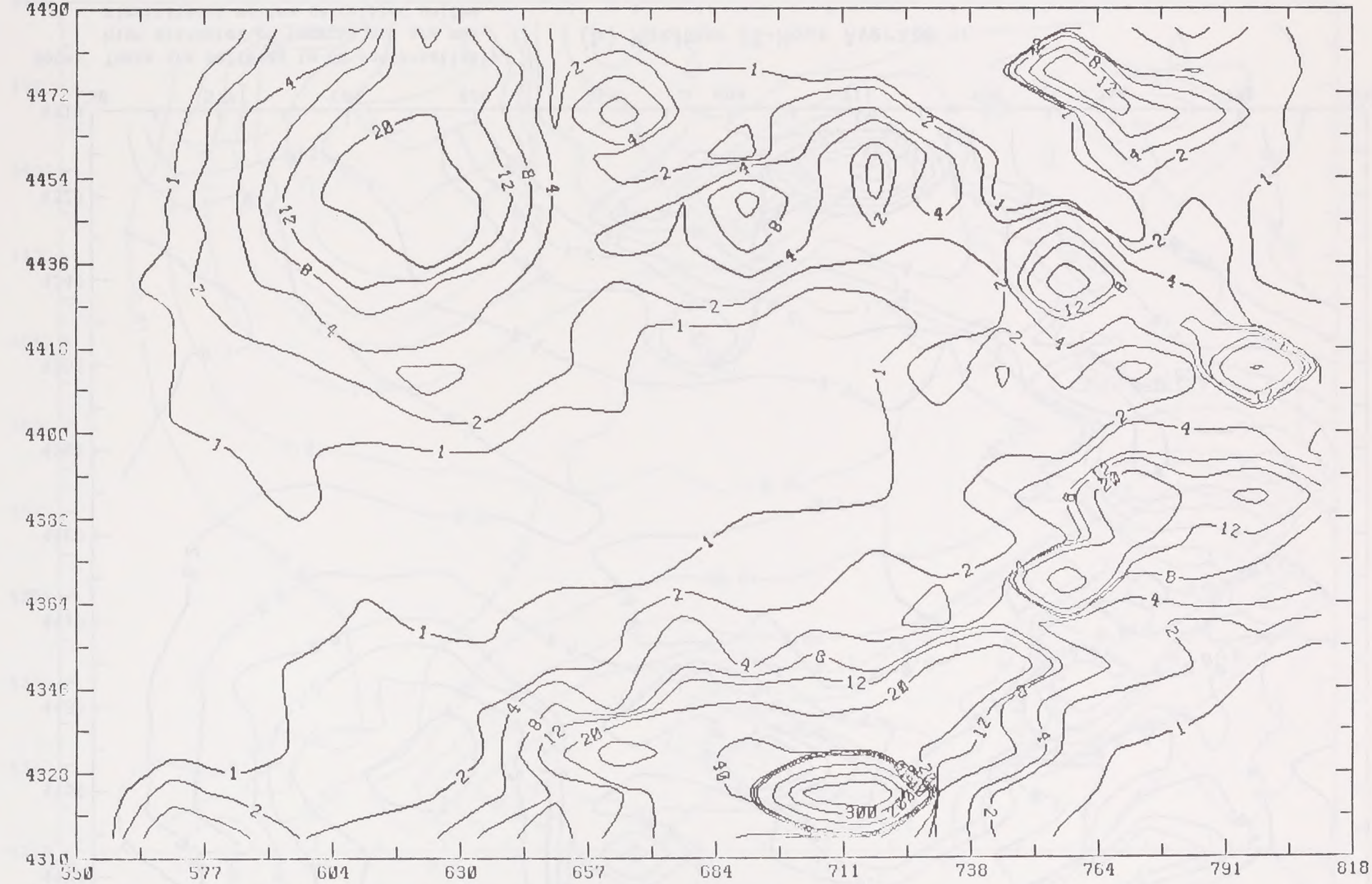

Note: These are believed to be conservatively high estimates of impacts and are non-simultaneous maxima calculated on the basis of one year's meteorological data.

(a) Maximum 3-Hour Average

FIGURE 5-26. IMPACT OF AREA SOURCE EMISSIONS ON GROUND-LEVEL SO_2 CONCENTRATIONS ($\mu g/m^3$) FOR THE LOW OIL PRODUCTION SCENARIO

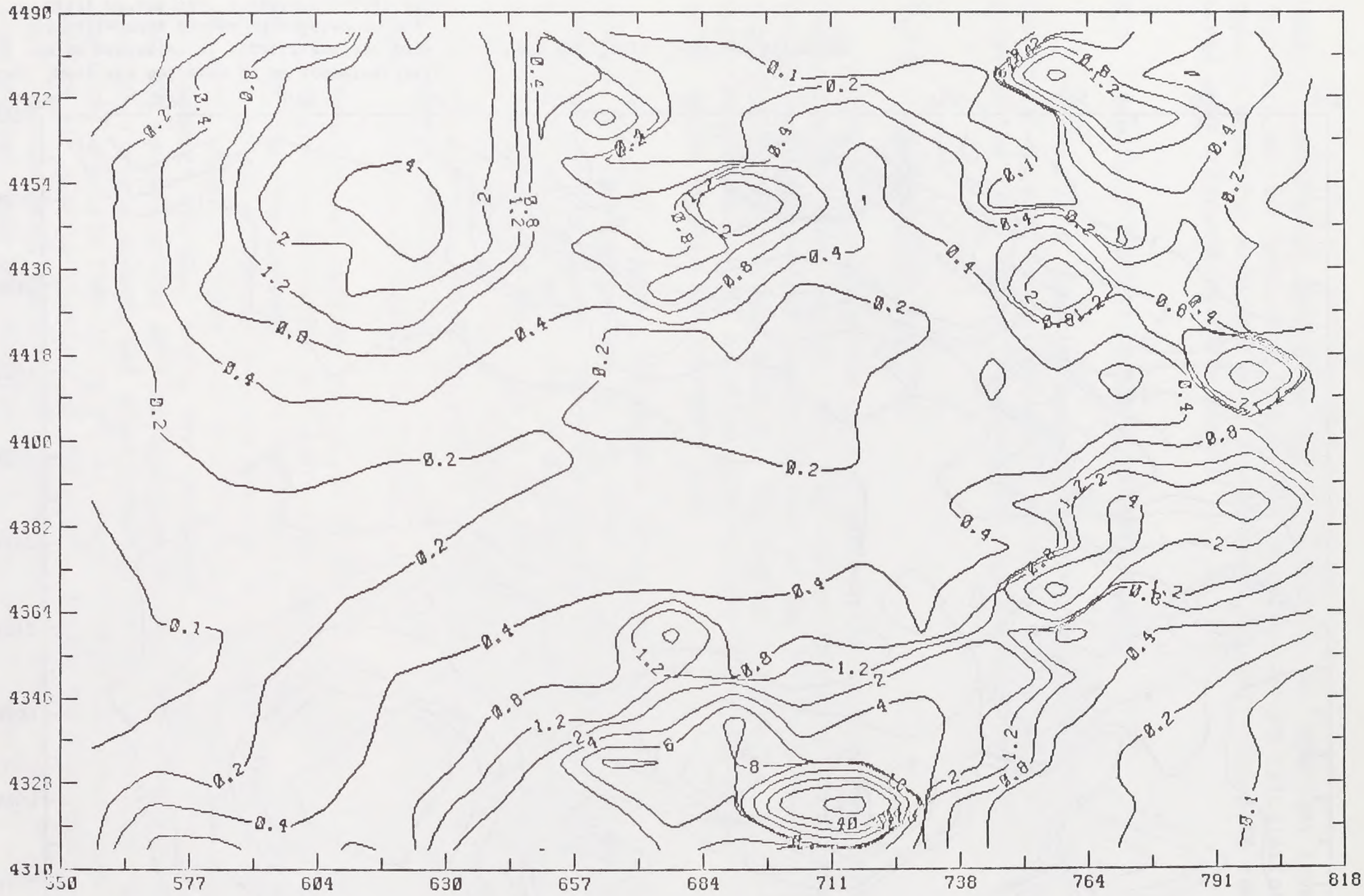

Note: These are believed to be conservatively high estimates of impacts and are non-simultaneous maxima calculated on the basis of one year's meteorological data.

(b) Maximum 24-Hour Average

FIGURE 5-26 (Continued)

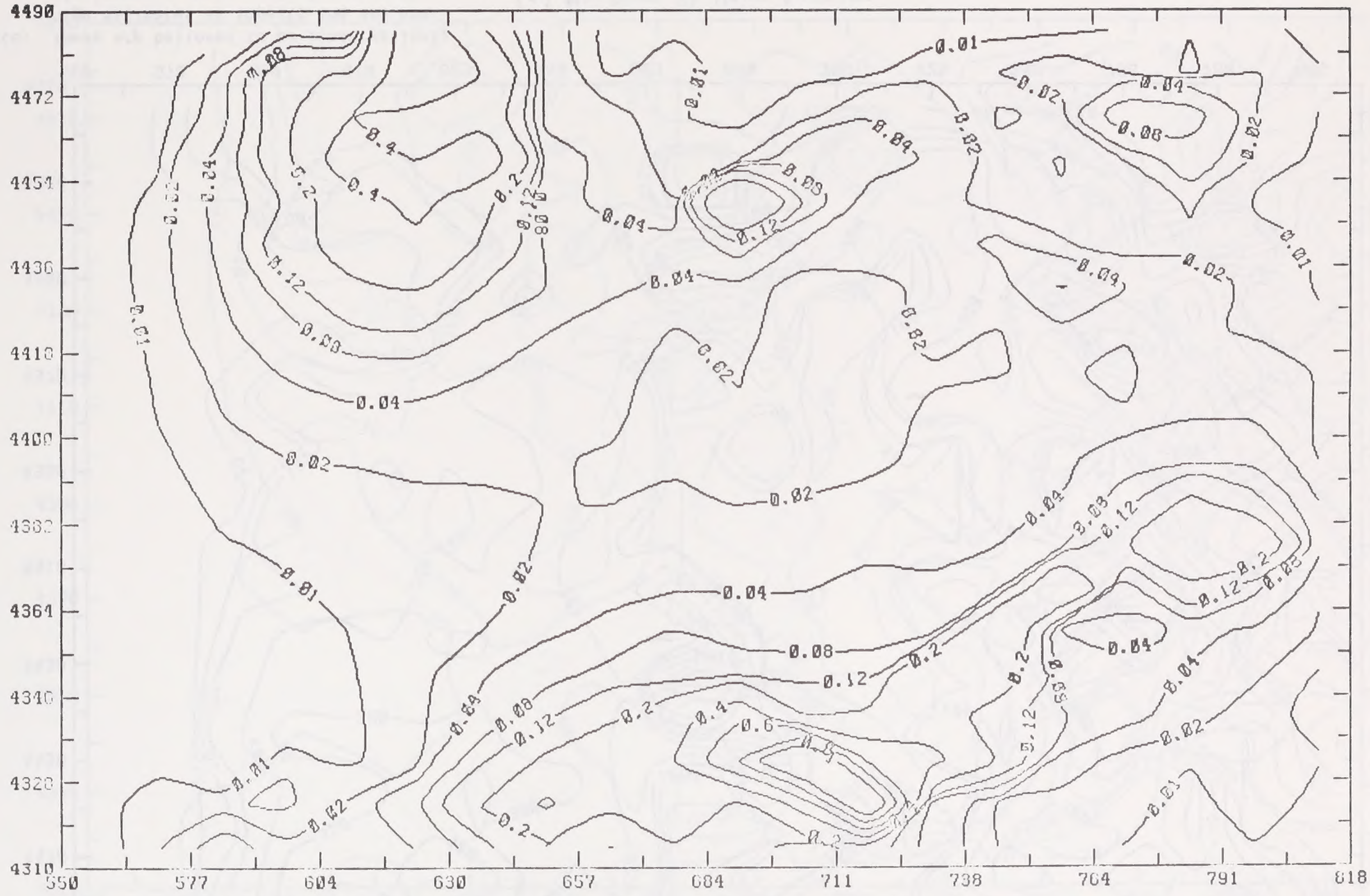

Note: These are believed to be conservatively high estimates of impacts.

(c) Annual Average

FIGURE 5-26 (Concluded)

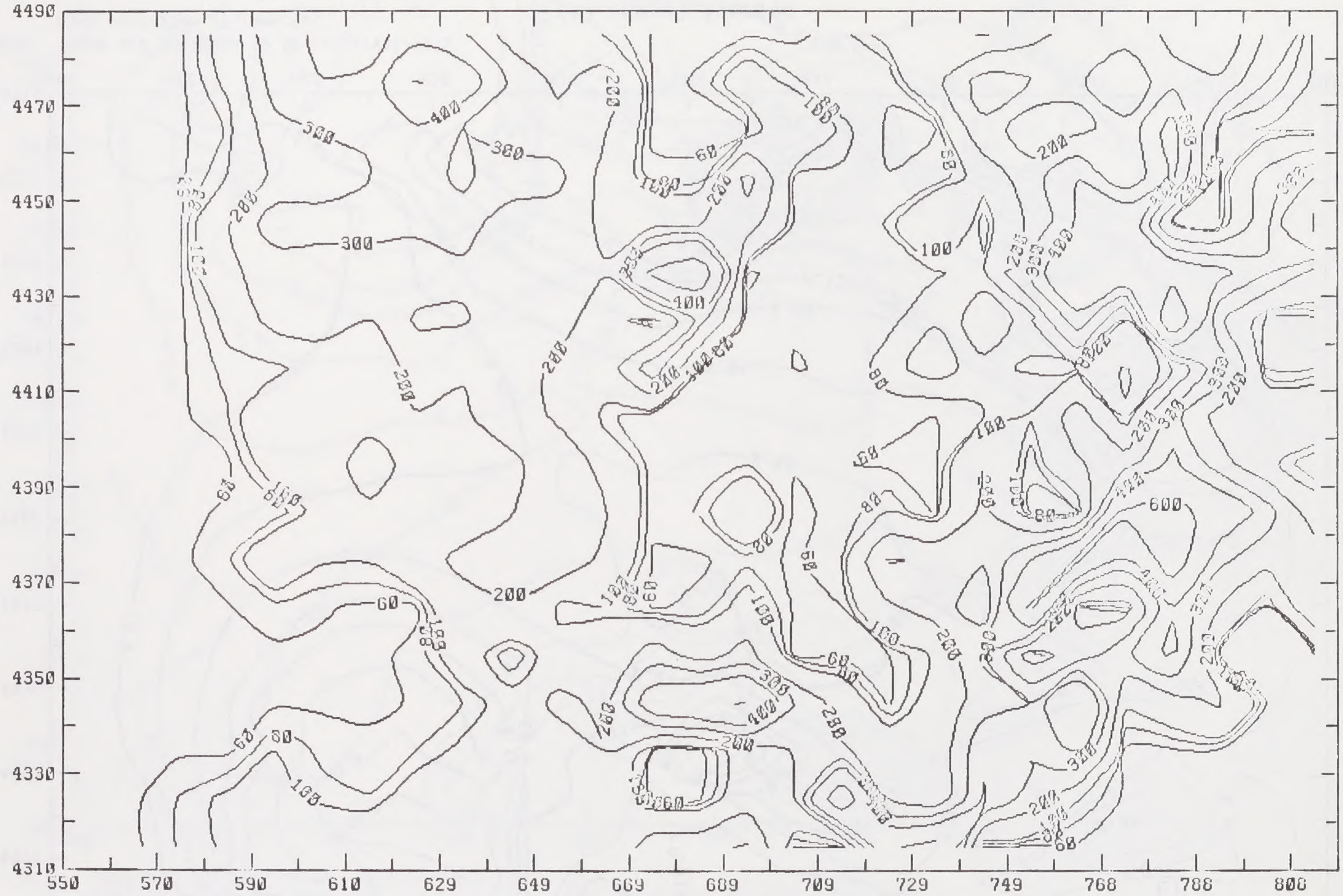

Note: These are believed to be conservatively high estimates of impacts and are non-simultaneous maxima calculated on the basis of one year's meteorological data.

(a) Maximum 24-Hour Average

FIGURE 5-27. IMPACT OF AREA SOURCE EMISSIONS ON GROUND-LEVEL TSP CONCENTRATIONS (μg/m^3) FOR THE LOW OIL PRODUCTION SCENARIO

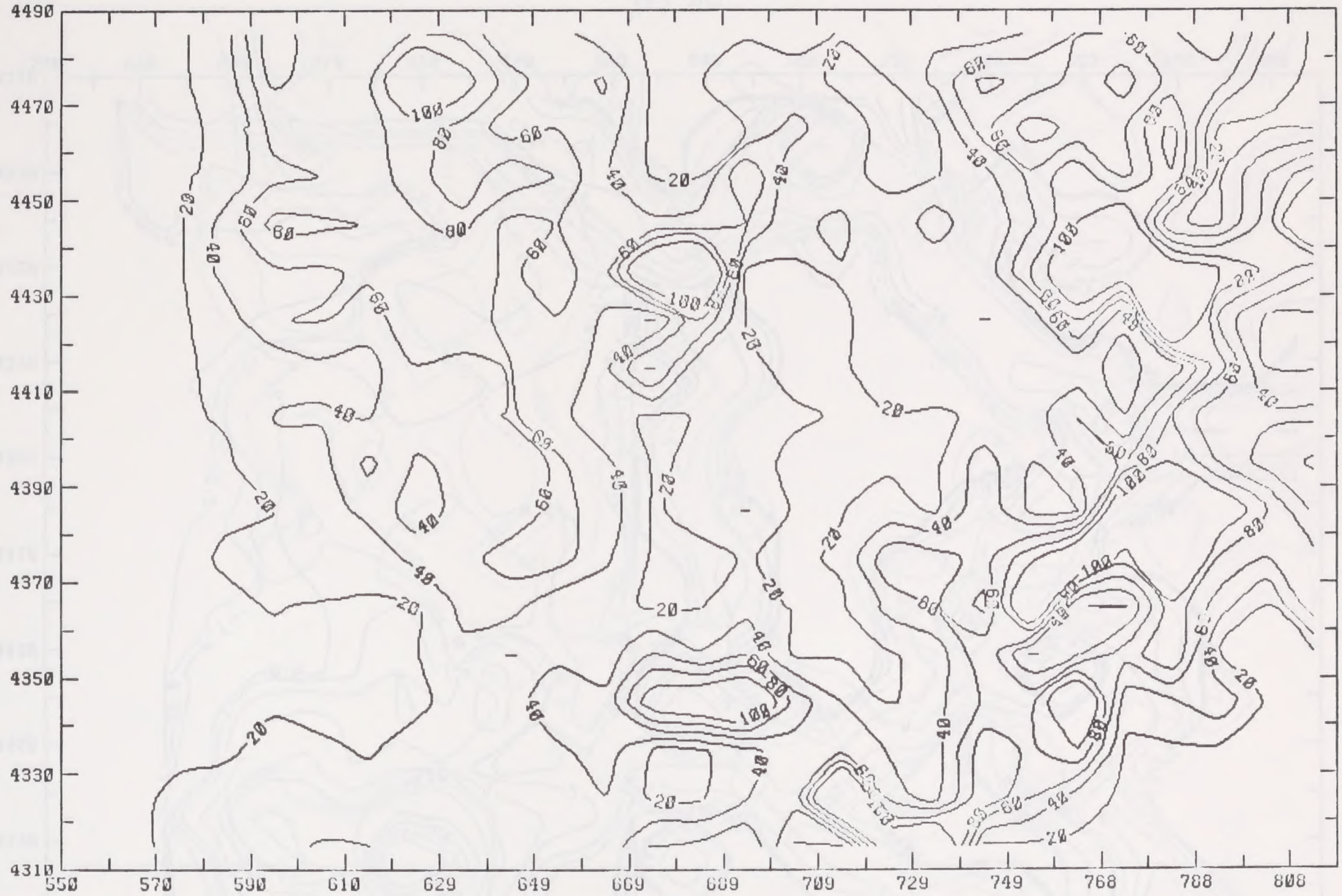

Note: These are believed to be conservatively high estimates of impacts and are non-simultaneous maxima calculated on the basis of one year's meteorological data.

(b) Annual Average

FIGURE 5-27 (Concluded)

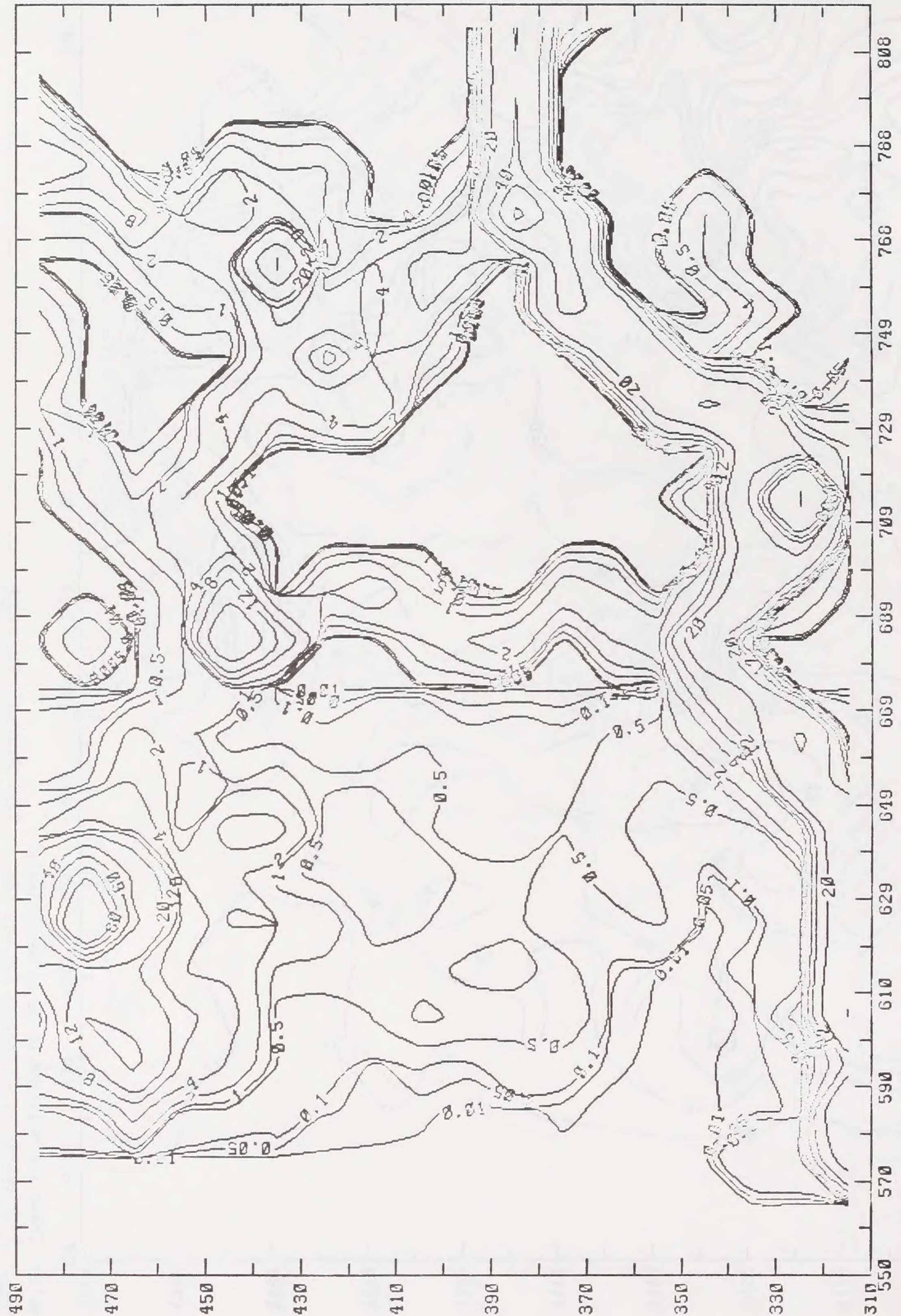

(a) SO_2

FIGURE 5-28. AREA SOURCE EMISSION DENSITIES FOR LOW OIL PRODUCTION SCENARIO (tons/yr/100 km^2)

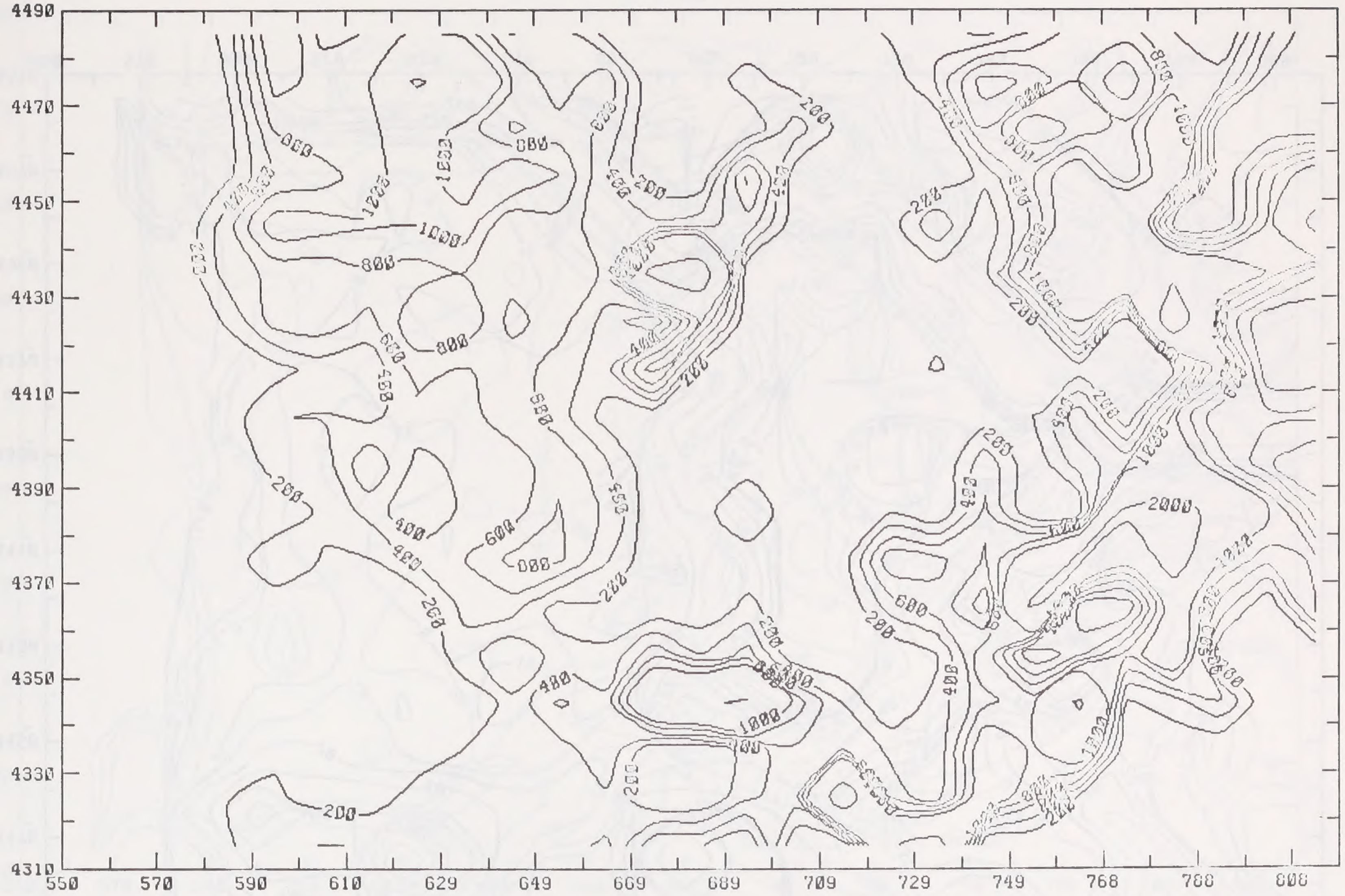

(b) TSP

FIGURE 5-28 (Continued)

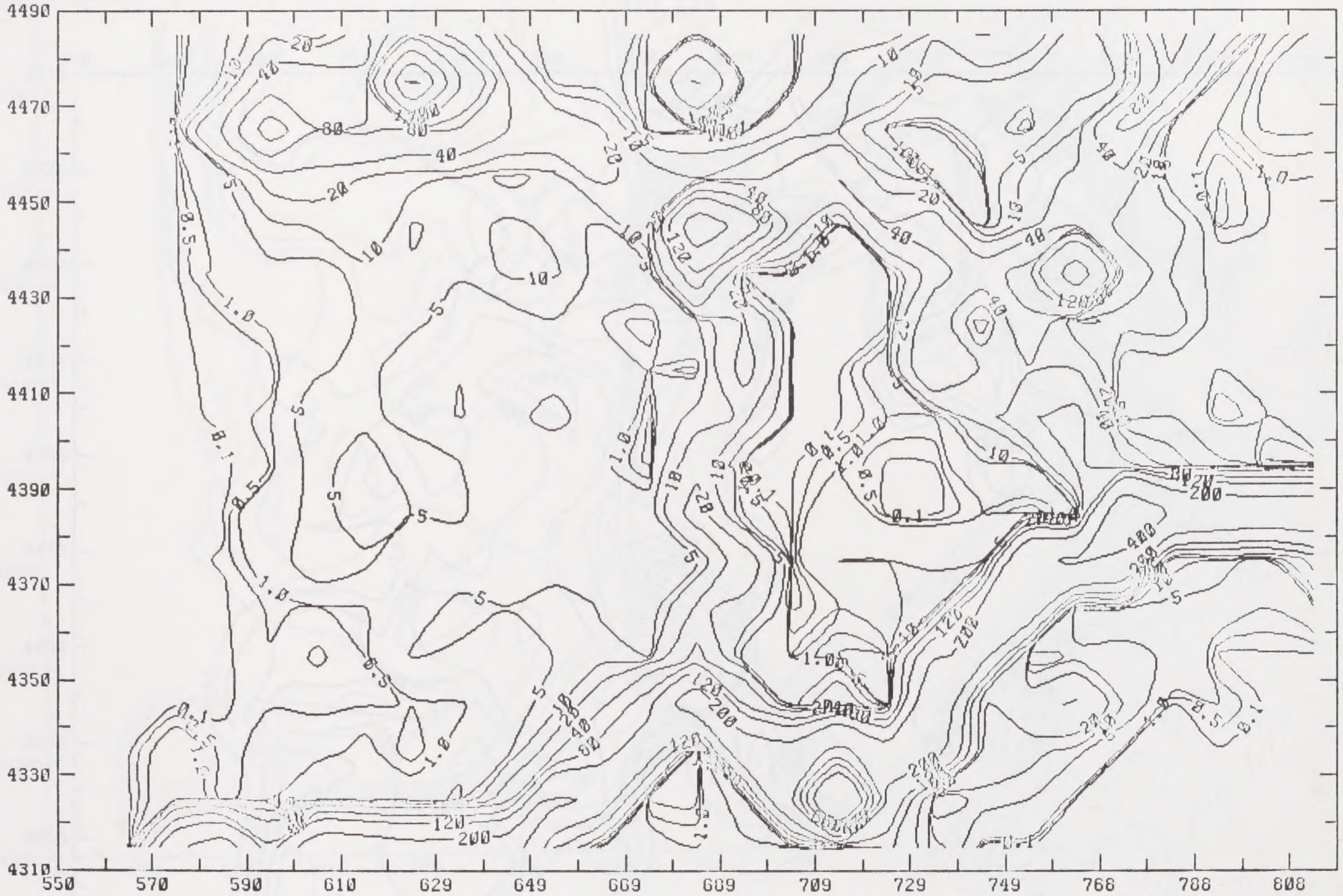

(c) NO_x

FIGURE 5-28 (Continued)

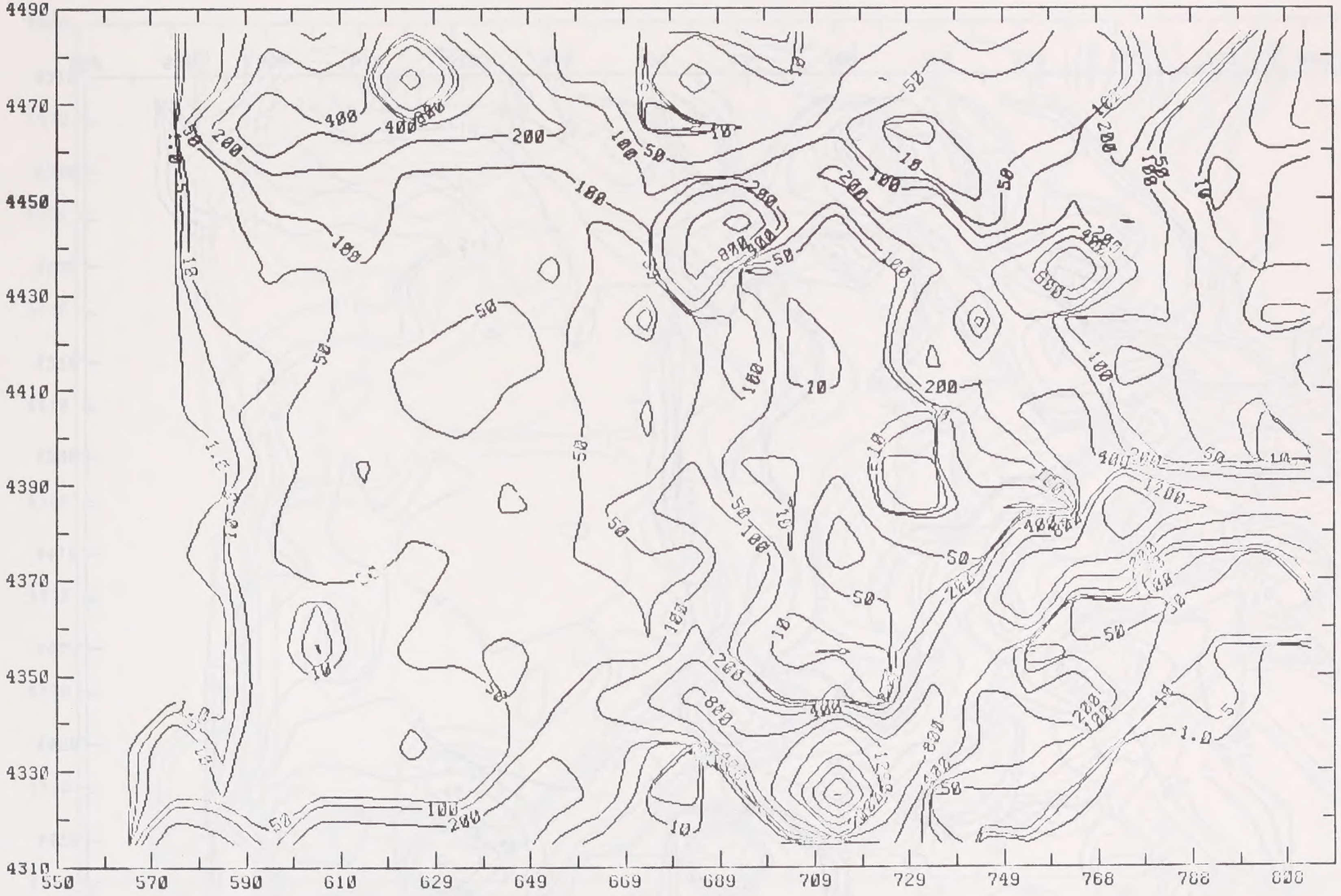

(d) CO

FIGURE 5-28 (Continued)

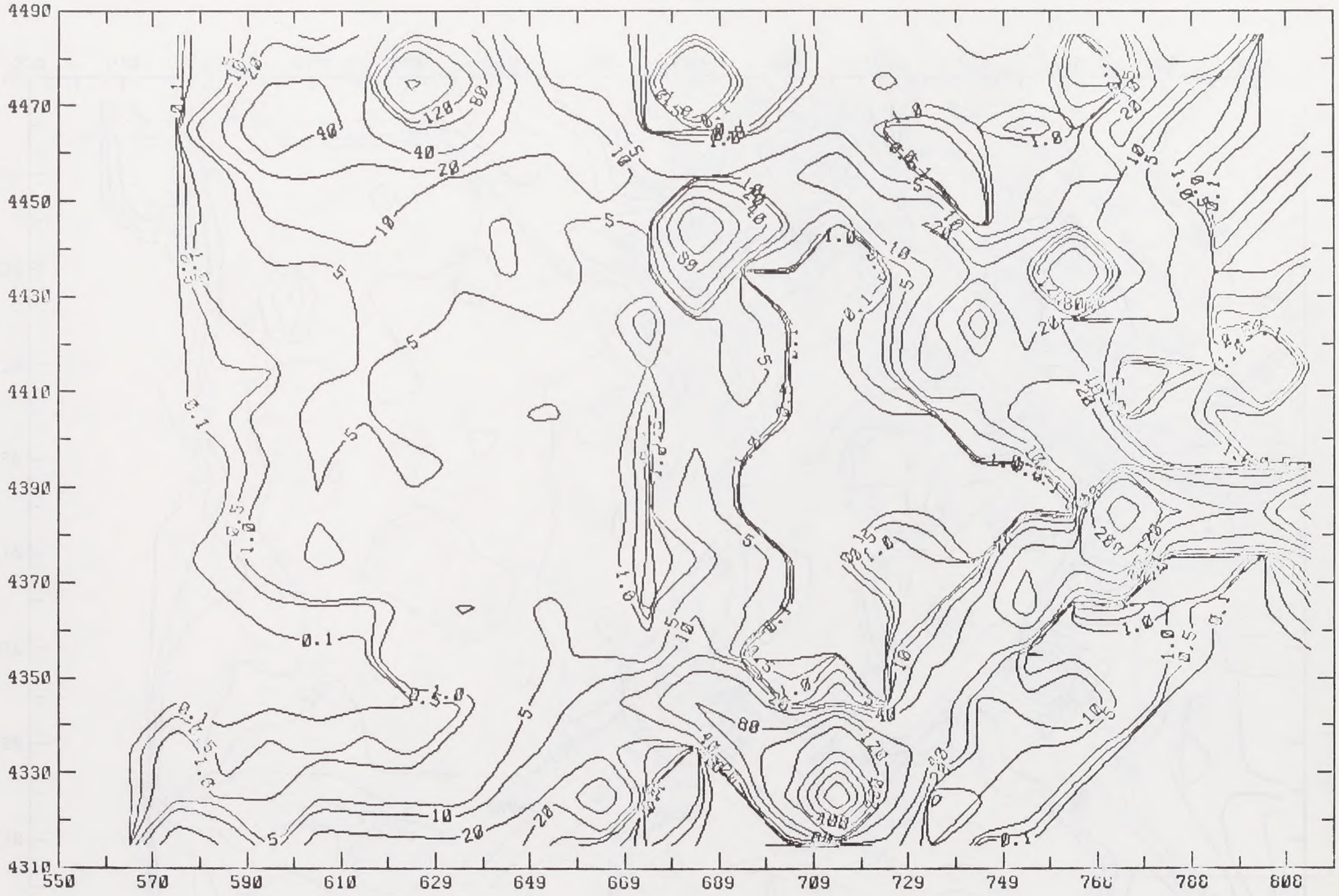

(e) Reactive Hydrocarbons

FIGURE 5-28 (Continued)

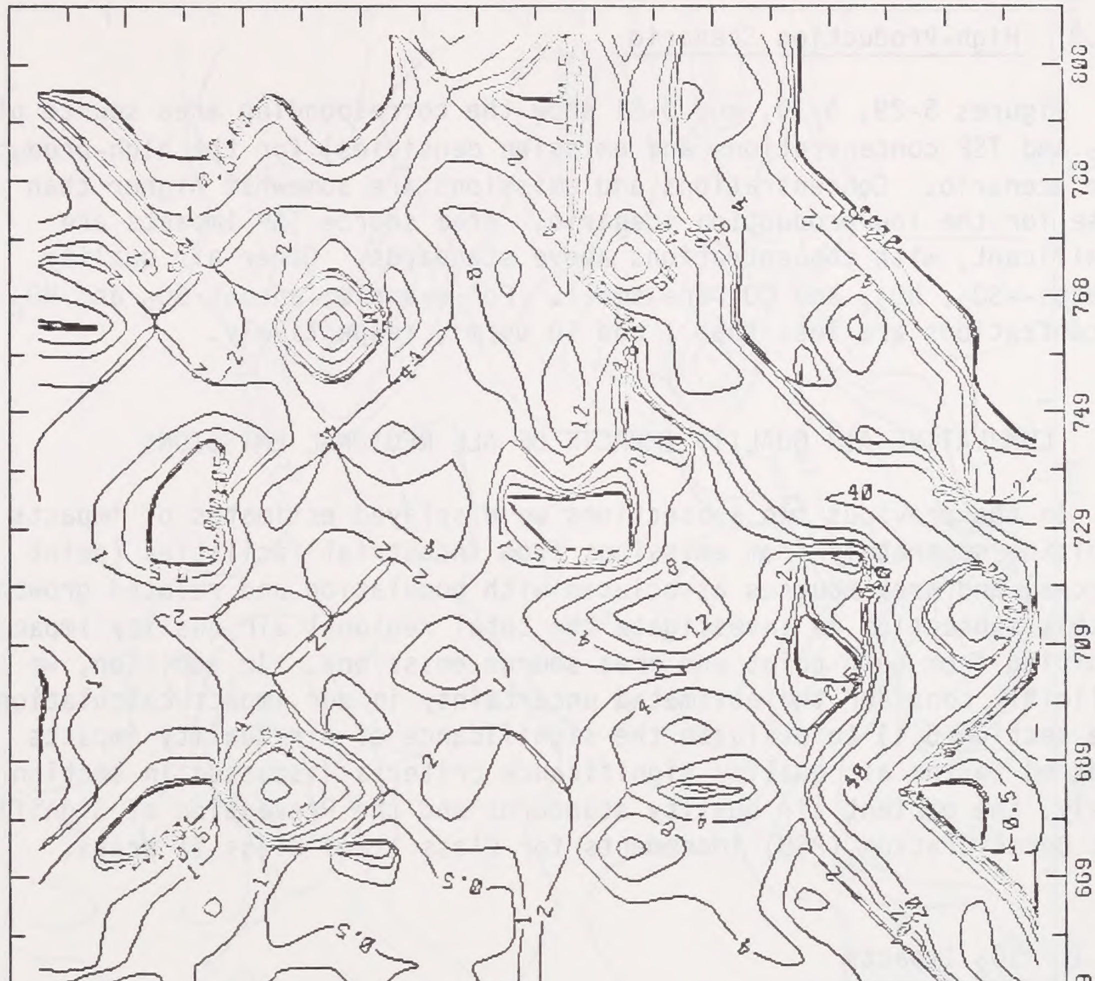

(f) Unreactive Hydrocarbons

FIGURE 5-28 (Concluded)

5.3.2 High-Production Scenario

Figures 5-29, 5-30, and 5-31 show the corresponding area source plots (SO_2 and TSP concentrations and emission densities) for the high-production scenario. Concentrations and emissions are somewhat higher than those for the low-production scenario. Area source TSP impacts are significant, with concentrations above standards. Other air quality impacts--SO_2, NO_2, and CO--are small. For example, annual SO_2 and NO_2 concentrations are less than 1 and 10 $\mu g/m^3$, respectively.

5.4 CUMULATIVE AIR QUALITY IMPACTS OF ALL REGIONAL EMISSIONS

In the previous two subsections we displayed estimates of impacts resulting separately from emissions from industrial facilities (point sources) and area sources associated with population and related growth. In this subsection we investigate the total regional air quality impacts resulting from both point and area source emissions. In addition, we explicitly consider the estimated uncertainty in our impact calculations (see section 5.1) to evaluate the significance of air quality impacts compared to the air quality significance criteria discussed in section 3, namely, the ambient air quality standards and the Prevention of Significant Deterioration (PSD) increments for Class I and Class II areas.

5.4.1 SO_2 Impacts

Tables 5-1 and 5-2 summarize the total SO_2 impacts of regional emission sources for a variety of receptors of interest for the low- and high-oil-production scenarios, respectively. Maximum 3-hour and 24-hour SO_2 concentrations (maximum concentrations in a year) as well as annual average concentrations are provided. Ranges of maximum concentrations are given for each receptor, taking into account the conservatism of the GPM calculations as discussed in subsection 5.1. From this table it is clear that impacts will be well within ambient air quality standards everywhere in the region; this conclusion is unambiguous within the estimated range of uncertainty since even the conservative, high estimates are within standards. The maximum SO_2 impacts are predicted in the Grand Junction area (including Colorado National Monument) with maximum 3-hour concentrations estimated to be in the range 66 to 664 $\mu g/m^3$. Most of this impact is the result of existing industrial or area source emissions on the Grand Junction area, not the projected emissions from the synthetic fuels industry.

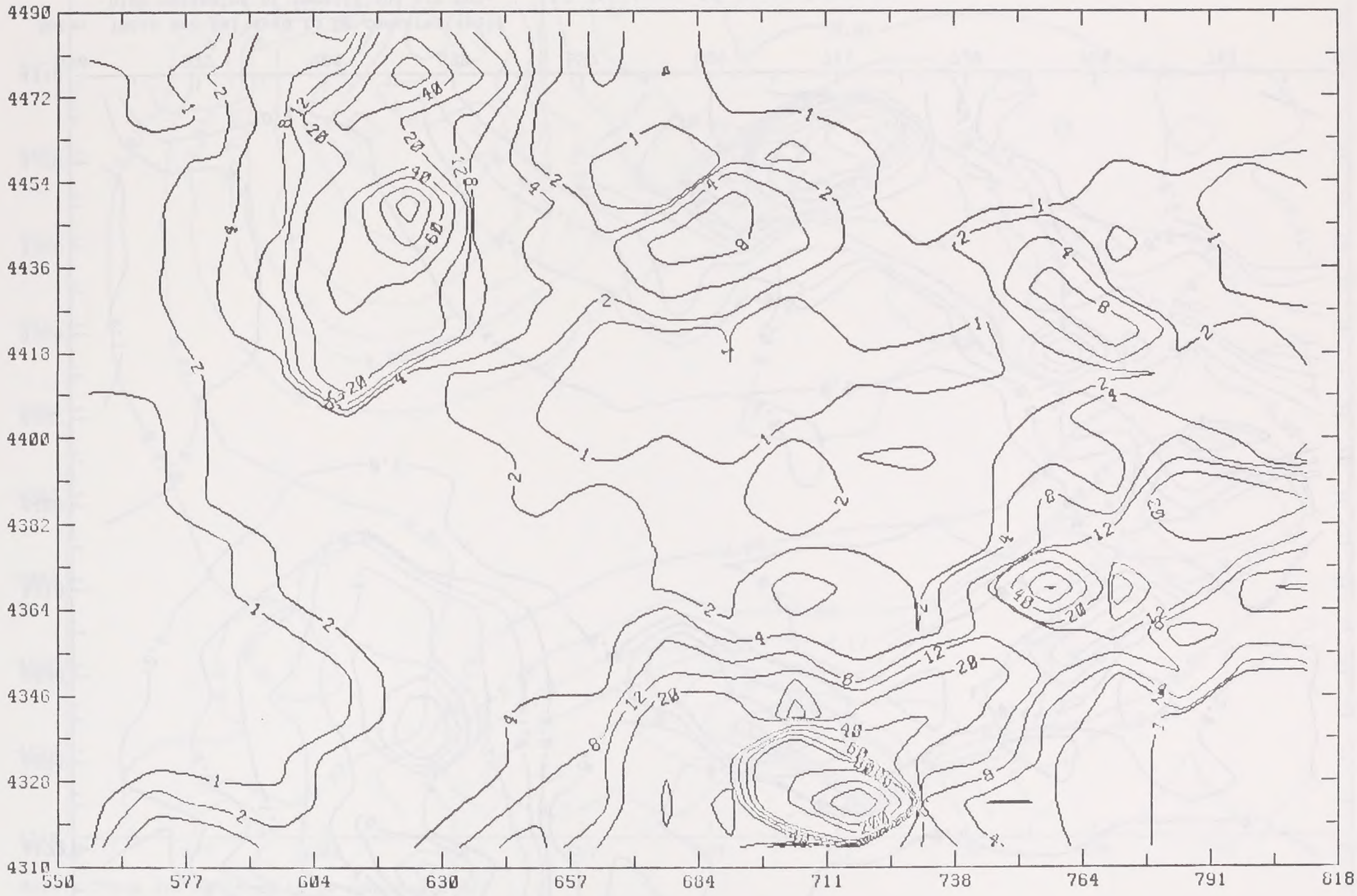

Note: These are believed to be conservatively high estimates of impacts and are non-simultaneous maxima calculated on the basis of one year's meteorological data.

(a) Maximum 3-Hour Average

FIGURE 5-29. IMPACT OF AREA SOURCE EMISSIONS ON GROUND-LEVEL SO_2 CONCENTRATIONS ($\mu g/m^3$) FOR THE HIGH OIL PRODUCTION SCENARIO

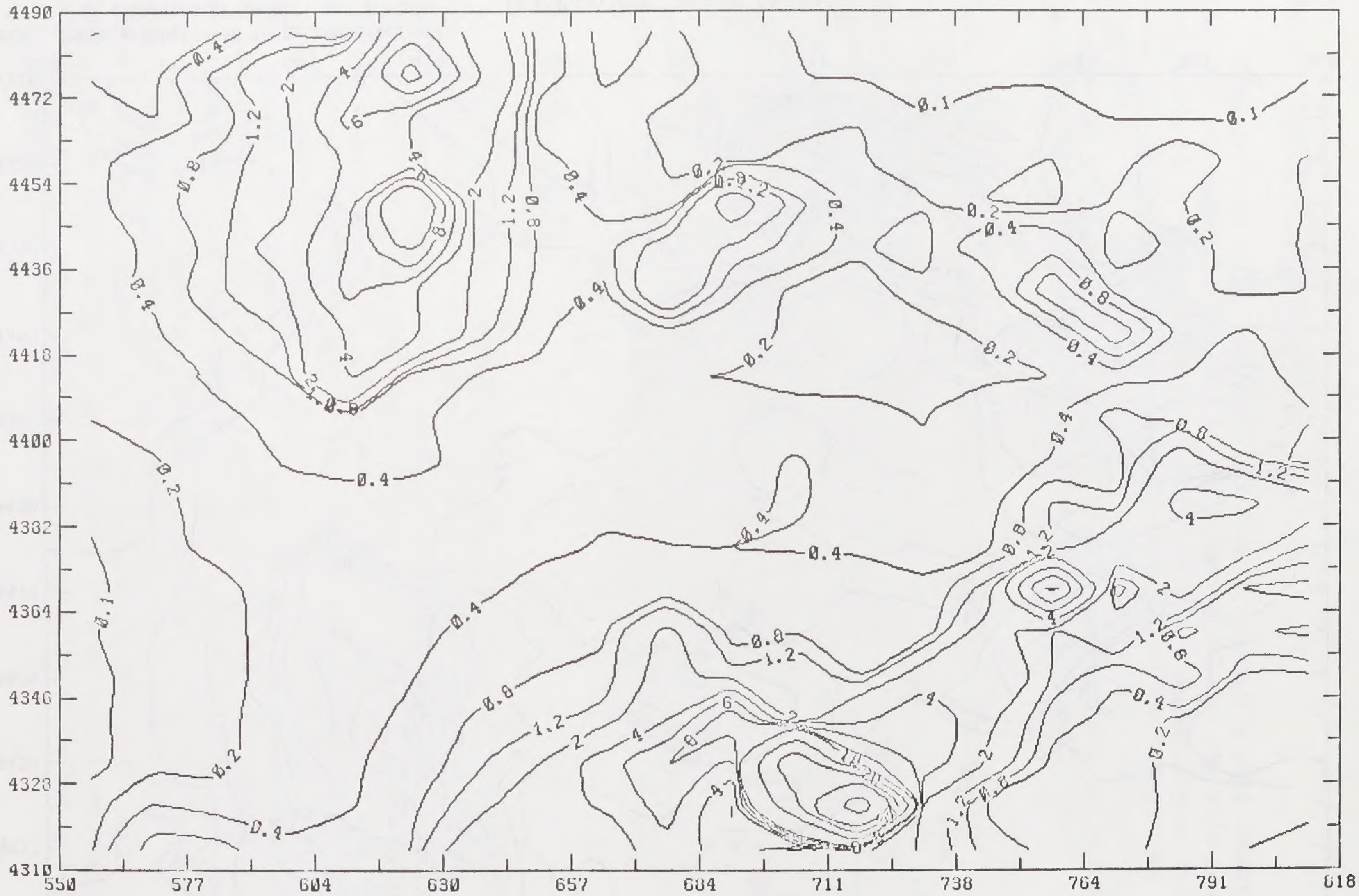

Note: These are believed to be conservatively high estimates of impacts and are non-simultaneous maxima calculated on the basis of one year's meteorological data.

(b) Maximum 24-Hour Average

FIGURE 5-29 (Continued)

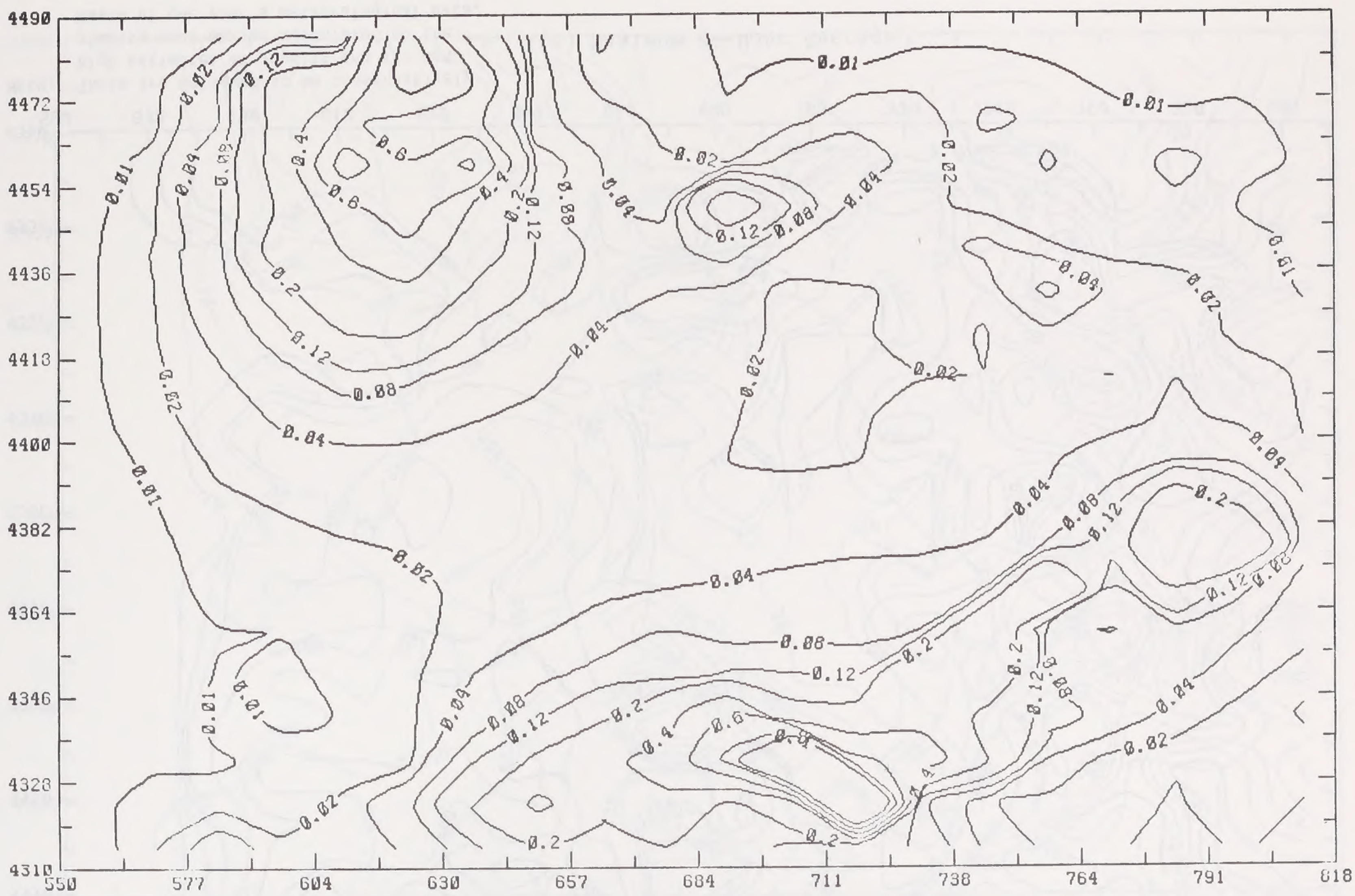

Note: These are believed to be conservatively high estimates of impacts.

(c) Annual Average

FIGURE 5-29 (Concluded)

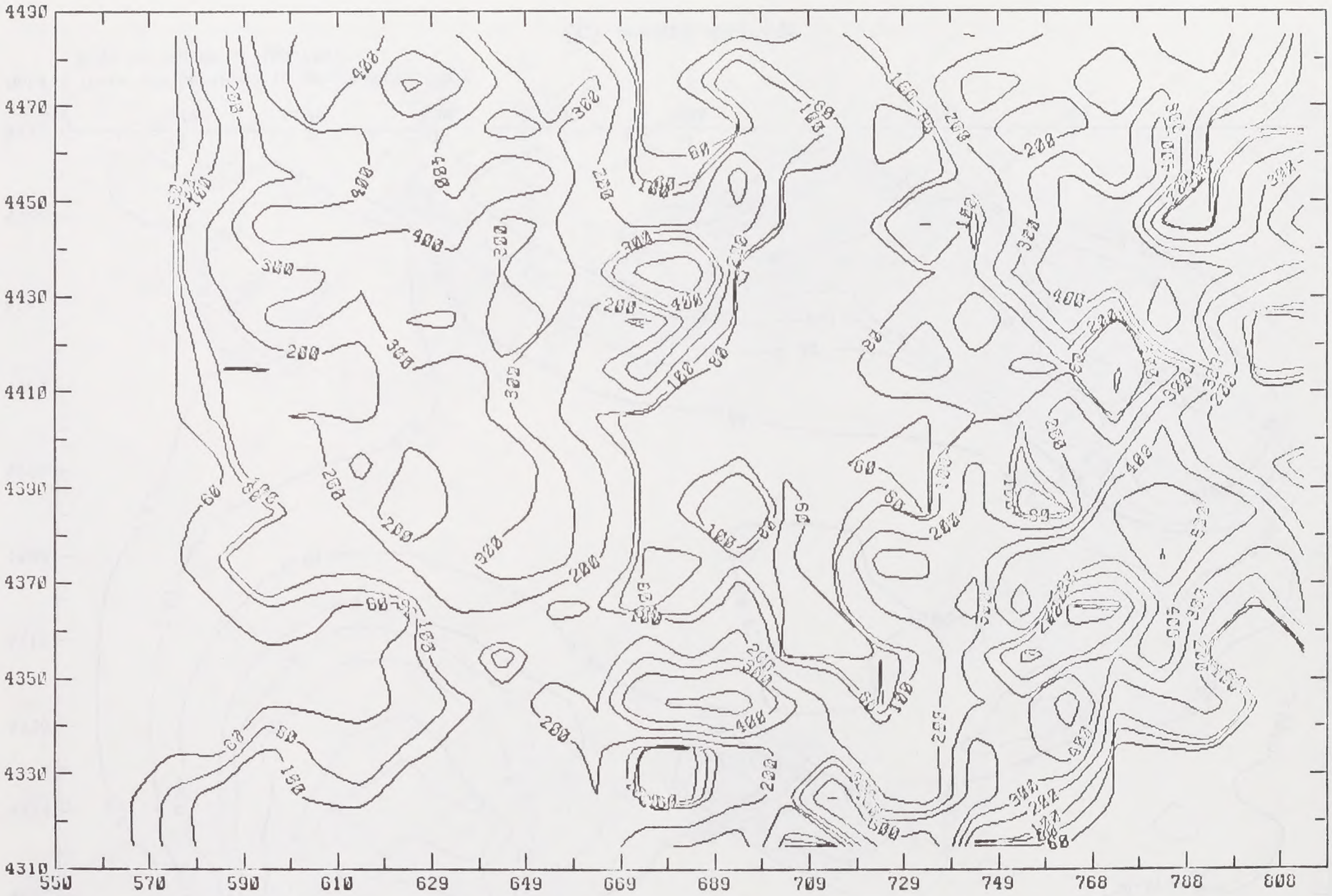

Note: These are believed to be conservatively high estimates of impacts and are non-simultaneous maxima calculated on the basis of one year's meteorological data.

(a) Maximum 24-Hour Average

FIGURE 5-30. IMPACT OF AREA SOURCE EMISSIONS ON GROUND-LEVEL TSP CONCENTRATIONS ($\mu g/m^3$) FOR THE HIGH OIL PRODUCTION SCENARIO

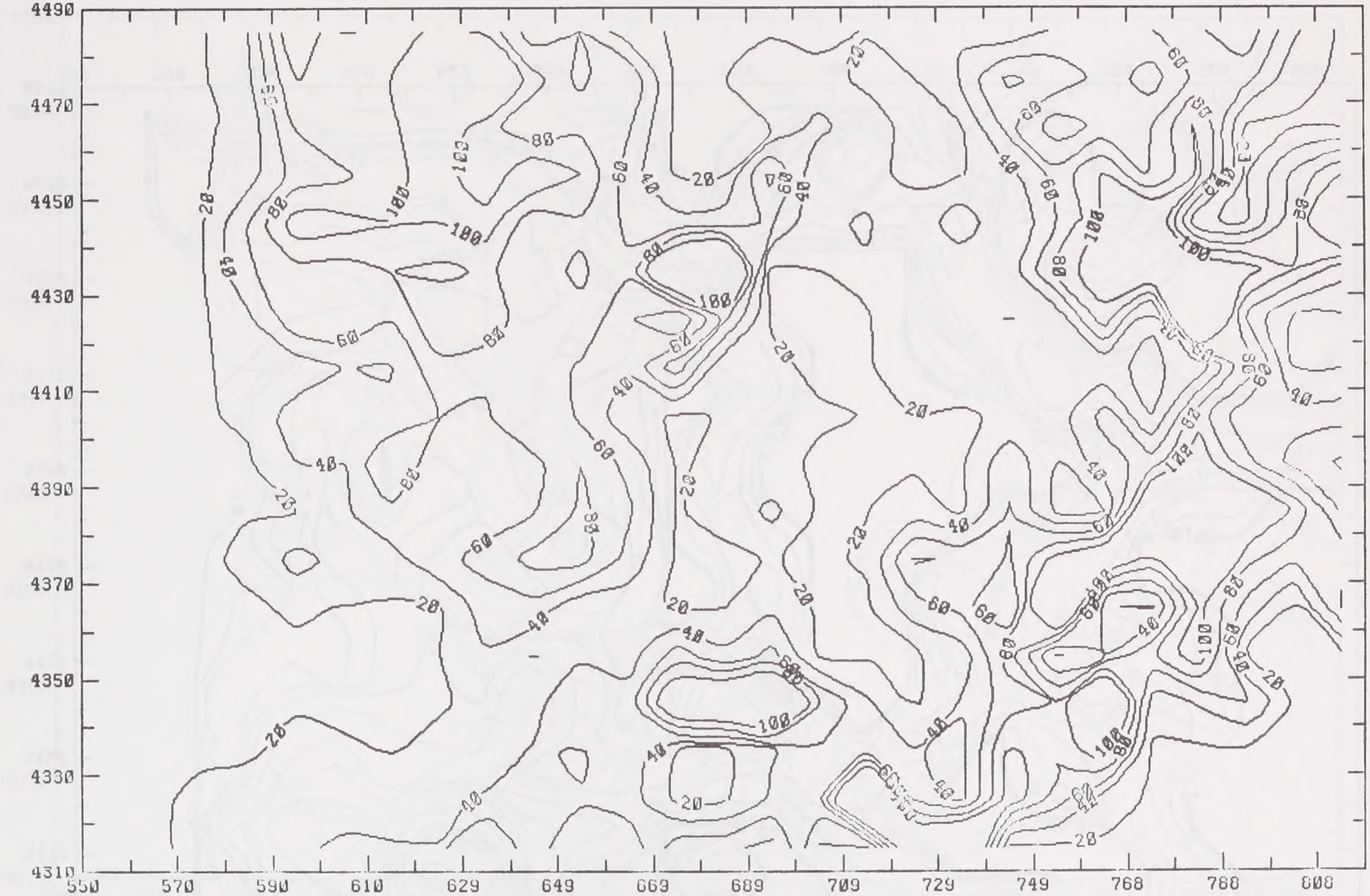

Note: These are believed to be conservatively high estimates of impacts and are non-simultaneous maxima calculated on the basis of one year's meteorological data.

(b) Annual Average

FIGURE 5-30 (Concluded)

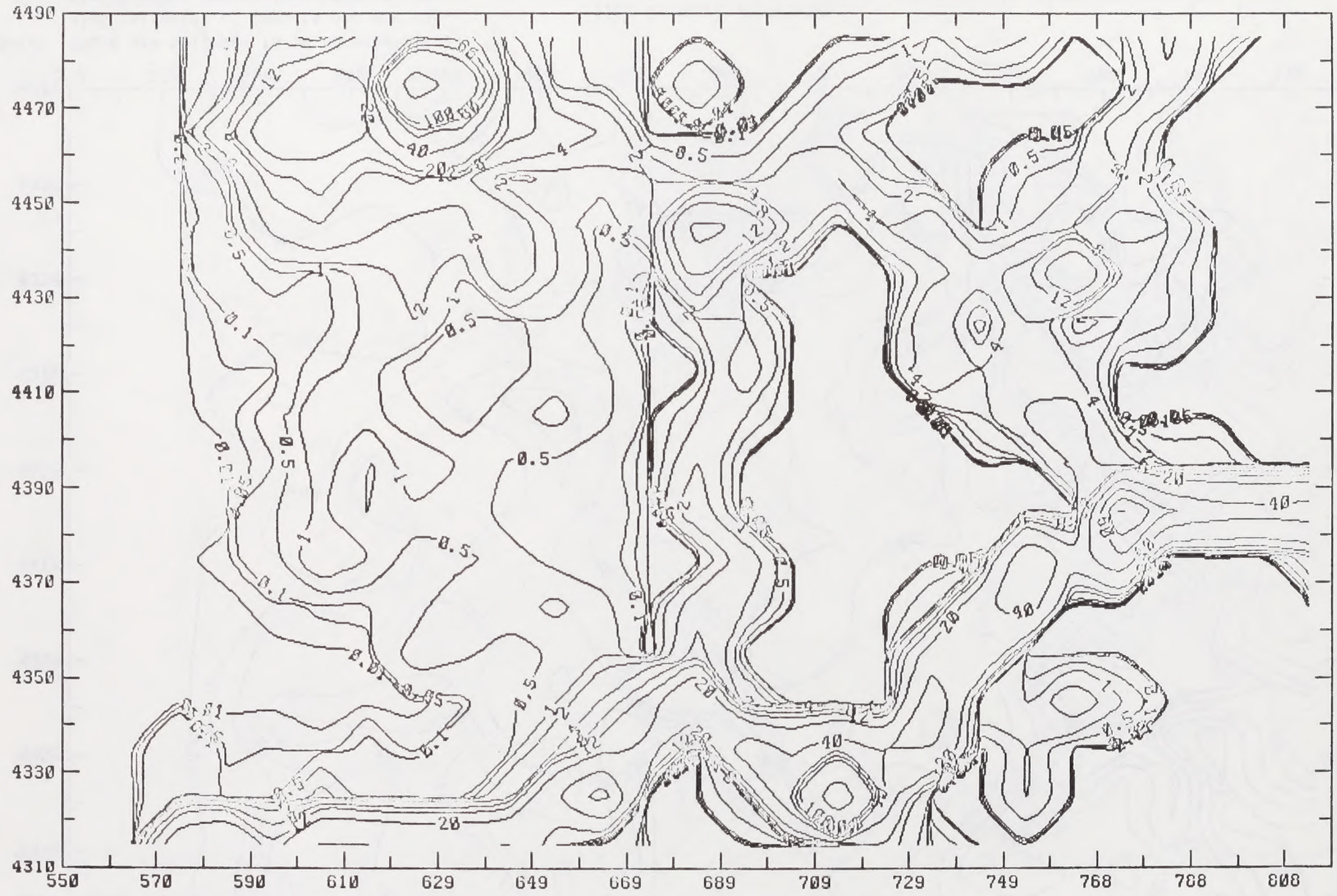

(a) SO_2

FIGURE 5-31. AREA SOURCE EMISSION DENSITIES FOR HIGH OIL PRODUCTION SCENARIO (tons/yr/100 km^2)

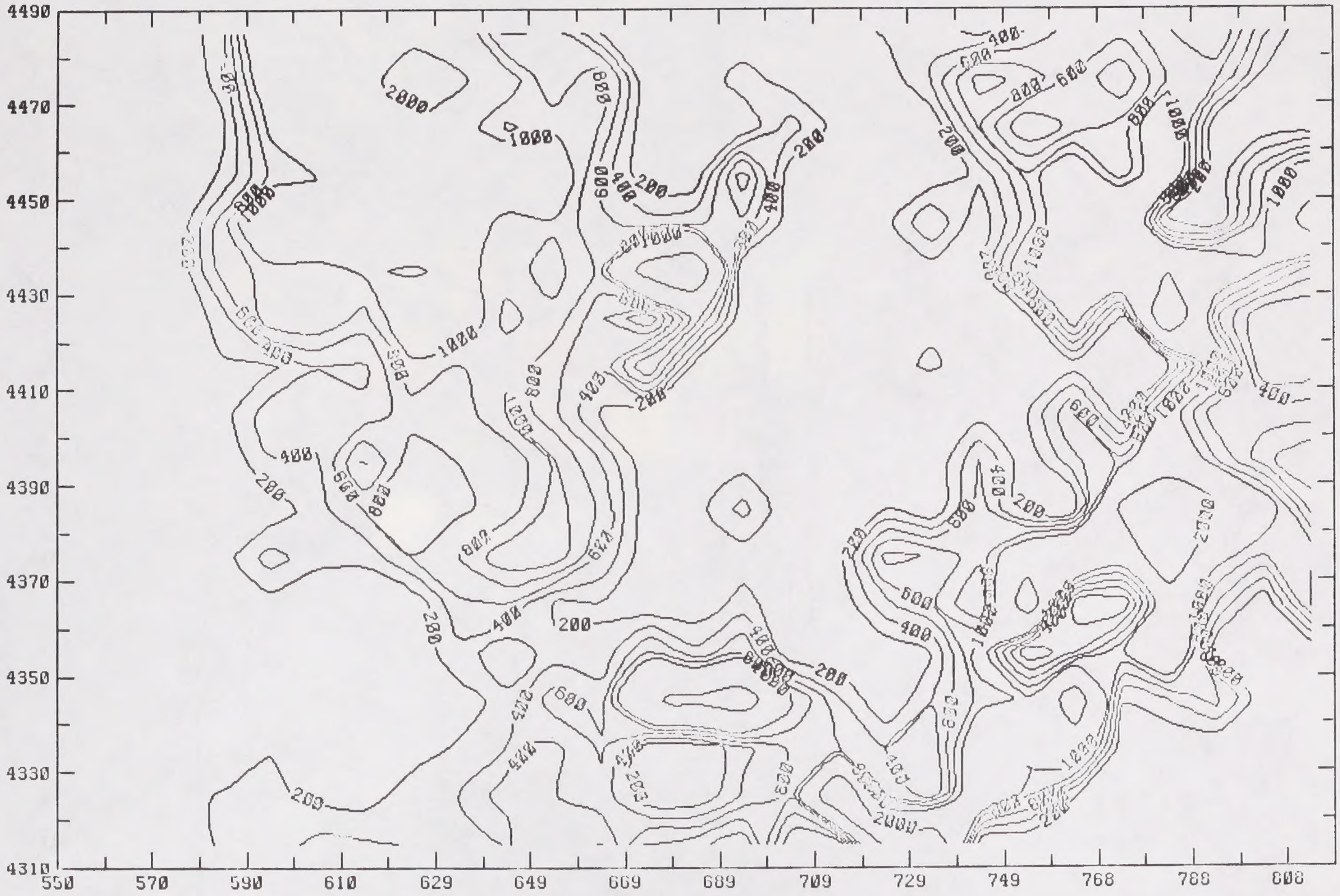

(b) TSP

FIGURE 5-31 (Continued)

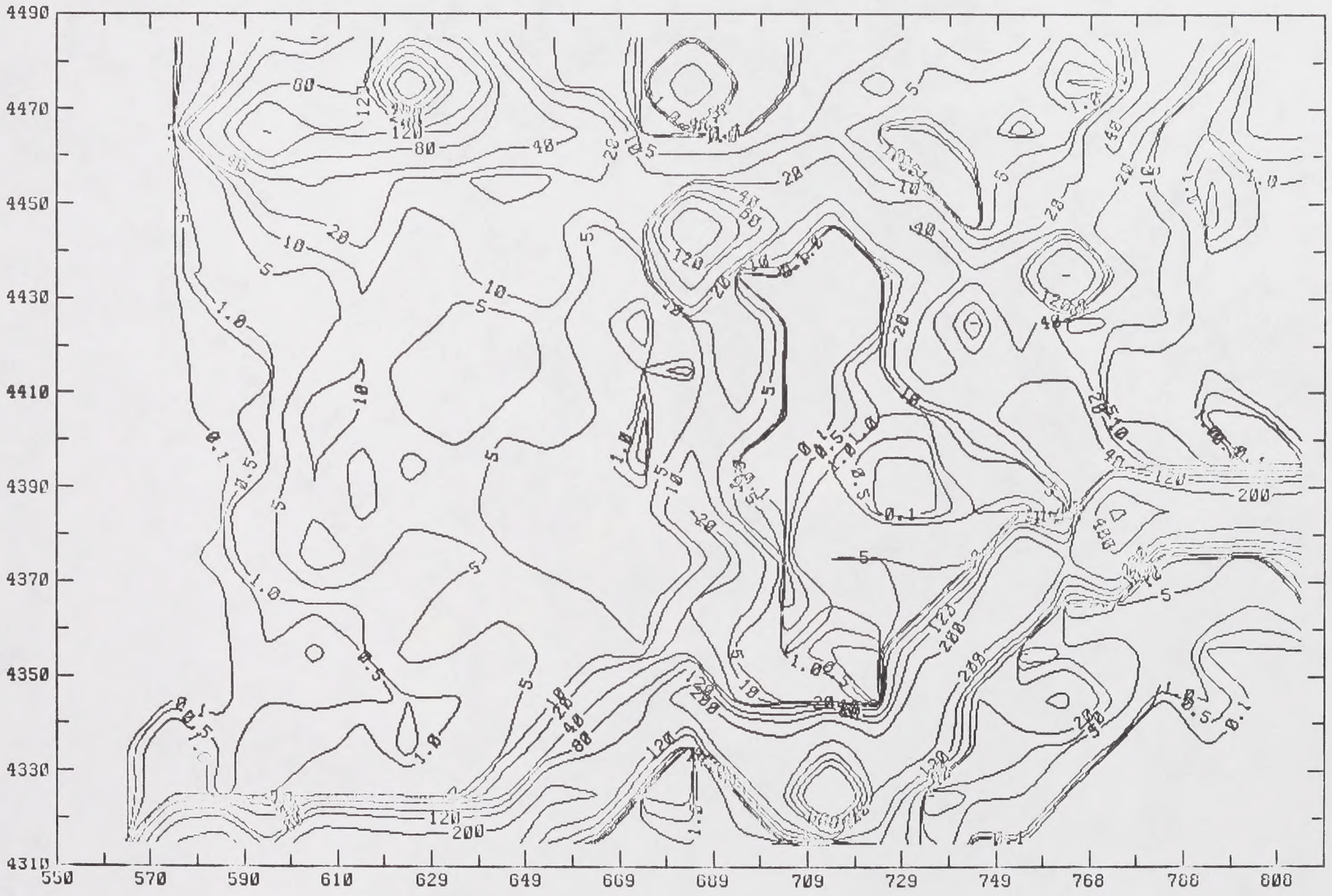

(c) NO_x

FIGURE 5-31 (Continued)

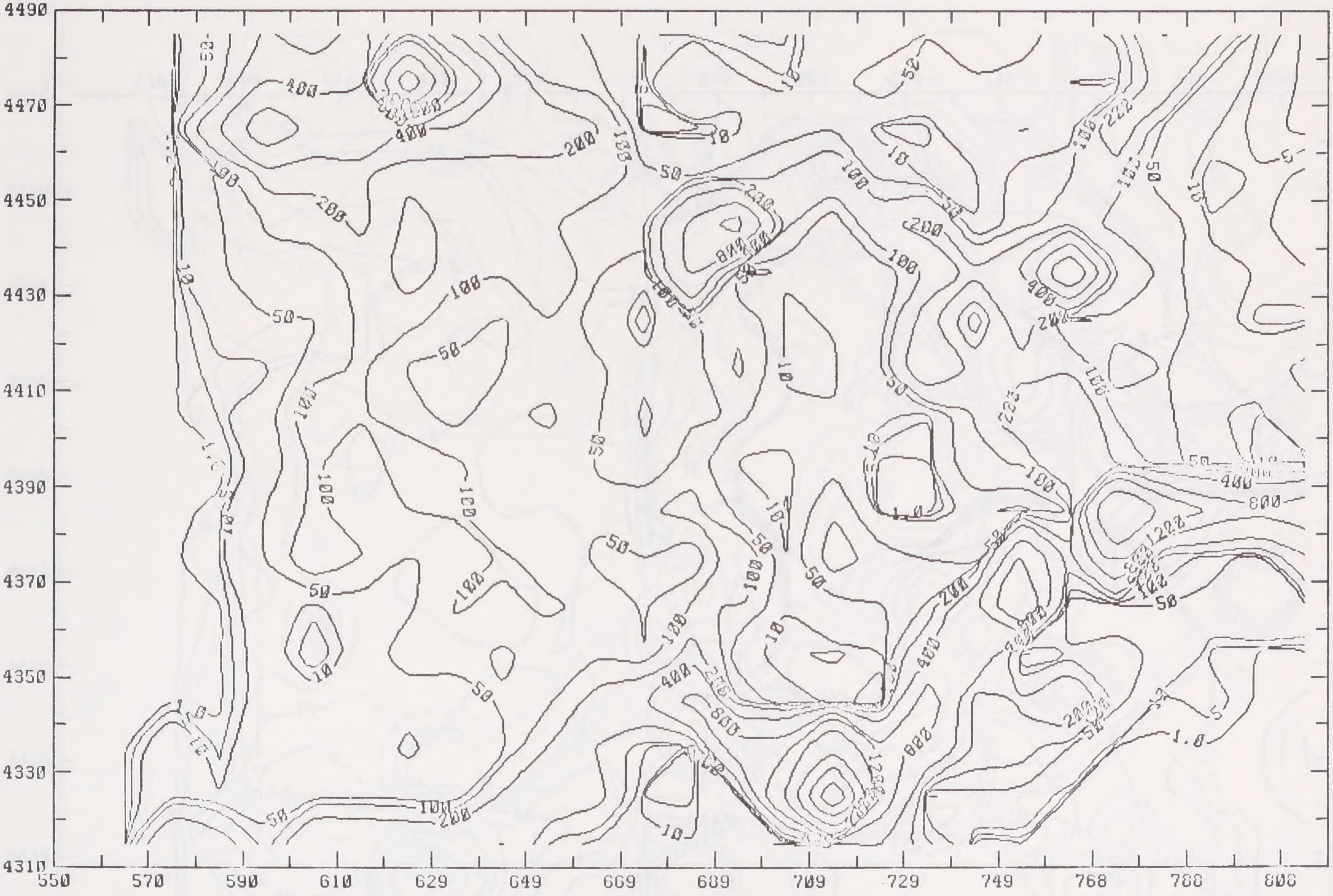

(d) CO

FIGURE 5-31 (Continued)

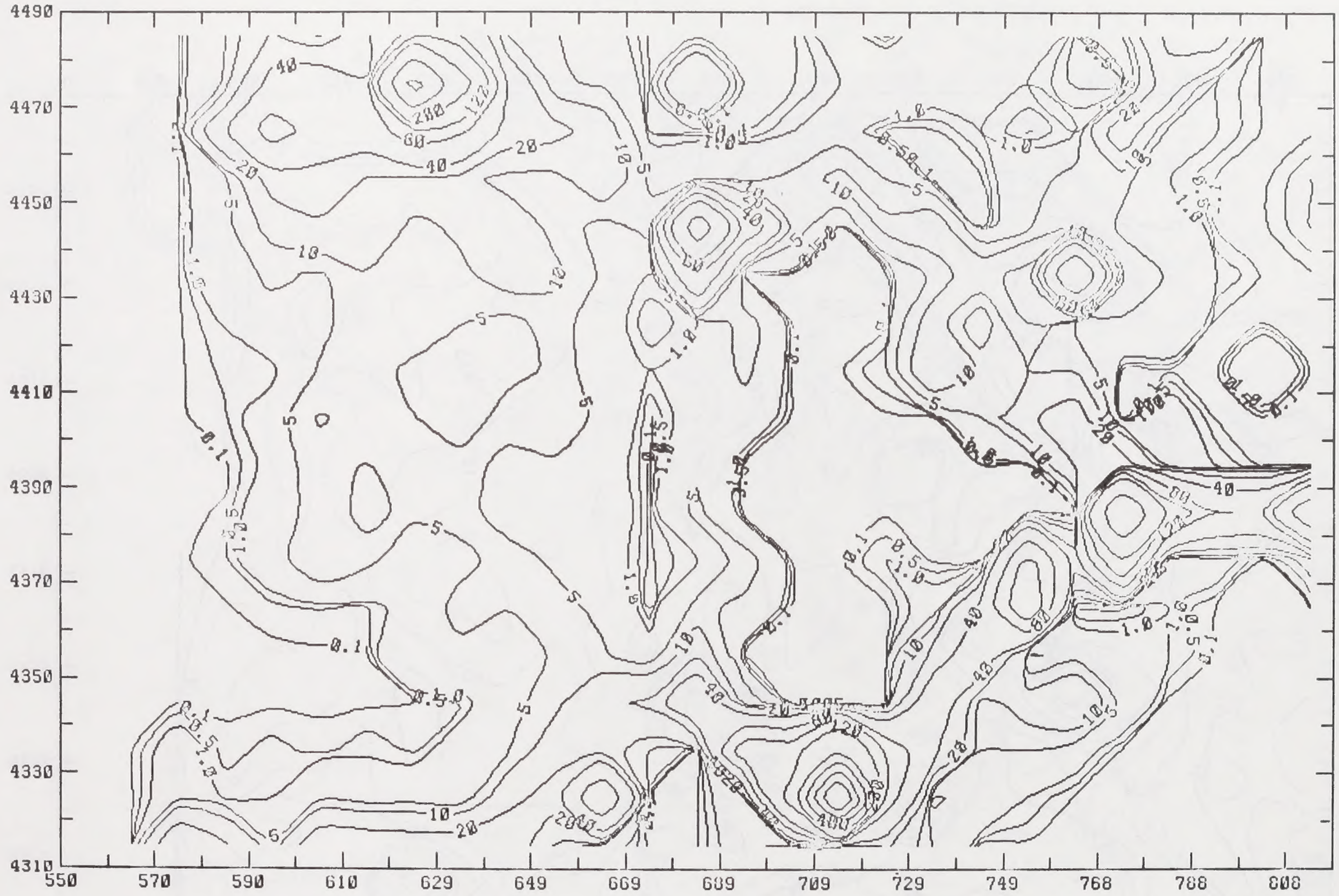

(e) Reactive Hydrocarbons

FIGURE 5-31 (Continued)

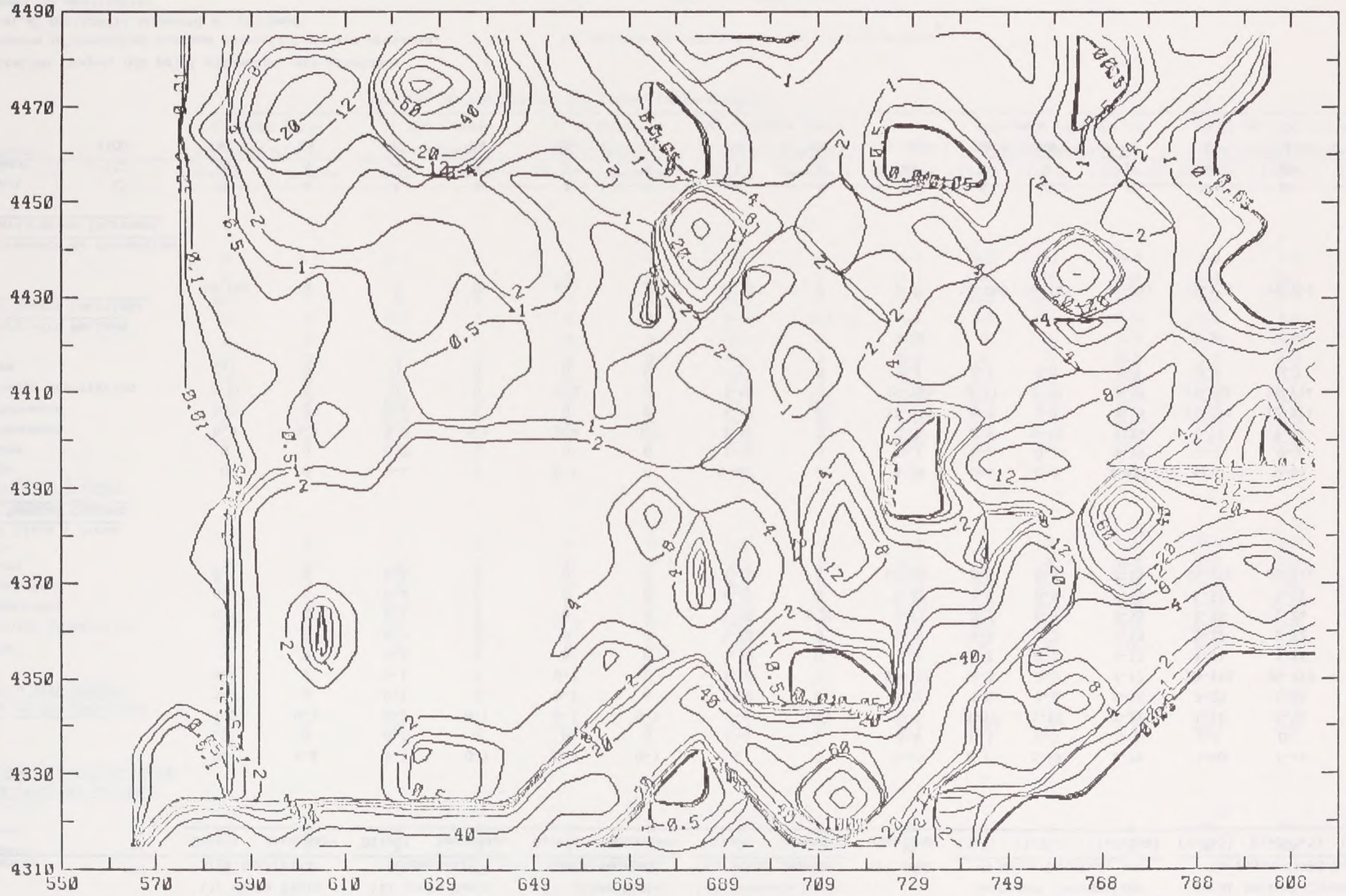

(f) Unreactive Hydrocarbons

FIGURE 5-31 (Concluded)

TABLE 5-1. SUMMARY OF AMBIENT AIR QUALITY IMPACTS ASSOCIATED WITH THE LOW OIL PRODUCTION SCENARIO

(a) Maximum 3-hour Average SO_2 Concentrations*

Maximum 3-hour Average SO_2 Concentrations ($\mu g/m^3$)

Receptor	(1) Uinta Basin Site-Specifics		(2) Uinta Basin Conceptuals		(3) Other Uinta Basin Sources		(4) Piceance Basin (Colorado Sources)		(5) 1980 Baseline	Increment Consumption Above Baseline			Total Ambient Concentration Including 1980 Baseline		
	Direct	Secondary	Direct	Secondary	Direct	Secondary	Direct	Secondary		(1+2)	(1+2+3)	(1+2+3+4)	(1+2+5)	(1+2+3+5)	(1+2+3+4+5)
Population Centers															
Vernal	0-1	1-6	1-5	0-3	0-1	0-3	0	0	5-45	2-15	2-19	2-19	7-60	7-64	7-64
Green River	0	0	0-3	0	0	0	0-4	0	0-4	0-3	0-3	0-7	0-7	0-7	0-11
Rangely	1-5	0-3	0-2	0-1	0-3	0-1	0-4	0-3	0-1	1-11	1-15	1-22	1-12	1-16	1-23
Meeker	1-3	0	0-1	0	0-2	0	5-50	0	2-16	1-4	1-6	6-56	3-20	3-22	8-72
Craig	0-1	0	0-1	0	0-1	0	1-10	0	20-196	0-2	0-3	1-13	20-198	20-199	21-209
Glenwood Springs	0	0	0-2	0	0	0	1-10	0	1-9	0-2	0-2	1-12	1-11	1-11	2-21
Rifle	0	0	0-3	0	0	0	1-10	0	2-19	0-3	0-3	1-13	2-22	2-22	3-32
Parachute	0-1	0	0-2	0	0	0	1-10	2-20	2-21	0-3	0-3	3-33	2-24	2-24	5-54
De Beque	0-1	0	0-4	0	0	0	1-10	0	5-52	0-5	0-5	1-15	5-57	5-57	6-67
Grand Junction	0-1	0	0-4	0	0	0	1-10	0	60-607	0-5	0-5	1-15	60-612	60-612	61-622
Existing or Potential Class I Areas and Other Areas of Special Concern															
Flat Tops Wilderness	0	0	0-4	0	0-1	0	4-40†	0	4-39	0-4	0-5	4-45†	4-43	4-44	8-84
Mt. Zirkel Wilderness	0	0	0-2	0	0	0	1-10	0	0-3	0-2	0-2	1-12	0-5	0-5	1-15
Dinosaur National Monument	0-3	0-2	0-3	0-1	0-4	0-1	1-10	0	1-5	0-9	0-14	1-24	1-14	1-19	2-29
Colorado National Monument	0-1	0	0-2	0	0	0	1-10	0	32-318	0-3	0-3	1-13	32-321	32-321	33-331
Uintah and Ouray Indian Reservation	2-21	0	0	0	0-8	0	1-10	0	19-185	2-21	2-29	3-39	21-206	21-214	22-224
Uinta Primitive Area	0-1	0	0	0	0	0	0	0	0-1	0-1	0-1	0-1	0-2	0-2	0-2
Class II Area Receptors with Maximum Impacts from Direct Source Emissions in Uinta Basin	14-140	0	0	0	0-5	0	0-10	0	1-10	14-140	14-145	15-155	15-150	15-155	16-165
Ambient Air Quality Standard or Prevention of Significant Deterioration Increment															
PSD Class I Increment 25	A	A	A	A	A	A	A	A	NA	A	A	A	NA	NA	NA
PSD Class II Increment 512	A	A	A	A	A	A	A	A	NA	A	A	A	NA	NA	NA
AAQS 1300	NA	NA	NA	NA	NA	NA	NA	NA	A	NA	NA	NA	A	A	A

---

* Note that concentration ranges, not point estimates, are provided; low and high estimates of predicted maximum concentration are provided.

† Indicates violation of applicable standard or increment.

A Standard or increment is applicable.

NA Standard or increment is not applicable.

TABLE 5-1 (Continued)

(b) Maximum 24-hour Average SO_2 Concentrations*

Receptor		Maximum 24-hour Average SO_2 Concentrations ($\mu g/m^3$)														
		(1) Uinta Basin Site-Specifics		(2) Uinta Basin Conceptuals		(3) Other Uinta Basin Sources		(4) Piceance Basin (Colorado Sources)		(5) 1980	Increment Consumption Above Baseline			Total Ambient Concentration Including 1980 Baseline		
		Direct	Secondary	Direct	Secondary	Direct	Secondary	Direct	Secondary	Baseline	(1+2)	(1+2+3)	(1+2+3+4)	(1+2+5)	(1+2+3+5)	(1+2+3+4+5)
Population Centers																
Vernal		0	0-1	0-1	0	0	0	0	0	1-6	0-2	0-2	0-2	1-8	1-8	1-8
Green River		0	0	0	0	0	0	0-1	0	0-1	0	0	0-1	0-1	0-1	0-2
Rangely		0-2	0	0	0	0	0	0-1	0	0-1	0-2	0-2	0-3	0-3	0-3	0-4
Meeker		0	0	0-1	0	0	0	1-14	0-1	1-5	0-1	0-1	1-16	1-6	1-6	2-21
Craig		0	0	0	0	0	0	0-2	0	3-28	0	0	0-2	3-28	3-28	3-30
Glenwood Springs		0	0	0	0	0	0	0-3	0	0-2	0	0	0-3	0-2	0-2	0-5
Rifle		0	0	0-1	0	0	0	0-3	0	0-3	0-1	0-1	0-4	0-4	0-4	0-7
Parachute		0	0	0-1	0	0	0	0-3	0-3	0-3	0-1	0-1	0-7	0-4	0-4	0-10
De Beque		0	0	0-1	0	0	0	0-3	0	1-11	0-1	0-1	0-4	1-12	1-12	1-15
Grand Junction		0	0	0-1	0	0	0	0-3	0	8-82	0-1	0-1	0-4	8-83	8-83	8-86
Existing or Potential Class I Areas and Other Areas of Special Concern																
Flat Tops Wilderness		0	0	0	0	0	0	1-6†	0	1-5	0	0	1-6†	1-5	1-5	2-11
Mt. Zirkel Wilderness		0	0	0	0	0	0	0-2	0	0-1	0	0	0-2	0-1	0-1	0-3
Dinosaur National Monument		0-1	0	0	0	0	0	0-1	0	1-5	0-1	0-1	0-2	1-6	1-6	1-7
Colorado National Monument		0	0	0-1	0	0	0	0-3	0	4-40	0-1	0-1	0-4	4-41	4-41	4-44
Uintah and Ouray Indian Reservation		0-3	0	0	0	0-2	0	0-2	0	2-23	0-3	0-5	0-7	2-26	2-28	2-30
Uinta Primitive Area		0	0	0	0	0	0	0	0	0-1	0	0	0	0-1	0-1	0-1
Class II Area Receptors with Maximum Impacts from Direct Source Emissions in Uinta Basin		2-22	0	0	0	0-1	0	0-1	0	0-1	2-22	2-23	2-24	2-23	2-24	2-25
Ambient Air Quality Standard or Prevention of Significant Deterioration Increment																
PSD Class I Increment	5	A	A	A	A	A	A	A	A	NA	A	A	A	NA	NA	NA
PSD Class II Increment	91	A	A	A	A	A	A	A	A	NA	A	A	A	NA	NA	NA
AAQS	365	NA	NA	NA	NA	NA	NA	NA	NA	A	NA	NA	NA	A	A	A

---

* Note that concentration ranges, not point estimates, are provided; low and high estimates of predicted maximum concentration are provided.

† Indicates violation of applicable standard or increment.

A Standard or increment is applicable.

NA Standard or increment is not applicable.

TABLE 5-1 (Concluded)

(c) Annual Average SO_2 Concentrations*

Receptor		Annaul Average SO_2 Concentrations ($\mu g/m^3$)														
		(1) Uinta Basin Site-Specifics		(2) Uinta Basin Conceptuals		(3) Other Uinta Basin Sources		(4) Piceance Basin (Colorado Sources)		(5) 1980	Increment Consumption Above Baseline			Total Ambient Concentration Including 1980 Baseline		
		Direct	Secondary	Direct	Secondary	Direct	Secondary	Direct	Secondary	Baseline	(1+2)	(1+2+3)	(1+2+3+4)	(1+2+5)	(1+2+3+5)	(1+2+3+4+5)
Population Centers																
Vernal		0	0	0	0	0	0	0	0	0	0	0	0	0	0	0
Green River		0	0	0	0	0	0	0	0	0	0	0	0	0	0	0
Rangely		0	0	0	0	0	0	0	0	0	0	0	0	0	0	0
Meeker		0	0	0	0	0	0	0-1	0	0	0	0	0-1	0	0	0-1
Craig		0	0	0	0	0	0	0	0	0	0	0	0	0	0	0
Glenwood Springs		0	0	0	0	0	0	0	0	0	0	0	0	0	0	0
Rifle		0	0	0	0	0	0	0	0	0-1	0	0	0	0-1	0-1	0-1
Parachute		0	0	0	0	0	0	0	0	0-1	0	0	0	0-1	0-1	0-1
De Beque		0	0	0	0	0	0	0	0	0-1	0	0	0	0-1	0-1	0-1
Grand Junction		0	0	0	0	0	0	0	0	0-9	0	0	0	0-9	0-9	0-9
Existing or Potential Class I Areas and Other Areas of Special Concern																
Flat Tops Wilderness		0	0	0	0	0	0	0	0	0	0	0	0	0	0	0
Mt. Zirkel Wilderness		0	0	0	0	0	0	0	0	0	0	0	0	0	0	0
Dinosaur National Monument		0	0	0	0	0	0	0	0	0	0	0	0	0	0	0
Colorado National Monument		0	0	0	0	0	0	0	0	0-1	0	0	0	0-1	0-1	0-1
Uintah and Ouray Indian Reservation		0	0	0	0	0	0	0	0	0	0	0	0	0	0	0
Uinta Primitive Area		0	0	0	0	0	0	0	0	0	0	0	0	0	0	0
Class II Area Receptors with Maximum Impacts from Direct Source Emissions in Uinta Basin		0	0	0-2	0	0	0	0	0	0-1	0-2	0-2	0-2	0-3	0-3	0-3
Ambient Air Quality Standard or Prevention of Significant Deterioration Increment																
PSD Class I Increment	2	A	A	A	A	A	A	A	A	NA	A	A	A	NA	NA	NA
PSD Class II Increment	20	A	A	A	A	A	A	A	A	NA	A	A	A	NA	NA	NA
AAQS	80	NA	NA	NA	NA	NA	NA	NA	NA	A	NA	NA	NA	A	A	A

---

* Note that concentration ranges, not point estimates, are provided; low and high estimates of predicted maximum concentration are provided.

† Indicates violation of applicable standard or increment.

A Standard or increment is applicable.

NA Standard or increment is not applicable.

TABLE 5-2. SUMMARY OF AMBIENT AIR QUALITY IMPACTS ASSOCIATED WITH THE HIGH OIL PRODUCTION SCENARIO

(a) Maximum 3-hour Average SO_2 Concentrations[*]

Receptor	Maximum 3-hour Average SO_2 Concentrations ($\mu g/m^3$)														
	(1) Uinta Basin Site-Specifics		(2) Uinta Basin Conceptuals		(3) Other Uinta Basin Sources		(4) Piceance Basin (Colorado Sources)		(5) 1980	Increment Consumption Above Baseline			Total Ambient Concentration Including 1980 Baseline		
	Direct	Secondary	Direct	Secondary	Direct	Secondary	Direct	Secondary	Baseline	(1+2)	(1+2+3)	(1+2+3+4)	(1+2+5)	(1+2+3+5)	(1+2+3+4+5)
Population Centers															
Vernal	0-4	1-10	3-30	1-5	0-1	1-5	0-4	0	5-45	5-49	6-55	6-59	10-94	11-100	11-104
Green River	0-1	0	1-6	0	0	0	0-4	0	0-4	1-7	1-7	1-11	1-11	1-11	1-15
Rangely	1-11	0-4	1-6	0-1	0-3	0-1	2-20	0-4	0-1	2-22	2-26	4-50	2-23	2-27	4-51
Meeker	1-5	0	1-7	0	0-2	0	8-80	0	2-16	2-12	2-14	10-94	4-28	4-30	12-110
Craig	0-2	0	1-6	0	0-1	0	12-120	0	20-196	1-8	1-9	13-129	21-204	21-205	33-325
Glenwood Springs	0-1	0	1-6	0	0	0	1-10	0	1-9	1-7	1-7	2-17	2-16	2-16	3-26
Rifle	0-2	0	1-7	0	0	0	1-10	0	2-19	1-9	1-9	2-19	3-28	3-28	4-38
Parachute	0-3	0	1-6	0	0	0	1-10	6-60	2-21	1-9	1-9	8-79	3-30	3-30	10-100
De Beque	0-2	0	1-11	0	0	0	1-10	0	5-52	1-13	1-13	2-23	6-65	6-65	7-75
Grand Junction	1-7	0	4-40	0	0	0	1-10	0	60-607	5-47	5-47	6-57	65-654	65-654	66-664
Existing or Potential Class I Areas and Other Areas of Special Concern															
Flat Tops Wilderness	0-2	0	1-6	0	0-1	0	8-80[†]	0	4-39	1-8	1-9	9-89[†]	5-47	5-48	13-128
Mt. Zirkel Wilderness	0-1	0	1-5	0	0	0	2-20	0	0-3	1-6	1-6	3-26[†]	1-9	1-9	3-29
Dinosaur National Monument	1-10	1-4	12-117[§]	0-2	0-4	0-2	1-10	0	1-5	14-133[§]	14-139[§]	15-149[§]	15-138	15-144	16-154
Colorado National Monument	1-6	0	4-40[§]	0	0	0	1-10	0	32-318	5-46[§]	5-46[§]	6-56[§]	37-364	37-364	38-374
Uintah and Ouray Indian Reservation	17-170	0	11-110	0	0-8	0	2-20	0	19-185	28-280	28-288	30-308	47-465	47-471	49-493
Uinta Primitive Area	0-2	0-1	1-8	0	0	0	0	0	0-1	1-11	1-11	1-11	1-12	1-12	1-12
Class II Area Receptors with Maximum Impacts from Direct Source Emissions in Uinta Basin	16-156	0	12-124	0	0-2	0	2-20	0	19-185	28-280	28-288	30-308	47-465	47-471	49-493
Ambient Air Quality Standard or Prevention of Significant Deterioration Increment															
PSD Class I Increment 25	A	A	A	A	A	A	A	A	NA	A	A	A	NA	NA	NA
PSD Class II Increment 512	A	A	A	A	A	A	A	A	NA	A	A	A	NA	NA	NA
AAQS 1300	NA	NA	NA	NA	NA	NA	NA	NA	A	NA	NA	NA	A	A	A

---

[*] Note that concentration ranges, not point estimates, are provided; low and high estimates of predicted maximum concentration are provided.

[†] Indicates violation of applicable standard or increment.

A Standard or increment is applicable.

NA Standard or increment is not applicable.

[§] Indicates violation of increment if monument is redesignated Class I.

TABLE 5-2 (Continued)

(b) Maximum 24-hour Average SO_2 Concentrations*

Maximum 24-hour Average SO_2 Concentrations ($\mu g/m^3$)

Receptor		(1) Uinta Basin Site-Specifics		(2) Uinta Basin Conceptuals		(3) Other Uinta Basin Sources		(4) Piceance Basin (Colorado Sources)		(5) 1980	Increment Consumption Above Baseline			Total Ambient Concentration Including 1980 Baseline		
		Direct	Secondary	Direct	Secondary	Direct	Secondary	Direct	Secondary	Baseline	(1+2)	(1+2+3)	(1+2+3+4)	(1+2+5)	(1+2+3+5)	(1+2+3+4+5)
Population Centers																
Vernal		0-1	0-2	1-9	0-1	0	0-1	0-1	0	1-6	1-13	1-14	1-15	2-19	2-20	2-21
Green River		0	0	0-2	0	0	0	0-1	0	0-1	0-2	0-2	0-3	0-3	0-3	0-4
Rangely		0-2	0	0-2	0	0	0	0-3	0	0-1	0-4	0-4	0-7	0-5	0-5	0-8
Meeker		0-1	0	0-2	0	0	0	1-14	0-1	1-5	0-3	0-3	1-18	1-8	1-8	2-23
Craig		0-1	0	0-1	0	0	0	2-15	0	3-28	0-2	0-2	2-17	3-30	3-30	5-45
Glenwood Springs		0	0	0-2	0	0	0	1-12	0	0-2	0-2	0-2	2-14	0-4	0-4	2-16
Rifle		0-1	0	0-1	0	0	0	1-6	0	0-3	0-2	0-2	1-8	0-5	0-5	1-11
Parachute		0-1	0	0-2	0	0	0	3-25	0-5	0-3	0-3	0-3	3-33	0-6	0-6	3-36
De Beque		0-1	0	0-2	0	0	0	0-3	0	1-11	0-3	0-3	0-6	1-14	1-14	1-17
Grand Junction		0-1	0	1-6	0	0	0	0-1	0	8-82	1-7	1-7	1-8	9-89	9-89	9-90
Existing or Potential Class I Areas and Other Areas of Special Concern																
Flat Tops Wilderness		0-1	0	0-1	0	0	0	1-10†	0	1-5	0-2	0-2	1-12†	1-7	1-7	2-17
Mt. Zirkel Wilderness		0	0	0-1	0	0	0	0-2	0	0-1	0-1	0-1	0-3	0-2	0-2	0-4
Dinosaur National Monument		0-2	0-1	1-10	0	0	0	0-1	0	1-5	1-13§	1-13§	1-14§	2-18	2-18	2-19
Colorado National Monument		0-2	0	0-4	0	0	0	0-1	0	4-40	0-6§	0-6§	0-7§	4-46	4-46	4-47
Uintah and Ouray Indian Reservation		2-21	0	3-34	0	0-2	0	0-3	0	2-23	5-55	5-57	5-60	7-78	7-80	7-83
Uinta Primitive Area		0-1	0	0-3	0	0	0	0	0	0-1	0-4	0-4	0-4	0-5	0-5	0-5
Class II Area Receptors with Maximum Impacts from Direct Source Emissions in Uinta Basin		2-21	0	3-34	0	0-2	0	0-3	0	2-23	5-55	5-57	5-60	7-78	7-80	7-83
Ambient Air Quality Standard or Prevention of Significant Deterioration Increment																
PSD Class I Increment	5	A	A	A	A	A	A	A	A	NA	A	A	A	NA	NA	NA
PSD Class II Increment	91	A	A	A	A	A	A	A	A	NA	A	A	A	NA	NA	NA
AAQS	365	NA	NA	NA	NA	NA	NA	NA	NA	A	NA	NA	NA	A	A	A

---

* Note that concentration ranges, not point estimates, are provided; low and high estimates of predicted maximum concentration are provided.

† Indicates violation of applicable standard or increment.

A Standard or increment is applicable.

NA Standard or increment is not applicable.

§ Indicates violation of increment if monument is redesignated Class I.

TABLE 5-2 (Concluded)

(c) Annual Average SO_2 Concentrations*

Annual Average SO_2 Concentrations ($\mu g/m^3$)

Receptor		(1) Uinta Basin Site-Specifics		(2) Uinta Basin Conceptuals		(3) Other Uinta Basin Sources		(4) Piceance Basin (Colorado Sources)		(5) 1980	Increment Consumption Above Baseline			Total Ambient Concentration Including 1980 Baseline		
		Direct	Secondary	Direct	Secondary	Direct	Secondary	Direct	Secondary	Baseline	(1+2)	(1+2+3)	(1+2+3+4)	(1+2+5)	(1+2+3+5)	(1+2+3+4+5)
Population Centers																
Vernal		0	0-1	0	0	0	0	0	0	0	0-1	0-1	0-1	0-1	0-1	0-1
Green River		0	0	0	0	0	0	0	0	0	0	0	0	0	0	0
Rangely		0	0	0-1	0	0	0	0	0	0	0-1	0-1	0-1	0-1	0-1	0-1
Meeker		0	0	0	0	0	0	0-1	0	0	0	0	0-1	0	0	0-1
Craig		0	0	0	0	0	0	0	0	0	0	0	0	0	0	0
Glenwood Springs		0	0	0	0	0	0	0	0	0	0	0	0	0	0	0
Rifle		0	0	0	0	0	0	0-1	0	0-1	0	0	0-1	0-1	0-1	0-2
Parachute		0	0	0	0	0	0	0-1	0	0-1	0	0	0-1	0-1	0-1	0-2
De Beque		0	0	0	0	0	0	0-1	0	0-1	0	0	0-1	0-1	0-1	0-2
Grand Junction		0	0	0	0	0	0	0-1	0	0-9	0	0	0-1	0-9	0-9	0-10
Existing or Potential Class I Areas and Other Areas of Special Concern																
Flat Tops Wilderness		0	0	0	0	0	0	0-1	0	0	0	0	0-1	0	0	0-1
Mt. Zirkel Wilderness		0	0	0	0	0	0	0	0	0	0	0	0	0	0	0
Dinosaur National Monument		0	0	0-1	0	0	0	0	0	0	0-1	0-1	0-1	0-1	0-1	0-1
Colorado National Monument		0	0	0	0	0	0	0	0	0-1	0	0	0	0-1	0-1	0-1
Uintah and Ouray Indian Reservation		0	0	0-2	0	0	0	0	0	0	0-2	0-2	0-2	0-2	0-2	0-2
Uinta Primitive Area		0	0	0	0	0	0	0	0	0	0	0	0	0	0	0
Class II Area Receptors with Maximum Impacts from Direct Source Emissions in Uinta Basin		0-1	0	1-3	0	0	0	0	0	0	1-4	1-4	1-4	1-4	1-4	1-4
Ambient Air Quality Standard or Prevention of Significant Deterioration Increment																
PSD Class I Increment	2	A	A	A	A	A	A	A	A	NA	A	A	A	NA	NA	NA
PSD Class II Increment	20	A	A	A	A	A	A	A	A	NA	A	A	A	NA	NA	NA
AAQS	80	NA	NA	NA	NA	NA	NA	NA	NA	A	NA	NA	NA	A	A	A

---

[*] Note that concentration ranges, not point estimates, are provided; low and high estimates of predicted maximum concentration are provided.

[†] Indicates violation of applicable standard or increment.

A Standard or increment is applicable.

NA Standard or increment is not applicable.

In the existing SO_2 mandatory Class I area most adversely affected by the projected emissions, the Flat Tops Wilderness Area, conclusions are more ambiguous since the projected ranges of SO_2 concentrations overlap the 3-hour and 24-hour SO_2 Class I PSD increments for the high-oil-production scenario. In other words, if the conservative, high estimate were used, the Class I increments would be exceeded; if the low estimate were used, the increments would not be exceeded. However, it should be pointed out that the conservative, high estimate of the impact of the Uinta Basin sources by themselves is well within the Class I increment. Piceance Basin sources, development plans for which are currently uncertain, cause most of the projected impact in Flat Tops. Indeed, the Cathedral Bluffs facility that has been recently shelved accounts for half of the increment consumption in Flat Tops.

In addition, for the high-oil-production scenario there is a similar probability that the Colorado Category I (PSD Class I) increments will be exceeded in Dinosaur National Monument. Although total impacts in Colorado National Monument are large, almost all the impact is due to existing point and area sources in the Grand Junction area that do not consume the increment. Figure 5-32 summarizes these impacts in a graphical representation.

5.4.2 TSP Impacts

Tables 5-3 and 5-4 summarize the total TSP impacts of regional emission sources for several important receptor areas for the low- and high-oil-production scenarios, respectively. It is clear from these tables that secondary TSP area emission sources (principally emissions from dirt and gravel roads) dominate the total impact and that impacts in many areas will be greater than ambient air quality standards. If secondary emissions from additional vehicles on dirt roads associated with development-induced population growth are included in the PSD increment consumption, there is little doubt that PSD Class II increments for TSP will be exceeded in many areas throughout the study area. (These impacts could possibly be mitigated by paving these roads.) If just the direct TSP emissions from the synthetic fuel facilities are considered to consume the PSD increment, and secondary emissions are excluded, it is quite likely that PSD Class I and II increments for TSP will not be consumed or exceeded in the region except for the potential problems near Sohio's conceptual tar sands facility noted in Section 5.2. Figure 5-33 summarizes these impacts.

82062r3 19

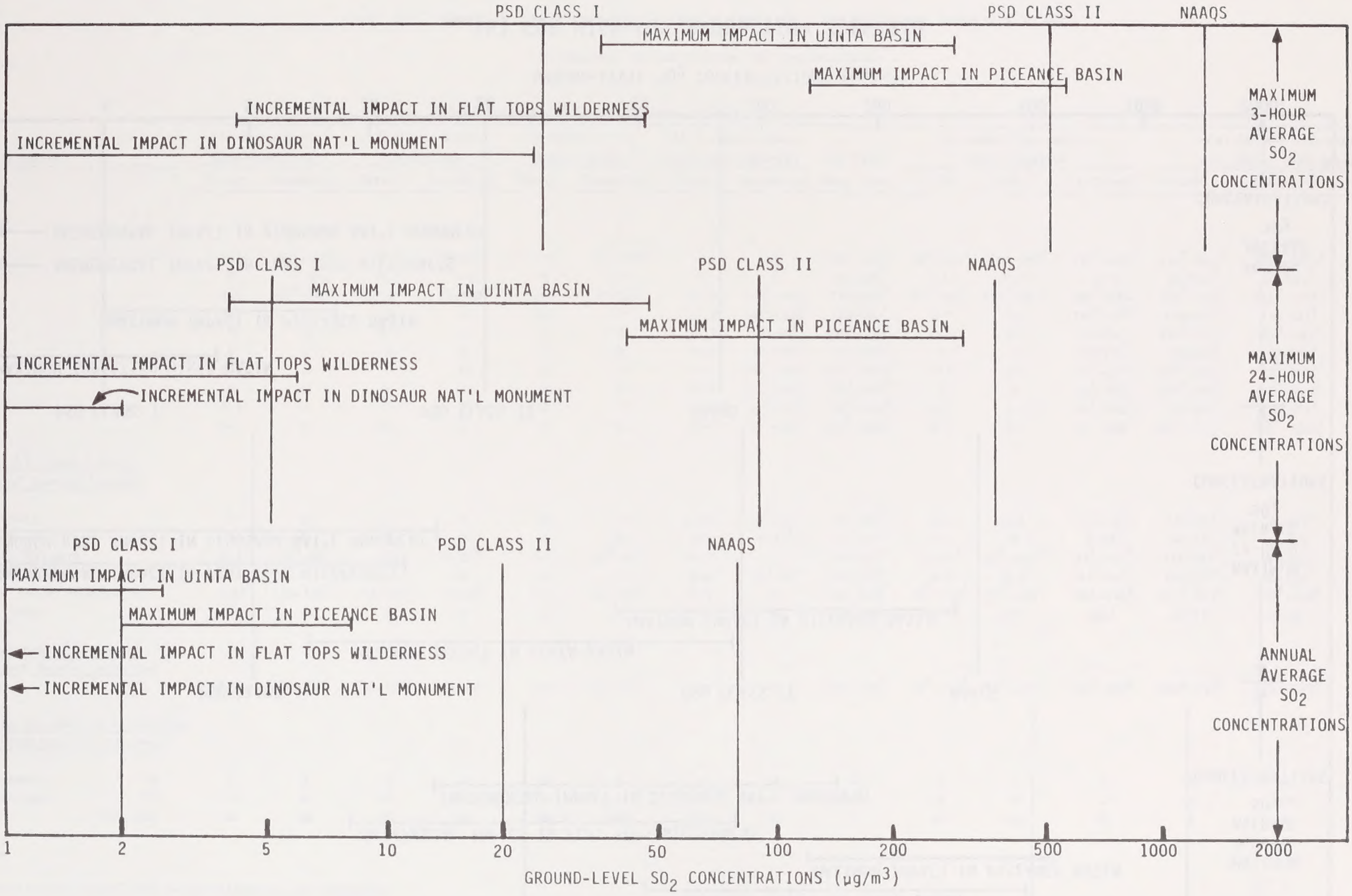

(a) FOR LOW-OIL-PRODUCTION SCENARIO

FIGURE 5-32. SUMMARY OF SO_2 CONCENTRATION ESTIMATES FOR VARIOUS AVERAGING TIMES COMPARED TO AIR QUALITY STANDARDS AND PSD INCREMENTS

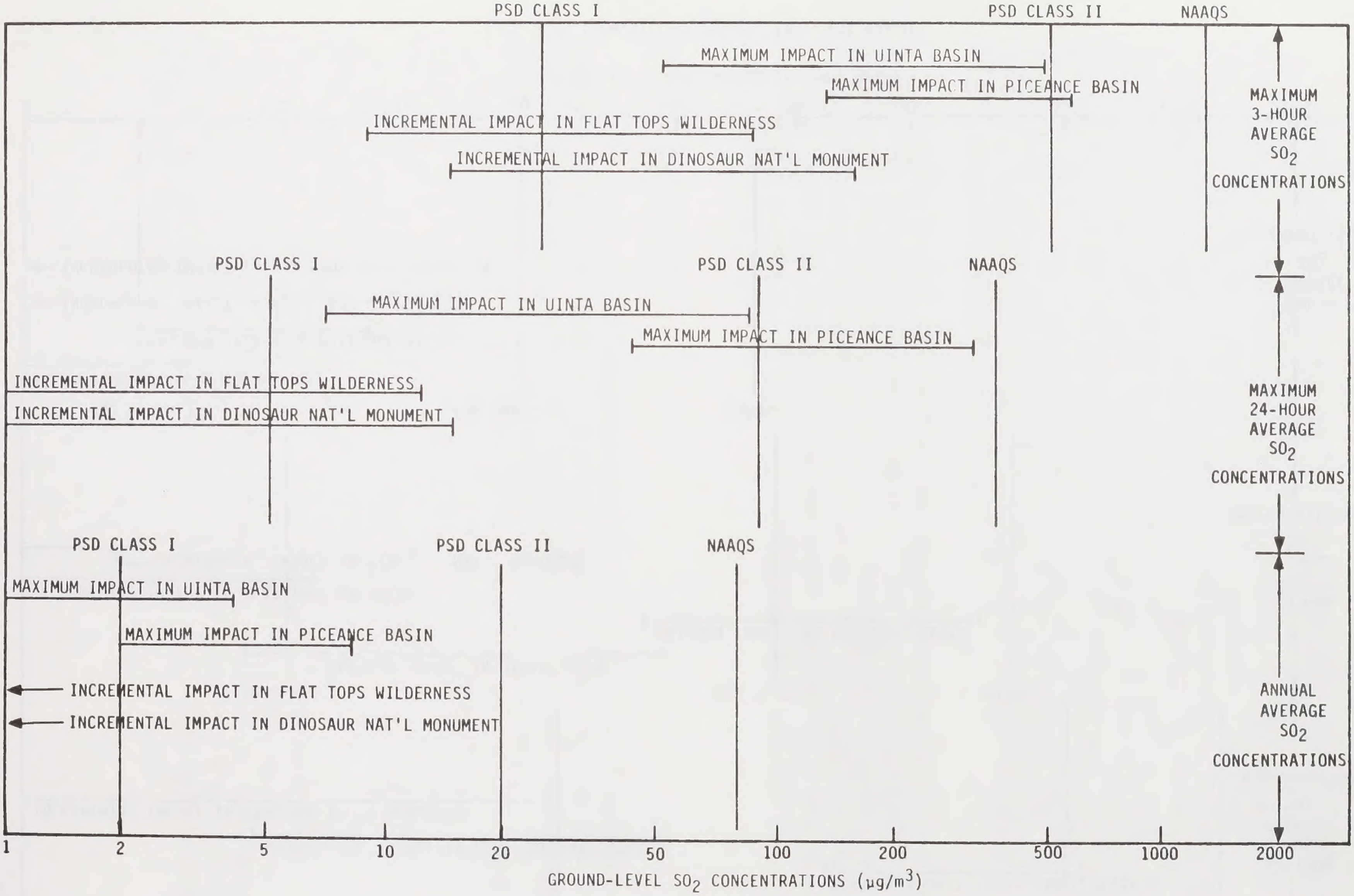

(b) FOR HIGH-OIL-PRODUCTION SCENARIO

FIGURE 5-32 (Concluded)

TABLE 5-3. SUMMARY OF AMBIENT AIR QUALITY IMPACTS ASSOCIATED WITH THE LOW OIL PRODUCTION SCENARIO

(a) Maximum 24-hour Average TSP Concentrations[*]

Receptor	Maximum 24-hour Average TSP Concentrations ($\mu g/m^3$)														
	(1) Uinta Basin Site-Specifics		(2) Uinta Basin Conceptuals		(3) Other Uinta Basin Sources		(4) Piceance Basin (Colorado Sources)		(5) 1980)	Increment Consumption Above Baseline			Total Ambient Concentration Including 1980 Baseline		
	Direct	Secondary	Direct	Secondary	Direct	Secondary	Direct	Secondary	Base line	(1+2)	(1+2+3)	(1+2+3+4)	(1+2+5)	(1+2+3+5)	(1+2+3+4+5)
Population Centers															
Vernal	0-1	40†-160†	0-3	20-80†	0-1	60†-240†	0	0	185†-740†	60†-244†	120†-485†	120†-485†	245†-984†	305†-1225†	305†-1225†
Green River	0	2-8	0-1	1-4	0	1-4	0	0	38-150†	3-13	4-17	4-17	41-163†	42-167†	42-167†
Rangely	1-5	60†-240†	0	30-120†	0-2	30-120†	0-3	120†-480†	135-540†	91†-365†	121†-487†	241†-970†	226†-905†	256†-1027†	376†-1510†
Meeker	0-1	0	0	0	0-1	0	2-17	140†-560†	110-440†	0-1	0-2	142†-579†	110-441†	110-442†	252†-1019†
Craig	0	0	0-1	0	0	0	1-13	10-40†	190†-760†	0-1	0-1	11-54†	190†-761†	190†-761†	201†-814†
Glenwood Springs	0	0	0	0	0	0	0-3	30-120†	110-450†	0	0	30-123†	110-450†	110-450†	140-573†
Rifle	0-1	0	0	0	0	0	1-6	60†-240†	300†-1200†	0-1	0-1	61†-247†	300†-1201†	300†-1201†	361†-1447†
Parachute	0	0	0	0	0	0	0-4	80†-320†	235†-940†	0	0	80†-324†	235†-940†	235†-940†	315†-1264†
De Beque	0-1	0	0	0	0	0	0-4	40†-160†	120†-480†	0-1	0-1	40†-165†	120-481†	120-481†	160†-645†
Grand Junction	0-1	0	0-1	0	0	0	0-4	70†-280†	310†-1200†	0-2	0-2	70†-286†	310†-1202†	310†-1202†	380†-1486†
Existing or Potential Class I Areas and Other Areas of Special Concern															
Flat Tops Wilderness	0	0	0-1	0	0	0	2-17†	13†-52†	75-300†	0-1	0-1	15†-70†	75-301†	75-301†	90-370†
Mt. Zirkel Wilderness	0	0	0	0	0	0	0-4	6-24†	30-110†	0	0	6-28†	30-110	30-110	36-138
Dinosaur National Monument	0-1	15§-60†	0-3	5-20§	0-1	20§-80†	0-2	0	100-400†	21-84†	41†-165†	41†-167†	121-484†	141-565†	141-567†
Colorado National Monument	0-1	0	0-1	0	0	0	0-4	15§-60†	80-320†	0-2	0-2	15§-66†	80-322†	80-322†	95-386†
Uintah and Ouray Indian Reservation	2-21	30-120†	13-131†	10-40†	0-2	35-140†	0-2	0	125-500†	55†-312†	90†-454†	90†-456†	180†-812†	215†-954†	215†-956†
Uinta Primitive Area	0-1	0	0	0	0	0	0	0	25-110	0-1	0-1	0-1	25-111	25-111	25-111
Class II Area Receptors with Maximum Impacts from Direct Source Emissions in Uinta Basin	2-21	30-120†	13-131†	10-40	0-2	35-140†	0-2	0	125-500†	55†-312†	90†-454†	90†-456†	180†-812†	215†-953†	215†-956†
Ambient Air Quality Standard or Prevention of Significant Deterioration Increment															
PSD Class I Increment 10	A	A	A	A	A	A	A	A	NA	A	A	A	NA	NA	NA
PSD Class II Increment 37	A	A	A	A	A	A	A	A	NA	A	A	A	NA	NA	NA
AAQS 150, 260	NA	NA	NA	NA	NA	NA	NA	NA	A	NA	NA	NA	A	A	A

---

[*] Note that concentration ranges, not point estimates, are provided; low and high estimates of predicted maximum concentration are provided.

† Indicates violation of applicable standard or increment.

A Standard or increment is applicable.

NA Standard or increment is not applicable.

§ Indicates violation of increment if monument is redesignated Class I.

TABLE 5-3 (Concluded)

(b) Annual Average TSP Concentrations[*]

	Annual Average TSP Concentrations ($\mu g/m^3$)														
Receptor	(1) Uinta Basin Site-Specifics		(2) Uinta Basin Conceptuals		(3) Other Uinta Basin Sources		(4) Piceance Basin (Colorado Sources)		(5) 1980	Increment Consumption Above Baseline			Total Ambient Concentration Including 1980 Baseline		
	Direct	Secondary	Direct	Secondary	Direct	Secondary	Direct	Secondary	Baseline	(1+2)	(1+2+3)	(1+2+3+4)	(1+2+5)	(1+2+3+5)	(1+2+3+4+5)
Population Centers															
Vernal	0	10-40[†]	0	3-12	0	15-60[†]	0	0	45-180[†]	13-52[†]	28[†]-112[†]	28[†]-112[†]	58-232[†]	73[†]-292[†]	73[†]-292[†]
Green River	0	0-1	0	0	0	1-2	0	0	10-40	0-1	1-3	1-3	10-41	11-43	11-43
Rangely	0-1	10-40[†]	0	5-20[†]	0	10-40[†]	0	30[†]-120[†]	30-120[†]	15-61[†]	25[†]-101[†]	55[†]-221[†]	45-181[†]	55-221[†]	85[†]-241[†]
Meeker	0	0	0	0	0	0	1-5	30[†]-120[†]	30-120[†]	0	0	31[†]-125[†]	30-120[†]	30-120[†]	61[†]-245[†]
Craig	0	0	0	0	0	0	0-1	3-12	45-180[†]	0	0	3-13	45-180[†]	45-180[†]	48-192[†]
Glenwood Springs	0	0	0	0	0	0	0	4-16	30-120[†]	0	0	4-16	30-120[†]	30-120[†]	34-136[†]
Rifle	0	0	0	0	0	0	0-1	15-60[†]	70[†]-280[†]	0	0	15-61[†]	70[†]-280[†]	70[†]-280[†]	85[†]-341[†]
Parachute	0	0	0	0	0	0	0-1	20[†]-80[†]	55-220[†]	0	0	20[†]-81[†]	55-220[†]	55-220[†]	75[†]-301[†]
De Beque	0	0	0	0	0	0	0-1	8-32[†]	30-120[†]	0	0	8-33	30-120[†]	30-120[†]	38-153[†]
Grand Junction	0	0	0	0	0	0	0-1	20[†]-80[†]	70[†]-280[†]	0	0	20[†]-81[†]	70[†]-280[†]	70[†]-280[†]	90[†]-361[†]
Existing or Potential Class I Areas and Other Areas of Special Concern															
Flat Tops Wilderness	0	0	0	0	0	0	0-1	3-10[†]	20-80[†]	0	0	3-11[†]	20-80[†]	20-80[†]	23-91[†]
Mt. Zirkel Wilderness	0	0	0	0	0	0	0	1-4	10-40	0	0	1-4	10-40	10-40	11-44
Dinosaur National Monument	0	4-16[§]	0	2-8[§]	0	5[§]-20[†]	0	0	25-100[†]	6[§]-24[†]	11[§]-44[†]	11[§]-44[†]	31-124[†]	36-144[†]	36-144[†]
Colorado National Monument	0	0	0	0	0	0	0-1	4-16[§]	20-80[†]	0	0	4-17[§]	20-80[†]	20-80[†]	24-97[†]
Uintah and Ouray Indian Reservation	0-1	5-20[†]	1-6	2-8	0	6-24[†]	0	0	35-140[†]	8-35[†]	14-59[†]	14-59[†]	43-175[†]	49-199[†]	49-199[†]
Uinta Primitive Area	0	0	0	0	0	0	0	0	10-40	0	0	0	10-40	10-40	10-40
Class II Area Receptors with Maximum Impacts from Direct Source Emissions in Uinta Basin	0-1	3-12	1-13	2-8	0	5-20[†]	0	0	28-110	6-34[†]	11-54[†]	11-54[†]	34-144[†]	39-164[†]	39-164[†]
Ambient Air Quality Standard or Prevention of Significant Deterioration Increment															
PSD Class I Increment 5	A	A	A	A	A	A	A	A	NA	A	A	A	NA	NA	NA
PSD Class II Increment 19	A	A	A	A	A	A	A	A	NA	A	A	A	NA	NA	NA
AAQS 60, 75	NA	NA	NA	NA	NA	NA	NA	NA	A	NA	NA	NA	A	A	A

---

[*] Note that concentration ranges, not point estimates, are provided; low and high estimates of predicted maximum concentration are provided.

[†] Indicates violation of applicable standard or increment.

A Standard or increment is applicable.

NA Standard or increment is not applicable.

[§] Indicates violation of increment if monument is redesignated Class I.

TABLE 5-4. SUMMARY OF AMBIENT AIR QUALITY IMPACTS ASSOCIATED WITH THE HIGH OIL PRODUCTION SCENARIO

(a) Maximum 24-hour Average TSP Concentrations[*]

Maximum 24-hour Average TSP Concentrations (µg/m³)

Receptor	(1) Uinta Basin Site-Specifics		(2) Uinta Basin Conceptuals		(3) Other Uinta Basin Sources		(4) Piceance Basin (Colorado Sources)		(5) 1980	Increment Consumption Above Baseline			Total Ambient Concentration Including 1980 Baseline		
	Direct	Secondary	Direct	Secondary	Direct	Secondary	Direct	Secondary	Baseline	(1+2)	(1+2+3)	(1+2+3+4)	(1+2+5)	(1+2+3+5)	(1+2+3+4+5)
Population Centers															
Vernal	0-2	125[†]-500[†]	1-14	60[†]-240[†]	0-1	60[†]-240[†]	0	0	185[†]-740[†]	186[†]-756[†]	246[†]-997[†]	246[†]-997[†]	371[†]-1496[†]	431[†]-1737[†]	431[†]-1737[†]
Green River	0-1	3-12	0-4	2-8	0	1-4	0	0	38-150	5-25	6-29	6-29	43-175[†]	44-179[†]	44-179[†]
Rangely	1-12	60[†]-240[†]	2-17	30-120[†]	0-2	30-120[†]	1-10	130[†]-520[†]	135-540[†]	93[†]-389[†]	123[†]-509[†]	254[†]-1039[†]	228[†]-929[†]	258[†]-1049[†]	389[†]-1579[†]
Meeker	0-2	0	0-3	0	0-1	0	7-70[†]	140[†]-560[†]	110-440[†]	0-5	0-6	147[†]-636[†]	110-445[†]	110-446[†]	257[†]-1076[†]
Craig	0-1	0	0	0	0	0	2-20	10-40[†]	190[†]-760[†]	0-1	0-1	12-61	190[†]-761[†]	190[†]-761[†]	202[†]-821[†]
Glenwood Springs	0-1	0	0	0	0	0	1-10	40[†]-160[†]	110-450[†]	0-1	0-1	41[†]-171[†]	110-451[†]	110-451[†]	151[†]-621[†]
Rifle	0-1	0	0	0	0	0	2-20	100[†]-400[†]	300[†]-1200[†]	0-1	0-1	102[†]-421[†]	300[†]-1201[†]	300[†]-1201[†]	402[†]-1621[†]
Parachute	0-1	0	0-3	0	0	0	1-10	135[†]-540[†]	235[†]-940[†]	0-4	0-4	136[†]-554[†]	235[†]-944[†]	235[†]-944[†]	371[†]-1494[†]
De Beque	0-1	0	1-6	0	0	0	1-10	60[†]-240[†]	120-480[†]	1-7	1-7	62[†]-257[†]	121-487[†]	121-487[†]	182[†]-737[†]
Grand Junction	0-1	0	1-6	0	0	0	1-10	120[†]-480[†]	310[†]-1200[†]	1-7	1-7	122[†]-497[†]	311[†]-1207[†]	311[†]-1207[†]	432[†]-1697[†]
Existing or Potential Class I Areas and Other Areas of Special Concern															
Flat Tops Wilderness	0-1	0	0-1	0	0	0	2-17[†]	22[†]-88[†]	75-300[†]	0-2	0-2	24[†]-107[†]	75-302[†]	75-302[†]	99-407[†]
Mt. Zirkel Wilderness	0-1	0	0-1	0	0	0	0-4	10[†]-40[†]	30-110	0-2	0-2	10[†]-46[†]	30-112	30-112	40-156[†]
Dinosaur National Monument	1-6	40[†]-60[†]	3-30[§]	20[§]-80[†]	0-1	20[§]-80[†]	0	0	100-400[†]	64[†]-276[†]	84[†]-357[†]	84[†]-357[†]	164[†]-676[†]	184[†]-757[†]	184[†]-757[†]
Colorado National Monument	0-2	0	1-7	0	0	0	1-10[§]	30[§]-120[†]	80-320[†]	1-9	1-9	32[§]-139[†]	81-329[†]	81-329[†]	112-459[†]
Uintah and Ouray Indian Reservation	17-171[†]	70[†]-280[†]	45[†]-453[†]	36-140[†]	0-2	35-140[†]	1-10	0	125-500[†]	167[†]-1044[†]	202[†]-1186[†]	203[†]-1196[†]	292[†]-1544[†]	327[†]-1686[†]	328[†]-1696[†]
Uinta Primitive Area	0-1	0	0-4	0	0	0	0	0	25-110	0-5	0-5	0-5	25-115	25-115	25-115
Class II Area Receptors with Maximum Impacts from Direct Source Emissions in Uinta Basin	1-11	70[†]-280[†]	61-613[†]	35-140[†]	0-1	35-140[†]	1-10	0	90-360[†]	167[†]-1044[†]	203[†]-1185[†]	204[†]-1195[*]	257[†]-1404[†]	293[†]-1545[†]	294[†]-1555[†]
Ambient Air Quality Standard or Prevention of Significant Deterioration Increment															
PSD Class I Increment 10	A	A	A	A	A	A	A	A	NA	A	A	A	NA	NA	NA
PSD Class II Increment 37	A	A	A	A	A	A	A	A	NA	A	A	A	NA	NA	NA
AAQS 150, 260	NA	NA	NA	NA	NA	NA	NA	NA	A	NA	NA	NA	A	A	A

---

[*] Note that concentration ranges, not point estimates, are provided; low and high estimates of predicted maximum concentration are provided.

[†] Indicates violation of applicable standard or increment.

A Standard or increment is applicable.

NA Standard or increment is not applicable.

[§] Indicates violation of increment if monument is redesignated Class I.

TABLE 5-4 (Concluded)

(b) Annual Average TSP Concentrations*

Annual Average TSP Concentrations ($\mu g/m^3$)

Receptor	(1) Uinta Basin Site-Specifics		(2) Uinta Basin Conceptuals		(3) Other Uinta Basin Sources		(4) Piceance Basin (Colorado Sources)		(5) 1980	Increment Consumption Above Baseline			Total Ambient Concentration Including 1980 Baseline		
	Direct	Secondary	Direct	Secondary	Direct	Secondary	Direct	Secondary	Baseline	(1+2)	(1+2+3)	(1+2+3+4)	(1+2+5)	(1+2+3+5)	(1+2+3+4+5)
Population Centers															
Vernal	0	30†-120†	0-1	10-40†	0	15-60†	0	0	45-180†	40†-161†	55†-221†	55†-221†	85†-341†	100†-401†	100†-401†
Green River	0	1-4	0	1-2	0	1-2	0	0	10-40	2-6	3-8	3-8	12-46	13-48	13-48
Rangely	0-2	15-60†	0-2	5-20†	0	10-40†	0	30†-120†	30-120†	20†-84†	30†-124†	60†-244†	50-204†	60†-244†	90†-364†
Meeker	0	0	0	0	0	0	1-7	30†-120†	30-120†	0	0	31†-127†	30-120†	30-120†	61†-247†
Craig	0	0	0	0	0	0	0-1	5-20†	45-180†	0	0	5-21†	45-180†	45-180†	50-201†
Glenwood Springs	0	0	0	0	0	0	0-1	8-32†	30-120†	0	0	8-33†	30-120†	30-120†	38-153†
Rifle	0	0	0	0	0	0	0-1	25†-100†	70†-280†	0	0	25†-101†	70†-280†	70†-280†	95†-381†
Parachute	0	0	0	0	0	0	0-1	30†-120†	55†-220†	0	0	30†-121†	55-220†	55-220†	85†-341†
De Beque	0	0	0	0	0	0	0-1	15-60†	30-120†	0	0	15-61†	30-120†	30-120†	45-181†
Grand Junction	0	0	0	0	0	0	0-1	30†-120†	70†-280†	0	0	30†-121†	70†-280†	70†-280†	100†-401†
Existing or Potential Class I Areas and Other Areas of Special Concern															
Flat Tops Wilderness	0	0	0	0	0	0	0-1	5†-20†	20-80†	0	0	5†-21†	20-80†	20-80†	25-101†
Mt. Zirkel Wilderness	0	0	0	0	0	0	0-1	2-10†	10-40	0	0	2-11†	10-40	10-40	12-51
Dinosaur National Monument	0	10§-40†	0-1	5§-20†	0	5§-20†	0	0	25-100†	5§-61†	20†-81†	20†-81†	40-161†	45-181†	45-181†
Colorado National Monument	0	0	0	0	0	0	0-1	8§-32†	20-80†	0	0	8§-33†	20-80†	20-80†	28-113†
Uintah and Ouray Indian Reservation	1-3	15-60†	2-19†	6-24†	0	6-24†	0	0	35-140†	24†-106†	30†-130†	30†-130†	59-246†	65†-270†	65†-270†
Uinta Primitive Area	0	0	0	0	0	0	0	0	10-40	0	0	0	10-40	10-40	10-40
Class II Area Receptors with Maximum Impacts from Direct Source Emissions in Uinta Basin	0	15-60†	6-61†	6-24†	0	6-24†	0	0	35-140†	27†-145†	33†-169†	33†-169†	62†-285†	68†-309†	68†-309†
Ambient Air Quality Standard or Prevention of Significant Deterioration Increment															
PSD Class I Increment 5	A	A	A	A	A	A	A	A	NA	A	A	A	NA	NA	NA
PSD Class II Increment 19	A	A	A	A	A	A	A	A	NA	A	A	A	NA	NA	NA
AAQS 60,75	NA	NA	NA	NA	NA	NA	NA	NA	A	NA	NA	NA	A	A	A

---

* Note that concentration ranges, not point estimates, are provided; low and high estimates of predicted maximum concentration are provided.

† Indicates violation of applicable standard or increment.

A Standard or increment is applicable.

NA Standard or increment is not applicable.

§ Indicates violation of increment if monument is redesignated Class I.

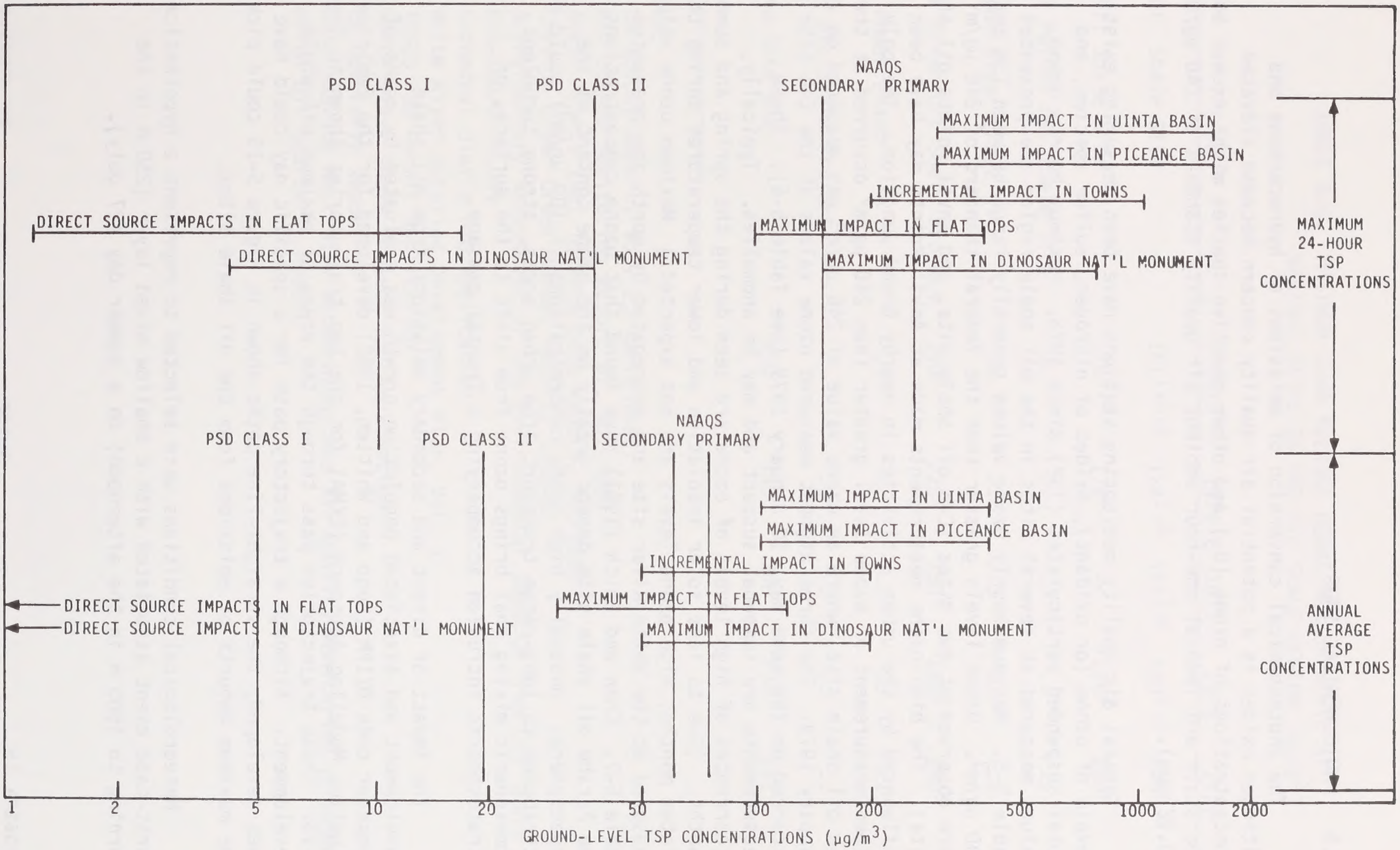

FIGURE 5-33. SUMMARY OF TSP CONCENTRATION ESTIMATES FOR VARIOUS AVERAGING TIMES COMPARED TO AMBIENT AIR QUALITY STANDARDS AND PSD INCREMENTS FOR BOTH THE LOW AND HIGH OIL PRODUCTION SCENARIOS

5.5 PHOTOCHEMICAL SMOG

The photochemical conversion of emissions of hydrocarbons and nitrogen oxides is a potential air quality concern because elevated concentrations of ozone (O_3) and other reactive species might exceed both the state and federal one-hour ambient air quality standard of 240 $\mu g/m^3$ (0.12 ppm).

Several air quality monitoring stations have been measuring existing levels of ozone (or oxidant), oxides of nitrogen, sulfur species, and total suspended particulates (TSP) since 1975. Maximum hourly ozone values measured at several sites in the oil shale region are presented in Table 5-5. Maximum hourly ozone values generally range between 136 and 200 $\mu g/m^3$. Ozone levels greater than the federal standard of 240 $\mu g/m^3$ were observed at two sites (C-b oil shale site, and Anvil Points oil shale site). The high ozone measurements made at Anvil Points may have been influenced by the urban activities in nearby Grand Junction. The only other measurement of ozone level greater than 240 $\mu g/m^3$ occurred at the C-b oil shale site, where an ozone value of 246 $\mu g/m^3$ was measured on 20 January 1979. The three highest measured ozone values at the C-b site all occurred on the same day, 20 January 1979 (see Table 5-6). These measurements are somewhat suspect and may be anomalies. Typically, occurrences of high levels of ozone are seen during the spring and summer months. (Due to less solar insolation and lower temperatures during the winter months, high ozone levels are not expected.) Maximum ozone values measured at the White River site and segregated by month are presented in Table 5-7. Chan and Smith (1981) have found that ozone concentrations at the Paraho oil shale site depend greatly on the ozone content of the troposphere. Unusually high ozone concentrations (> 100 $\mu g/m^3$) could be attributed to long-range transport from urban areas, strong turbulent atmospheric mixing that brings ozone from aloft to the surface, or stratospheric intrusion accompanying a frontal passage.

The impact of direct and secondary emissions from oil shale development and associated population growth was evaluated by means of the computer code OZIPM (Hogo and Whitten, 1982) developed for the Empirical Kinetics Modeling Approach (EKMA) for the two trajectories shown in figure 5-15. These trajectories pass through the areas of maximum oil shale development. Although a trajectory path for a specific day could have been developed, the straight-line paths shown in Figure 5-15 could pick up the maximum amounts of emissions from the oil shale sites.

Meteorological conditions were selected to represent a hypothetical, worst-case event associated with a shallow mixed layer (250 m in the morning to 1500 m in the afternoon) on a summer day (27 July).

TABLE 5-5. MAXIMUM 1-HR AVERAGE OZONE MEASUREMENTS AT VARIOUS SITES IN THE OIL SHALE REGION ($\mu g/m^3$)

Site	1975	1976	1977	1978	1979	1980	1981
C-b Oil Shale Site	151[1,5,6]	124[1,6]	164[1,6]	160[1,6]	246[1,6]	154[1,6]	155[10]
C-a Oil Shale Site	178[2,5]	178[2,5]	--	176[2]	160[2]	--	--
Anvil Points Oil Shale Site	--	--	--	--	--	206[3]	265[3]
Chevron Clear Creek Site	--	--	--	--	--	94[4]	152[4]
White River Oil Shale Project	190[5]	220[7]	160[9]	160[9]	160[9]	160[9]	160[9]
Mack Power Plant	--	--	--	--	--	--	150[11]
Union Oil Shale Project	--	--	--	--	--	--	136[12]
Paraho Site A-6	150	140	160	137	151	143	--

Sources:
1. Cb Annual Report, Vol. 2, April 1981
2. Rio Blanco Monitoring Report #7, No. 1980
3. Anvil Points 1981 Interim Data Report, No. 1981
4. Chevron Clear Creek Annual Report, 1980-81
5. A Preliminary Assessment of the Environmental Impacts from Oil Shale Developments, EPA-600/7-77-069
6. Cathedral Bluffs PSD Application
7. White River Detailed Development Plan, Vol. 1
8. TOSCO PSD Permit Application
9. White River Shale Project PSD Application
10. Ca Quarterly Report #7
11. Colorado-Ute Mack Site Meteorology and Air Quality Monitoring Program
12. Union Oil Quarterly Report

TABLE 5-6. Ozone measurements at the C-b tract (trailer 023) from 1975 to 1980

1975

Number Hourly Observations: 7160

Annual Arithmetic Mean (ug/m^3): 69.0

5-Highest Hourly Averages (ug/m^3):

1.	151.3	6/26	HOUR ENDING	1400
2.	147.9	6/26	" "	1500
3.	142.4	2/23	" "	2300
4.	136.9	5/22	" "	0300
5.	136.9	5/22	" "	0400

Number of Hourly Concentrations In Ranges:

RANGE:	NO. OF VALUES:
0.0 - 2.9 (ug/m^3)	3
3.0 - 20.9	39
21.0 - 40.9	1160
41.0 - 60.9	1752
61.0 - 80.9	1385
81.0 - 100.9	2205
101.0 - 120.9	530
121.0 - 140.9	83
141.0 - 160.0	3
GREATER THAN 160.0	0

1976

Number Hourly Observations: 8239

Annual Arithmetic Mean (ug/m^3): 62.0

5-Highest Hourly Averages (ug/m^3):

1.	124.0	4/26	HOUR ENDING	1500
2.	123.0	4/26	" "	1600
3.	122.4	4/26	" "	1700
4.	120.3	4/26	" "	1300
5.	119.3	4/26	" "	1400

Number of Hourly Concentrations In Ranges:

RANGE:	NO. OF VALUES:
0.0 - 2.9 (ug/m^3)	15
3.0 - 20.9	50
21.0 - 40.9	1197
41.0 - 60.9	2611
61.0 - 80.9	2890
81.0 - 100.9	1232
101.0 - 120.9	241
121.0 - 140.9	3
141.0 - 160.0	0
GREATER THAN 160.0	0

1977

Number Hourly Observations: 7874

Annual Arithmetic Mean (ug/m^3): 79.0

5-Highest Hourly Averages (ug/m^3):

1.	164.0	8/24	HOUR ENDING	1100
2.	163.8	8/24	" "	1200
3.	162.6	8/24	" "	1300
4.	162.5	8/24	" "	1000
5.	158.1	7/31	" "	0900

Number of Hourly Concentrations In Ranges:

RANGE:	NO. OF VALUES:
0.0 - 2.9 (ug/m^3)	2
3.0 - 20.9	4
21.0 - 40.9	105
41.0 - 60.9	1232
61.0 - 80.9	3405
81.0 - 100.9	2066
101.0 - 120.9	842
121.0 - 140.9	179
141.0 - 160.0	35
GREATER THAN 160.0	4

1978

Number Hourly Observations: 8081

Annual Arithmetic Mean (ug/m^3): 81.6

5-Highest Hourly Averages (ug/m^3):

1.	160.9	8/27	HOUR ENDING	1800
2.	157.0	8/27	" "	1700
3.	153.0	8/27	" "	1900
4.	153.0	9/8	" "	1500
5.	149.1	9/8	" "	1800

Number of Hourly Concentrations In Ranges:

RANGE:	NO. OF VALUES:
0.0 - 2.9 (ug/m^3)	0
3.0 - 20.9	2
21.0 - 40.9	104
41.0 - 60.9	1290
61.0 - 80.9	2097
81.0 - 100.9	2203
101.0 - 120.9	1165
121.0 - 140.9	320
141.0 - 160.0	34
GREATER THAN 160.0	1

1979

Number Hourly Observations: 8693

Annual Arithmetic Mean (ug/m^3): 76.0

5-Highest Hourly Averages (ug/m^3):

1.	245.8	1/20
2.	203.5	1/20
3.	195.2	1/20
4.	192.5	1/20
5.	154.6	1/20

Number of Hourly Concentrations In Ranges:

RANGE:	NO. OF VALUES:
0.0 - 2.9 (ug/m^3)	0
3.0 - 20.9	0
21.0 - 40.9	115
41.0 - 60.9	1335
61.0 - 80.9	3622
81.0 - 100.9	3167
101.0 - 120.9	443
121.0 - 140.9	6
141.0 - 160.0	0
GREATER THAN 160.0	5

1980

Number Hourly Observations: 8448

Annual Arithmetic Mean (ug/m^3): 76.3

5-Highest Hourly Averages (ug/m^3):

1.	153.6	1/3
2.	133.5	1/3
3.	129.5	5/24
4.	129.5	6/5
5.	127.5	5/24

Number of Hourly Concentrations In Ranges:

RANGE:	NO. OF VALUES:
0.0 - 2.9 (ug/m^3)	5
3.0 - 20.9	6
21.0 - 40.9	157
41.0 - 60.9	1559
61.0 - 80.9	3685
81.0 - 100.9	2505
101.0 - 120.9	303
121.0 - 140.9	27
141.0 - 160.0	1
GREATER THAN 160.0	0

Source: Cb Annual Report, Vol. 2, 1981

TABLE 5-7. PEAK HOURLY OZONE VALUES AT WHITE RIVER OIL SHALE PROJECT IN 1976 SEPARATED BY SEASON ($\mu g/m^3$)

Season	Site A2	Site A3	Site S6
Winter	170	130	130
Spring	180	150	200
Summer	220	130	150
Fall	120	150	110

For photochemical modeling purposes, initial and aloft boundary conditions of ozone, hydrocarbons, and NO_x must be defined to initialize the simulations. Procedures such as those recommended by EPA (1981) involve the use of early morning (6-9 am) concentrations measured at monitoring stations on the day of interest. Typically, maximum ozone levels are observed during the afternoon hours. Therefore, maximum ozone levels are not recommended to initialize model simulations. Also, use of maximum ozone levels to initialize model simulations may lead to overpredictions of baseline values. Since the trajectories developed for the present study do not represent any specific day, an alternate procdure recommended by EPA (1981), involving the use of median (or mean) ozone levels, was used to define the initial and aloft ozone concentrations. (Table 2-3 shows mean ozone values observed over a five-year period from a few monitoring sites. Mean ozone values generally range from 60 to 110 $\mu g/m^3$.)

Based on the range of mean ozone observations, two initial and aloft conditions were used in the analysis. The first (or low) condition consists of low ozone and hydrocarbon levels representative of pristine areas. The ozone value for the low condition is set at 0.035 ppm (~ 69 $\mu g/m^3$) with associated hydrocarbon levels around 0.033 ppmC. The second (or high) condition, representative of air masses found upwind of isolated urban areas, is set at 0.06 ppm (~ 117 $\mu g/m^3$) ozone and 0.058 ppmC hydrocarbon. The hydrocarbon conditions are those recommended by Killus (1982). Due to the paucity of airborne measurements, the ozone and hydrocarbon conditions for the aloft layer were the same as those used for the surface layer. Airborne measurements in other regions of the United States by independent study groups, such as Singh, Ludwig, and Johnson (1978), do not show aloft ozone values (within 1000 m) to be significantly higher than surface measurements. Under extreme adverse conditions (e.g., storm fronts and turbulent vertical mixing) aloft ozone values may be much higher than surface values. Since these types of situations are associated with some sorts of transport phenomena, and the OZIPM trajectory model can only account for photochemical processes, extremely different surface and aloft ozone values were not used.

The Rio Blanco and Garfield county areas and existing point source emissions were assumed to be concentrated along the trajectory paths shown in figure 5-34, while the Uintah County area and existing point source emissions were assumed to be spread out over the entire county. Thus, the land areas used to determine emission densities are as follows:

Uintah -- 1.16×10^{10} m^2 (county area)
Rio Blanco -- 2.88×10^9 m^2 (20-km x 144-km strip)
Garfield -- 2.8×10^9 m^2 (20-km x 140-km strip)

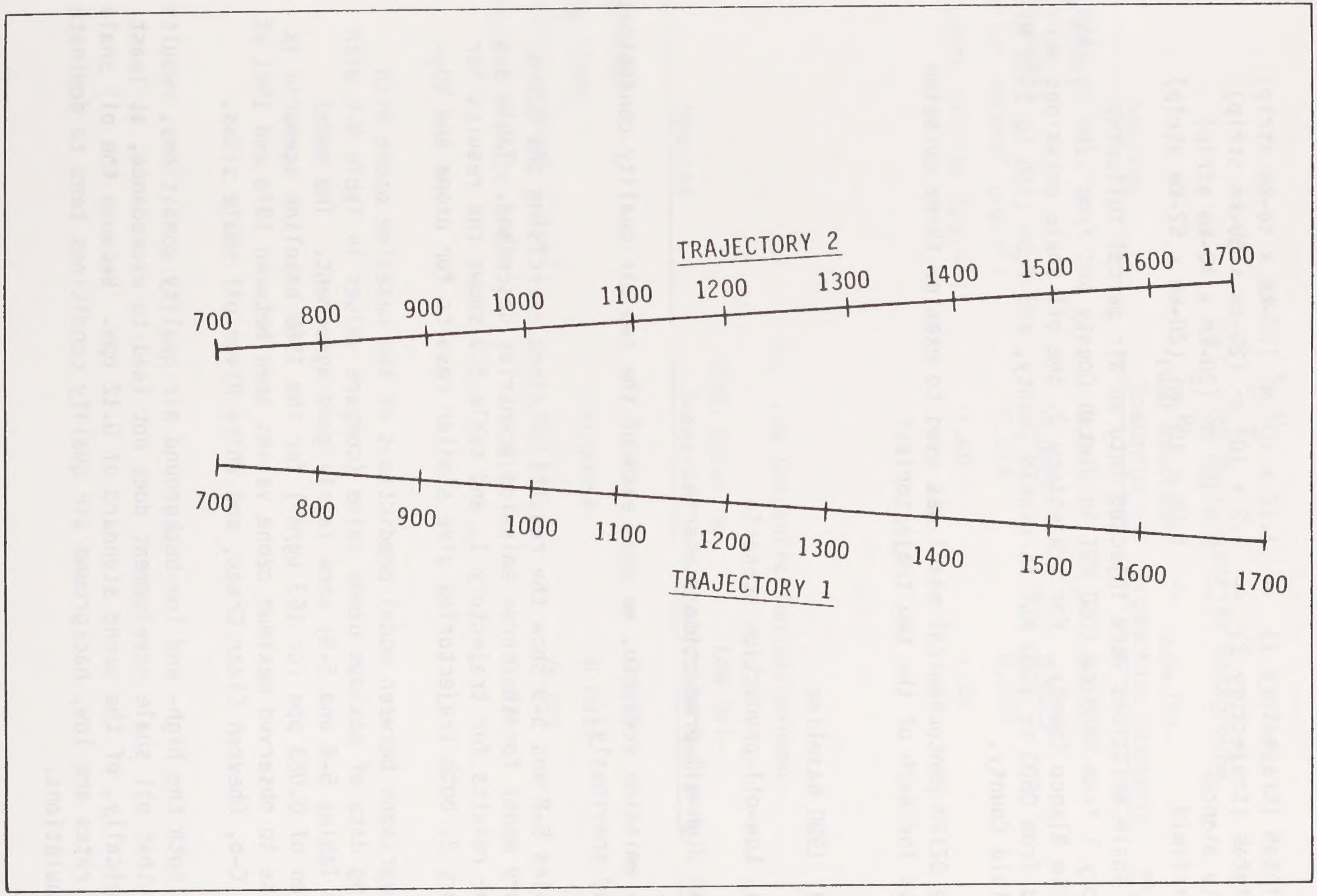

FIGURE 5-34. TWO TRAJECTORIES MODELED FOR WORST-CASE PHOTOCHEMICAL OXIDANT (OZONE) IMPACT

Note: Reader can use clear plastic overlay (see back cover) to indicate locations of sources and counties.

Emissions from oil shale developments were distributed over smaller regions:

Uintah (trajectory 1) -- 1.12×10^9 m^2 (20-km x 56-km strip)
Uintah (trajectory 2) -- 1.2×10^9 m^2 (20-km x 60-km strip)
Rio Blanco -- 8×10^8 m^2 (20-km x 40-km strip)
Garfield -- 1.04×10^9 m^2 (20-km x 52-km strip)

The oil shale emissions were injected into an air parcel following trajectory 1 from 0800 to 1000 MST in Uintah County and from 1200 to 1400 MST in Rio Blanco County. For trajectory 2, the oil shale emissions were injected from 0800 to 1000 MST in Uintah County, and from 1300 to 1500 MST in Garfield County.

The OZIPM photochemical model was used to examine three emission scenarios for each of the two trajectories:

(1) 1980 baseline

(2) Low-oil-production scenario

(3) High-oil-production scenario.

For each emission scenario, we used each of the two air quality conditions discussed previously.

Tables 5-8 and 5-9 show the results obtained exercising the OZIPM trajectory model for the three emission scenarios described. Table 5-8 shows the results for trajectory 1, and table 5-9 shows the results for trajectory 2; both trajectories give similar results for ozone and NO_2.

Comparisons between model predictions of the baseline ozone with monitoring data of maximum ozone value (compare values in Table 5-5 with those in Tables 5-8 and 5-9) show fairly good agreement. The model prediction of 0.083 ppm (or 163 $\mu g/m^3$) for the 1980 baseline scenario is very close to observed maximum ozone values seen between 1978 and 1981 at the C-a, C-b, Chevron Clear Creek, and White River oil shale sites.

For both the high- and low-background air quality conditions, results indicate that oil shale development does not lead to exceedance, at least photochemically, of the ozone standard of 0.12 ppm. Because the oil shale emissions rates are low, background air quality conditions tend to dominate these simulations.

TABLE 5-8. SUMMARY OF EKMA RESULTS FOR TRAJECTORY 1

(a) High Concentration Background

Species	1980 Baseline Scenario	Low Oil-Production Scenario	High Oil-Production Scenario
O_3 (ppm)	0.083	0.091	0.093
NO_2 (ppm)	0.0025	0.0029	0.0040
Sulfur aerosol ($\mu g/m^3$)	0.314	0.628	1.34
Organic nitrate ($\mu g/m^3$)	1.40	1.86	1.98

(b) Low Concentration Background

Species	1980 Baseline Scenario	Low Oil-Production Scenario	High Oil-Production Scenario
O_3 (ppm)	0.042	0.048	0.042
NO_2 (ppm)	0.00054	0.0034	0.0053
Sulfur aerosol ($\mu g/m^3$)	0.213	0.748	0.700
Organic nitrate ($\mu g/m^3$)	0.518	0.974	0.703

TABLE 5-9. SUMMARY OF EKMA RESULTS FOR TRAJECTORY 2

(a) High Concentration Conditions

Species	1980 Baseline Scenario	Low Oil-Production Scenario	High Oil-Production Scenario
O_3 (ppm)	0.083	0.088	0.092
NO_2 (ppm)	0.0025	0.0027	0.0027
Sulfur aerosol ($\mu g/m^3$)	0.314	0.55	1.58
Organic nitrate ($\mu g/m^3$)	1.44	1.69	2.18

(b) Low Concentration Conditions

Species	1980 Baseline Scenario	Low Oil-Production Scenario	High Oil-Production Scenario
O_3 (ppm)	0.043	0.051	0.049
NO_2 (ppm)	0.00054	0.0014	0.0042
Sulfur aerosol ($\mu g/m^3$)	0.235	0.759	1.16
Organic nitrate ($\mu g/m^3$)	0.585	1.07	1.03

5.6 VISIBILITY IMPAIRMENT

Some visibility impairment will occur as a result of emissions from oil shale facilities of particulate matter, sulfur dioxide (which is converted in the atmosphere to sulfate aerosol), and nitric oxide (which is converted to nitrogen dioxide). Particulate matter (both primary emissions and secondary aerosol) scatters light and thereby causes white or gray plumes, reduces the contrast of terrain features, and reduces visual range. Nitrogen dioxide discolors the sky, causing yellow or brown hazes. As noted in Section 3, the judgment as to whether projected emissions are adverse is subjective since there are no specific criteria for such adversity judgments, which are made by the federal land managers and the states.

We performed an EPA Level-1 visibility screening analysis (Latimer and Ireson, 1980) for each of the synthetic fuel facilities in the study region. Screening was done for maximum emissions from each facility associated with the high oil production scenario. Screening was performed for the only existing mandatory Class I area in the study region, the Flat Tops Wilderness Area; for two potential Class I areas, the Dinosaur and Colorado National monuments; and two other areas of special concern, the Uintah/Ouray Indian Reservation and the Uinta Primitive Area.

The Level-1 analysis allows one to determine the likelihood that visibility impairment will be considered to be adverse. This analysis functions as a screening test in that it overestimates (by design) impacts to the extent that if the test is passed, there is little possibility that significant visibility impairment will take place.

Level-1 screening contrast parameters (C_1, C_2, C_3) were calculated to indicate potential problems for three scenarios: a dark (NO_2) plume visible against the sky, a light (particulate) plume visible against terrain, and regional reductions in terrain/sky contrast and visual range. Appendix D summarizes the results. If any of these contrast parameters is greater or less than -0.1, a potentially adverse problem cannot be ruled out.

This screening analysis suggests that the possibility of adverse visibility impairment due to the Uinta Basin sources on Flat Tops can be ruled out, although the screening identifies several proposed oil shale facilities in Colorado that could cause potentially adverse visibility impairment in this existing mandatory Class I area. The screening identified, however, that adverse impacts in Dinosaur National Monument, a potential Class I area, cannot be ruled out as a result of emissions from Moon Lake and White River, both existing or other (interrelated) projects in the Uinta Basin; Syntana, a site-specific Uinta Basin project; and

Sohio, a Uinta Basin conceptual. Similar, potential problems were also indicated by screening to occur in the Uintah/Ouray Indian Reservation, an area of special concern which is very close to several of the proposed Uinta Basin facilities. Potential visual impacts identified by the screening are associated with the perceptibility of nitrogen dioxide or particulate plumes during worst-case, stable, light-wind meteorological conditions. In addition to these potential plume discoloration (so-called plume blight) concerns in these areas close to the Uinta Basin sources, Level-1 screening identified that, although Uinta Basin sources, both separately and together would not cause potentially adverse regional reduction in visual range, all regional emissions, including Colorado sources, could do so. (The third screening test gave C_3 values of 0.09, 0.06, and 0.14, respectively, for the cumulative Uinta Basin, Piceance Basin, and combined emissions for the high-oil-production scenario.)

To investigate these potential local plume discoloration and regional haze (visual range reduction) problems, we performed more detailed (and less conservative) Level-2 and Level-3 analyses for

> Worst-case plume discoloration due primarily to nitrogen oxide emissions.

> Worst-case incremental contributions to regional haze.

5.6.1 Plume Discoloration

An analysis of the magnitude and frequency of occurrence of plume visual impact (a Level-3 analysis) was performed. It was reasoned that although the Level-1 screening test identified potential problems with both nitrogen oxide (C_1) and particulate (C_2) plumes, the principal plume visual impact will be associated with the former. Particle emissions from scattered, ground-level fugitive dust sources within a synfuel facility are expected to be in a size range having large settling velocities and low light-scattering efficiencies. Therefore, ground-level particulates from fugitive dust sources will probably not be a significant visual impact in the region, although the possibility of local dust clouds being perceptible at the development sites cannot be ruled out. The most likely visual impact associated with individual plumes from facilities is yellow or brown discoloration resulting from atmospheric conversion of emissions of nitric oxide to nitrogen dioxide, a dark brown gas. Near-source, quite perceptible visual impacts caused by this colored gas are probable. Nitrogen oxide is emitted in hot flue gas emissions from stacks at synfuel facilities, along with some particulate and SO_2 emissions. The stack emission rates of the largest of the Uinta Basin synfuel facilities are similar to those of a modern, well-controlled 300 Mwe coal-fired power plant. Experience with existing power plants of this size suggests that yellow or brown plume discoloration will be perceptible during stable, light-wind conditions that occur most frequently in the morning.

The magnitude of plume discoloration for each of the Uinta Basin sources was evaluated using PLUVUE (see Appendix C) for three worst-case meteorological scenarios. These scenarios assume that a plume is transported within a 22.5° sector centered on the observer with a 2.5 meter per second wind and D, E, and F stability conditions. Table 5-10 provides values of the plume perceptibility parameter, $\Delta E(L^*a^*b^*)$, calculated for observers located in Dinosaur National Monument and on the Uintah/Ouray Indian Reservation. Various studies suggest that plume discoloration will be perceptible when ΔE is greater than 1 to 4.

The frequency with which these worst-case meteorological conditions would occur and the resulting visual impacts would be perceived was estimated using upper-air meteorological data collected at effective stack height near the Moon Lake Power Plant (Burns & McDonnell, 1980). These pibal and radiosonde measurements were made twice daily, one-half hour after sunrise and at 2:00 p.m. LST, every other day for the period October 1976 through January 1978. Although the year 1977 may be atypical because of drought conditions, it is believed that this data base is most representative of stability conditions at plume height for the Uinta Basin synfuel facilities. Figures 5-35 and 5-36 show cumulative frequencies of ΔE at Dinosaur and the reservation. Depending on whether one selects a ΔE of 1 or 4 as the perceptibility threshold, plumes are predicted to be visible from one or more synfuel facilities at Dinosaur or the reservation from about 5 to 50 mornings per year. Impacts in the afternoon are much less frequent. It should be noted that the magnitude and frequency of occurrence of plume discoloration from the Moon Lake Power Plant will be much greater than that resulting from a single synfuel facility. However, because there may be a number of discolored plumes visible at any one time from the Uinta Basin synfuel facilities, it is difficult to judge whether the adversity of perceived plume visual impact of the many synfuel facilities will be greater or less than the single plume from the Moon Lake Power Plant.

One final caveat is in order with regard to these estimates. A recent intensive field measurement program in the vicinity of a large coal-fired power plant suggests that the PLUVUE model reasonably accurately predicts observed plume discoloration. However, there is considerable uncertainty in individual model calculations and the model tends to overpredict, on the average, by a factor of two (Bergstrom et al., 1981).

TABLE 5-10. MAGNITUDE [ΔE(L*a*b*)] OF PLUME DISCOLORATION

(a) Observed in Dinosaur National Monument

Emission Source	Distance (km)	Dispersion Condition*		
		F, 2.5 m/s	E, 2.5 m/s	D, 2.5 m/s
Enercor-Mono Power	80	0.6	0.3	0.2
Geokinetics				
Agency Draw	80	1.0	0.6	0.3
LOFRECO	60	0.3	0.2	0.1
Magic Circle	60	4.2	3.1	1.7
Moon Lake 1 & 2	40	10.5	8.3	4.9
Paraho	50	2.4	1.8	1.0
Sohio	20	1.6	1.4	1.1
Syntana	40	3.9	3.1	1.8
Tosco	50	4.0	2.9	1.6
White River	50	4.2	3.1	1.7

TABLE 5-10 (Concluded)

(b) Observed in the Uintah/Ouray Indian Reservation

Emission Source	Distance (km)	Dispersion Condition* F, 2.5 m/s	E, 2.5 m/s	D, 2.5 m/s
Enercor-Mono Power	40	0.6	0.5	0.3
Geokinetics				
Agency Draw	40	1.1	0.9	0.5
LOFRECO	20	0.3	0.2	0.1
Magic Circle	10	4.2	3.3	2.7
Moon Lake 1 & 2	10	8.9	8.0	6.7
Paraho	30	2.5	2.1	1.4
Sohio	30	1.7	1.4	0.9
Syntana	30	3.9	3.3	2.1
Tosco	10	3.1	2.8	2.5
White River	30	4.3	3.6	2.4

---

[*] Worst-case dispersion scenario with low wind speed and transport within 22.5° sector directly toward the observer.

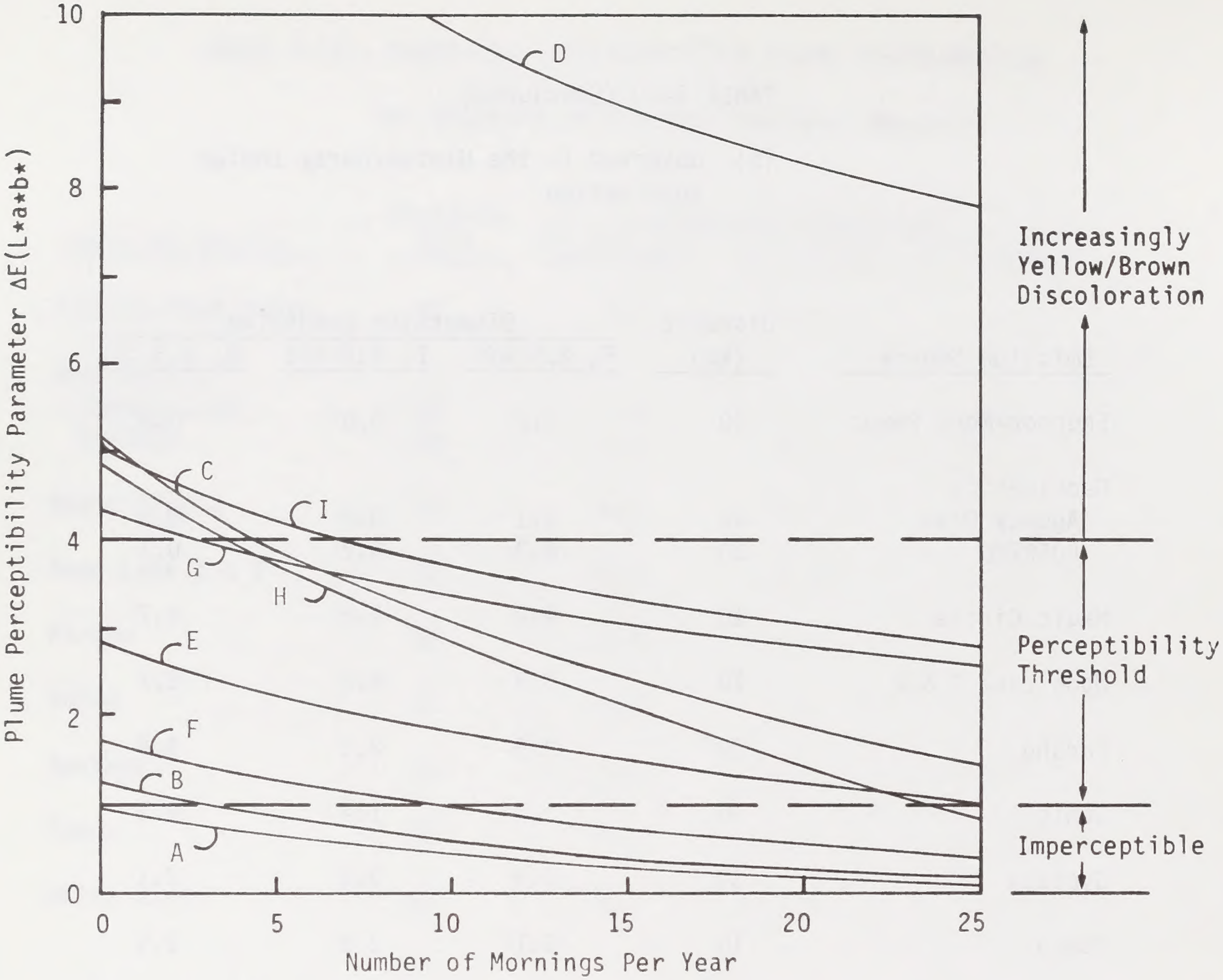

Key to Emission Sources:

A - Enercor-Mono Power
B - Geokinetics
C - Magic Circle
D - Moon Lake Power Plant Units 1 and 2
E - Paraho
F - Sohio
G - Syntana
H - Tosco
I - White River

(a) Morning impacts

FIGURE 5-35. CUMULATIVE FREQUENCY OF PERCEPTIBLE PLUME DISCOLORATION RESULTING FROM EMISSIONS FROM VARIOUS UINTA BASIN SOURCES AT DINOSAUR NATIONAL MONUMENT

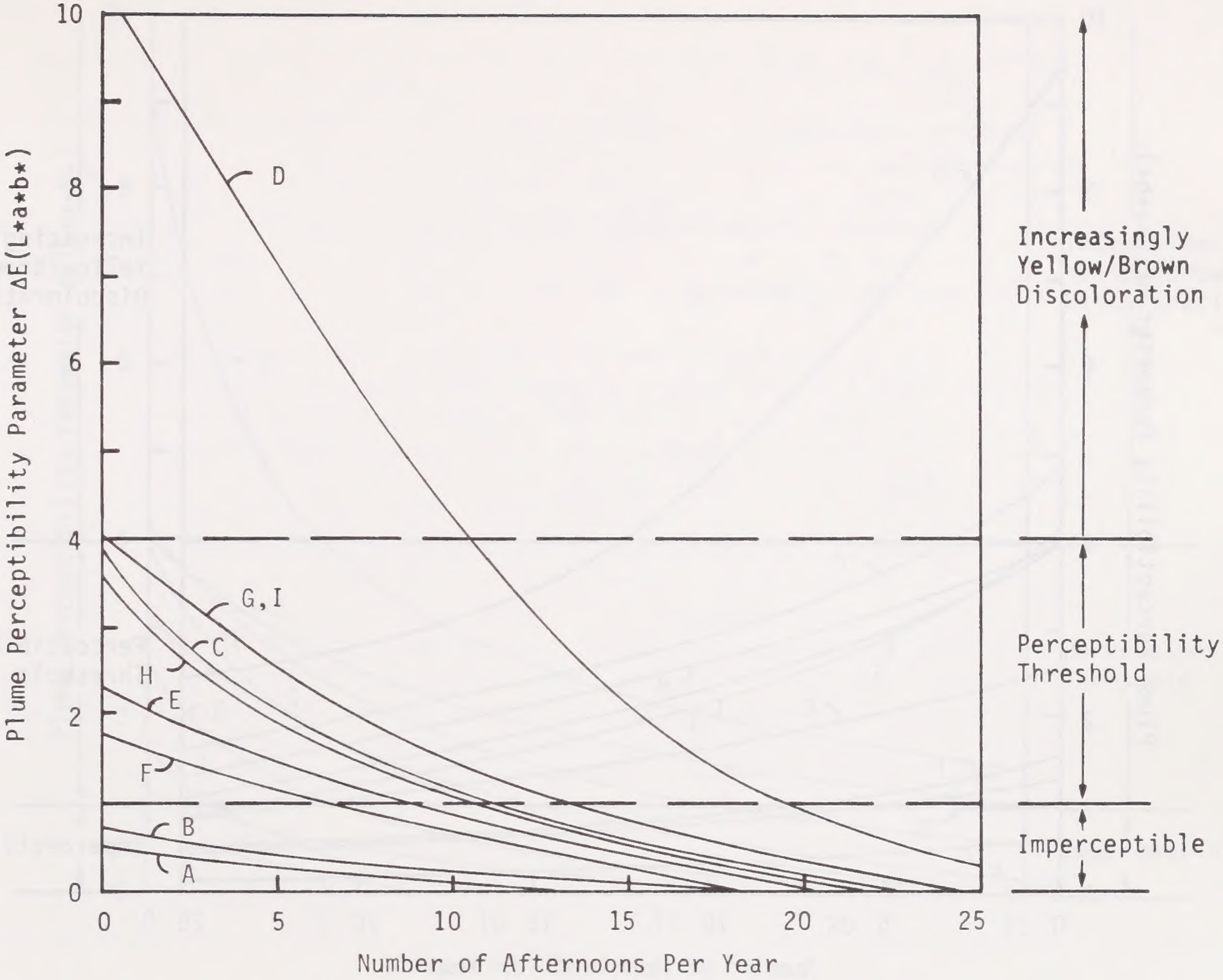

Key to Emission Sources:

A - Enercor-Mono Power
B - Geokinetics
C - Magic Circle
D - Moon Lake Power Plant Units 1 and 2
E - Paraho
F - Sohio
G - Syntana
H - Tosco
I - White River

(b) Afternoon impacts

FIGURE 5-35 (Concluded)

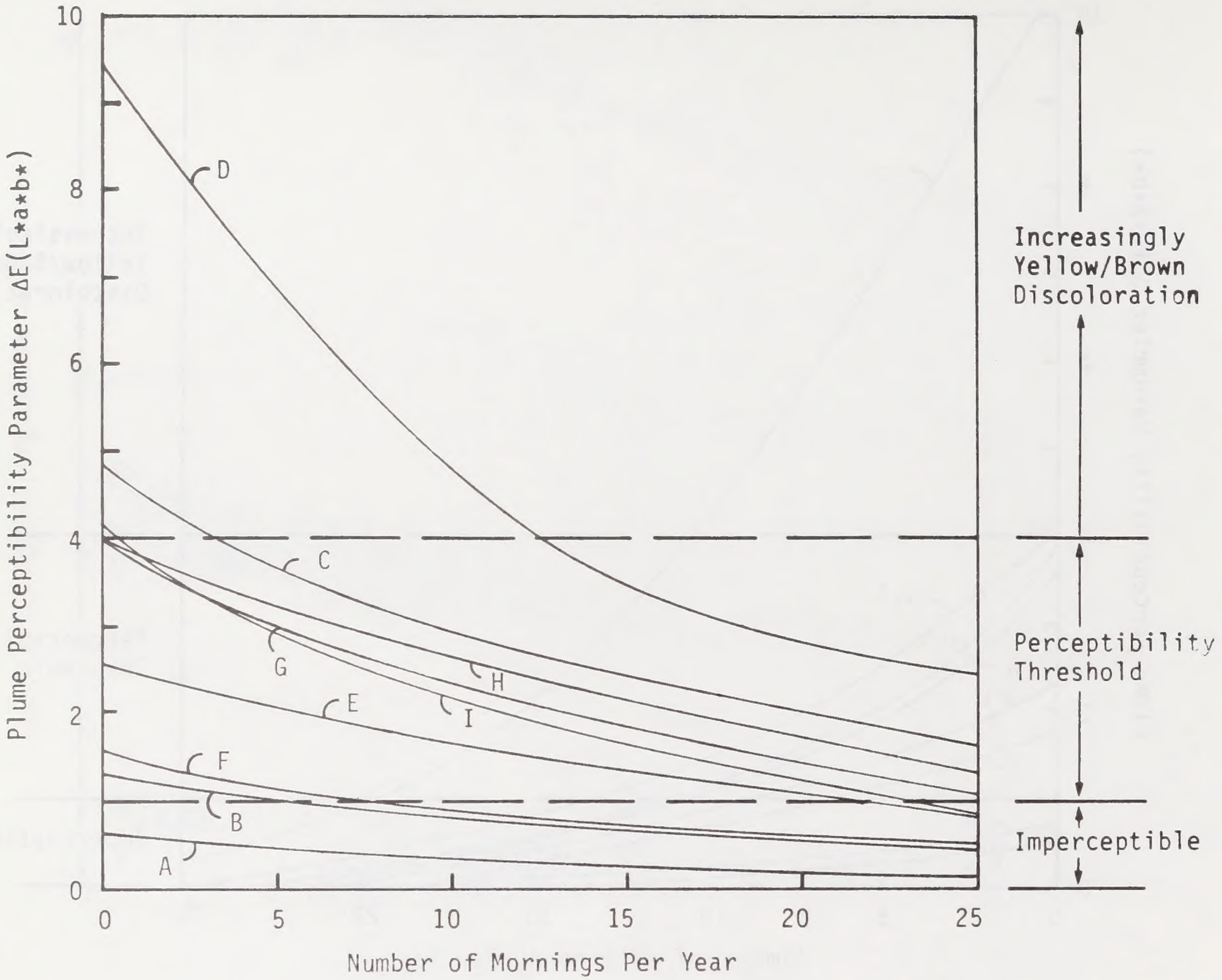

Key to Emission Sources:

A - Enercor-Mono Power
B - Geokinetics
C - Magic Circle
D - Moon Lake Power Plant Units 1 and 2
E - Paraho
F - Sohio
G - Syntana
H - Tosco
I - White River

(a) Morning impacts

FIGURE 5-36. CUMULATIVE FREQUENCY OF PERCEPTIBLE PLUME DISCOLORATION RESULTING FROM EMISSIONS FROM VARIOUS UINTA BASIN SOURCES AT UINTAH AND OURAY INDIAN RESERVATION

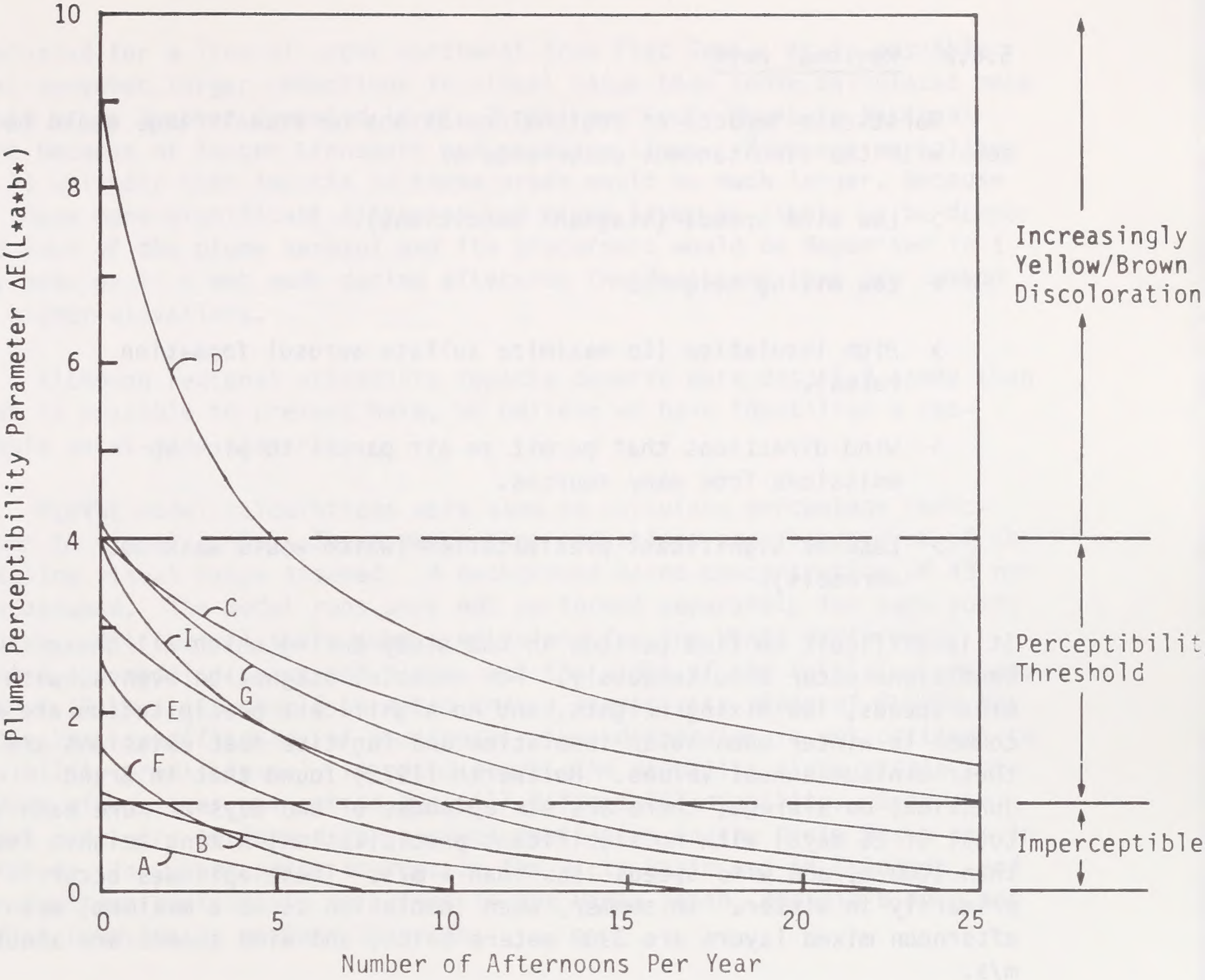

Key to Emission Sources:

A - Enercor-Mono Power
B - Geokinetics
C - Magic Circle
D - Moon Lake Power Plant Units 1 and 2
E - Paraho
F - Sohio
G - Syntana
H - Tosco
I - White River

(b) Afternoon impacts

FIGURE 5-36 (Concluded)

5.6.2 Regional Haze

Worst-case impacts of regional emissions on visual range would be seen with the simultaneous occurrence of

> Low wind speeds (stagnant conditions).

> Low mixing heights.

> High insolation (to maximize sulfate aerosol formation rates).

> Wind directions that permit an air parcel to pick up emissions from many sources.

> Lack of significant precipitation (which would wash out aerosols).

It is difficult to find periods in the study during which all these conditions occur simultaneously. For example, stagnation events, with low wind speeds, low mixing heights, and no significant precipitation are most common in winter when solar insolation and fugitive dust emissions are at their minimum annual values. Holzworth (1972) found that in Grand Junction, on average, there are six episodes of two days or more each (a total of 26 days) with no significant precipitation, mixing heights less than 1000 m, and wind speeds less than 4 m/s. These episodes occur primarily in winter. In summer, when insolation is at a maximum, mean afternoon mixed layers are 3900 meters thick, and wind speeds are about 6 m/s.

Although it must be noted that it is possible that significant regional visual range reduction would occur in the winter in populated areas due to fireplace and stove emissions trapped in stagnant layers, the magnitude of such impacts is difficult to quantify at this time.

We selected a summertime worst-case meteorological scenario for evaluation of regional visual range reduction. We choose a conservatively low summertime mixing height of 1000 meters and a low wind speed of 3 meters per second. We assumed that an air parcel was transported over the population centers and synfuel development areas of the Uinta and Piceance basins picking up emissions as it progressed eastward. Unlike plume discoloration effects, regional visual range reduction increases with transport time and the rate of plume mixing with reactive background species (primarily the hydroxyl radical). We therefore selected a C stability for plumes (trapped within the 1000-m mixed layer) and a long transport time of about 10 hours for Uinta Basin emissions. Impacts were evaluated for a line of sight northwest from Flat Tops. It is possible that somewhat larger reductions in visual range than those calculated here could occur further downwind in Mt. Zirkel and Rocky Mountain National Park because of longer transport and reaction times. However, we believe it is unlikely that impacts in these areas would be much larger, because at these more significant distances the mixed layer is likely to be deeper and much of the plume aerosol and its precursors would be deposited in a dry mode or in a wet mode during afternoon thunderstorms that are common at higher elevations.

Although regional visibility impacts deserve more detailed study than what is possible to present here, we believe we have identified a reasonble worst-case scenario.

PLUVUE model calculations were used to calculate percentage reductions in visual range. These percentage reductions are independent of the baseline visual range assumed. A background ozone concentration of 43 ppb was assumed. The model runs were not performed separately for each point source. All the oil shale source emissions for the Uinta Basin were summed and modeled using one plume, and the width of the initial plume was set at 10 km. (It should be noted that a sensitivity study of PLUVUE has shown that specification of horizontal plume dispersion is not critical to visibility predictions.) As noted above, the stability class within the 1000-m mixed layer was set to Pasquill-Gifford "C" stability. Separate model runs were performed for synfuel facilities in the Uinta Basin and in Colorado, for other point sources in the Uinta Basin and in Colorado, and for fugitive particulate emissions in the Uinta Basin, and Rio Blanco and Moffat counties in western Colorado.

Specification of the size distribution of the aerosol is very important in obtaining accurate estimates of visibility impacts due to scattering by particulate matter or secondary aerosol. We used size distributions specified by EPA (1981). Table 5-11 shows the size distributions and deposition velocities of the primary and secondary aerosols used in the various simulations. We have assumed a particle size distrbution with a mass median diameter of 6 µm for direct TSP emissions from oil shale facilities. Although stack emissions might be smaller than this (say, 1-2 µm), fugitive dust emissions would probably be larger (> 10 µm). The only area source emissions considered were emissions of fugitive dust (TSP) from unpaved roads, which amount to more than 90 percent of the total area source TSP emissions.

A PLUVUE model simulation was performed for each source type, level of emissions, and location. For each simulation, the reduction in visual range from the background value was determined for an observer at the Flat Tops Wilderness Area looking toward the northwest horizon sky. The total

TABLE 5-11. PARTICLE SIZE DISTRIBUTIONS AND DEPOSITION VELOCITIES ASSUMED IN VISIBILITY MODEL SIMULATIONS

Type of Particle	Mass Median Diameter (μm)	Geometric Standard Deviation	Deposition Velocity (cm/sec)
Oil shale and other point source particulate emissions	6.0	2.0	0.19
Area source emissions (unpaved roads)	5.0*	2.0	0.19
	10.0†	2.0	0.75
Secondary aerosol	0.1	2.0	0.10

---

[*] 8 percent of TSP emissions.

[†] 24 percent of TSP emissions (the remaining 68 percent of TSP emissions are in an optically inactive size range, 30 to 100 μm, with large deposition rates).

visual-range reduction was obtained by adding the fractional visual-range reductions for all the different sources. The contributions of each source, and the total visual-range reduction for the three emission levels are shown in table 5-12. The visual-range reductions are 2.86 percent, 7.25 percent, and 9.48 percent for the 1980 baseline year, and for the low- and high-oil-shale-production scenarios, respectively.

Most of the visual-range reduction in the worst-case scenario results from sulfate aerosol formed from SO_2 emissions from oil shale facilities and other point sources. Little of the visual-range reduction is due to secondary emissions associated with population growth.

5.7 ACID DEPOSITION

The potential impact of air pollution on acid deposition in such forms as sulfurous, sulfuric, and nitric acid through both wet and dry processes is currently a growing concern. For the high-oil-production scenario, we estimated dry deposition in the study region from annual-average concentration isopleth maps. The annual dry deposition is determined through multiplication of the annual-average concentration by the deposition velocity, which for SO_2 and NO_x is on the order of 1 cm/sec. Figures 5-37 and 5-38 summarize these calculations. Since these plots were derived from GPM calculations, they are expected to be conservative.

Wet deposition was estimated from precipitation statistics for Grand Junction and the surrounding region. Grand Junction has 69 days per year during which precipitation is greater than 0.01 inch, and has a total annual precipitation of 8.4 inches. However, higher elevations receive greater amounts of precipitation. For example, annual precipitation in the Flat Tops Wilderness Area is estimated to be as high as 40 to 50 inches. Assuming conservatively that virtually all SO_x and NO_x is scavenged in significant rainfall events, we estimated that annual wet deposition rates would be on the same order as dry deposition rates, though short-term wet deposition rates would be higher. These estimates are likely to be conservative--extremely conservative in the low-elevation areas that receive less precipitation than the high-elevation areas. Thus, these wet deposition estimates are upper-bound estimates. Wet deposition clearly deserves more detailed study than that possible in this study.

Wet deposition was estimated by calculating an annual effective deposition velocity by assuming that all emissions in the mixed layer throughout the region are deposited during one-hour precipitation events on the 69 days per year with measured precipitation in Grand Junction of

TABLE 5-12. WORST-CASE REDUCTION OF VISUAL RANGE FOR A VIEW FROM FLAT TOPS WILDERNESS AREA LOOKING TOWARD THE NORTHWEST

	Percentage Visual Range Reduction		
Source	Year 1980 Baseline	Low-Oil-Production Scenario	High-Oil-Production Scenario
Uinta Basin synfuel facilities			
site specifics	0.00%	0.31%	0.53%
conceptuals	0.00	0.64	1.75
Other Uinta Basin point sources	0.45	1.56	1.56
Piceance Basin oil shale	0.00	0.99	1.64
Other Piceance Basin point sources	1.96	2.95	2.97
Uintah County area sources*			
5 µm aerosol	0.04	0.08	0.12
10 µm aerosol	0.17	0.36	0.54
Rio Blanco County area sources*			
5 µm aerosol	0.03	0.03	0.03
10 µm aerosol	0.15	0.15	0.15
Moffat County area sources*			
5 µm aerosol	0.01	0.03	0.03
10 µm aerosol	0.05	0.14	0.15
Total visual range reduction	2.86%	7.25%	9.48%

---

* Only particulate emissions from unpaved roads, which are more than 90 percent of total particulate emissions, were considered in the visibility analysis.

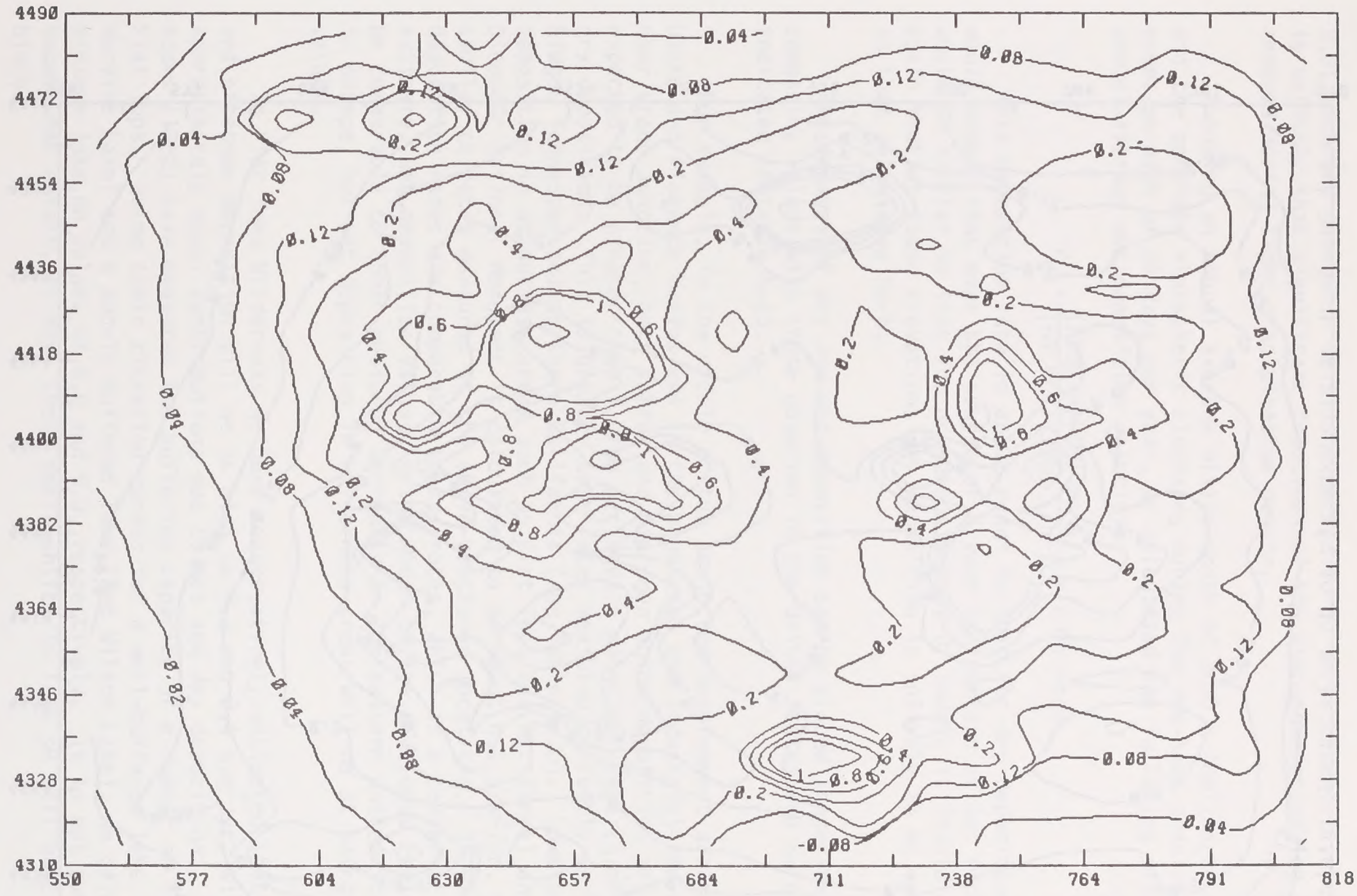

FIGURE 5-37. ANNUAL SULFUR ANION DRY DEPOSITION ($G/M^2/YR$) FOR THE HIGH OIL PRODUCTION SCENARIO

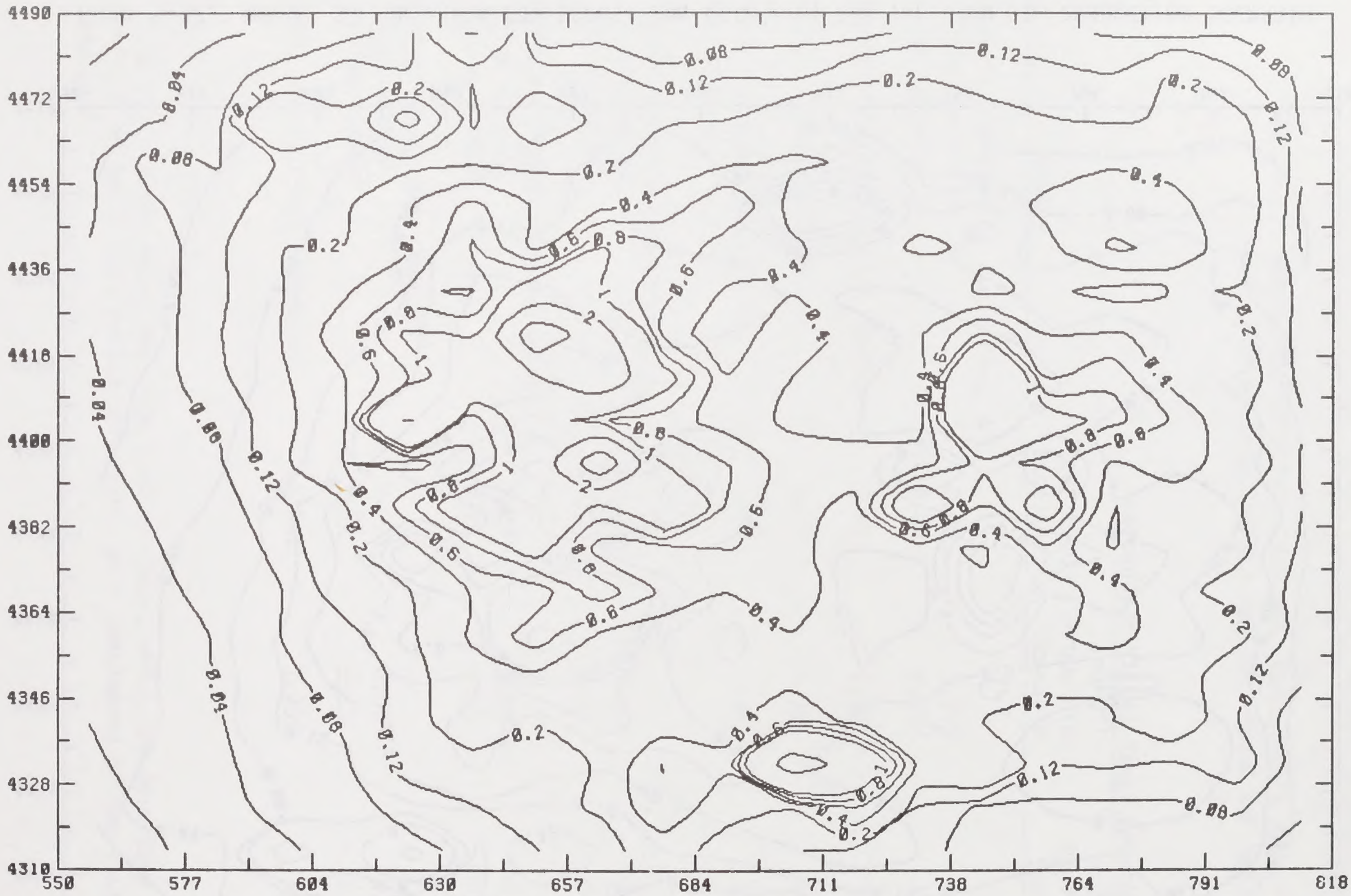

FIGURE 5-38. ANNUAL NITROGEN ANION DRY DEPOSITION ($G/M^2/YR$) FOR THE HIGH OIL PRODUCTION SCENARIO

0.01 inch and greater. This is expected to be very conservative since it is unlikely that significant fractions of the atmospheric loading would be removed during light precipitation events.

Assuming an annual average mixing depth of 2600 m (Holzworth, 1972) and the complete atmospheric cleansing during the one-hour precipitation event on each of 69 days per year, we calculated the following effective, annual-average wet deposition velocity:

$$V_d = \frac{(2600\ \mathrm{m})(100\ \mathrm{cm/m})}{(69\ \mathrm{hrs})(3600\ \mathrm{s/hr})} = 1.05\ \mathrm{cm/s}$$

This deposition rate is about equal to that for dry deposition. One would expect that over the course of a year the pattern of wet deposition would be similar to that for dry deposition. Of course it should be noted again that at lower elevations wet deposition is unlikely to be as great as that calculated here.

These rates of dry and wet deposition can be placed in perspective by comparing values with those observed in the United States and Europe, as indicated in table 5-13.

For example, in the middle of the projected development areas in the Uinta and Piceance basins and in the populated and industrialized area near Grand Junction, both sulfur and nitrogen anion deposition are expected to be greater than 1 gram per square meter per year ($g/m^2/yr$) by dry deposition. This is greater than rates measured currently in Oak Ridge, Tennessee and northern California (see Table 5-10). However, dry deposition in wilderness areas such as Flat Tops and Mt. Zirkel and at Dinosaur National Monument is calculated to be about 0.1 $g/m^2/yr$, which is similar to rates measured at the above-mentioned locations. If wet deposition rates are comparable to dry rates, which is a conservative estimate, wet deposition values in the midst of the developed regions will be comparable to those measured currently in the eastern United States and in Europe, but wet deposition in wilderness areas will be at background values.

In Flat Tops Wilderness we have conservatively estimated that sulfur and nitrogen deposition will be as high as 0.2 and 0.4 $g/m^2/yr$, with approximately equal contributions due to wet and dry deposition. Turk and Adams (1982) have measured the buffering capacity of a number of lakes in Flat Tops. Using their titration curves for a well-buffered lake (Lower Marvine Lake) and a poorly buffered lake (Ned Wilson Lake), we calculated minimum lake pH values of 8.0 and 6.0, respectively. It is not currently known what effect, if any, these small shifts in lake pH will have on biota.

TABLE 5-13. SUMMARY OF WORLD-WIDE WET AND DRY, SULFURIC AND NITRIC ACID DEPOSITION MEASUREMENTS

Location	Annual Deposition* ($g/m^2/yr$)
Background	0.2 N (wet) 0.2 S (wet)
Berkeley, California (1974-1975)	0.48 S (wet) 0.03 N (wet)
Central Europe (circa 1970)	0.6 N (wet)
Eastern United States (1977-1978)	1.2 S (wet)
Oak Ridge, Tennessee (1975-1976)	1.4 S (wet) 0.4 S (dry)
Sweden (1975)	2.5 S (wet)
Northern California (1978-1979)	0.1-0.3 S (wet) 0.1-0.4 N (wet) 0.0-0.1 S (dry) 0.0-0.2 N (dry)

---

[*] Stated in terms of mass of sulfur (S) or nitrogen (N).

5.8 AIR QUALITY IMPACTS ASSOCIATED WITH CONSTRUCTION ACTIVITIES

Although it is difficult at this time to quantify construction impacts, they are expected to be small compared to impacts associated with the operation of synfuel facilities. The air quality impacts associated with construction activities will be temporary, lasting only a few years. Impacts will include fugitive dust emissions resulting from the use of large earth-moving equipment and small quantities of emissions from the exhaust of such equipment. Impacts resulting from population growth associated with construction activities will be proportional to such population growth and will be similar to those predicted for other secondary emissions, as discussed in Section 5.3.

6 AIR QUALITY IMPACTS OF SPECIFIC PROPOSED ACTIONS

In the previous section, the cumulative impacts of synthetic fuel development, other projects, and associated growth were discussed. In this section we discuss the impacts at maximum production rates of the following specific proposed actions:

> Enercor-Mono Power

> Magic Circle

> Paraho

> Syntana-Utah

> Tosco.

Whereas we studied regional impacts within the large study region, we examine in this section individual site impacts on a smaller scale in the Uinta Basin, and impacts of ground-level releases of total suspended particulates (TSP) within 5 kilometers of each source. The Prevention of Significant Deterioration (PSD) increment consumption of each source is evaluated separately and together with other projects (primarily the White River oil shale project and the Moon Lake power plant). The impact of the emissions from facilities (together with the existing baseline, other project impacts, and secondary growth impacts) is evaluated with respect to applicable ambient air quality standards.

In this analysis, subregional Gaussian Puff Model (GPM) runs and COMPLEX-I model runs, as discussed in Section 4, were used to make best estimates of air quality impacts. These results are expected to be conservative, but not nearly as conservative as the regional results presented in Section 5. For this reason we provide the model results directly without any estimated error bounds. The TSP concentration calculations using GPM are overly conservative within 10 to 20 km of each source because multiple ground-level releases were aggregated into one point (see Section 4); we therefore supplemented the GPM calculations with COMPLEX-I calculations.

Clear plastic overlays showing the locations of the synthetic fuel facilities and terrain elevations in the small Uinta Basin modeling subregion are provided inside the back cover of this report.

A discussion of proposed mitigation measures for controlling emissions from these synthetic fuel facilities is provided in Appendix E.

6.1 ENERCOR-MONO POWER

Enercor-Mono Power proposes to operate tar sands synthetic fuel facilities at two locations to produce 55,000 barrels per day. The northern location, the Rainbow site, is just west of Three Mile Canyon at approximately 7000 feet MSL. At this site, local drainage winds to the north into Evacuation Creek are likely to compete with the prevailing westerly winds in causing worst-case impacts. The southern location, called the PR Springs, or Cedar Camp site, is located on Meadow Creek at about 8000 feet MSL right at the ridgeline above the Colorado River. This site should be quite well ventilated; drainage winds, if they exist at all, would carry emissions to the west and then to the north.

As indicated in tables 6-1 and 6-2 and figures 6-1 and 6-2, impacts are extremely small and well within air quality criteria. Visibility impairment resulting from this proposed project will be insignificant, with the facility passing EPA Level-1 screening tests at all mandatory and potential Class I areas (see table 6-3).

6.2 MAGIC CIRCLE

Magic Circle proposes to construct an oil shale facility to produce 31,500 barrels per day at a site in terrain gently sloping to the north and west toward the White and Green rivers, respectively. Drainage flows in the local area would carry emissions to the northeast.

Tables 6-4 and 6-5 and figures 6-3 and 6-4 summarize the impacts. Except for TSP impacts on-site, impacts are predicted to be well within criteria. Local TSP impacts are quite large on-site, but concentrations drop off rapidly with distance. On the basis of the more realistic COMPLEX model results, impacts beyond 5 km downwind are within PSD increments. Near-source (< 5 km downwind) impacts were calculated using EPA's COMPLEX model, taking into account the spatial distribution of TSP point sources. The facility passes the conservative EPA Level-1 visibility screening test for all mandatory and potential Class I areas (see table 6-6); thus, visibility impairment due to this source is not expected to be significant.

TABLE 6-1. SUMMARY OF PSD INCREMENT CONSUMPTION BY ENERCOR-MONO POWER

	SO_2 Concentration ($\mu g/m^3$)			TSP Concentration ($\mu g/m^3$)	
PSD Increments/Increment Consumption	3-Hour Average	24-Hour Average	Annual Average	24-Hour Average	Annual Average
Class II Areas					
Allowable PSD Class II increment	512	91	20	37	19
Increment consumption at receptors of maximum impacts					
Impact alone	12	3	0	7	0
Impact with Moon Lake Unit 1	13	3	0	7	0
Impact with all interrelated (other) sources	14	3	0	8	0
Maximum increment consumption on Uintah/Ouray Indian Reservation					
Impact alone	0	0	0	0	0
Impact with Moon Lake Unit 1	6	1	0	1	0
Impact with all interrelated (other) sources	14	3	0	3	0
Maximum increment consumption in Colorado					
Impact alone	3	1	0	1	0
Class I Areas					
Allowable PSD Class I increment	25	5	2	10	5
Increment consumption at Flat Tops Wilderness Area (federal Class I)					
Impact alone	0	0	0	0	0
Impact with Moon Lake Unit 1	0	0	0	0	0
Impact with all interrelated (other) sources	1	0	0	0	0
Increment consumption at Maroon Bells-Snowmass Wilderness Area (federal Class I)					
Impact alone	0	0	0	0	0
Impact with Moon Lake Unit 1	0	0	0	0	0
Impact with all interrelated (other) sources	0	0	0	0	0
Increment consumption at Dinosaur National Monument (Colorado category I and potential federal Class I)					
Impact alone	0	0	0	0	0
Impact with Moon Lake Unit 1	2	0	0	0	0
Impact with all interrelated (other) sources	6	1	0	1	0

TABLE 6-2. SUMMARY OF MAXIMUM AMBIENT AIR QUALITY IMPACTS OF ENERCOR-MONO POWER COMPARED WITH APPLICABLE STANDARDS

	Maximum Ground-Level Concentration ($\mu g/m^3$)					
Pollutant/Averaging Time	Baseline	Source Impact	Subtotal	Impact of Other Sources	Total	NAAQS* ($\mu g/m^3$)
Sulfur dioxide (SO_2)						
3-Hour	16	12	28	1	29	1300
24-hour	9	3	12	0	12	365
Annual	1	0	1	0	1	80
Total suspended particulate (TSP)						
24-Hour	127	7	134	1	135	150
Annual	20	0	20	0	20	60
Nitrogen dioxide (NO_2)						
Annual	2	0	2	0	2	100
Carbon monoxide (CO)						
1-Hour	2500	1	2501	0	2501	40,000
8-Hour	1500	1	1501	0	1501	10,000
Ozone (O_3)						
1-Hour	143	2	145	0	145	240

---

* National Ambient Air Quality Standards.

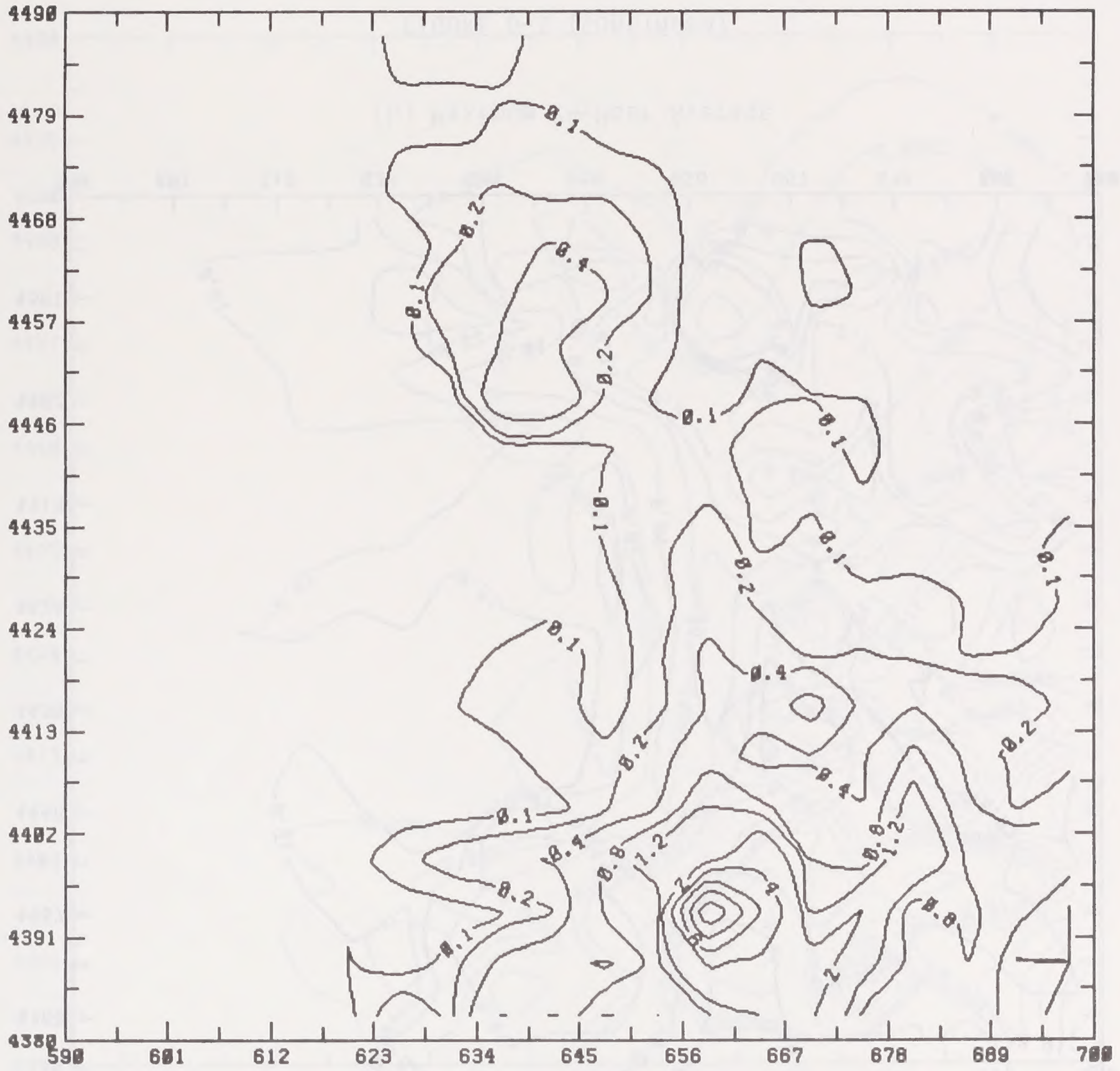

Maximum: 12 µg/m^3

(a) Maximum 3-Hour Average

FIGURE 6-1. GROUND-LEVEL SO_2 CONCENTRATIONS (µg/m^3) DUE TO ENERCOR-MONO POWER EMISSIONS

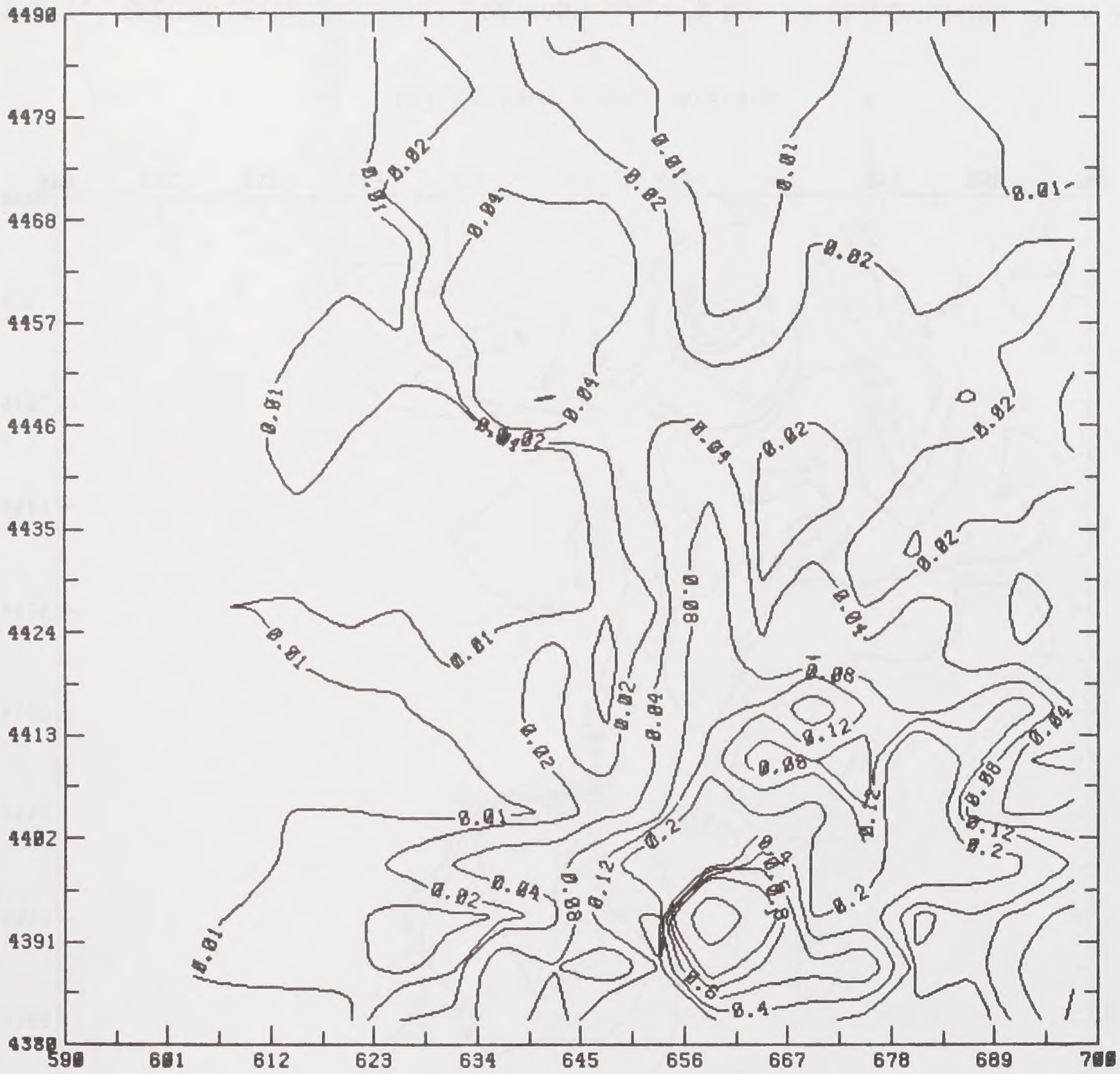

Maximum: 3 µg/m^3

(b) Maximum 24-Hour Average

FIGURE 6-1 (Continued)

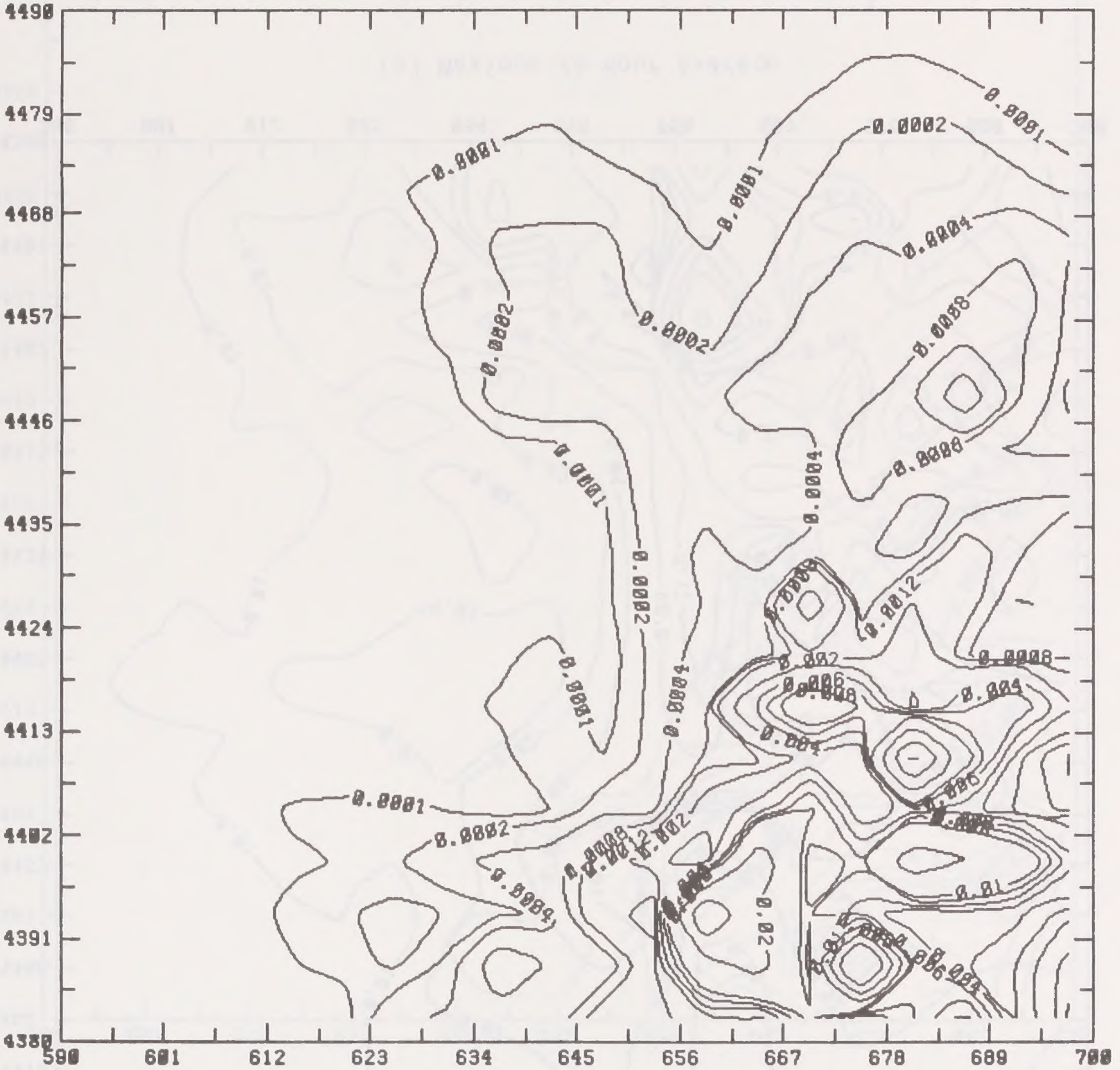

Maximum: 0.1 μg/m^3

(c) Annual Average

FIGURE 6-1 (Concluded)

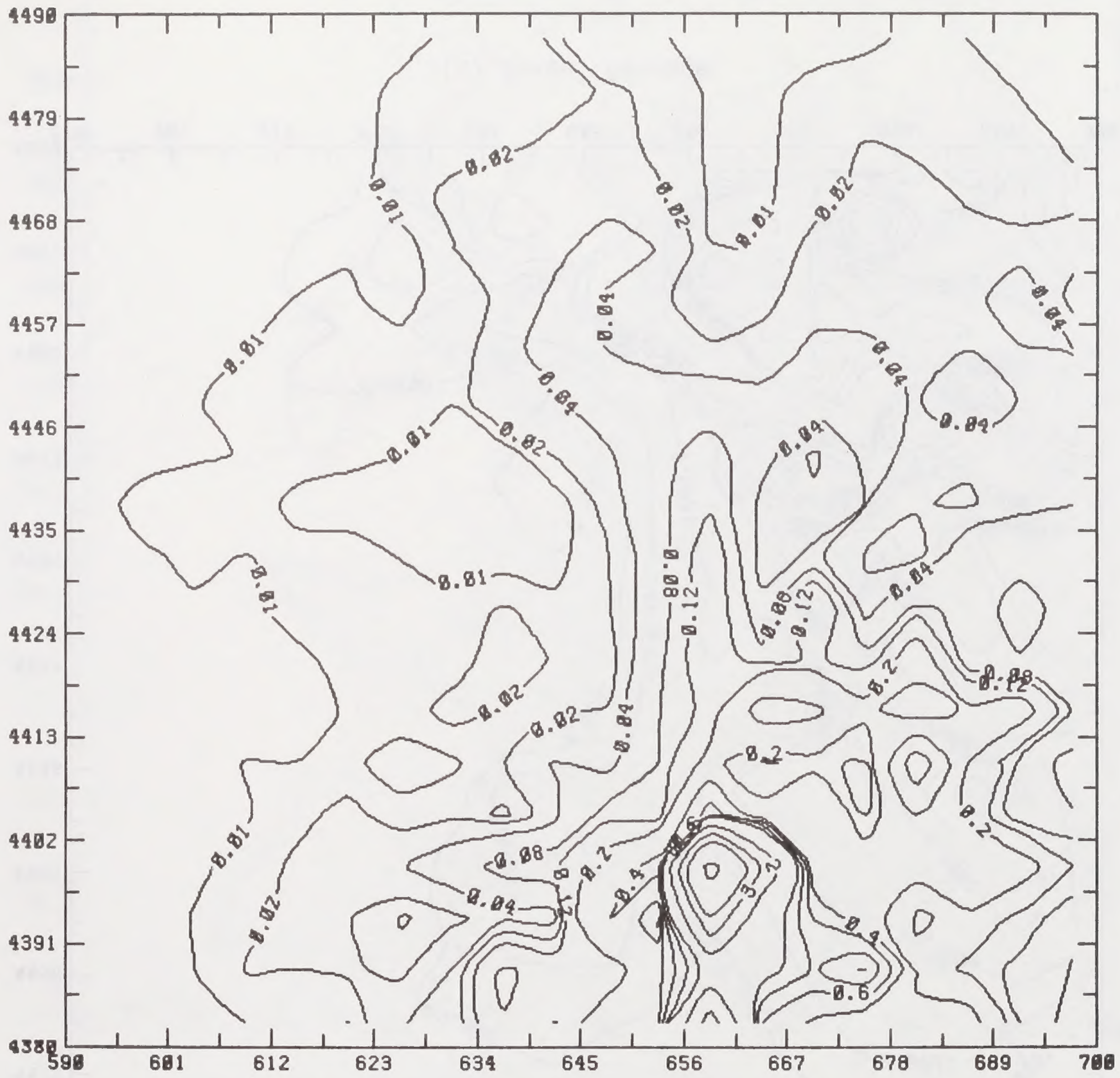

Maximum: 6.7 μg/m^3

(a) Maximum 24-Hour Average

FIGURE 6-2. GROUND-LEVEL TSP CONCENTRATIONS (μg/m^3) DUE TO ENERCOR-MONO POWER EMISSIONS

82062r3 24

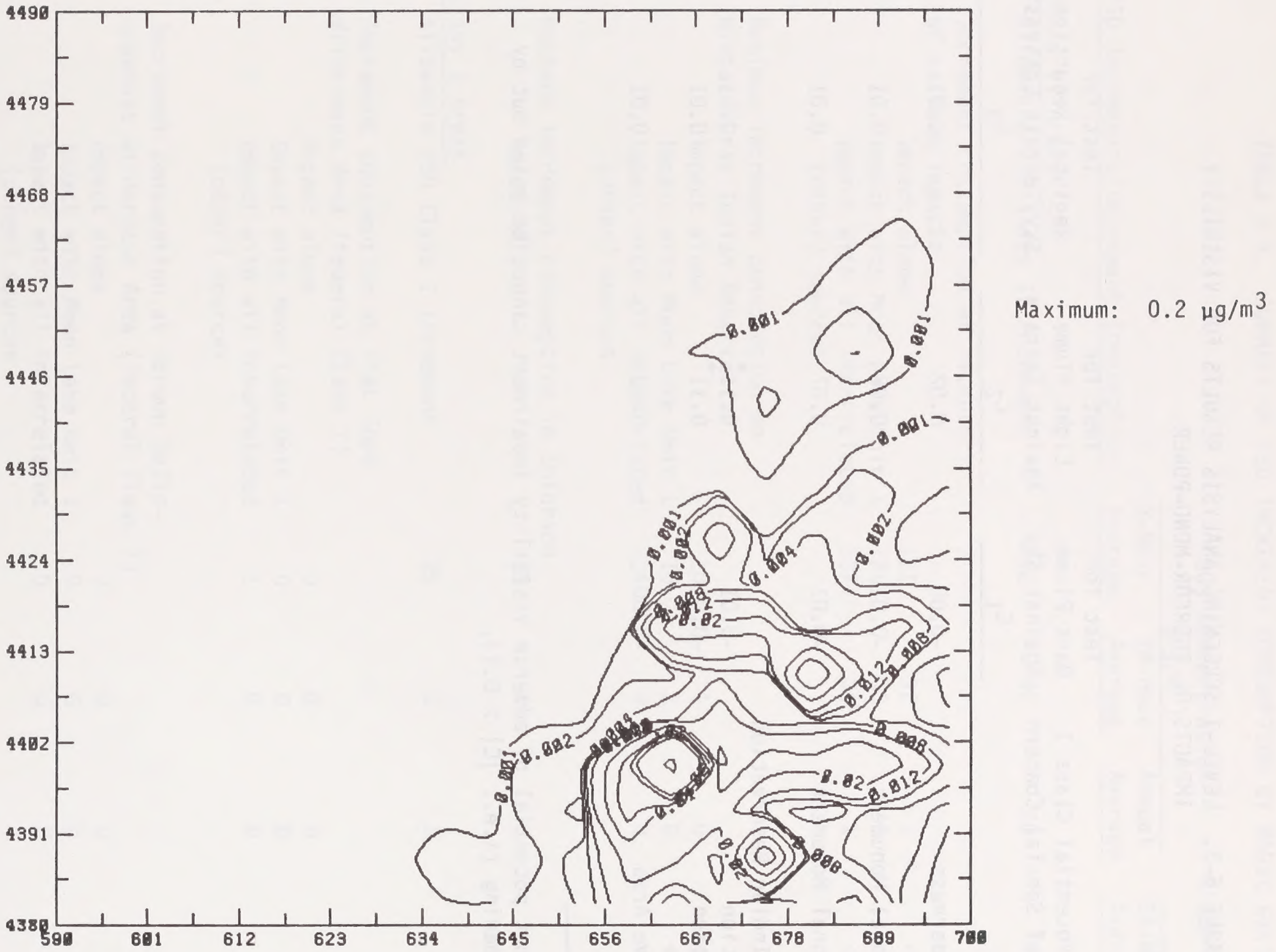

(b) Annual Average

FIGURE 6-2 (Concluded)

TABLE 6-3. LEVEL-1 SCREENING ANALYSIS RESULTS FOR VISIBILITY IMPACTS OF ENERCOR-MONO-POWER

Existing or Potential Class I Area or Area of Special Concern	Test for Dark Plume Against Sky C_1	Test for Light Plume Against Terrain C_2	Test for Regional Reduction Sky/Terrain Contrast C_3
Flat Tops Wilderness	-0.00	0.02	0.01
Dinosaur National Monument	-0.01	0.08	0.01
Colorado National Monument	-0.01	0.07	0.01
Uintah/Ouray Indian Reservation			
- North portion	-0.01	0.11*	0.01
- South portion	-0.01	0.11*	0.01
Uinta Primitive Area	-0.00	0.02	0.01

---

* Indicates that potential of adverse visibility impairment cannot be ruled out by Level-1 screening (i.e., $|C| > 0.1$).

TABLE 6-4. SUMMARY OF PSD INCREMENT CONSUMPTION BY MAGIC CIRCLE

	SO_2 Concentration ($\mu g/m^3$)			TSP Concentration ($\mu g/m^3$)	
PSD Increments/Increment Consumption	3-Hour Average	24-Hour Average	Annual Average	24-Hour Average	Annual Average
Class II Areas					
Allowable PSD Class II increment	512	91	20	37	19
Increment consumption at receptors of maximum impacts					
Impact alone	121	32	1	<32	<4
Impact with Moon Lake Unit 1	129	33	1	<34	<4
Impact with all interrelated (other) sources	137	34	1	<34	<4
Maximum increment consumption on Uintah/Ouray Indian Reservation					
Impact alone	10	1	0	<32	<4
Impact with Moon Lake Unit 1	16	2	0	<33	<4
Impact with all interrelated (other) sources	24	4	0	<35	<4
Maximum increment consumption in Colorado					
Impact alone	15	4	0	4	0
Class I Areas					
Allowable PSD Class I increment	25	5	2	10	5
Increment consumption at Flat Tops Wilderness Area (federal Class I)					
Impact alone	0	0	0	0	0
Impact with Moon Lake Unit 1	0	0	0	0	0
Impact with all interrelated (other) sources	1	0	0	0	0
Increment consumption at Maroon Bells-Snowmass Wilderness Area (federal Class I)					
Impact alone	0	0	0	0	0
Impact with Moon Lake Unit 1	0	0	0	0	0
Impact with all interrelated (other) sources	0	0	0	0	0
Increment consumption at Dinosaur National Monument (Colorado category I and potential federal Class I)					
Impact alone	1	0	0	0	0
Impact with Moon Lake Unit 1	3	0	0	0	0
Impact with all interrelated (other) sources	7	1	0	1	0

TABLE 6-4 (Concluded)

PSD Increments/Increment Consumption	SO_2 Concentration ($\mu g/m^3$)			TSP Concentration ($\mu g/m^3$)	
	3-Hour Average	24-Hour Average	Annual Average	24-Hour Average	Annual Average
Increment consumption at Colorado National Monument (Colorado category I and potential federal Class I)					
Impact alone	0	0	0	0	0
Impact with Moon Lake Unit 1	0	0	0	0	0
Impact with all interrelated (other) sources	0	0	0	0	0

TABLE 6-5. SUMMARY OF MAXIMUM AMBIENT AIR QUALITY IMPACTS OF MAGIC CIRCLE COMPARED WITH APPLICABLE STANDARDS

	Maximum Ground-Level Concentration ($\mu g/m^3$)					
Pollutant/Averaging Time	Baseline	Source Impact	Subtotal	Impact of Other Sources	Total	NAAQS* ($\mu g/m^3$)
Sulfur dioxide (SO_2)						
3-Hour	5	121	126	8	134	1300
24-hour	2	32	34	1	35	365
Annual	1	1	2	0	2	80
Total suspended particulate (TSP)						
24-Hour	84	< 32	< 116	2	< 118	150
Annual	19	< 4	< 23	0	< 23	60
Nitrogen dioxide (NO_2)						
Annual	1	6	7	0	7	100
Carbon monoxide (CO)						
1-Hour	7400	44	7444	0	7444	40,000
8-Hour	4500	44	4544	0	4544	10,000
Ozone (O_3)						
1-Hour	160	2	162	0	162	240

---

* National Ambient Air Quality Standards.

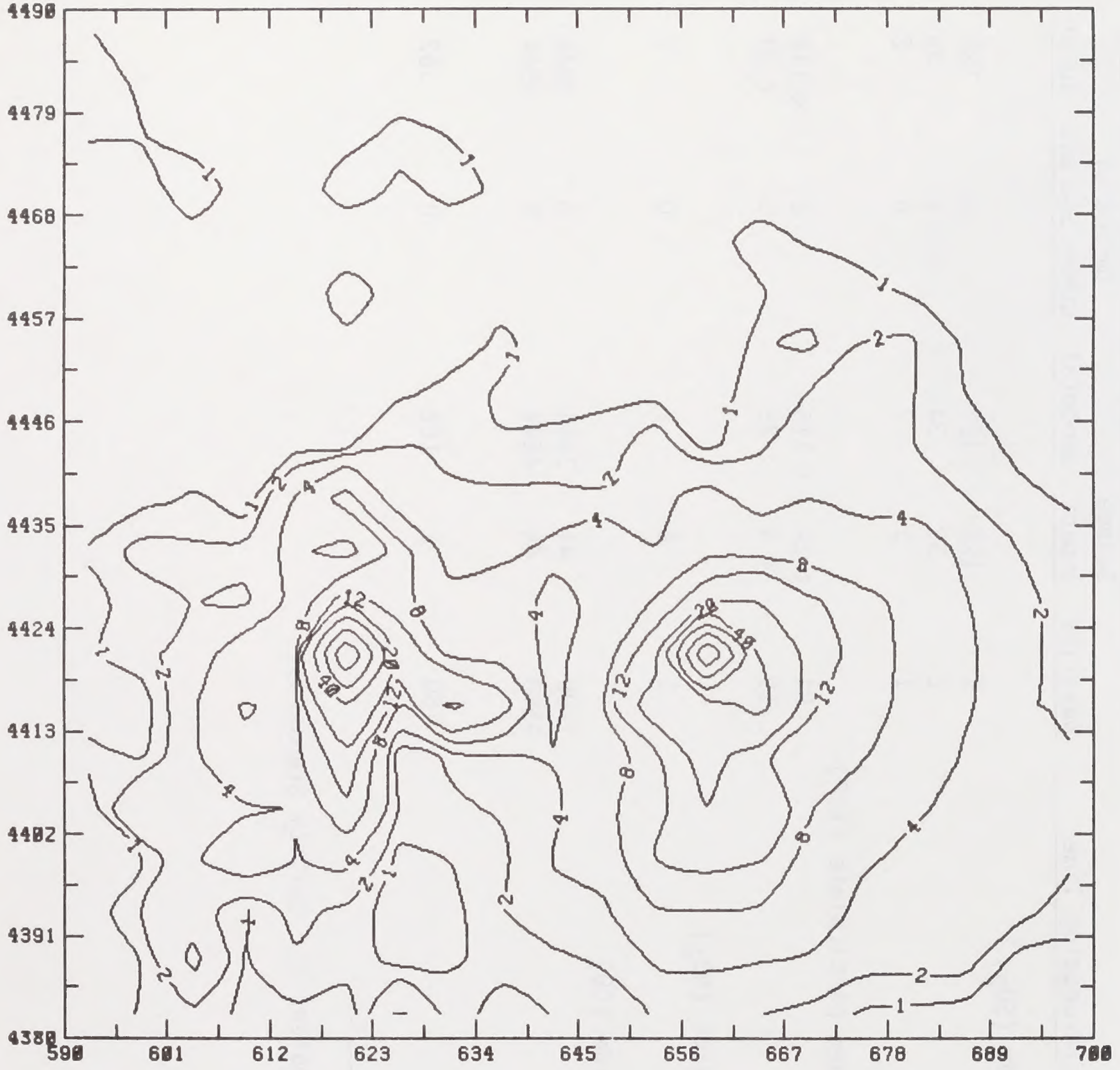

Maximum: 121 $\mu g/m^3$

(a) Maximum 3-Hour Average

FIGURE 6-3. GROUND-LEVEL SO_2 CONCENTRATIONS ($\mu g/m^3$) DUE TO MAGIC CIRCLE EMISSIONS

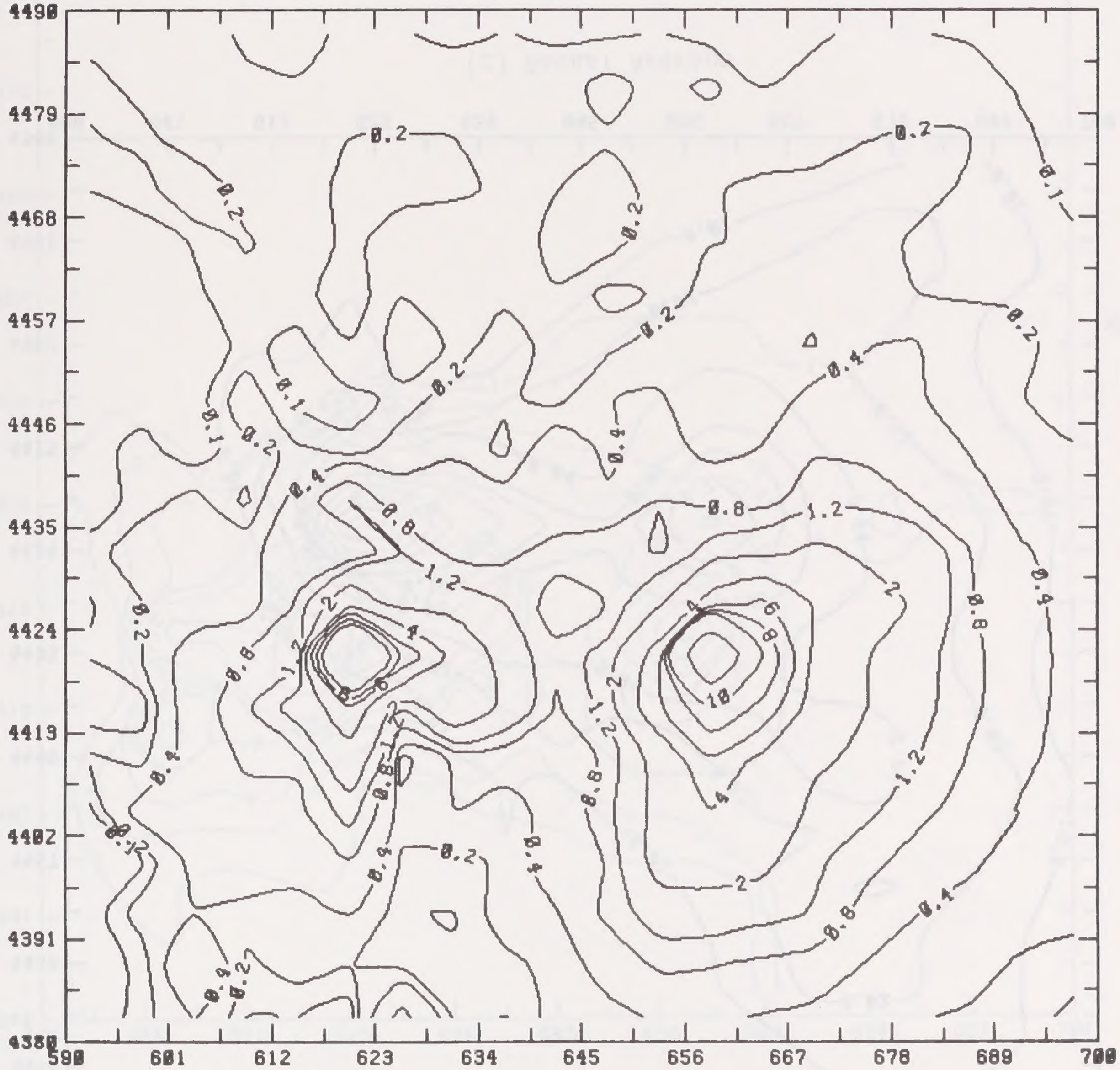

Maximum: 32 µg/m^3

(b) Maximum 24-Hour Average

FIGURE 6-3 (Continued)

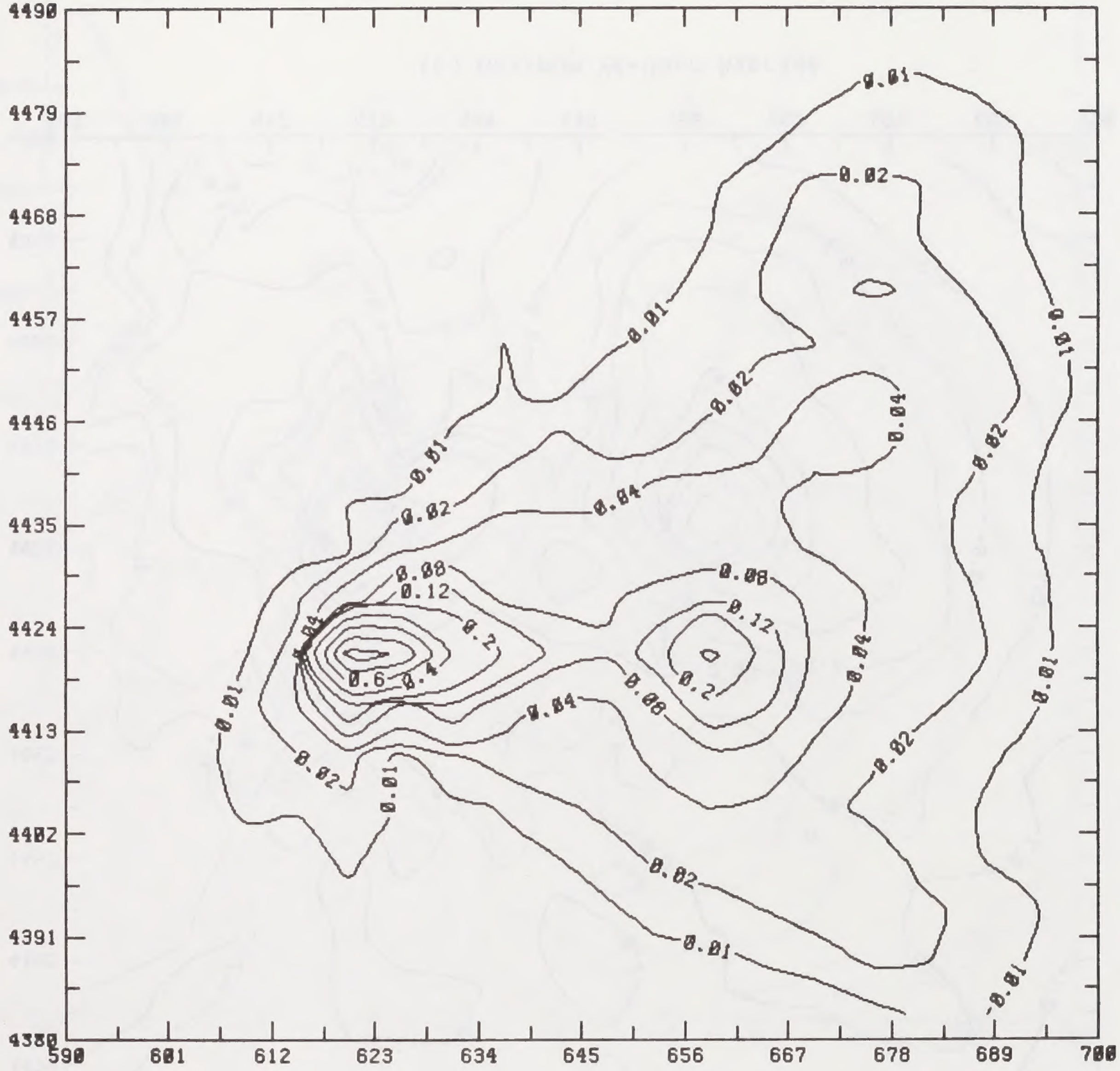

Maximum: 1.1 µg/m^3

(c) Annual Average

FIGURE 6-3 (Concluded)

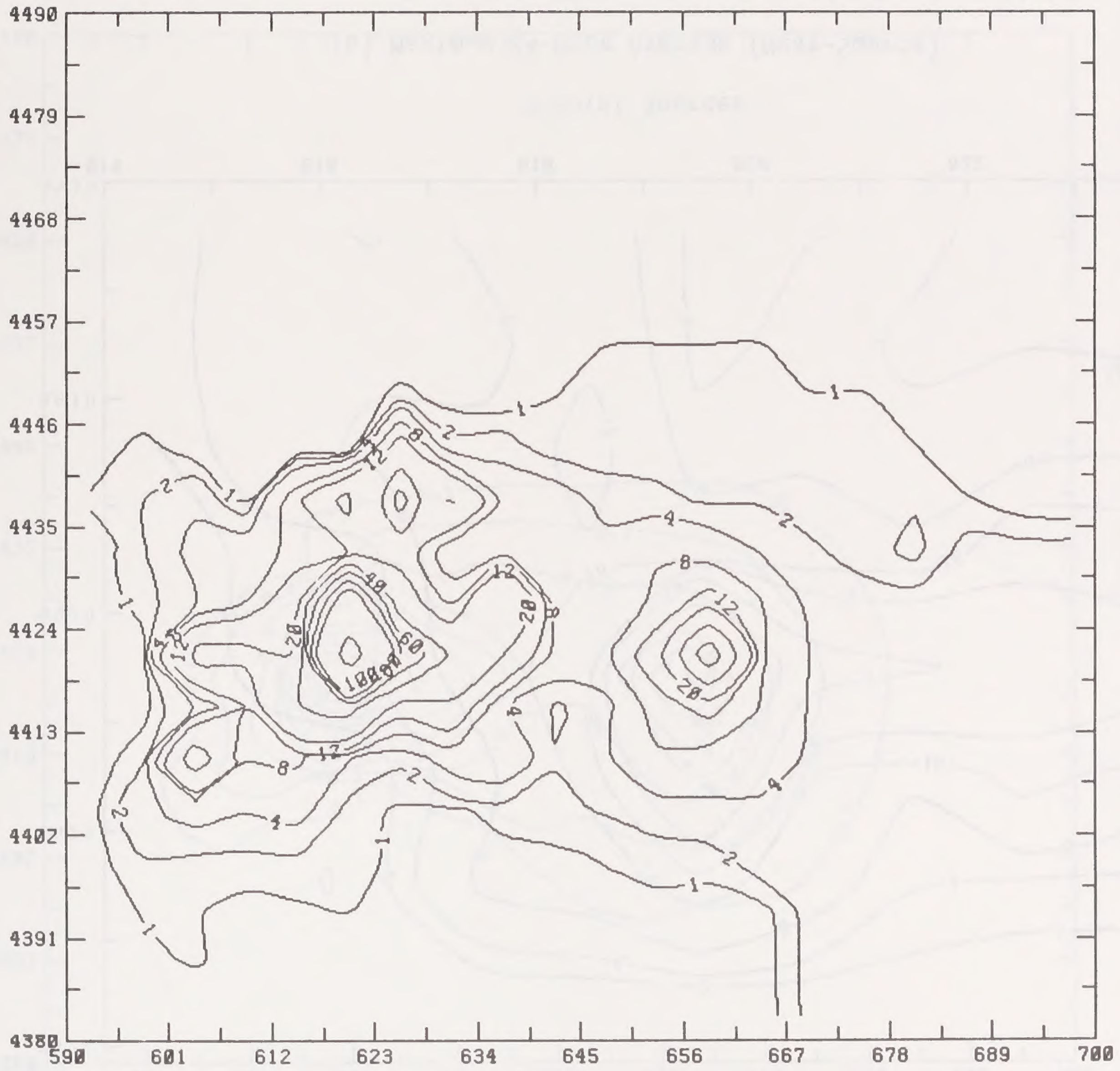

Maximum: 285 μg/m^3 (on-site)
<32 μg/m^3 (off-site)

Note: These GPM results are overly conservative near the source because of source emission aggregation; see COMPLEX-I results in Figure 6-4(b).

(a) Maximum 24-Hour Average

FIGURE 6-4. GROUND-LEVEL TSP CONCENTRATIONS (μg/m^3) DUE TO MAGIC CIRCLE EMISSIONS

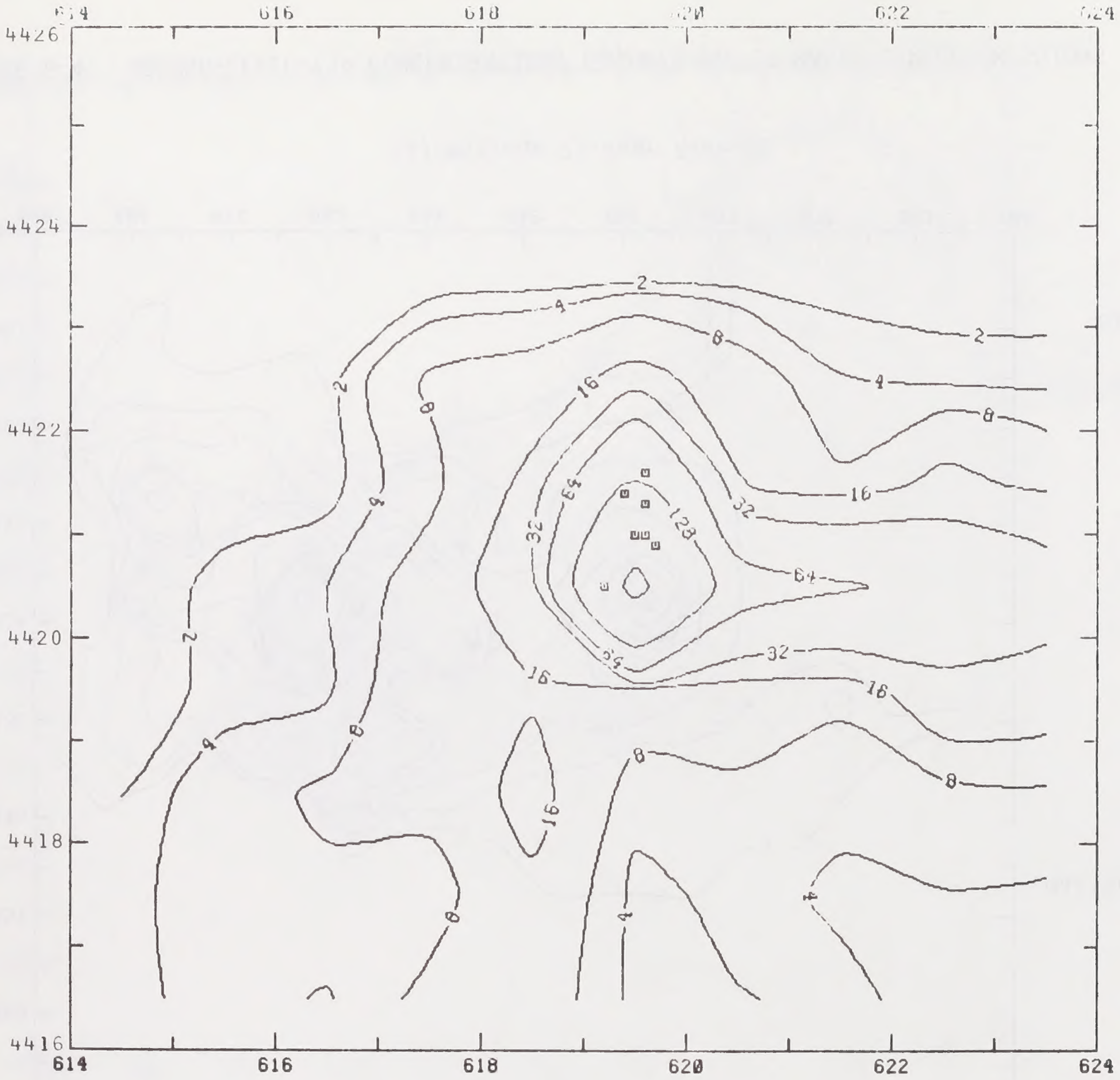

⊡ Point Sources

(b) Maximum 24-Hour Average (Near-Source)

FIGURE 6-4 (Continued)

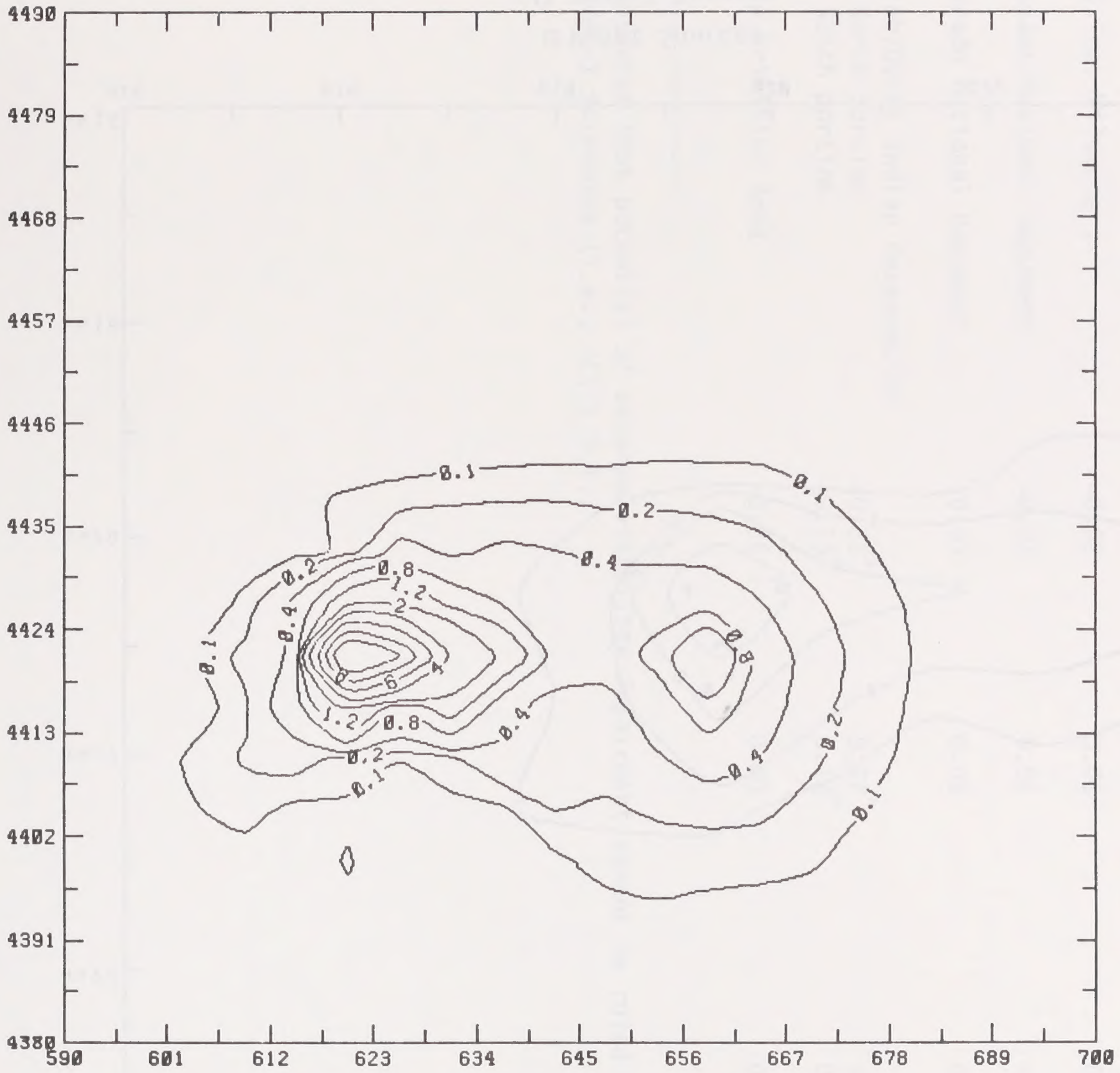

Maximum: 27 μg/m^3 (on-site)
<4 μg/m^3 (off-site)

Note: These GPM results are overly conservative near the source because of source emission aggregation; see COMPLEX-I results in Figure 6-4(d).

(c) Annual Average

FIGURE 6-4 (Continued)

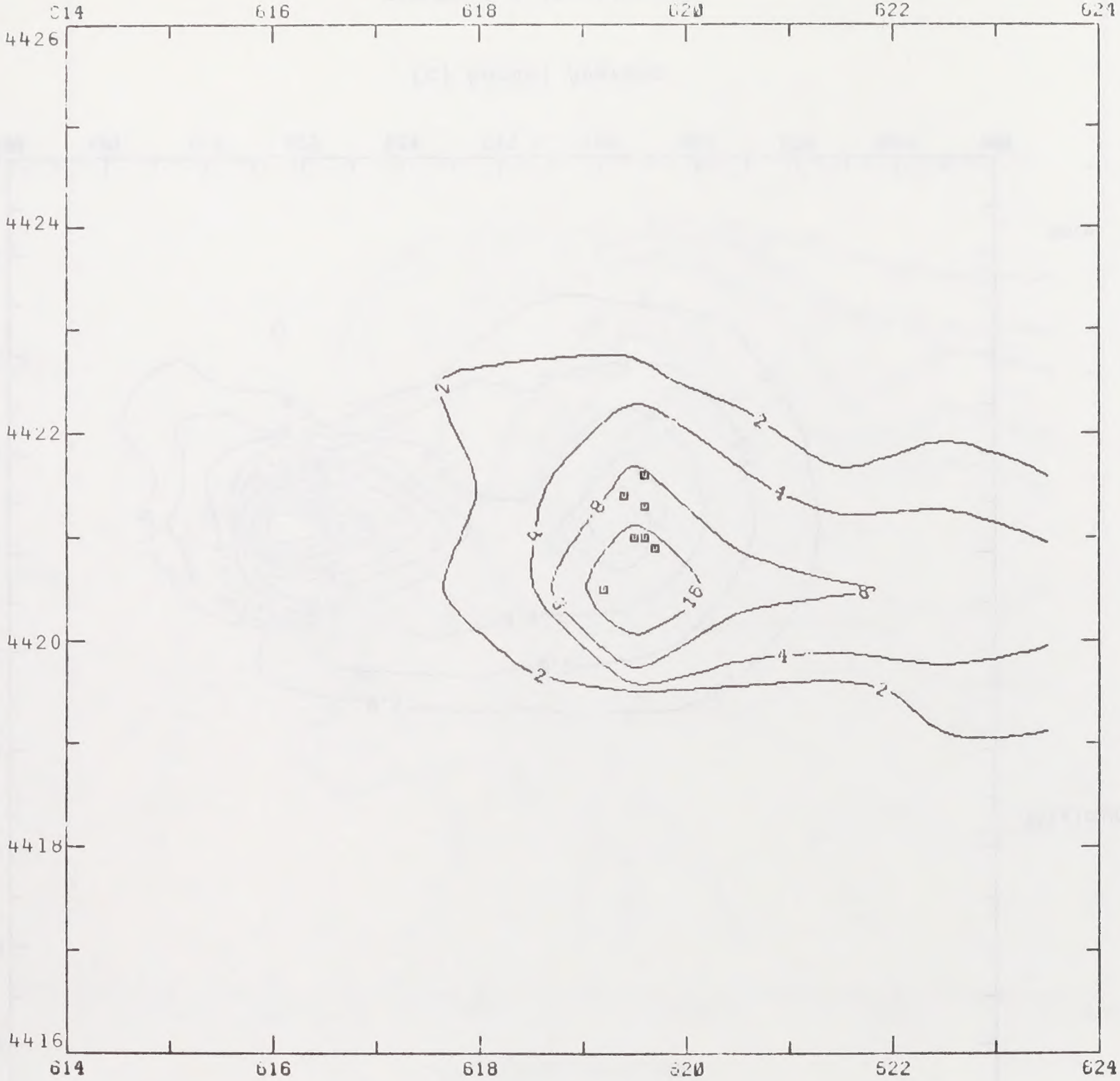

⊡ Point Sources

(d) Annual Average

FIGURE 6-4 (Concluded)

TABLE 6-6. LEVEL-1 SCREENING ANALYSIS RESULTS FOR VISIBILITY IMPACTS OF MAGIC CIRCLE

Existing or Potential Class I Area or Area of Special Concern	Test for Dark Plume Against Sky C_1	Test for Light Plume Against Terrain C_2	Test for Regional Reduction Sky/Terrain Contrast C_3
Flat Tops Wilderness	-0.02	0.01	0.01
Dinosaur National Monument	-0.07	0.05	0.01
Colorado National Monument	-0.03	0.02	0.01
Uintah/Ouray Indian Reservation			
- North portion	-0.32*	0.37*	0.01
- South portion	-0.13*	0.12*	0.01
Uinta Primitive Area	-0.04	0.03	0.01

---

* Indicates that potential of adverse visibility impairment cannot be ruled out by Level-1 screening (i.e., |C| > 0.1).

6.3 PARAHO

The proposed Paraho oil shale facility would produce 42,000 barrels per day and would be located just north of the confluence of Evacuation Creek and the White River at 5400 feet MSL. Drainage flows in the area are easterly, while general prevailing flows are westerly. Maximum ground-level impacts are predicted to the east of the facility.

Tables 6-7 and 6-8 and figures 6-5 and 6-6 summarize the impacts, which are well within criteria. On-site TSP concentrations are above PSD increments, but off-site concentrations are well within the increments. Given the results of the EPA Level-1 visibility screening test, there is no possibility of adverse visibility impairment occurring as a result of Paraho emissions in any mandatory or potential Class I areas (see table 6-9).

6.4 SYNTANA-UTAH

Syntana-Utah is a proposed 57,000 barrel-per-day oil shale facility to be located just north of the White River at 5800 feet MSL.

Tables 6-10 snd 6-11 and figures 6-7 and 6-8 summarize the projected air quality impacts, which are well within criteria. Although the Gaussian Puff Model (GPM) indicates that maximum 24-hour-average TSP concentrations near the source are greater than 60 $\mu g/m^3$, the more realistic COMPLEX model, with distributed point source treatment, indicates a maximum of 13 $\mu g/m^3$, a factor of 5 less than the GPM result. The EPA Level-1 visibility screening test indicates that the possibility of adverse visibility impairment due to Syntana emissions can be ruled out in all mandatory and potential Class I areas, except Dinosaur National Monument. In this area the screening test indicates that a particulate and NO_x plume might be visible from Dinosaur during stable, light-wind conditions a few times per year (see table 6-12). This was confirmed with the analysis presented in Section 5.6, which indicated that plume discoloration would be observed between 0 and 15 mornings per year in Dinosaur.

6.5 TOSCO

Tosco proposes to produce 45,000 barrels of shale oil per day at a facility located at 5000 feet MSL, south of the White River and east of the Green River.

TABLE 6-7. SUMMARY OF PSD INCREMENT CONSUMPTION BY PARAHO

	SO_2 Concentration ($\mu g/m^3$)			TSP Concentration ($\mu g/m^3$)	
PSD Increments/Increment Consumption	3-Hour Average	24-Hour Average	Annual Average	24-Hour Average	Annual Average
Class II Areas					
Allowable PSD Class II increment	512	91	20	37	19
Increment consumption at receptors of maximum impacts					
Impact alone	317	40	1	<16	<4
Impact with Moon Lake Unit 1	319	40	1	<16	<4
Impact with all interrelated (other) sources	322	41	1	<25	<5
Maximum increment consumption on Uintah/Ouray Indian Reservation					
Impact alone	4	1	0	4	0
Impact with Moon Lake Unit 1	10	2	0	5	0
Impact with all interrelated (other) sources	18	4	0	7	0
Maximum increment consumption in Colorado					
Impact alone	26	4	0	12	1
Class I Areas					
Allowable PSD Class I increment	25	5	2	10	5
Increment consumption at Flat Tops Wilderness Area (federal Class I)					
Impact alone	0	0	0	0	0
Impact with Moon Lake Unit 1	0	0	0	0	0
Impact with all interrelated (other) sources	1	0	0	0	0
Increment consumption at Maroon Bells-Snowmass Wilderness Area (federal Class I)					
Impact alone	0	0	0	0	0
Impact with Moon Lake Unit 1	0	0	0	0	0
Impact with all interrelated (other) sources	0	0	0	0	0
Increment consumption at Dinosaur National Monument (Colorado category I and potential federal Class I)					
Impact alone	4	0	0	0	0
Impact with Moon Lake Unit 1	6	0	0	0	0
Impact with all interrelated (other) sources	10	1	0	1	0

TABLE 6-7 (Concluded)

PSD Increments/Increment Consumption	SO_2 Concentration ($\mu g/m^3$) 3-Hour Average	SO_2 Concentration ($\mu g/m^3$) 24-Hour Average	SO_2 Concentration ($\mu g/m^3$) Annual Average	TSP Concentration ($\mu g/m^3$) 24-Hour Average	TSP Concentration ($\mu g/m^3$) Annual Average
Increment consumption at Colorado National Monument (Colorado category I and potential federal Class I)					
Impact alone	0	0	0	0	0
Impact with Moon Lake Unit 1	0	0	0	0	0
Impact with all interrelated (other) sources	0	0	0	0	0

TABLE 6-8. SUMMARY OF MAXIMUM AMBIENT AIR QUALITY IMPACTS OF PARAHO COMPARED WITH APPLICABLE STANDARDS

	Maximum Ground-Level Concentration ($\mu g/m^3$)					
Pollutant/Averaging Time	Baseline	Source Impact	Subtotal	Impact of Other Sources	Total	NAAQS* ($\mu g/m^3$)
Sulfur dioxide (SO_2)						
3-Hour	16	317	333	5	338	1300
24-hour	9	40	49	1	50	365
Annual	1	1	2	0	2	80
Total suspended particulate (TSP)						
24-Hour	127	< 16	< 143	9	< 152	150
Annual	20	< 4	< 24	1	< 25	60
Nitrogen dioxide (NO_2)						
Annual	2	3	5	0	5	100
Carbon monoxide (CO)						
1-Hour	2500	125	2625	2	2627	40,000
8-Hour	1500	125	1625	2	1627	10,000
Ozone (O_3)						
1-Hour	143	2	145	0	145	240

---

* National Ambient Air Quality Standards.

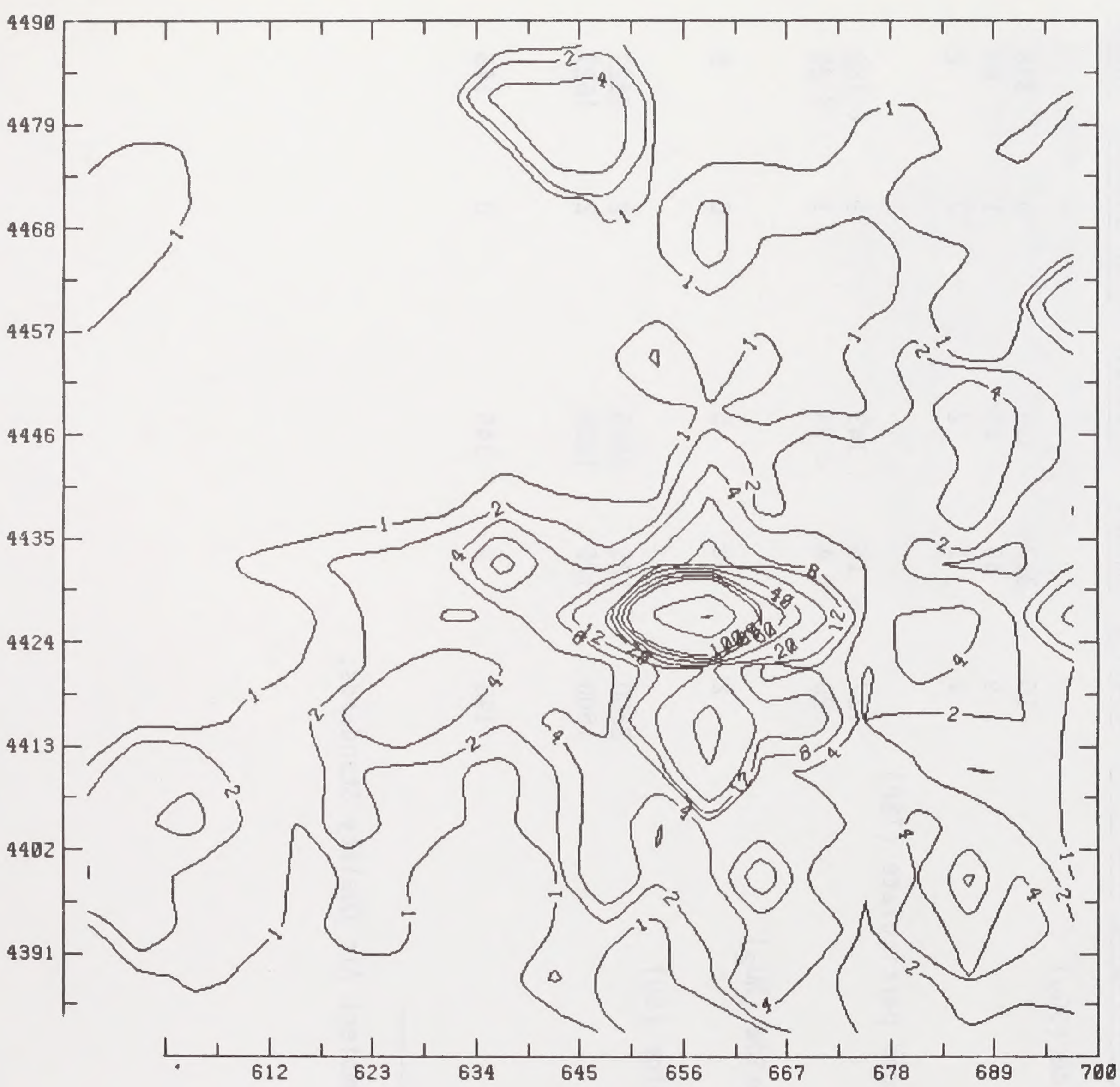

Maximum: 317 μg/m^3

(a) Maximum 3-Hour Average

FIGURE 6-5. GROUND-LEVEL SO_2 CONCENTRATIONS (μg/m^3) DUE TO PARAHO EMISSIONS

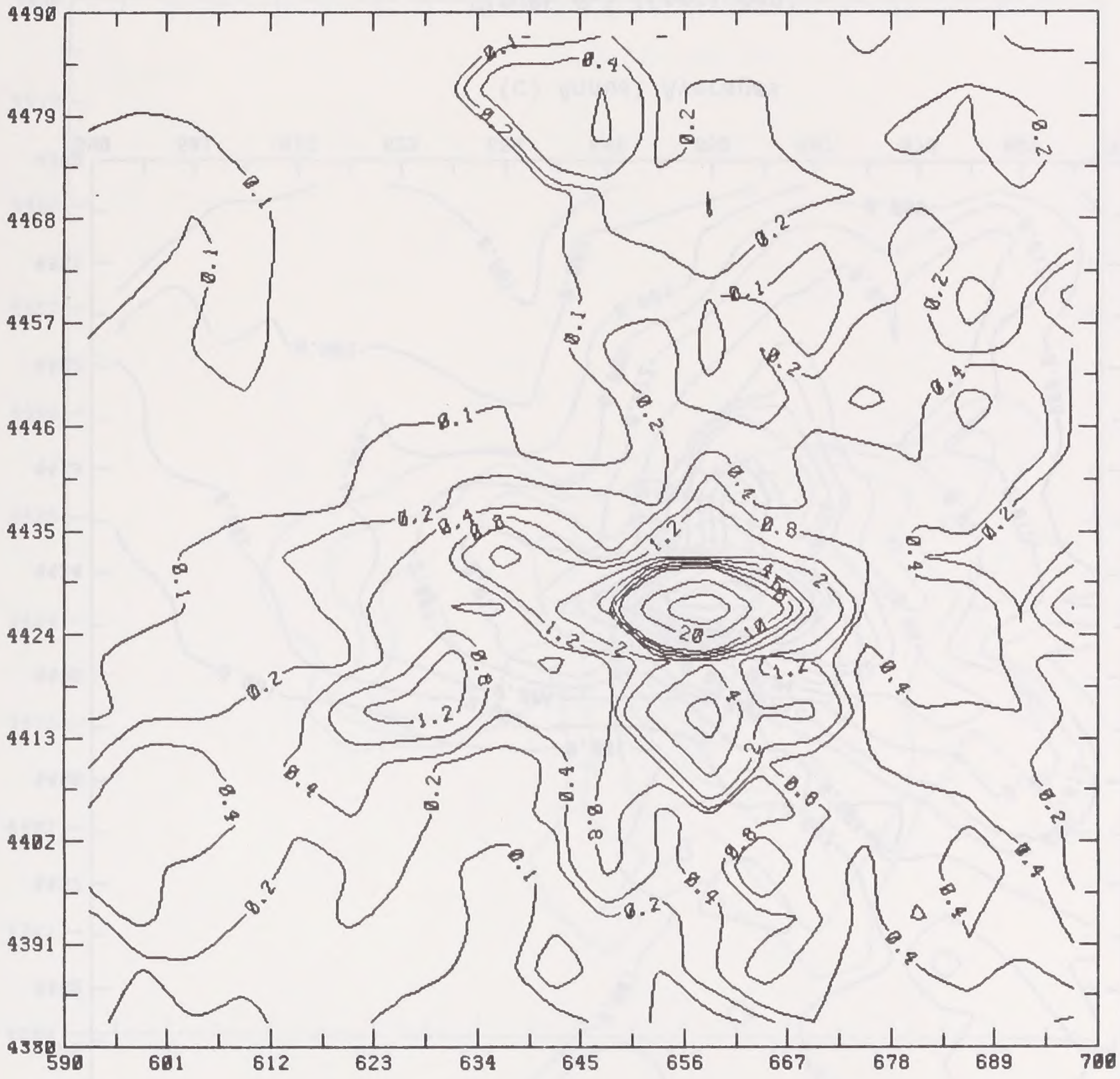

Maximum: 40 μg/m^3

(b) Maximum 24-Hour Average

FIGURE 6-5 (Continued)

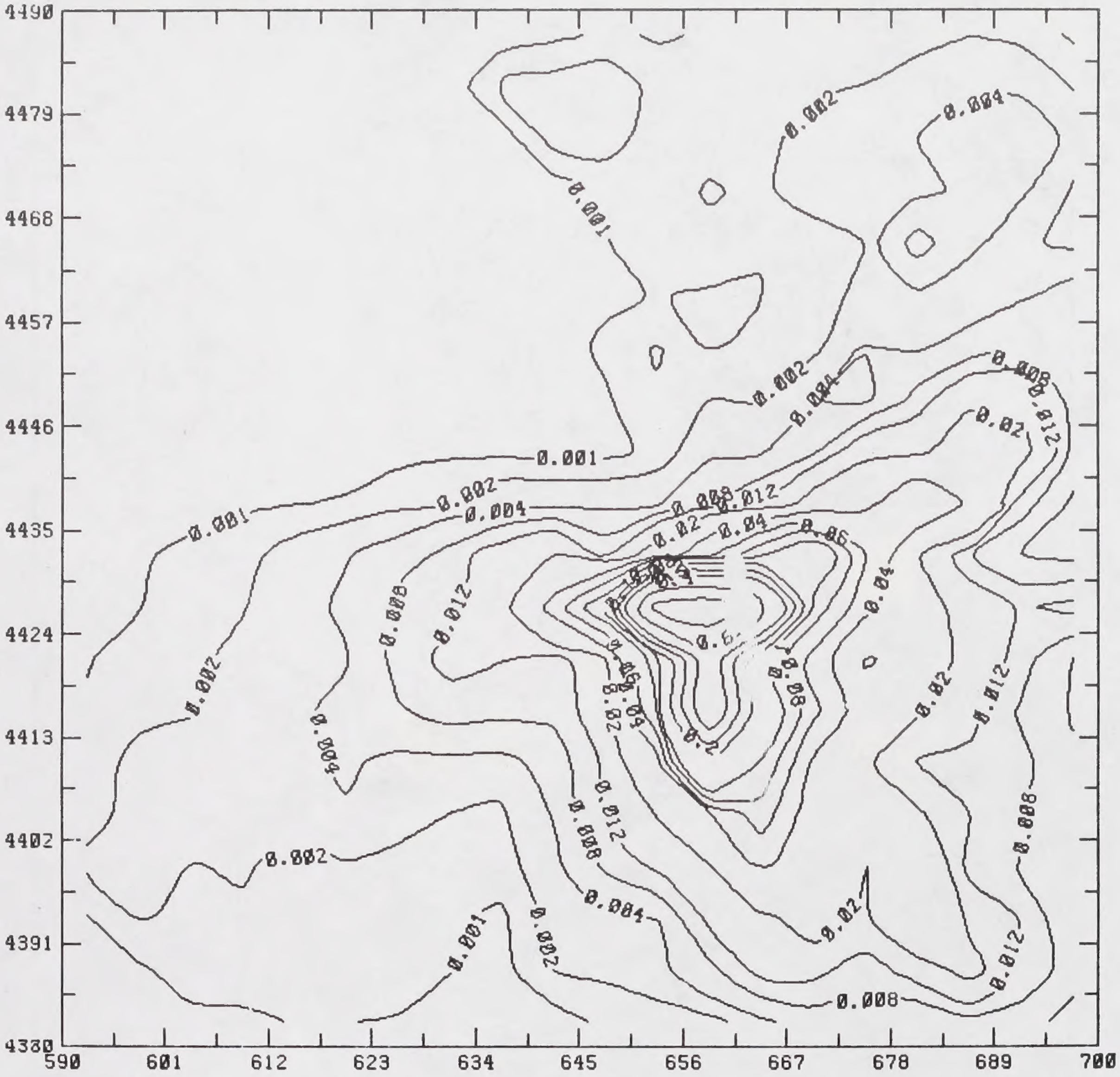

Maximum: 1.0 µg/m^3

(c) Annual Averages

FIGURE 6-5 (Concluded)

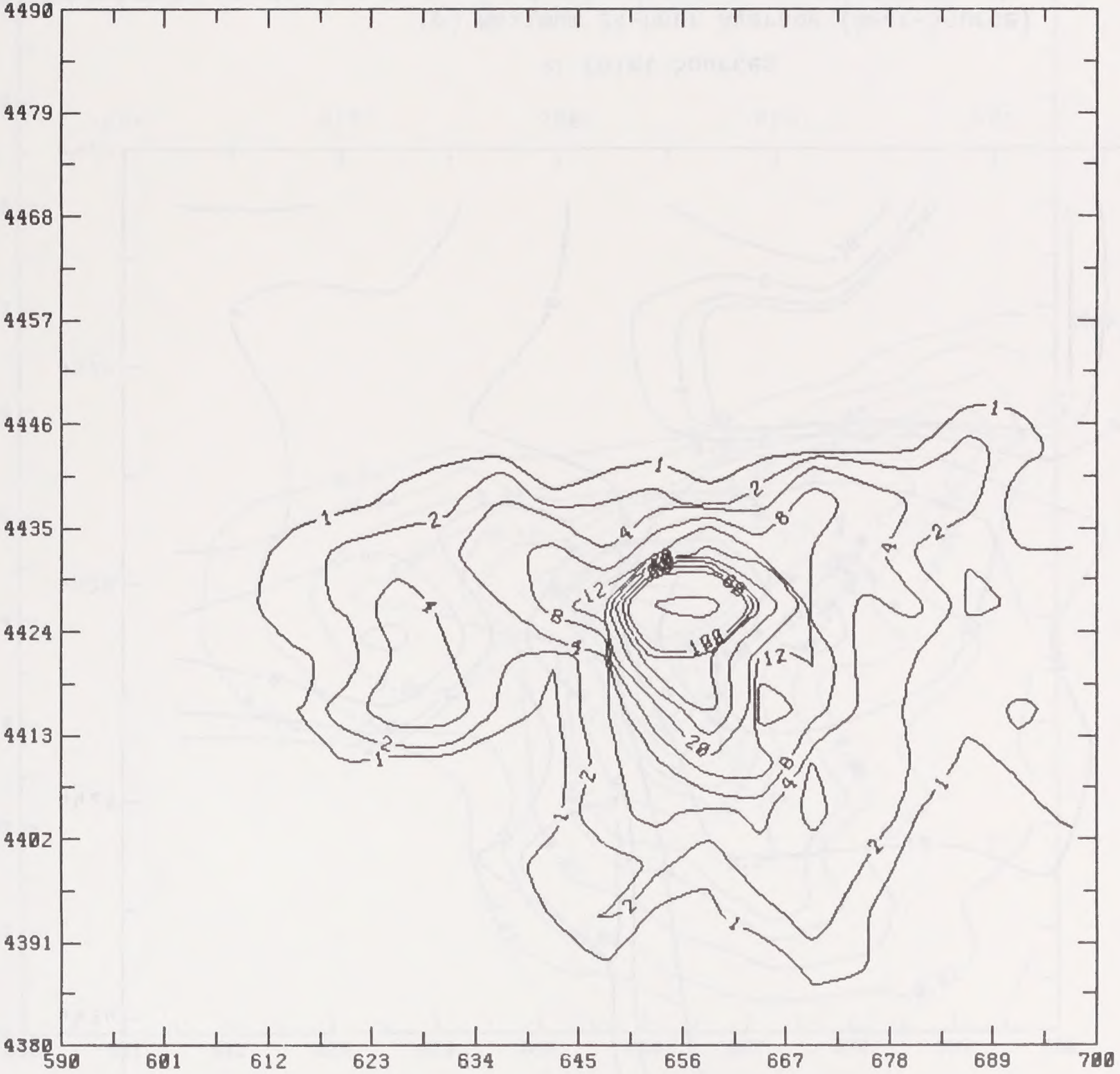

Maximum: 69 μg/m^3 (on-site)
<16 μg/m^3 (off-site)

Note: These GPM results are overly conservative near the source because of source emission aggregation; see COMPLEX-I results in Figure 6-6(b).

(a) Maximum 24-Hour Average

FIGURE 6-6. GROUND-LEVEL TSP CONCENTRATIONS (μg/m^3) DUE TO PARAHO EMISSIONS

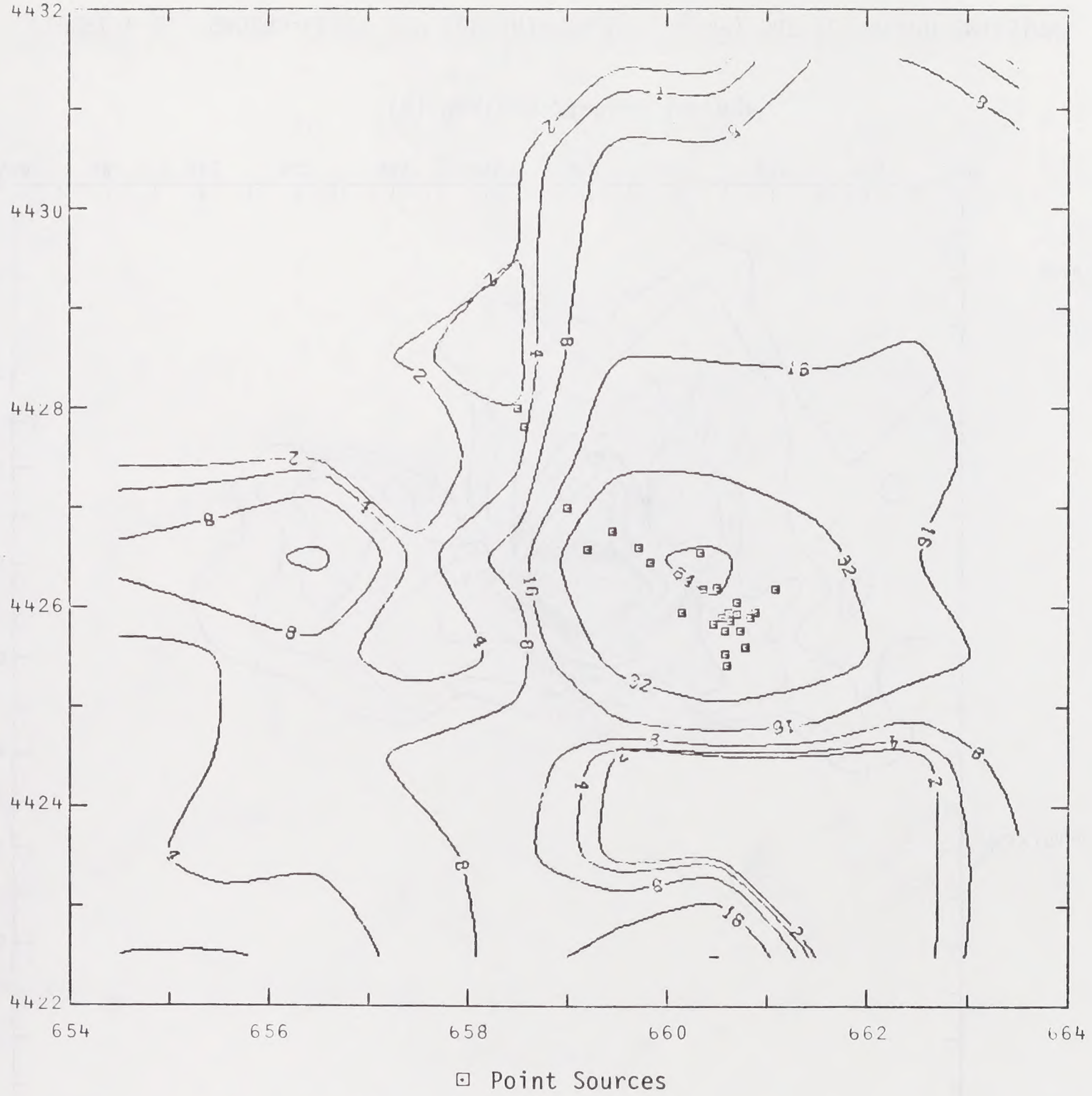

(b) Maximum 24-Hour Average (Near-Source)

FIGURE 6-6 (Continued)

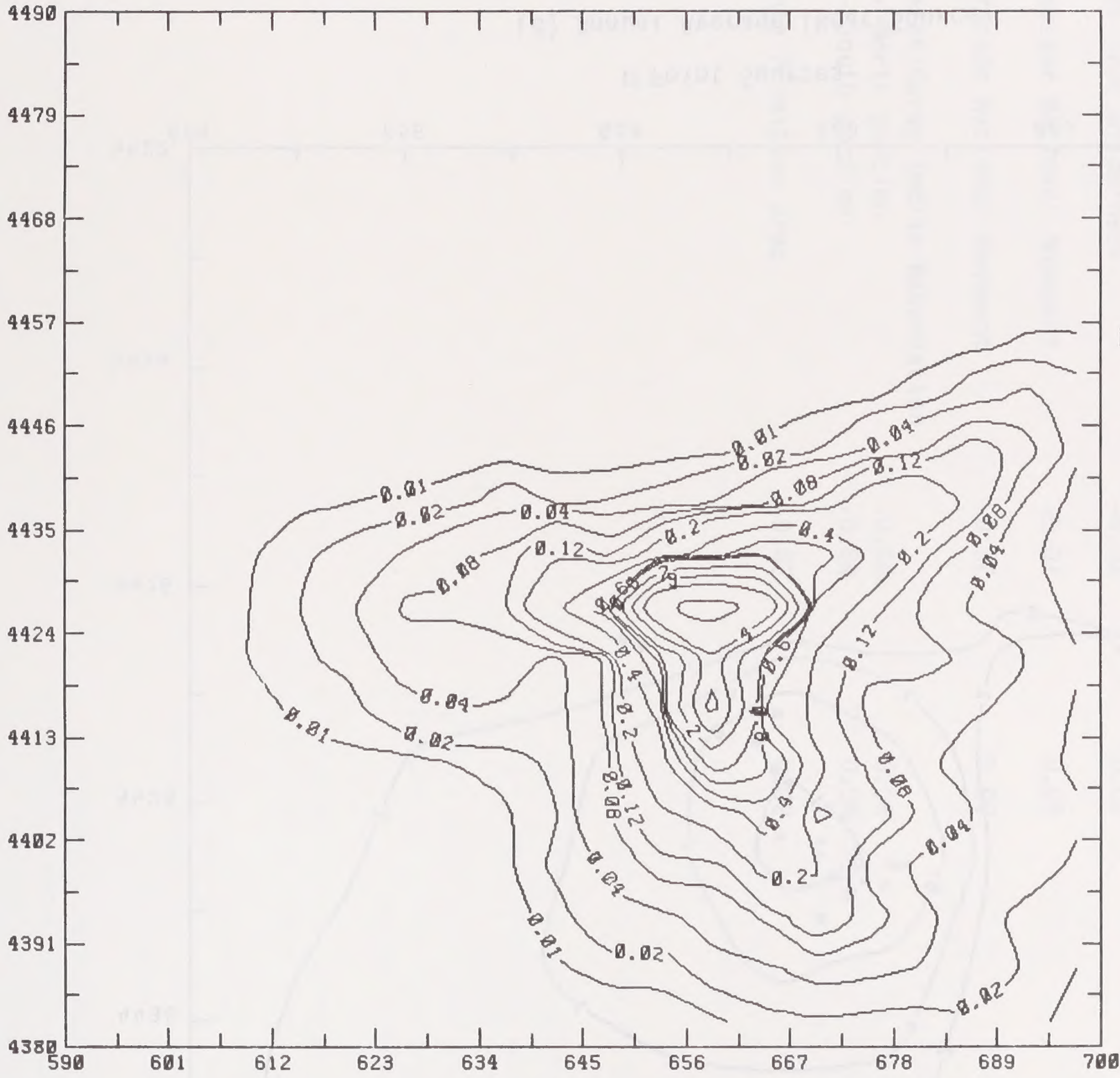

Maximum: 19 µg/m^3 (on-site)
<4 µg/m^3 (off-site)

Note: These GPM results are overly conservative near the source because of source emission aggregation; see COMPLEX-I results in Figure 6-6(d).

(c) Annual Average

FIGURE 6-6 (Continued)

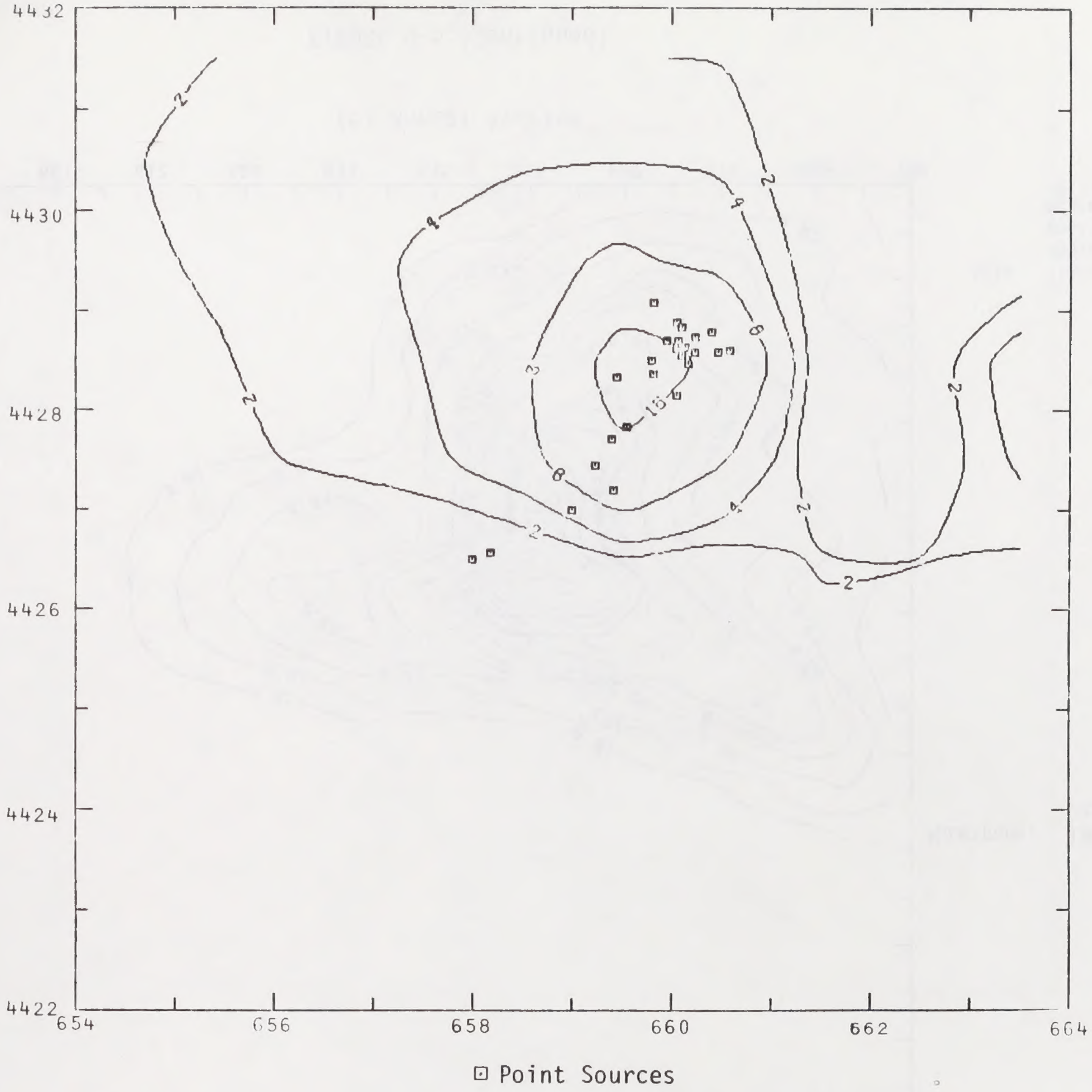

(d) Annual Average (Near-Source)

FIGURE 6-6 (Concluded)

TABLE 6-9. LEVEL-1 SCREENING ANALYSIS RESULTS FOR VISIBILITY IMPACTS OF PARAHO

Existing or Potential Class I Area or Area of Special Concern	Test for Dark Plume Against Sky C_1	Test for Light Plume Against Terrain C_2	Test for Regional Reduction Sky/Terrain Contrast C_3
Flat Tops Wilderness	-0.02	0.01	0.01
Dinosaur National Monument	-0.07	0.09	0.01
Colorado National Monument	-0.02	0.02	0.01
Uintah/Ouray Indian Reservation			
- North portion	-0.06	0.06	0.01
- South portion	-0.04	0.04	0.01
Uinta Primitive Area	-0.02	0.02	0.01

TABLE 6-10. SUMMARY OF PSD INCREMENT CONSUMPTION BY SYNTANA

	SO_2 Concentration ($\mu g/m^3$)			TSP Concentration ($\mu g/m^3$)	
PSD Increments/Increment Consumption	3-Hour Average	24-Hour Average	Annual Average	24-Hour Average	Annual Average
Class II Areas					
Allowable PSD Class II increment	512	91	20	37	19
Increment consumption at receptors of maximum impacts					
Impact alone	41	8	1	13	1
Impact with Moon Lake Unit 1	44	8	1	13	1
Impact with all interrelated (other) sources	47	9	1	18	1
Maximum increment consumption on Uintah/Ouray Indian Reservation					
Impact alone	8	1	0	<13	0
Impact with Moon Lake Unit 1	14	2	0	<14	0
Impact with all interrelated (other) sources	22	4	0	<16	0
Maximum increment consumption in Colorado					
Impact alone	15	2	0	13	1
Class I Areas					
Allowable PSD Class I increment	25	5	2	10	5
Increment consumption at Flat Tops Wilderness Area (federal Class I)					
Impact alone	0	0	0	0	0
Impact with Moon Lake Unit 1	0	0	0	0	0
Impact with all interrelated (other) sources	1	0	0	0	0
Increment consumption at Maroon Bells-Snowmass Wilderness Area (federal Class I)					
Impact alone	0	0	0	0	0
Impact with Moon Lake Unit 1	0	0	0	0	0
Impact with all interrelated (other) sources	0	0	0	0	0
Increment consumption at Dinosaur National Monument (Colorado category I and potential federal Class I)					
Impact alone	1	0	0	0	0
Impact with Moon Lake Unit 1	3	0	0	0	0
Impact with all interrelated (other) sources	7	1	0	1	0

TABLE 6-10 (Concluded)

PSD Increments/Increment Consumption	SO_2 Concentration ($\mu g/m^3$) 3-Hour Average	SO_2 Concentration ($\mu g/m^3$) 24-Hour Average	SO_2 Concentration ($\mu g/m^3$) Annual Average	TSP Concentration ($\mu g/m^3$) 24-Hour Average	TSP Concentration ($\mu g/m^3$) Annual Average
Increment consumption at Colorado National Monument (Colorado category I and potential federal Class I)					
Impact alone	0	0	0	0	0
Impact with Moon Lake Unit 1	0	0	0	0	0
Impact with all interrelated (other) sources	0	0	0	0	0

TABLE 6-11. SUMMARY OF MAXIMUM AMBIENT AIR QUALITY IMPACTS OF SYNTANA COMPARED WITH APPLICABLE STANDARDS

Pollutant/Averaging Time	Maximum Ground-Level Concentration ($\mu g/m^3$) Baseline	Source Impact	Subtotal	Impact of Other Sources	Total	NAAQS* ($\mu g/m^3$)
Sulfur dioxide (SO_2)						
3-Hour	16	41	57	6	63	1300
24-Hour	9	8	17	1	18	365
Annual	1	1	2	0	2	80
Total suspended particulate (TSP)						
24-Hour	127	13	140	5	145	150
Annual	20	1	21	0	21	60
Nitrogen dioxide (NO_2)						
Annual	2	6	8	0	8	100
Carbon monoxide (CO)						
1-Hour	2500	20	2520	0	2520	40,000
8-Hour	1500	20	1520	0	1520	10,000
Ozone (O_3						
1-Hour	143	2	72	0	72	240

---

* National Ambient Air Quality Standards.

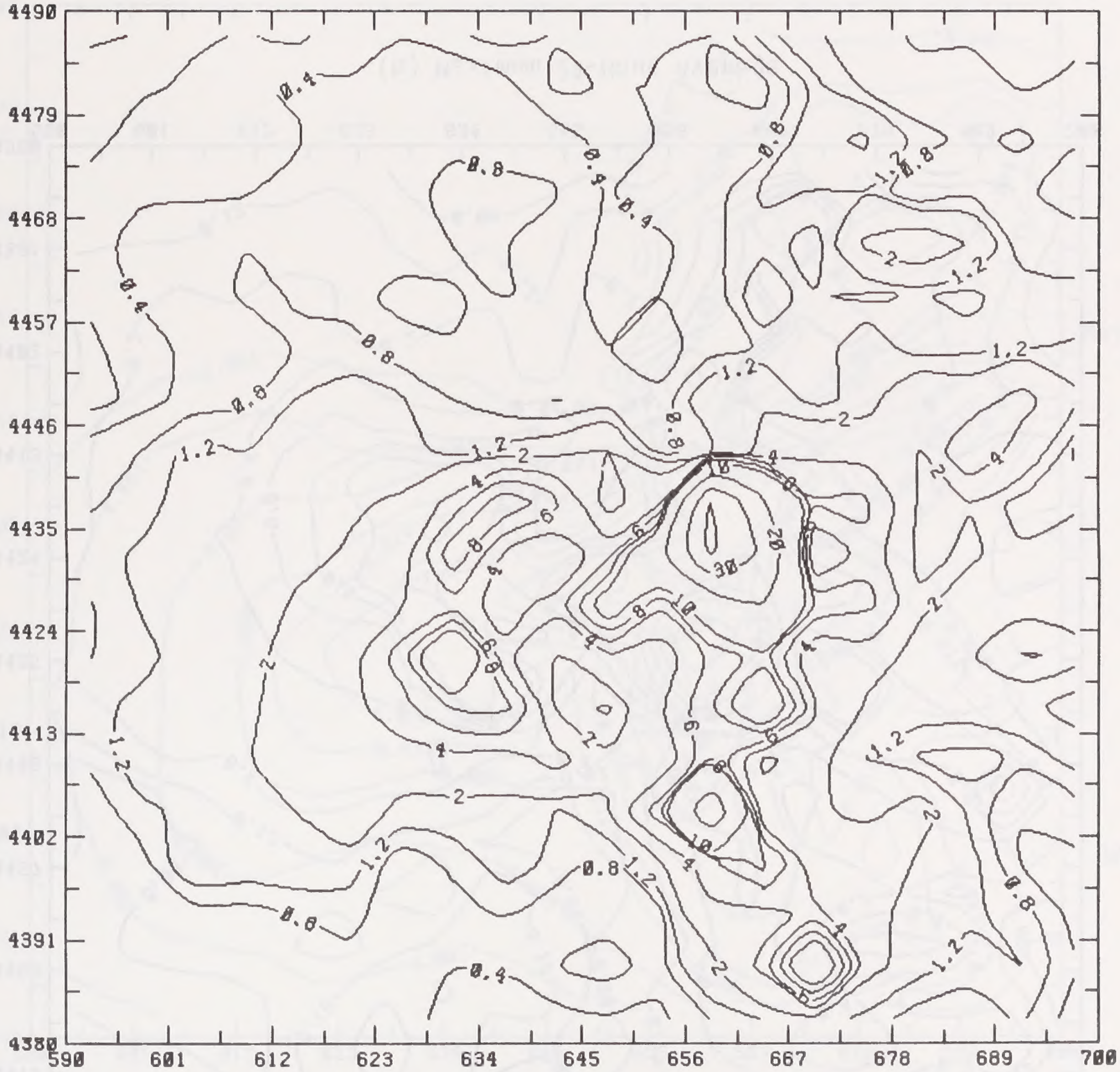

Maximum: 41 $\mu g/m^3$

(a) Maximum 3-Hour Average

FIGURE 6-7. GROUND-LEVEL SO_2 CONCENTRATIONS ($\mu g/m^3$) DUE TO SYNTANA-UTAH EMISSIONS

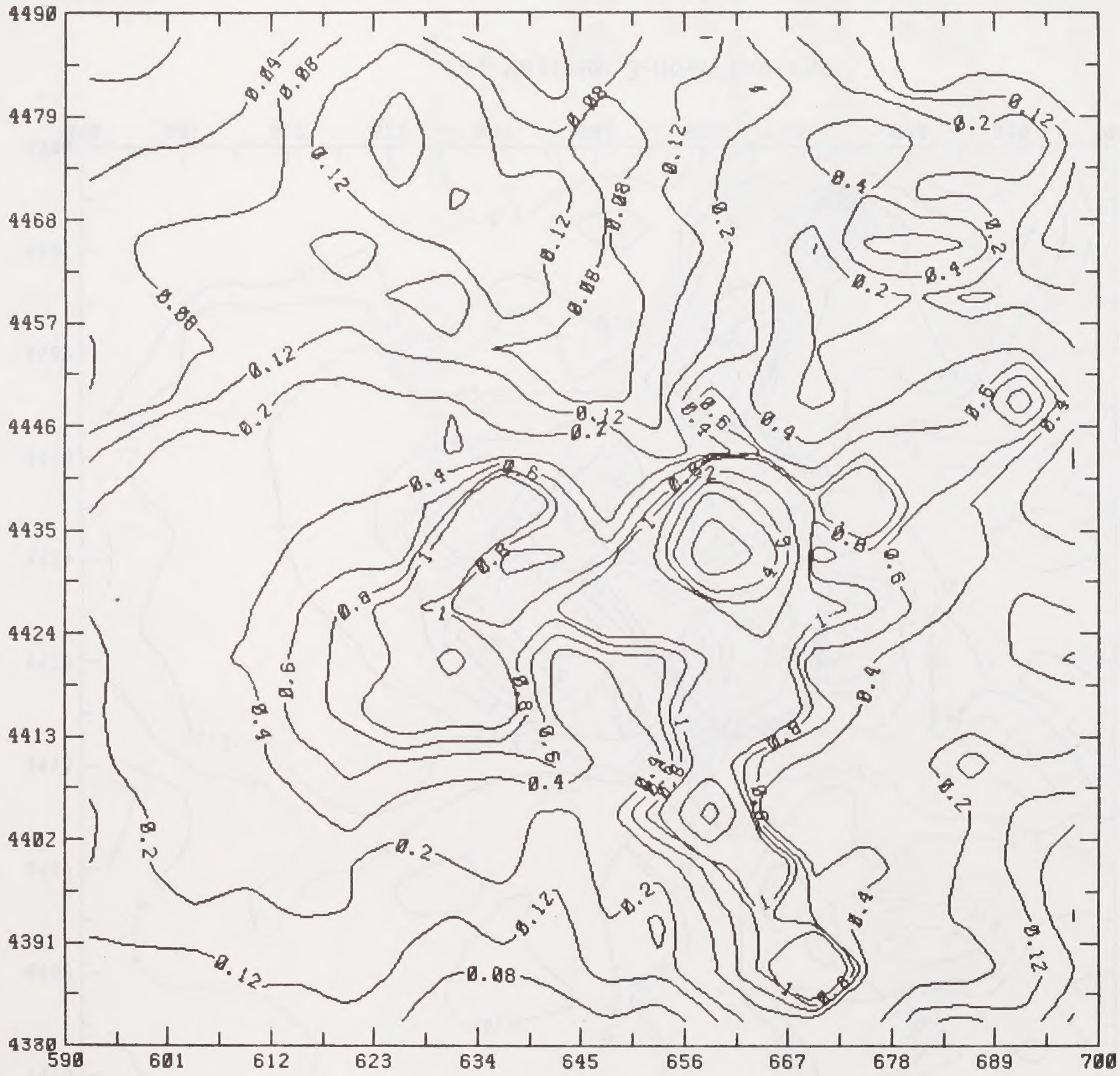

Maximum: 8 µg/m^3

(b) Maximum 24-Hour Average

FIGURE 6-7 (Continued)

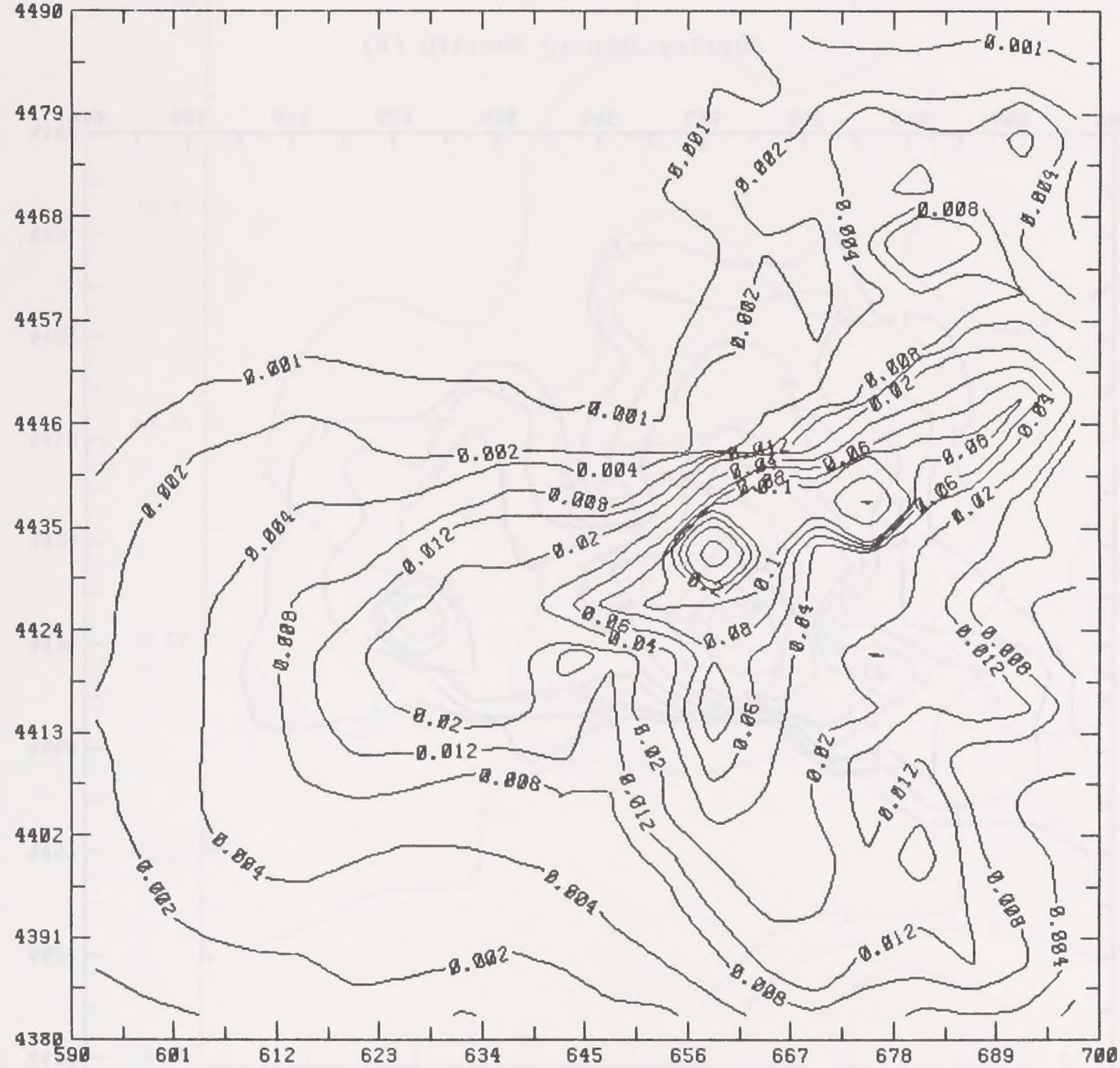

Maximum: 0.8 µg/m^3

(c) Annual Average

FIGURE 6-7 (Concluded)

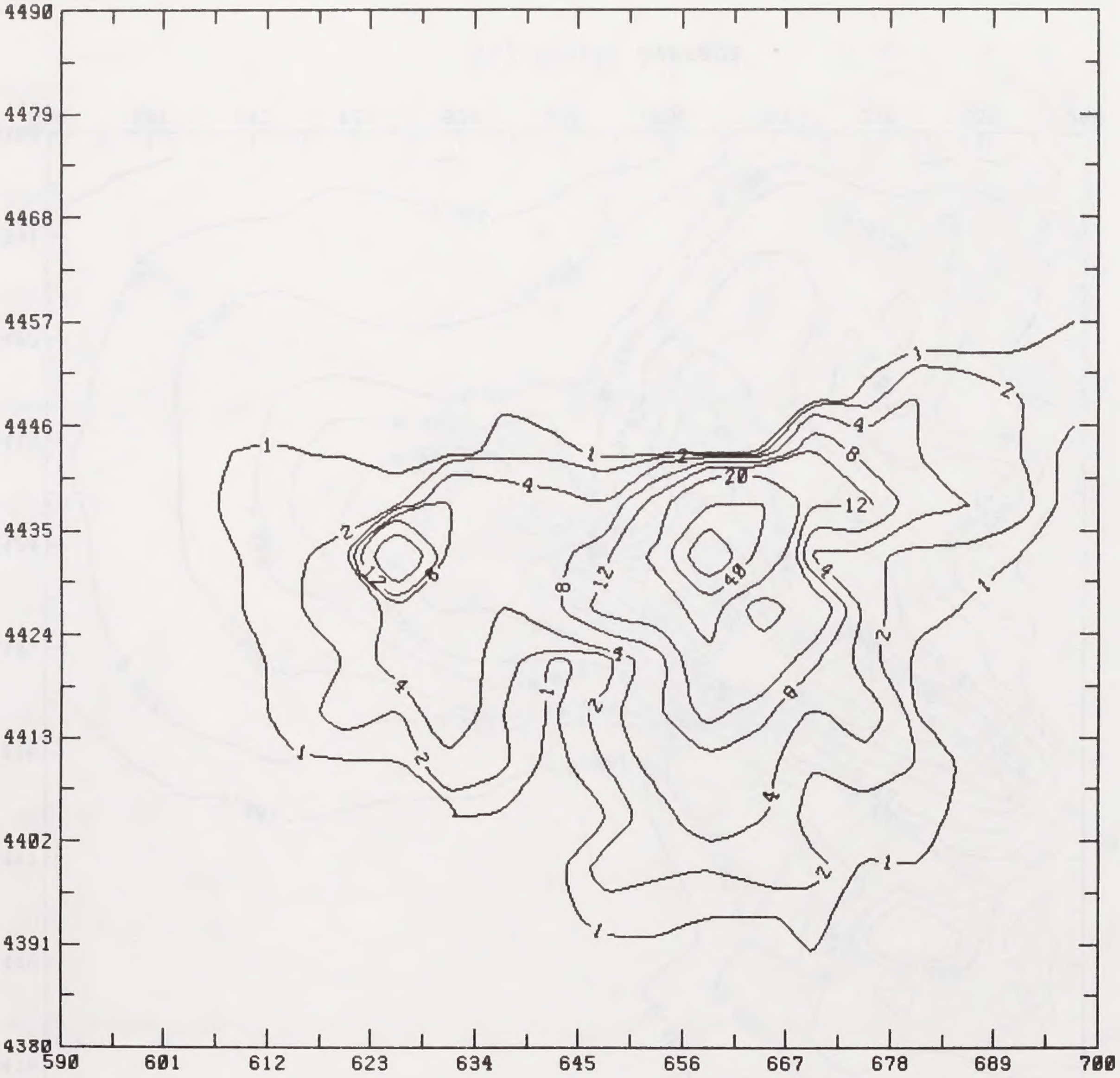

Maximum: 13 μg/m^3

Note: These GPM results are overly conservative near the source because of source emission aggregation; see COMPLEX-I results in Figure 6-8(b).

(a) Maximum 24-Hour Average

FIGURE 6-8. GROUND-LEVEL TSP CONCENTRATIONS (μg/m^3) DUE TO SYNTANA-UTAH EMISSIONS

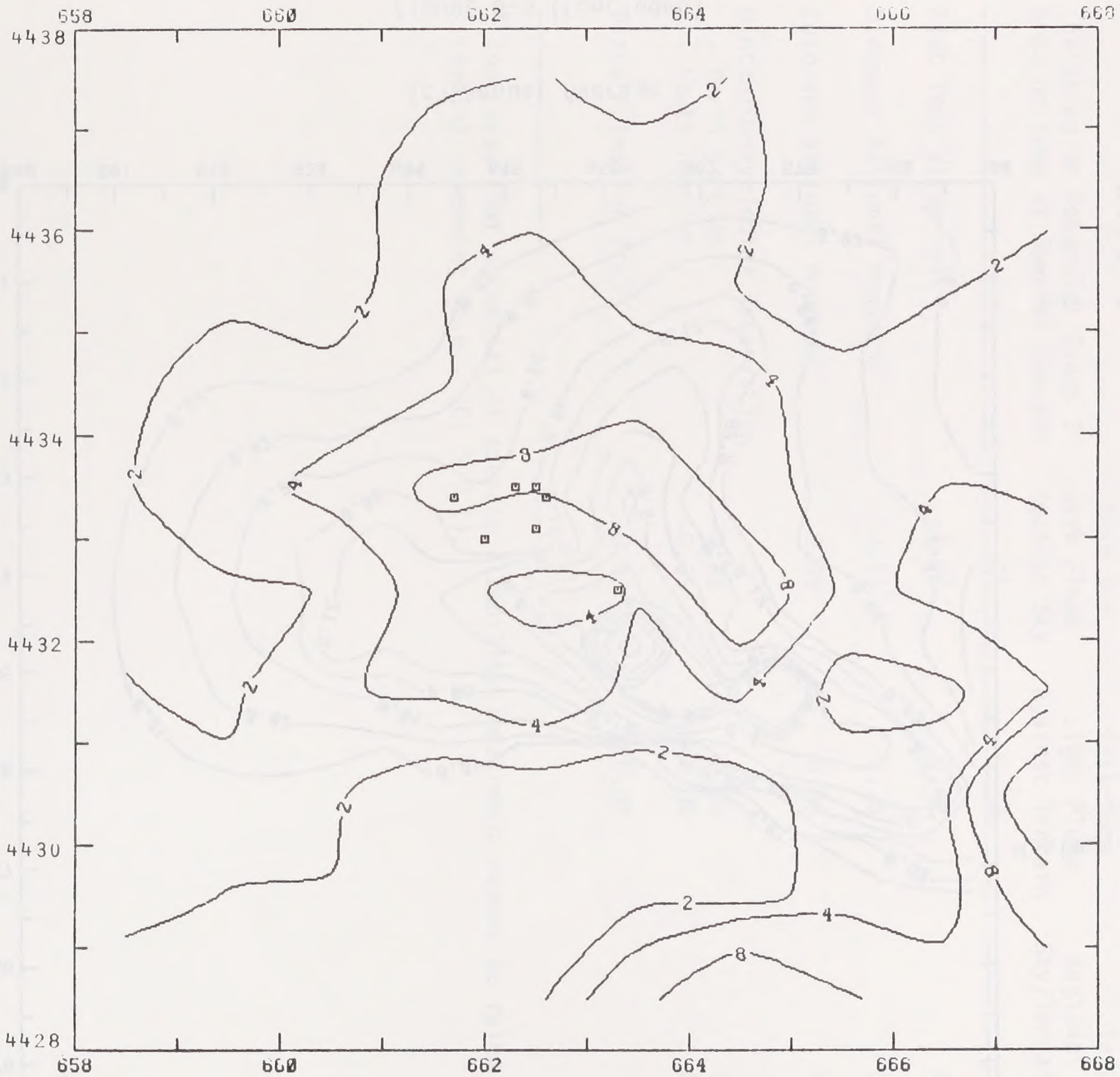

⊡ Point Sources

(b) Maximum 24-Hour Average (Near-Source)

FIGURE 6-8 (Continued)

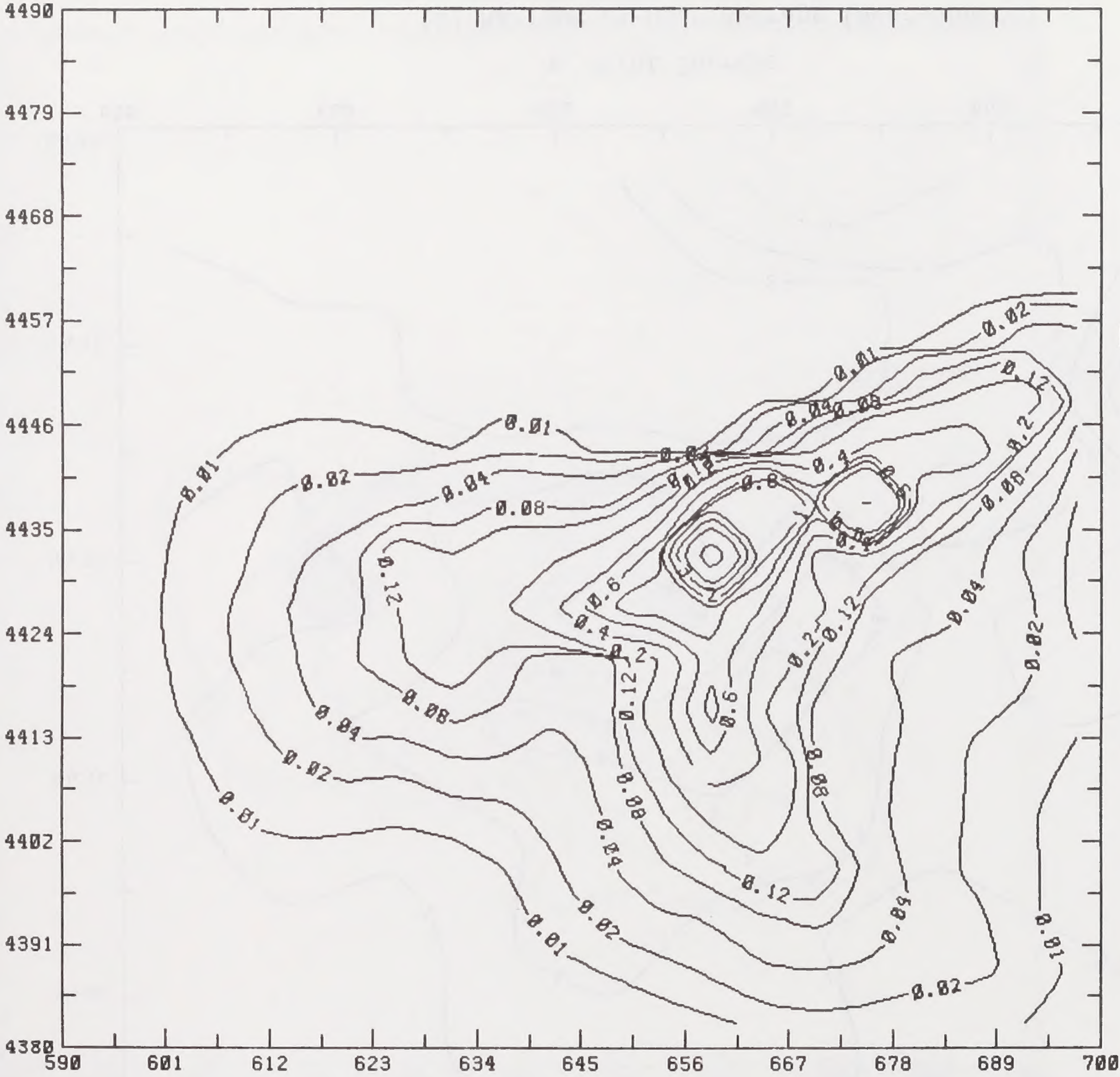

Maximum: 1 μg/m^3

Note: These GPM results are overly conservative near the source because of source emission aggregation. COMPLEX-I results indicated the maximum concentration was 1 μg/m^3.

(c) Annual Average

FIGURE 6-8 (Concluded)

TABLE 6-12. LEVEL-1 SCREENING ANALYSIS RESULTS FOR VISIBILITY IMPACTS OF SYNTANA

Existing or Potential Class I Area or Area of Special Concern	Test for Dark Plume Against Sky C_1	Test for Light Plume Against Terrain C_2	Test for Regional Reduction Sky/Terrain Contrast C_3
Flat Tops Wilderness	-0.02	0.02	0.01
Dinosaur National Monument	-0.13*	0.15*	0.01
Colorado National Monument	-0.03	0.03	0.01
Uintah/Ouray Indian Reservation			
- North portion	-0.08	0.08	0.01
- South portion	-0.05	0.05	0.01
Uinta Primitive Area	-0.03	0.02	0.01

---

* Indicates that potential of adverse visibility impairment cannot be ruled out by Level-1 screening (i.e., $|C| > 0.1$).

Tables 6-13 and 6-14 and figures 6-9 and 6-10 summarize the air quality impacts, which are well within criteria values. The on-site maximum 24-hour-average TSP concentration is predicted to be higher than the Class II increment of 37 μg/m^3; however, off-site impacts are predicted to be less than 16 μg/m^3. Tosco passes the EPA Level-1 visibility screening analysis at all mandatory and potential Class I areas (see table 6-15).

6.6 SUMMARY AND COMPARISON WITH OTHER ANALYSES

The air quality modeling studies performed by the applicants were reviewed. Only the following three provided model estimates of air quality impacts: Paraho, Syntana-Utah, and Tosco. Table 6-16 summarizes the air quality model approaches used by these applicants. Table 6-17 compares results of the current study, previous screening analyses performed by Systems Applications, Inc. for the EPA (Latimer and Doyle, 1981), and the applicant studies. This table compares maximum 24-hour-average SO_2 and TSP concentrations. This averaging time is of particular interest because the 24-hour-average SO_2 and TSP PSD Class II increments are most restrictive. Note that all the model estimates of impacts are reasonably close and that all impacts are within PSD increments.

TABLE 6-13. SUMMARY OF PSD INCREMENT CONSUMPTION BY TOSCO

	SO_2 Concentration ($\mu g/m^3$)			TSP Concentration ($\mu g/m^3$)	
PSD Increments/Increment Consumption	3-Hour Average	24-Hour Average	Annual Average	24-Hour Average	Annual Average
Class II Areas					
Allowable PSD Class II increment	512	91	20	37	19
Increment consumption at receptors of maximum impacts					
Impact alone	54	13	1	<16	<1
Impact with Moon Lake Unit 1	57	14	1	<17	<1
Impact with all interrelated (other) sources	60	15	1	<18	<1
Maximum increment consumption on Uintah/Ouray Indian Reservation					
Impact alone	40	8	0	<16	<1
Impact with Moon Lake Unit 1	46	9	0	<17	<1
Impact with all interrelated (other) sources	54	11	0	<19	<1
Maximum increment consumption in Colorado					
Impact alone	5	1	0	2	0
Class I Areas					
Allowable PSD Class I increment	25	5	2	10	5
Increment consumption at Flat Tops Wilderness Area (federal Class I)					
Impact alone	0	0	0	0	0
Impact with Moon Lake Unit 1	0	0	0	0	0
Impact with all interrelated (other) sources	1	0	0	0	0
Increment consumption at Maroon Bells-Snowmass Wilderness Area (federal Class I)					
Impact alone	0	0	0	0	0
Impact with Moon Lake Unit 1	0	0	0	0	0
Impact with all interrelated (other) sources	0	0	0	0	0
Increment consumption at Dinosaur National Monument (Colorado category I and potential federal Class I)					
Impact alone	1	0	0	0	0
Impact with Moon Lake Unit 1	3	0	0	0	0
Impact with all interrelated (other) sources	7	1	0	1	0

TABLE 6-13 (Concluded)

PSD Increments/Increment Consumption	SO_2 Concentration ($\mu g/m^3$) 3-Hour Average	SO_2 Concentration ($\mu g/m^3$) 24-Hour Average	SO_2 Concentration ($\mu g/m^3$) Annual Average	TSP Concentration ($\mu g/m^3$) 24-Hour Average	TSP Concentration ($\mu g/m^3$) Annual Average
Increment consumption at Colorado National Monument (Colorado category I and potential federal Class I)					
Impact alone	0	0	0	0	0
Impact with Moon Lake Unit 1	0	0	0	0	0
Impact with all interrelated (other) sources	0	0	0	0	0

TABLE 6-14. SUMMARY OF MAXIMUM AMBIENT AIR QUALITY IMPACTS OF TOSCO COMPARED WITH APPLICABLE STANDARDS

Pollutant/Averaging Time	Maximum Ground-Level Concentration ($\mu g/m^3$) Baseline	Source Impact	Subtotal	Impact of Other Sources	Total	NAAQS* ($\mu g/m^3$)
Sulfur dioxide (SO_2)						
3-Hour	5	54	59	3	62	1300
24-Hour	2	13	15	1	16	365
Annual	1	1	2	0	2	80
Total suspended particulate (TSP)						
24-Hour	84	< 16	< 100	1	< 101	150
Annual	19	< 1	< 20	0	< 20	60
Nitrogen dioxide (NO_2)						
Annual	1	8	9	0	9	100
Carbon monoxide (CO)						
1-Hour	7400	5	7405	0	7405	40,000
8-Hour	4500	5	4505	0	4505	10,000
Ozone (O_3)						
1-Hour	160	2	162	0	162	240

---

[*] National Ambient Air Quality Standards.

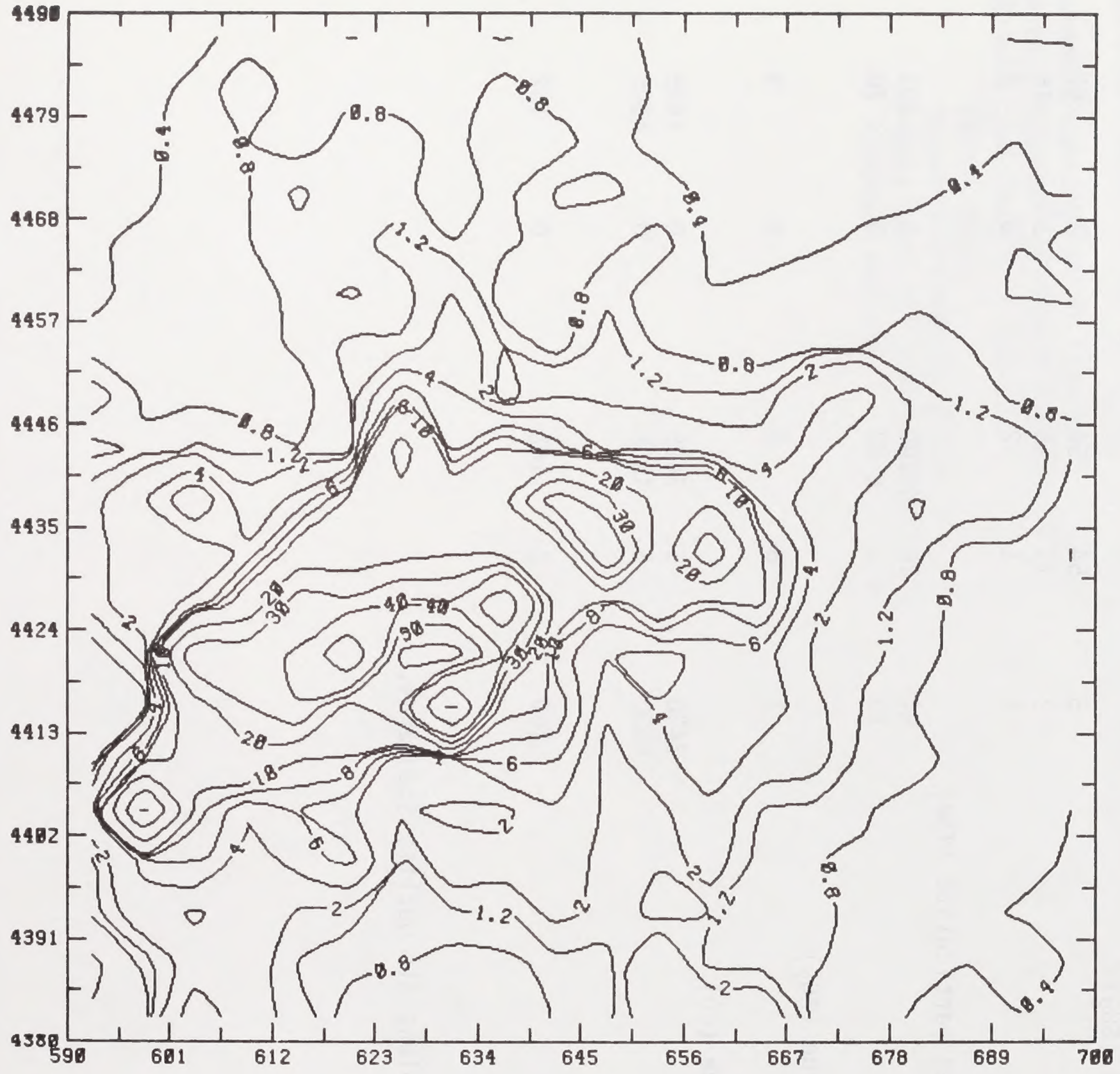

Maximum: 54 µg/m^3

(a) Maximum 3-Hour Average

FIGURE 6-9. GROUND-LEVEL SO_2 CONCENTRATIONS (µg/m^3) DUE TO TOSCO EMISSIONS

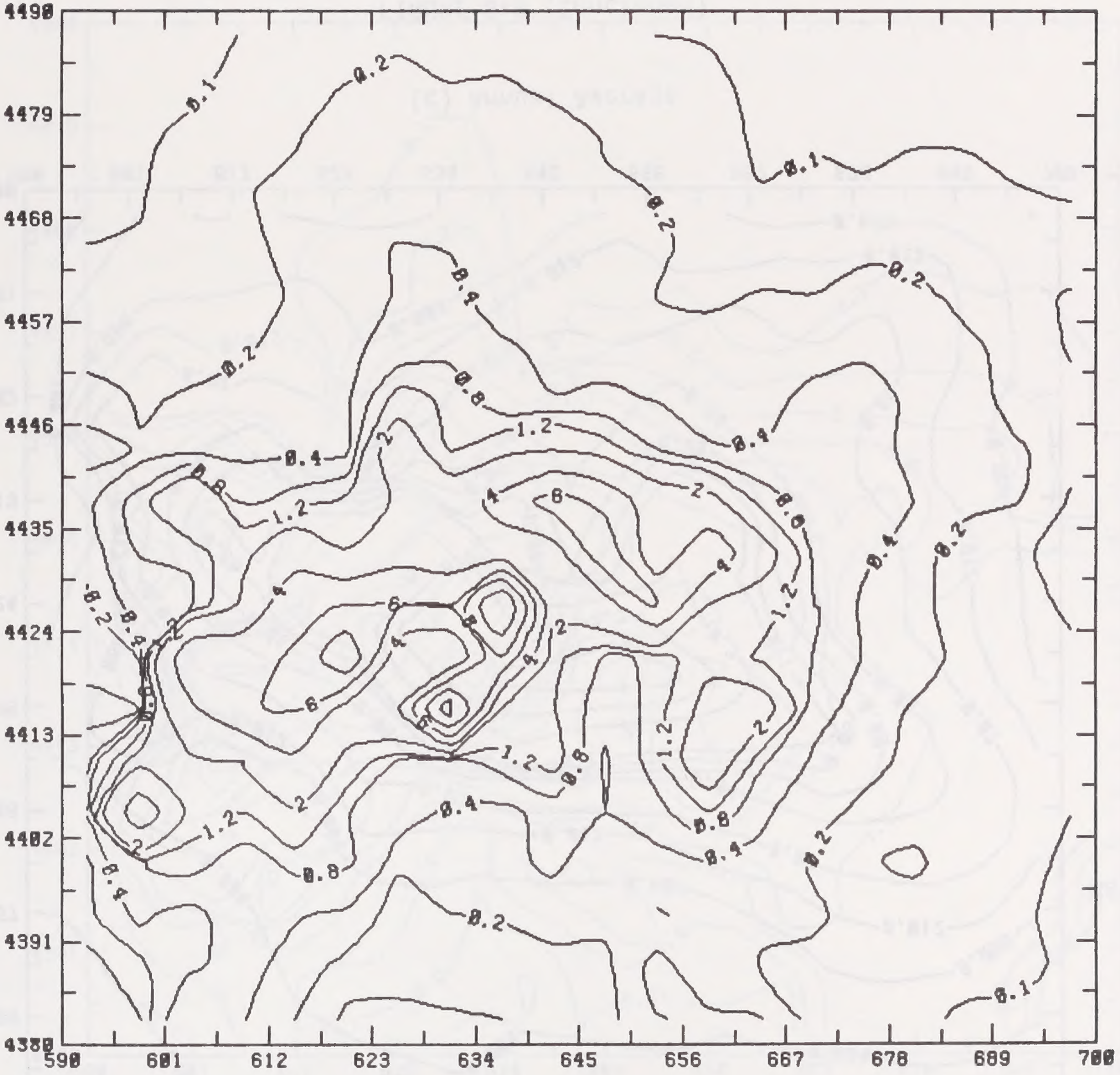

Maximum: 13 µg/m^3

(b) Maximum 24-Hour Average

FIGURE 6-9 (Continued)

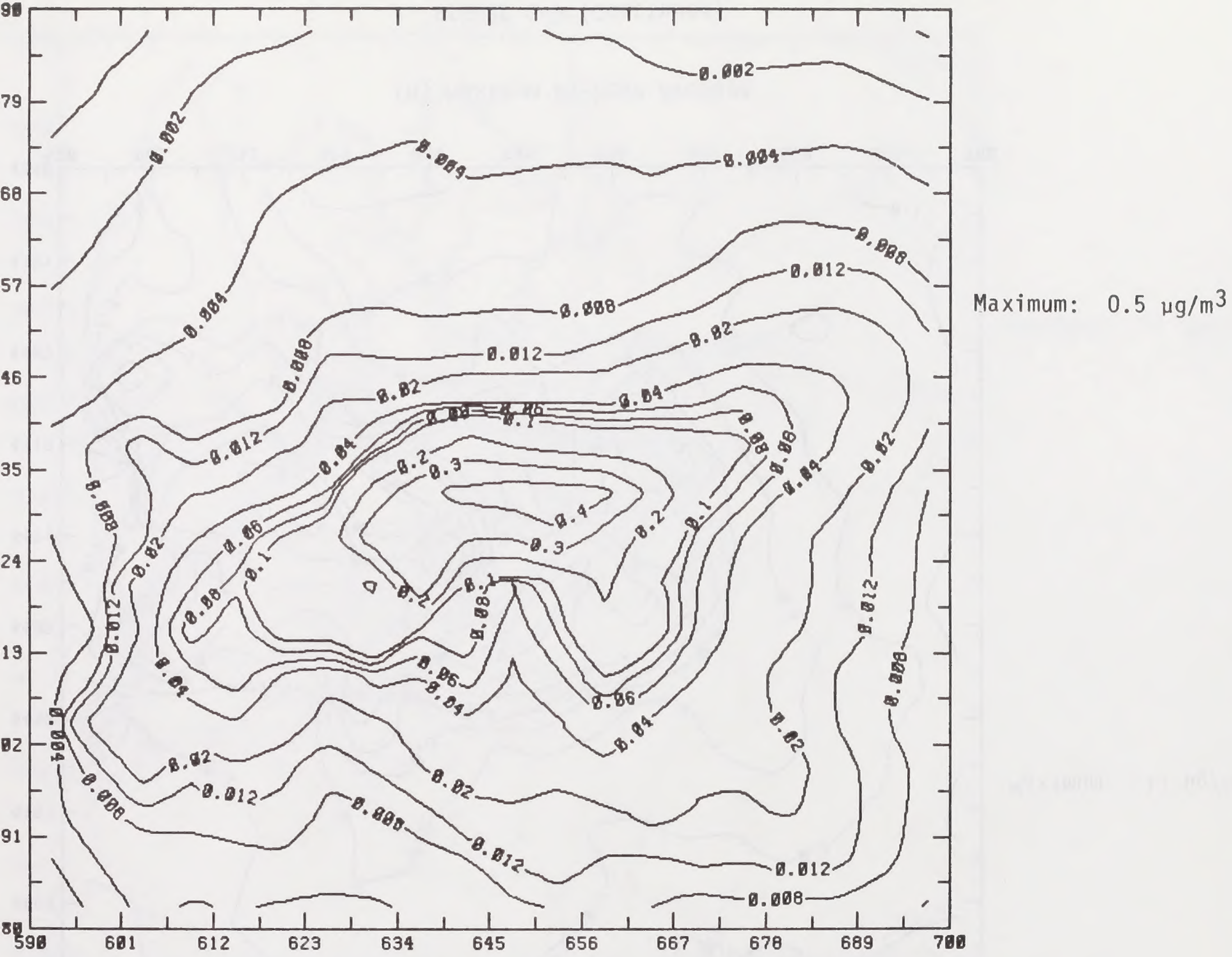

(c) Annual Average

FIGURE 6-9 (Concluded)

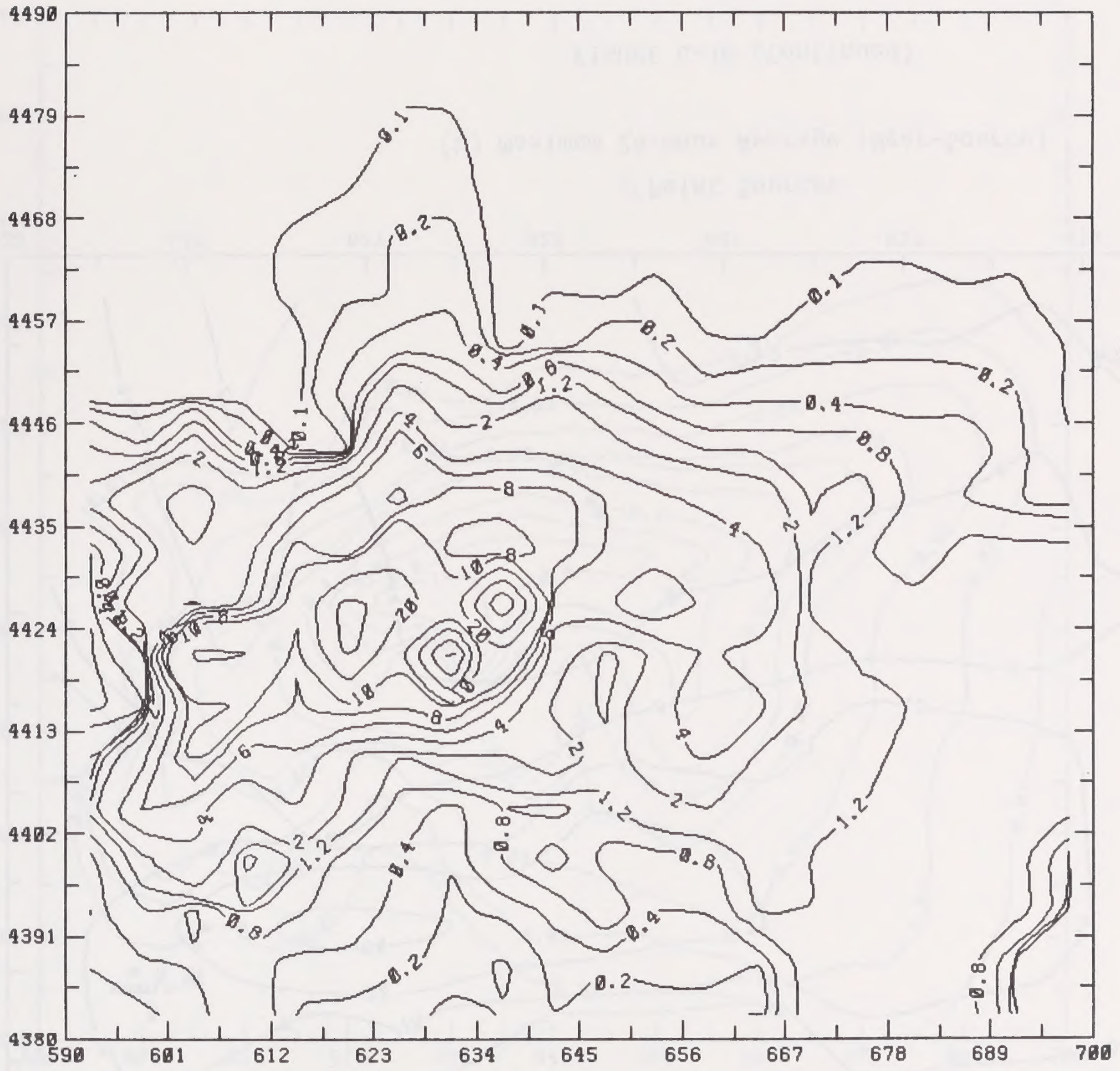

Maximum: 80 μg/m^3 (on-site)
<16 μg/m^3 (off-site)

Note: These GPM results are overly conservative near the source because of source emission aggregation; see COMPLEX-I results in Figure 6-10(b).

(a) Maximum 24-Hour Average

FIGURE 6-10. GROUND-LEVEL TSP CONCENTRATIONS (μg/m^3) DUE TO TOSCO EMISSIONS

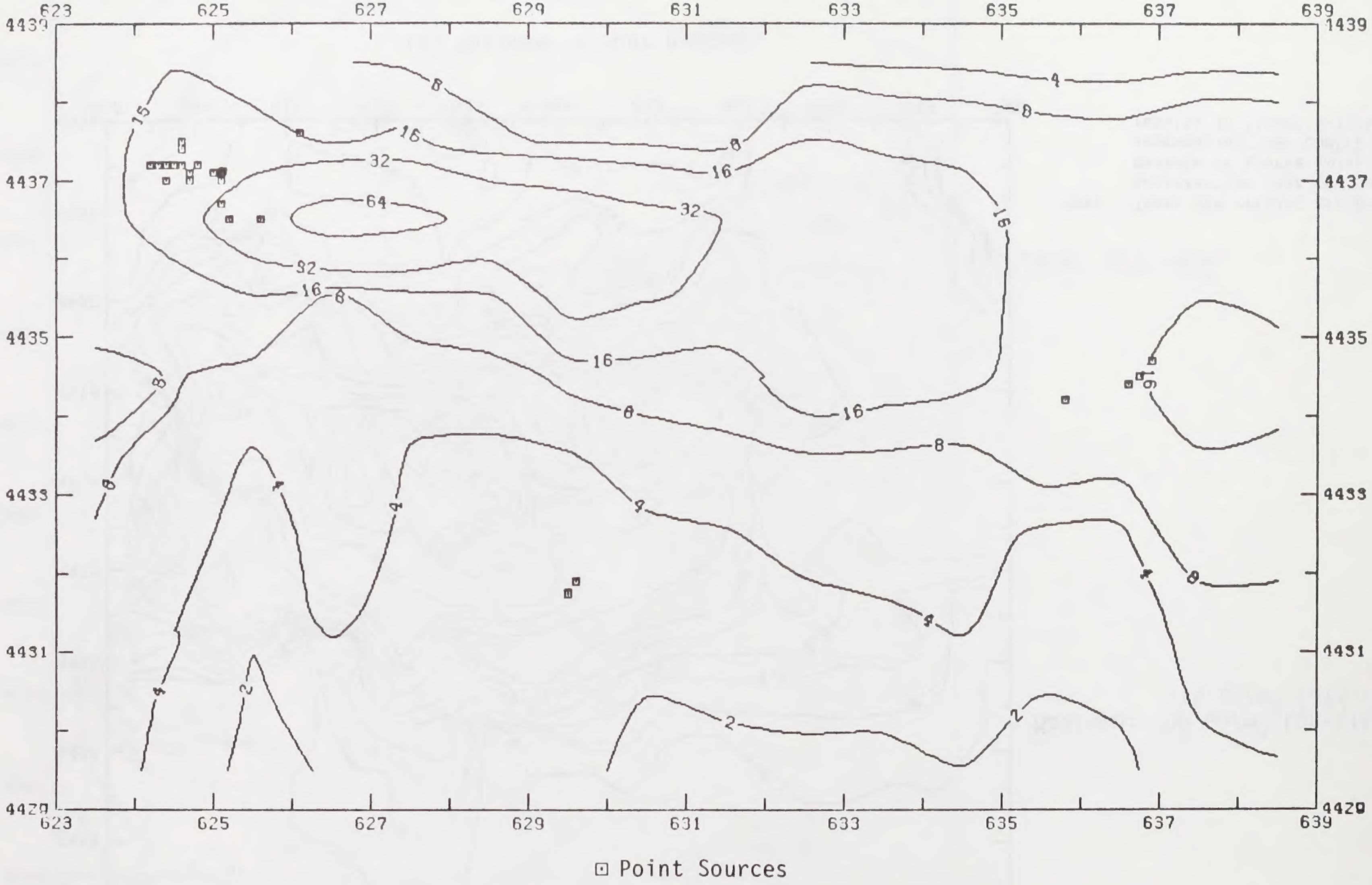

(b) Maximum 24-Hour Average (Near-Source)

FIGURE 6-10 (Continued)

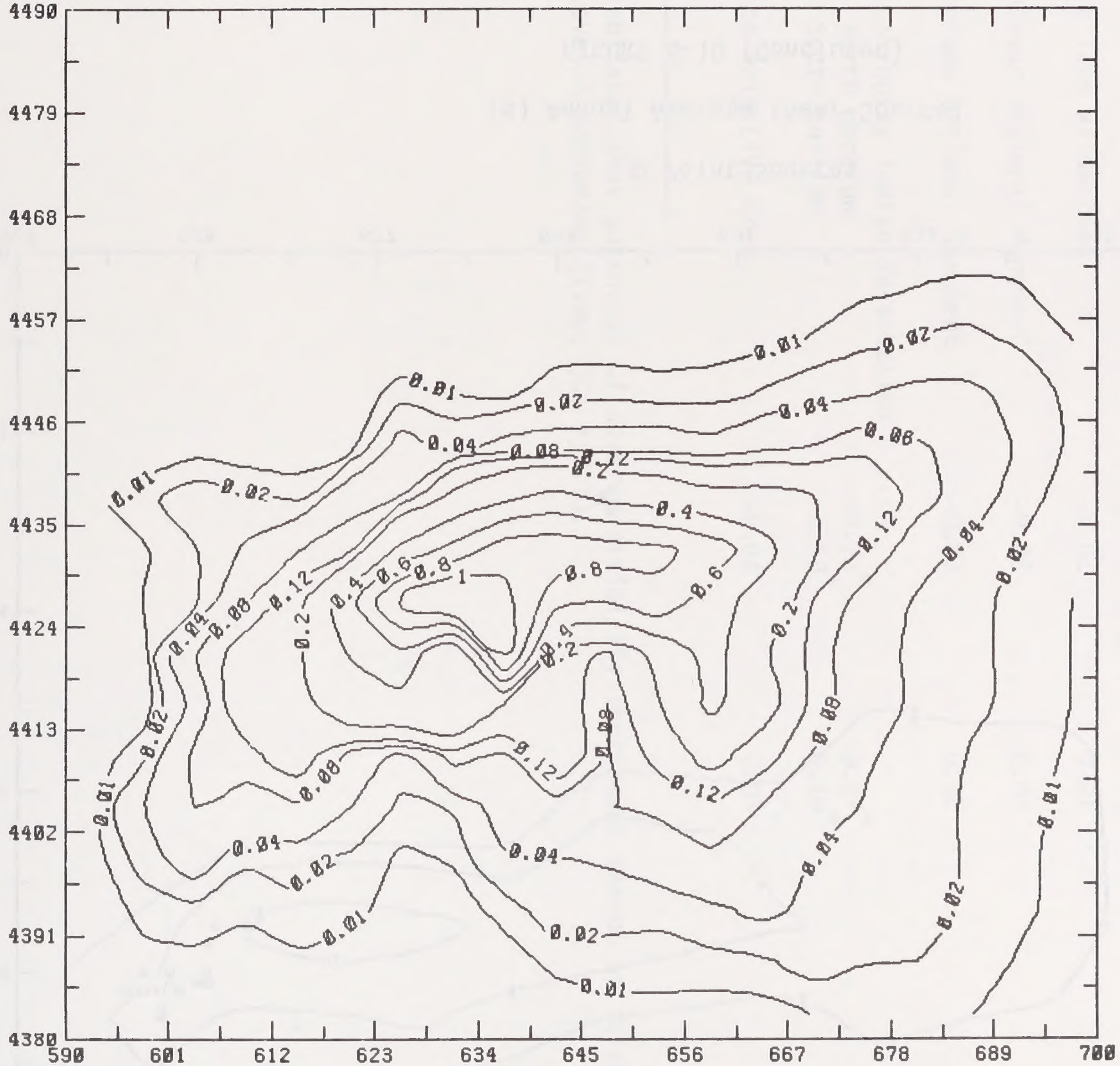

Maximum: 11 μg/m^3 (on-site)
<1 μg/m^3 (off-site)

(c) Annual Average

FIGURE 6-10 (Continued)

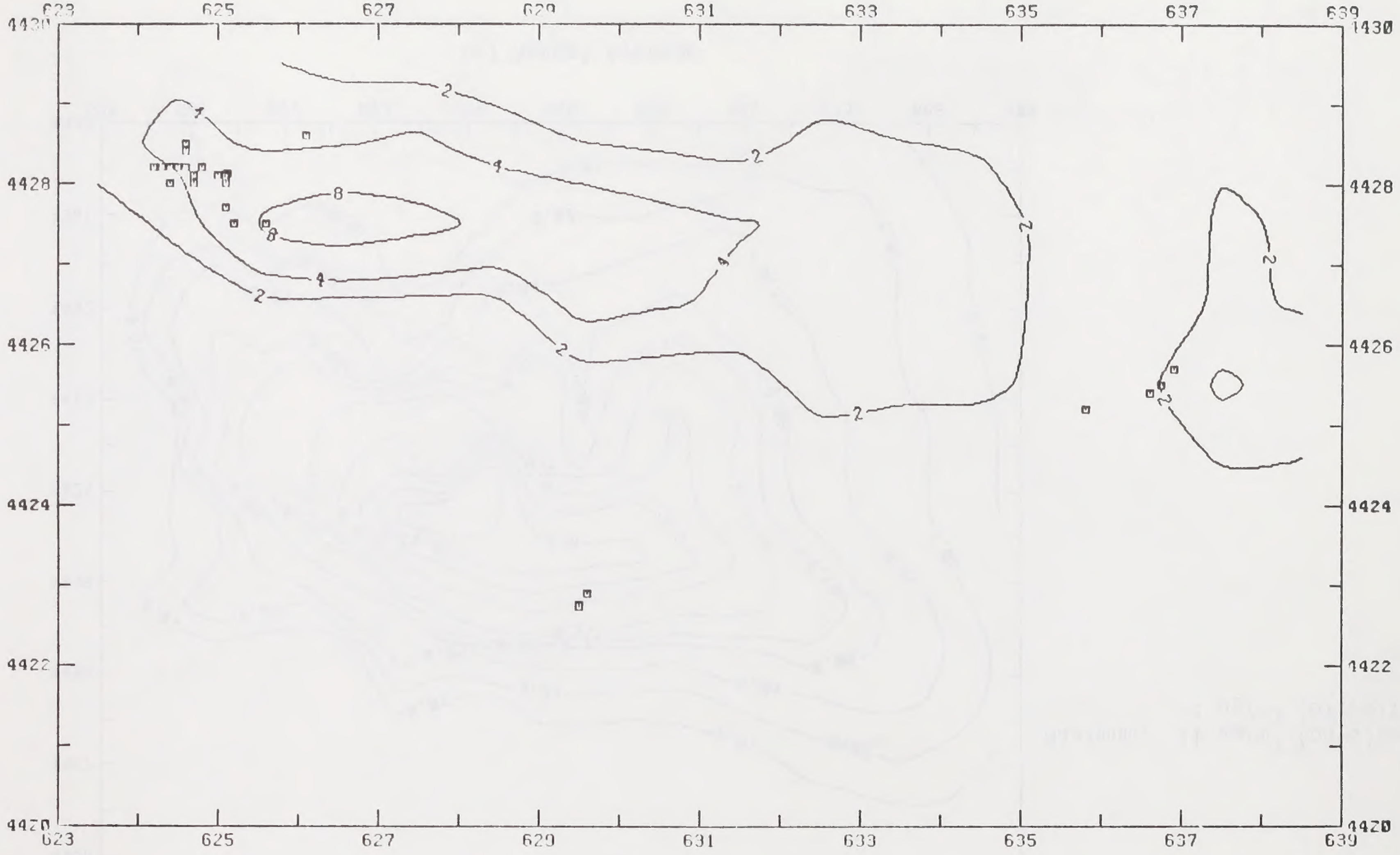

⊡ Point Sources

(d) Annual Average (Near-Source)

FIGURE 6-10 (Concluded)

TABLE 6-15. LEVEL-1 SCREENING ANALYSIS RESULTS FOR VISIBILITY IMPACTS OF TOSCO

Existing or Potential Class I Area or Area of Special Concern	Test for Dark Plume Against Sky C_1	Test for Light Plume Against Terrain C_2	Test for Regional Reduction Sky/Terrain Contrast C_3
Flat Tops Wilderness	-0.02	0.01	0.00
Dinosaur National Monument	-0.08	0.07	0.00
Colorado National Monument	-0.03	0.02	0.00
Uintah/Ouray Indian Reservation			
- North portion	-0.23*	0.27*	0.00
- South portion	-0.10*	0.10*	0.00
Uinta Primitive Area	-0.04	0.03	0.00

---

* Indicates that potential of adverse visibility impairment cannot be ruled out by Level-1 screening (i.e., |C| > 0.1).

TABLE 6-16. SUMMARY OF MODEL APPROACHES USED BY APPLICANTS

Site	Methods
Paraho	> WRSP baseline air quality data > VALLEY runs for annual means of SO_2, TSP, and NO_2; 24-hour averages of SO_2, TSP, and H_2SO_4; 3-hour SO_2 average; and 1-hour and 8-hour CO averages > REM2 was run to model O_3 hourly in a Lagrangian trajectory methodology > Visibility screening (EPA Level-1) for Dinosaur National Monument
Syntana-Utah	> White River Shale Project (WRSP) baseline air quality data > VALLEY used for 24-hour worst-case mode screening (with F stability, 2.5 m/s wind speed, and 6 hours of persistence in each sector); for annual mode, with STAR data from WRSP sites > Visibility screening (EPA Level-1) for Flat Tops Wilderness Area
Tosco	> VALLEY for complex terrain; standard assumptions for 24-hour worst-case mode screening > TSP and CO obtained via χ/Q scaling from SO_2 results > CDM for flat terrain for 24-hour SO_2, TSP, and annual average TSP > Sand Wash 1980 baseline air quality data > Visibility screening (EPA Level-1) for Dinosaur National Monument

TABLE 6-17. COMPARISON OF WORST-CASE CALCULATIONS OF 24-HOUR CONCENTRATIONS NEAR SPECIFIC PROPOSED SYNTHETIC FUEL FACILITIES

Pollutant/Source	Ambient Air Quality Standard	PSD Class II Increment	EPA/Systems Applications Screening Study		Applicant's Air Quality Modeling	Current BLM/ Systems Applications Study
			Original Estimate	Corrected Estimate*		
Sulfur dioxide	365	91				
(maximum 24-hour average)						
Enercor-Mono Power			--	--	--	3
Magic Circle			16	14	--	32
Paraho			16	18	44	40
Syntana-Utah			27	12	6	8
Tosco			14	9	32	13
Total suspended particulates	150	37				
(maximum 24-hour average)						
Enercor-Mono Power			--	--	--	7
Magic Circle			16	30	--	< 32
Paraho			16	27	25	< 16
Syntana-Utah			26	33	18	13
Tosco			71	35	33	< 16

---

* Original (Latimer and Doyle, 1981) concentration estimates, corrected for current production capacity and emission inventory.

Appendix A

UPPER LEVEL WIND ROSE STRATIFIED BY SEASON AND TIME OF DAY FOR STUDY REGION IN 1978

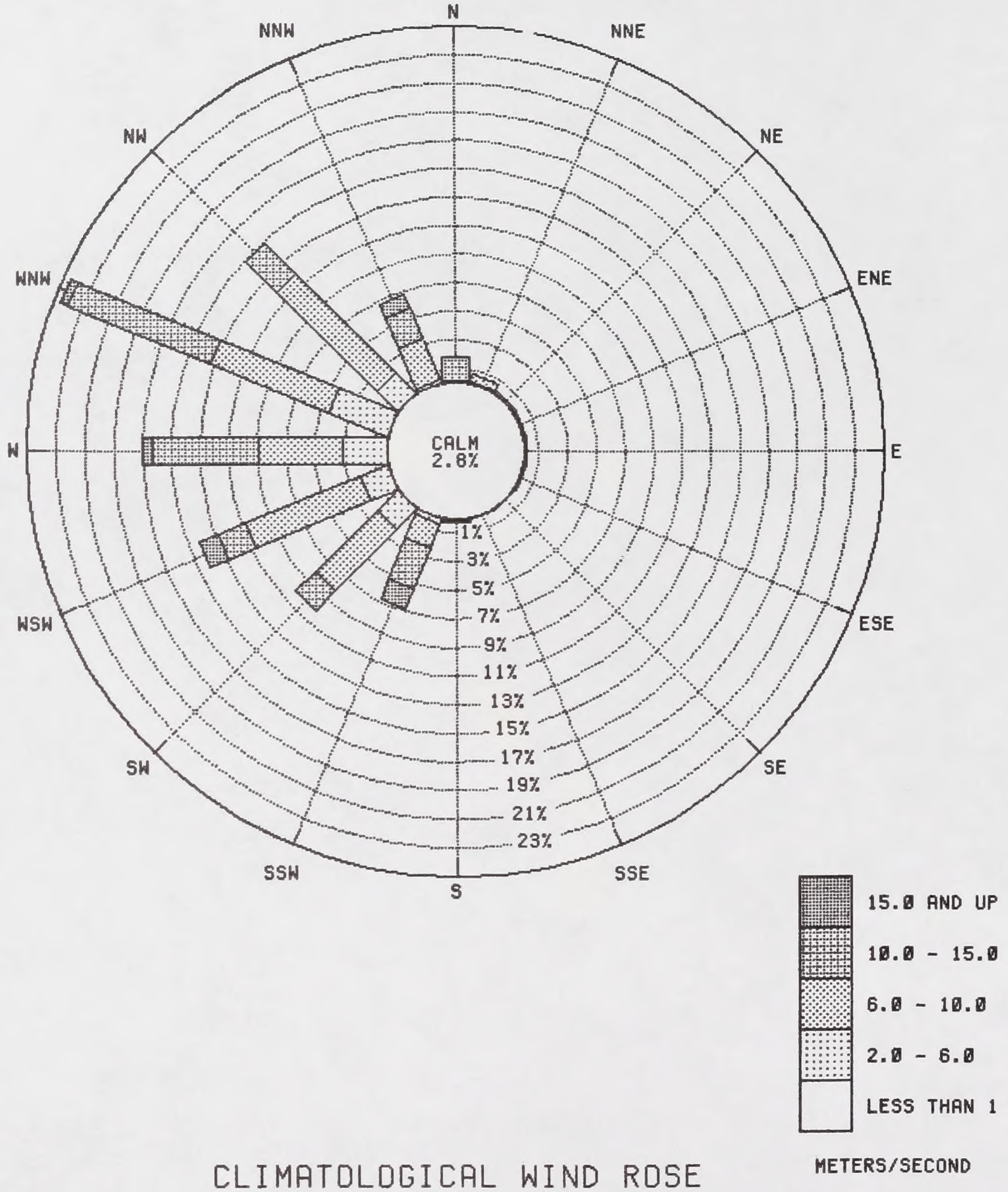

CLIMATOLOGICAL WIND ROSE
SPRING DAY
(MARCH - APRIL, 6 AM - 6 PM)

1104 VALID DATA POINTS

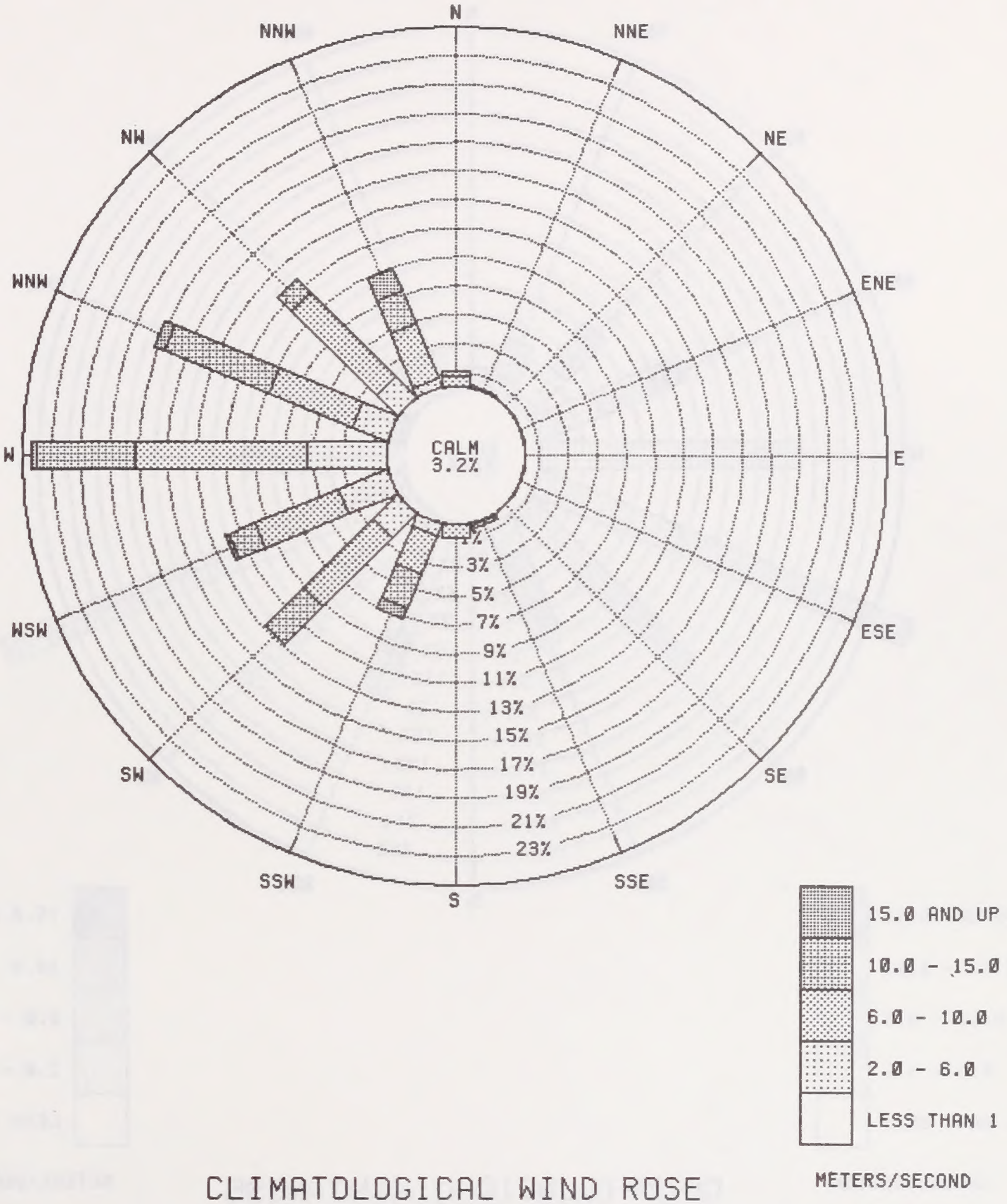

CLIMATOLOGICAL WIND ROSE
SPRING NIGHT
(MARCH - APRIL, 6 PM - 6 AM

1104 VALID DATA POINTS

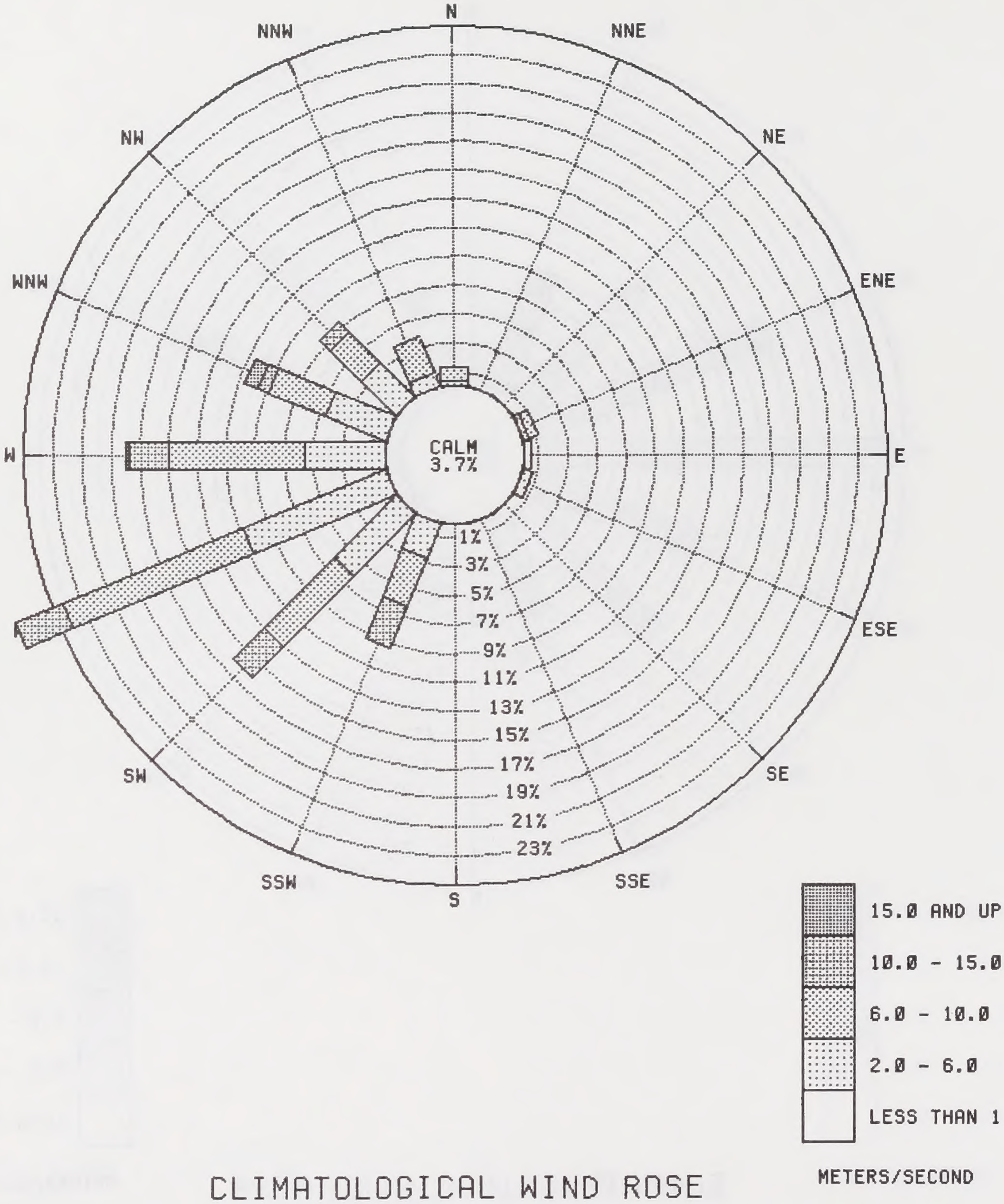

CLIMATOLOGICAL WIND ROSE
SUMMER DAY
(JUNE - AUGUST, 6 AM - 6 PM)

1104 VALID DATA POINTS

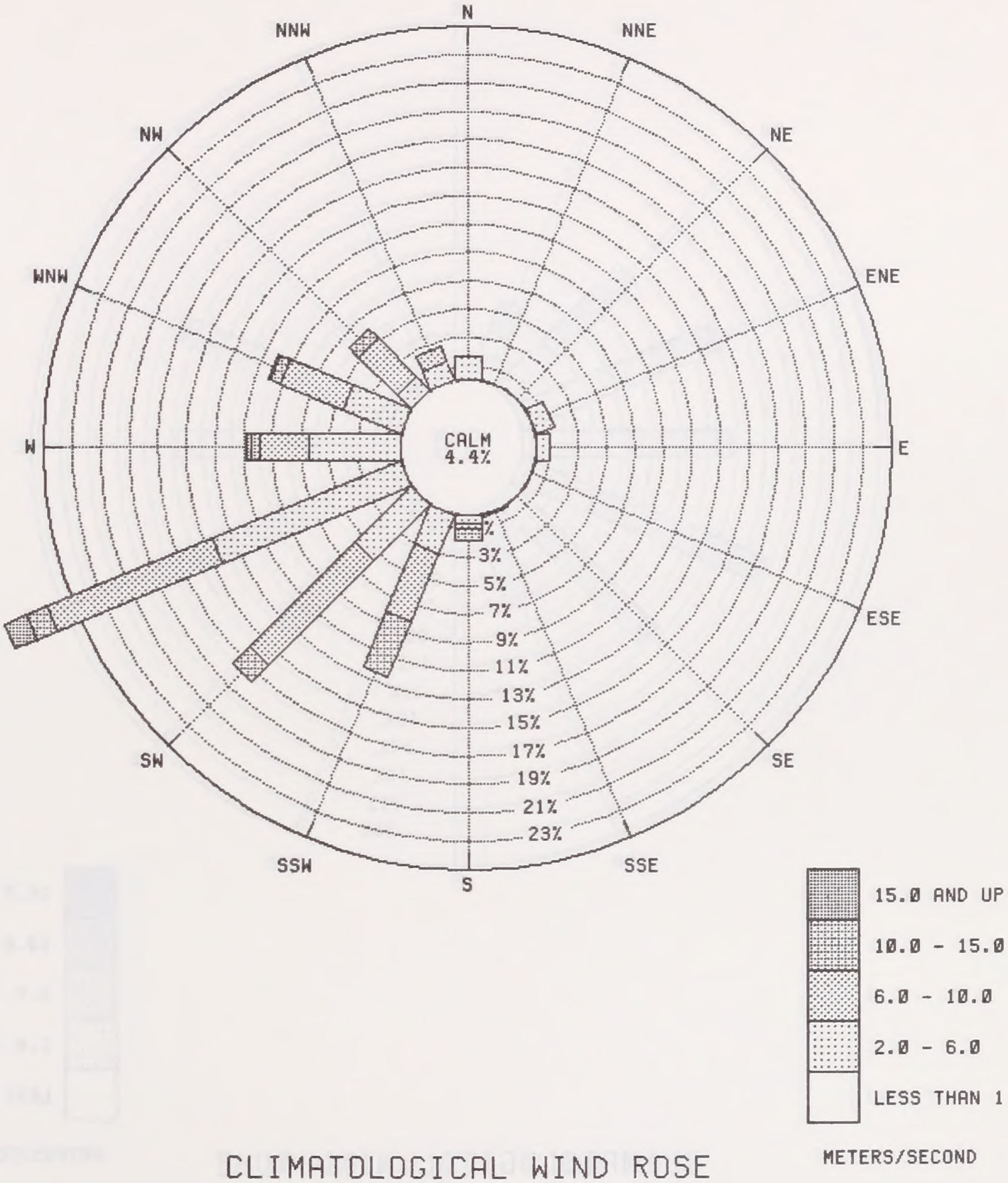

CLIMATOLOGICAL WIND ROSE
SUMMER NIGHT
(JUNE - AUGUST, 6 PM - 6 AM

1104 VALID DATA POINTS

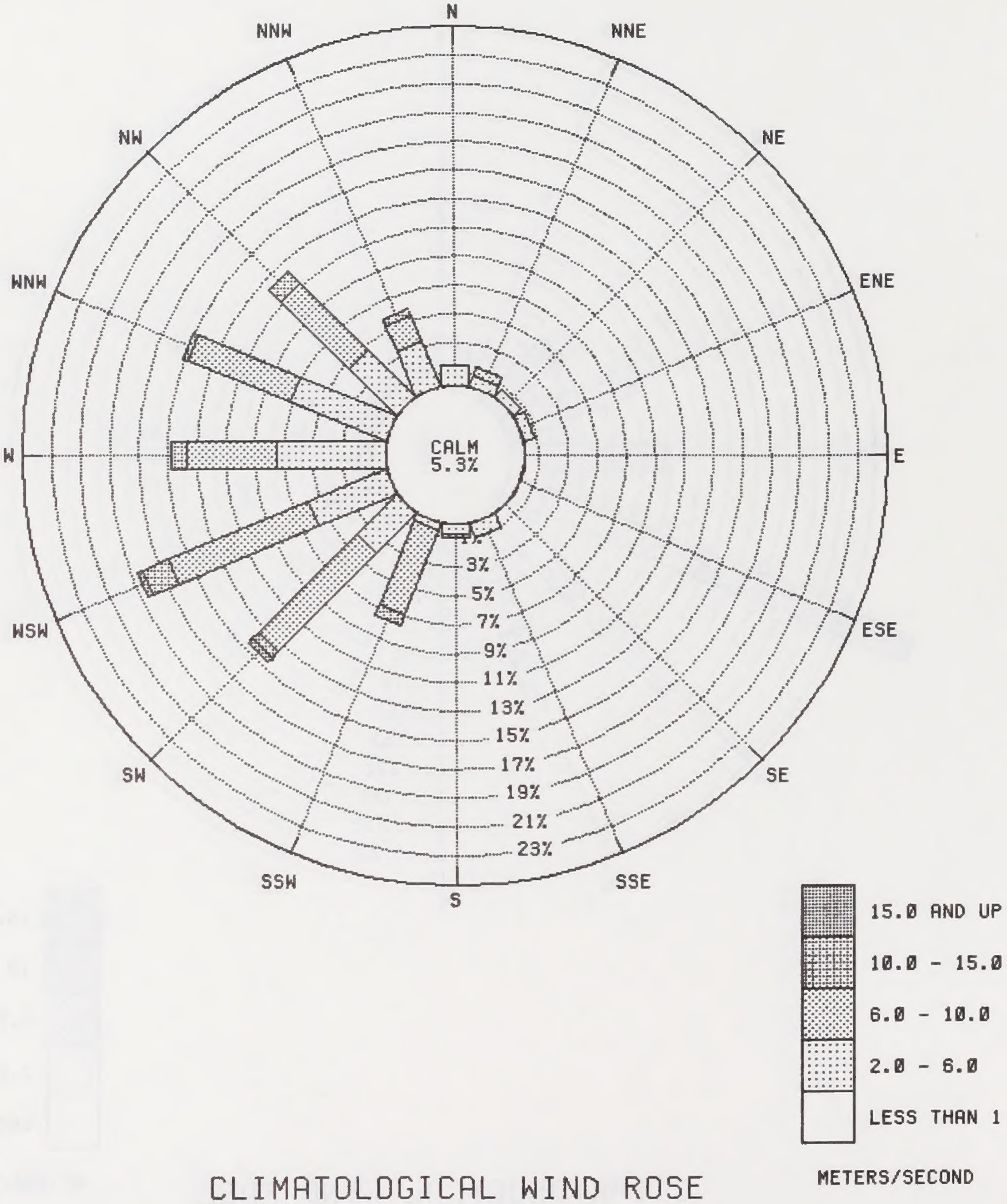

CLIMATOLOGICAL WIND ROSE
FALL DAY
(SEPT - NOV, 6 AM - 6 PM)

1092 VALID DATA POINTS

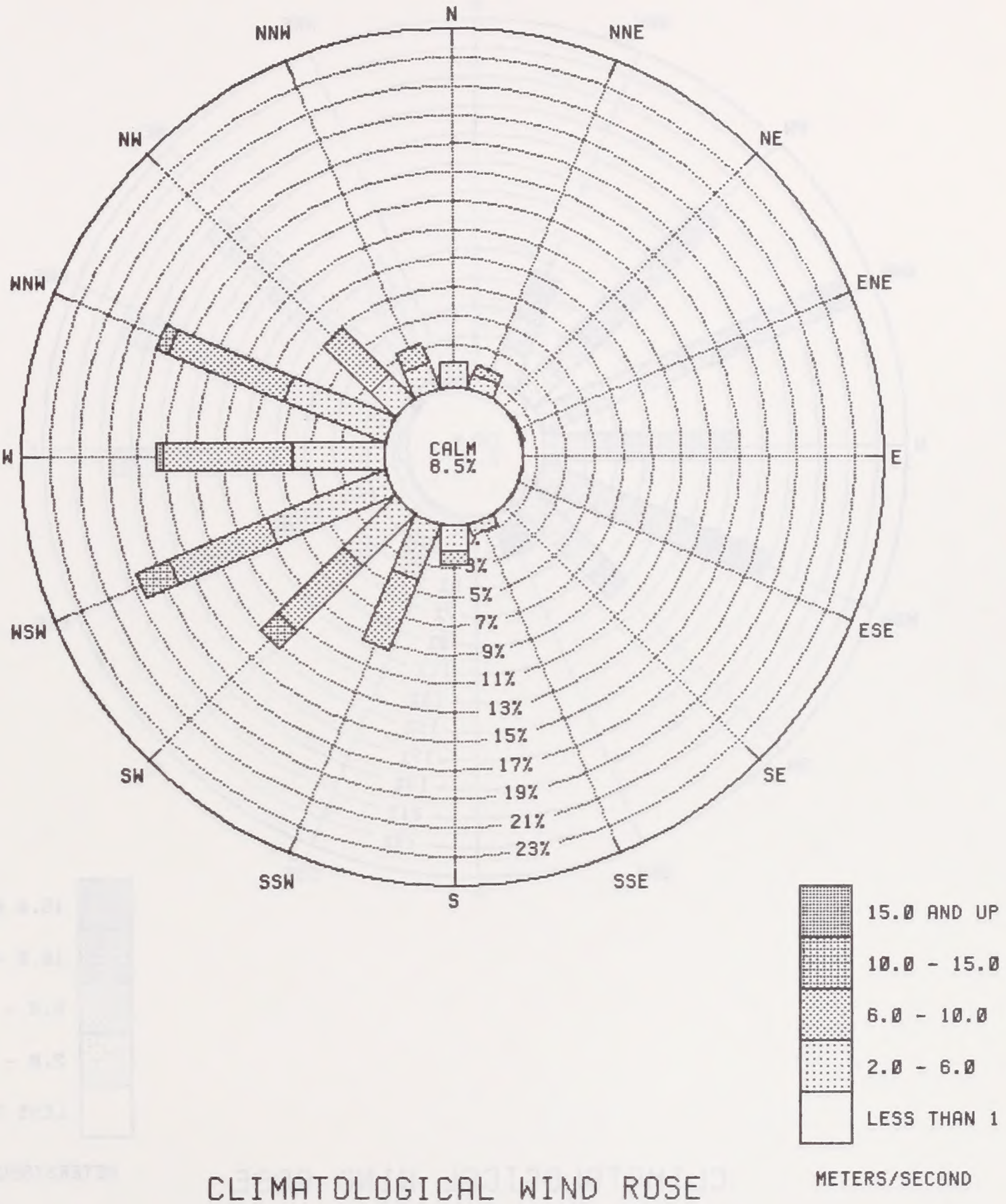

CLIMATOLOGICAL WIND ROSE
FALL NIGHT
(SEPT - NOV. 6 PM - 6 AM

1092 VALID DATA POINTS

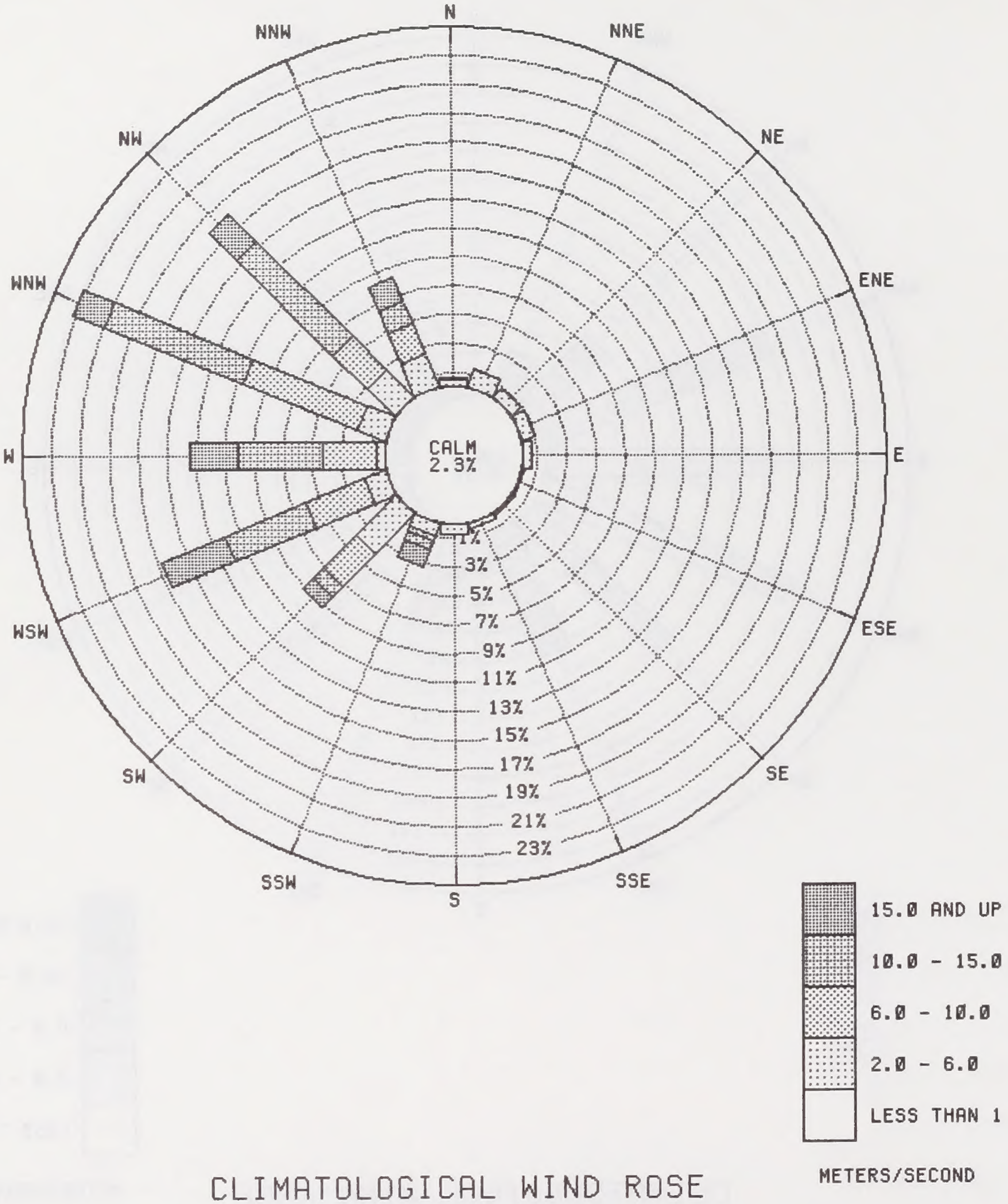

CLIMATOLOGICAL WIND ROSE
WINTER DAY
(DEC - FEB, 6 AM - 6 PM)

1080 VALID DATA POINTS

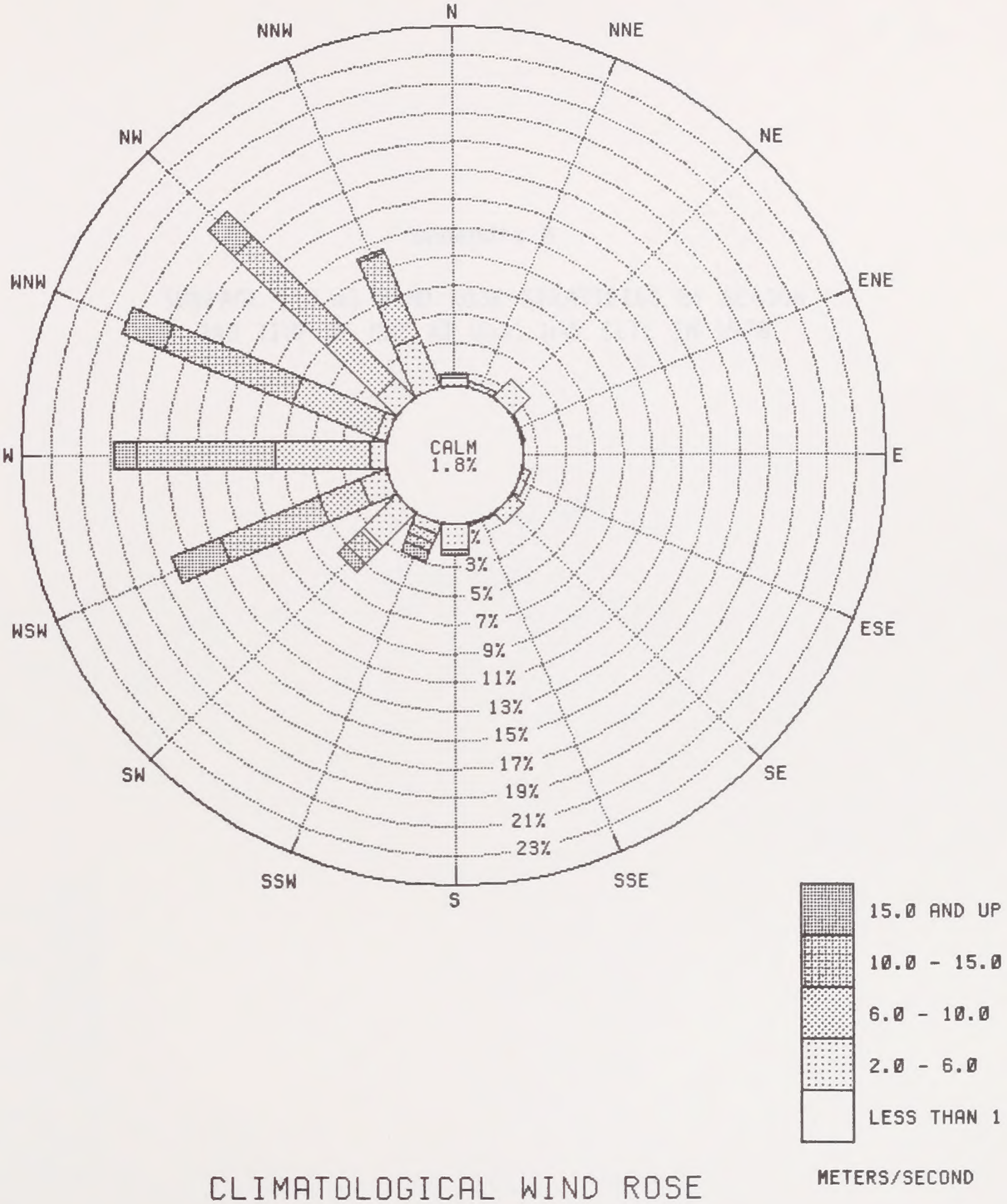

CLIMATOLOGICAL WIND ROSE
WINTER NIGHT
(DEC - FEB, 6 PM - 6 AM

1080 VALID DATA POINTS

[illegible]

Appendix B

SURFACE (10-m) WIND ROSE STRATIFIED BY SEASON AND TIME OF DAY AT U-A, U-B SITE IN 1978

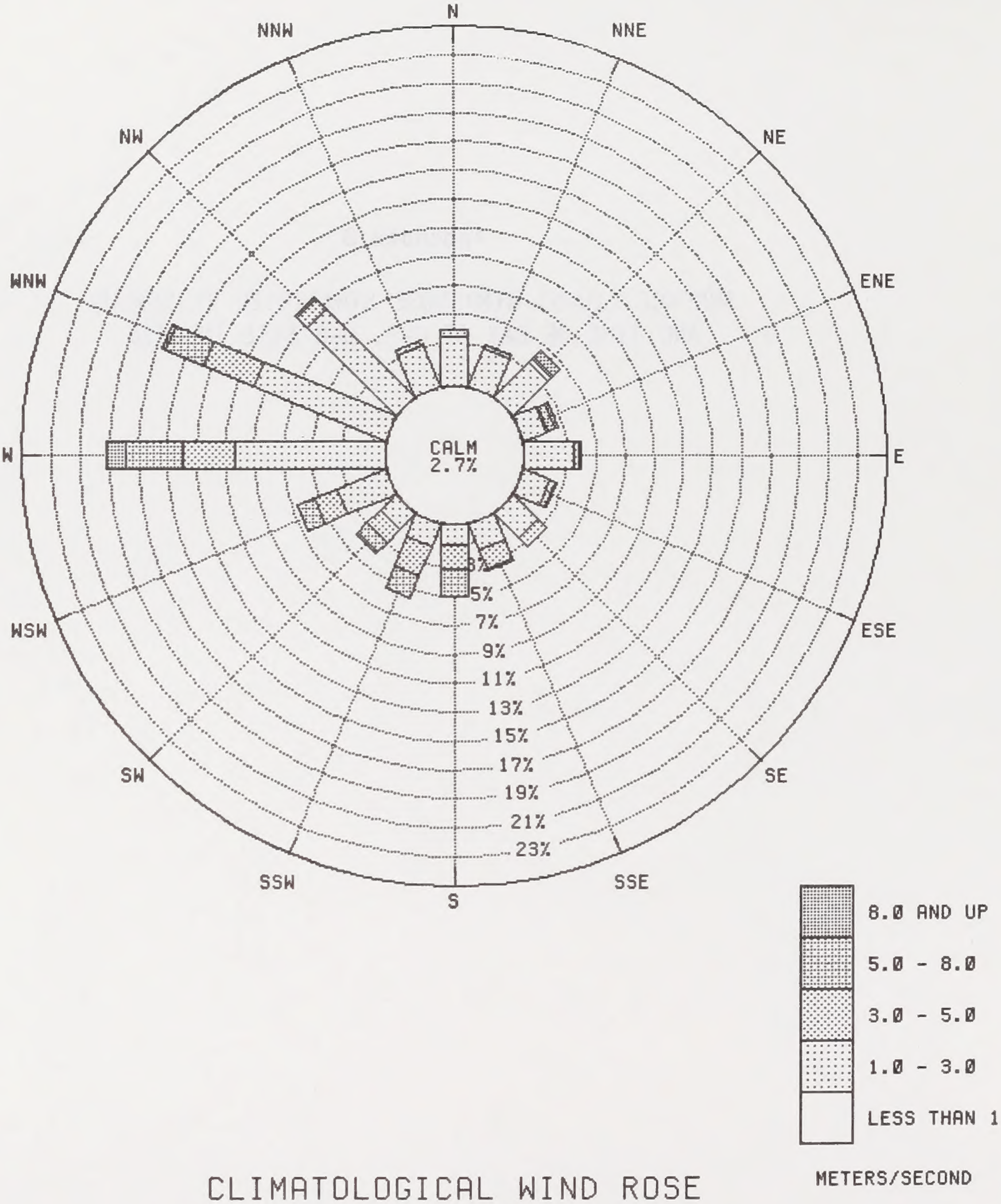

CLIMATOLOGICAL WIND ROSE
SPRING DAY
(MARCH - APRIL, 6 AM - 6 PM)

1031 VALID DATA POINTS

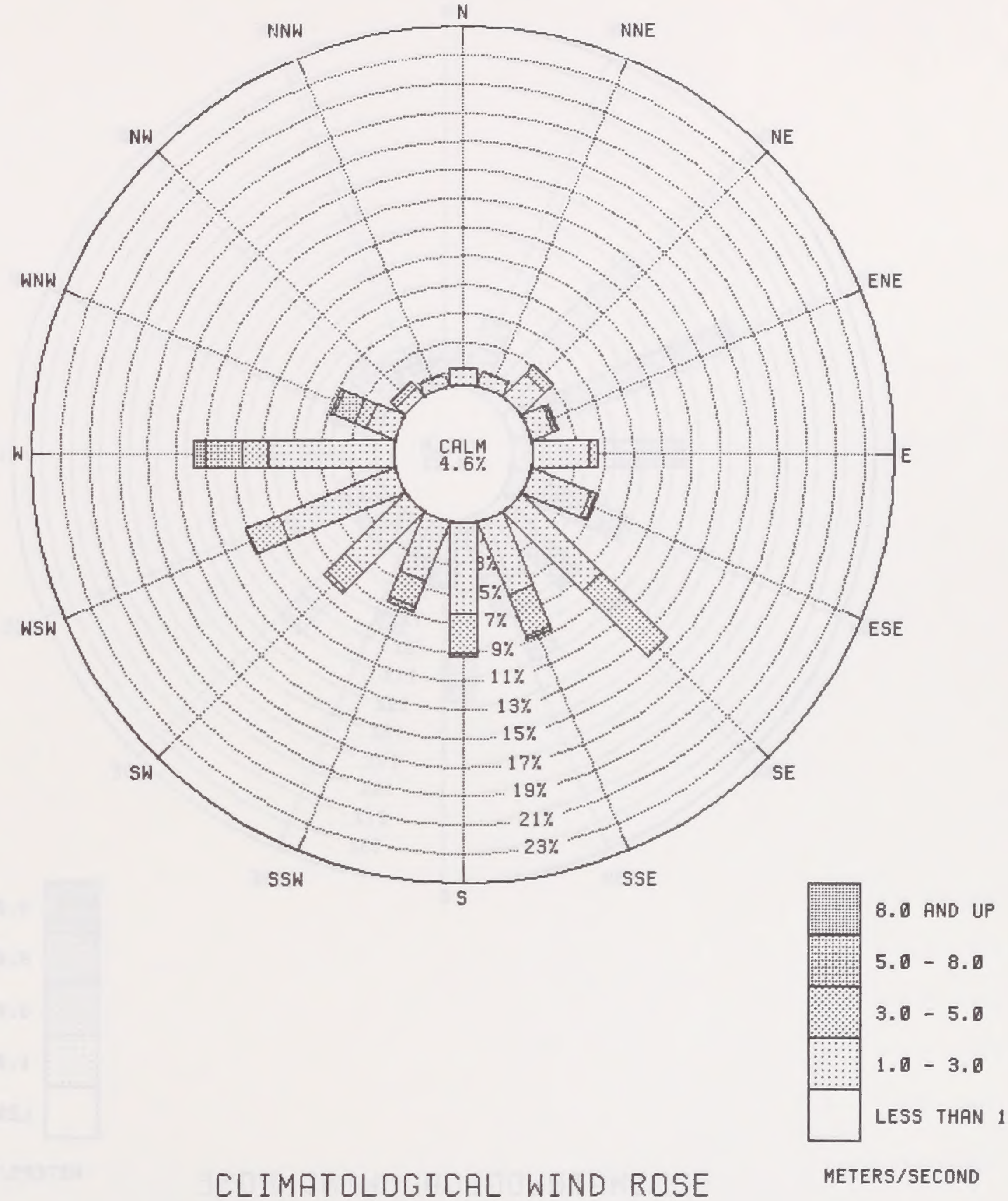

CLIMATOLOGICAL WIND ROSE
SPRING NIGHT
(MARCH - APRIL, 6 PM - 6 AM

1007 VALID DATA POINTS

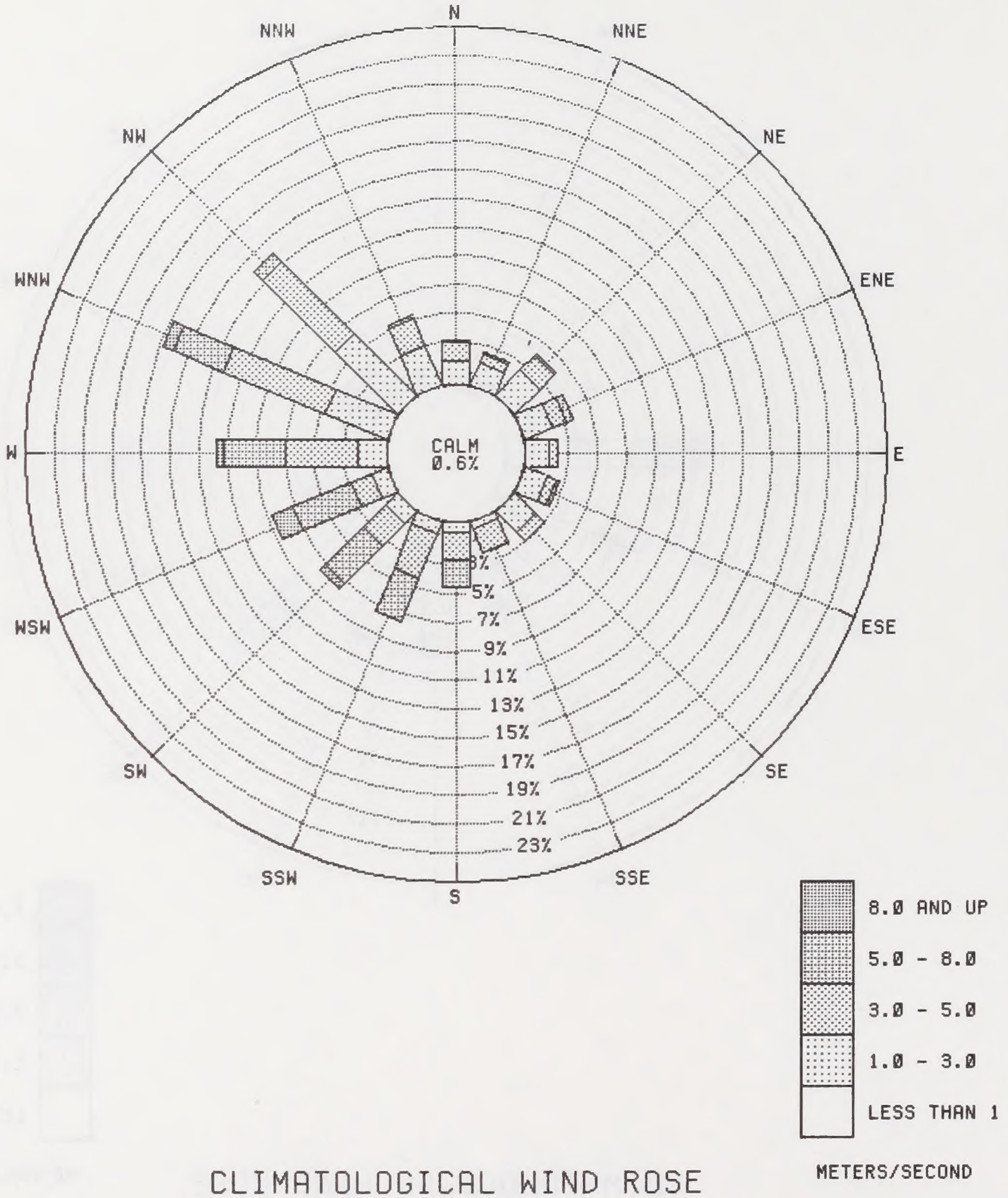

CLIMATOLOGICAL WIND ROSE
SUMMER DAY
(JUNE - AUGUST, 6 AM - 6 PM)

1048 VALID DATA POINTS

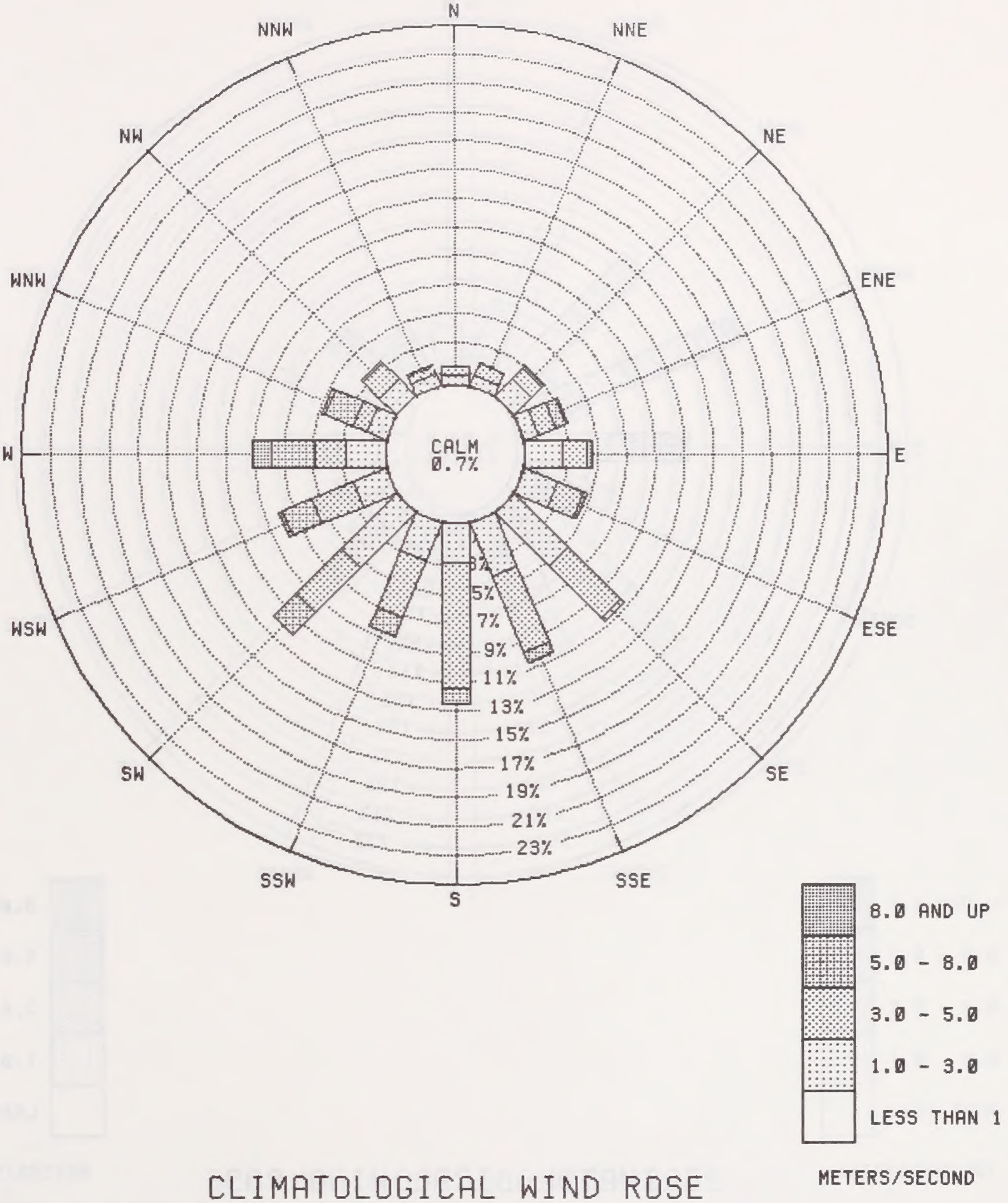

CLIMATOLOGICAL WIND ROSE
SUMMER NIGHT
(JUNE - AUGUST, 6 PM - 6 AM

1037 VALID DATA POINTS

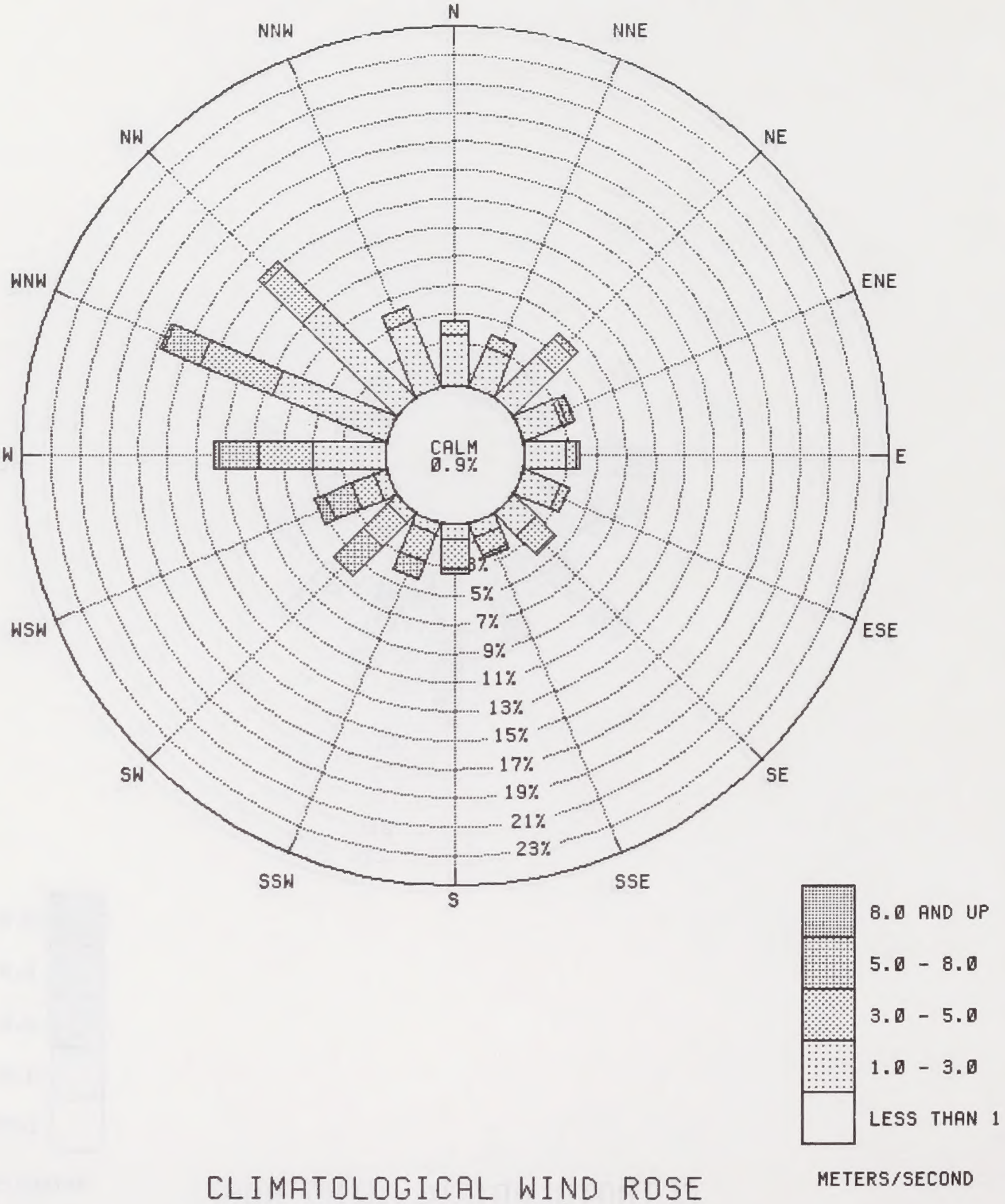

CLIMATOLOGICAL WIND ROSE
FALL DAY
(SEPT - NOV, 6 AM - 6 PM)

1030 VALID DATA POINTS

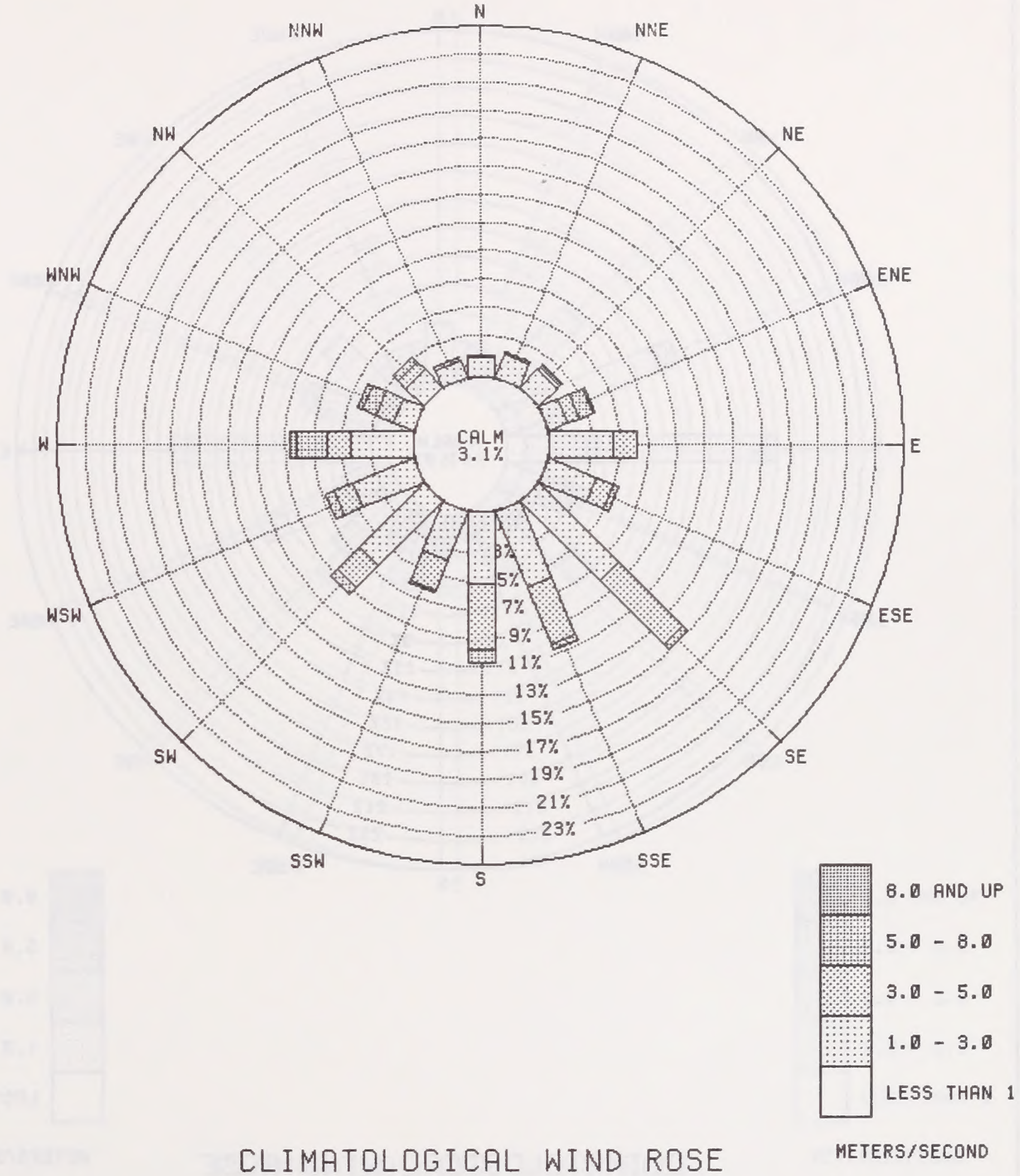

CLIMATOLOGICAL WIND ROSE
FALL NIGHT
(SEPT - NOV, 6 PM - 6 AM

994 VALID DATA POINTS

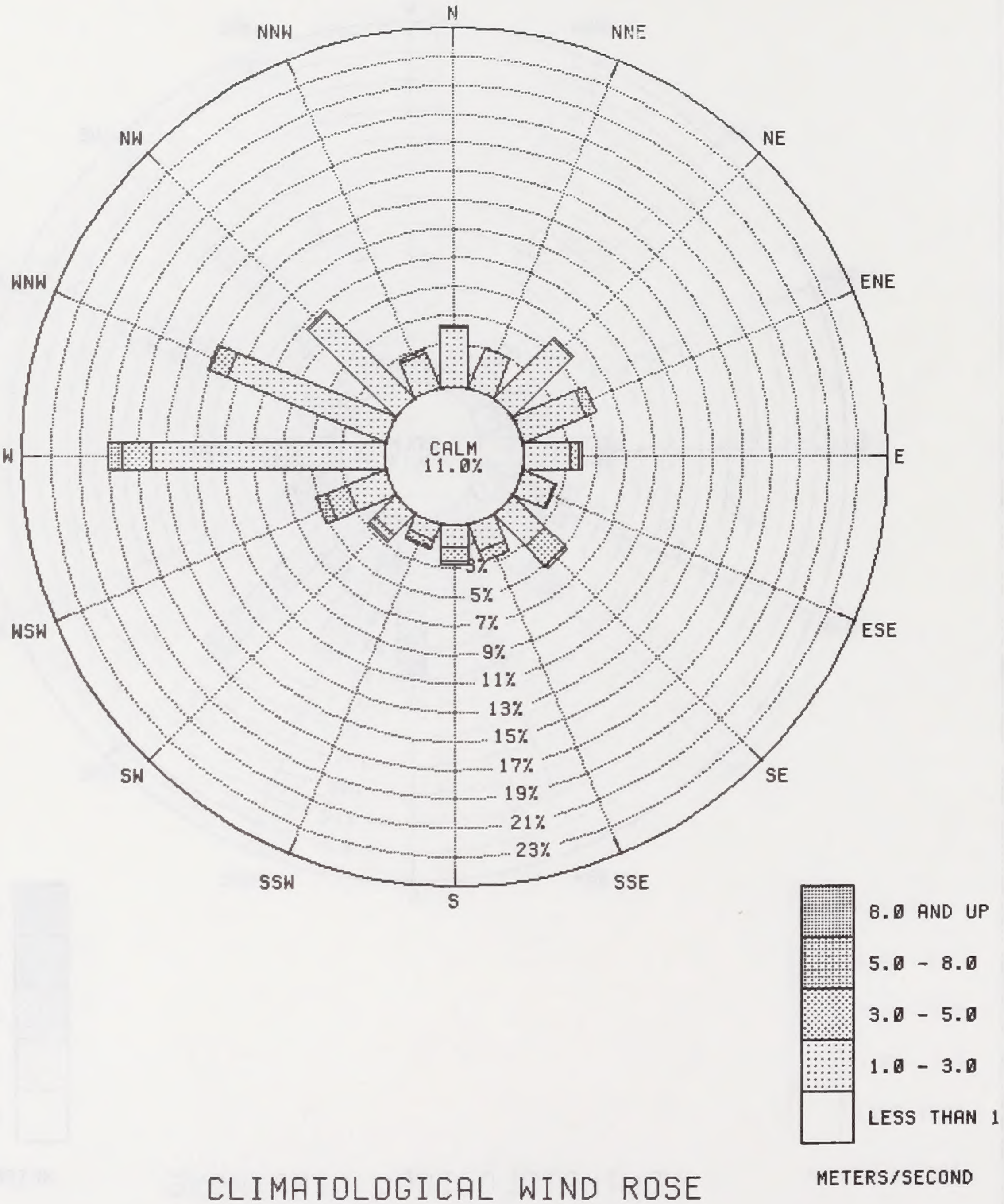

CLIMATOLOGICAL WIND ROSE
WINTER DAY
(DEC - FEB, 6 AM - 6 PM)

900 VALID DATA POINTS

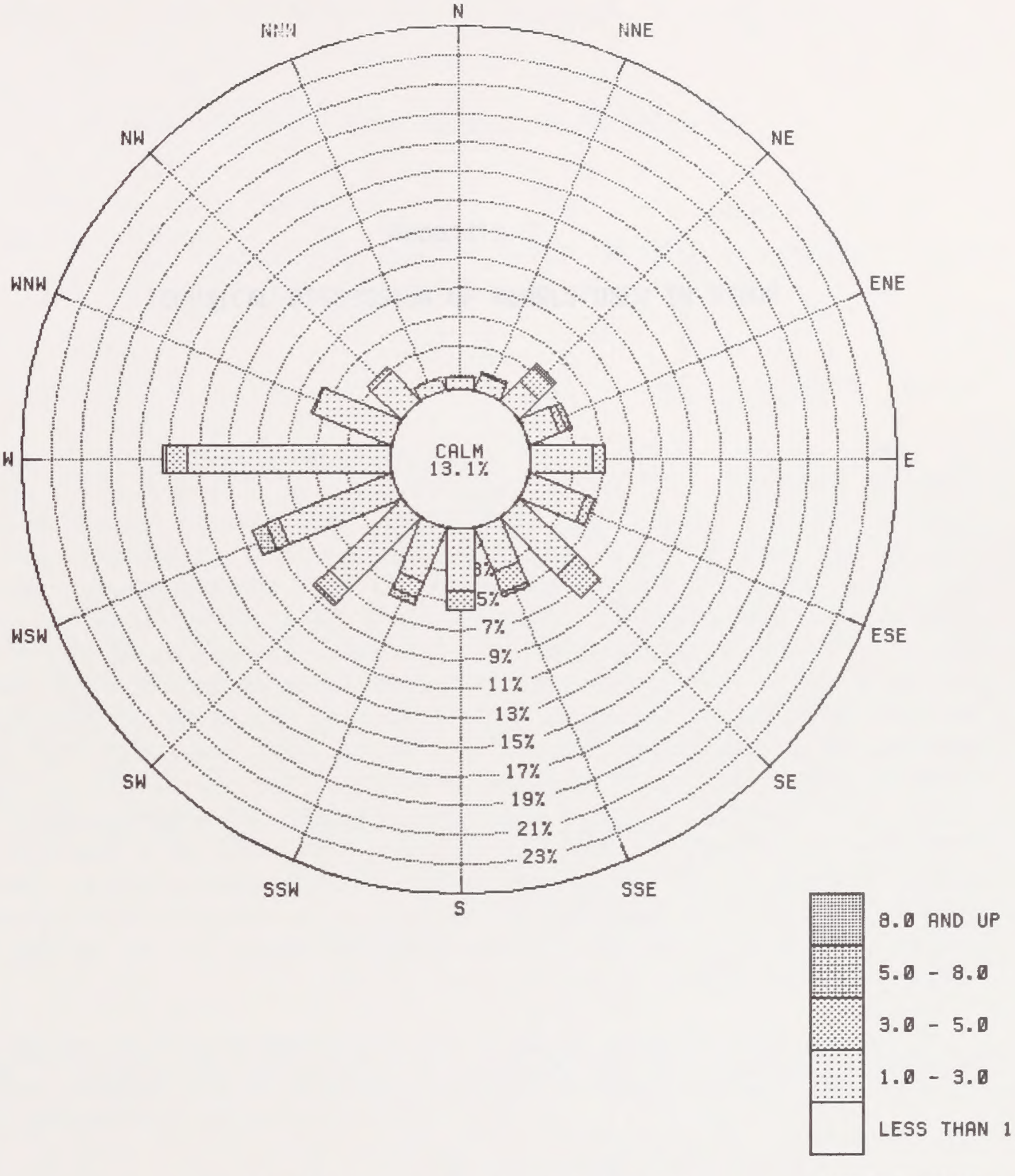

CLIMATOLOGICAL WIND ROSE
WINTER NIGHT
(DEC - FEB, 6 PM - 6 AM

854 VALID DATA POINTS

Appendix C

TECHNICAL DISCUSSION OF MODELS USED IN STUDY

Appendix C

TECHNICAL DISCUSSION OF MODELS USED IN STUDY

C.1 TECHNICAL DISCUSSION OF THE SYSTEMS APPLICATIONS THREE-DIMENSIONAL COMPLEX TERRAIN WIND MODEL

C.1.1 Model Equations

Modeling wind fields in the lower atmosphere is essentially tantamount to simulating the interactions between the free atmosphere and the surface boundary layer of the atmosphere. Depending on the characteristic spatial and temporal scales and other environmental parameters, such as the prevailing wind, the thermal stability, and the topography, these interactions take place at different levels of significance. For example, for a region having a characteristic horizontal dimension on the order of 10^3 km or larger and a characteristic time scale on the order of days, the surface layer can be viewed as a layer feeding energy to the free atmosphere. As a result, any successful model on this scale must include the dynamic changes in the large-scale motion that are due to the surface layer. In contrast, on the scale of interest to this study, with a horizontal dimension of about 200 km and a time scale of a few hours, the synoptic-scale air motion can be viewed as nearly steady-state. Consequently, the surface layer can be regarded as a passive system driven by the synoptic-scale flow and surface perturbations. This is the approach adopted in this model.

The model equation is based on the three-dimensional steady-state equation expressing the conservation of mass for an incompressible fluid:

$$\frac{\partial u}{\partial x} + \frac{\partial v}{\partial y} + \frac{\partial w}{\partial z} = 0 \quad , \qquad \text{(C-1)}$$

where x, y, and z are the orthogonal Cartesian coordinates and u, v, and w are the corresponding wind components. As shown in figure C-1, the modeling region is first divided into vertical layers. Note that the terrain is allowed to intersect the modeling region; consequently, portions of the modeling region (shaded in figure C-1) must be excluded in the calculations. Note also that it is not necessary to assume that the vertical layers are equally divided. By integrating Eq. (C-1) over each vertical slab, one can obtain the following set of equations:

$$\nabla \cdot v = \frac{\partial \bar{u}_i}{\partial x} + \frac{\partial \bar{v}_i}{\partial y} = - \Omega_i(x,y) \quad , \quad i = 1, 2, \ldots, N \quad , \qquad \text{(C-2)}$$

where N is the total number of vertical layers and $\bar{u}_i$ and $\bar{v}_i$ are the vertically averaged wind in the i-th layer, defined as follows:

$$\bar{u}_i = \frac{1}{\Delta z_i} \int_{z_{i-1}}^{z_i} u \, dz \quad , \qquad \text{(C-3)}$$

$$\bar{v}_i = \frac{1}{\Delta z_i} \int_{z_{i-1}}^{z_i} v \, dz \quad , \qquad \text{(C-4)}$$

where

$$\Delta z_i = z_i - z_{i-1} \quad ,$$

and Ω_i is the wind divergence in the i-th layer:

$$\Omega_i(x,y) = \frac{w(z_i) - w(z_{i-1})}{\Delta z_i} \quad . \qquad \text{(C-5)}$$

In its most general form, any velocity vector can be decomposed into two parts, one of which represents potential flow and the other rotational flow (Helmholtz's decomposition):

$$\bar{v} = \bar{A} + \bar{B} = \nabla\phi + \bar{B} \quad . \qquad \text{(C-6)}$$

This decomposition is obviously not unique, because any potential flow can be used for $\bar{A}$. By imposing the additional condition,

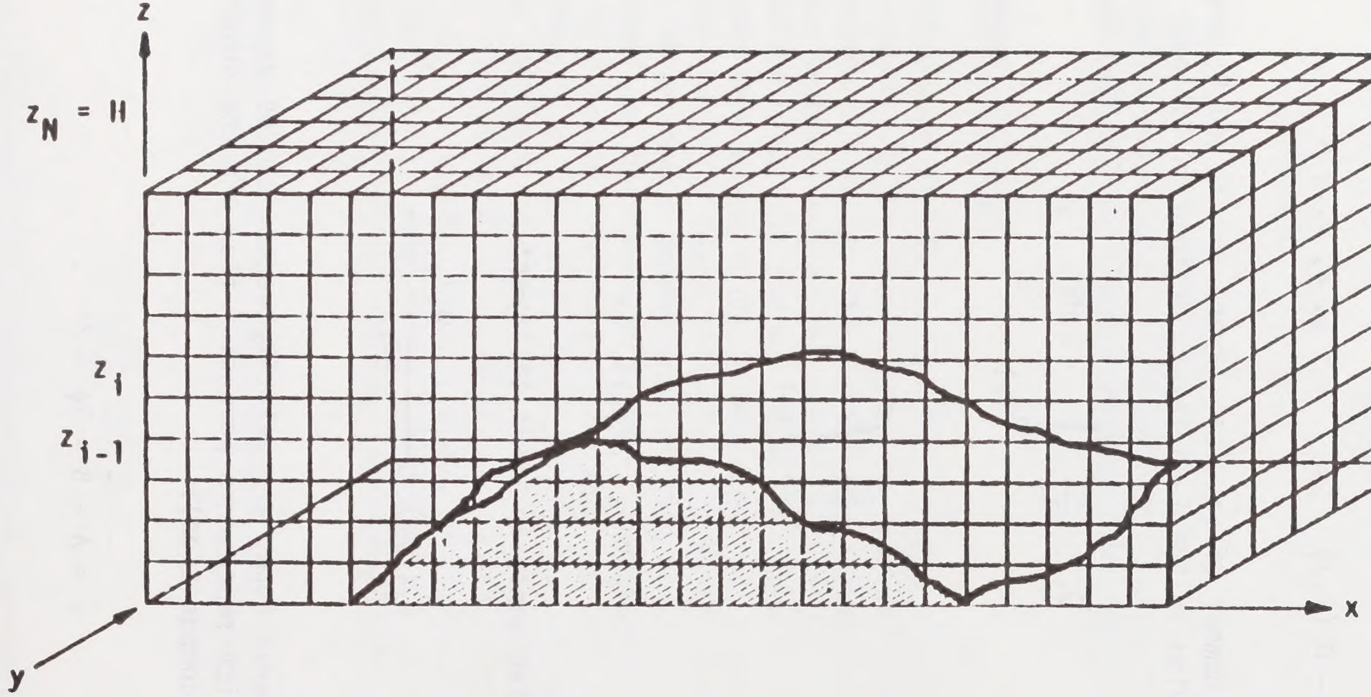

FIGURE C-1. CROSS-SECTIONAL VIEW OF THE INTERSECTION (SHOWN AS SHADED, DASHED GRID) OF A HYPOTHETICAL TERRAIN WITH A THREE-DIMENSIONAL MODELING GRID

$$\nabla \cdot \bar{B} = 0 \quad , \tag{C-7}$$

one can show that a unique decomposition can be constructed, and the second vector $\bar{B}$ can be given by a vector potential $\bar{\beta}$ (Aris, 1962):

$$\bar{B} = \nabla \times \bar{\beta} \quad . \tag{C-8}$$

This vector potential will satisfy Poisson's equation,

$$\nabla^2 \bar{\beta} = -\bar{\omega} \quad , \tag{C-9}$$

where $\bar{\omega}$ is the vorticity of the flow. This is the well-known Helmholtz expression of decomposition for incompressible flow.

Although in prior analyses of surface winds it was conventional to assume that the flow field can be derived from a velocity potential, the validity of such an assumption is predicated on the irrotational nature of the flow field, namely,

$$\nabla \times \bar{v} \equiv \bar{i}\Gamma_{yz} + \bar{j}\Gamma_{zx} + \bar{k}\Gamma_{xy} = 0 \quad ,$$

where

$$\Gamma_{yz} \equiv \frac{\partial w}{\partial y} - \frac{\partial v}{\partial z} \quad , \quad \Gamma_{zx} \equiv \frac{\partial u}{\partial z} - \frac{\partial w}{\partial x} \quad , \quad \Gamma_{xy} \equiv \frac{\partial v}{\partial x} - \frac{\partial u}{\partial y} \quad . \tag{C-10}$$

Since wind flows in the planetary boundary layer are not likely to be irrotational, particularly in the vertical plane, a slightly different approach is used in this model for the decomposition of the velocity vector. For each layer, a two-dimensional velocity potential ϕ is introduced such that

$$\bar{v} = \bar{i}u + \bar{j}v + \bar{k}w = \nabla_2\phi + \bar{k}w \quad , \tag{C-11}$$

where ∇_2 denotes the two-dimensional gradient vector,

$$\nabla_2 = \bar{i}\frac{\partial}{\partial x} + \bar{j}\frac{\partial}{\partial y} \quad .$$

As illustrated in figure C-2, the existence of the two-dimensional velocity potential would be contingent upon the condition that the wind flow is only weakly rotational in the horizontal plane, i.e.,

$$\Gamma_{xy} = \frac{\partial v}{\partial x} - \frac{\partial u}{\partial y} \approx 0 \quad . \tag{C-12}$$

With this approximation, it then follows from the incompressibility condition that

$$\nabla \cdot \bar{v} = \nabla_2^2 \phi + \frac{\partial w}{\partial z} = 0 \quad . \tag{C-13}$$

Therefore, by defining the following two-dimensional potential functions for each of the vertical layers, assuming that the flow is only weakly rotational in the horizontal plane,

$$\bar{u}_i = \frac{\partial \phi_i}{\partial x} \quad , \tag{C-14}$$

$$\bar{v}_i = \frac{\partial \phi_i}{\partial y} \quad , \tag{C-15}$$

Eq. (C-2) can be cast into the conventional Poisson form:

$$\nabla_2^2 \phi_i = \frac{\partial^2 \phi_i}{\partial x^2} + \frac{\partial^2 \phi_i}{\partial y^2} = -\Omega_i \quad . \tag{C-16}$$

Once the distribution of the wind convergence is specified, solutions to these equations with appropriate boundary conditions can be readily computed using numerical techniques discussed in section C.1.4.

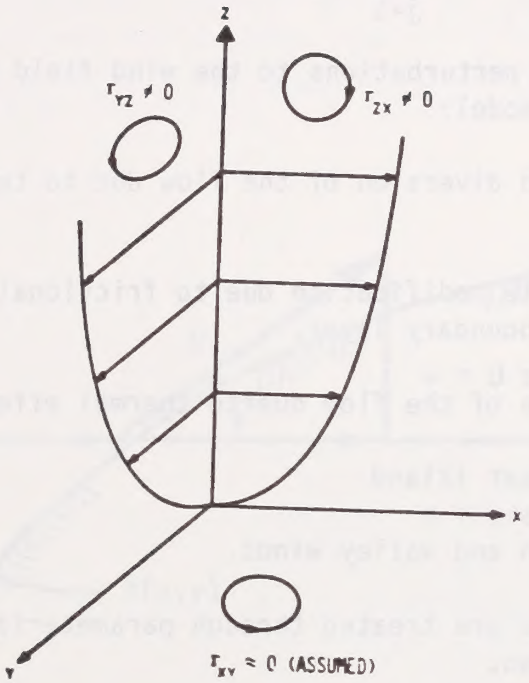

FIGURE C-2. DECOMPOSITION OF VELOCITY VECTORS IN PLANETARY BOUNDARY LAYER

C.1.2 Parameterization of the Vertical Fluxes

The specification of wind convergence is the key feature of this model. It is proposed that the overall wind convergence is the sum of many components, Ω_{ij}, as weighted by coefficients, α_j,

$$\Omega_i = \sum_{j=1}^{n} \alpha_j \omega_{ij} \quad . \tag{C-17}$$

The following perturbations to the wind field over rugged terrain are considered in the model:

> Lifting and diversion of the flow due to topographic effects.

> Wind profile modification due to frictional effects in the planetary boundary layer.

> Convergence of the flow due to thermal effects.

- Urban heat island
- Mountain and valley winds.

These perturbations are treated through parameterization of the pertinent processes as follows.

C.1.2.1 Topographic Effects

Because the terrain is part of the modeling region in the present model formulation, certain aspects of the topographic effects are included indirectly as boundary conditions. For example, the no-slip condition is imposed whenever the flow encounters a solid surface. The often observed lifting and diversion of the flow is, however, handled by parameterizing the vertical fluxes.

For high wind speeds and neutral and unstable conditions, it is perhaps logical to view an airflow contacting the slope of a hill to be perfectly elastic. Based on kinematic considerations, the vertical velocity can be expressed as (see figure C-3)

$$w = U \cdot \sin\left[\arctan \nabla h(x,y)\right] \cdot e^{-k_1 z} \quad , \tag{C-18}$$

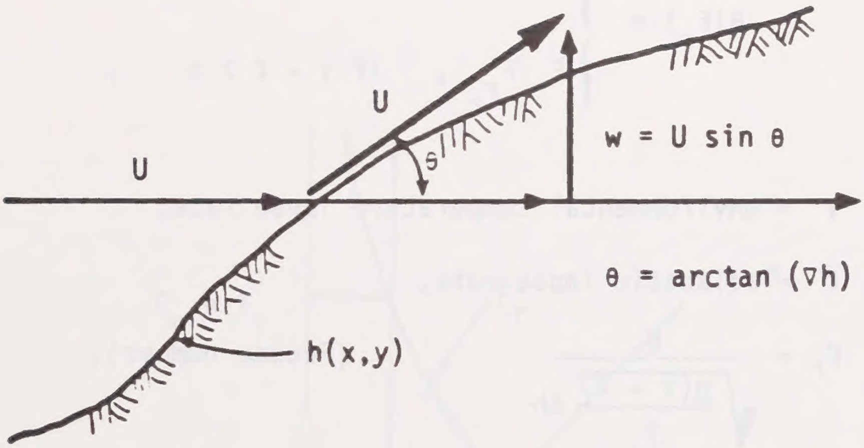

FIGURE C-3. SCHEMATIC DIAGRAM OF A FLOW CONTACTING THE SLOPE OF A HILL where h(x,y) is the terrain height as a function of location. The exponential term has been added to allow for the decay of the topographic influence away from the surface.

For low winds and stable conditions, the kinetic energy of the airstream approaching a hill may be too small to overcome the potential energy required to lift it over the obstacle. As a result, the flow is diverted around the hill. The physical processes governing the occurrence of these phenomena are rather complex, and they have only recently received the attention of researchers. To characterize this effect, Eq. (C-18) was further modified by a multiplicative factor (as shown in figure C-4),

$$B(F_r) = \begin{cases} 1 , & \text{if } \gamma - \Gamma \leq c \quad ; \\ F_r/F_{r_c} , & \text{if } \gamma - \Gamma > c \quad , \end{cases} \tag{C-19}$$

where

γ = environmental temperature lapse rate,

Γ = adiabatic lapse rate,

$$F_r = \frac{U}{\sqrt{\frac{g(\gamma - \Gamma)}{T_\infty}} \Delta h} \qquad \text{(Froude number),}$$

$\Delta h = h_{max} - h(x,y)$,

T_∞ = free-stream temperature,

g = acceleration of gravity,

$$c = \frac{U^2}{\frac{g}{T_\infty} (F_c \Delta h)^2} \qquad \text{(a cut-off constant),}$$

F_c = a critical Froude number where no flow diversion takes place.

Modification of the temperature lapse rate, γ, as air flows over a hill has been neglected as a first approximation herein. According to an analysis by Lilly (1973), the critical Froude number can be taken as 0.5 for an ellipsoidal mountain and 1.0 for a conical mountain.

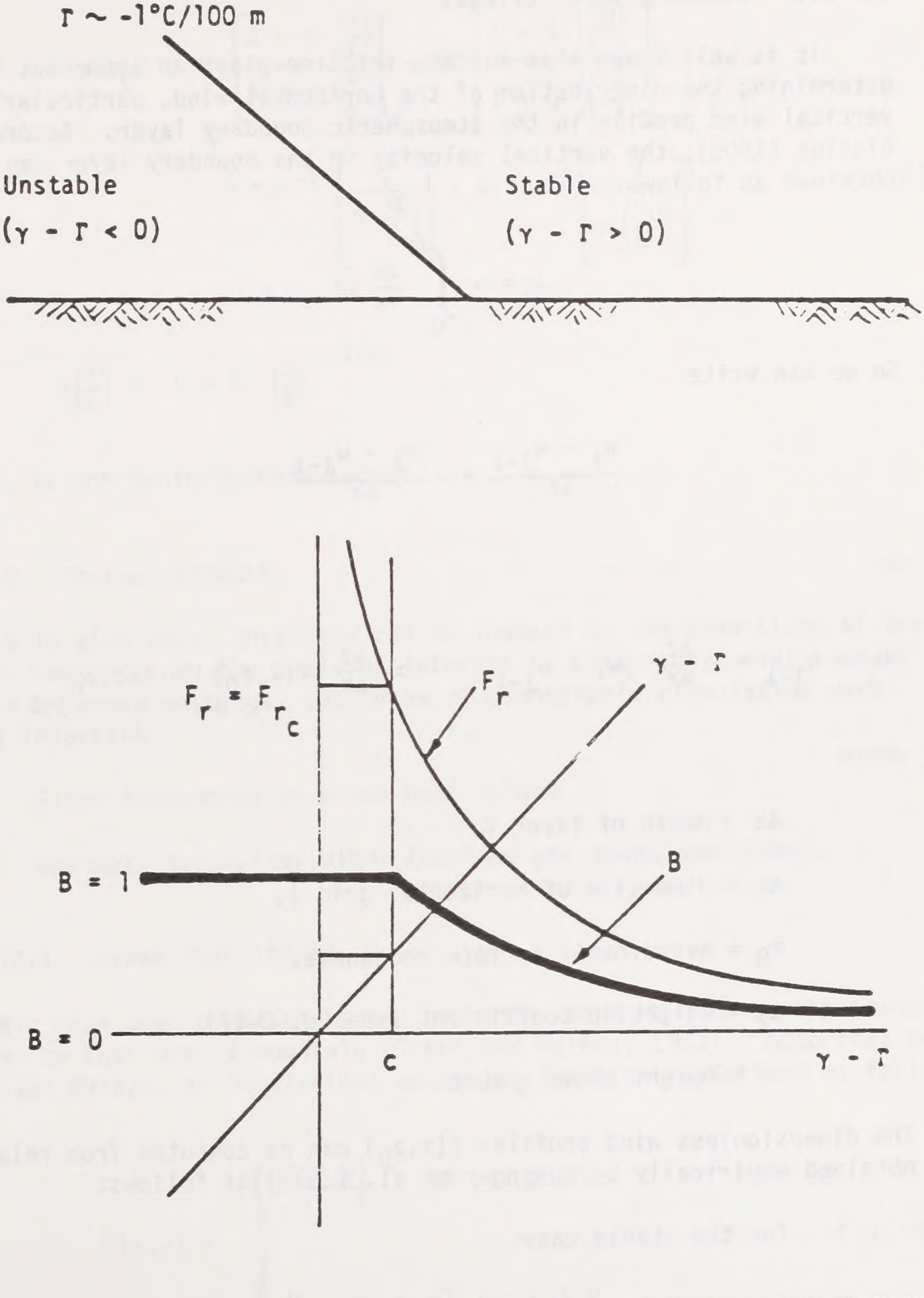

FIGURE C-4. PARAMETERS USED IN DEFINING THE DIVERSION EFFECT

C.1.2.2 Boundary Layer Effects

It is well known that surface friction plays an important role in determining the distribution of the horizontal wind, particularly the vertical wind profile in the atmospheric boundary layer. According to Blasius (1908), the vertical velocity in the boundary layer can be obtained as follows:

$$w = - \int_0^z \frac{\partial w}{\partial x} \partial z \quad . \qquad \text{(C-20)}$$

So we can write

$$\frac{w_i - w_{j-1}}{\Delta z} = - \frac{u_j - u_{j-1}}{\Delta x} \quad , \qquad \text{(C-21)}$$

or

$$w_i - w_{i-1} = - \frac{\Delta z}{\Delta x} \left(w_j - u_{j-1}\right) = - \alpha_2 \frac{\Delta z}{\Delta x} \; f(z,z_0)_j - f(z,z_0)_{j-1} \quad , \qquad \text{(C-22)}$$

where

Δz = depth of layer i,

Δx = dimension of horizontal grid j,

z_0 = aerodynamic surface roughness,

α_2 = weighting coefficient (see Eq. C-17),

z = height above ground.

The dimensionless wind profiles $f(z,z_0)$ can be computed from relationships obtained empirically by Businger et al. (1973) as follows:

> for the stable case,

$$f(z,z_0) = \ell n\left(\frac{z}{z_0}\right) + 4.7 \left(\frac{z - z_0}{L}\right) \quad ; \qquad \text{(C-23)}$$

> for the unstable case,

$$f(z,z_0) = \ell n \left[\frac{1 - g\left(\frac{z}{L}\right)}{1 + g\left(\frac{z}{L}\right)} \right] - \ell n \left[\frac{1 - g\left(\frac{z_0}{L}\right)}{1 + g\left(\frac{z_0}{L}\right)} \right]$$

$$+ 2 \tan^{-1} \left[\frac{1}{g\left(\frac{z}{L}\right)} \right] - 2 \tan^{-1} \left[\frac{1}{g\left(\frac{z_0}{L}\right)} \right] \quad , \qquad \text{(C-24)}$$

and

$$g\left(\frac{z}{L}\right) = \left[1 - 15 \left(\frac{z}{L}\right)\right]^{-1/4} ,$$

where L is the Monin-Obukhov length.

C.1.2.3 Thermal Effects

It is also known that flow can be induced by the conditions of uneven surface heating. On the scale of interest to this study, over complex terrain in urban settings, two types of atmospheric circulation were deemed important:

> Flows induced by an urban heat island

> Mountain and valley winds (upslope and downslope flows).

C.1.2.3.1 Urban heat island

Air flow over a heated island has been shown to have an appearance similar to that over a mountain (Stern and Malkus, 1953). According to Stern and Malkus, an "equivalent mountain" function is defined as follows:

$$M(x,y) = \begin{cases} \dfrac{T(x,y)}{\gamma - \Gamma} & \text{if } \gamma - \Gamma > 0 \\ 0 & \text{if } \gamma - \Gamma < 0 \end{cases} \qquad \text{(C-25)}$$

where T(x,y) is the spatial distribution of surface temperature. In parallel to the discussions that led to Eq. (C-18), it can be assumed that the vertical motion generated by heat island effects is

$$w = U \cdot \sin(\arctan \nabla M) \cdot e^{-k_2 z} \quad . \tag{C-26}$$

The reader should note that in the absence of a driving wind, U, vertical fluxes due to the urban heat island are zero. Furthermore, the equivalent mountain formulation was derived for flat terrain situations; therefore, this parameterization is used only for flat portions of the modeling grid. In sloping terrain, the treatment described in the following section is used.

C.1.2.3.2 Mountain-valley winds

Slope winds are micro/mesoscale breezes that blow normal to the topographic gradients due to temperature-dependent density differences. During the night, radiative cooling of the slope cools the air just above it. This process causes the air close to the ground to become denser than the air at the same altitude but farther above the sloping surface. As a result, the cold air slides down the slope. The reverse process occurs during the day when the sun's radiation warms the slope and the air just above the slope.

Defant (1933) proposed the following expression to describe the steady-state, average speed of a cold current gliding down a slope of average elevation angle α:

$$U_{slope} = \left[\frac{g\bar{h}(T_C - T_E)\sin\alpha}{C_D T_C} \right]^{1/2} \quad , \tag{C-27}$$

where

C_D = a drag coefficient,

$\bar{h}$ = the mean height of the cold current,

g = gravitational acceleration,

T_C, T_E = the temperatures of the current and environment, respectively.

The reader will note that a driving wind is not necessary to induce down-slope flow using Eq. (C-27).

Adapting Eq. (C-27) to our grid system, but retaining the important functional dependences, one can obtain the following expression for both up-slope and down-slope flow:

$$U_{slope} = \alpha_4 \left[\left(\frac{T_C - T_E}{T_C} \right) \left(\frac{H_{max} - H}{H_{max}} \right) \right]^{1/2} , \qquad \text{(C-28)}$$

where H is the average surface elevation in the grid cell and H_{max} is the highest terrain elevation affecting local flow. The term involving the terrain heights is substituted for the "sin α" term in Eq. (C-27) because this is qualitatively correct only for estimating average slope velocity and only if the elevation angle is uniform along the entire slope. In the modeling grid, however, the velocity is computed at any point along a slope, not just the average slope velocity, and elevation angles are rarely uniform along a slope. The substitution allows qualitatively realistic, spatially resolved estimates of up-slope and down-slope flow behavior. With a proper selection of the constant in Eq. (C-28), quantitatively correct estimates should also be possible.

As in Defant's algorithm, Eq. (C-28) contains no dependence on driving wind. In this model, therefore, the vertical fluxes for the mountain-valley winds are self-generating. Since down-slope and up-slope flows have both horizontal and vertical components, to maintain consistency the model must account for the self-generating horizontal component as well as the vertical component. Therefore, the parameterization of mountain-valley winds is entered through the vertical flux term and through the horizontal boundary conditions. All previous parameterizations of vertical fluxes described are dependent on the horizontal wind and are intrinsically consistent with the horizontal flow component; thus, no adjustments to boundary conditions are necessary for them.

C.1.3 Specification of Parametric Coefficients

Equation (C-17) calls for the specification of a weighting coefficient for each of the four parameterized vertical fluxes discussed in the last section. A user may wish to vary these empirically to improve the model's performance for a given application. However, it is possible to determine values analytically for sample cases. In this section the specification of these coefficients is described.

C.1.3.1 Coefficient for Topographic Effects

As indicated earlier, on the basis of kinematic considerations, the empirical coefficient for topographic effect, α_1, should be unity for a perfectly elastic wind flow. This will probably correspond to the neutrally stratified atmospheric conditions. For stable or unstable stratifications corresponding to the inelastic situations, this empirical coefficient is expected to be less or greater than 1, namely,

$$\alpha_1 \begin{cases} < 1 & \text{stable stratification} \\ = 1 & \text{neutral stratification} \\ > 1 & \text{unstable stratification} \end{cases} .$$

From model sensitivity tests, it was found that the resultant wind field is extremely sensitive to the specification of this coefficient.

C.1.3.2 Coefficient for Boundary Layer Effects

The parameterization scheme outlined earlier for the boundary layer effect essentially provides a correspondence between the horizontal and vertical wind velocities. The derivation of the expression given in Eq. (C-22) involves substitution of the dimensionless $f(z,z_0)$ term for u_j and u_{j-1} since

$$f(z,z_0) = \frac{ku(z)}{u_*} ,$$

where k is von Karman's constant and u_* is the friction velocity. Therefore, the frictional coefficient is given by

$$\alpha_2 = \alpha_f = \frac{u_*}{k} . \qquad \text{(C-29)}$$

Typically, k is about 0.35 in the atmosphere (Businger et al., 1973) and an average u_* is about 0.316 m/sec (Tennekes, 1973). Substituting these values into Eq. (C-29) yields

$$\alpha_2 \approx 1.0 .$$

C.1.3.3 Coefficient for Urban Heat Island Effects

It can be seen from Eqs. (C-25) and (C-26) that the parameterization for the urban heat island effect is parallel to that for the topographic effects. For this reason, one would expect that the specification of the coefficients for the effects are the same. Therefore, the coefficient is given by

$$\alpha_3 \begin{cases} < 1 & \text{stable} \\ \cong 1 & \text{neutral} \\ > 1 & \text{unstable} \end{cases} .$$

C.1.3.4 Coefficient for the Slope Wind Effect

To derive the range of values for this coefficient, we begin with the vertical momentum equation, assuming hydrostatic, steady-state conditions:

$$w \frac{\partial w}{\partial z} = - \frac{1}{\rho} \left(\frac{\partial p}{\partial z}\right) - g \quad . \tag{C-30}$$

Following Rao and Snodgrass (1981), Eq. (C-30) can be expressed in the following form:

$$w \frac{\partial w}{\partial z} = \left(\frac{g}{\theta_0}\right) \theta' \sin \alpha \quad , \tag{C-31}$$

where g is the gravitational constant, θ_0 is the reference-state temperature, θ' is the deviation of the mean potential temperature from the reference-state temperature, and α is the terrain slope angle. Integrating Eq. (C-32) from the surface to the top of the slope flow, h, one obtains

$$w = \sqrt{2g\theta' h \sin\alpha/\theta_0} \quad . \tag{C-32}$$

A comparison of Eqs. (C-27) and (C-32) yields the following expression:

$$\alpha_4 = \sqrt{gh/C_D} \quad . \tag{C-33}$$

Using a range of values between 10 and 50 meters for h (given by Defant [1951]) and between 0.001 and 0.005 for C_D (given by Munn [1966]), the following range is obtained for α_4:

$$140 \leqslant \alpha_4 \leqslant 700 \quad .$$

C.1.4 Numerical Solution Procedure

To obtain a solution to Eq. (C-16) with complex boundary conditions, a numerical technique is required. Several direct Poisson solvers are available that are based on block-cyclic reduction of a set of finite difference equations (Buzbee, Golub, and Nielson, 1970; Swarztrauber and Sweet, 1975). Although these solvers are convenient and inexpensive to use, their application is restricted to simple rectangular modeling regions. This restriction presents a rather serious drawback for our formulation because, as described earlier, the terrain may intersect the modeling region.

Thus, an alternative solution technique was chosen that can accommodate the exclusion of portions of the modeling region having irregular shapes and yet incur only a modest increase in computation time over the direct solution techniques. The general form of the Poisson equation can be written as

$$\nabla^2 \phi = \frac{\partial^2 \phi}{\partial x^2} + \frac{\partial^2 \phi}{\partial y^2} = f(x,y) \quad , \tag{C-34}$$

and the five-point difference approximation to Eq. (C-34) is

$$\frac{\phi_{i-1,j} - 2\phi_{i,j} + \phi_{i+1,j}}{(\Delta x)^2} + \frac{\phi_{i,j-1} + 2\phi_{i,j} + \phi_{i,j+1}}{(\Delta y)^2} = f_{i,j} \quad , \tag{C-35}$$

$$i = 1, \ldots, M \text{ and } J = 1, \ldots, N \quad ,$$

where

ϕ = the potential function,

$f(x,y)$ = the forcing function,

x, y = orthogonal Cartesian coordinates, i, j = the grid cell indices of a grid system that is superimposed on the modeling region and that has M grid cells in the x- (i-) direction and N grid cells in the y- (j-) direction.

Equation (C-35) is valid for all points within the modeling region, but for those along the modeling boundary some additional computations are required. Along the boundaries, the normal derivatives of ϕ (i.e., $d\phi/dx$ or $d\phi/dy$--often referred to as Neumann-type boundary conditions) are specified, and these are used to compute values of ϕ at fictitious grid points outside the modeling region. For example, consider a grid cell (i,j) that forms part of the left boundary of the modeling region as shown in figure C-5. To solve Eq. (C-35) for this point, one must specify some value for $\phi_{i-1,j}$, which exists at a point outside the modeling region. One can simply compute $\phi_{i-1,j}$ using

$$\phi_{i-1,j} = \phi_{i,j} - \frac{d\phi}{dx}_{ij} \Delta x \quad , \tag{C-36}$$

and substitute this expression in Eq. (C-35).

The commonly used modified Gauss-Seidel iterative solution method was selected because it is very well suited to the solution of the five-point operator [Eq. (C-35)] for the Poisson equation (Dahlquist and Björck, 1974). Like all iterative techniques, it starts from a first approximation, which is successively improved until a sufficiently accurate solution is obtained. To simplify the description of this method, consider the linear system of equations

$$Ax = b \quad , \tag{C-37}$$

instead of the system described in Eq. (C-35). Equation (C-37) can be written as

$$x_i = \frac{-\sum_{\substack{j=1 \\ j \neq i}}^{N} (a_{ij}x_j + b_j)}{a_{ii}} \quad , \quad i = 1, 2, \ldots, n, \text{ and } a_{ii} \neq 0 \quad . \tag{C-38}$$

In Gauss-Seidel's method, a sequence of approximations $x^{(1)}$, $x^{(2)}$, $x^{(3)}$, ... is computed by

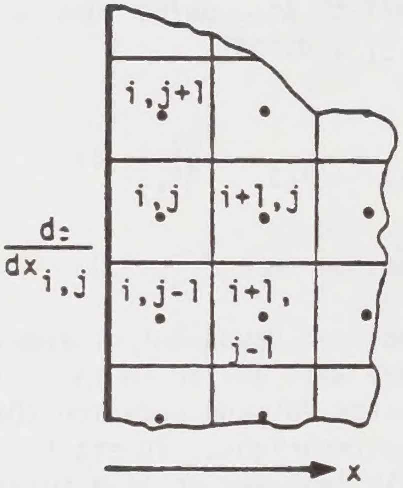

FIGURE C-5. SKETCH SHOWING A GRID CELL (i,j) ALONG THE LEFT BOUNDARY OF THE MODELING REGION

$$x_i^{(k+1)} = \frac{-\sum_{j=1}^{i-1} a_{ij} x_j^{(k+1)} - \sum_{j=i+1}^{n} a_{ij} x_j^{(k)} + b_i}{a_{ii}} , \qquad \text{(C-39)}$$

Note that Eq. (C-39) can also be written as

$$x_i^{(k+1)} = x_i^{(k)} + r_i^{(k)} , \qquad \text{(C-40)}$$

where $r_i^{(k)}$ is the current residual of the i-th equation and

$$r_i^{(k)} = \frac{-\sum_{j=1}^{i=1} a_{ij} x_j^{(k+1)} - \sum_{j=1}^{n} a_{ij} x_j^{(k)} + b_i}{a_{ii}} . \qquad \text{(C-41)}$$

Now, to improve the rate of convergence, one can slightly modify Eq. (C-40) to give

$$x_i^{(k+1)} = x_i^{(k)} + \omega\, r_i^{(k)} , \qquad \text{(C-42)}$$

where ω is called the relaxation parameter, which is chosen so that the rate of convergence is maximized. This improved iteration procedure is called the "successive overrelaxation method" (Dahlquist and Björck, 1974).

For this model, $\omega = 1.7$ is found to give the best rate of stable convergence in tests of the modified Gauss-Seidel solution to Eq. (C-35). The criterion for complete convergence is defined so that

$$\max r_i^{(k)} < 0.01\, x_i^{(k)} . \qquad \text{(C-43)}$$

C.2 TECHNICAL DISCUSSION OF THE SYSTEMS APPLICATIONS GAUSSIAN PUFF MODEL

The Gaussian Puff Model (GPM) is a multiple-source Gaussian dispersion model utilizing temporally and spatially varying meteorological data that include temperature, exposure class, a three dimensional wind field, and height of the mixing layer.* As many as five species can be simulated. The GPM also treats time varying emissions. Complex advection and dispersion situations, such as plume backtracking or plume-terrain interactions, can also be accommodated with the GPM.

GPM contains two main sections. In the first, a plume rise model is used to predict the height of the plume. This model calculates either the height of a source from which the plume emanates, or the plume trajectory near the source. In the second section, the plume is treated as a series of segments or puffs, a puff being a part of the plume emitted during one time step.

The model keeps track of all of the puffs emitted from a source until they leave the modeling region. The model stores information about the location of the center of each puff (in three dimensions), the pollutant mass in the puff, and the standard deviation of the puff mass distribution in the vertical direction (σ_z), and in the horizontal direction perpendicular to the motion of the puff (σ_y). Each puff is advected according to the winds at the center of the puff, and the mass distribution of any cross-section of the plume is determined by the dispersion coefficients σ_z and σ_y and the Gaussian formulation. An area source is treated as a point source, but without plume rise, having an initial σ_y equal to one-half the diameter of the area source.

A display program plots ground-level concentration iospleths, plume paths, instantaneous concentrations, or average concentrations. Also, subgrid concentrations can be printed for any times within the interval of the simulation, and for any subregion of the modeling region.

GPM uses gridded two- or three-dimensional wind fields supplied by the user. In this study, three-dimensional wind fields were generated using the SAI Complex-Terrain Wind Model in a computer mode. In this mode, hourly gridded wind fields are generated by scaling one of sixteen cardinal wind direction flow patterns and then superimposing one of six slope wind flow patterns, if appropriate (see section 4.2.1.4). Since the flow patterns were categorized within only 16 cardinal wind directions, the resolution of the wind fields was, at best, 22.5°. Therefore, each time a wind vector is selected by GPM for use in the advection algorithm, it is first randomized. The randomization occurs uniformly with a ±12° sector.

---

* The reader will note many similarities between GPM and the Gaussian puff submodel within RTM.

Another feature added to GPM for this study is a "trajectory look-ahead" option. "Trajectory look-ahead" is accomplished by subdividing the time step into sub-time steps sufficiently small that puffs are prevented from traveling more than 3/4 the length of a wind model grid cell during the sub-time step. The puffs' trajectories are then computed using the gridded winds at each sub-time step and are assembled to form an effective trajectory for the larger time step. This allows the model to use all the spatial resolution available in the gridded winds while permitting a large time step for greatest economy. The added economy of the option is most important for the year-long GPM runs required in this study.

The model accounts for several occurrences at each time step: all the old puffs are advected downwind; new values for puff location, mass, and dispersion coefficients are calculated. In addition, a new puff is created with a center a half-step downwind, at a height determined by the following plume rise equation (Briggs, 1971):

$$H_e = H_s + [1.6\, F^{1/3} \cdot (10H_s)^{2/3} \,/U] \qquad \text{(C-44)}$$

$$\text{where } F = 9.8\,\frac{\Delta T}{T_s} \cdot V_s R_s^{\,2} \quad ,$$

where

$\Delta T = T_s - T_a$

H_e = effective release height

H_s = stack height

U = wind velocity

F = buoyancy flux

V_s = exit velocity from stack

R_s = stack radius

T_s = temperature in stack

T_a = ambient temperature.

Vertical winds are conservatively assumed to be zero; therefore, this height is used for the center of the puff downwind except in the vicinity of high terrain. Near high terrain, the height of the puff above local ground level is governed by the following expression (Queney, 1947), which is also used in the wind model (see section C.1.1):

$$H_P = H_T \exp\,[-K_S H_E] + H_E \qquad \text{(C-45)}$$

where

H_P = local height of puff

H_E = effective stack height of puff at release

H_T = local height of terrain above terrain height at source

K_S = s/u

$s = \left(\frac{g}{\theta}\frac{\partial\theta}{\partial z}\right)^{1/2} \quad ; \quad \frac{\partial\theta}{\partial z} \geqslant 0$

u = local wind speed

θ = potential temperature

g = gravitational constant.

The reader will note that the vertical displacement of a puff caused by the terrain is dependent on the stability in such a manner that displacement decreases with increasing stability and with increasing effective stack height. For neutral or unstable conditions, puff displacement is identical to the terrain height displacement. For added conservatism in the regional GPM applications (in which neutral stability is assumed), puffs are allowed to approach terrain to within one-half their effective stack height rather than maintaining their original terrain separation, as would be calculated using the expression above.

Two methods are implemented to calculate the dispersion coefficients within 40 km of the source: Pasquill-Gifford Turner (PGT) and TVA. For each point source, one of the methods is prescribed by the user. For this study, the PGT curves were used. These dispersion coefficients are functions of atmospheric stability class, downwind distance, and dispersion coefficient history. Although the stability class is a discrete function of meteorological conditions and, therefore, can vary discontinuously in space or time, the dispersion coefficients are calculated to increase smoothly with time. The rate of change of the coefficients at the appropriate stability class and downwind distance is used to calculate increments that are added to the coefficients at each time step.

Fundamental diffusion theory (Taylor, 1921) indicates that plume growth becomes dependent on time after sufficient time. Therefore, beyond 40 km, GPM uses the following time-dependent algorithm (Heffter, 1965):

$$\Delta\sigma_y = 1800\ dt$$
$$\Delta\sigma_z = 94.8\ dt/VT \quad ,$$

where

dt = time step (hours)

T = age of puff (hours)

Time-dependent stability class information is supplied by the user. In the regional-scale applications of GPM, stability class was assumed to be neutral (Pasquill-Gifford Class D) at all times, because it is more appropriate for long-range transport than are the time-varying stabilities derived from micrometeorological (small-scale) measurements. In the near-source GPM applications, stability class is time-dependent and derived from sigma-theta measurements made at Tracts U-a and U-b.

Changes in each puff's mass, caused by deposition and oxidation, are also calculated during each time step. To calculate the percentage of plume mass near the ground, deposition is calculated using the vertical dispersion coefficient and the Gaussian distribution in the vertical direction. Deposition is then calculated using a first-order decay model. Oxidation is also calculated using a simple first-order decay approximation and user-specified decay rate.

The first-order decay or loss of mass in a puff due to chemical transformation and surface deposition is given by

$$\text{Mass Loss} = \text{Current Puff Mass} \times \left\{1 - \exp\left[-(K1 + K2)\Delta t\right]\right\}$$

where K1 = chemical conversion rate in (s^{-1}); SO_2 to SO_4 conversion rates 1.5%/hr in daytime and 0.1%/hr at night were assumed.

K2 = deposition rate (s^{-1}) deposition velocity/puff depth. (Deposition velocities for SO_2 and TSP were assumed to be 1 and 0.5 cm/s, respectively. The puff depth was taken to be the minimum of $4\sigma_z$, $H + 2\sigma_z$, and the assumed 3600 m mixing depth.)

Δt = time step

The usual Gaussian equation is

$$\chi(P) = \frac{Q}{U} F(Y, \sigma_y)\ G(Z, S_c, \sigma_z, L) \tag{C-46}$$

where

χ = the concentration at P due to the plume (g/m^3),

X = the downwind distance of point P from the source,

Y = the crosswind distance from P to the plume centerline (m),

Z = the vertical coordinate of the point P (m),

S = the vertical coordinate of the point (X_c, Y_c, Z_c) on the plume centerline that is closest to P (m),

Q = the rate of emission (g/sec),

U = the wind speed (m/sec),

σ_y = the horizontal (transverse) dispersion coefficient (m),

σ_z = the vertical dispersion coefficient (m),

L = the mixing height (m).

σ_y and σ_z are calculated at (X_c, Y_c, Z_c).

$$F(Y, \sigma_y) = \frac{1}{\sqrt{2\pi}\ \sigma_y} \exp\left[\frac{-Y^2}{2\sigma_y^{\ 2}}\right] \tag{C-47}$$

$$G(Z, S, \sigma, L) = \frac{1}{\sqrt{2\pi}\ \sigma} \Bigg\{ \exp -\left[\frac{(S - Z)^2}{2\ \sigma^2}\right]$$

$$+ \exp -\left[\frac{(ZL - S - Z)^2}{2\ \sigma^2}\right] + \exp -\left[\frac{(2a - S - Z)^2}{2\ \sigma^2}\right]$$

$$\sum_{\substack{n\ \text{even} \\ n > 0}} \Bigg(\exp -\left[\frac{(na - nL + S - Z)^2}{2\ \sigma^2}\right] + \exp -\left[\frac{[n + 2]\ L - na - S - Z)^2}{2\ \sigma^2}\right]$$

$$+ \exp \left[\frac{(nL - na + S - Z)^2}{2\,\sigma^2} \right] + \exp - \left[\frac{[n + 2]\,a - nL - S - Z)^2}{2\,\sigma^2} \right] \Bigg) \Bigg\} \quad \text{(C-48)}$$

where a is the height of the ground (or lower barrier). If a = Z = 0, this reduces to

$$G(0,\ S,\ \sigma,\ L) = \frac{2}{\sqrt{2\pi}\ \sigma} \sum_{n=-\infty}^{\infty} \exp - \left[\frac{(S + 2nL)^2}{2\,\sigma^2} \right] \quad . \quad \text{(C-49)}$$

When σ_z/L is large enough, the pollutant is considered to be uniformly distributed in the mixing layer, and then G = 1/L.

Equations (C-47) and (C-48) are implemented as shown in Eq. (C-46). The concentration due to a puff is calculated in ppm:

$$C(P) = \frac{A \cdot 10^6}{\phi \cdot dx}\ F(y,\ \sigma_y)\ G(Z,\ Z_c,\ \sigma_z,\ L) \quad , \quad \text{(C-50a)}$$

$$C(P) = \frac{A \cdot 10^6}{(\phi \cdot dx \cdot 4\sigma_y,\ \text{mixing depth})} \quad . \quad \text{(C-50b)}$$

where

C = the concentration at the point P (ppm),

A = the number of moles of pollutant in the puff,

dx = the distance the puff traveled during the current time step (m),

ϕ = the number of models per cubic meter (air) = 40.82,

F, G = the same as above (except we use a finite sum).

Beyond 50 km, concentrations are calculated by Eq. (C-50b) assuming uniform mixing. The concentration at P due to the plume is then the result of summing Eq. (C-50b) over all puffs, with the following two exceptions:

> If the point P is at P_1, then the contribution at P due to puff B is ignored (see figure C-6).

> If P is at P_2, then Eq. (C-50b) gives zero contribution at P from both puffs A and B. In this case, Eq. (C-50b) is used with y equal to the horizontal distance from X to P, and (X_c, Y_c, Z_c) equal to X.

C.3 OVERVIEW OF THE EPA/SYSTEMS APPLICATIONS PLUME VISIBILITY MODEL

The design objective of the plume visibility model (PLUVUE) used in this analysis is to calculate visual range reduction and atmospheric discoloration caused by plumes consisting of primary particulates, nitrogen oxides, and sulfur dioxides emitted by a single emissions source. Primary emissions of sulfur dioxide (SO_2) and nitric oxide (NO) do not scatter or absorb light and therefore do not cause visibility impairment. However, these emissions are converted in the atmosphere to secondary species that do scatter or absorb light and have the potential to cause visibility impairment. SO_2 emissions are converted to sulfate ($SO_4^=$) aerosol, such as sulfuric acid and acid ammonium sulfates. These aerosols are generally formed or grow to a size (0.1 to 1.0 µm) that is effective in scattering light. Nitric oxide (NO) emissions are converted to nitrogen dioxide (NO_2) gas, which is effective in absorbing light. In turn, NO_2 is converted to nitric acid vapor (HNO_3), which neither absorbs nor scatters light. In some situations, nitric acid may form ammonium nitrate or organic nitrate aerosol, which scatters light. However, in many nonurban plumes nitrate probably remains as HNO_3 vapor without visual effects. Eventually, all primary particulates, secondary aerosol, and gases in a plume are removed from the atmosphere as a result of surface deposition and precipitation scavenging. PLUVUE is designed to predict the transport, atmospheric diffusion, chemical conversion, optical effects, and surface deposition of point-source emissions. Figure C-7 shows schematically the logic flow of PLUVUE.

The model uses a Gaussian formulation for transport and dispersion. The spectral radiance $I(\lambda)$ (i.e., the intensity of light) at 39 visible wavelengths ($0.36 < \lambda < 0.75$ µm) is calculated for views with and without the plume; the changes in the spectrum are used to calculate various parameters that predict the perceptibility of the plume and contrast reduction caused by the plume (see Latimer et al., 1978). The four key perception parameters for predicting visual impact are

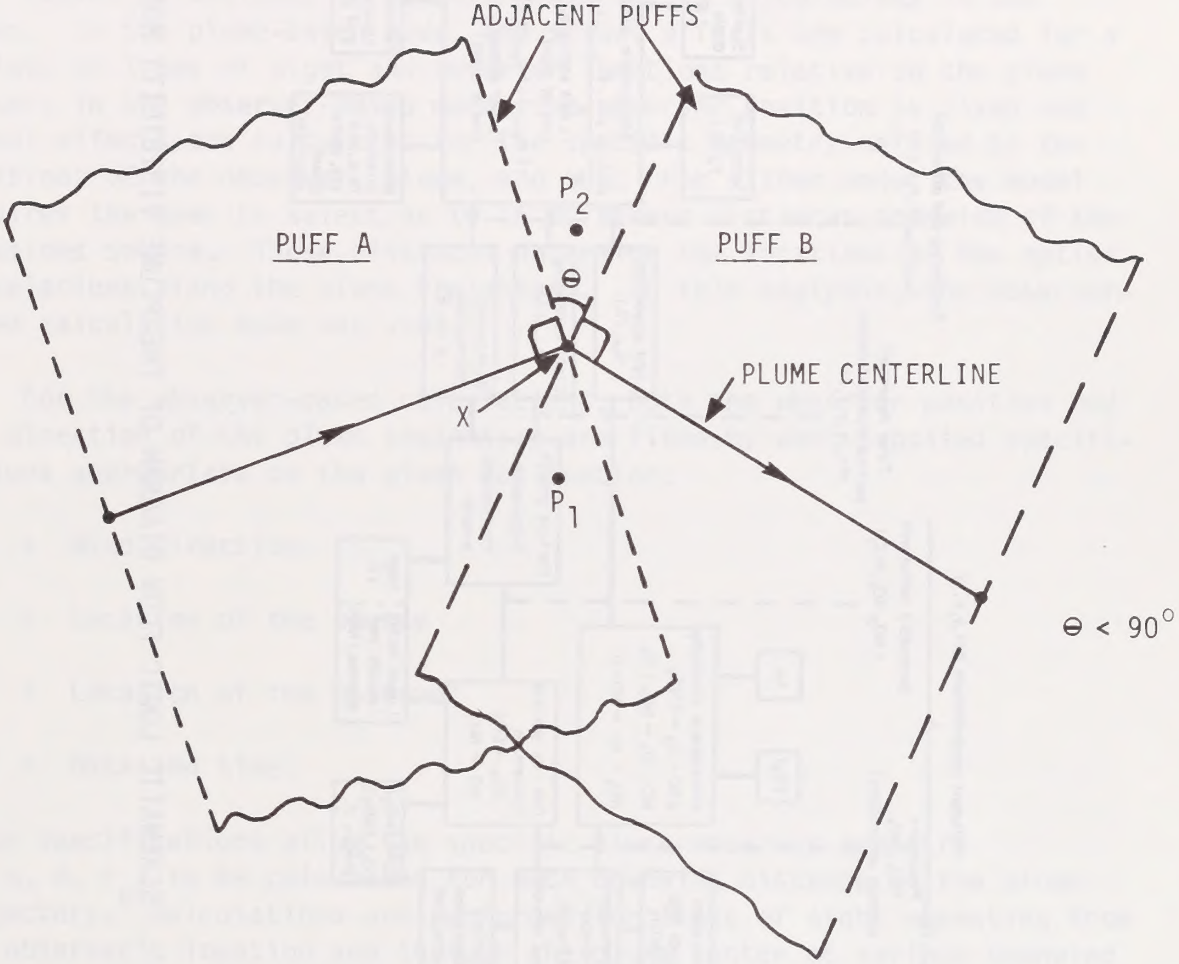

FIGURE C-6. DIAGRAM OF GPM TREATMENT OF PUFF INTERSECTIONS

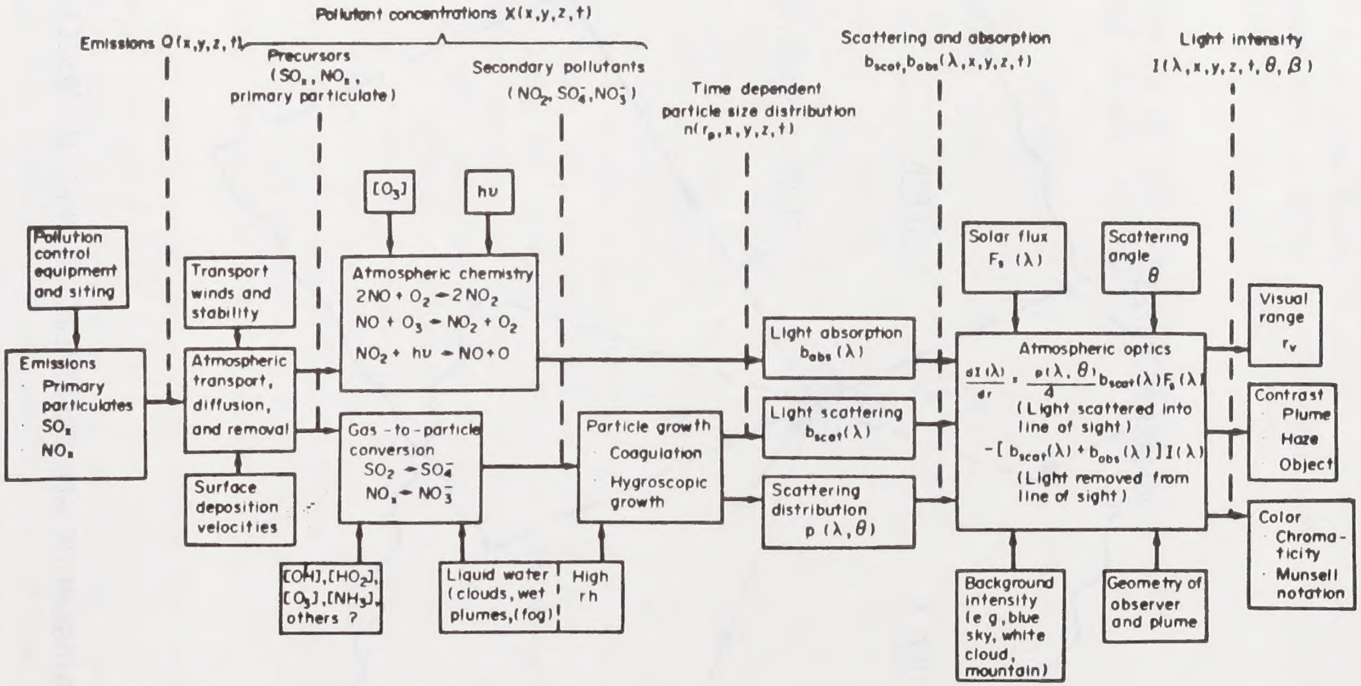
Pollutant concentrations X(x,y,z,t)
Emissions Q(x,y,z,t)
Precursors (SOx, NOx, primary particulate)
Secondary pollutants (NO2, SO4=, NO3-)
Time dependent particle size distribution n(rp,x,y,z,t)
Scattering and absorption bscat,babs(λ,x,y,z,t)
Light intensity I(λ,x,y,z,t,θ,β)
Pollution control equipment and siting
Emissions · Primary particulates · SOx · NOx
Transport winds and stability
Atmospheric transport, diffusion, and removal
Surface deposition velocities
[O3]
hν
Atmospheric chemistry 2NO + O2 → 2NO2 NO + O3 → NO2 + O2 NO2 + hν → NO+O
Gas-to-particle conversion SO2 → SO4= NOx → NO3-
[OH],[HO2],[O3],[NH3], others ?
Liquid water (clouds, wet plumes,(fog)
High rh
Particle growth · Coagulation · Hygroscopic growth
Light absorption babs(λ)
Light scattering bscat(λ)
Scattering distribution p(λ,θ)
Solar flux Fs(λ)
Scattering angle θ
Atmospheric optics dI(λ)/dr = p(λ,θ)/4 bscat(λ)Fs(λ) (Light scattered into line of sight) -[bscat(λ) + babs(λ)]I(λ) (Light removed from line of sight)
Background intensity (e g, blue sky, white cloud, mountain)
Geometry of observer and plume
Visual range rv
Contrast · Plume · Haze · Object
Color · Chromaticity · Munsell notation

FIGURE C-7. SCHEMATIC LOGIC FLOW DIAGRAM OF THE PLUME VISIBILITY MODEL

> Reduction in visual range.

> Contrast of the plume against a viewing background at the 0.55 μm wavelength.

> The blue-red ratio (color shift) of the plume.

> The color change perception parameter ΔE(L*a*b*).

PLUVUE is designed to perform plume optics calculations in two modes. In the plume-based mode, the visual effects are calculated for a variety of lines of sight and observer locations relative to the plume parcel; in the observer-based mode, the observer position is fixed and visual effects are calculated for the specific geometry defined by the positions of the observer, plume, and sun. For either mode, the model requires the user to select up to 16 different distances downwind of the emissions source. These distances determine the locations of the optics calculations along the plume trajectory. In this analysis, the observer-based calculation mode was used.

For the observer-based calculations, both the observer position and the direction of the plume trajectory are fixed by user-supplied specifications appropriate to the given application:

> Wind direction

> Location of the source

> Location of the observer

> Date and time.

These specifications allow the specific plume observer geometry (θ, α, β, r_p) to be calculated for each downwind distance on the plume trajectory. Calculations are performed for lines of sight emanating from the observer's location and through the plume center at various downwind distances. Each line of sight is matched with its particular set of these specifications.

Several types of calculations can be performed at each downwind distance. One calculates the effects for horizontal lines of sight with a clear sky background. Plume-based calculations include a range of scattering angles (θ), azimuthal angles between the line of sight and the plume centerline (α), and observer-to-plume distances (r_p). The observer-based computation uses the specific values of these variables for each downwind point appropriate for the given plume-observer geometry.

Another type of calculation evaluates the effect of the plume on horizontal views with white, gray, and black viewing object (terrain) backgrounds with uniform spectral reflectances of 1.0, 0.3, and 0.0, respectively. The plume-based calculations are done for the range of scattering angles (θ), observer-to-plume distances (r_p), and observer-to-background object distances (r_o) assuming the line of sight is perpendicular to the plume centerline ($\alpha = 90°$). However, in the observer-based calculations, the values of the angles and distances for the specific geometry are used. In this analysis, appropriate viewing object colors and distances were used to characterize terrain-viewing backgrounds.

Figure C-8 illustrates five situations in which air pollution is visually perceptible. There are two basic kinds of visibility impacts. In one case, of which figures C-8(b), (c), and (e) are examples, air pollution is perceptible as a result of the comparison of two objects viewed simultaneously by an observer. The haze layer and plume in figures C-8(b) and (c), for example, are perceptible because they contrast with the background atmosphere. The plume in figure C-8(e) is perceptible because it contrasts with the viewed objects; in other words, it is brighter or darker or colored differently from the viewed object. In the other case, of which figures C-8(a) and (d) are examples, perception of pollution results from the difference between the currently observed scene and the scene remembered under clear conditions. For example, the haze in figure C-8(c) may be perceptible because it is colored differently from what is considered to be normal sky color; it appears white, gray, yellow, or brown instead of blue. The situation shown in figure C-8(d) is similar. The scene may appear hazy because the contrast of viewed objects is decreased from that observed on a clear day.

Visual impacts associated with oil shale development are best characterized by the situations shown in figure C-8(a), (b), and (d), where well-mixed emissions within a surface-based layer affect the coloration of the horizon sky or the contrast of distant landscape features. Since TSP and NO_x emissions from individual oil shale facilities are relatively low, plume visual impacts as shown in figure C-8(c) and (e), will be localized near the individual oil shale facilities and will occur rarely on stable, stagnant mornings. The visual impacts of greatest regulatory concern are those that occur in mandatory Class I areas. Flat Tops, which is 60 km from the Piceance Basin and 140 km from the Uinta Basin, is the nearest Class I area to the projected oil shale developments. At this distance, plumes from oil shale facilities will be relatively well mixed and, if perceptible at all, will be perceived as haze (see figure C-8(a), (b), and (d).

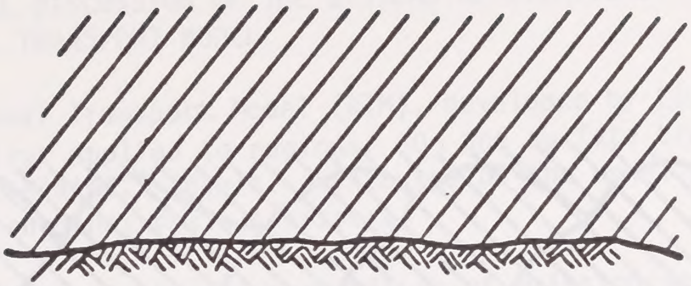

(a) General, uniformly discolored haze

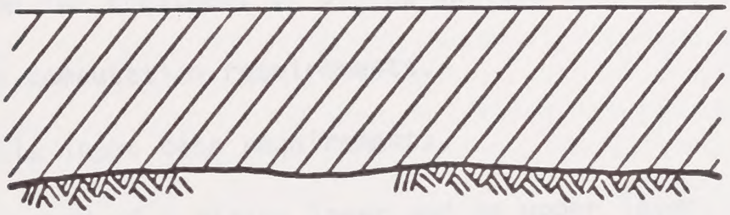

(b) Surface-based haze layer contrasting with background atmosphere above

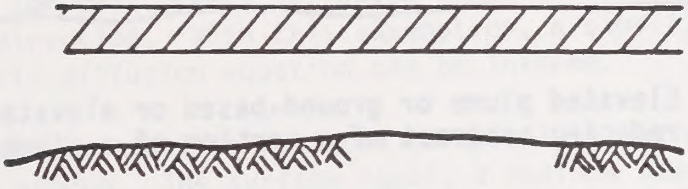

(c) Elevated plume or haze layer contrasting with background atmosphere above and below

FIGURE C-8. FIVE BASIC SITUATIONS IN WHICH AIR POLLUTION IS VISUALLY PERCEPTIBLE

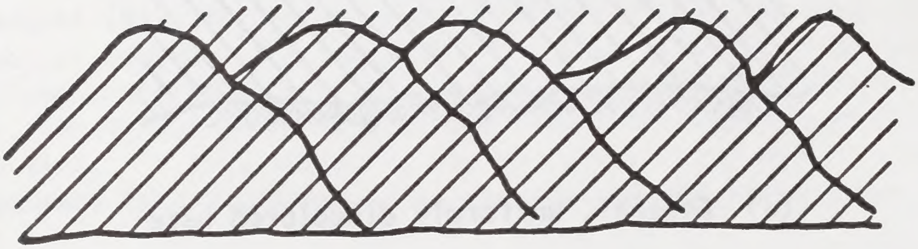

(d) General haze reducing contrast of viewed objects

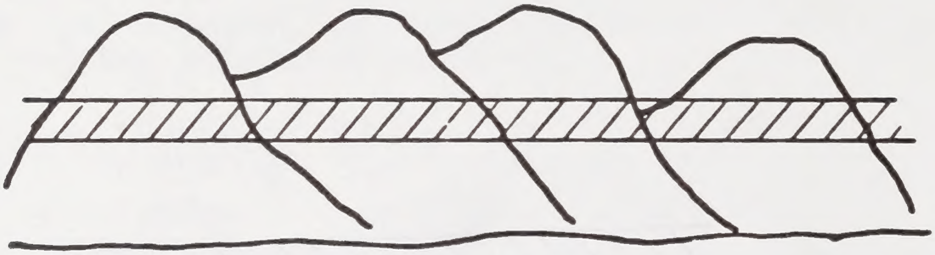

(e) Elevated plume or ground-based or elevated haze layer reducing contrast of a portion of a viewed object

FIGURE C-8. (Concluded)

C.4 TECHNICAL DISCUSSION OF THE SYSTEMS APPLICATIONS REGIONAL TRANSPORT MODEL

The Regional Transport Model (RTM), developed by Liu and Durran (1977), was first applied to regional SO_2 and sulfate transport in the northern Great Plains. Several attributes of the model are essential to simulation of regional-scale transport:

> The ability to handle a multitude of emission sources.

> Adequate treatment of pollutant transport over large distances.

> Adequate treatment of pollutant surface depletion processes.

> Provision for treatment of SO_2-to-sulfate transformations.

> Moderate computation requirements.

> Reasonable input data requirements.

The model is composed of a mixing layer and an upper layer, and has a nested surface layer treatment contained in the mixing layer.

The mixing-layer model is designed to treat transport and diffusion above the surface and below the mixing height. A second (upper) layer above the mixing height is intended to treat transport and diffusion of pollutants released above the mixing height. It also tracks mass that is vented out of the mixing layer when the mixing height decreases. A grid approach was adopted for this model to facilitate the handling of multiple sources and complex chemistry. The major feature of this model is its assumption that, for each layer, pollutant distribution is nearly uniform in the vertical direction. With this assumption, a simplified form of the general atmospheric diffusion equation can be invoked.

The surface-layer model is designed to calculate the pollutant flux deposited on the ground. The surface layer, a shallow layer immediately above the terrain, is embedded within the mixing layer. For pollutants originating from either elevated sources or distant ground-level sources, most of the pollutant mass is contained in the mixing layer. The removal processes consist of the diffusion of the pollutants through the surface layer to the ground, followed by absorption or adsorption at the atmosphere-ground interface. A unique feature of the surface layer is its diurnal variation in surface temperature, which is a result of daytime heating and nighttime cooling. This variation affects the vertical pollutant distribution through atmospheric stabilities and, consequently, affects the rate of surface uptake of pollutants.

The three layers--surface layer, mixing layer, and upper layer--are discussed in the following sections. It should be emphasized that RTM contains most of the basic and most desirable elements of an ideal regional air quality model, but it does not address several important issues:

> Predictions from the regional grid model in its basic form are not likely to be applicable within, say, a few kilometers downwind of a major emission source. Sub-grid-scale concentration distributions must be dealt with by portions of the computer code intended to deal with sub-grid-scale concentration distributions are described in section C.4.1.3.

> The only pollutant removal process treated by this version of the model is dry deposition at the surface. Other important removal processes such as rainout and washout are not considered. Unless these processes are included, the present model is, strictly speaking, applicable only during periods of no precipitation.

> The treatment of chemical reactions is limited to a first-order overall reaction between SO_2 and sulfate. Although computational time is the only constraint that imposes a problem, the inclusion of complex chemistry awaits the development of a kinetic model capable of simulating both chemical transformations during nighttime and the effects of natural emissions of hydrocarbons.

C.4.1 The Mixing Layer and Upper Layer

The mixing layer and upper layer are designed to treat the transport and diffusion of air pollutants over long distances. The model formulation is discussed in section C.4.1.1. As stated earlier, the grid approach was adopted in the present study. There are a number of significant advantages to the grid approach--it is quite versatile and can easily handle time- and space-varying emissions and meteorological variables, complex chemistry, and surface sinks. There is one major disadvantage associated with this approach: pseudo-diffusion involved in the numerical solution of the governing equation can be overwhelming if not properly treated (the numerical solution method is discussed in section C.4.1.2). Furthermore, an accurate scheme is required for the simulation of the advection term.

There is no vertical diffusion between the mixing layer and the upper layer. The only pollutant transfer between the mixing layer and the upper layer is associated with either temporal or spatial variations in the mixing height.

C.4.1.1 The Model Equations

Within the framework of the so-called gradient-transport theory,* the concentration distributions of N reactive species can be described by the atmospheric diffusion equation of the following form (Monin and Yaglom, 1971):

$$\frac{\partial c_i}{\partial t} + u\frac{\partial c_i}{\partial x} + \frac{\partial c_i}{\partial y} + w\frac{\partial c_i}{\partial z} = \frac{\partial}{\partial x}\left(K_x\frac{\partial c_i}{\partial x}\right) + \frac{\partial}{\partial y}\left(K_y\frac{\partial c_i}{\partial y}\right) + \frac{\partial}{\partial x}\left(K_z\frac{\partial c_i}{\partial x}\right) + R_i(c_1, c_2, \ldots, c_N) + S_i(c_i) \qquad i = 1, 2, \ldots, N \quad , \tag{C-51}$$

where c_i denotes concentration for pollutant species i, u, v, w, and K_x, K_y, K_z represent wind speeds and turbulent eddy diffusivities in the x, y, and z directions, respectively, and R and S are the chemical reaction and source (and/or sink) terms.

One of the major simplifications in this model is the assumption of vertical homogeneity in the concentration distribution. One of the reasons for choosing this simplification is that the vertical diffusion term, based on the dimensional analysis shown above, is about 100 times greater than the transport term, and the horizontal diffusion term is only a fraction of the transport term. Thus, retaining the vertical variation

---

[*] The gradient-transport theory, analogous to molecular diffusion theory, states that a pollutant flux in the direction of decreasing concentration is established as a result of turbulent fluctuations. The magnitude of this flux is assumed to be proportional to the gradient of the average concentration. The limitations of models based on the gradient-transport theory, also known as K-theory, were examined by Corrsin (1974).

terms in the diffusion equation will compound difficulties in the numerical solution of the governing equation, without necessarily improving the accuracy of the model's prediction. As shown in figure C-9 measurements of the vertical distributions of sulfur compounds over central Germany (Georgii, 1970) show that in these remote areas the profiles are fairly uniform beneath the temperature inversion. Similar observations were also reported by Rodhe (1971) in southern Sweden.

Assuming that the concentration distribution in the vertical is nearly uniform below the base of the temperature inversion, a vertically averaged concentration can be defined as

$$\bar{c}_i = \frac{1}{H} \int_0^H c_i \, dz \quad , \qquad \text{(C-52)}$$

where H is the height of the layer. Performing the same operation on Eq. (C-51) and imposing the appropriate vertical boundary conditions, one obtains

$$\frac{\partial \bar{c}_i}{\partial t} + \bar{u}\frac{\partial \bar{c}_i}{\partial x} + \bar{v}\frac{\partial \bar{c}_i}{\partial y} = \frac{\partial}{\partial x} K_x \frac{\partial \bar{c}_i}{\partial x} + \frac{\partial}{\partial y} K_y \frac{\partial \bar{c}_i}{\partial y} + R_i(\bar{c}_1, \bar{c}_2, \ldots, \bar{c}_N) + S_i(\bar{c}_i)$$

$$+ D \cdot \zeta(D) \quad i = 1, 2, \ldots, N \quad , \qquad \text{(C-53)}$$

where

c_{0_i} = the upper-layer concentration for species i for the mixing layer and the background concentration of species i for the upper layer.

$\bar{u}$ and $\bar{v}$ = the vertically averaged horizontal wind components

$$(\bar{u} = {}_0^H\, u\,dz/H, \ \bar{v} = {}_0^H\, v\,dz/H),$$

D = the two-dimensional divergence

$D = [(\partial \bar{u}/\partial x) + (\partial \bar{v}/\partial y)]$, and

$\zeta(D)$ = a step function defined by

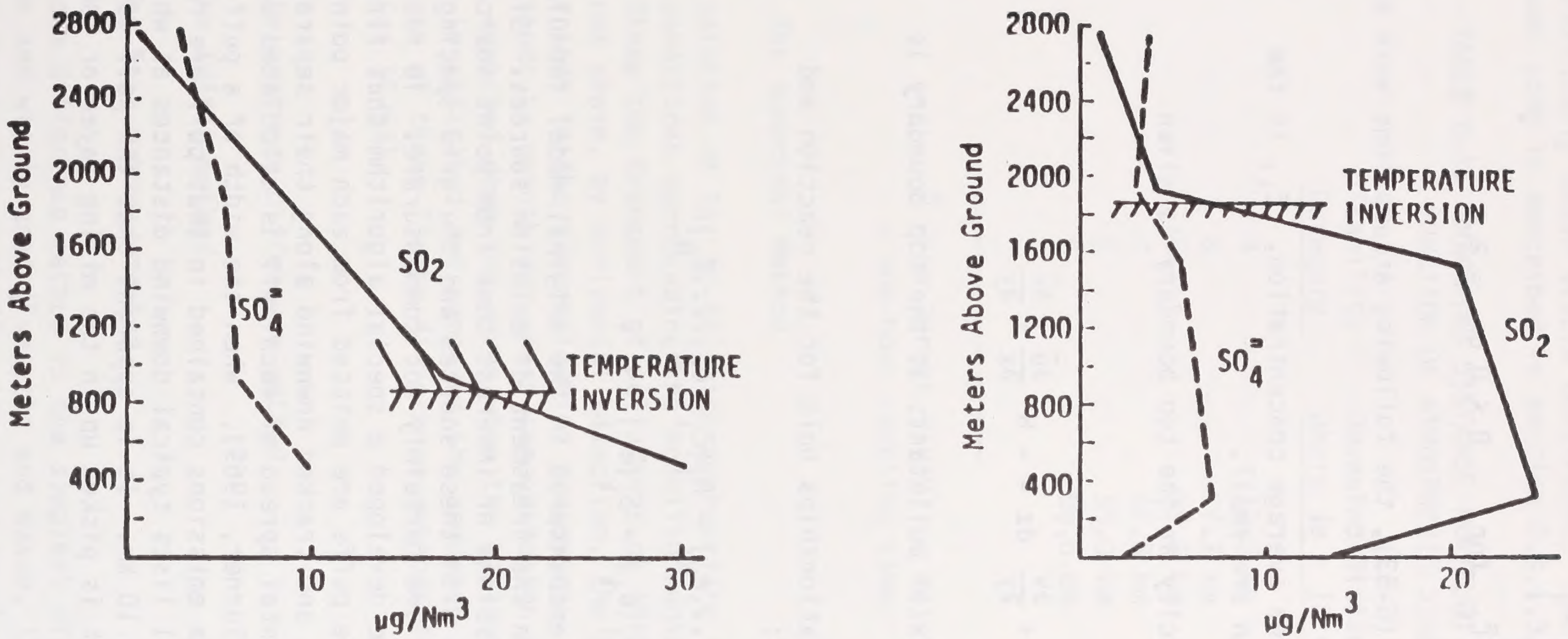

(a) 25 February 1967

(b) 26 April 1967

Source: Georgii (1970).

FIGURE C-9. VERTICAL DISTRIBUTION OF SO_2 AND $SO_4^=$ OVER CENTRAL GERMANY

$$\zeta(D) = \begin{cases} \bar{C}_{o_i} & \text{for} \quad D > 0 \text{ or, } \omega < o \\ \bar{C}_i & \text{for} \quad D \leq 0 \text{ or, } \omega \geq o \end{cases} \quad . \tag{C-54}$$

In the derivation of Eq. (C-53), the following assumptions were made:

- > Deviations from the average concentration, $\bar{c}_i$, in the vertical direction are small.
- > The vertical velocity at the top boundary is given approximately by

$$w = - \int_0^H \frac{\partial u}{\partial x} + \frac{\partial v}{\partial y} \; dz \simeq - H \; \frac{\partial \bar{u}}{\partial x} + \frac{\partial \bar{v}}{\partial y} \quad . \tag{C-55}$$

- > The diffusive flux of pollutants at the top boundary is negligible.
- > The following relationships hold for the reaction and source/sink terms:

$$R_i(c_1, c_2, \ldots, c_N) = R_i(\bar{c}_1, \bar{c}_2, \ldots, \bar{c}_N) \tag{C-56}$$

$$\bar{S}_i(c_i) = S_i(\bar{c}_i) \quad . \tag{C-57}$$

One of the problems encountered in the original model formulation was the disparity of scales in the treatment of emission sources. Since most of the sulfur dioxide emissions of interest come from point sources, the spatial scales associated with these sources and the grid spacings adopted in the mixing-layer model are certainly not commensurate. To resolve this sub-grid-scale problem, we developed a special algorithm that first treats emissions as puffs. These puffs are emitted from each major point source at regular time intervals and tracked downwind along their separate trajectories. The horizontal spread of each puff is calculated according to the Gaussian formula (Turner, 1969). When the width of a puff reaches that of one grid cell, the emissions contained in that puff are released into that cell. Table C-1 lists typical downwind distances at which the width of the puff* equals 10 km. It is apparent that the puff can travel a few grid cells before it is picked up in the mixing layer or the upper layer, particularly under stable conditions. The treatment of puffs used in the model code is described in section C.4.1.3.

---

* The width has been chosen to be 4σ, within which the puff contains more than 95 percent of the pollutant mass.

TABLE C-1. DOWNWIND DISTANCE TRAVELED BY A PUFF AS A FUNCTION OF ATMOSPHERIC STABILITY

Stability Category	Downwind Distance Where 4σ = 10 km*
A	13.3 km
B	17.7 km
C	25.8 km
D	42.8 km
E	59.0 km
F	88.5 km

---

* From Turner (1969); σ adjusted for a one-hour sampling time.

C.4.1.2 The Numerical Method

The solution of Eq. (C-53) with appropriate initial conditions and boundary conditions surrounding the modeling region requires a numerical method. Since the transport of pollutants on this scale is dominated, as demonstrated above, by horizontal advection, the problem of numerical solution arises in the discretization processes. That is, the numerical solution tends to smooth any sharp concentration profiles as the pollutants are advected downwind, even when the horizontal diffusivity is zero. We investigated and compared the accuracy and computing time requirements of three finite difference methods for solving simplified forms of Eq. (C-53):

> The upstream difference method

> The SHASTA method

> The Egan-Mahoney method.

The upstream difference method is the simplest of the three. It is also well known and widely used (Forsythe and Wasow, 1960). The SHASTA method (Sharp and Smooth Transport Algorithm) was developed by Boris and Book (1973). The method proposed by Egan and Mahoney (1972a, 1972b) has the distinctive feature that the first and second moments of the mass distribution in each cell are also calculated. The performance of each method was examined by means of hypothetical situations. Considering accuracy and computing speed, the SHASTA method appeared to be most suitable to the needs of regional modeling; it was thus selected for treating the horizontal advection terms. In the following paragraphs we present a brief description of the numerical method used in the mixing layer and upper layer.

Let the continuous variables be represented on a grid with mesh widths Δx and Δy so that $x_{ij} = x(i\Delta x, j\Delta y)$. Define the operators

$$D_{\pm}^{(1)} c_{ij} = \pm (c_{i\pm1,j} - c_{ij}) \qquad D_{\pm}^{(2)} c_{ij} = \pm (c_{i,j\pm1} - c_{ij}) \tag{C-58}$$

$$D_{0}^{(1)} c_{ij} = c_{i+1,j} - c_{i-1,j} \qquad D_{0}^{(2)} c_{ij} = c_{i,j+1} - c_{i,j-1}$$

$$Q_{\pm}^{(1)} u_{ij} = \frac{\frac{1}{2} \pm u_{ij} \frac{\Delta t}{\Delta x}}{1 \pm (u_{i\pm1,j} - u_{ij}) \frac{\Delta t}{\Delta x}} \qquad Q_{\pm}^{(2)} v_{ij} = \frac{\frac{1}{2} \pm v_{ij} \frac{\Delta t}{\Delta x}}{1 \pm (v_{i,j+1} - v_{ij}) \frac{\Delta t}{\Delta x}} \quad . \tag{C-59}$$

Then our numerical method is given by the following three fractional steps (Yanenko, 1971):

Step 1--x-direction

$$c^{*} = \alpha_1 + \frac{1}{2} (Q_{+}^{(1)} u)^2 \; D_{+}^{(1)} c^n - \alpha_1 + \frac{1}{2} (Q_{-}^{(1)} u)^2 \; D_{-}^{(1)} c^n$$

$$+ Q_{+}^{(1)} u + Q_{-}^{(1)} u + (r - d) \Delta t \, c^n$$

$$\tilde{c} = \frac{1}{2} \; Q_{+}^{(1)} u^{\;\;2} \; D_{+}^{(1)} c^n - \frac{1}{2} \; Q_{-}^{(1)} u^{\;\;2} \; D_{-}^{(1)} c^n + Q_{+}^{(1)} u + Q_{-}^{(1)} u \;\; c^n$$

$$c^{**} = c^{*} - \frac{1}{8} D_{+}^{(1)} D_{-}^{(1)} \tilde{c} \quad , \tag{C-60}$$

Step 2--y-direction

$$c^{***} = \alpha_2 + \frac{1}{2} (Q_+^{(2)} v)^2 \quad D_+^{(2)} c^{**} - \alpha_2 + \frac{1}{2} (Q_-^{(2)} v)^2 \quad D_-^{(2)} c^{**}$$

$$+ \quad Q_+^{(2)} v + Q_-^{(2)} v - \frac{w \Delta t}{\Delta H} c^{**}$$

$$\tilde{\tilde{c}} = \frac{1}{2} (Q_+^{(2)} v)^2 D_+^{(2)} c^{**} - \frac{1}{2} (Q_-^{(2)} v)^2 D_-^{(2)} c^{**} + (Q_+^{(2)} v + Q_-^{(2)} v) c^{**}$$

$$c^+ = c^{***} - \frac{1}{8} D_+^{(2)} D_-^{(2)} \tilde{\tilde{c}} \; , \qquad \text{(C-61)}$$

Step 3--point sources

$$c^{n+1} = c^+ + S \quad ,$$

$$\text{where } \alpha_1 = \frac{K_x \Delta t}{\Delta x^2} \; , \; \alpha_2 = \frac{K_y \Delta t}{\Delta y^2} \quad . \qquad \text{(C-62)}$$

The chemical reaction rate is r, and d is the surface deposition rate. The advection terms are treated with at least second-order accuracy, while the fractionalized scheme as a whole is accurate to the second order in space and to the first order in time.

An estimate of the accuracy of the numerical method adopted is useful. Table C-2 gives the effective pseudo-diffusivities produced by the model on a 10-km grid with an optimum step size. The pseudo-diffusion generated appears to be small when compared with the physical diffusivity in the horizontal plane, which is estimated to be on the order of $10^4 m^2$/sec (Randerson, 1972). With a 10-km-square grid cell, the most restrictive stability constraint derives from the advection terms [Eq. (C-63)] if K_x and K_y are less than 10^5 m^2/sec. For higher horizontal diffusivities, Eq. (C-64) becomes more stringent. The time step used in the model is chosen so that these conditions are always satisfied. Thus, accurate and stable solutions are obtained. A more thorough analysis of the problem of pseudo-diffusion is presented in Liu and Durran (1977).

Wave Type	Wave Number (m^{-1})	Pseudo-Diffusivity (m^2/sec)
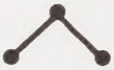	$60\pi/10^6$	2.5×10^3
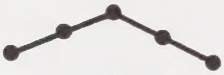	$30\pi/10^6$	1.6×10^2
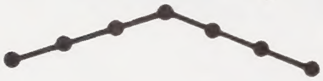	$15\pi/10^6$	40

Computational stability is guaranteed when

$$\max\left(\frac{u\Delta t}{\Delta x}, \frac{v\Delta t}{\Delta y}\right) < 0.6 \qquad \text{(C-63)}$$

$$\max\left(\frac{K_x\Delta t}{\Delta x^2}, \frac{K_y\Delta t}{\Delta y^2}\right) < 0.15 \quad . \qquad \text{(C-64)}$$

TABLE C-2. PSEUDO-DIFFUSIVITY IN ADVECTIVE TRANSPORT FOR A 10 KILOMETER GRID AND $v\Delta t/\Delta x = 1/2$

C.4.1.3 The Gaussian Puff Sub-Model

Although not used in this study a Gaussian Puff Model (GPM) was used for the near-source plume simulation within the mixing layer. In this model, the plume is considered to be composed of a series of puffs. A puff, illustrated in figure C-10, is that part of the plume emitted during one time step.

The model keeps track of all of the puffs emitted from a source until they are released into the larger grid. The model stores information about the location of the center of each puff (in 3 dimensions), the mass of SO_2 and SO_4 in the puff, and the standard deviation of the puff mass distribution in the vertical direction (σ_z) and in the horizontal direction perpendicular to the motion of the puff (σ_y). Each puff is advected according to the winds at the center of the puff, and the mass distribution of any cross section of the plume is determined by the dispersion coefficients σ_z and σ_y and the Gaussian formulation.

The model accounts for several occurrences at each time step: all the old puffs are advected downwind; new values for puff location, SO_2 and SO_4 mass, and dispersion coefficients are calculated; and a puff, if it is sufficiently dispersed, is released into the regular grid model. In addition, a new puff is created with a center a half-step downwind, at a height determined by the following plume rise equation (Briggs, 1971):

$$H_e = H_s + [1.6\ F^{1/3} \cdot (10H_s)^{2/3}\ /U] \qquad \text{(C-65)}$$

$$\text{where } F = 9.8\,\frac{\Delta T}{T_s} \cdot V_s\, R_s^{\,2} \quad ,$$

where

$\Delta T = T_s - T_a$

H_e = effective release height

H_s = stack height

U = wind velocity

F = buoyancy flux

V_s = exit velocity from stack

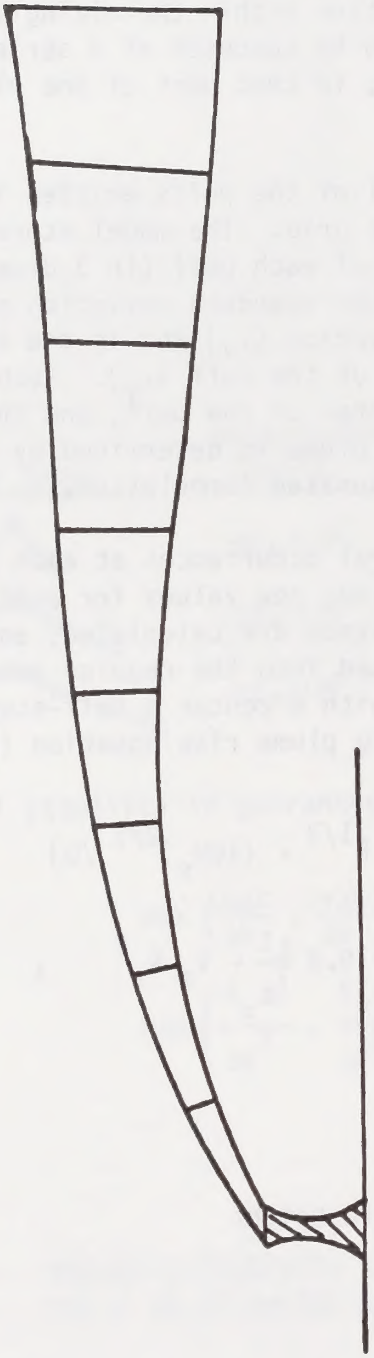

FIGURE C-10. ILLUSTRATION OF A PLUME COMPOSED OF PUFFS

R_s = stack radius

T_s = temperature in stack

T_a = ambient temperature.

Vertical winds are assumed to be zero; therefore, this height is used for the center of the puff downwind.

Dispersion coefficients for the puffs are calculated using the Pasquill-Turner-Gifford (Turner, 1969) method. The dispersion coefficients are functions of atmospheric stability class, downwind distance of the puff, and dispersion coefficient history. The coefficients are calculated to increase smoothly with time. The rate of change of coefficients at the appropriate stability class and downwind distance is used to calculate increments that are added to the coefficient with each time step.

Changes in each puff's SO_2 and SO_4 mass, caused by deposition and SO_2 and SO_4 oxidation, are also calculated for each time step. To calculate the percentage of plume mass near the ground, deposition is calculated using the vertical dispersion coefficient and the Gaussian normal distribution in the vertical direction. Then deposition is calculated from the surface-layer model equations. Oxidation is calculated as it is throughout the grid model. This process is described in section C.4.1.4.

When a puff is dispersed sufficiently so that its dimensions reach those of a grid cell, the mass of the puff is released into the grid cell containing the puff's center. This condition is met when

$$4\,\sigma_y \geqslant \mathrm{MAX}\,(\Delta X,\ \Delta Y),$$

or when

$4\,\sigma_z \geqslant$ mixing height in that cell or depth of the upper layer if the puff's height is above the mixing layer.

The RTM plume model stores information about the history of the puffs from each source and determines when and where to release these puffs into the grid model and how much to deposit and oxidize from each puff. The near-source concentrations can be calculated in two ways at the option of the user: by adding the mass of the puff into the grid cell in which the puff was centered; the mass is then divided by the full volume of that cell, or, as explained in the following section, by the Gaussian equation method for calculating puff concentrations at a point.

C.4.1.3.1 Gaussian plume equation

The usual Gaussian equation is

$$\chi(P) = \frac{Q}{U} F(Y, \sigma_y) \; G(Z, S_c, \sigma_z, L) \quad , \qquad \text{(C-66)}$$

where

χ = the concentration at P due to the plume (g/m^3),

X = the downwind distance of point P from the source,

Y = the crosswind distance from P to the plume centerline (m),

Z = the vertical coordinate of the point P (m),

S = The vertical coordinate of the point (X_c, Y_c, Z_c) on the plume centerline that is closest to P (m).

Q = the rate of emission (g/sec),

U = the wind speed (m/sec),

σ_y = the horizontal (transverse) dispersion coefficient (m),

σ_z = the vertical dispersion coefficient (m),

L = the mixing height (m).

σ_y and σ_z are calculated at (X_c, Y_c, Z_c).

$$F(Y, \sigma_y) = \frac{1}{\sqrt{2\pi}\,\sigma_y} \exp\left(\frac{-Y^2}{2\sigma_y^2}\right)$$

$$G(Z, S, \sigma, L) = \frac{1}{\sqrt{2\pi}\,\sigma} \left\{ \exp\left(- \frac{(S - Z)^2}{2\,\sigma^2}\right) \right.$$

$$\left. + \exp\left(- \frac{(ZL - S - Z)^2}{2\,\sigma^2}\right) + \exp\left(- \frac{(2a - S - Z)^2}{2\,\sigma^2}\right) \right.$$

$$+ \sum_{\substack{n \text{ even} \\ n > 0}} \left(\exp\left[- \frac{(na - nL + S - Z)^2}{2\sigma^2} \right] + \exp\left[- \frac{[n + 2]\, L - na - S - Z)^2}{2\sigma^2} \right] + \exp\left[\frac{(nL - na + S - Z)^2}{2\sigma^2} \right] + \exp\left[- \frac{[n + 2]\, a - nL - S - Z)^2}{2\sigma^2} \right] \right) \Bigg\}$$

where a is the height of the ground (or lower barrier). If a = Z = 0, this reduces to

$$G(0, S, \sigma, L) = \frac{2}{\sqrt{2\pi}\,\sigma} \sum_{\substack{n=Z \\ n=-\infty}}^{\infty} \exp -\left[\frac{(S + 2nL)^2}{2\sigma^2} \right] \quad .$$

When σ_z/L is large enough, the pollutant is considered to be uniformly distributed in the mixing layer, and then G = 1/L.

Equation (C-86) is implemented as shown in Eq. (C-87). The concentration due to a puff is calculated in ppm:

$$C(P) = \frac{A \cdot 10^6}{\phi \cdot dx} F(y, \sigma_y)\, G(Z, Z_c, \sigma_z, L) \quad , \qquad \text{(C-67)}$$

where

C = the concentration at the point P (ppm),

A = the number of moles of pollutant in the puff,

dx = the distance the puff traveled during the current time step (m),

ϕ = the number of moles per cubic meter (air) = 40.82,

F, G = the same as above (except we use a finite sum).

The concentration at P resulting from the plume is then the result of summing Eq. (C-87) over all puffs.

C.4.1.4 Oxidation of SO_2 to SO_4

Another feature of the RTM is its capability to vary the rate of oxidation of SO_2 to SO_4 diurnally, according to changes in the intensity of solar radiation. Altshuller (1979) presented clean-air homogeneous oxidation rates of SO_2 by latitude and by the month of the year. The maximum noontime values calculated are shown in table C-3.

The oxidation rate r(t) at time t used in the model is calculated by

$$r(t) = r_{night} + \frac{\sin[\Theta_z(t)]}{\sin[\Theta_z(noon)]} \cdot (r_{noon} - r_{night}) \quad , \qquad (C\text{-}68)$$

where $\Theta_z(t)$ is the solar zenith angle at time t, and $\sin[\Theta_z(t)]$ is thus proportional to the solar radiation intensity. $\Theta_z(t)$ is calculated in the model from inputs of latitude and longitude of the modeling region and of the time zone, and $\Theta_z(noon)$ is calculated as the maximum daily solar zenith angle that can occur in that particular standard time. r_{noon} is the peak oxidation rate at 1200 local time for a given latitude (Altshuller, 1979), and r_{night} accounts for the slow oxidation that continues after sunset.

It should be noted that this oxidation rate calculation assumes relatively clear skies. With substantial cloud cover or high humidities, and as heterogeneous reactions take on more importance, SO_2 oxidation to SO_4 becomes more complex. Accounting for cloud cover in the calculation would involve a considerable increase in the levels of model complexity and input preparation. Since the method chosen uses maximum and minimum rates of oxidation, the user can adjust these inputs to allow the use of reasonable values in the model.

C.4.2 The Surface-Layer Model

Pollutants are removed from the atmosphere via both dry and wet deposition. Only dry deposition at the earth's surface is considered by this model. The importance of the effects of surface deposition on pollutant concentrations at large distances has been well established (e.g., Bolin and Granat, 1973, 1974; Scriven and Fisher, 1975). Thus, an indispensable element in the regional air pollution model is the treatment of pollutant depletion processes near the surface. In this section, we describe the surface-layer model. We begin with a discussion of previous studies concerning surface deposition and conclude with a description of the approach adopted.

TABLE C-3. HOMOGENEOUS OXIDATION OF SULFUR DIOXIDE*

(Percent reaction per hour at noontime of sulfur dioxide of HO, HO_2, and CH_3O_2, at 0.1 km)

	Latitude (°N)						
Month	5	15	25	35	45	55	65
January	1.81	1.10	0.61	0.26	0.08	0.01	<0.01
February	1.81	1.21	0.74	0.32	0.13	0.04	0.01
March	2.06	1.55	1.01	0.48	0.21	0.09	0.03
April	2.01	1.79	1.36	0.73	0.35	0.17	0.07
May	1.82	1.68	1.48	1.01	0.58	0.30	0.16
June	1.81	1.72	1.56	1.22	0.74	0.42	0.25
July	1.78	1.80	1.58	1.30	0.88	0.52	0.31
August	1.86	1.78	1.61	1.31	0.82	0.45	0.26
September	1.91	1.68	1.50	1.15	0.65	0.34	0.17
October	1.79	1.54	1.29	0.84	0.39	0.17	0.06
November	1.56	1.33	0.98	0.48	0.19	0.06	0.02
December	1.58	1.16	0.74	0.33	0.11	0.02	<0.01

---

* Taken from Altshuller (1979).

C.4.2.1 Dry Deposition on Surfaces

In most studies, removal of pollutants by the ground surface is generally characterized by

$$F = V_d c \quad , \qquad \text{(C-69)}$$

where F is the mass flux to the surface, c is the concentration measured at an unspecified reference height, and V_d, having the units of velocity, is commonly referred to as the deposition velocity. In this expression, the deposition velocity is viewed as a proportionality constant whose magnitude is empirically established. The surface deposition is governed by many complex physical processes that depend primarily on

- > The state of the atmosphere near the ground
- > The types and configurations of the surface.

For example, Bolin, Aspling, and Persson (1974) noted that for a perfect sink of a particular gas, in which all molecules of that gas that reach the surface are absorbed, the ground-level concentration is zero and the deposition velocity is theoretically infinite. In this case the flux is diffusion-limited. Consequently, the simple concept of the deposition velocity is generalized.

In analogy with electrical circuits, surface deposition is treated in terms of resistance to mass transfer (Owen and Thompson, 1963; Chamberlain, 1966). The transfer of gases from the atmosphere to a surface is described by three resistances in parallel:

- > The resistance to momentum transfer, r_m
- > The excess resistance to mass or heat transfer, r_h
- > The resistance at the ground surface, r_s.

The total resistance, R, which is defined as the reciprocal of the deposition velocity, is then given by

$$v_d = \frac{1}{R} = \frac{1}{r_m} + \frac{1}{r_h} + \frac{1}{r_s} \quad . \qquad \text{(C-70)}$$

Within the framework of the surface boundary layer (Owen and Thompson, 1963)

$$r_m = \frac{u(z)}{u^* \; 14} \quad , \tag{C-71}$$

where u(z) is the vertical wind profile and u* is the friction velocity. The deviation between momentum and mass/heat transfer is characterized by

$$r_h = \frac{1}{\beta u^*} \quad , \tag{C-72}$$

where β is dependent on the surface roughness, a Reynolds number appropriate to the flow in the roughness layer, and the ratio of the kinematic viscosity of air to the molecular diffusion coefficient of the pollutant gas. This correction is necessary because the process of mass transfer is generally less efficient than that of momentum transfer, resulting in a nonzero concentration of the gas at the surface. On the basis of a study of heat transfer to roughened glass plates, Owen and Thompson (1963) suggested

$$\beta^{-1} = \alpha (u^* z_0/\nu)^{0.45} \; \frac{\nu}{D} \;\; 0.8 \quad , \tag{C-73}$$

where u*, z_0, υ, and D are the friction velocity, surface roughness, kinematic viscosity, and molecular diffusivity, respectively, and α is an empirical constant determined by the shape of the roughness elements. In further investigations by Chamberlain (1966) and Thom (1972), little functional relation was found between β and z_0. Thus, Thom proposed

$$\beta^{-1} = \alpha_1 u^{*\,1-3} \quad \alpha_2 \; \frac{\upsilon}{D} \;\; 2/3 \; - 1 \quad , \tag{C-74}$$

where α_1 and α_2 are empirical constants determined primarily by the surface roughness elements.

C.4.2.2 The Formulation of a Surface Deposition Model

For pollutants originating from either elevated sources or distant ground-level sources, most of the pollutant mass is contained in the mixing layer. The removal processes, as discussed above, consist of diffusion of the pollutants through the surface layer to the ground and absorption or adsorption at the atmosphere-ground interface. As illustrated in figure C-11, the diurnal variation of temperature in the surface

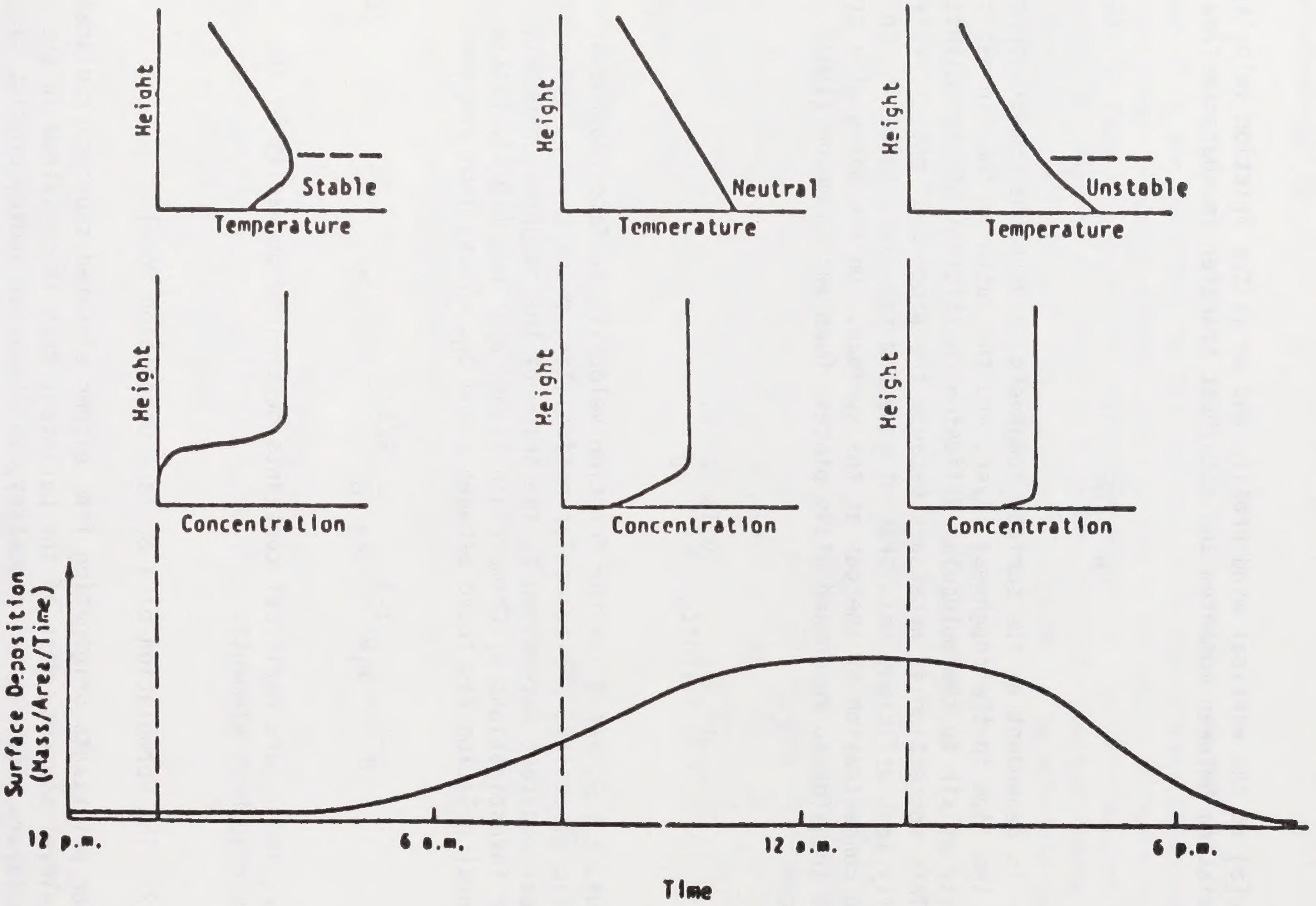

FIGURE C-11. SCHEMATIC ILLUSTRATION OF DIURNAL VARIATIONS IN SURFACE DEPOSITION layer affects the vertical pollutant distribution through atmospheric stabilities and, consequently, affects the rate of surface uptake of pollutants (Högström, 1975). As a result, an algorithm that can account for these variations must be included as part of the surface-layer model.

The surface-layer model used here for the prescription of pollutant fluxes is similar to those discussed by Bolin and Granat (1973) and Galbally (1974), but it was extended to included

> Diabatic atmospheric conditions

> Nonlinear surface reactions.

This approach is favored over the relatively simple resistance approach primarily because the latter is restricted to linear surface reactions, which may not fit all situations of interest. For example, Hill (1971) observed that the adsorption of ozone by leaves does not vary linearly with concentration at high concentration levels.

The model assumes that the transfer of pollutant gases from the atmosphere to a surface is accomplished via three stages (Sehmel, Sutter, and Dana, 1973; Galbally, 1974):

> The gases are transported, primarily by turbulent diffusion, to a laminar sublayer just above the surface.

> The gases are transported, primarily by molecular diffusion, through this laminar sublayer.

> The gases interact by adsorption or chemical reaction with the surface.

Thus, as shown in figure C-12, the surface layer is divided into two parts: the turbulent layer and the laminar sublayer. In the turbulent layer, after the atmosphere reaches an equilibrium state, the atmospheric diffusion equation becomes

$$\frac{\partial}{\partial z} K_V \frac{\partial c}{\partial z} = 0 \quad , \qquad \text{(C-75)}$$

with the following boundary conditions,

$$c = \bar{c} \text{ at } z = h \quad ,$$

$$K_V \frac{\partial c}{\partial z} = F \text{ at } z = z_0 \quad ,$$

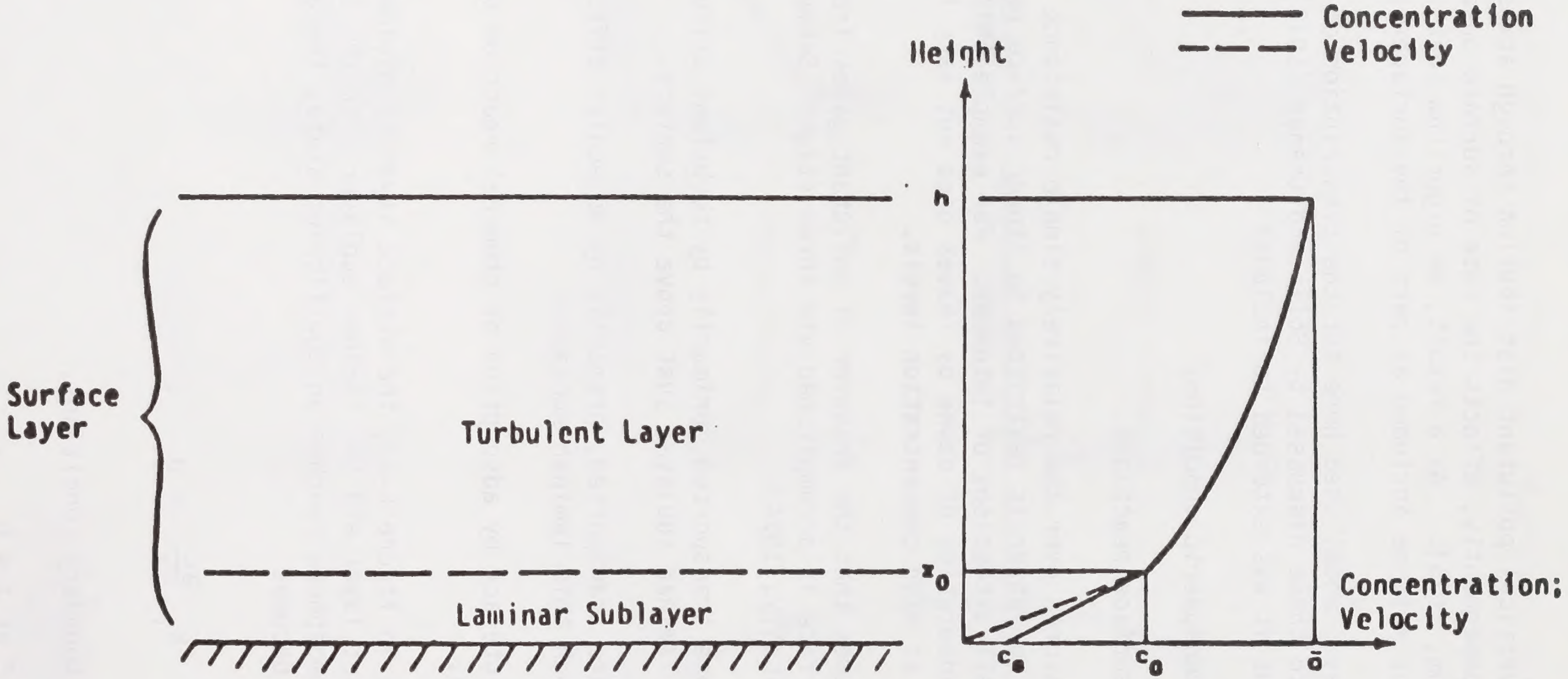

FIGURE C-12. SCHEMATIC ILLUSTRATION OF THE SURFACE LAYER where $\bar{c}$ is the cell-averaged concentration in the mixing layer, F is the pollutant flux across the turbulent layer-laminar sublayer interface, and z_0 is the height of the surface roughness element. The vertical diffusivity K_V can be prescribed as

$$K_V = \frac{Ku_* z}{\phi\left(\frac{z}{L}\right)} , \qquad \text{(C-76)}$$

where

k = von Karman constant (= 0.35)

u_* = friction velocity

z = height

L = Monin-Obukhov length.

This formula is the result of the similarity theory for the constant-flux surface layer (Businger et al., 1971). For the neutral case, the ϕ-function equals unity. For the stable and unstable cases, the ϕ-function is greater and less than one, respectively. The following empirical expressions for the ϕ-function were proposed by Businger et al. (1971) on the basis of observational data:

For the stable case (L > 0)

$$\phi_s\left(\frac{z}{L}\right) = 1 + 4.7\left(\frac{z}{L}\right) . \qquad \text{(C-77)}$$

For the unstable case (L < 0)

$$\phi_u\left(\frac{z}{L}\right) = \left[1 - 15\left(\frac{z}{L}\right)\right]^{-1/4} . \qquad \text{(C-78)}$$

The friction velocity is determined by

$$u_* = \frac{ku_r}{f} , \qquad \text{(C-79)}$$

where u_r denotes a reference wind speed measured at a reference height, z_r, and

$$f = \ln\left(\frac{z_r}{z_0}\right) + 4.7\left(\frac{z_r - z_0}{L}\right) \text{ (stable)} \quad , \qquad \text{(C-80)}$$

$$f = \ln\left[\frac{1 - \phi_u\left(\frac{z_r}{L}\right)}{1 + \phi_u\left(\frac{z_r}{L}\right)}\right] - \ln\left[\frac{1 - \phi_u\left(\frac{z_0}{L}\right)}{1 + \phi_u\left(\frac{z_0}{L}\right)}\right]$$

$$+ 2 \tan^{-1}\left[\frac{1}{\phi\left(\frac{z_r}{L}\right)}\right] - 1 \tan^{-1}\left[\frac{1}{\phi_u\left(\frac{z_0}{L}\right)}\right] \text{ (unstable).} \qquad \text{(C-81)}$$

For either the stable or unstable case, the solution of Eq. (C-81) is simply

$$c = \bar{c} - F \cdot \int_z^h \frac{\phi(z)}{k u_* z}\, dz \quad . \qquad \text{(C-82)}$$

Across the laminar sublayer, it is assumed that the pollutant flux can be written as

$$F = \beta u_* \left(c_0 - c_s\right) \quad , \qquad \text{(C-83)}$$

where c_0 and c_s denote the concentrations at the interface and the surface, respectively, and β, analogous to the Stanton number in heat transfer, is the inverse of a dimensionless resistance for the laminar sublayer. If it is further assumed that mass and momentum are transferred in an identical manner in the turbulent layer, but differently through the laminar sublayer, then the relationships established by Owen and Thompson (1963) and Thom (1972) discussed above can be used:

$$\beta^{-1} = \alpha \left(u_* \frac{z_0}{\nu}\right)^{0.45} \left(\frac{\nu}{d}\right)^{0.8} \quad \text{(Owen-Thompson)} \quad , \qquad \text{(C-84)}$$

$$\beta^{-1} = \alpha_1 u_*^{1/3} \left[\alpha_2 \left(\frac{\nu}{D}\right)^{2/3} - 1\right] \quad \text{(Thom)} \quad . \qquad \text{(C-85)}$$

Equation (C-81) is used in the model. To complete the description of the surface-layer model, a boundary condition is required at the surface.

Uptake of air pollutants occurs by chemical reaction with, or catalytic decomposition within, either the soil or vegetation, or it can occur by these processes at soil or vegetation surfaces. These processes are generally dependent on the gas concentration at the surface. A general equation for the gas loss per unit area per unit time can be written as (Benson, 1968),

$$F = \gamma\, c_s^a \quad , \qquad \text{(C-86)}$$

where F is the pollutant flux, γ is a reaction rate constant, and c_s is the concentration of the gas at the soil or vegetation surface. The exponent, a, denotes the reaction order. Eliminating c_0 and c_s from Eq. (C-82), (C-83), and (C-86), the following transcendental equation is obtained for F,

$$I \cdot F + \gamma^{-1/a} \cdot F^{1/a} - \bar{c} = 0 \quad , \qquad \text{(C-87)}$$

where

$$I \equiv \frac{1}{\beta u_*} + \int_{z_0}^{h} \frac{\phi(z)}{k u_* z}\, dz \quad .$$

Although the reaction order is most likely to be 1, closed-form solutions can be found for the cases of a = 1, 2, and 3,

$$F = \begin{cases} \dfrac{\bar{c}}{I + \dfrac{1}{\gamma}} & a = 1 \\[2ex] \dfrac{-\dfrac{1}{\sqrt{\gamma}} + \dfrac{1}{\gamma} + 4I\bar{c}^{\,1/2}}{2I} & a = 2 \\[2ex] A_+ + A_-{}^{3} & a = 3 \quad , \end{cases} \qquad \text{(C-88)}$$

where

$$A_\pm = 3 \left[\frac{\bar{c}}{I} \pm \left(\frac{\bar{c}}{2I}^{2} + \frac{1}{27\gamma I^3} \right)^{1/2} \right]^{1/2} \quad .$$

It is interesting to note that these formulas reduce to that of Chamberlain (1966) or Galbally (1974) for the special case of (1) a first-order surface reaction, and (2) a neutrally stratified atmosphere.

C.5 TECHNICAL DESCRIPTION OF EKMA

The Empirical Kinetic Modeling Approach (EKMA) has been developed as a procedure for relating photochemical oxidants (expressed as ozone) to organic compounds and oxides of nitrogen (EPA, 1977). The EKMA calculates maximum afternoon concentrations of ozone as a function of the following parameters:

> Morning concentrations of nonmethane hydrocarbons (NMHC) and oxides of nitrogen (NO_x).

> Emissions of NMHC and NO_x occurring during the day.

> Meteorological conditions.

> Reactivity of the NMHC mix.

Detailed documentation of the EKMA and its associated computer programs is given by EPA (1977); Whitten and Hogo (1978a, 1978b); and EPA (1981).

C.5.1 Kinetic Mechanism

The EKMA uses a two-hydrocarbon/NO_x mechanism to describe the photochemical formation of ozone (Dodge, 1977). This mechanism contains two hydrocarbons (propylene and butane) to represent typical urban emissions. Studies by Whitten and Hogo (1981), Hogo, Whitten, and Reynolds (1981), and Whitten, Hogo, and Johnson (1981) have shown that different chemical mechanisms can behave differently with changing hydrocarbon reactivity. For this study the Carbon-Bond Mechanism is used instead of the propylene/butane mechanism for the following reasons:

> The Carbon-Bond Mechanism is more responsive to a wider range of reactivity than is the propylene/butane mechanism.

> It is harder to define reactivity as a function of propylene and butane.

> The Carbon-Bond Mechanism is based on more recent measurements of rate constants.

Table C-4 shows the Carbon-Bond Mechanism used in this study. Further discussions of the Carbon-Bond Mechanism are reported by Whitten, Hogo, and Killus (1980) and Killus and Whitten (1981).

C.5.2 Concepts

The physical model underlying the EKMA is similar in concept to a trajectory-type photochemical model. A column of air consisting of initial concentrations of ozone and precursors is transported along an assumed trajectory. As the column moves, it can encounter fresh precursor emissions, which are assumed to be mixed uniformly within the column. The column is assumed to act like a large smog chamber in which the precursors react according to the kinetic mechanism in table C-4 to form ozone and other products. The column extends from the earth's surface to the base of an elevated inversion. Because the diameter of the column is such that concentrations inside and just outside the column are similar, the horizontal exchange of air in and out of the column can be ignored. The volume of the column increases only as the inversion rises. Thus, the pollutants within the column are diluted as they are mixed with the air aloft. If the air aloft is polluted, the inversion rise also introduces ozone and precursors. The EKMA mathematically simulates these physical and chemical processes.

The "trajectory" mode of the EKMA computer code can be used to consider impacts due to specific sources in rural areas of the horizontal area (or size) of the parcel is small in relation to the size of the source. In this situation the horizontal exchange of reactants is not important.

C.5.3 Summary of Input Data

Values of the parameters that can be input to EKMA include the following:

> Latitude.

> Longitude.

> Time zone.

> Date.

> Morning and afternoon inversion heights (also called mixing depths) or hourly mixing depths.

> Times at which the inversion starts and stops rising.

> Concentrations of HMHC, NO_x, and ozone in the air above the inversion layer due to transport aloft.

> Concentrations of NMHC, NO_x and ozone initially in the surface layer.

> NMHC and NO_x emissions.

> NMHC reactivity.

> Initial ratio of aldehydes to NMHC.

> NO_x reactivity (initial fraction of NO_x that is NO_2).

C.5.4 Output

As previously described, the major function of EKMA is to calculate ozone concentrations. The output includes a table summarizing the simulation conditions, a table summarizing the results of each simulation performed. The user also has the option to obtain detailed information for the simulation (e.g., concentrations of all species, rates of reactions, etc.).

C.5.5 Conceptual Basis for the EKMA Kinetics Model

As previously described, the physical model underlying the kinetics model in OZIPM is similar in concept to a trajectory-type photochemical model. In the kinetics model, a column of air transported along an assumed trajectory is modeled. The column is assumed to extend from the earth's surface to the base of a temperature inversion. The horizontal dimensions of this column are such that the concentration gradients are small. This makes it unnecessary to consider horizontal exchange of air between the column and its surroundings. The air within the column is assumed to be uniformly mixed at all times.

At the beginning of a simulation, the column is assumed to contain some specified initial concentrations of NMHC and NO_x. These pollutants, sometimes called background, are in this report termed pollutants "transported in the surface layer." As the column moves along the assumed trajectory, the height of the column can change because of temporal and spatial variations in mixing height. The height of the column is assumed to change with time during a user-selected period, and to be constant before and after that period. As the height of the column increases, its volume increases, and air above the inversion layer is mixed in. Pollutants in the inversion layer are described as "transported above the surface layer" or "transported aloft" in this report. Any ozone or ozone precursors from the inversion layer that are mixed into the column as it expands are assumed to be immediately mixed uniformly throughout the column.

The kinetics model in EKMA can also consider emissions of NMHC and NO_x into the column as it moves along its trajectory. The concentrations of the species within the column are physically decreased by dilution due to the inversion rise, and physically increased by entrainment of pollutants transported aloft and by fresh emissions. All species react chemically according to the kinetic mechanism shown in table C-4. Certain photolysis rates within that mechanism are functions of the intensity and spectral distribution of sunlight, and they vary diurnally according to time of year and location.

The assumptions and specifications that describe the kinetics model are

> The air mass of interest is an imaginary air parcel (column) of fixed horizontal area at a constant temperature, within which pollutants are well mixed.

> There is sufficient homogeneity that horizontal diffusion does not affect pollutant concentrations within the column.

> The height of the column varies with time during a specified period and is constant at other times.

> The column contains specified initial concentrations of NMHC and NO_x prior to the simulation starting time.

> Pollutants transported within the surface layer from outside the area of interest (sometimes called background) may be present in the column at the start of each simulation. The pollutant concentrations due to transport in the surface layer are normally assumed to be zero, but the user may specify other values for the NMHC, NO_x, and ozone concentrations transported within this layer.

> The changes in pollutant concentrations within the column are calculated, by computer simulation, from a user-specified period. The chemical reactions involving these pollutants are listed in table C-4.

> Entrainment of pollutants transported aloft is possible during the rise of the inversion layer. EKMA only permits entrainment of constant concentrations of NMHC, NO_x, and ozone.

> Pollutants emitted into the column after the starting time can be represented by specifying additions of NMHC and NO_x each hour.

> The rate constants of all chemical reactions in the kinetic mechanism are as shown in table C-4, except for the photolysis reactions. Photolytic rate constants vary according to the time of day, date, and location being simulated. (Default photolysis rate constants are intended to represent the period from 0800 to 1800 PDT on the summer solstice in Los Angeles.)

> Zero cloud cover is assumed.

Other assumptions relating to the use of EKMA to predict control requirements or changes in urban ozone concentrations as a result of changes in precursor emissions are discussed by EPA (1981).

C.5.6 Mathematical Formulation of Kinetics Model

The kinetics model in EKMA mathematically simulates physical and chemical processes taking place in the atmosphere. This simulation is accomplished by numerically solving a system of ordinary, nonlinear differential equations that describe the effects of these processes on pollutant concentrations. The solution gives the concentration of pollutants as a function of time. The mathematical formulation of the system of differential equations is described in this section.

In EKMA, there are four processes that are assumed to affect pollutant concentrations:

(1) Chemical reactions

(2) Dilution

(3) Entrainment of pollutants transported aloft

(4) Emissions.

Differential equations have been formulated to describe the time rate of change of pollutant concentrations due to each process, and these are presented below. The total time rate of change of each pollutant's concentration is then simply equal to the sum of all these effects. Thus, the system of equations consists of one equation for each species in the kinetic mechanism shown in table C-4.

C.5.6.1 Chemical Reaction Effects

The change in pollutant concentration due to chemical reaction is a function of the rates of the chemical reactions in table C-4. The rate of each reaction is the product of a rate constant and a concentration term. The rate constants for the nonphotolytic reactions are shown in table C-4. The photolytic rate constants are calculated by the procedures described above. The concentration term for unimolecular or pseudo-first-order reactions (such as photolytic reactions) is simply the concentration of the reactant. Bimolecular reaction rates are calculated similarly, except that the concentration term is the product of the two reactant concentrations. For example, the reaction rate (RT) for the first reaction in table C-4 would be expressed as follows:

$$(RT)_1 = k_1 \, C_{NO_2} \quad , \tag{C-89}$$

where

$(RT)_1$ = rate of reaction, ppm min^{-1}

k_1 = photolytic rate constant for reaction

C_{NO_2} = concentration of NO_2, ppm

The time rate of change of a species due to chemical reaction is simply equal to the sum of all rates for those reactions in which the species is a product minus the sum of the rates for those reactions in which the species is a reactant. Thus,

$$\frac{\Delta C_i}{\Delta t} R = \Sigma \, (RT)_{PROD} - \Sigma \, (RT)_{REAC} \tag{C-90}$$

where

$\frac{\Delta C_i}{\Delta t} R$ = reaction rate contribution to the time rate of change of species i

$\Sigma(RT)_{PROD}$ = the sum of all reaction rates in which species i appears as a product

$\Sigma(RT)_{REAC}$ = the sum of all reaction rates in which species i appears as a reactant

C.5.6.2 Dilution Effects

The mathematical representation for simple dilution due to inversion rise is a first-order decay process. The rate of change due to this effect can be represented as follows:

$$\frac{\Delta C_i}{\Delta t} D = -DC_i \qquad \text{(C-91)}$$

where

$\frac{\Delta C_i}{\Delta t} D$ = dilution effect contribution to the time rate of change of pollutant species i, ppm min^{-1}

D = dilution factor, min^{-1}

C_i = concentration of species i, ppm

The dilution factor is calculated from the following equation:

$$D = \frac{\ln(Z_2/Z_1)}{\Delta t} \qquad \text{(C-92)}$$

where

D = dilution factor, min^{-1}

Z_2 = afternoon mixing height

Z_1 = morning mixing height

Δt = total time during which the inversion rise takes place, minutes

Note that, before and after the inversion rise period, the dilution factor is zero since there are no dilution effects for those periods.

When hourly mixing depths are specified, the dilution factor is calculated as follows:

$$D_t = \dot{H}T/HT_t$$

where

D_t = dilution factor at time t, min^{-1}

$\dot{H}T$ = the change in mixing depth from the previous time to the current time

HT_t = current mixing depth

The dilution factor is not constant when hourly mixing depths are specified.

C.5.6.3 Entrainment Effects

Only hydrocarbons, NO_x, and O_3 are subject to being entrained from pollutants transported aloft. The mathematical treatment of entrainment assumes that the concentrations aloft do not change with time and extend uniformly to at least the height of the afternoon mixed layer. The pollutants entrained are assumed to be instantaneously mixed within the enlarged surface layer. The mathematical expressions for the rates of change for the pollutants are shown below:

$$\frac{\Delta C_{O_3}}{\Delta t}\, AL = D(C_{O_3})_{AL} \qquad \text{(C-93)}$$

$$\frac{\Delta C_{NO_2}}{\Delta t}\, AL = D(C_{NO_2})_{AL} \qquad \text{(C-94)}$$

$$\frac{\Delta C_{HC_i}}{\Delta t}\, AL = D(C_{NMHC})_{AL} \quad R_{HC_i} \quad C_{HC_i} \qquad \text{(C-95)}$$

where

$\frac{\Delta C_{O_3}}{\Delta t}\, AL,\ \frac{\Delta C_{NO_2}}{\Delta t}\, AL,\ \frac{\Delta C_{HC_i}}{\Delta t}\, AL,$ = entrainment effect contribution to the time rates of change of ozone, nitrogen dioxide, and hydrocarbons, respectively, ppm min^{-1}

D = dilution factor (i.e., the rate constant for the mixing height rise), $\min^{-1}$

$C_{O_3\ AL}$ = concentration of ozone trapped aloft, ppm

$C_{NO_2\ AL}$ = concentration of NO_2 trapped aloft, ppm

$(C_{NMHC})_{AL}$ = concentration of total nonmethane hydrocarbon trapped aloft, ppmC

It should be noted that the effect of the change in mixing height is the sum of the dilution and the entrainment effects.

C.5.6.4 Emissions Effects

The fourth factor affecting the rate of change of pollutant concentration is emissions. The rates of change due to emissions are equal to the additional concentrations produced by the emissions.

Because equivalent emissions into different volumes will produce different concentrations, it is necessary to adjust the relative emissions to reflect the change in the column volumes due to the inversion rise. This is done internally by EKMA by first calculating the ratio of the starting inversion height to the current inversion height. (This is equivalent to the ratio of initial volume to the current volume.) Before the inversion rise begins, this ratio is simply one. After the inversion rise has ceased, the ratio is the starting mixing height divided by the final mixing height. For the period during which the inversion rises, the ratio (f_t) is calculated as follows:

$$f_t = \exp[-(D)(\Delta t)] \quad , \qquad \text{(C-96)}$$

where

f_t = ratio of the starting mixing height to the mixing height at time t

D = dilution factor (i.e., the rate constant for the mixing height rise, min^{-1})

Δt = elapsed time between the start of the mixing height rise and the current time, minutes.

The rates of change due to the emissions are calculated from the values of the emission rates (calculated using the polynomial spline functions described earlier), the f_t ratio described above, and the reactivity assumptions. The equations for the rates of change due to emissions for each of the affected species are shown below:

$$\frac{\Delta C_i}{\Delta t}_E = f_t (E_i)_t [C_i] \quad . \qquad \text{(C-97)}$$

$\frac{\Delta C_i}{\Delta t}_E$ = emissions contribution to the rates of change of species i, ppm min^{-1}

f_t = defined above (Eq. C-97)

$(E_i)_t$ = value of emission rate, ppm per minute

Note that, in the above formulations, a conversion from ppmC to ppm is performed for hydrocarbon species, and the reactivity of the hydrocarbons is taken into account.

Under the EPA guidelines for the use of EKMA, trajectories are assumed to be straight-line to the maximum observed ozone. The column of air is assumed to be moving at uniform speed throughout the day. Thus, although it seems that the wind speed is an important factor in determining emission rates, a simple calculation shows otherwise. As an example, we define an air parcel moving through an area of length L meters as illustrated in figure C-13.

The fractional emissions contained in the air parcel after moving through the area of length L are:

$$\text{fractional emissions} = \frac{qs\ L}{\rho a\ HV}$$

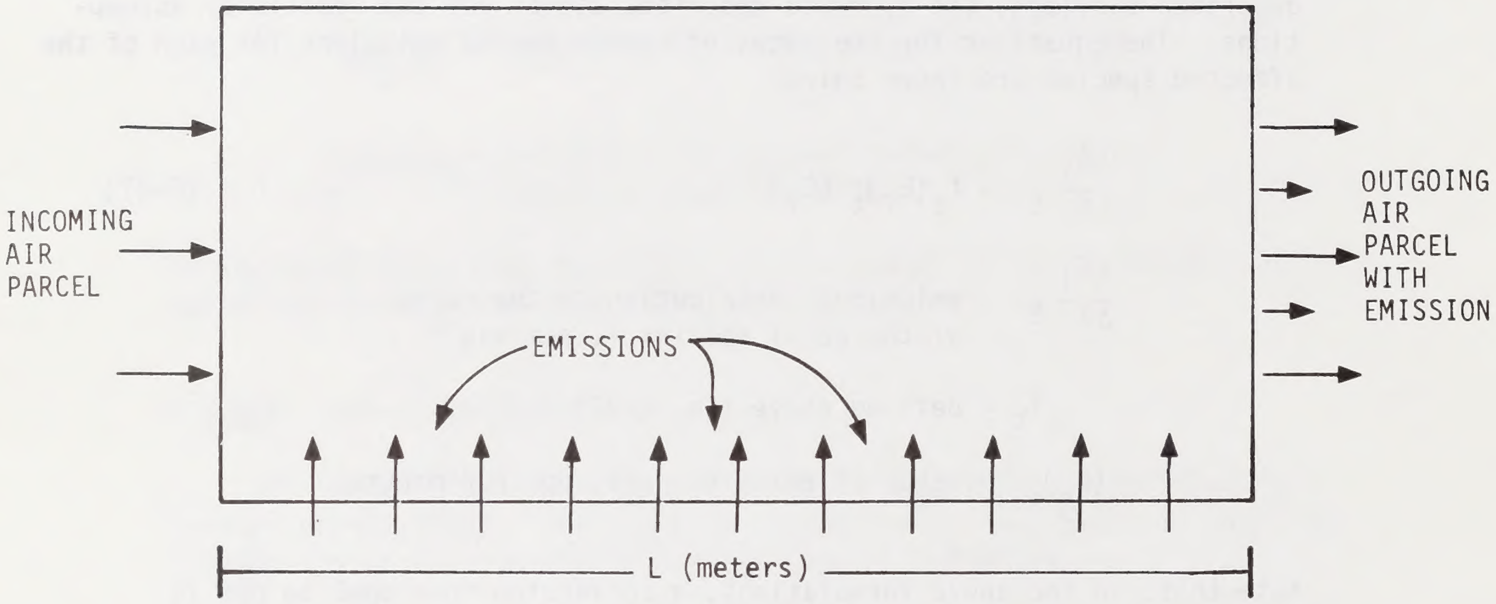

FIGURE C-13. SCHEMATIC OF AN AIR COLUMN MOVING THROUGH AN AREA CONTAINING EMISSIONS where

qs = the emission rate in mol/m^2 sec

L = length of the area

ρa = density of air (mol/m^3)

H = the vertical height in meters

V = wind speed (m/sec)

The emissions in ppm would be

(fractional emissions) x 10^6/L/V
or
$[qs/\rho a\ H] \times 10^6$,

which is the emissions in units of ppm/sec. Thus, we see that the emission rate required for the OZIPM is independent of wind speed.

To determine an emission rate for EKMA in units of ppm/hr, the emissions in mols per unit time is assumed to be evenly distributed spatially within a certain area (usually the county area since emissions are most often reported as county totals). The emissions density is divided by the initial mixing height and multiplied by 24450 m^3/mol to convert to ppm units. As described above, the factor f_t readjusts the emissions for the increase in mixing depth.

C.5.7 Description of Numerical Integration

The kinetics model in EKMA employs a Gear-type integration scheme to numerically solve the set of differential equations described in the previous section. A detailed description is not given here because the method is not unique to EKMA, and the procedure has been described elsewhere (Gear, 1971; Spellman and Hindmarsh, 1975; and Sherman, 1975). The integration scheme initially uses a time step of 1×10^{-10} minutes (i.e., pollutant concentrations are to be calculated 1×10^{-10} minutes after the start time). Subsequent time steps are computed by the Gear-type integration scheme according to the estimated error at each step. However, since the onset and cessation of dilution represent changing conditions, it is necessary for maximal numerical accuracy to begin or end a time step at precisely these points (i.e., the times at which onset and cessation of dilution take place). The pollutant concentrations are calculated at each time step throughout the simulation period. (Once the time reaches the final hour, there is no restriction on precisely matching the final time step, since the concentrations can be interpolated back to exactly the last hour.) A typical simulation in EKMA takes from 150 to 200 times steps for a ten-hour simulation period; about one-half of these time steps are used in simulating the first minute.

The total rate of change of any species is the sum of the rates of change due to dilution, entrainment, emission, and chemical reaction described above. At each time step, the concentrations of all species are calculated along with the current rates of change for each species. The Gear method utilizes a Taylor series polynomial for each species to predict the species concentration at the end of the time step. The order of the polynomial is varied internally for optimum efficiency and is based on the values at the beginning of the time step. A corrective scheme then "corrects" the new concentration values, updates the Taylor polynomials, and estimates the average error. The corrector is a set of linear equations based on a matrix whose elements are the set of partial derivatives of the rate of change of concentrations of each species with respect to all other species. EKMA utilizes a linear system solving package for sparse matrices (i.e., those matrices in which most elements are equal to zero). The integration method used in EKMA has been modified somewhat from the version published by Spellman and Hindmarsh (1975). In particular, the error estimation is performed relative to the current concentration of a species rather than to its maximum concentration. The method utilizes the error estimate to determine the optimum step size and order, so that the allowable error specified by the user is met with the minimum number of integration steps.

The final task performed by the differential equations integrator is the calculation of the maximum one-hour average ozone concentration. Ozone concentrations are calculated for precisely every minute of the simulation. This calculation is performed by interpolation between the time step solutions to the differential equations. Running one-hour average concentrations are calculated using Simpson's rule. The largest one-hour average concentration is then selected as the maximum.

C.5.8 Description of a Sample Simulation

This section describes in considerable detail the mathematical procedures used in EKMA to calculate the maximum one-hour average ozone concentration that results from given initial concentrations of NMHC and NO_x. The procedures are based on the physical and chemical processes described in the last section. Before the beginning of a simulation, data-preparation steps are performed. A simulation is conducted by first determining concentrations at the starting time and then numerically integrating the equations that form the basis of the model. The numerical solution yields species concentration as a function of time for each hour of the simulation period. The following discussion describes the data-preparation steps, the calculation of initial concentrations, model formulation, and the numerical integration technique.

C.5.8.1 Data-Preparation Steps

Because all simulations performed by EKMA in generating an ozone isopleth diagram have identical conditions except for the initial NMHC and NO_x concentrations, a data-preparation step is performed before any simulation is commenced. The purpose of this step is to eliminate abrupt changes in photolytic rate constants and emission rates. Elimination of these abrupt changes (i.e., discontinuities) is desirable for three reasons:

> The integration scheme requires less computer time (discontinuities require the use of small time steps).

> The results are more accurate numerically (stepping past discontinuities can lead to error).

> The atmosphere does not normally have discontinuities. (The simulation of intermittent cloud cover or sudden changes in emissions is outside the scope of EKMA.)

The photolytic rate constants are evaluated every hour using an algorithm developed by Schere and Demerjian (1977). The algorithm uses input data of latitude, longitude, time zone, and date to calculate photolytic constants. A set of third-order polynomial spline functions is then generated so that photolytic constants can be easily calculated from a smooth curve for any time of the day. A set of four coefficients for each of the eight photolytic rate constants in the kinetic mechanism shown in table 3-7 is prepared for each hour of the ten-hour simulation period. Thus, at any time during the simulation period, the photolytic rate constants can be calculated from a simple third-order polynomial equation.

If emissions are to be considered, it is necessary to specify the emission rate(s) of NMHC and/or NO_x injected into the column each hour after the simulation start time. These emission rates are expressed as concentrations in ppm per hour. A set of cubic spline coefficients is determined each hour so that the instantaneous emission rate(s) can be evaluated for any time during the simulation period. For the first hour, a straight line is used, and for each subsequent hour a simple cubic (or lower order) polynomial is used subject to the following limitations:

> The total, or integrated, emissions for each hour must equal the input value.

> The spline functions at each hour must match in value, slope, and curvature unless lower-order functions are used.

> At the end of the last hour of emissions, the emissions must be zero with zero curvature.

> If cubic splines lead to any minima (points of zero slope) that are less than zero, then a lower-order spline function is used for that hour.

C.5.8.2 Determination of Initial Concentrations

Before a simulation can begin, the concentrations of all pollutant species at the starting time must be determined. These initial concentrations are based on assumed initial concentrations of NMHC and NO_x and on the concentrations of pollutants transported in the surface layer. The concentrations of transported pollutants are assumed to be zero unless otherwise specified.

The concentrations of the nonzero species are calculated as described below.

(1) NO_2 is set to the initial NO_x concentration multiplied by the NO_2/NO_x fraction (default is 0.25).

(2) NO is set to the initial NO_x concentration multiplied by the quantity one minus the NO_2/NO_x fraction.

(3) O_3 is set to the concentration transported in the surface layer (default is zero).

(4) The concentrations of the hydrocarbon species are determined from the assumed initial NMHC concentration and the assumed reactivity fraction. Mathematically,

$$[HC]_i = [NMHC]\ (R_i)/C_i \qquad \text{(C-98)}$$

where

$[HC]_i$ = i-th hydrocarbon species in ppm

[NMHC] = initial NMHC concentration, ppmC

R_i = fraction of initial NMHC that is species i

C_i = number of carbon atoms in species i.

(5) Species other than hydrocarbon, NO_x, and O_3 are specified explicitly in the inputs in units of ppm as described by Whitten and Hogo (1978b).

C.6 TECHNICAL DESCRIPTION OF COMPLEX-I

COMPLEX-I is a multiple point source model developed by the U.S. Environmental Protection Agency for application to situations in rural complex terrain settings. The model is based upon the EPA MPTER model (Pierce and Turner, 1980) but has several optional treatments of plume-terrain interactions not included in MPTER.

As applied in this study, COMPLEX-I was developed by EPA but is not an EPA approved model. This version used here has three plume-terrain interaction options. We have used option 3 because it has been shown to perform better than options 1 and 2 (New Mexico EID, 1981). The version of COMPLEX-I that is currently being evaluated by the EPA for approval uses a different treatment of the terrain effect (optional) than that used here. COMPLEX-I can estimate concentrations from sources for one simulated hour for one or more receptors, either at ground-level or varying heights above the ground, or it can simulate concentrations hour-by-hour for a year that result from up to 250 point sources at as many as 180 receptors.

COMPLEX-I is most applicable within 10 km of the source (EPA, 1980). Its use beyond this distance will be less accurate due to mesoscale influences, such as wind change with height, and to meteorological conditions that may vary during the time of transport. COMPLEX-I is suited to the same types of multiple-source applications for which MPTER and CRSTER are.

C.6.1 Model Formulation

The following assumptions are made in COMPLEX-I's formulation: (1) continuous plumes are diluted upon release by the wind speed at stack top;

(2) dispersion from continuous plumes results in time averaged Gaussian distributions in both the horizontal and vertical directions through the dispersing plume; (3) concentration estimates may be made for each hourly period using the mean meteorological conditions appropriate for each hour; (4) the total concentration at a receptor is the sum of the concentrations estimated at the receptor from each source, i.e., concentrations are additive; and (5) concentrations at a receptor for periods longer than an hour can be determined by averaging the hourly concentrations over the period.

The downwind distance x and the crosswind distance y of the source from the receptor is determined as a function of the mean hourly wind direction. Dispersion parameter values are determined as functions of stability class and upwind distance. Equations to estimate concentrations are selected dependent upon stability class, and, for neutral or unstable conditions, upon the relation of dispersion parameter value to mixing height.

The contribution to the concentration, χ_p, from a single point source to a receptor is given by one of the three following equations where the expressions g_2 and g_3, are defined below

Component:

$$\chi_p \cdot Q \cdot \frac{1}{u\sqrt{2\pi}\, w} \cdot \frac{g_2}{\sqrt{2\pi}\,\sigma_z} \qquad \text{(C-99)}$$

$$\chi_p = Q \cdot \frac{1}{u\sqrt{2\pi}\, w} \cdot \frac{1}{L} \qquad \text{(C-100)}$$

$$\chi_p = Q \cdot \frac{1}{u\sqrt{2\pi}\, w} \cdot \frac{g_3}{\sqrt{2\pi}\,\sigma_z} \qquad \text{(C-101)}$$

where:

χ_p, concentration, g m^{-3}

Q, emission rate, g s^{-1}

u, wind speed, m s^{-1}

w, horizontal plume distribution width = 392.7 x (evaluated at the distance x assuming 22.5° sector spread).

σ_z, standard deviation of plume concentration vertical distribution (evaluated at the distance x and for appropriate stability), m

L, mixing height, m

H, effective height of emission, m

z, receptor height above ground, m

y, crosswind distance, m

For stable conditions or unlimited mixing equation (C-99) is used. For unstable or neutral conditions, where σ_z is equal to or greater than 1.6 L, equation (C-100) is used. For unstable or neutral conditions where σ_z is less than 1.6 L, equation (C-102) is selected, provided that both H and z are less than L.

Definitions for expressions g_2 and g_3 follow:

$$g_2 = \exp\left[-0.5(z-H)^2/\sigma_z^2\right] + \exp\left[-0.5(z+H)^2/\sigma_z^2\right] \qquad \text{(C-102)}$$

$$g_3 = \sum_{N=-\infty}^{\infty} \left\{ \exp\left[-0.5(zH+2NL)^2/\sigma_z^2\right] + \exp\left[-0.5(z+H+2NL)^2/\sigma_z^2\right] \right\} \qquad \text{(C-103)}$$

Sensitivity tests using equation (C-101) have indicated that for all H and all z between the ground and the mixing height, the vertical distribution of concentration with height is uniform when σ_z has increased to 1.6 L. Therefore, when σ_z is equal to or greater than 1.6 L for neutral or unstable conditions, use equation (C-100). For special cases such as z = 0, equation (C-100) may given appropriate concentrations for σ_z much less than 1.6 L. However, the above recommendation covers the more general case. (Note that is recommendation differs from that of Pasquill (1976) which indicates that σ_z should not be allowed to increase beyond 0.8 L.) For ground level receptors, z = 0, the use of $\sigma_z = 0.8L$ in equation (C-99) reduces to equation (C-101). However, the above recommendation allows σ_z to increase beyond the value of L, specifically as large as 1.6 L; it also allows for a smooth transition to a uniform vertical profile for receptors above the ground, $z \neq 0$, and for effective heights of emission approaching the mixing height.

C.6.1.1 Dispersion Parameter Values

The vertical dispersion parameter values used in COMPLEX-I are the Pasquill-Gifford (P-G) parameters (Pasquill, 1961; Gifford, 1960) representative for open country (a roughness of approximately 0.03 m). The subroutines used to determined the parameter values are the same as in the UNAMAP programs PTDIS, PTMTP, and RAMR. A 22.5° sector spread is assumed in the horizontal, as in VALLEY.

Except for stable layers aloft, which inhibit vertical dispersion, the atmosphere is treated as a single layer in the vertical that has the same rate of vertical dispersion throughout. Complete eddy reflection is assumed both from the ground and from the stable layer aloft (except in option 3 and some option 2 cases), given by the mixing height for neutral and unstable stabilities.

C.6.1.2 Plume Rise

Plume rise is calculated using the methods of Briggs (1969, 1971, 1972, and 1975). Although the plume rise from point sources is usually dominated by buoyancy, plume rise due to momentum is also considered. (merging of nearby buoyant plumes is not considered).

C.6.1.3 Input Data

All input data are assumed to be representative for the area being modeled. Since concentration estimates are proportional to emissions, consideration of variations may be necessary, such as diurnal or weekday vs. weekend. COMPLEX-I can utilize hourly emissions as an option. The meteorological data consisting of wind direction, wind speed, temperature, stability class, and mixing height for each hour should be representative of region being modeled. Wind speed is measured at the anemometer height and then extrapolated to the stack top, using power law wind speed profiles with the exponent dependent upon stability.

C.6.1.4 Mixing Height

Except in option 3 and option 2 cases, the entire plume is completely eddy-reflected if the effective plume height is below the mixing height. The entire plume is assumed to be within the stable layer aloft if the effective plume height is above the mixing height.

COMPLEX-I does not include calculations for the transitional phenomenon of fumigation, which is the elimination of an inversion layer containing a stable plume from below (which causes mixing of pollutants downward, resulting in uniform concentrations with height beneath the original plume centerline).

C.6.1.5 Removal or Depletion

Transformations of a pollutant resulting in loss of that pollutant throughout the entire depth of each plume can be approximated by COMPLEX-I. If the loss to be simulated is realistic and occurs through the whole plume without dependence upon concentration, then this exponential loss may provide a reasonable simulation. If, however, the loss mechansim is selective, the loss mechanism built into the model will not approximate the atmospheric chemistry very well. Examples of selective loss mechanisms include impaction with features on the ground surface, reactions with materials on the ground, or dependence on a given small parcel of air for concentration (requiring consideration of contributions from all sources to this parcel).

C.6.2 Special Features

COMPLEX-I has the following special plume terrain interaction options. Option 1 entails the following adjustments:

> In stable conditions, plume centerline height is set to 10 m whenever the effective stack height is less than or equal to 10 m above a ground-level receptor height.

> In neutral or unstable conditions, the plume centerline is not allowed to approach the terrain closer than one-half the effective-stack height.

Option 2 includes all the provisions of option 1 but in addition:

> Calculated ground-level concentrations are not allowed to exceed the corresponding centerline plume concentrations (without ground or inversion reflections). This ensures that the second law of thermodynamics is not violated.

Features associated with option 3 are:

> Ground reflection is regarded to be an inappropriate assumption under stable impaction conditions (as is also the treatment in option 2 in some cases).

> Final plume elevation is assumed to be unmodified by terrain.

Verification studies have shown that all three options yield conservative concentration estimates in complex terrain settings (New Mexico EID, 1981). However, option 1 and option 2 consistently over-predict concentrations by wider margins than option 3.

TABLE C-4. CARBON-BOND MECHANISM III USED IN THIS STUDY

	Reaction	Rate Constant at 298K ($ppm^{-1}min^{-1}$)	Activation Energy (K)
1	$NO_2 \rightarrow NO + O$	*	0
2	$O + (O_2) + (M) \rightarrow O_3$	$4.40 \times 10^{6\dagger}$	0
3	$NO + O_3 \rightarrow NO_2 + O_2$	26.6	1450
4	$NO_2 + O_3 \rightarrow NO_3 + O_2$	0.048	2450
5	$NO_2 + O \rightarrow NO + O_2$	1.3×10^4	0
6	$OH + O_3 \rightarrow HO_2 + O_2$	100	1000
7	$HO_2 + O_3 \rightarrow OH + 2O_2$	2.40	1525
8	$OH + NO_2 \rightarrow HNO_3$	1.60×10^4	0
9	$OH + CO \xrightarrow{O_2} HO_2 + CO_2$	440	0
10	$NO + NO + (O_2) \rightarrow NO_2 + NO_2$	$1.50 \times 10^{-4\dagger}$	0
11	$NO + NO_3 \rightarrow NO_2 + NO_2$	2.80×10^4	0
12	$NO_2 + NO_3 + H_2O \rightarrow 2HNO_3$	§	-1.06×10^4
13	$NO + HO_2 \rightarrow NO_2 + OH$	1.20×10^4	0
14	$HO_2 + HO_2 \rightarrow H_2O_2 + O_2$	1.50×10^4	0
15	$X + PAR \rightarrow$	10^5	0
16	$OH + PAR \xrightarrow{O_2} MEO_2 + H_2O$	1300	0
17	$O + OLE \xrightarrow{O_2} MEO_2 + ACO_3 + X$	2700	0
18	$O + OLE \rightarrow CARB + PAR$	2700	0
19	$OH + OLE \xrightarrow{O_2} RAO_2$	3.70×10^4	0
20	$O_3 + OLE \rightarrow CARB + CRIG$	0.008	1900
21	$O_3 + OLE \rightarrow CARB + MCRG + X$	0.008	1900
22	$O + ETH \xrightarrow{O_2} MEO_2 + HO_2 + CO$	600	800
23	$O + ETH \rightarrow CARB + PAR$	600	800

	Reaction	Rate Constant at 298K ($ppm^{-1}min^{-1}$)	Activation Energy (K)
24	$OH + ETH \xrightarrow{O_2} RBO_2$	1.20×10^4	0
25	$O_3 + ETH \rightarrow CARB + CRIG$	0.0024	0
26	$NO + ACO_3 \xrightarrow{O_2} NO_2 + MEO_2$	1.04×10^4	0
27	$NO + RBO_2 \xrightarrow{O_2} NO_2 + CARB + HO_2 + CARB$	1.20×10^4	0
28	$NO + RAO_2 \xrightarrow{O_2} NO_2 + CARB + HO_2 + CARB$	1.20×10^4	0
29	$NO + MEO_2 \xrightarrow{O_2} NO_2 + CARB + MEO_2 + X$	3800	0
30	$NO + MEO_2 \xrightarrow{O_2} NO_2 + CARB + HO_2$	7700	0
31	$NO + MEO_2 \rightarrow NRAT$	500	0
32	$O_3 + RBO_2 \rightarrow CARB + CARB + HO_2 + O_2$	500	0
33	$O_3 + RAO_2 \rightarrow CARB + CARB + HO_2 + O_2$	200	0
34	$OH + CARB \rightarrow CRO_2 + X$	1000	0
35	$OH + CARB \xrightarrow{O_2} HO_2 + CO$	7000	0
36	$OH + CARB \xrightarrow{O_2} ACO_3 + X$	6000	0
37	$CARB \rightarrow CO + H_2$	$(\approx 0.001\ K_1)^*$	0
38	$CARB + (O_2) \xrightarrow{O_2} 2/3\ (2HO_2 + CO)$ $1/3\ (2MEO_2 + CO + 2X)$	$(\approx 0.002\ K_1)^*$	0
39	$NO_2 + ACO_3 \rightarrow PAN$	7000	0
40	$PAN \rightarrow ACO_3 + NO_2$	0.022	1.35×10^4
41	$HO_2 + ACO_3 \rightarrow$ Stable products	1.50×10^4	0
42	$HO_2 + MEO_2 \rightarrow$ Stable products	9000	0

TABLE C-4 (Continued)

	Reaction	Rate Constant at 298K ($ppm^{-1}min^{-1}$)	Activation Energy (K)
43	$NO + CRIG \rightarrow NO_2 + CARB$	1.20×10^4	0
44	$NO_2 + CRIG \rightarrow NO_3 + CARB$	8000	0
45	$CARB + CRIG \rightarrow Ozonide$	2000	0
46	$NO + MCRG \rightarrow NO_2 + CARB + PAR$	1.20×10^4	0
47	$NO_2 + MCRG \rightarrow NO_3 + CARB + PAR$	8000	0
48	$CARB + MCRG \rightarrow Ozonide$	2000	0
49	$CRIG \rightarrow CO + H_2O$	670^{**}	0
50	$CRIG \rightarrow Stable\ products$	240^{**}	0
51	$CRIG \xrightarrow{O_2} HO_2 + HO_2 + CO$	90^{**}	0
52	$MCRG \rightarrow Stable\ products$	150^{**}	0
53	$MCRG \xrightarrow{O_2} MEO_2 + OH + CO$	340^{**}	0
54	$MCRG \xrightarrow{O_2} MEO_2 + HO_2$	425^{**}	0
55	$MCRG \xrightarrow{O_2} CARB + HO_2 + CO + HO_2$	85^{**}	0
56	$OH + ARO \xrightarrow{O_2} RARO + H_2O$	8000	600
57	$OH + ARO \xrightarrow{O_2} HO_2 + OPEN$	1.45×10^4	400
58	$NO + RARO \xrightarrow{O_2} NO_2 + PHEN + HO_2$	4000	0
59	$OPEN + NO \xrightarrow{O_2} NO_2 + DCRB + X + APRC$	6000	0
60	$APRC \xrightarrow{O_2} DCRB + CARB + CO$	10^{4**}	0
61	$APRC \xrightarrow{O_2} CARB + CARB + CO + CO$	10^{4**}	0
62	$PHEN + NO_3 \rightarrow PHO + HNO_3$	5000	0
63	$PHO + NO_2 \rightarrow NPHN$	4000	0

TABLE C-4 (Concluded)

	Reaction	Rate Constant at 298K ($ppm^{-1}min^{-1}$)	Activation Energy (K)
64	$PHO + HO_2 \rightarrow PHEN$	5.00×10^4	0
65	$OPEN + O_3 \rightarrow DCRB + X + APRC$	40	0
66	$OH + PHEN \xrightarrow{O_2} HO_2 + APRC + PAR + CARB$	3.00×10^4	0
67	$DCRB \xrightarrow{O_2} 1/2\ (HO_2 + ACO_3 + CO)$ $1/2\ (MEO_2 + HO_2 + 2CO)$	$(\approx 0.04\ K_1)^*$	0
68	$PHEN + OH \rightarrow PHO$	10^4	0
69	$CRO_2 + NO \xrightarrow{O_2} NO_2 + HO_2 + DCRB$	1.20×10^4	0
70	$DCRB + OH \rightarrow ACO_3$	7000	0
71	$HONO \rightarrow OH + NO$	$(\approx 0.06\ K_1)^*$	0
72	$OH + NO \rightarrow HONO$	9770	0
73	$O_3 \rightarrow O^1D$	$(\approx 10^{-3} K_1)^*$	0
74	$O^1D \xrightarrow{+(M)} O$	4.44×10^{10}	0
75	$OH + SO_2 \rightarrow HSO_5$	2.00×10^3	0
76	$NO + HSO_5 \rightarrow NO_2 + HSO_4$	8.00×10^2	0
77	$NO_2 + HSO_4 \rightarrow SULF + HNO_3$	1.00×10^4	0

---

* Sunlight-dependent; units of min^{-1}.

† Units of $ppm^{-2}min^{-1}$.

§ Heterogeneous; pseudo third order. Equal to 591 x $N_2O_5 + H_2O$.

** Units of min^{-1}.

Appendix D

LEVEL-1 VISIBILITY SCREENING RESULTS FOR EMISSIONS FROM ALL SYNTHETIC FUEL FACILITIES IN THE REGION AT THE HIGH OIL PRODUCTION RATES

LEVEL I VISIBILITY SCREENING ANALYSIS

FOR FLAT TOPS WILDERNESS

UTAH SYNFUEL PROJECTS - HIGH LEVEL SCENARIO

EMISSION SOURCE	SKY/PLUME	PLUME/TERRAIN	SKY/TERRAIN
ENERCOR-MONO POWER	-0.004	0.024	0.006
GEOKINETICS	-0.019	0.016	0.033
MAGIC CIRCLE	-0.017	0.010	0.005
PARAHO	-0.015	0.014	0.003
SOHIO	-0.006	0.035	0.012
SYNTANA-UTAH	-0.024	0.019	0.005
TOSCO	-0.017	0.012	0.004

LEVEL I VISIBILITY SCREENING ANALYSIS

FOR DINOSAUR NATIONAL MONUMENT

UTAH SYNFUEL PROJECTS - HIGH LEVEL SCENARIO

EMISSION SOURCE	SKY/PLUME	PLUME/TERRAIN	SKY/TERRAIN
ENERCOR-MONO POWER	-0.010	0.078	0.006
GEOKINETICS	-0.057	0.066	0.038
MAGIC CIRCLE	-0.066	0.052	0.005
PARAHO	-0.072	0.086	0.005
SOHIO	-0.039	0.381	0.019
SYNTANA-UTAH	-0.129	0.145	0.001
TOSCO	-0.075	0.072	0.004

LEVEL I VISIBILITY SCREENING ANALYSIS

FOR COLORADO NATIONAL MONUMENT

UTAH SYNFUEL PROJECTS - HIGH LEVEL SCENARIO

EMISSION SOURCE	SKY/PLUME	PLUME/TERRAIN	SKY/TERRAIN
ENERCOR-MONO POWER	-0.009	0.073	0.006
GEOKINETICS	-0.042	0.045	0.033
MAGIC CIRCLE	-0.031	0.022	0.005
PARAHO	-0.022	0.022	0.005
SOHIO	-0.008	0.048	0.01[illegible]
SYNTANA-UTAH	-0.032	0.028	0.005
TOSCO	-0.029	0.023	0.004

LEVEL I VISIBILITY SCREENING ANALYSIS
FOR UINTAH & OURAY RES - NORTH

UTAH SYNFUEL PROJECTS - HIGH LEVEL SCENARIO

EMISSION SOURCE	SKY/PLUME	PLUME/TERRAIN	SKY/TERRAIN
ENERCOR-MONO POWER	-0.013	0.111	0.006
GEOKINETICS	-0.126	0.169	0.033
MAGIC CIRCLE	-0.323	0.371	0.005
PARAHO	-0.056	0.064	0.005
SOHIO	-0.034	0.325	0.015
SYNTANA-UTAH	-0.076	0.078	0.005
TOSCO	-0.226	0.274	0.004

LEVEL I VISIBILITY SCREENING ANALYSIS

FOR UINTAH & OURAY RES - SOUTH

UTAH SYNFUEL PROJECTS - HIGH LEVEL SCENARIO

EMISSION SOURCE	SKY/PLUME	PLUME/TERRAIN	SKY/TERRAIN
ENERCOR-MONO POWER	-0.013	0.112	0.006
GEOKINETICS	-0.111	0.146	0.038
MAGIC CIRCLE	-0.131	0.117	0.005
PARAHO	-0.040	0.043	0.005
SOHIO	-0.018	0.144	0.010
SYNTANA-UTAH	-0.053	0.051	0.005
TOSCO	-0.098	0.099	0.004

LEVEL I VISIBILITY SCREENING ANALYSIS
FOR UINTA PRIMITIVE AREA

UTAH SYNFUEL PROJECTS - HIGH LEVEL SCENARIO

EMISSION SOURCE	SKY/PLUME	PLUME/TERRAIN	SKY/TERRAIN
ENERCOR-MONO POWER	-0.003	0.021	0.006
GEOKINETICS	-0.024	0.024	0.038
MAGIC CIRCLE	-0.036	0.027	0.005
PARAHO	-0.018	0.017	0.005
SOHIO	-0.023	0.203	0.018
SYNTANA-UTAH	-0.028	0.024	0.005
TOSCO	-0.037	0.031	0.004

LEVEL I VISIBILITY SCREENING ANALYSIS

FOR FLAT TOPS WILDERNESS

UTAH OTHER PLANNED PROJECTS

EMISSION SOURCE	SKY/PLUME	PLUME/TERRAIN	SKY/TERRAIN
MOON LAKE	-0.052	0.022	0.006
WHITE RIVER	-0.025	0.024	0.006

LEVEL I VISIBILITY SCREENING ANALYSIS

FOR DINOSAUR NATIONAL MONUMENT

UTAH OTHER PLANNED PROJECTS

EMISSION SOURCE	SKY/PLUME	PLUME/TERRAIN	SKY/TERRAIN
MOON LAKE	-0.284	0.163	0.006
WHITE RIVER	-0.097	0.130	0.006

LEVEL I VISIBILITY SCREENING ANALYSIS

FOR COLORADO NATIONAL MONUMENT

UTAH OTHER PLANNED PROJECTS

EMISSION SOURCE	SKY/PLUME	PLUME/TERRAIN	SKY/TERRAIN
MOON LAKE	-0.073	0.034	0.006
WHITE RIVER	-0.040	0.045	0.006

LEVEL I VISIBILITY SCREENING ANALYSIS
FOR UINTAH & OURAY RES - NORTH

UTAH OTHER PLANNED PROJECTS

EMISSION SOURCE	SKY/PLUME	PLUME/TERRAIN	SKY/TERRAIN
MOON LAKE	-0.259	0.145	0.006
WHITE RIVER	-0.103	0.140	0.006

LEVEL I VISIBILITY SCREENING ANALYSIS
FOR UINTAH & OURAY RES - SOUTH

UTAH OTHER PLANNED PROJECTS

EMISSION SOURCE	SKY/PLUME	PLUME/TERRAIN	SKY/TERRAIN
MOON LAKE	-0.155	0.079	0.006
WHITE RIVER	-0.076	0.097	0.006

LEVEL I VISIBILITY SCREENING ANALYSIS

FOR UINTA PRIMITIVE AREA

UTAH OTHER PLANNED PROJECTS

EMISSION SOURCE	SKY/PLUME	PLUME/TERRAIN	SKY/TERRAIN
MOON LAKE	-0.087	0.042	0.006
WHITE RIVER	-0.030	0.031	0.006

LEVEL I VISIBILITY SCREENING ANALYSIS FOR FLAT TOPS WILDERNESS

COLORADO OIL SHALE PROJECTS - 2000 SCENARIO

EMISSION SOURCE	SKY/PLUME	PLUME/TERRAIN	SKY/TERRAIN
COLONY	-0.105	0.169	0.006
UNION/LONG RIDGE	-0.017	0.023	0.002
CATHEDRAL BLUFFS	-0.313	0.296	0.022
CHEVRON	-0.018	0.023	0.004
RIO BLANCO	-0.051	0.085	0.005
MOBIL	-0.016	0.021	0.002
EXXON	-0.085	0.129	0.006
SUPERIOR	-0.009	0.021	0.004
GETTY	-0.011	0.014	0.002
MULTIMINERAL	-0.011	0.014	0.002
NAVAL OIL SHALE	-0.076	0.172	0.004

LEVEL I VISIBILITY SCREENING ANALYSIS
FOR DINOSAUR NATIONAL MONUMENT

COLORADO OIL SHALE PROJECTS - 2000 SCENARIO

EMISSION SOURCE	SKY/PLUME	PLUME/TERRAIN	SKY/TERRAIN
COLONY	-0.035	0.043	0.006
UNION/LONG RIDGE	-0.004	0.005	0.002
CATHEDRAL BLUFFS	-0.165	0.124	0.022
CHEVRON	-0.013	0.015	0.004
RIO BLANCO	-0.066	0.117	0.005
MOBIL	-0.004	0.004	0.002
EXXON	-0.043	0.056	0.006
SUPERIOR	-0.007	0.014	0.004
GETTY	-0.005	0.006	0.002
MULTIMINERAL	-0.010	0.013	0.002
NAVAL OIL SHALE	-0.017	0.028	0.004

LEVEL I VISIBILITY SCREENING ANALYSIS

FOR COLORADO NATIONAL MONUMENT

COLORADO OIL SHALE PROJECTS - 2000 SCENARIO

EMISSION SOURCE	SKY/PLUME	PLUME/TERRAIN	SKY/TERRAIN
COLONY	-0.062	0.087	0.006
UNION/LONG RIDGE	-0.009	0.012	0.002
CATHEDRAL BLUFFS	-0.170	0.128	0.022
CHEVRON	-0.023	0.030	0.004
RIO BLANCO	-0.038	0.059	0.005
MOBIL	-0.010	0.012	0.002
EXXON	-0.066	0.095	0.006
SUPERIOR	-0.003	0.005	0.004
GETTY	-0.012	0.016	0.002
MULTIMINERAL	-0.006	0.006	0.002
NAVAL OIL SHALE	-0.035	0.067	0.004

LEVEL I VISIBILITY SCREENING ANALYSIS

FOR UINTAH & OURAY RES - NORTH

COLORADO OIL SHALE PROJECTS - 2000 SCENARIO

EMISSION SOURCE	SKY/PLUME	PLUME/TERRAIN	SKY/TERRAIN
COLONY	-0.022	0.024	0.006
UNION/LONG RIDGE	-0.003	0.003	0.002
CATHEDRAL BLUFFS	-0.087	0.054	0.022
CHEVRON	-0.008	0.009	0.004
RIO BLANCO	-0.027	0.039	0.005
MOBIL	-0.003	0.003	0.002
EXXON	-0.025	0.028	0.006
SUPERIOR	-0.002	0.004	0.004
GETTY	-0.003	0.004	0.002
MULTIMINERAL	-0.004	0.004	0.002
NAVAL OIL SHALE	-0.011	0.015	0.004

LEVEL I VISIBILITY SCREENING ANALYSIS
FOR UINTAH & OURAY RES - SOUTH

COLORADO OIL SHALE PROJECTS - 2000 SCENARIO

EMISSION SOURCE	SKY/PLUME	PLUME/TERRAIN	SKY/TERRAIN
COLONY	-0.022	0.024	0.006
UNION/LONG RIDGE	-0.003	0.003	0.002
CATHEDRAL BLUFFS	-0.085	0.052	0.022
CHEVRON	-0.008	0.009	0.004
RIO BLANCO	-0.024	0.034	0.005
MOBIL	-0.003	0.003	0.002
EXXON	-0.026	0.029	0.006
SUPERIOR	-0.002	0.003	0.004
GETTY	-0.004	0.004	0.002
MULTIMINERAL	-0.004	0.004	0.002
NAVAL OIL SHALE	-0.012	0.016	0.004

LEVEL I VISIBILITY SCREENING ANALYSIS FOR UINTA PRIMITIVE AREA

COLORADO OIL SHALE PROJECTS - 2000 SCENARIO

EMISSION SOURCE	SKY/PLUME	PLUME/TERRAIN	SKY/TERRAIN
COLONY	-0.012	0.010	0.006
UNION/LONG RIDGE	-0.001	0.001	0.002
CATHEDRAL BLUFFS	-0.052	0.027	0.022
CHEVRON	-0.004	0.003	0.004
RIO BLANCO	-0.015	0.018	0.005
MOBIL	-0.001	0.001	0.002
EXXON	-0.013	0.012	0.006
SUPERIOR	-0.001	0.002	0.004
GETTY	-0.002	0.001	0.002
MULTIMINERAL	-0.002	0.002	0.002
NAVAL OIL SHALE	-0.006	0.007	0.004

Appendix E

AVAILABLE CONTROL MEASURES FOR SYNFUEL INDUSTRY RELATED EMISSIONS

Appendix E
AVAILABLE CONTROL MEASURES FOR SYNFUEL INDUSTRY RELATED EMISSIONS

E.1 INTRODUCTION

The mining of oil shale and tar sands and their subsequent processing produce a variety of pollutant emissions with varying impacts on the air quality of the region. Pollutants due to the mining and processing of oil shale and tar sands include particulate matter, hydrogen sulfide, sulfur dioxide, oxides of nitrogen, hydrocarbons, and carbon monoxide. This appendix identifies available controls for emissions from the synfuel industry and discusses the mitigation measures proposed by the seven project applicants in the Uinta Basin.

A number of techniques are available for the mitigation of particulate matter and gaseous pollutant emissions, though the applicability of some of these techniques to large-scale oil shale development projects has yet to be demonstrated. In Section 2 of this appendix we discuss pollutant abatement methods that are pertinent to the synfuel industry. Abatement procedures proposed for specific projects in the Uinta Basin are reviewed in Section 3. A summary is provided in Section 4.

E.2 TECHNOLOGIES AVAILABLE FOR EMISSION CONTROL

E.2.1 Particulate Matter Control

Particulate matter is emitted, in many cases, as fugitive dust during the mining, transportation, crushing, and retorting of the ore and during the subsequent refining of the crude oil. Disposal of spent shale can also be a cause of significant fugitive emissions.

E.2.1.1. Water Sprays

Water spraying is a simple and effective means of controlling fugitive dust from mining and blasting, surface haul vehicles, wind erosion, and material dumping. Water spraying without the aid of chemical additives has a control efficiency of about 80 percent for particle sizes equal to or greater than 5 μm (EPA, 1980). The control efficiency declines sharply with decreasing particle size. Wetting agents are frequently added to increase the control efficiency. Water spraying can, however, cause clogging of some equipment and is not suitable during freezing weather.

E.2.1.2 Chemical Binders

Chemical binders, such as polymers and inorganic salts, can be employed to control fugitive dust. These are generally applied in solution and form a crust when dry. This protective crust prevents a large amount of particulate matter from becoming airborne. No data are available to quantitatively assess the control efficiency of this technique.

E.2.1.3 Cyclones

Cyclones are widely used in chemical and mineral industries to separate particles from a gas stream. Centrifugal forces in a rotating parcel of air move the particulate matter toward the cyclone wall. The removal efficiency is directly proportional to the square of the velocity and inversely proportional to the cyclone radius. It is customary to increase the control efficiency by using a series of cyclones. Such techniques can lead to efficiencies of up to 90 percent for particles of 5 μm diameter. However, in view of the design and operation costs, cyclones are not suitable for particles smaller than 10 μm in diameter.

E.2.1.4 Baghouses

Fabric filters are one of the most effective devices for the removal of particulate matter from a gas stream. Filters are typically made in a bag form and thus are commonly known as baghouses. Particles are removed by inertial impaction, direct interception, diffusion, and electrostatic forces. Once a layer of dust is collected on the fiber, the dust itself acts as a filter medium. Control efficiences of more than 99 percent can be achieved for particles as small as 1 μm in diameter.

E.2.1.5 Scrubbers

Particulate matter can be washed out of gas streams by water sprays. Particles are removed primarily by collision with water droplets; small particles may also provide sites for condensation of water. Among all wet collection techniques available (spray towers, wet cyclones, mechanical scrubbers, and venturi scrubbers), venturi scrubbers have the highest efficiency--99 percent for particles of diameter 1 µm or more--and are the most widely recommended and used.

E.2.1.6 Electrostatic Precipitators

Electrostatic precipitators are particularly useful for removal of particulate matter from large volumes of gases. A high voltage is used to electrically charge suspended matter in the incoming stream, which is then passed through electrode plates. Charged particles migrate to the electrode of opposite polarity. Collected particles are regularly removed from the collecting surface to ensure high efficiency. A removal efficiency of up to 99 percent can be obtained for particles as small as 1 µm in diameter.

E.2.1.7 Baffled Settling

This is an effective technique for controlling fugitive dust from underground mines. Air masses are made to flow through tortuous paths to accelerate the settling of larger particles unable to negotiate the bends. In underground mines mined-out production panels can be utilized for baffled settling.

E.2.1.8 Covering of Conveyors

As much as 97 percent of particulate matter from conveyors can be controlled by simply covering them. Enclosed and hooded transfer points increase the level of control.

E.2.1.9 Spent Shale Watering

Spent shale can be moisturized to a reasonable moisture content (say, 10 percent) to prevent a large amount of fugitive dust from being generated during handling and disposal.

E.2.1.10 Minimization of the Distance of Fall

Dust released during the dumping of material by trucks (raw oil shale, spent shale, etc.) can be reduced by minimizing the distance of fall (or drop leg).

E.2.1.11 Revegetation

Wind erosion of storage piles, not intended for future use, can be abated by planting indigenous vegetation.

E.2.2 Hydrogen Sulfide Control

Although oil shale contains a small amount of sulfur, normally less than one percent, a large amount of oil shale must be processed to generate crude shale oil in appreciable quantities. If uncontrolled, processing could lead to significant emissions of sulfurous gases. Hydrogen sulfide (H_2S) is produced during shale retorting.

E.2.2.1 The Stretford Process

In the Stretford process, H_2S is dissolved in an alkaline solution of sodium carbonate and sodium bicarbonate and catalytically oxidized to water and elemental sulfur by air. Vanadium and sodium derivatives of anthraquinone disulfonic acid (ADA) are used to promote the oxidation step, which can be written as:

$$2H_2S + O_2 \rightleftarrows 2H_2O + 2S \quad .$$

This process can reduce the concentration of H_2S in the gas stream to 100 ppm.

E.2.2.2 The Claus Process

The Claus process involves oxidation of H_2S to sulfur dioxide (SO_2), which in turn reacts with the remaining H_2S, in the presence of a catalyst, to produce elemental sulfur:

$$2H_2S + 3O_2 \rightleftarrows 2H_2O + 2SO_2$$

$$SO_2 + 2H_2S \rightleftarrows 2H_2O + 3S \quad .$$

The stoichiometric ratio of H_2S to SO_2, as these gases come in contact with the catalyst, is very important in determining removal efficiency. The effluent or tail gas from a Claus plant contains significant quantities of H_2S and SO_2 and needs additional sulfur removal before it can be released into the atmosphere. In the SCOT (Shell Claus Off-Gas Treating) process, the sulfurous compounds in the tail gas are catalytically reduced to H_2S by hydrogen. This H_2S is separated from the gas stream by absorption and the concentrated H_2S, produced by heating the solution, is recycled to the Claus unit. The Beavon process is similar in that the sulfur compounds in the tail gas are catalytically converted to H_2S. The tail gas is mixed with the combustion products of fuel gas and air before passing through the catalyst. The effluent stream from the converter is cooled and directly sent to a Stretford unit.

E.2.3 Sulfur Dioxide Control

Sulfur dioxide is generated during the oxidation of H_2S from the retort facility as well as from the combustion of fuels. The use of desulfurized fuel is expected to limit SO_2 emission from combustion to a small amount, making retorting the primary source of SO_2 pollutant. Many technologies are available for removal of SO_2 from the gas stream before it is discharged into the atmosphere. The Claus process, used for H_2S control, is also effective in controlling SO_2 emission.

E.2.3.1 The Wellman-Lord Process

In the Wellman-Lord process, SO_2 is absorbed by a solution of sodium sulfite. The following reaction takes place:

$$SO_2 + Na_2SO_3 + H_2O \rightleftarrows 2NaHSO_3 \quad .$$

The bisulfite solution is heated to reverse the reaction and sodium sulfite solution is recycled to the absorption column. The resultant concentrated SO_2 can be used to make sulfur or sulfuric acid.

E.2.3.2 The Citrate Process

The citrate process uses citric acid or sodium citrate as a buffer. Hydrogen sulfide is added to the absorber to yield the following liquid phase transformation:

$$HSO_3^- + H^+ + 2H_2S \rightleftarrows 3S + 3H_2O \quad .$$

Flotation is used to separate the elemental sulfur.

E.2.3.3 Alkali Scrubbing

Lime (or limestone), magnesium oxide, or sodium hydroxide and sodium sulfite are commonly used chemical agents for alkali scrubbing. The limestone process produces a slurry of calcium sulfite or sulfate as a result of SO_2 absorbtion by limestone. Notwithstanding its widespread use, some aspects of this process are not very well understood; the process therefore may be somewhat unreliable for the synfuel industry. The dual alkali ($NaOH - Na_2SO_3$) process is reliable and economical. The sodium bisulfite solution formed during scrubbing is converted back to $NaOH$ and Na_2SO_3 by treating it with lime or limestone. In magnesium oxide scrubbing, magnesium hydroxide, the hydrolyzed product, reacts with SO_2 dioxide to produce insoluble magnesium sulfite or sulfate. This product is calcined to regenerate concentrated SO_2 that can be used to produce sulfuric acid or elemental sulfur.

A naturally occurring mineral known as nahcolite can be effectively used for SO_2 absorption. Sodium bicarbonate, its main constituent, can be converted to sodium carbonate by heating; the dry sodium carbonate can then be used to remove SO_2 by absorption. This process may be of special interest to the oil shale industry because some reserves of nahcolite are available near oil shale deposits.

E.2.4 Nitrogen Oxides Control

Oxides of nitrogen are formed by the reaction of nitrogen and oxygen in air at high temperatures. Since conditions of high temperature usually occur in or near fossil fuel flames, most conventional combustion processes produce this class of pollutants. Emissions can be controlled either by designing the combustion process so as to minimize the oxidation of nitrogen or by removing the nitrogen oxides from gas streams.

E.2.4.1 The Minimization of NO_x Formation

E.2.4.1.1 Combustion Process Modification

Combustion processes can be modified to reduce NO_x formation, e.g., by prevention of very high temperature zones and minimization of turbulence. However, such modifications generally diminish combustion efficiency.

In two-stage combustion the amount of air is tightly controlled to prevent conditions favoring the oxidation of nitrogen. About 80-95 percent of the air needed for combustion is supplied in the first stage.

The remaining air is supplied in a second stage to complete the combustion. This process is capable of reducing NO_x emissions by 50 percent without significantly affecting combustion efficiency.

In tangential firing the burners are arranged in a circle and combustion takes place on a tangent to that circle. This controls NO_x formation by preventing flame interaction and by improving heat transfer.

E.2.4.1.2 Flue Gas Recirculation

Flue gas can be recirculated into the combustion chamber to control NO_x. The introduction of exhaust gases limits peak combustion temperatures, thereby limiting NO_x formation. Moreover, compared to air, this recycled gas is lean in oxygen and hence the oxidation is limited.

E.2.4.1.3 Low NO_x Burners

The burner design can be altered to achieve NO_x control. Internal recirculation of gases, stratified combustion, and good mixing of gases are examples of desirable conditions.

E.2.4.2 Flue Gas NO_x Removal

E.2.4.2.1 The Chiyoda Thoroughbred 102 Process

The NO/NO_2 mixture in NO_x is oxidized to NO_2 by ozone in the Chiyoda Thoroughbred 102 process. This NO_2 is absorbed by dilute sulfuric acid in the presence of a catalyst in a packed column. Removal efficiencies of 60 percent have been reported for this process.

E.2.4.2.2 Selective Catalytic Reduction Processes

A very high control efficiency of 90 percent has been achieved by one such process, known as the Kurabo process. This process involves catalytic reduction of NO_x by ammonia to nitrogen. Alumina and copper are typical catalysts. This process has been developed and successfully used on a large scale in Japan.

E.2.4.2.3 Limestone Scrubbing

The limestone scrubbing process used to absorb SO_2 from gases is also effective for NO_x removal. Up to 20 percent of NO_x emissions can be removed by this process. The only disadvantage is the increase of calcium nitrate, a soluble compound, in the scrubbing slurry.

E.2.5 Hydrocarbon and Carbon Monoxide Control

Hydrocarbons and carbon monoxide are formed during the retorting of oil shale and the subsequent refining of crude shale oil. These can be removed from gas streams by destruction (incineration), recovery and recycling, adsorption, or conversion. In addition, volatile organic compounds are released as fugitive emissions from storage tanks, pumps, and valves and from portions of several tar sands processes.

E.2.5.1 Incineration

Incineration involves the direct combustion of hydrocarbons and carbon monoxide from exhaust gases in a refractory-lined incinerator. External fuel may be added if the fuel value of the process gas is not high enough to sustain combustion. It may also be necessary to introduce air into the combustion chamber to maintain an oxidizing atmosphere. Over 99 percent control efficiency for hydrocarbon removal can be achieved by direct incineration. Catalysts are also used in incineration. Catalytic incineration has the advantage of lowering the combustion temperature and increasing combustion efficiency. However, catalysts may be selective and therefore may not convert all components. Control efficiencies of over 99 percent can be obtained from catalytic incinerators for some compounds.

E.2.5.2 Compression/Condensation

Hydrocarbons can be recovered and recycled by a number of techniques involving compression, refrigeration and condensation, or absorption. The gas stream is first saturated with hydrocarbons to avoid explosion during compression and then compressed. In the CRC (compression/refrigeration/condensation) system the compressed gas is passed through a condenser, where the hydrocarbons are removed by condensation. In the CRA (compression/refrigeration/absorption) system the compressed gas is first cooled in a heat exchanger and then sent to an absorber, where hydrocarbons are absorbed by a chilled liquid. CRA and CRC systems have control efficiencies up to 90 percent and 96 percent, respectively.

E.2.5.3 Adsorption

Highly porous solids are used to capture vapor on a surface by adsorption. Activated carbon can be used to efficaciously remove hydrocarbons from process gases. Vapor and adsorbent can be regenerated.

E.2.5.4 Shift Conversion

Carbon monoxide is catalytically oxidized to carbon dioxide by steam in a shift converter. Chromium and iron oxides are suitable catalysts. The by-product hydrogen can be used as a fuel.

E.2.5.5 Control of Fugitive Hydrocarbon Emissions

Floating-roof tanks are commonly used to control evaporative hydrocarbon emissions from relatively volatile liquids in storage tanks. In addition, nitrogen blankets, i.e, filling of empty space with inert nitrogen, can be used to control hydrocarbon emissions from both floating- and fixed-roof tanks. Other control measures include the use of dual seals for pumps and regular maintenance.

E.3 MITIGATION MEASURES PROPOSED BY THE APPLICANTS

A variety of control techniques, based largely upon BACT (Best Available Control Technology) and NSPS (New Source Performance Standards), have been proposed by the oil shale and tar sands companies. These are summarized in Tables E-1 through E-6. The site-specific review presented in these tables is based upon information provided to Systems Applications by each applicant. The information from some applicants was not as detailed or complete as that from others and this is evident in the tables. This may be due to the fact that the projects are in various stages of planning. For example, most emission control measures for mining in the Enercor-Mono Power project are yet to be identified. The emission data for Geokinetics were transmitted to Systems Applications by telephone, and we do not have any information on the specific mitigation measures this applicant intends to use; thus, no summary table is provided for Geokinetics. Furthermore, it must be emphasized that in general there is a large degree of uncertainty in the estimates of hydrocarbon emissions from solvent extraction processes in the tar sands industry. This uncertainty makes the determination of control technology for this process difficult.

E.4 SUMMARY

We have discussed various control technologies for gaseous and particulate pollutants that are commonly used in the mining, minerals, and chemical industries and are applicable to the synfuel industry as well. Many of these pollution abatement methods were found to be included in the project plans of the applicants, as discussed in the third section.

All projects proposed for the Uinta Basin include some types of mitigation measures, although in some projects only general control strategies have been identified because of the embryonic state of the project. Additional control of both particulate matter and gaseous emissions is possible. If additional control becomes desirable, effective and economical measures can be selected from the overview of existing control technologies in Section 2. The limited information given to us on each applicant's processes, equipment, and proposed mitigation measures did not allow us to make a thorough analysis of individual control technologies proposed by the applicants nor to recommend additional measures.

TABLE E-1. MITIGATION MEASURES FOR ENERCOR-MONO POWER

Source	Pollutant	Control Measure	Control Efficiency (%)
Plant flue gases	SO_2	Dry absorption type scrubber (Na_2CO_3)	90
Combustion and scrubber solids	TSP	Baghouse	--
Unpaved roads	TSP	Wet suppression	--
Spoils piles	TSP	Reclamation	--

In addition:

> All gas emissions are expected to be controlled according to BACT as specified by EPA and the Utah Bureau of Air Quality. Measurement of mining related emissions is proposed. Based upon the results of these measurements, appropriate action will be taken to mitigate the emissions. However, none of the control measures has yet been identified.

> The crusher building will have a dust suppression system (details not available).

> A dust suppression technique will be used for storage piles, if necessary (details not available).

TABLE E-2. MITIGATION MEASURES FOR MAGIC CIRCLE

Source	Pollutant	Control Measure	Control Efficiency (%)
Mining	TSP	Wet suppression, water curtain, baffled settling	80
In-Mine crushing and transfer points	TSP	Wet suppression, baffled settling, dust collectors	80
Raw shale stock pile	TSP	None	--
Screening plant	TSP	Baghouse	99.7
Spent shale disposal:			
Load in, dumping, road dust	TSP	Moisture, chemical stablizer	15-20
Wind erosion	TSP	Revegetation	85
Grooming and compaction	TSP	Watering	50
Conveyors	TSP	Baghouse	99.7
Retort gas combustion	NO_x	None	--
	SO_2	Stretford unit	97
	CO	Incinerator	99
Fines combustion	TSP	Baghouse	90

TABLE E-3. MITIGATION MEASURES FOR PARAHO

Source	Pollutant	Control Measure	Control Efficiency (%)
Drilling, bolting, scaling and hauling	TSP	Wet suppression, baffled settling	87.5
Roof bolting unit and drill	TSP	Self-contained with water, detergent tanks	--
Muck piles and working area	TSP	Wet suppression, baffled settling	87.5
Blasting	TSP	Baffled settling	50
	NO_x	None	--
	CO	None	--
	SO_2	None	--
Crushing and screening	TSP	Baghouse, baffled settling, wet scrubbing	99
Conveyors	TSP	Enclosure, baghouses	99
Diesel exhaust	NO_x	Catalytic converter or wet scrubbing	--
	HC		--
	CO		--
	TSP		--
Live storage piles	TSP	Complete enclosure	99.5
Retorted shale storage and handling	TSP	Moisture content of 10%	90
Surficial soil storage piles	TSP	Vegetation	75
Raw shale emergency storage (wind erosion)	TSP	None	--

Continued

TABLE E-3 (Concluded)

Source	Pollutant	Control Measure	Control Efficiency (%)
Hydrogen plant reformer furnace	TSP	None	--
	CO	None	--
	HC	None	--
	NO_x	None	--
	SO_2	Holmes Stretford	99.6
Hydrotreater feed furnace	TSP	None	--
	CO	None	--
	HC	None	--
	NO_x	None	--
	SO_2	None	--
Power generation (gas turbines)	TSP	None	--
	CO	None	--
	HC	None	--
	NO_x	NH_3 removal by water scrubbing before combustion	97
	SO_2	Holmes Stretford	97.1
Package boiler	TSP	None	--
	CO	None	--
	HC	None	--
	NO_x	None	--
	SO_2	Low-sulfur fuel	--
Day tanks	HC	Internal floating roof with a single seal	--
Crude shale oil and hydrotreated shale oil storage	HC	Floating roof with primary and secondary seals	--
Other storage tanks	HC	Fixed roof	--
Pumps, compressors, and valves	HC	Double mechanical seals, regular maintenance	--

TABLE E-4. MITIGATION MEASURES FOR SOHIO

Source	Pollutant	Control Measure	Control Efficiency (%)
Tar sand stock pile	TSP	None	--
Topsoil (removal)	TSP	None	--
Topsoil (wind erosion)	TSP	Windbreakers, revegetation	75
Overburden (removal)	TSP	None	--
Overburden (wind erosion)	TSP	None	--
Tar sands (removal)	TSP	None	--
Spent sand (wind erosion)	TSP	None	--
Blasting	TSP	None	--
Railroad loading	TSP	Drop leg	--
Truck hauling	TSP	Watering	50
Truck dump	TSP	Spraying	50
Conveyors	TSP	Partial covering	90
Grizzlies	TSP	Baghouse	99
Crushers, pulverizers	TSP	Spraying	50
Storage piles	TSP	Partial enclosure	90
Oil/water separator	TSP	Covered	96
Truck loadout (mine waste)	TSP	Drop leg	--
Diluent (kerosene) and diluted bitumen storage tanks	HC	N_2 blanket, cone roof	--

Continued

TABLE E-4 (Concluded)

Source	Pollutant	Control Measure	Control Efficiency (%)
Hydrotreated oil storage tanks	HC	Floating roof	--
Slop oil tanks	HC	None	--
Process plant exhauster	HC	None	--
Diluent recovery, delayed coker, hydrotreater, and hydrogen plant	TSP CO HC NO_x SO_2	Meet NSPS for refinery-related sources	
Sulfur recovery	SO_2	SCOT (tail gas)	99.9
Steam generator	TSP	Not specified by applicant	97.6
	SO_2		23.5
	NO_x		74.0
Seven-day coke storage pile	TSP	Covered	--
Long-term coke storage pile and truck hauling	TSP	Watering	--
Sulfur pile and truck hauling	TSP	None	--

TABLE E-5. MITIGATION MEASURES FOR SYNTANA-UTAH

Source	Pollutant	Control Measure	Control Efficiency (%)
Mining, blasting	TSP	Baffled settling	75
Blasting	CO	None	--
In-mine transfer	TSP	Wet suppression, baffled settling	87.5
Primary crushing	TSP	Wet suppression, baffled settling	87.5
Mine mobile equipment	TSP	Wet suppression, baffled settling	87.5
	CO	None	--
	HC	None	--
	NO_x	None	--
	SO_2	None	--
Load-in (to coarse storage pile)	TSP	Wet suppression, drop leg	90
Storage pile (wind erosion)	TSP	Water spray (live storage)	50
		Chemical supression (dead storage)	90
Conveyors, secondary crushers, screens	TSP	Baghouse	99.5
Retorted shale:			
Conveyor feed	TSP	Wet suppression, water bath	98
Conveyor transfer, hopper load-in	TSP	Water spray	75
Truck loading and spreading	TSP	None	--
Wind erosion	TSP	Chemical suppression	90
Pile maintenance	TSP	Water spray	75

Continued

TABLE E-5 (Concluded)

Source	Pollutant	Control Measure	Control Efficiency (%)
Road dust from hauling	TSP	Chemical suppression	90
Flue gas desulfurization (FGD) unit	SO_2	FGD	90
	NO_x	None	--
	CO	Combustion control	--
	HC	Combustion control	--
	TSP	Baghouse	99.5
Tosco elutriator	TSP	Cyclone, venturi scrubber	99.5
Processed shale moisturizer	TSP	Venturi scrubber	99.5
Ball heater and lift pipe flue gas	SO_2	FGD	90
	NO_x	None	--
	CO	None	--
	HC	Incinerator	85
	TSP	Cyclone, venturi scrubber	99.5
Hydrogen reformer furnace	SO_2	None	--
	NO_x	Low NO_x burner	--
	CO	Combustion control	--
	HC	Combustion control	--
	TSP	None	--
Raw shale oil storage	HC	Floating roof	--
Product oil storage tanks	HC	Floating roof	--
Valves, flanges, pump, seals, etc.	HC	Regular maintenance	50

TABLE E-6. MITIGATION MEASURES FOR TOSCO

Source	Pollutant	Control Measure	Control Efficiency (%)
Mining	TSP	None	--
Coarse ore handling	TSP	Water spray	--
Conveyors	TSP	Covers, baghouse	99
Transfer points	TSP	Enclosure, baghouse	99
Storage piles (wind erosion and maintenance)	TSP	Wet suppression, polymer dust suppression	--
Spent shale (haul roads, dumping)	TSP	Water spray	--
Spent shale (handling and compaction)	TSP	Moisture content of 13%	--
Spent shale (wind erosion)	TSP	Moisture content of 13%	83
Raw shale preheaters and ceramic ball heaters	SO_2	Low-sulfur fuel, chemical absorption by solids in the ore	95
	NO_x	Good combustion practices	--
	HC	Incinerator	85
	CO	Incinerator	99.9
	TSP	Cyclones and venturi scrubber	99.9
Elutriators and steam superheaters	SO_2	Chemical absorption by shale fines	--
	NO_x	Good combustion practices	
	HC	" " "	
	CO	" " "	
	TSP	Cyclones and venturi scrubbers	99.9

Continued

TABLE E-6 (Concluded)

Source	Pollutant	Control Measure	Control Efficiency (%)
Shale moisturizers	TSP	Venturi scrubber	98.4
Sulfur plant and tail gas unit	SO_2	Tail gas scrubber	99.6
High-volatility material storage tanks	HC	Floating roof	--
Low-volatility material storage tanks	HC	Fixed roof	--
Valves, flanges, pumps, and compressors	HC	Seals, regular maintenance	--

REFERENCES

Altshuller, A. P. (1979), "Model Predictions of the Rates of Homogeneous Oxidation of Sulfur Dioxide to Sulfate in the Troposphere," Atmos. Environ., Vol. 13, pp. 1653-1661.

Anderson, G. E., et al. (1981), "Air Quality Impacts of Anticipated Development in Oil Shale Operations in Western Colorado and Eastern Utah," Systems Applications, Inc., San Rafael, California.

Anderson, G. E., et al. (1980), "Air Quality Interrelationships in the Piceance Basin with Massive Oil Shale Development," SAI No. ES80-152, Systems Applications, Inc., San Rafael, California.

Aris, R. (1962), Vectors, Tensors, and the Basic Equations of Fluid Mechanics (Prentice-Hall, Incorporated, Englewood Cliffs, New Jersey).

Bass, A., D. G. Strimaitis, and B. A. Egan (1981), "Potential Flow Model for Gaussian Plume Interaction with Simple Terrain Features," EPA-600/4-81-008, U.S. Environmental Protection Agency, Research Triangle Park, North Carolina.

Baur, E. (1973), "Dispersion of Tracers in the Atmosphere: Survey of Meteorological Data," Institute of Defense Analysis, Paper P-925, Arlington, Virginia.

Bergstrom, R. W., et al. (1981), "Comparison of the Observed and Predicted Visual Effects Caused by Power Plant Plumes," Atmos. Environ., Vol. 15, pp. 2135-2150.

Blasius, H. (1908), Z. Angew. Math. Phys., Vol. 56, pp. 1-37 (English translation, NACA Tech. Mem., 1256).

Bolin, B., G. Aspling, and C. Persson (1974), "Residence Time of Atmospheric Pollutants as Dependent on Source Characteristics, Atmospheric Diffusion Processes, and Sink Mechanisms," Tellus, Vol. 26, pp. 185-194.

Bolin, B., and L. Granat (1973), "Local Fallout and Long Distance Transport of Sulfur," Ambio, Vol. 2, pp. 87-90.

Boris, J. P., and D. L. Book (1973), "Flux Corrected Transport--I. SHASTA, A Fluid Transport Algorithm That Works," J. Comput. Phys., Vol. 11, pp. 38-69.

Briggs, G. A. (1975), "Plume Rise Predictions," in Lectures on Air Pollution and Environmental Impact Analysis, Duane A. Haugen, ed., pp. 59-111 (American Meteorological Society, Boston, Massachusetts).

Briggs, G. A. (1973), "Diffusion Estimation for Small Emissions," Atmospheric Turbulence and Diffusion Laboratory, Contribution File No. (Draft) 79. Oak Ridge, Tennessee, p. 59.

Briggs, G. A. (1972), "Discussion on Chimney Plumes in Neutral and Stable Surroundings," Atmos. Environ., Vol. 6, pp. 507-510.

Briggs, G. A. (1971), "Some Recent Analyses of Plume Rise Observation," Proc. Second International Clean Air Congress, H. H. Englund and W. T. Beery, eds., pp. 1029-1032 (Academic Press, New York, New York).

Briggs, G. A. (1969), "Plume Rise," USAEC Critical Review Series, TID-25075, National Technical Information Service, Springfield, Virginia.

Burns and McDonnell (1980), "Assessment of Visibility Impairment for the Deseret Generation and Transmission Cooperative, Inc. Moon Lake Power Plant Units 1 and 2," Burns & McDonnell Engineers, Kansas City, Missouri.

Burt, E. W. (1977), Valley Model User's Guide, EPA-450/2-77-018, U.S. Environmental Protection Agency, Research Triangle Park, North Carolina.

Chamberlain, A. C. (1966), "Transport of Gases to and from Grass and Grass-Like Surfaces," Proc. Roy. Soc., Vol. 3, pp. 63-88.

Chan, M. W., and M. E. Smith (1981), "Long-Term Variations in Ozone Measurements in a Remote Area in Northeastern Utah," AeroVironment, Inc. AV-TP-81/523.

Dahlquist, G., and A. Björck (1974), Numerical Methods (Prentice-Hall, Englewood Cliffs, New Jersey).

Defant, A. (1951), "Local Winds," in Compendium of Meteorology, pp. 655-672 (American Meteorological Society, Boston, Massachusetts).

Defant, A. (1933), "Der Abfluss Schwerer Luftmassen auf geneigtem Boden, nebst einigen Bemerkungen zu der Theorie stationarer Luftstrome," Sitzungberichte der Preuss. Akad. Wiss. Phys.-Math. Klasse, Vol. 18, No. 3, pp. 624-635.

DOC (1981), "1978 Census of Agriculture, Volume 1, State and County Data," U.S. Department of Commerce, Washington, D.C.

DOC (1980), "County Business Patterns--1979," U.S. Department of Commerce, Washington, D.C.

Dodge, M. C. (1977), "Effect of Selected Parameters on Predictions of a Photochemical Model," EPA-600/3-77-048, U.S. Environmental Protection Agency, Research Triangle Park, North Carolina.

DOE (1981), "Energy Data Reports--1979," U.S. Department of Energy, Washington, D.C.

Egan, B. A. (1975), "Turbulent Diffusion in Complex Terrain," Lectures on Air Pollution and Environmental Impact Analyses., American Meteorological Society, Boston, Massachusetts.

Egan, B. A., and J. R. Mahoney (1972), "Numerical Modeling of Advection and Diffusion of Urban Area Source Pollutants," J. Appl. Meteorol., Vol. 11, pp. 312-322.

EPA (1981a), "Guideline for Use of City-Specific EKMA in Preparing Ozone SIPs," EPA-450/4-80-027, U.S. Environmental Protection Agency, Research Triangle Park, North Carolina.

EPA (1981b), "Compilation of Air Pollution Emission Factors (Including Supplements 1-12)," AP-42, U.S. Environmental Protection Agency, Research Triangle Park, North Carolina.

EPA (1981c), "Control Strategy Demonstration: New Mexico Air Quality Control Regulation 602, Coal Burning Equipment--Sulfur Dioxide," Air Quality Bureau, Health and Environment Department, New Mexico Environmental Improvement Division, Santa Fe, New Mexico.

EPA (1980), "Environmental Perspective on the Emerging Oil Shale Industry," EPA-600/2-80-205a, U.S. Environmental Protection Agency, Cincinnati, Ohio.

EPA (1980), "Procedures for the Preparation of Emission Inventories for Volatile Organic Compounds," Volume I, EPA-450/2-77-028, U.S. Environmental Protection Agency, Research Triangle Park, North Carolina.

EPA (1978), "Workbook for Comparison of Air Quality Models," EPA 450/2-78-028a, Research Triangle Park, North Carolina.

EPA (1977), "Uses, Limitations and Technical Basis of Procedures for Quantifying Relationships between Photochemical Oxidants and Precursors," EPA-450/2-77-021a, U.S. Environmental Protection Agency, Research Triangle Park, North Carolina.

Forsythe, G. E., and W. R. Wasow (1960), Finite-Difference Methods for Partial Differential Equations (John Wiley & Sons, New York, New York).

Galbally, I. E. (1974), "Gas Transfer near the Earth's Surface," Adv. in Geophysics, Vol. 18B, pp. 329-340.

Garratt, J. R. (1977), "Review of Dry Coefficients over Oceans and Continents," Monthly Weather Review, Vol. 105, pp. 915-929.

Gear, C. W. (1971), "The Automatic Integration of Ordinary Differential Equations," in Communication of the Association for Computing Machinery, Vol. 14, No. 3, pp. 176-179.

Geiger, R. (1971), The Climate near the Ground, Third Printing (Harvard University Press, Cambridge, Massachusetts).

Georgii, H. W. (1970), "Contributions to the Atmospheric Sulfur Budget," J. Geophys. Res., Vol. 75, pp. 2365-2371.

Gifford, F. A., Jr. (1960), "Atmospheric Dispersion Calculations Using the Generalized Gaussian Plume Model," Nucl. Saf., Vol. 2, No. 2, pp. 56-59.

Heffter, J. (1965), "The Variations of Horizontal Diffusion Parameters with Time for Travel Periods of One Hour or Longer," J. Appl. Meteorol., Vol. 4.

Hill, A. C. (1971), "A Sink for Atmospheric Pollutants," J. Air Pollut. Control Assoc., Vol. 21, pp. 946-947.

Hogo, H. and G. Z. Whitten (1982), "Level II EKMA User's Manual for a HP-3000 Computer: Volume I," No. 82236, Systems Applications, Inc., San Rafael, California.

Hogo, H., G. Z. Whitten, and S. D. Reynolds (1981), "Application of the Empirical Kinetic Modeling Approach to Urban Areas, Volume II: Tulsa," EPA-450/4-81-005b, Systems Applications, Inc., San Rafael, California.

Högström , U. (1975), "Further Comments on the Long Range Transport of Airborne Material and Its Removal by Deposition and Washout," Atmos. Environ., Vol. 9, pp. 946-947.

Holzworth, G. C. (1972), "Mixing Heights, Wind Speeds, and Potential for Urban Air Pollution throughout the Contiguous United States," AP-101, Office of Air Programs, Environmental Protection Agency, Research Triangle Park, North Carolina.

Hovind, E. L., T. C. Spangler, and A. J. Anderson (1974), "The Influence of Rough Mountainous Terrain upon Plume Dispersion from an Elevated Source," Proc. Symposium on Atmospheric Diffusion and Air Pollution, Santa Barbara, California, pp. 214-217.

Irwin, J. S., and D. B. Turner, "An Analysis of Complex I and Complex II--Candidate Screening Models," U.S. Environmental Protection Agency, Research Triangle Park, North Carolina.

Johnson, C. D., et al. (1980), "User's Manual for the Plume Visibility Model (PLUVUE)," EPA-450/4-80-032, Systems Applications, Inc., San Rafael, California.

Kao, S. K., and G. H. Taylor (1976), "An Airborne QIR Pollution Monitoring Experiment in an Area of Mountain-Valley Terrain," University of Utah, Salt Lake City, Utah.

Killus, J. P. (1982), "Background Reactivity Estimates for Atmospheric Modeling Studies," paper presented at the XV Informal Conference on Photochemistry, Stanford, California, June 27-July 1, 1982.

Killus, J. P., and G. Z. Whitten (1981), "A New Carbon-Bond Mechanism of Air Quality Simulation Modeling," SAI No. 81245, Systems Applications, Inc., San Rafael, California.

Lantz, R. B., and G. F. Hoffnagle (1976), "Comparison of Several Models with Ambient Sulfur Dioxide Measurements Near the Navajo Generating Station," paper for 69th Annual Meeting of the Air Pollution Control Association, Portland, Oregon, 1976.

Lavery, T. F., A. Bass, D. G. Strimaitis, Venkatram, B. R. Green, P. J. Drivas, and B. A. Egan (1982), "EPA Complex Terrain Model Development; First Milestone Report--1981," EPA-600/3-82-036, U.S. Environmental Protection Agency, Research Triangle Park, North Carolina.

Latimer, D. A., and J. R. Doyle (1981), "Prevention of Significant Deterioration Policy Implications for Projected Oil Shale Development," report for U.S. Environmental Protection Agency, Systems Applications, Inc., San Rafael, California.

Latimer, D. A., and R. G. Ireson (1980), "Workbook for Estimating Visibility Impairment," EPA-450/4-80-031, Systems Applications, Inc., San Rafael, California.

Latimer, D. A., et al. (1980), "An Assessment of Visibility Impairment in Capitol Reef National Park Caused by Emissions from the Hunter Power Plant," EF80-43, Systems Applications, Inc., San Rafael, California.

Latimer, D. A., et al. (1978), "The Development of Mathematical Models for the Prediction of Anthropogenic Visibility Impairment," EPA-450/3-78-110 a, b, c, Systems Applications, Inc., San Rafael, California.

Lilly, D. K. (1973), "Calculation of Stably Stratified Flow around Complex Terrain," Research Note No. 40, Flow Research, Incorporated, Kent, Washington.

Liu, M. K., and D. R. Durran (1977), "The Development of a Regional Air Pollution Model and Its Application to the Northern Great Plains," EPA-908/1-77-001, Systems Applications, Inc., San Rafael, California.

McMahon, T. A., and P. J. Denison (1979), "Empirical Atmospheric Deposition Parameters--A Survey," Atmos. Environ., Vol. 13, pp. 571-585.

Monin, A. S., and A. M. Yaglom (1971), Statistical Fluid Mechanics: Mechanics of Turbulence, Vol. 1 (MIT Press, Cambridge, Massachusetts).

Munn, R. E. (1966), Descriptive Micrometeorology (Academic Press, New York, New York).

NPS (1982), Socioeconomic data for Uintah and Grand counties, private communication, National Park Service, Denver, Colorado.

New Mexico EID (1981), "Control Strategy Demonstration: New Mexico Air Quality Control Regulation 602, Coal Burning Equipment--Sulfur Dioxide," Air Quality Bureau, New Mexico Environmental Improvement Division, Santa Fe, New Mexico.

ORNL (1982), "Agricultural Production in the United States by County," Oak Ridge National Laboratory, Oak Ridge, Tennessee.

Owen, P. R., and W. R. Thompson (1963), "Heat Transfer across Rough Surfaces," J. Fluid Mech., Vol. 15, pp. 321-324.

Pasquill, F. (1976), "Atmospheric Dispersion Parameters in Gaussian Plume Modeling. Part II. Possible Requirements for Change in the Turner Workbook Values," EPA-600/4-76-030b, U.S. Environmental Protection Agency, Research Triangle Park, North Carolina.

Pasquill, F. (1961), "The Estimation of the Dispersion of Windborne Material," Meteorol. Mag., Vol. 90, No. 1063, pp. 33-49.

PEDCo (1981), "Emission Inventory: Secondary Impacts (Draft)," PEDCo Environmental, Inc., Kansas City, Missouri.

Pierce, T. E., and D. B. Turner (1980), "User's Guide for MPTER, A Multiple Point Gaussian Dispersion Algorithm with Optional Terrain Adjustment," EPA-600/8-80-016, Environmental Sciences Research Laboratory, Office of Research and Development, U.S. Environmental Protection Agency, Research Triangle Park, North Carolina.

Queney, P. (1947), "The Problem of Air Flow over Mountains: A Summary of Theoretical Studies," Bull. Am. Meteorol. Soc., Vol. 29, pp. 16-27.

Randerson, D. (1972), "Temporal Changes in Horizontal Diffusion Parameters of a Single Nuclear Debris Cloud," J. Appl. Meteorol., Vol. 11, pp. 670-673.

Rao, K. S., and H. F. Snodgrass (1981), "A Nonstationary Nocturnal Drainage Flow Model," Boundary-Layer Meteorol., Vol. 20, pp. 309-320.

Reid, J. D. (1976), "Dispersion in a Mountain Environment," Paper No. 253, Department of Atmospheric Science, Colorado State University, Fort Collins, Colorado.

Schere, K. L., and K. L. Demerjian (1977), "Calculation of Selected Photolytic Rate Constants over a Diurnal Range," EPA-600/4-77-015, U.S. Environmental Protection Agency, Research Triangle Park, North Carolina.

Schock, M. R. (1981), "The Selection of a Computer Modeling Procedure for the Simulation of Mesoscale Ground-Level Air Quality Concentrations," Division of Environmental Waste Management and Research, North Dakota State Department of Health, Bismarck, North Dakota.

Scriven, R. A., and B.E.A. Fisher (1975), "The Long Range Transport of Airborne Material and Its Removal by Deposition and Washout--I. General Considerations," Atmos. Environ., Vol. 9, pp. 49-58.

Sehmel, G. A., S. L. Sutter, and M. T. Dana (1973), "Dry Deposition Processes," in Pacific Northwest Laboratory Annual Report for 1971, to the USAEC, Division of Biomedical and Environmental Research, Vol. II: Physical Sciences, Part 1, Atmospheric Science, BNWL-1751, pp. 150-153 (Battelle Northwest Laboratories, Richland, Washington).

Shearer, D. L., D. H. Minott, and G. R. Hilst (1977), "Development of Vertical Dispersion Coefficients for Rolling Terrain Environments," The Research Corporation of New England, Wethersfield, Connecticut.

Sherman, A. H. (1975), "Yale Sparse Matrix Package User's Guide," UCID-30114, University of California, Livermore, California.

Singh, H. B., F. L. Ludwig, and W. B. Johnson (1978), "Tropospheric Ozone: Concentrations and Variabilities in Clean Remote Atmospheres," Atmos. Environ., Vol. 12, No. 11, pp. 2045-2242.

Smagorinsky, J. (1963), "General Circulation Experiments with the Primitive Equations. I. The Basic Experiments," Monthly Weather Review, Vol. 91, pp. 99-164.

Spellman, J. W., and A. C. Hindmarsh (1975), "GEARS: Solution of Ordinary Differential Equations Having a Sparse Jacobian Matrix," UCID-30116, University of California, Livermore, California.

Start, G. E., C. R. Dickson, and N. R. Ricks (1974), "Effluent Dilutions over Mountainous Terrain and Within Mountain Canyons," Proc. Symposium on Atmospheric Diffusion and Air Pollution, Santa Barbara, California, pp. 226-232.

Start, G. E., N. R. Ricks, and C. R. Dickson (1974), "Effluent Dilutions over Mountainous Terrain," ERL ARL-51, National Oceanic and Atmospheric Administration, U.S. Department of Commerce, Idaho Falls, Idaho.

Stern, M. E., and J. S. Malkus (1953), "The Flow of a Stable Atmosphere over a Heated Island, Part II," J. Meteorol., Vol. 10, pp. 105-120.

Taylor, G. I. (1921), "Diffusion by Continuous Movements," Proc. London Math. Soc., Vol. 2, No. 20, pp. 196-202.

Tennekes, H. (1973), "A Model for the Dynamics of the Inversion above a Convective Layer," J. Atmos. Sci., Vol. 30, p. 558.

Tesche, T. W., and M. A. Yocke (1978), "Numerical Modeling of Wind Fields Over Mountainous Regions in California," paper sponsored by Systems Applications, Inc., San Rafael, California, presented at Conference on Sierra Nevada Meteorology, American Meteorological Society, South Lake Tahoe, NV, June 19-21, 1978.

Tesche, T. W., and M. A. Yocke (1976), "Application of Numerical Wind Models to Snow Avalanche Forecasting," Proc. Avalanche Workshop, National Research Council of Canada and Environment, Banff, Alberta, Canada, 1976.

Thom, A. S. (1972), "Momentum, Mass and Heat Exchange of Vegetation," Q. J. Roy. Meteorol. Soc., Vol. 98, pp. 124-134.

Turk, J. T., and D. B. Adams (1982), "Sensitivity to Acidification of Lakes in the Flat Tops Wilderness Area, Colorado," unpublished manuscript prepared for submission to Water Resources Research.

Turner, D. B. (1969), "Workbook of Atmospheric Dispersion Estimates," 999-AP-26, U.S. Public Health Service, Cincinnati, Ohio.

UDOT (1982), Estimates of traffic counts on county and class "D" roads, private communication, Utah Department of Transportation, Salt Lake City, Utah.

UDOT (1979), "Traffic on Utah Highways--1979," Utah Department of Transportation, Salt Lake City, Utah.

Utah State Planning Coordinator's Office (1982), "Economic and Demographic Projections," State Planning Coordinator's Office, Salt Lake City, Utah.

VanWagoner (1980), "Uinta Basin Transportation Study," Wayne T. VanWagoner and Associates, Inc., Salt Lake City, Utah.

Walther, E. G., and R. M. Newburn (1980), "Standard Visual Range Measured in the NPS/EPA Regional Visibility Network from December 1978 through August 1979," Visibility Research Center, Las Vegas, Nevada.

Whitten, G. Z., and H. Hogo (1981), "Comparative Applications of the EKMA in the Los Angeles Area," SAI No. 10R2-EF80-73, Systems Applications, Inc., San Rafael, California.

Whitten, G. Z., and H. Hogo, (1978a), "User's Manual for Kinetics Model and Ozone Isopleth Plotting Package," EPA-600/8-78-014a, Systems Applications, Inc., San Rafael, California.

Whitten, G. Z., and H. Hogo (1978b), "User's Manual for Ozone Isopleth Plotting with Optional Mechanism (OZIPM)," SAI No. EF78-30, Systems Applications, Inc., San Rafael, California.

Whitten, G. Z., H. Hogo, and R. G. Johnson (1981), "Application of the Empirical Kinetic Modeling Approach (EKMA) to Urban Areas, Volume 1: San Francisco/Sacramento," EPA-450/4-81-005a, Systems Applications, Inc., San Rafael, California.

Whitten, G. Z., H. Hogo, and J. P. Killus (1980), "The Carbon-Bond Mechanism: A Condensed Kinetic Mechanism for Photochemical Smog," Environ. Sci. Technol., Vol. 14, pp. 690-700.

Williams, M. D., et al. (1981), "NCAQ Report 2, Air Quality in the Four Corners Region, Vol. I: Local Analysis," Report No. LA-UR-81-1145 to National Commission on Air Quality, Los Alamos National Laboratory, Los Alamos, New Mexico.

Yocke, M. A. (1981), "A Three-Dimensional Wind Model for Complex Terrain," dissertation, University of California, Berkeley.

Yocke, M. A., and M. K. Liu (1978), "Modeling Wind Distributions over Complex Terrain," EF78-78, Systems Applications, Inc., San Rafael, California.

Yocke, M. A., M. K. Liu, and M. L. McElroy (1977), "The Development of a Three-Dimensional Wind Model for Complex Terrain," Proc. Conference on Applications on Air Pollution Meteorology, American Meteorological Society, 28 November-2 December 1977.

☆ U.S. GOVERNMENT PRINTING OFFICE: 1983—677-915 REGION No. 8

BLM LIBRARY
RS 150A BLDG. 50
DENVER FEDERAL CENTER
P.O. BOX 25047
DENVER, CO 80225

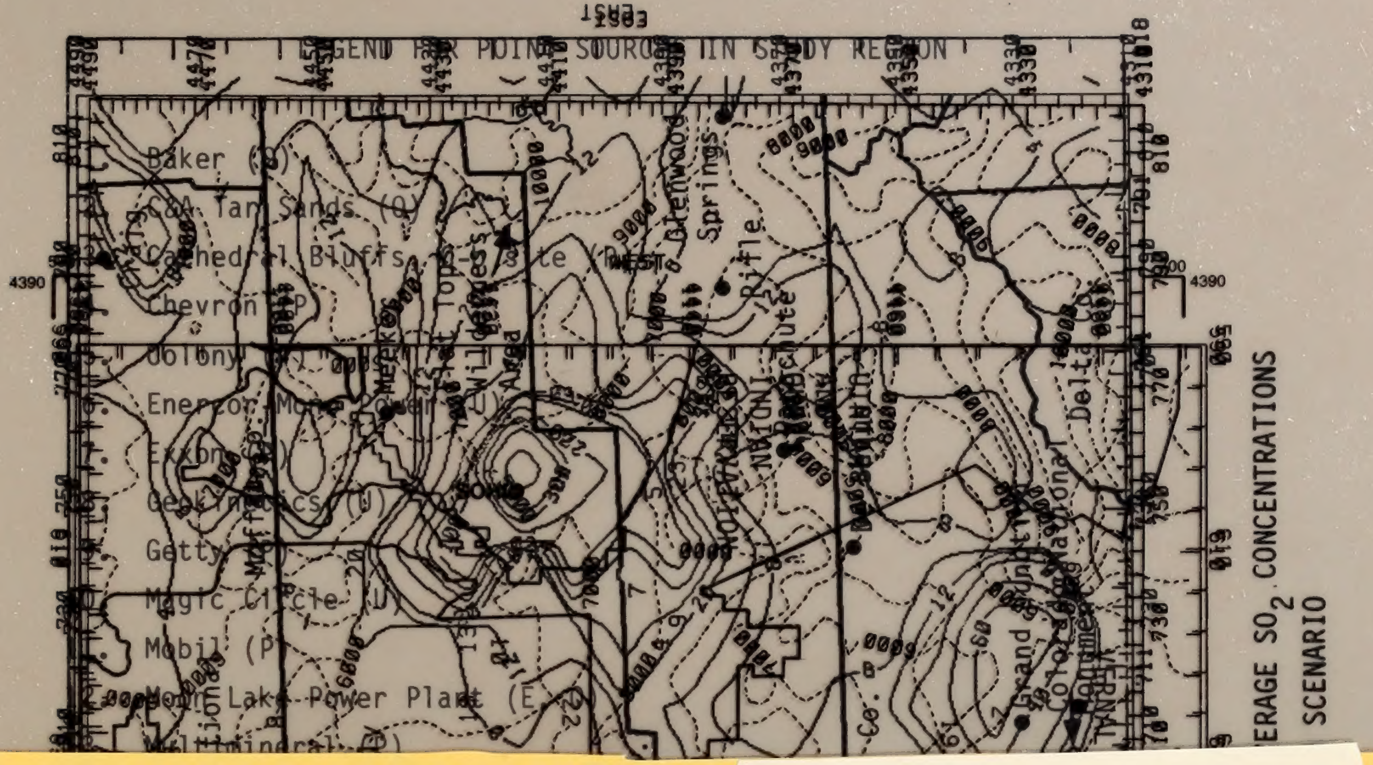

R'S CARD

TD 195 .S95 U35 1983 suppl.

Final air quality technical
report for the Uintah Basin

OFFICE	DATE RETURNED

(Continued on reverse)

BLM LIBRARY
RS 150A BLDG. 50
DENVER FEDERAL CENTER
P.O. BOX 25047
DENVER, CO 80225

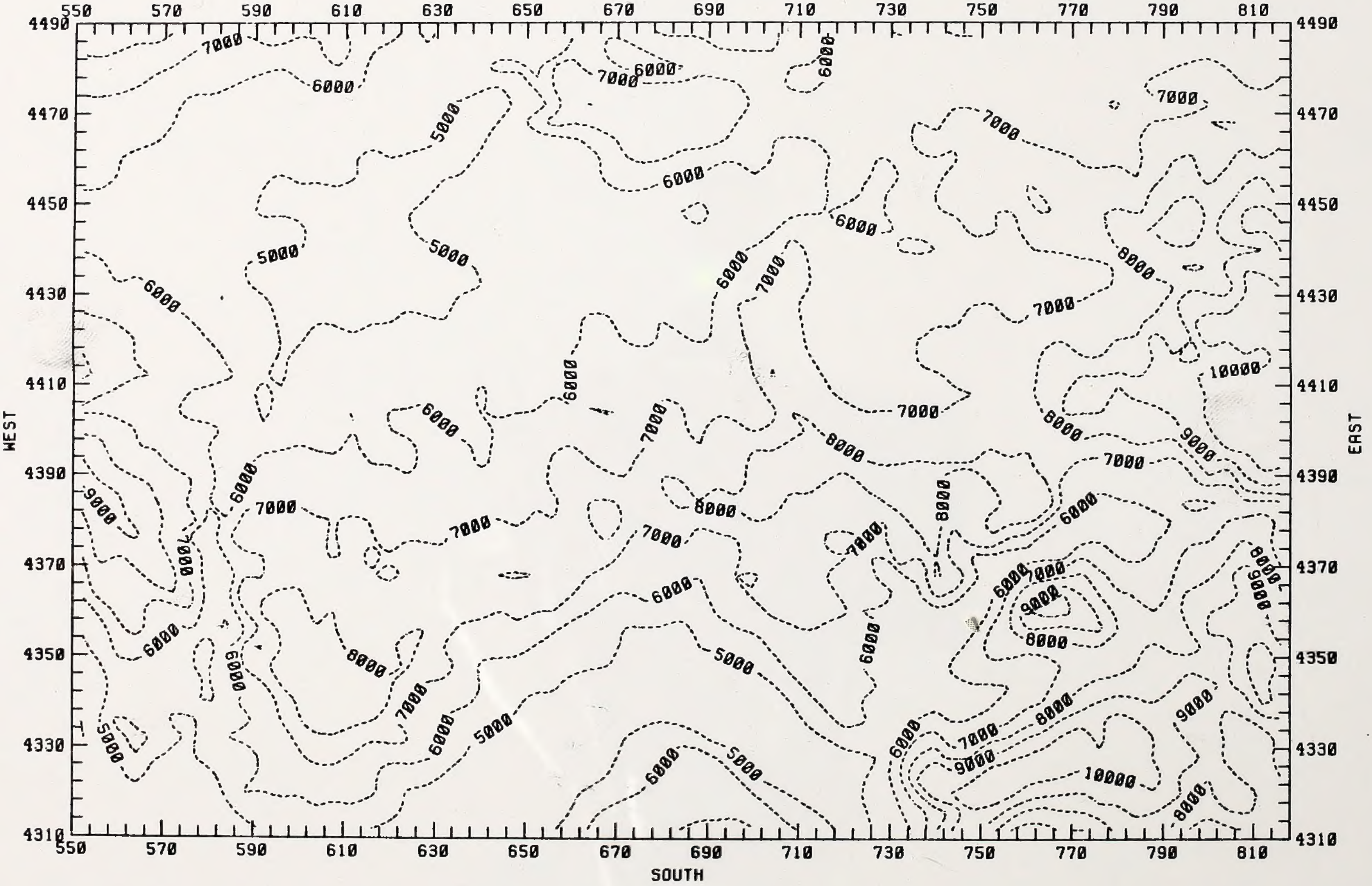

TERRAIN HEIGHTS IN FEET ABOVE SEA LEVEL

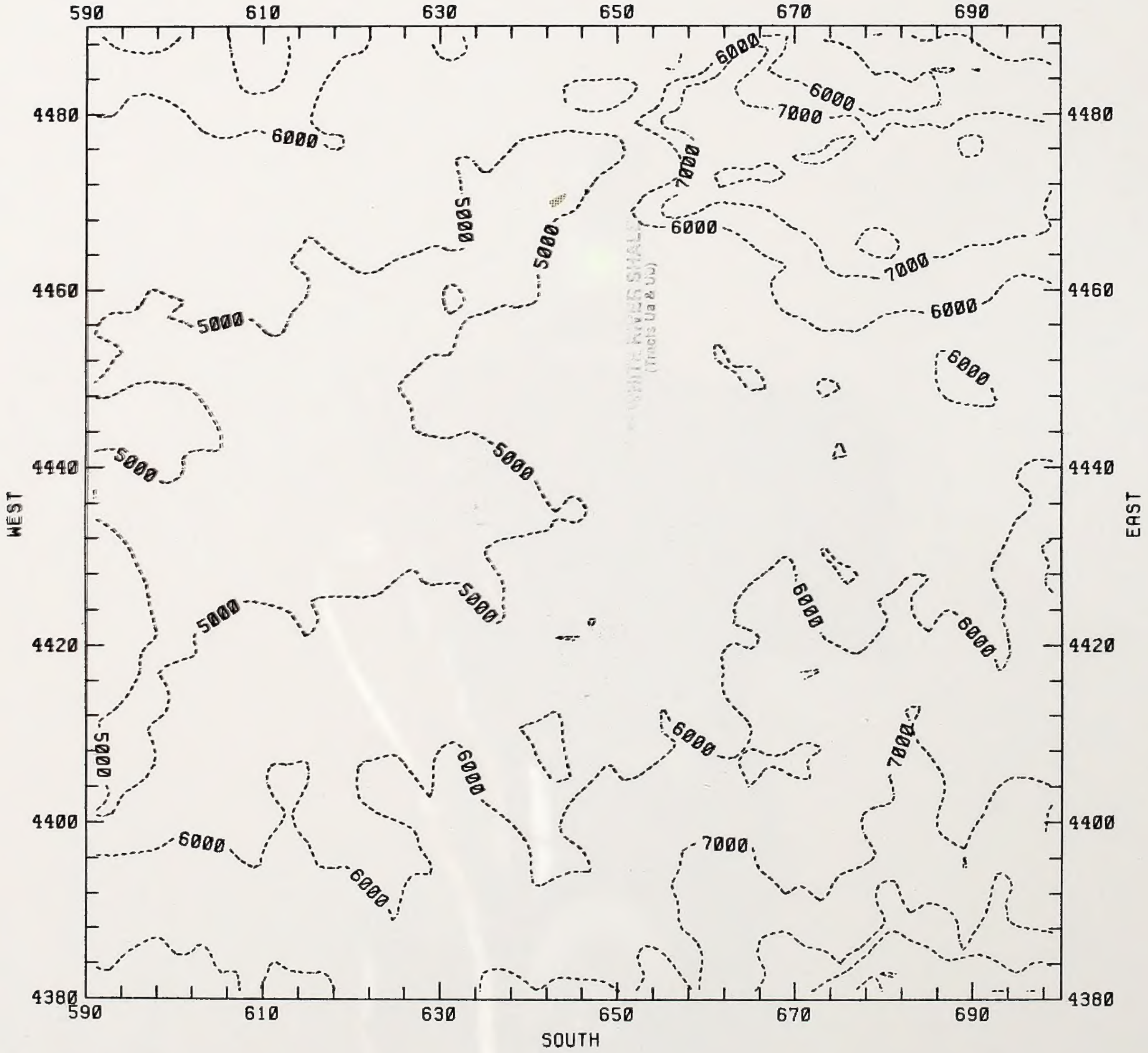
590
610
630
650
670
690
4480
4460
4440
4420
4400
4380
WEST
EAST
SOUTH
5000
6000
7000
WHITE RIVER SHALE
(Tracts Ua & Ub)

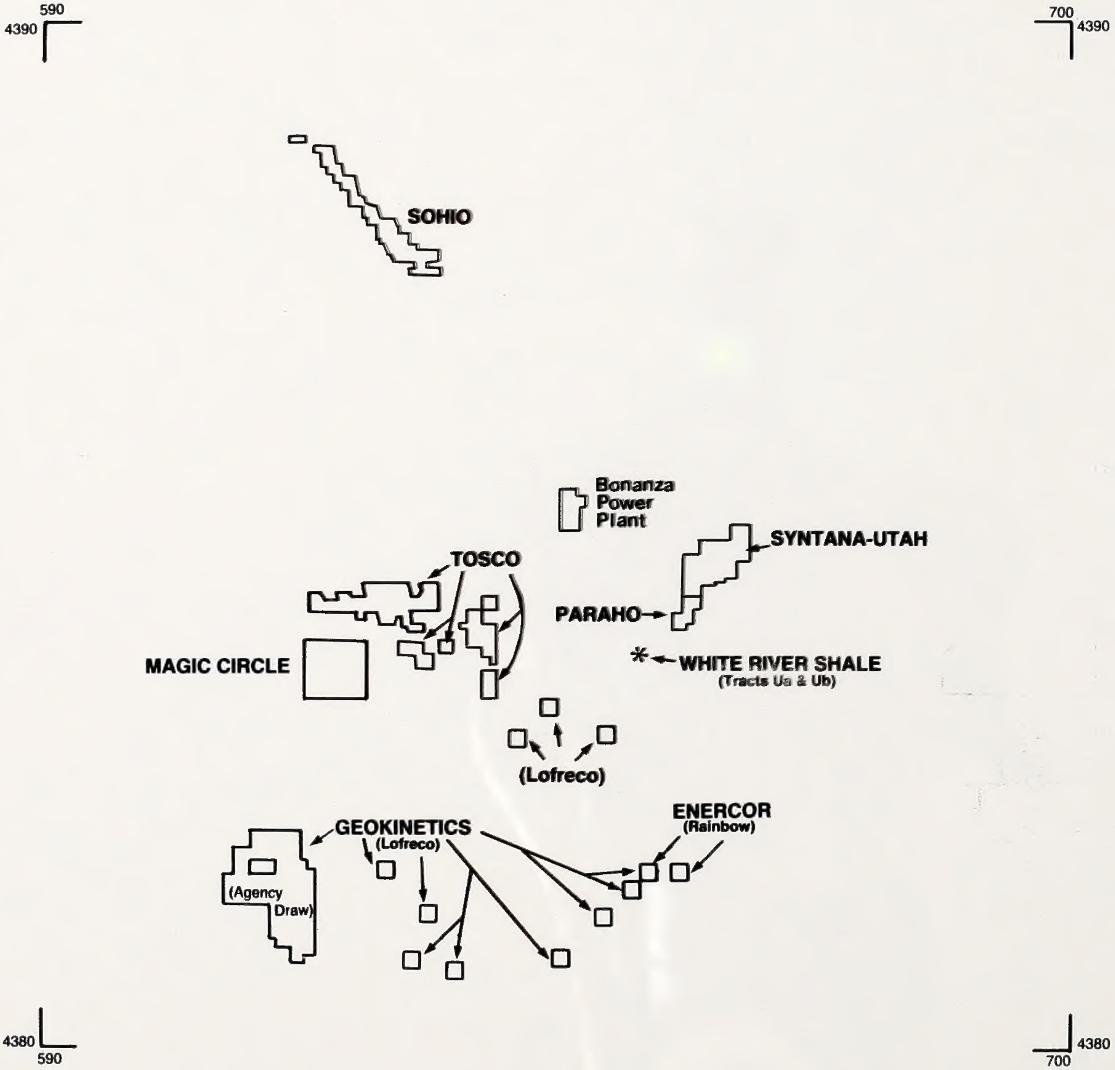
590
4390
700
4390
SOHIO
Bonanza
Power
Plant
SYNTANA-UTAH
TOSCO
PARAHO
MAGIC CIRCLE
WHITE RIVER SHALE
(Tracts Ua & Ub)
(Lofreco)
GEOKINETICS
(Lofreco)
ENERCOR
(Rainbow)
(Agency
Draw)
4380
590
4380
700

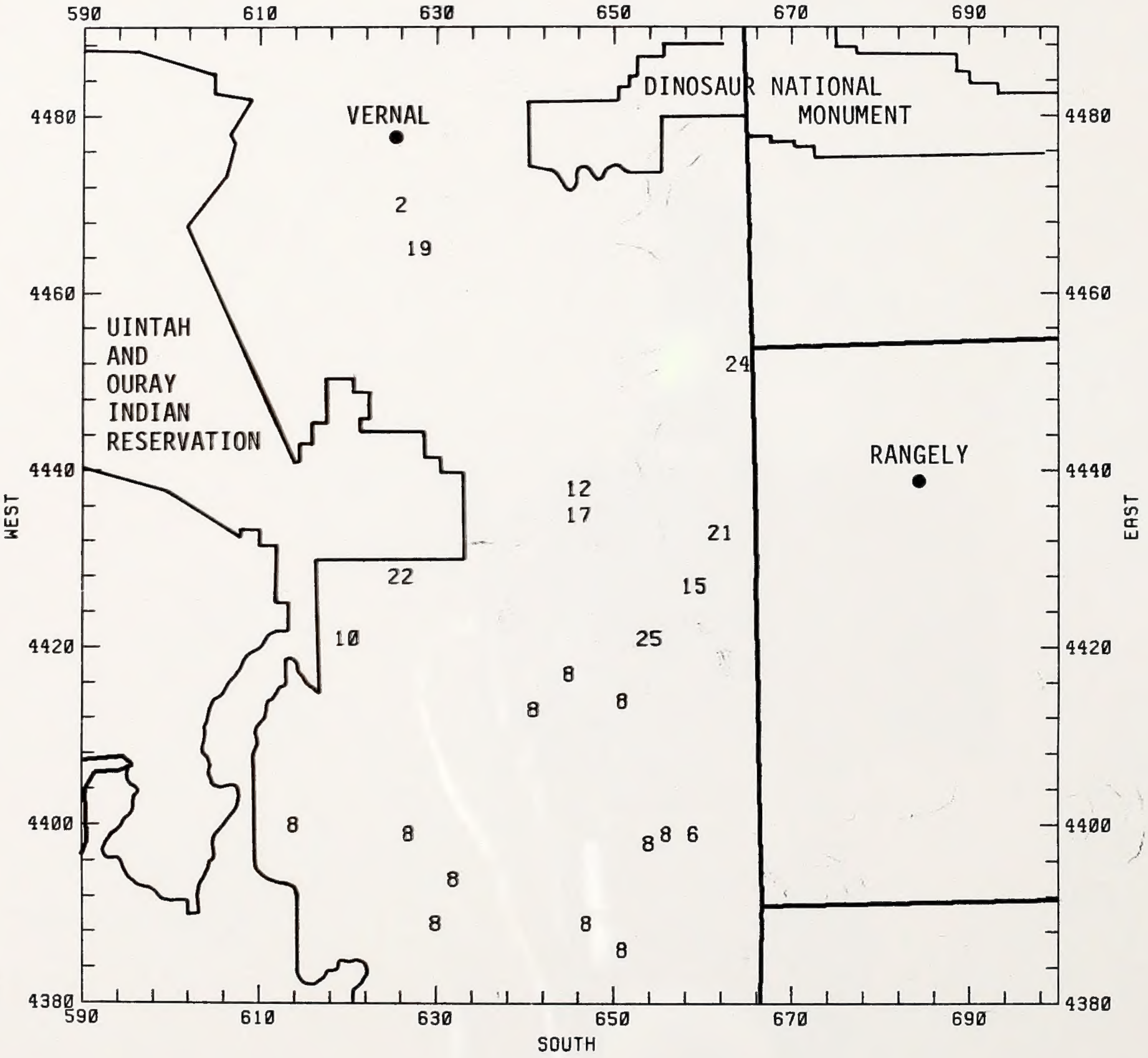
590
610
630
650
670
690
4480
4460
4440
4420
4400
4380
WEST
EAST
SOUTH
VERNAL
DINOSAUR NATIONAL MONUMENT
UINTAH AND OURAY INDIAN RESERVATION
RANGELY
2
19
24
12
17
21
22
15
10
25
8
8
8
8
8
8
8
6
8
8
8
8

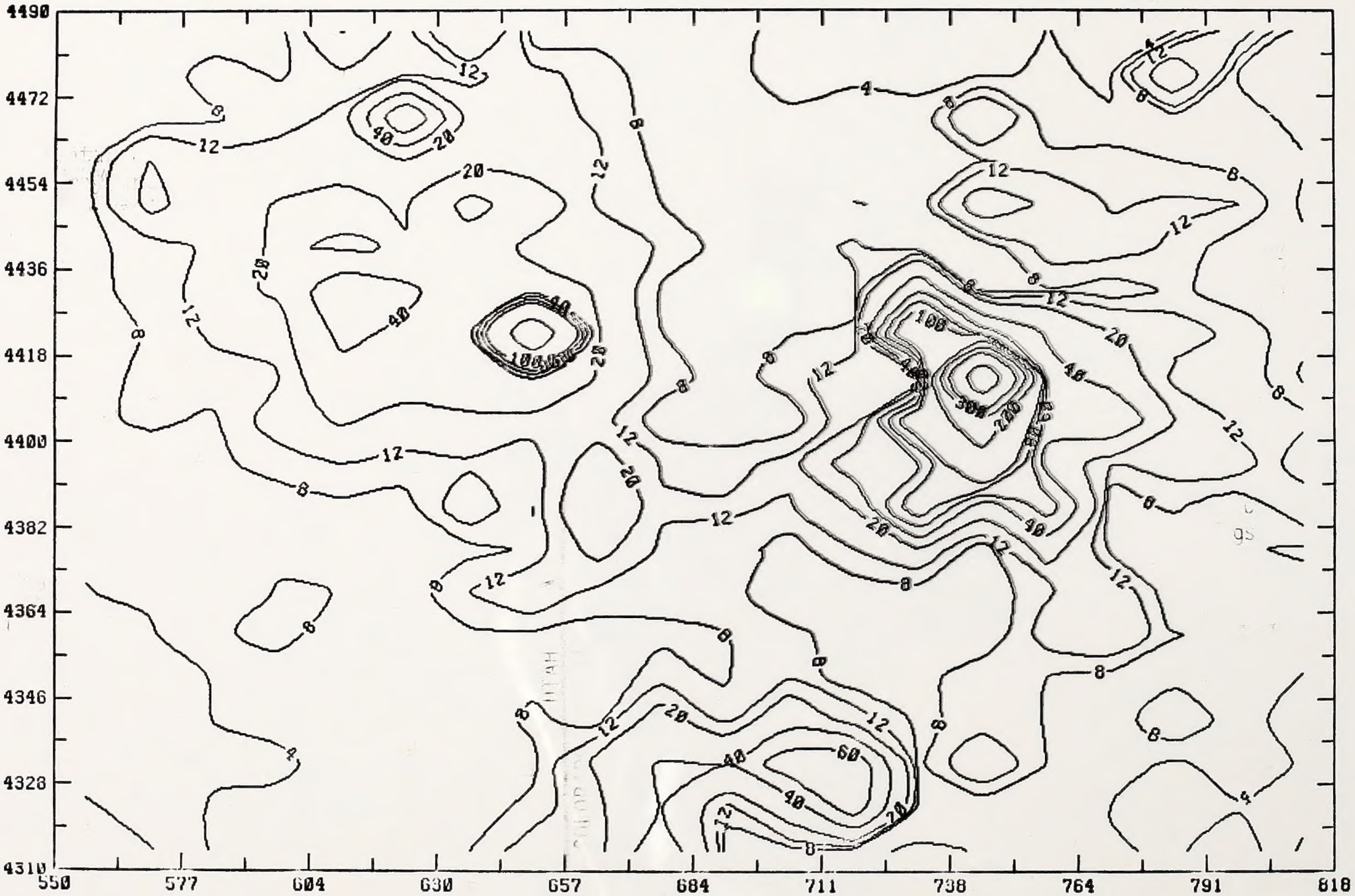

GPM ESTIMATES OF MAXIMUM 24-HOUR AVERAGE SO_2 CONCENTRATIONS ($\mu g/m^3$) FOR THE HIGH-OIL-PRODUCTION SCENARIO

82062r3 19
82062 4

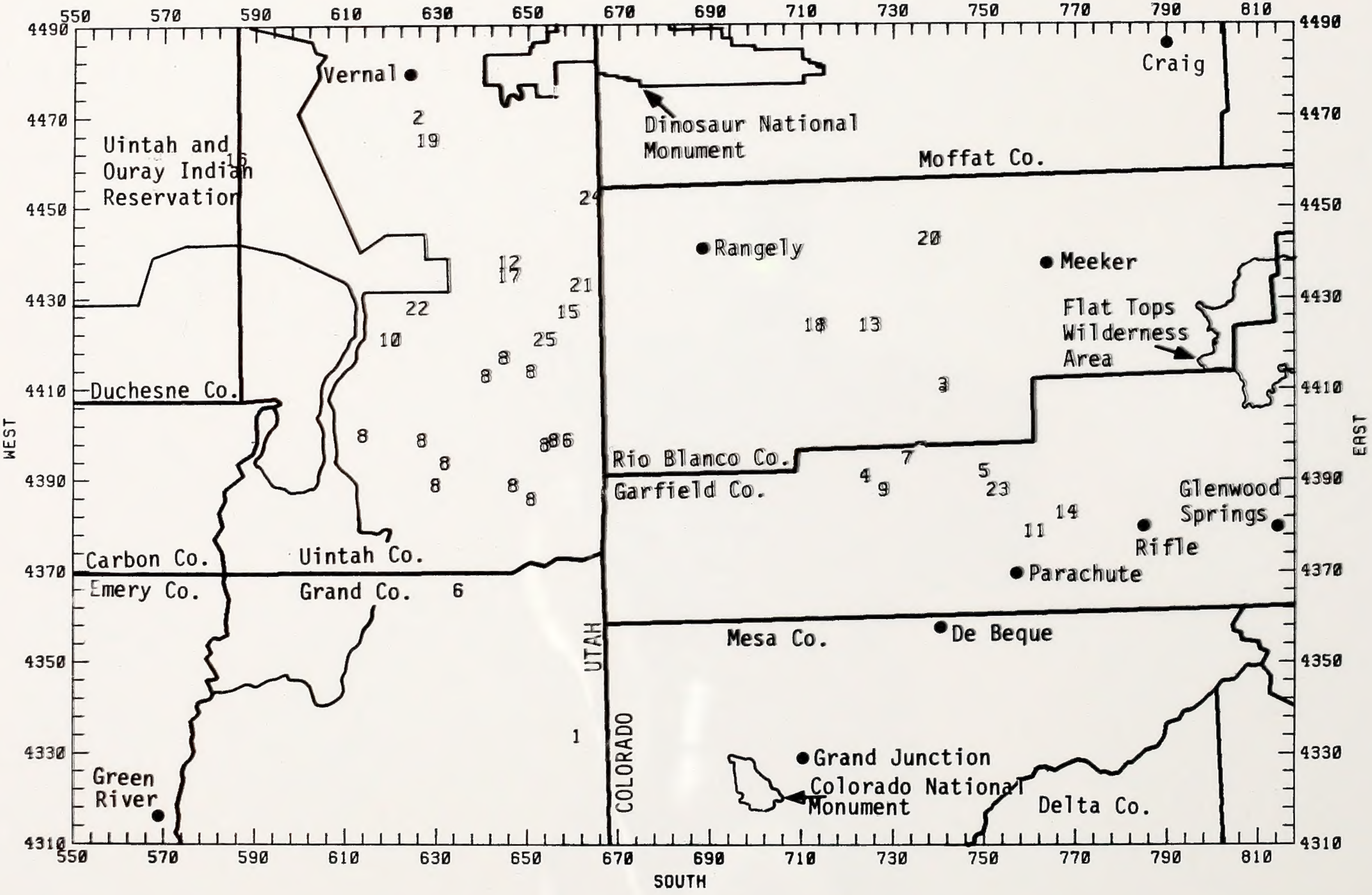

LEGEND FOR POINT SOURCES IN STUDY REGION

1. Baker (O)
2. C&A Tar Sands (O)
3. Cathedral Bluffs, C-b site (P)
4. Chevron (P)
5. Colony (P)
6. Enercor-Mono Power (U)
7. Exxon (P)
8. Geokinetics (U)
9. Getty (P)
10. Magic Circle (U)
11. Mobil (P)
12. Moon Lake Power Plant (E, O)
13. Multimineral (P)
14. Naval Oil Shale (P)
15. Paraho (U)
16. Plateau refinery (E, O)
17. Ramex (O)
18. Rio Blanco, C-a site (P)
19. Sohio (U)
20. Superior (P)
21. Syntana (U)
22. Tosco (U)
23. Union (P)
24. Western Tar Sands (O)
25. White River, U-a, U-b site (O)

Legend:
(E) Existing source in 1980
(O) Other planned sources (Uinta Basin)
(U) Uinta Basin synfuel facilities
(P) Piceance Basin oil shale facilities